

# **Exploration of Catalytic Activities of Some Transition Metal Borates for Green Synthesis of Nitrogen Containing Heterocyclic Compounds**

*A thesis submitted to the*  
**University of North Bengal**

*For the award of*  
**DOCTOR OF PHILOSOPHY (Ph.D.)**

*In*  
**CHEMISTRY**

*By*  
**SAILESH CHETTRI**  
(M.Sc. in Chemistry)

**Principal Supervisor**  
**Dr. Biswajit Sinha**  
Professor, Department of Chemistry  
University of North Bengal

**Co-Supervisor**  
**Dr. Dhiraj Brahman**  
Assistant Professor, Department of Chemistry  
St. Joseph's College, Darjeeling

**DEPARTMENT OF CHEMISTRY**  
**UNIVERSITY OF NORTH BENGAL**  
**DARJEELING, PIN 734013**  
**WEST BENGAL, INDIA**

July, 2022

*Dedicated*

*to*

*AAMA AND BABA*

## DECLARATION

I declare that the thesis entitled "**Exploration of Catalytic Activities of Some Transition Metal Borates for Green Synthesis of Nitrogen Containing Heterocyclic Compounds**" has been prepared by me under the supervision of Dr. Biswajit Sinha, Professor, Department of Chemistry, University of North Bengal and Dr. Dhiraj Brahma, Assistant Professor, Department of Chemistry, St. Joseph's College, Darjeeling. No part of this thesis has formed the basis for the award of any degree or fellowship previously.

*Sailesh Chettri*  
.....

**SAILESH CHETTRI**

Department of Chemistry

University of North Bengal

Darjeeling- 734013

West Bengal, India

Date: 19/07/2022.

## UNIVERSITY OF NORTH BENGAL

Prof. Biswajit Sinha, Ph. D  
Professor  
Department of Chemistry  
E-mail: biswachem@nbu.ac.in  
biswachem@gmail.com  
M: 9932738973, 9641967211



স্বদেশী মনঃ কামিনি স্বদেশী  
Accredited by NAAC with  
Grade B<sup>++</sup>

Ph: +91-353-2776381  
University of North  
Bengal  
Darjeeling 734 013  
INDIA

### CERTIFICATE

I declare that **Mr. SAILESH CHETTRI** has prepared the thesis entitled **“Exploration of Catalytic Activities of Some Transition Metal Borates for Green Synthesis of Nitrogen Containing Heterocyclic Compounds”** for the award of Ph. D degree of University of North Bengal under joint supervision of me and Dr. Dhiraj Brahman of Department of Chemistry, St. Joseph College, Darjeeling. He has carried out most of the work at the Department of Chemistry, University of North Bengal.

*Bis*

.....  
**Prof. Biswajit Sinha**

Department of Chemistry  
University of North Bengal  
Darjeeling-734013  
West Bengal,  
India

*Prof. Biswajit Sinha  
Department of Chemistry  
University of North Bengal*

Date: 19-07-2022



# St. Joseph's College

P.O. North Point, Darjeeling - 734104

E-mail: [dhirajslg2@gmail.com](mailto:dhirajslg2@gmail.com)

Accredited by the National Assessment and Accreditation Council, Bangalore, with Grade 'B' (3<sup>rd</sup> Cycle)

From:

**Dr. Dhiraj Brahman**

**Assistant Professor**

## CERTIFICATE

I declare that **Mr. Sallish Chettri** has prepared the thesis entitled "**Exploration of Catalytic Activities of Some Transition Metal Borates for Green Synthesis of Nitrogen Containing Heterocyclic Compounds**" for the award of Ph.D degree on University of North Bengal under joint supervision of me and **Prof. Biswajit Sinha** of Department of Chemistry, University of North Bengal. He has carried out some of the work at the Department of Chemistry, St. Joseph's College, Darjeeling.

*Dhiraj Brahman*  
10.9.2022

(Dhiraj Brahman)

Dr. Dhiraj Brahman  
Assistant Professor  
Department of Chemistry  
St. Joseph's College  
Darjeeling-734104

## Anti-Plagiarism Report of the Ph. D Thesis

### Title of the Thesis:

**Exploration of Catalytic Activities of Some Transition Metal Borates for Green Synthesis of Nitrogen Containing Heterocyclic Compounds**

Original

#### Document information

Analyzed document	Sailesh Chetti_Chemistry.pdf (0141972347)
Submitted	7/12/2022 @ 10:00 AM
Submitted by	University of North Bengal
Submitter email	nou@gnou.ac.in
Similarity	3%
Analysis address	nou@gnou.ac.in

Sailesh Chetti

(Signature of the Candidate)

19-09-2022

(Signature of the Supervisor)

*Prof. Biswajit Sinha*  
Department of Chemistry  
University of North Bengal

Dhiraj Brahma 19.07.2022

(Signature of the Supervisor)  
Co-

*Dr. Dhiraj Brahma*  
Assistant Professor  
Department of Chemistry  
St. Joseph's College  
Darjeeling-734104

## Abstract

Solvent-free multicomponent reactions are very important tools to carry out organic synthesis and functional group transformations rapidly thus opening up the possibility of synthesis of a wide variety of organic compounds in a very clean and an efficient manner according to the postulates of Green Chemistry. There are several methods for the synthesis of Nitrogen Containing Heterocyclic Compounds but most of the methods suffer from various drawbacks like low yield, harsh reaction conditions, use of toxic solvents, long reaction time and tedious work up procedures. Taking all these facts into consideration, we have tried to synthesize few Nitrogen containing Heterocyclic Compounds in a clean and efficient manner using solvent free multi-component approach taking some of the Transition Metal Borates as catalysts.

The entire thesis has been segregated into 6 (six) broad chapters and many chapters are further divided into sections for better discussion of the outcomes of the research work.

**Chapter-I** includes a brief introduction to the concept of Solvent free multicomponent reactions and the postulates of Green Chemistry. An idea about the Nitrogen Containing Heterocyclic compounds which have been prepared in this work is given in the chapter along with the recent literature review and their various biological applications. This chapter also includes a brief introduction to the transition metal borates under study and their applications in various fields of science.

**Chapter-II** is the experimental section where the sources and purity of various chemicals used in this research work is documented. It also includes the details of the various analytical and spectroscopic techniques like Melting Point determination, FT-IR spectroscopy, NMR spectroscopy, X-Ray Crystallography, etc., used for physicochemical characterization of the synthesized compounds. This chapter also includes the details of the theoretical works carried out on the selected synthesized compounds like DFT, Molecular Docking and Pharmacokinetic studies.

**Chapter-III** has been divided into three sections. **Section-A** contains the multi-component green synthesis of 2,4,5-triaryl imidazole derivatives using Copper Borate ( $\text{CuB}_4\text{O}_7$ ) as a catalyst wherein a variety of 2,4,5 triaryl imidazoles have been prepared using Benzil, aromatic aldehyde and ammonium acetate). The reaction proceeded in a milder way with excellent yield of the products. The products were characterized by FT-IR and  $^1\text{H}$ NMR spectroscopic techniques. **Section-B** comprises of the Synthesis, X-ray Diffraction study, Hirshfeld surface analysis and catalytic activity of Bis[2-(4,5-diphenyl-1H-imidazol-2-yl)-4-nitro-phenolato] copper (II) dihydrate complex. This chapter is also important from the view that the evidence of in-situ conversion of  $\text{CuB}_4\text{O}_7$  into  $\text{Cu}(\text{OAc})_2 \cdot 2\text{H}_2\text{O}$  in presence of  $\text{NH}_4\text{OAc}$  is discussed here. **Section-C** of the chapter mostly focusses on the DFT, Molecular Docking and Pharmacokinetic study of some selected synthesized 2, 4, 5-triarylimidazole derivatives.

**Chapter-IV** is divided into two sections. **Section-A** of the chapter deals with the green synthesis of 3,4-dihydropyrimidine-2-(1H)-ones (DHPMs) using Iron Borate as an efficient catalyst using substituted Benzaldehyde, Ethyl acetoacetate and Urea. The reaction provides a method for the synthesis of a variety of 3, 4-dihydropyrimidine-2-ones with good to excellent yields and the catalyst has been versatile for a wide range of aromatic aldehydes. The products were characterized by FT-IR and <sup>1</sup>HNMR spectroscopic techniques. **Section-B** of the chapter includes the DFT, Molecular Docking and Pharmacokinetic study of some selected 3, 4-dihydropyrimidin-2(1H)-one (DHPM) derivatives.

**Chapter-V** contains two sections. **Section-A** of the chapter includes an efficient and green protocol for the synthesis of 1-hydroxy-2-arylimidazole-3-oxide derivatives under solvent free condition using inexpensive Copper borate (CuB<sub>4</sub>O<sub>7</sub>) catalyst using a mixture of diacetyl monoxime, substituted benzaldehyde and hydroxylamine hydrochloride and the products were characterized by FT-IR and <sup>1</sup>HNMR spectroscopic techniques. **Section-B** includes DFT, Molecular Docking and Pharmacokinetic study of some selected 1-hydroxy-2-arylimidazole-3-oxide derivatives.

**Chapter-VI** deals with the solvent free green synthesis of 2-substituted benzimidazole and 1, 2-disubstituted benzimidazole derivatives using Nickel Borate as a catalyst with excellent yield of products. The synthesized products were characterized by FT-IR and <sup>1</sup>HNMR spectroscopic techniques.

Finally, the thesis ends with concluding remarks of the research work embodied in the thesis.



## Preface

*With the development of the idea of Green Chemistry as given by Prof.P.T.Anastas, solvent free multicomponent reactions are becoming very popular in the present days. Keeping this theme in mind and also with an enthusiasm of exploring the catalytic activity of some selected transition metal borates, this research work is carried out by the author under the joint guidance of Dr.Biswajit Sinha, Professor, Department of Chemistry, University of North Bengal and Dr. Dhiraj Brahman, Assistant Professor, Department of Chemistry, St. Joseph's College, Darjeeling.*

*While going through the literatures it was observed that there were numerous applications of transition metal borates in various fields, however, it was observed that the catalytic activity of these borates were very poorly explored. Therefore, this encouraged us to explore the catalytic activity of these borates in some famous organic reactions involving the synthesis of 2,4,5-triaryl imidazoles, 3,4-dihydropyrimidine-2[1H]-ones, 1-hydroxy-2-arylimidazole-3-oxide and 2-substituted benzimidazoles and 1, 2-disubstituted benzimidazoles. Looking at the diverse applications of these Nitrogen Containing Heterocyclic Compounds, the synthesis of these compounds in a cleaner and milder way following the principles of Green Chemistry with the transition metal borates as catalysts may evolve as an attractive field of research in the field of chemical sciences.*

*Transition metal borates have been used profoundly in glass industries and have tremendous applications in lithium-ion batteries, glass electrodes, non linear optical devices and optical communication devices. Taking inspiration from the famous scientists like Hawthorne, Grimes and Braunschweig who have done various works in the field of borates, the present dissertation was undertaken for exploring the catalytic activity of some selected transition metal borates, namely Copper Borate, Iron Borate and Nickel Borate for the green synthesis of Nitrogen Containing Heterocyclic Compounds and the results of this work are quite promising.*

*Density Functional Theory (DFT), Molecular Docking, Computer Aided Drug Design (CADD) are widely used now-a-days for investigating the physical properties as well as for identification of suitable and specific drug target molecules. An attempt has been made to study the theoretical properties and drug likeliness of some of the selected synthesized compounds using DFT and Molecular Docking Studies and some of the theoretical parameters have also been compared with experimental results to get into a deep insight into the structures of the selected compounds.*

## ***Acknowledgements...***

*First and foremost, I would like to thank the **Supreme Power of the Universe “Almighty God”** for giving me power and strength to complete this work. When I started with my research work, it was a completely a new experience for me but the support, motivation and blessings of some great souls made this experience a great and an enjoyable one and the knowledge that I have gained from this work is completely ineffable.*

*It goes without saying, I would like to thank and acknowledge the efforts put in this research work by my Principal Supervisor, **Prof. Biswajit Sinha**, Department of Chemistry, University of North Bengal. He has always been a kind-hearted person whose constant motivation and words of wisdom never made me feel uncomfortable with my work. It’s a blessing to work with such a great person of vision and knowledge. The success of this research work is the result of his constant dedication towards his students.*

*From the bottom of my heart, I would like to thank my Co-Supervisor, **Dr. Dhiraj Brahman**, Assistant Professor, St. Joseph’s College, Darjeeling. Sir has always been my “**Genie-The Genius**” always there with his magical gesture to protect me and take me out from almost all the kinds of trouble that came to me. Without him, my research career would not have been possible. He has been a friend, a philosopher and a guide whose hard work and sincerity is reflected in this work. I shall always remain indebted to him and “No words” can describe my feeling of gratitude towards him.*

*Most respectfully I would like to thank **Prof. Pranab Ghosh**, Department of Chemistry, University of North Bengal for his valuable help and suggestions which played a great role in completion of my research work.*

*With deep sense of gratitude and respect, I would like to thank respected **Fr. Dr. Donatus Kujur**, Principal, St. Joseph’s College, Darjeeling for his blessings and constant support which has played a crucial and a pivotal role in my personal as well as my research life. Without his guidance and help this work would have never been a successful one.*

*I am extremely thankful to **Dr. Kiran Pradhan**, Associate Professor, Department of Chemistry, University of North Bengal for his guidance, motivation and support right from my student life to my research career.*

*I would like to thank the support and help that I received from all the faculty members, Scientific Officers and all the staffs of the Department of Chemistry, University of North Bengal.*

*I am extremely thankful to all the faculty members and my teachers **Dr. Rupa Bhowmick, Dr. Rajendra Pradhan, Ms. Antara Sharma, Dr. Rajani Dewan** from*

*the Department of Chemistry, St. Joseph's College, Darjeeling for their teachings and guidance and making me what I am today. I would also like to thank **Mr. Meghraj Tamang** and **Mr. Roshan Rizal** from the Department of chemistry, St. Joseph's College, Darjeeling for their valuable help and support.*

*My heartfelt gratitude to my friends and lab mates **Mr. Sudarshan Pradhan**, **Mr. Anmol Chettri** and **Ms. Pritika Gurung**. My life would not have been easy without the support of you all.*

*I would also like to thank my seniors **Mr. Uttam. Kr. Singha**, **Dr. Ananya Das**, **Dr. Dipu. Kr. Mishra**, **Dr. Amarjit Kamath**, **Mr. Dhrubajyoti Roy**, **Dr. Kaushik Acharjee** and my junior lab mate **Mr. Prajal Chhetri**. I would also like to acknowledge the support provided by my dear brothers and sisters from the Department of Chemistry, University of North Bengal namely **Mr. Munna Mukhia** (Munna Bhai), **Mr. Sangharaj Diyali** (Shankee), **Ms. Yachna Rai** and **Ms. Prasansha Rai**.*

*My parents are my pillars of success. This work is dedicated to my father **Mr. Bikram Kumar Chettri** and my mother **Mrs. Rupa Chettri** as without their blessings and support I would not have made it through*

*This acknowledgement note would not be complete without mentioning my junior lab mate and my dear bhai **Mr. Sumiran Tamang**. The hardwork and enthusiasm that he has shown for helping me out in my research work is highly acknowledged and shall be forever remembered. I would also like to thank my friends and my well-wishers especially **Miss Nikita Chhetri**, **Mr. Shivanand Chettri** and **Mr. Bikram Gurung** for their love, support and constant motivation.*

*. I would like to thank my teachers **Dr. Ramesh Sharma**, **Prof. Nayan Kamal Bhattacharyya**, **Dr. Joydeep Biswas**, **Prof. Sanjay Dahal** and **Mr. Suraj Tamang** for their valuable guidance and support in every step of my life.*

*Finally, I gracefully acknowledge the analytical services for the characterization of synthesized products provided by*

- 1. **Incubation Centre, St. Joseph's College, Darjeeling***
- 2. **CDRI Lucknow***
- 3. **SAIF NEHU Shillong***
- 4. **Central University of Sikkim***
- 5. **Department of Microbiology, St. Joseph's College, Darjeeling and***
- 6. **Research Centre for Crystalline Material, Sunway University, Malaysia.***

*-Sailesh Chettri  
Research Scholar  
Department of Chemistry  
University of North Bengal.*

## TABLE OF CONTENTS

<b>TOPICS</b>	<b>Page No.</b>
Abstract	i-ii
Preface	iii
Acknowledgement	iv-v
Table of Contents	vi-vii
List of Tables	viii-xi
List of Figures	xii-xix
List of Schemes	xx-xxiv
List of Appendices	xxv
<b>Chapter-I</b>	<b>1-96</b>
1.1 Introduction	1-7
1.2 Green Chemistry	7-24
1.3 Brief information about the studied N-heterocyclic scaffolds	24-68
1.4 Brief information about the Transition Metal Borates	69
1.5 Objectives of the Research work	70
1.5 References	71-96
<b>Chapter-II</b>	<b>97-110</b>
2.1 General Remarks	97
2.2 General procedure for the synthesis of different N-containing heterocyclic derivatives.	97-104
2.3 Theoretical Study of some selected N-heterocyclic compounds	104-107
2.4 References	108-110
<b>Chapter III-Section A</b>	<b>111-134</b>
3.A.1 Background of the present investigation	111-113
3.A.2 Results and discussion	113-119
3.A.3 Plausible Mechanism	120
3.A.4 Experimental section	121
3.A.5 Conclusion	121
3.A.6 Analytical and Spectroscopic data	122-124
3.A.7 Supporting spectra	125-129
3.A.8 References	130-134
<b>Chapter III-Section B</b>	<b>135-161</b>
3.B.1 Background of the present investigation	135-136
3.B.2 Results and discussion	136-158
3.B.3 Experimental section	158
3.B.4 Conclusion	159
3.B.5 References	160-161
<b>Chapter III-Section-C</b>	<b>162-203</b>
3.C.1 Background of the present investigation	162-163

3.C.2 Results and discussion	164-198
3.C.3 References	199-203
<b>Chapter IV-Section A</b>	<b>204-234</b>
4.A.1 Background of the present investigation	204-206
4.A.2 Results and Discussions	206-212
4.A.3 Plausible Mechanism	213
4.A.4 Experimental Section	214
4.A.5 Conclusions	214
4.A.6 Analytical and Spectroscopic data	215-217
4.A.7 Supporting spectra:	218-230
4.A.8 References	231-234
<b>Chapter IV-Section-B</b>	<b>235-268</b>
4.B.1 Background of the present investigation	235-237
4.B.2 Results and Discussions	238-263
4.B.3 References	264-268
<b>Chapter V-Section A</b>	<b>269-300</b>
5.A.1 Background of the present investigation	269-271
5.A.2 Result and Discussions	271-284
5.A.3 Experimental section	284-285
5.A.4 Analytical and Spectroscopic data	285-287
5.A.5 Supporting spectra	288-297
5.A.6 References	298-300
<b>Chapter-V-Section B</b>	<b>301-340</b>
5.B.1 Background of the present investigation	301
5.B.2 Results and Discussion	301-336
5.B.3 References	337-340
<b>Chapter VI</b>	<b>341-363</b>
6.1 Background of the present investigation	341-342
6.2. Results and discussions	343-353
6.3 Experimental Section	353-354
6.4. Conclusion	354
6.5 Analytical and Spectroscopic data	355-358
6.6 Supporting spectra	359-360
6.7 References	361-363
<b>Chapter VII</b>	<b>364-366</b>
7.1 Concluding Remarks	364-366
Appendix-I	367-371
Appendix-II	372
Appendix-III	373
Appendix-IV	374
Bibliography	375-422
INDEX	423-424

## LIST OF TABLES

<b>Tables</b>		<b>Page No.</b>
Table 2.1	Provenance and purity of Chemicals	98-99
Table 2.2	Particulars of the catalyst	100
Table 2.3	Provenance and purity of the solvent used	101
Table 3.A.1	Screening of the solvent for model reaction	113
Table 3.A.2	Screening of the amount of the catalyst for the model reaction	114
Table 3.A.3	CuB <sub>4</sub> O <sub>7</sub> catalyzed solvent free synthesis of 2,4,5-triarylimidazole derivatives (4a-4w)	116
Table 3.A.4.	Comparision of Catalytic efficacy of CuB <sub>4</sub> O <sub>7</sub> with other reported Catalysts	118-119
Table 3.B.1	Crystallographic parameters of complex (1)	141
Table 3.B.2.	Selected geometric parameters of complex (1)	142
Table 3.B.3	Hydrogen Bond geometry for complex (1)	144
Table 3.B.4	Summary of short interatomic contacts (Å) in complex (1)	146
Table 3.B.5	Percentage contributions of interatomic contacts to the Hirschfield surface for the complex in (i) and overall (II)	150
Table 3.B.6	Crystal data collection and structure refinement for compound (2)	152
Table 3.B.7	The selected bond lengths (Å) and bond angles (°) for compound (2)	153
Table 3.B.8	Hydrogen bonded geometries in compound (2)	154
Table 3.B.9	Optimization of catalyst loading	155
Table 3.B.10	Optimization of reaction parameters for the C-S coupling reaction	156
Table 3.C.1	Structural parameters (bond lengths, bond angle and dihedral angle) of the studied compounds (IM-1 to IM-6)	165-170
Table 3.C.2	Energies of HOMO and LUMO orbitals, ionization energy (I), electron affinity (A), Chemical potential ( $\mu$ ), Electronegativity ( $\chi$ ), Global hardness ( $\eta$ ) and Global electrophilicity power ( $\omega$ ) of the studied compounds (IM-1 to IM-6)	174
Table 3.C.3	Experimental and theoretical vibrational frequencies of compounds (IM-1 to IM-6) (with B3LYP/6-31G+(d,2p)) with proposed assignments	175-178
Table 3.C.4	Detailed description of MEP surface for compounds IM-1 to IM-6	181

Table 3.C.5	Dipole moments, dipole polarizabilities, anisotropic polarizabilities and First order hyperpolarizabilities of the studied compounds (IM-1 to IM-6)	183
Table 3.C.6	Second order hyperpolarizabilities of studied compounds IM-1 to IM-6	185
Table 3.C.7	Summary of docking of the compound (IM-1 to IM-6) against insulin receptor protein 1IR3 with corresponding binding energy ( $\Delta G$ ), predicted inhibitory constant ( $pK_i$ ), interacting amino acid residues and type of interactions	188
Table 3.C.8.	Lipinski's properties and pharmacokinetic properties (ADME) of 2, 4, 5-triarylimidazole derivatives (IM-1 to IM-6)	196
Table 4.A.1	Screening of the solvent for control reaction	206
Table 4.A.2	Screening of the amount of the catalyst for the model reaction	207
Table 4.A.3	Iron Borate catalyzed solvent free neat synthesis of 3,4-dihydropyrimidine-2-one derivatives (4a-4q)	209
Table 4.A.4.	Study on the recyclability of the catalyst	210
Table 4.A.5.	Comparison of Catalytic efficiency of Iron Borate with other reported catalysts for the synthesis of 3,4-dihydropyrimidine-2-one derivatives (4a-4q).	211
Table 4.B.1.	Structural parameters (bond lengths, bond angles and dihedral angles) of the studied compounds (DP-1 to DP-3)	241-243
Table 4.B.2.	Energies of HOMO and LUMO orbitals, ionization energy ( $I$ ), electron affinity ( $A$ ), Chemical potential ( $\mu$ ), Electronegativity ( $\chi$ ), Global hardness ( $\eta$ ) and Global electrophilicity power ( $\omega$ ) of the studied compounds (DP-1 to DP-3)	245
Table 4.B.3.	FT-IR analysis of studied compounds DP-1 to DP-3	246-247
Table 4.B.4	Detailed description of MEP surface for compounds DP-1 to DP-3	251
Table 4.B.5	Computed Dipole moments, dipole polarizabilities and anisotropic Polarizabilities and first-order hyperpolarizabilities of compounds DP-1 to DP-3	253
Table 4.B.6	Second order hyperpolarizabilities of studied compounds DP-1 to DP-3	254
Table 4.B.7	Summary of docking of the compound (IM-1 to IM-6) against insulin receptor protein 1IR3 with corresponding binding energy ( $\Delta G$ ), predicted inhibitory constant ( $pK_i$ ), interacting amino acid residues and type of interactions.	256
Table 4.B.8	Lipinski's properties and pharmacokinetic properties (ADME) of studied compounds DP-1 to DP-3	261

Table 5.A.1	Screening of the reaction condition (solvent) for model reaction	274
Table 5.A.2	Screening of the amount of catalyst loading for the model reaction	275
Table 5.A.3	CuB <sub>4</sub> O <sub>7</sub> catalyzed solvent free synthesis of 1-hydroxy-2-(aryl)-4,5-dimethylimidazole-3-oxide (4a-4m)	276
Table 5.A.4	Recyclability of copper borate in model reaction	278
Table 5.A.5	Crystal data collection and structure refinement for (4m)	281
Table 5.A.6	Selected bond lengths (Å), bond angles (°) and torsion angles (°) for (4m)	282
Table 5.A.7	Hydrogen bonded geometries in (4m)	282
Table 5.A.8	X–H···Cg interactions in (4m)	282
Table 5.B.1.	Structural parameters (bond lengths, bond angle and dihedral angle) of the studied compounds (IMO-1 to IMO-6)	303-307
Table 5.B.2.	Energies of HOMO and LUMO orbitals, ionization energy (I), electron affinity (A), Chemical potential (μ), Electronegativity (χ), Global hardness (η) and Global electrophilicity power (ω) of the studied compounds (IMO-1 to IMO-6)	311
Table 5.B.3.	Theoretical vibrational spectra of the studied compounds (IMO-1 to IMO-6)	313-316
Table 5.B.4	Detailed description of MEP surface for compounds IMO-1 to IMO-6	321
Table 5.B.5	Dipole moments, dipole polarizabilities, anisotropic polarizabilities and First order hyperpolarizabilities of IMO-1 to IMO-6	323
Table 5.B.6	Second order hyperpolarizabilities of compound IMO-1 to IMO-6	325
Table 5.B.7.	Summary of docking of the compound (IM-1 to IM-6) against insulin receptor protein IIR3 with corresponding binding energy (ΔG), predicted inhibitory constant (pK <sub>i</sub> ), interacting amino acid residues and type of interactions.	327
Table 5.B.8.	Lipinski's properties and pharmacokinetic properties (ADME) of 1-hydroxy-2-arylimidazole-3-oxide derivatives (IMO-1 to IMO-6)	334
Table 6.1.1	Optimization of reaction temperature for the model reaction	345
Table 6.1.2	Optimization of catalyst loading for the model reaction	345
Table 6.1.3.	Isolated yield and melting point of the synthesized benzimidazole derivatives (3a-3j)	346
Table 6.1.4	Recyclability of the catalyst	347



Table 6.2.1.	Optimization of reaction temperature for the model reaction	349
Table 6.2.2	Optimization of catalyst loading for the model reaction	350
Table 6.2.3	Isolated yield and melting point of the synthesized benzimidazole derivatives (3a'-3k')	351
Table 6.2.4	Recyclability of the catalyst	352

## LIST OF FIGURES

Figure		Page No.
Fig. 1.1	Examples of naturally occurring N-containing heterocyclic compounds	1
Fig. 1.2	Molecular structures of some of the prescribed drugs containing N-heterocyclic scaffold	2
Fig. 1.3	Molecular structures of nitrogenous bases of DNA and RNA	3
Fig. 1.4	Molecular structures of some of the N-heterocyclic scaffolds	3
Fig. 1.5	Molecular structures of amino acids containing N-heterocyclic motifs	4
Fig. 1.6	Molecular structures of Penicillin, Cephalosporin and Puromycin	5
Fig. 1.7	Structures of some of the biologically active N-heterocyclic motifs	6
Fig. 1.8	Wohler's Synthesis of ammonia	10
Fig. 1.9	Bayer-Villiger oxidation of ketones with mCPBA	10
Fig. 1.10	Claisen rearrangement	10
Fig. 1.11	Important organic reactions in solvent free condition.	11
Fig. 1.12	Solventless reaction protocols for synthesis of some N-containing heterocyclic compounds	13
Fig. 1.13	Historical development of Multi Component Reactions	22
Fig. 1.14	Molecular structures of 2,4,5-triarylimidazole, 3,4-dihydropyrimidin-2(1 <i>H</i> )-one, 1-hydroxyimidazole 3-oxide and 1,2-disubstituted benzimidazoles	24
Fig. 1.15	Structures of few drugs containing imidazole scaffold	25
Fig. 1.16	Structures of few naturally occurring biomolecules	25
Fig. 1.17	Structures of some biologically important substituted imidazoles	26
Fig. 1.18	Structures of few drugs having Imidazole Scaffold.	27
Fig. 1.19	Structures of 3,4-dihydropyrimidin-2(1 <i>H</i> )-ones and 3,4-dihydropyrimidine-2-(1 <i>H</i> )-thiones	37
Fig. 1.20	Some biologically important Bigenelli Compounds	38
Fig. 1.21	Structure of Benzimidazole	51
Fig. 1.22	Some of the biologically important benzimidazole derivatives	52
Fig. 1.23	Some of the important drugs containing benzimidazole nucleus	52
Fig. 2.1	a. Pulverization of reactant and catalyst in agate motor and pestle	98
	b. Heating the reaction mixture in oil bath.	98
Fig. 2.2	Determination of melting point by open capillary method	102
Fig. 2.3	Bruker Alpha-II FT-IR spectrophotometer	102
Fig. 2.4	Bruker Advance neo-FT-NMR spectrometer	103

Fig. 3.A.1	Structures of commercially available drugs containing imidazole core	111
Fig. 3.A.2	2,4,5 triarylimidazole derivatives	115
Fig.3.A.7.1	<sup>1</sup> H NMR spectra of 2,4,5-triphenyl-1H-imidazole	125
Fig. 3.A.7.2	FT-IR spectra of 2,4,5-triphenyl-1H-imidazole	125
Fig. 3.A.7.3	<sup>1</sup> H NMR spectra of 2-(2-nitrophenyl)-4,5-diphenyl-1H-imidazole	126
Fig. 3.A.7.4	FT-IR spectra of 2-(2-nitrophenyl)-4,5-diphenyl-1H-imidazole	126
Fig. 3.A.7.5	<sup>1</sup> H NMR of 2-(3-bromophenyl)-4,5-diphenyl-1H-imidazole	127
Fig. 3.A.7.6	FT-IR spectra of 2-(3-bromophenyl)-4,5-diphenyl-1H-imidazole	127
Fig. 3.A.7.7	<sup>1</sup> H NMR of 4-(4,5-diphenyl-1H-imidazol-2-yl)benzotrile	128
Fig. 3.A.7.8	FT-IR spectra of 4-(4,5-diphenyl-1H-imidazol-2-yl)benzotrile	128
Fig. 3.A.7.9	<sup>1</sup> H NMR of 4-chloro-2-(4,5-diphenyl-1H-imidazol-2-yl)phenol	129
Fig. 3.A.7.10	FT-IR spectra of 4-chloro-2-(4,5-diphenyl-1H-imidazol-2-yl)phenol	129
Fig. 3.B.1	Structure of plastocyanin	135
Fig.3.B.2	a. Molecular structure of complex (1)	136
	b. Crystal structure of the complex molecule (1), showing the atom-labeling scheme and with displacement ellipsoids drawn at the 70% probability level	137
Fig. 3.B.3	1. FT-IR spectra of the reaction mixture of CuSO <sub>4</sub> and NH <sub>4</sub> OAc	139
	2. FT-IR spectra of the reaction mixture of CuCl <sub>2</sub> and NH <sub>4</sub> OAc	139
	3. FT-IR spectra of the reaction mixture of CuO and NH <sub>4</sub> OAc	139
	4. FT-IR spectra of commercially available Cu(OAc) <sub>2</sub> ·2H <sub>2</sub> O	139
Fig. 3.B.4.	A view of the molecular structure of the complex molecule in (1), highlighting the distorted coordination geometry about the copper (II) atom.	141
	a. The molecular packing in the crystal of (1): a supramolecular layer parallel to (101) sustained by O—H...O, N—H...O and C—H...O interactions shown as orange, blue and green dashed lines, respectively	143
	b. a view of the unit-cell contents in projection down the c axis, with π-π and C—H...π interactions shown as purple and pink dashed lines, respectively	143

Fig. 3.B.5.	Different views of the Hirshfeld surfaces for the constituents of (I) mapped over $d_{\text{norm}}$ for the:	
	a. water-O1W molecule [in the range -0.2369 to +1.2173 arbitrary units (au)]	144
	b. water-O2W molecule (-0.2114 to +0.7500 au)	144
	c-e. complex molecule (-0.1170 to +1.6287 au).	144
Fig.3.B.6	Two views of the Hirshfeld surface mapped with the shape-index property for the complex molecule in (1) from 1.0 to +1.0 arbitrary units highlighting:	
	a. the donor and acceptor atoms of the C—H... $\pi$ interaction through a blue bump near the H34 atom and bright-orange curvature, enclosed within the black circle,	146
	b. the O2W—H4W... $\pi$ interaction by the bright-orange region enclosed within the black circle.	146
Fig. 3.B.7	Different views of the Hirschfeld surfaces for the constituents of (1) mapped over the electrostatic potential (the red and blue regions represent negative and positive electrostatic potentials, respectively) for the:	
	a. water-O1W molecule [in the range -0.1001 to +0.1943 atomic units (a.u.)],	146
	b. water-O2W molecule (-0.1013 to +0.1751 a.u.)	146
	c. complex molecule (-0.1209 to +0.2076 a.u.).	146
Fig. 3.B.8	Two views of the Hirschfeld surface mapped over curvedness for the complex molecule in (1), highlighting flat regions enclosing symmetry related imidazole and nitrobenzene rings involved in $\pi$ - $\pi$ stacking, labelled Cg1 and Cg3 for one pair of rings in (a), and Cg2 and Cg4 for the other pair in (b).	146
Fig. 3.B.9	Different views of the Hirschfeld surfaces calculated for the copper (II) centre in (I) highlighting the coordination by the N <sub>2</sub> O <sub>4</sub> donor set mapped over (a)/(b) shape-index in the range -1.0 to +1.0 arbitrary units and (c)/(d) curvedness in the range -4.0 to +0.4 arbitrary units.	147
Fig. 3.B.10	The two-dimensional fingerprint plot taking into account only the Hirschfeld surface calculated about the copper (II) atom	148
Fig.3.B.11a-f	A comparison of the full two-dimensional fingerprint plot for (1) and those delineated into (b) H---H, (c) O---H/H---O, (d) C---H/H---C, (e) C---C and (f) C---O/O---C contacts.	149
Fig.3.B.12	a. Asymmetric unit of compound (2)	152

	b. ortep diagram of (2) with 50% probability	152
Fig.3.B.13	Hydrogen bonding pattern in compound (2)	153
Fig.3.B.14	C-S coupled product (2a-t)	156
Fig. 3.C.1	Molecular structure of 2, 4, 5-triarylimidazole derivatives (IM-1 to IM-6)	163
Fig. 3.C.2	Optimized gas phase molecular geometry of the compounds (IM-1 to IM-6) with atom labelling scheme.	171
Fig. 3. C.3	Labelling of different phenyl ring attached to imidazole ring	172
Fig. 3.C.4	Energies of HOMO and LUMO orbitals of the studied compounds (IM-1 to IM-6)	173
Fig 3.C.5	Theoretical and experimental FT-IR spectra of IM-1 to IM-6	179
Fig.3.C.6	MEP plot of studied compounds (IM-1 to IM-6)	180
Fig. 3.C.7	The N-terminal and C-terminal lobe in the protein 1IR3	186
Fig.3.C.8	Molecular structure of SB202190	187
Fig. 3.C.9	Visualisation of docking results of ligand IM-1 with the protein kinase 1IR3	189
Fig. 3.C.10	Visualisation of docking results of ligand IM-2 with the protein kinase 1IR3	190
Fig.3.C.11	Visualisation of docking results of ligand IM-3 with the protein kinase 1IR3	191
Fig. 3.C.12	Visualisation of docking results of ligand IM-4 with the protein kinase 1IR3	192
Fig.3.C.13	Visualisation of docking results of ligand IM-5 with the protein kinase 1IR3	193
Fig.3.C.14	Visualisation of docking results of ligand IM-6 with the protein kinase 1IR3	194
Fig. 4.A.1	a. Structure of 3,4-dihydropyrimidine-2-(1H)-one	204
	b. Structure of 3,4-dihydropyrimidine-2-(1H)-thione	204
Fig 4.A.2	Structures of few drugs that contain the DHPM moiety	204
Fig 4.A.3	Pictorial representation of the Biginelli products (4a-4q).	208
Fig.4.A.4	Recyclability of the catalyst	208
Fig.4.A.7.1	<sup>1</sup> H NMR spectra of Ethyl 1,2,3,4-tetrahydro-6-methyl-2-oxo-4-phenylpyrimidine-5-carboxylate(4a)	217
Fig.4.A.7.2	FT-IR spectra of Ethyl 1,2,3,4-tetrahydro-6-methyl-2-oxo-4-phenylpyrimidine-5-carboxylate(4b)	217
Fig.4.A.7.3	<sup>1</sup> H NMR spectra of Ethyl 1,2,3,4-tetrahydro-6-methyl-4-(2-nitrophenyl)-2-oxopyrimidine-5-carboxylate(4b)	218
Fig.4.A.7.4	FT-IR spectra of Ethyl 1,2,3,4-tetrahydro-6-methyl-4-(2-nitrophenyl)-2-oxopyrimidine-5-carboxylate (4b)	218
Fig.4.A.7.5	<sup>1</sup> H NMR spectra of Ethyl 1,2,3,4-tetrahydro-6-methyl-4-(3-nitrophenyl)-2-oxopyrimidine-5-carboxylate (4c)	219

Fig.4.A.7.6	FT-IR spectra of Ethyl 1,2,3,4-tetrahydro-6-methyl-4-(3-nitrophenyl)-2-oxopyrimidine-5-carboxylate (4c)	219
Fig.4.A.7.7	<sup>1</sup> H NMR spectra of Ethyl 1,2,3,4-tetrahydro-6-methyl-4-(4-nitrophenyl)-2-oxopyrimidine-5-carboxylate (4d).	220
Fig.4.A.7.8	FT-IR spectra of Ethyl 1,2,3,4-tetrahydro-6-methyl-4-(4-nitrophenyl)-2-oxopyrimidine-5-carboxylate (4d)	220
Fig.4.A.7.9	<sup>1</sup> H NMR spectra of Ethyl 4-(3-bromophenyl)-1,2,3,4-tetrahydro-6-methyl-2-oxopyrimidine-5-carboxylate (4e)	221
Fig.4.A.7.10	FT-IR spectra of Ethyl 4-(3-bromophenyl)-1,2,3,4-tetrahydro-6-methyl-2-oxopyrimidine-5-carboxylate (4e)	221
Fig.4.A.7.11	<sup>1</sup> H NMR spectra of Ethyl 1,2,3,4-tetrahydro-4-(2,4-dihydroxyphenyl)-6-methyl-2-oxopyrimidine-5-carboxylate (4i)	222
Fig.4.A.7.12	FT-IR spectra of Ethyl 1,2,3,4-tetrahydro-4-(2,4-dihydroxyphenyl)-6-methyl-2-oxopyrimidine-5-carboxylate (4i)	222
Fig.4.A.7.13	<sup>1</sup> H NMR spectra of Ethyl 4-(5-chloro-2-hydroxyphenyl)-1,2,3,4-tetrahydro-6-methyl-2-oxopyrimidine-5-carboxylate (4k)	223
Fig.4.A.7.14	FT-IR spectra of Ethyl 4-(5-chloro-2-hydroxyphenyl)-1,2,3,4-tetrahydro-6-methyl-2-oxopyrimidine-5-carboxylate (4k)	223
Fig.4.A.7.15	<sup>1</sup> H NMR spectra of Ethyl 1,2,3,4-tetrahydro-4-(2-hydroxy-5-nitrophenyl)-6-methyl-2-oxopyrimidine-5-carboxylate (4l)	224
Fig.4.A.7.16	FT-IR spectra of Ethyl 1,2,3,4-tetrahydro-4-(2-hydroxy-5-nitrophenyl)-6-methyl-2-oxopyrimidine-5-carboxylate (4l)	224
Fig.4.A.7.17	<sup>1</sup> H NMR spectra of Ethyl 1,2,3,4-tetrahydro-4-(4-hydroxy-3-methoxyphenyl)-6-methyl-2-oxopyrimidine-5-carboxylate (4m)	225
Fig.4.A.7.18	FT-IR spectra of Ethyl 1,2,3,4-tetrahydro-4-(4-hydroxy-3-methoxyphenyl)-6-methyl-2-oxopyrimidine-5-carboxylate (4m).	225
Fig.4.A.7.19	<sup>1</sup> H NMR spectra of Ethyl 1,2,3,4-tetrahydro-4-(3-hydroxyphenyl)-6-methyl-2-oxopyrimidine-5-carboxylate (4n)	226
Fig.4.A.7.20	FT-IR spectra of Ethyl 1,2,3,4-tetrahydro-4-(3-hydroxyphenyl)-6-methyl-2-oxopyrimidine-5-carboxylate (4n)	226
Fig.4.A.7.21	<sup>1</sup> H NMR spectra of Ethyl 1,2,3,4-tetrahydro-4-(3,4,5-trimethoxyphenyl)-6-methyl-2-oxopyrimidine-5-carboxylate (4o)	227
Fig.4.A.7.22	FT-IR spectra of Ethyl 1,2,3,4-tetrahydro-4-(3,4,5-trimethoxyphenyl)-6-methyl-2-oxopyrimidine-5-carboxylate(4o)	227
Fig.4.A.7.23	<sup>1</sup> H NMR spectra of Ethyl 1,2,3,4-tetrahydro-4-(4-hydroxy-3,5-dimethoxyphenyl)-6-methyl-2-oxopyrimidine-5-carboxylate (4p)	228

Fig.4.A.7.24	FT-IR spectra of Ethyl 1,2,3,4-tetrahydro-4-(4-hydroxy-3,5-dimethoxyphenyl)-6-methyl-2-oxopyrimidine-5-carboxylate (4p)	228
Fig.4.A.7.25	<sup>1</sup> H NMR spectra of Ethyl 1,2,3,4-tetrahydro-4-(1H-indol-3-yl)-6-methyl-2-oxopyrimidine-5-carboxylate (4q)	229
Fig.4.A.7.26	FT-IR spectra of Ethyl 1,2,3,4-tetrahydro-4-(1H-indol-3-yl)-6-methyl-2-oxopyrimidine-5-carboxylate (4q)	229
Fig.4.B.1	DHPMs as essential building blocks	236
Fig. 4.B.2	Molecular Structures of selected 3, 4-dihydropyrimidin-(2H)-one derivatives (DP-1 to DP-3)	237
Fig.4.B.3	Atom labelling of the DHPM nucleus (1) and the phenyl ring (2) in the studied compounds	239
Fig.4.B.4	Optimized gas phase molecular geometry of the compounds (DP-1 to DP-3) with atom labelling scheme.	240
Fig.4.B.5	Pictorial representation of the HOMO-LUMO of selected compounds (DP-1 to DP-3)	243
Fig.4.B.6	Theoretical and experimental FTIR spectra of DP-1 to DP-3	249
Fig.4.B.7	MEP plots of studied compounds (DP-1 to DP-3)	250
Fig 4.B.8	Visualisation of docking results of ligand DP-1 within a receptor site in the protein 3DH4	257
Fig.4.B.9	Visualisation of docking results of ligand DP-2 with receptor protein 3DH4	258
Fig.4.B.10	Visualisation of docking results of ligand DP-3 within a receptor site in the protein 3DH4	259
Fig. 5.A.1	. Examples of drugs containing imidazole scaffold	270
Fig.5.A.2	Examples of 1-hydroxyimidazole compounds having biological activities	271
Fig.5.A.3	Schematic representation of product formed under the stated reaction condition	277
Fig 5.A.4	Recyclability of the catalyst	278
Fig.5.A.5	Prototropic tautomeric equilibrium of 1-hydroxyimidazole and N-hydroxybenzimidazole, a/a') N-hydroxy form and b/b') N-oxide form.	279
Fig.5.A.6	Structure of 1,3-dihydroxy-2-(4-methoxyphenyl)-4,5-dimethyl-1 <i>H</i> -imidazol-3-ium chloride (4m).	279
Fig. 5.A.7	Asymmetric unit of 4m with displacement ellipsoids drawn at 50% probability level.	280
Fig. 5.A.8	The molecular arrangement of 4m in the <i>ac</i> plane	282
Fig. 5.A.9	Hydrogen bonding interaction in 4m, (dotted lines indicate the interionic C–H···Cl interactions in 4m).	283
Fig. 5.A.10	C–H···C <sub>g</sub> interaction in the cationic unit of 4m (Dotted line indicates the C–H···C <sub>g</sub> interaction)	283
Fig.5.A.5.1	<sup>1</sup> H NMR spectra of 1-hydroxy-2-phenyl-4,5-dimethylimidazole-3-oxide (4a)	288
Fig. 5.A.5.2	FT-IR spectra of 1-hydroxy-2-phenyl-4,5-dimethylimidazole-3-oxide(4a)	288

Fig.5.A.5.3	<sup>1</sup> H NMR spectra of 1-hydroxy-2-(3-nitrophenyl)-4,5-dimethylimidazole-3-oxide (4b)	289
Fig. 5.A.5.4	FT-IR spectra of -hydroxy-2-(3-nitrophenyl)-4,5-dimethylimidazole-3-oxide (4b)	289
Fig.5.A.5.5	<sup>1</sup> HNMR spectra of 1-hydroxy-2(4-fluorophenyl)-4, 5-dimethylimidazole-3-oxide (4c)	290
Fig. 5.A.5.6	FT-IR spectra of -hydroxy-2(4-fluorophenyl)-4,5-dimethylimidazole-3-oxide (4c)	290
Fig.5.A.5.7	<sup>1</sup> HNMR spectra of 1-hydroxy-2-(3-hydroxyphenyl)-4, 5-dimethylimidazole-3- oxide (4d).	291
Fig. 5.A.5.8	FT-IR spectra of 1-hydroxy-2-(3-hydroxyphenyl)-4,5-dimethylimidazole-3-oxide (4d)	291
Fig.5.5.A.9	<sup>1</sup> HNMR spectra of 1-hydroxy-2-(2, 4-dihydroxyphenyl)-4, 5-dimethylimidazole-3- oxide (4e).	292
Fig.5.A.5.10	FT-IR spectra of 1-hydroxy-2-(2, 4-dihydroxyphenyl)-4, 5-dimethylimidazole-3- oxide (4e).	292
Fig.5.A.5.11	<sup>1</sup> HNMR spectra of 1-hydroxy-2-(2-hydroxyphenyl)-4, 5-dimethylimidazole-3- oxide (4f).	293
Fig.5.A.5.12	FT-IR spectra of 1-hydroxy-2-(2-hydroxyphenyl)-4, 5-dimethylimidazole-3- oxide (4f).	293
Fig.5.A.5.13	<sup>1</sup> HNMR spectra of 1-hydroxy-2-(5-chloro-2-hydroxyphenyl)-4, 5-dimethylimidazole-3- oxide (4h).	294
Fig.5.A.5.14	FT-IR spectra of 1-hydroxy-2-(5-chloro-2-hydroxyphenyl)-4, 5-dimethylimidazole-3- oxide (4h).	294
Fig.5.A.5.15	<sup>1</sup> HNMR spectra of 1-hydroxy-2(5-bromo-2-hydroxyphenyl)-4, 5-dimethylimidazole-3- oxide (4i).	295
Fig.5.A.5.16	FT-IR spectra of 1-hydroxy-2(5-bromo-2-hydroxyphenyl)-4, 5-dimethylimidazole-3- oxide (4i).	295
Fig.5.A.5.17	<sup>1</sup> HNMR spectra of 1-hydroxy-2(2-hydroxy-3-methoxyphenyl)-4, 5-dimethylimidazole-3- oxide (4j).	296
Fig.5.A.5.18	FT-IR spectra of 1-hydroxy-2(2-hydrox-3-methoxyphenyl)-4, 5-dimethylimidazole-3- oxide (4j).	296
Fig. 5.A.5.19	<sup>1</sup> HNMR spectra of 1-hydroxy-2(3, 4, 5-trimethoxyphenyl)-4, 5-dimethylimidazole-3- oxide(4l).	297
Fig.5.A.5.20.	FT-IR spectra of 1-hydroxy-2(3, 4, 5-trimethoxyphenyl)-4, 5-dimethylimidazole-3- oxide (4l).	297
Fig. 5.B.1	Labeling of the phenyl ring and the imidazole ring in the studied compounds	308
Fig. 5.B.2	DFT optimized geometry of the compounds IMO-1 to IMO-6 with atom labeling scheme	308
Fig. 5.B.3	Pictorial representation of the HOMO-LUMO of selected compounds (IMO-1 to IMO-6)	310
Fig.5.B.4	Theoretical and experimental FTIR spectra of IMO-1 to IMO-6	318
Fig. 5.B.5	MEP plot of studied compounds (IMO-1 to IMO-6)	320
Fig 5.B.6	Visualisation of docking results of ligand IMO-1 with the protein 3ERT	328
Fig.5.B.7	Visualization of docking results of ligand IMO-2 with the protein 3ERT	329



Fig 5.B.8	Visualization of docking results of ligand IMO-3 with the protein 3ERT	330
Fig 5.B.9.	Visualization of docking results of ligand IMO-4 with the protein 3ERT	331
Fig 5.B.10	Visualization of docking results of ligand IMO-5 with the protein 3ERT	332
Fig 5.B.11	Visualization of docking results of ligand IMO-6 with the protein 3ERT	333
Fig.6.1.1	Structures of some clinically approved drugs containing the benzimidazole scaffold	342
Fig.6.1.2	Structures of some new drugs containing the benzimidazole scaffold	342
Fig 6.1.3	Synthesized benzimidazole derivatives (3a-3j)	347
Fig 6.1.4	Recyclability of the catalyst	347
Fig 6.2.1	Synthesized 1, 2-benzimidazole derivatives (3a'-3k')	352
Fig 6.2.2	Recyclability of the catalyst	353
Fig.6.6.1	<sup>1</sup> HNMR of 1-(3-nitrobenzyl)-2-(3-nitrophenyl)-1H-benzo[d]imidazole (3c')	359
Fig.6.6.2	<sup>1</sup> HNMR of 1-(4-nitrobenzyl)-2-(4-nitrophenyl)-1H-benzo[d]imidazole (3d')	359
Fig.6.6.3	<sup>1</sup> HNMR of 1-((1 <i>H</i> -Indol-3-yl)methyl)-2-(1 <i>H</i> -indol-3-yl)-1 <i>H</i> -benzimidazole (3j')	360
Fig 6.6.4	<sup>1</sup> HNMR of 1-(2-chlorobenzyl)-2-(2-chlorophenyl)-1H-benzo[d]imidazole (3l')	360

## LIST OF SCHEMES

Schemes		Page No.
Scheme 1.1	Graphical illustration of the classes of MCRs	15
Scheme 1.2	Strecker's Reaction	15
Scheme 1.3	Debus-Raziszewski Synthesis	16
Scheme 1.4	Hantzsch Synthesis of substituted dihydropyridines	16
Scheme 1.5	Hantzsch Synthesis of pyrrole	16
Scheme 1.6	Bigenelli synthesis of dihydropyrimidinones	17
Scheme 1.7	Mannich Reaction	17
Scheme 1.8	Robinson's synthesis of bioactive alkaloid	18
Scheme 1.9	Bucherer and Bergs synthesis	18
Scheme 1.10	Asinger Reaction	18
Scheme 1.11	Ugi Reaction	19
Scheme 1.12	Povarov's reaction	19
Scheme 1.13	Gewald's Synthesis	19
Scheme 1.14	Petasis Multicomponent Reaction	20
Scheme 1.15	Synthesis of perfluoroalkyl isoxazoles by using perfluoroalkyl reagents	20
Scheme 1.16	Synthesis of 1,4-dihydropyridines under green condition using PEG-400	21
Scheme 1.17	Sequential One-Pot Ugi/Heck Carbocyclization/Sonogashira/Nucleophilic Addition reaction.	21
Scheme 1.18	Ugi-Mumm and Ugi Smiles Reaction	22
Scheme 1.19	<b>a)</b> Radziszewski and <b>b)</b> Japp imidazole synthesis	28
Scheme 1.20	Modern synthetic route for the synthesis of 2, 4, 5-triarylimidazole derivatives	29
Scheme 1.21	Synthesis of 2,4,5-triarylimidazole derivatives under solvent free conditions	30
Scheme 1.22	Synthesis of 2,4,5-triaryl imidazoles under microwave irradiation	32
Scheme 1.23	<b>(a)</b> Synthesis of Lepidiline, <b>(b)</b> Synthesis of Trifenagrel	32
Scheme 1.24	Synthesis of substituted tri-aryl imidazole from keto-oxime	33
Scheme 1.25	Microwave assisted synthesis of 2-substituted-4,5-di(2-furyl)-1-H-imidazole	34
Scheme 1.26	Microwave assisted, solvent and catalyst free synthesis of tri-aryl imidazole	34

Scheme 1.27	Synthesis of tri-substituted imidazoles containing carboxamido and cyano groups	35
Scheme 1.28	Synthesis of 2,4,5-triaryl imidazoles under Ultrasound irradiation	35
Scheme 1.29	Synthesis of 3,4-dihydropyrimidine-2-(1H)-ones	36
Scheme 1.30	Classical method for the synthesis of 3, 4-dihydropyrimidin-2(1H)-one	39
Scheme 1.31	Synthesis of 3, 4-dihydropyrimidin-2(1H)-one	39
Scheme 1.32	Synthesis of 3, 4-dihydropyrimidin-2(1H)-one from Cinnamaldehyde and Furfural.	40
Scheme 1.33	Solvent free synthesis of 3, 4-dihydropyrimidin-2(1H)-one derivatives	42
Scheme 1.34	Ultrasound assisted synthesis of 3, 4-dihydropyrimidin-2(1H)-one derivatives	44
Scheme 1.35	Ultrasound assisted synthesis of 3, 4-dihydropyrimidin-2(1H)-one derivatives using CAN catalyst	45
Scheme 1.36	Synthesis of novel 4-(2-phenyl-1,2,3-triazol-4-yl)-3,4-dihydropyrimidin-2(1H)-(thio)ones	46
Scheme 1.37	Synthesis of Imidazole-N-oxide by using 2,2'-diimidazolyl	46
Scheme 1.38	Synthesis of Imidazole-N-oxide from 1-aryl-4-dimethylamino-1,3-diaza-1, 3-butadienes	47
Scheme 1.39	Synthesis of imidazole-N-oxides from $\alpha$ -amino oximes and triethyl orthoformate	47
Scheme 1.40	Synthesis of enantiomerically pure imidazole-N-oxide	48
Scheme 1.41	Synthesis of enantiomerically pure imidazole-N-oxide	48
Scheme 1.42	Synthesis of imidazole-N-oxide from 3-hydroxyamino-2-butanone oxime	49
Scheme 1.43	Synthesis of bulky bulky imidazole-N-oxide using 1-amino admantane	49
Scheme 1.44	Synthesis of aryl imidazole-N-oxides	50
Scheme 1.45	Solvent free, self catalysed reaction for the synthesis of N-substituted imidazole-3-oxides	50
Scheme 1.46	Numerous methods for the synthesis of disubstituted benzimidazoles	53
Scheme 1.47	Synthesis of 1,2-disubstituted Benzimidazole	54
Scheme 1.48	Hoebrecker's synthesis of Benzimidazole	54
Scheme 1.49	Synthesis of 1,2 disubstituted imidazoles using <i>N, N'</i> -disubstituted- <i>o</i> -phenylenediamine	55
Scheme 1.50	Synthesis of 1,2 disubstituted benzimidazole using Bismuth nitrate as catalyst	55
Scheme 1.51	Synthesis of benzimidazole derivatives from chloroacetyl chloride	55

Scheme 1.52	Synthesis of benzimidazole derivatives from tertiary butane sulfoxide	56
Scheme 1.53	Synthesis of benzimidazole derivatives using Ammonium chloride catalyst	56
Scheme 1.54	Synthesis of benzimidazole derivatives using SDS catalyst	57
Scheme 1.55	Two separate procedures for synthesis of benzimidazole derivatives	57
Scheme 1.56	Synthesis of 1-(2-aryl-2-oxoethyl)-2-aryloylbenzimidazoles	58
Scheme 1.57	Synthesis of two regio isomers of 1,2-Disubstituted benzimidazoles	58
Scheme 1.58	Synthesis of Benzimidazoles using Palladium based catalyst	59
Scheme 1.59	Synthesis of benzimidazole scaffold by using an active deep eutectic solvent	59
Scheme 1.60	Synthesis of Benzimidazoles from amidine	59
Scheme 1.61	Synthesis of benzimidazoles by using CuO nanoparticle as catalyst	60
Scheme 1.62	Synthesis of benzimidazoles using ortho-bromo-amidines	60
Scheme 1.63	Synthesis of benzimidazole derivatives using diarylcarbodiimides	61
Scheme 1.64	Synthesis of benzimidazole from ortho-halo anilines	61
Scheme 1.65	Synthesis of 2 fluoroalkylbenzimidazoles	61
Scheme 1.66	Synthesis of substituted benzimidazoles using DABCO as a catalyst	62
Scheme 1.67	Synthesis of substituted benzimidazoles from dibromomethylarenes	62
Scheme 1.68	Synthesis of 1,2 disubstituted benzimidazole by dehydrogenative coupling	63
Scheme 1.69	Synthesis of benzimidazole derivatives using (ZrO <sub>2</sub> -β-CD) catalyst	64
Scheme 1.70	Synthesis of 1,2-disubstituted benzimidazole using PIL	64
Scheme 1.71	Synthesis of 1,2-disubstituted benzimidazole using microwave irradiation	65
Scheme 1.72	Synthesis of 1, 2-disubstituted benzimidazole derivatives from orthophenylene diamine	65
Scheme 1.73	Synthesis of 1, 2-disubstituted benzimidazole by using molecular I <sub>2</sub> as catalyst	66

Scheme 1.74	Synthesis of 1, 2-disubstituted benzimidazole derivatives under Ultrasound irradiation	67
Scheme 1.75	Synthesis of 1, 2-disubstituted benzimidazoles using $YCl_3$	67
Scheme 1.76	Synthesis of 1, 2-disubstituted benzimidazole derivatives using CuI as an efficient catalyst	68
Scheme 1.77	Synthesis of 1, 2-disubstituted benzimidazoles using aqueous hydrotropic solution	68
Scheme 3.A.1	A. Debus-Radziszewski imidazole synthesis	113
	B. Synthesis of tri-substituted imidazole using $\alpha$ -hydroxyketone.	113
Scheme 3.A.2.	Model reaction for the synthesis of 2,4,5 triaryl imidazole	114
Scheme 3.A.3	Proposed mechanism for the synthesis of 2,4,5 -triarylimidazole	121
Scheme 3.B.1	a. Reaction between ligand 4n and $CuB_4O_7$	138
	b. Reaction between ligand 4n and $CuB_4O_7$ in presence of $NH_4OAc$ for the synthesis of (1)	138
	c. Reaction between $CuB_4O_7$ and $NH_4OAc$ to form compound (2)	138
	d. Reaction between ligand 4n and compound (2) to form compound (1)	138
Scheme 3.B.2	C-S cross-coupling between aryl halide and aryl thiols using complex (1) as a catalyst.	155
Scheme 4.A.1	Schematic representation of Bigenelli reaction catalyzed by Fe borate catalyst	209
Scheme 4.A.2	Proposed mechanism for the synthesis of 3, 4-dihydropyrimidine-2-one catalyzed by Fe-borate	215
Scheme 5.A.1	Method of synthesis of N-alkylimidazole-3-oxide (4)	271
Scheme 5.A.2	Synthesis of 1-hydroxyimidazole derivatives (4)	272
Scheme 5.A.3	Synthesis of 1-hydroxy-2-(aryl)-4,5-dimethylimidazole-3-oxide (4).	272
Scheme 5.A.4	Model reaction for the synthesis of 1-hydroxy-2-(aryl)-4,5-dimethylimidazole-3-oxide	273
Scheme 5.A.5	Optimized reaction condition for the synthesis of 1-hydroxy-2-(aryl)-4,5-dimethylimidazole-3-oxide	274

Scheme 6.1.1	Synthetic methodology for the synthesis of 2-substituted benzimidazole derivatives	343
Scheme 6.1.2	Model reaction for the synthesis of 2-substituted benzimidazole	344
Scheme 6.2.1	Classical method for the synthesis of 1,2-disubstituted benzimidazole	348
Scheme 6.2.2	Modern methods for the synthesis of 1, 2-disubstituted benzimidazole derivatives.	348
Scheme 6.2.3	Model reaction for the synthesis of 1, 2-disubstituted benzimidazole	349
Scheme 6.2.4	Optimization of reaction condition for model reaction to synthesize (3a'-3k')	350

## LIST OF APPENDICES

<b>Appendix</b>	<b>Page No.</b>
I. Supplementary spectra of Chapter III-A	367-371
II. List of Publications	372
III. List of communicated Articles	373
IV. List of Seminars, Webinars, Symposiums and Conferences attended	374

# CHAPTER-I

## 1.1 Introduction

Heterocyclic compounds are cyclic organic compounds with one or more heteroatom such as oxygen, sulfur or nitrogen in ring structure in addition to carbon atom. Owing to immense biological, pharmaceutical, and industrial applications, heterocyclic compounds among many organic molecules, have gained lot of interest in past few decades<sup>1</sup>. Amongst the various heterocyclic compounds available, N-containing heterocyclic compounds finds an extensive range of applications in numerous fields like pharmacology, drug industry, and analytical chemistry<sup>2-4</sup>. N-containing heterocyclic compounds serves as a fundamental subunit in many natural products such as hormones, vitamins and antibiotics<sup>5</sup>. Interestingly, the core structure of several natural products such as serotonin (1)<sup>6</sup>, thiamine (2)<sup>7</sup>, morphine (3)<sup>8</sup>, codeine (4)<sup>9</sup>, coniine (5)<sup>10</sup>, caffeine (6)<sup>11</sup>, nicotine (7)<sup>12</sup> etc. contains N-containing heterocyclic compounds (Fig 1.1).

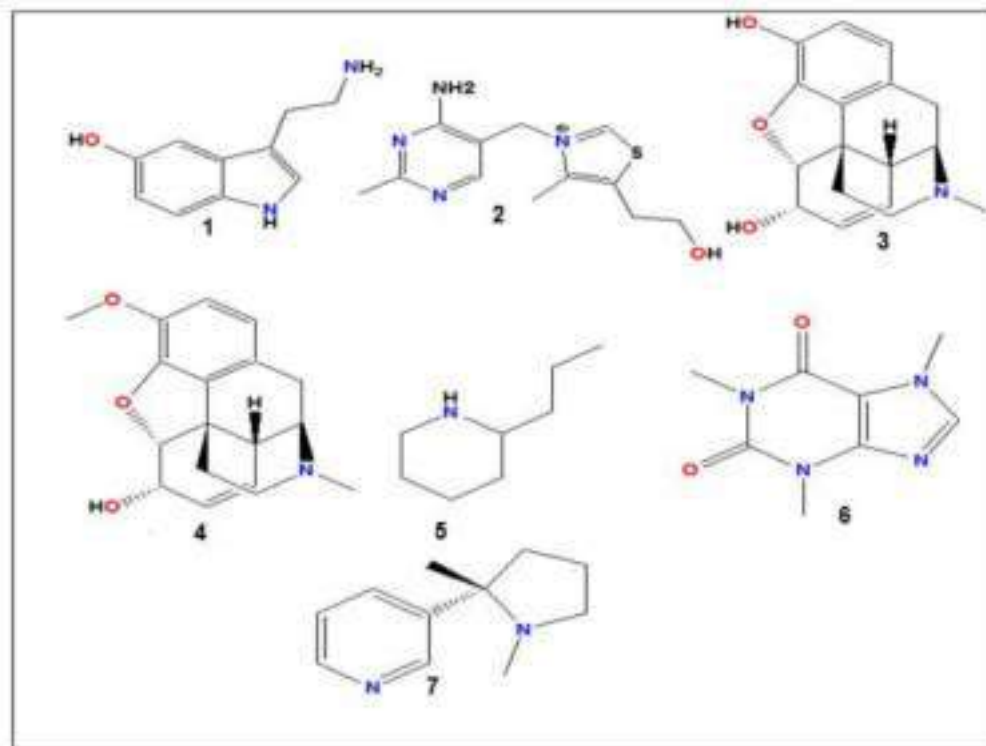


**Fig. 1.1.** Examples of naturally occurring N-containing heterocyclic compounds.

During the past few decades, N-containing heterocyclic compounds have been an active field of research due to their diverse and numerous biological activities and therefore, they have become an active target to the synthetic chemist in the field of total synthesis of natural products<sup>13-14</sup>. Moreover, several prescribed drugs like Risperidone (8) (Schizophrenia)<sup>15</sup>, Timolol (9) (Anti-glaucoma agent)<sup>16</sup>,



Sunitinib (10) (Renal cell carcinoma and gastrointestinal stromal tumors)<sup>17</sup>, Anastrozole (11) (Migraine)<sup>18</sup> and Rufinamide (12) (Anticonvulsant)<sup>19</sup> etc. contains N-containing heterocyclic scaffold (Fig. 1.2).

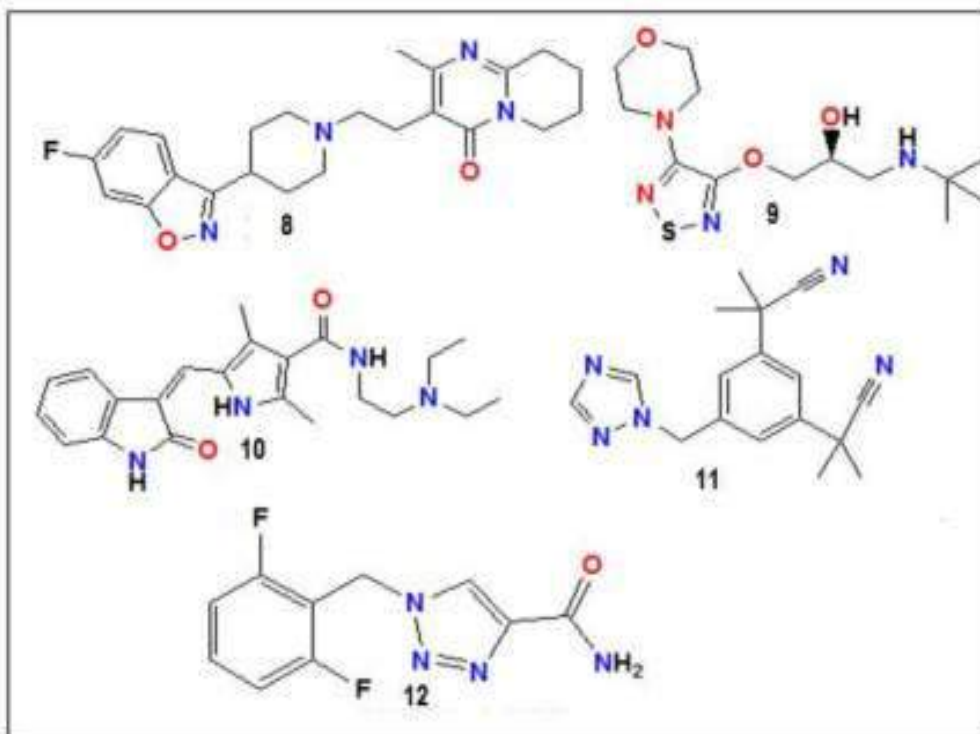


**Fig. 1.2.** Molecular structure of some of the prescribed drugs containing N-heterocyclic scaffold.

The worth of the heterocyclic compounds in medicinal field and biological systems can be understood from their presence in amino acids like histidine and tryptophan to DNA and RNA<sup>20</sup>. Purine and Pyrimidine skeleton of thymine (13), cytosine (14), uracil (15), guanine (16) and adenine (17) contain N-heterocyclic scaffold (Fig.1.3) and they are essential building blocks of nucleic acids, DNA and RNA<sup>21</sup>. According to FDA database nearly 75% unique small-molecule drugs contain a nitrogen heterocycle<sup>22</sup>.

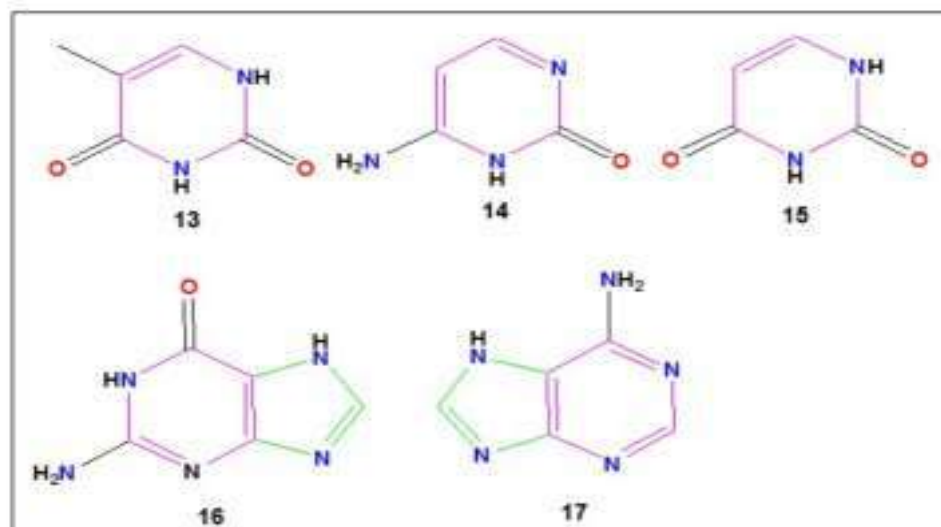


**Fig. 1.3.** Molecular structures of nitrogenous Bases of DNA and RNA.

Interesting structural features of the N-containing heterocyclic compounds allows them to establish a diverse type of weak interactions such as hydrogen bonding, dipole-dipole interaction, hydrophobic effect and  $\pi$ - $\pi$  stacking etc., with the enzymes and receptors of the biological targets with high affinity which in turn is essential in the field of medicinal chemistry for the discovery of new therapeutic agents/drug molecules<sup>23-25</sup>. Looking at the diverse applications of heterocyclic compounds in the pharmaceutical industries, many think tanks are engaged in synthesising biologically active heterocyclic compounds for the betterment of humans and the society as a whole<sup>26-30</sup>. Structures of some of the N-containing heterocyclic scaffolds such as imidazole (18), indole (19), pyrazole (20), pyrimidine (21), pyrazine (22), morpholine (23), triazole (24), quinoline (25) and isoquinoline (26) are depicted in Fig. 1.4.

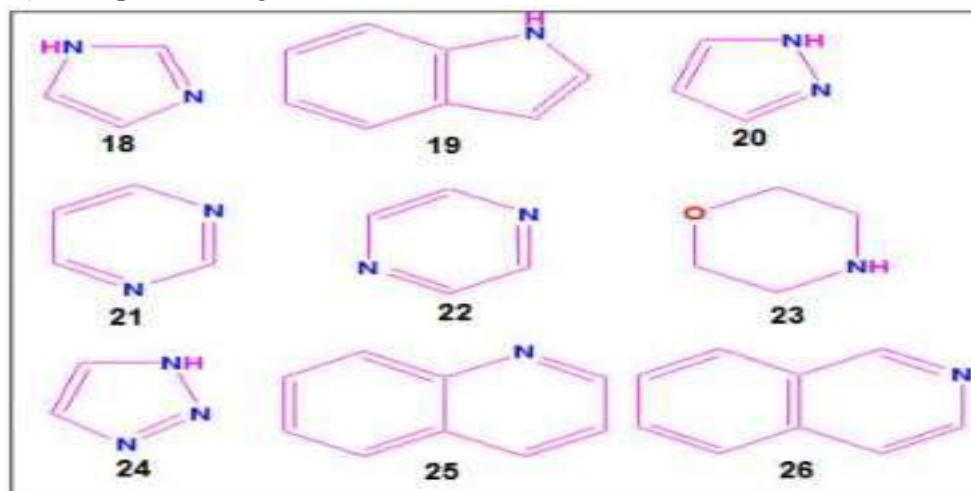


**Fig. 1.4.** Molecular structure of some of the N-Heterocyclic scaffolds.

Also, biologically important amino acid, namely histidine (27), tryptophan (28) and proline (29) contain N-heterocyclic motifs in their main structure (Fig. 1.5).

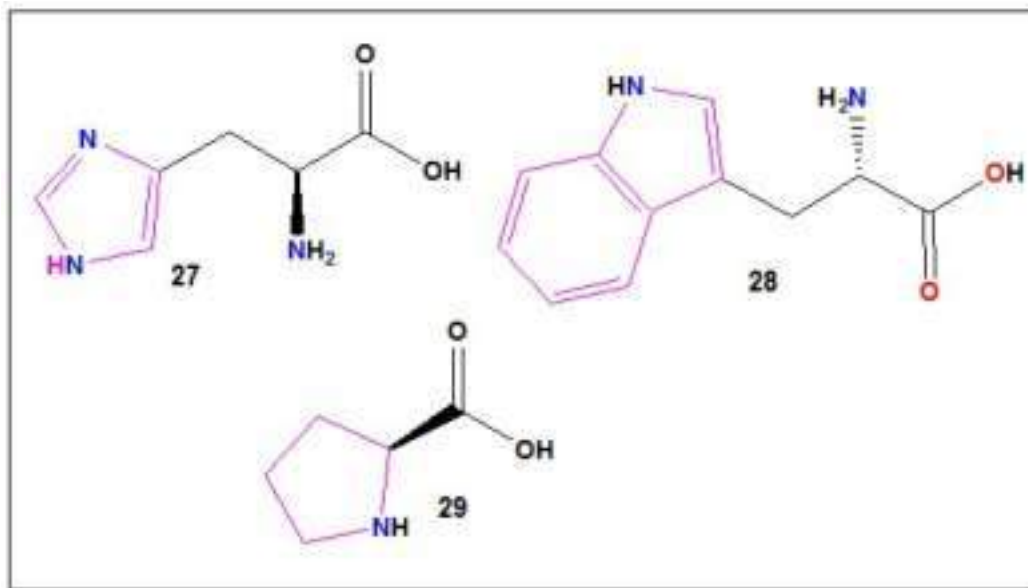


**Fig. 1.5.** Molecular structures of amino acids containing N-heterocyclic motifs.

Hemoglobin and Chlorophyll are the best examples of Metal Porphyrins which contains N- heterocycle and they are responsible for transport of Oxygen in animals and photosynthesis in plants respectively. The ability of N atom in N-heterocyclic compounds to form hydrogen bonds with potential biological targets has been fully exploited by the medicinal chemists to develop pharmaceutically important therapeutic agents/ drugs for the treatment of various diseases<sup>31-32</sup>. Penicillin (30)<sup>33</sup>, Cephalosporins (31)<sup>34</sup>, Puromycins (32)<sup>35</sup> are important classes of Antibiotics which contain N-heterocyclic scaffold in their skeleton structure (Fig. 1.6). N-heterocyclic compounds having 5 or 6 membered rings play a key role in metabolism of all living cells<sup>36</sup>. Nitrogen containing heterocyclic scaffold are present in a wide variety of drug such as antidiabetic<sup>37</sup>, anti-inflammatory<sup>38</sup>, antidepressant<sup>39</sup>, antitumor<sup>40</sup>, antimalarial<sup>41</sup>, anti-HIV<sup>42</sup>, antibacterial<sup>43</sup>, antifungal<sup>44</sup>, antiviral<sup>45</sup>, herbicidal<sup>46</sup> and insecticidal<sup>47</sup> etc. Structures of some of the biologically active compounds having N-heterocyclic motif are Clotrimazole (33), Fluconazole (34), Flucytosine (35), Piroxicam (36), Celecoxib (37), Sparfloxacin (38), Furalazine (39), Nitrofurantoin (40), Levetiracetam (41), Phenytoin (42) and Phenobarbital (43)) are shown in Fig. 1.7.

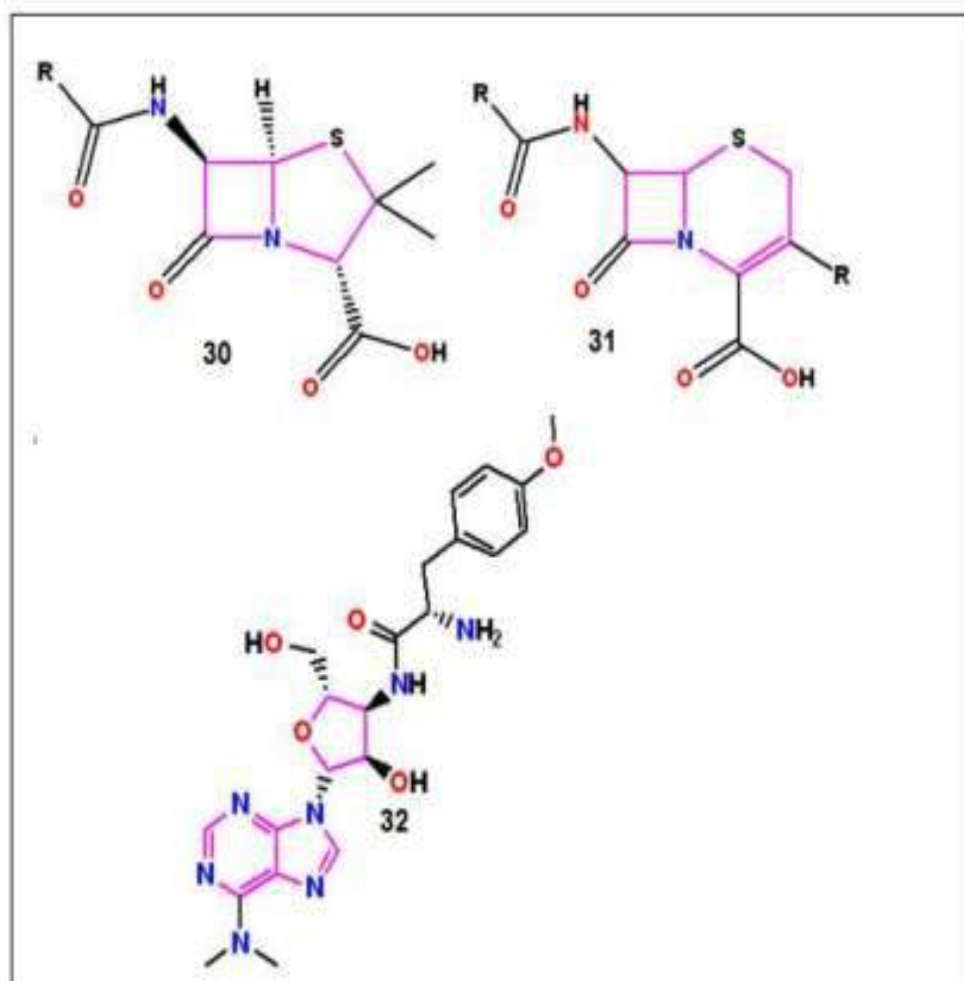
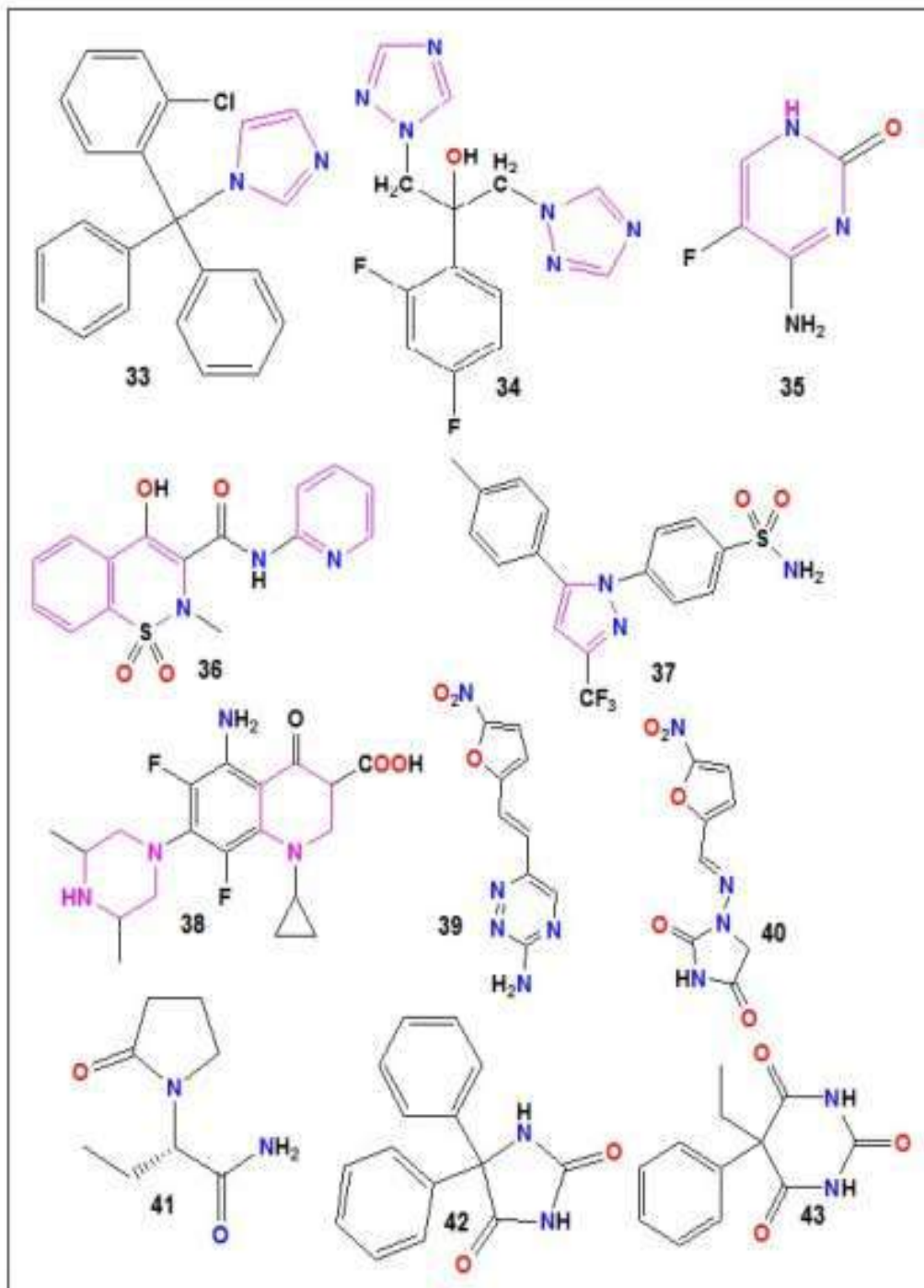


Fig. 1.6. Molecular structure of Penicillin, Cephalosporin and Puromycin.



**Fig. 1.7.** Structures of some of the biologically active N-heterocyclic motifs

Though the N-heterocyclic compounds are ubiquitous in nature, but their expense is not sufficient to meet the necessities of the increasing demand every day. Therefore, chemists are always looking for a novel and cost-effective synthetic procedure for the synthesis of these naturally occurring valuable heterocyclic

scaffolds in the laboratories as well as in industries to fulfill the ever-increasing demand of these heterocyclic compounds<sup>48</sup>.

Thus, the synthesis of N-heterocyclic compounds is one of the most attractive areas of research due to their unique structures with the extensive applications in the fields of organic, pharmaceutical and material chemistry<sup>49</sup>. During the last few decades, much of the work is focused on the development of new reaction methodology for the synthesis of N-heterocyclic compounds in the laboratory and in industrial scale and current literature survey revealed that a vast number of works are documented in this field<sup>50-55</sup>. However, these documented methodologies/ procedures have associated with some drawbacks such as use of expensive and toxic solvents, non-ecofriendly processes, expensive/incompetent catalysts, poor yields, incompatibility with other functional groups, difficult product purification and isolation techniques etc<sup>56,57</sup>.

## 1.2 Green chemistry

The concept of green chemistry was coined by Prof. Paul. T. Anastas in early 1990s in a special program launched by the US Environmental Protection Agency (EPA) to implement sustainable development in chemistry and chemical technology by industry, academia and government<sup>58</sup>. Green chemistry is a new philosophical approach which exclusively utilizes a set of principles to develop process and products to reduce or eliminate hazardous substances and this new approach may also be known as “*Environmentally benign*” chemistry, “*Clean chemistry*” and “*benign-by-design chemistry*”<sup>59</sup>.

The term Green chemistry may be defined as “*design of chemical products and processes to reduce or eliminate the use and generation of hazardous substances*”<sup>60</sup>.

Alternatively, green chemistry may also be defined as the “*utilization of a set of principles that eliminates or reduces the use or the generation of hazardous substances in the design, manufacture and application of chemical products or materials*”<sup>58</sup>.

Prof. Anastas highlighted that the green chemistry is all about redesigning of chemical processes i.e., making industrial chemistry safer, cleaner and more energy efficient starting from synthesis to clean-up to disposal<sup>58</sup>. The main aim of green chemistry is to develop products and processes in energy efficient way, less waste generation, use of less organic solvents or no use of solvents, have no environmental or health problems, recycling of the products or environmental degradation to harmless materials<sup>61</sup>. One of the key goals of green chemistry is to prevent pollution at its source than dealing with pollution after it has occurred. The Green chemistry also known as sustainable chemistry encourages the design of the products and processes that minimize the use and generation of hazardous chemicals<sup>62</sup>.

Green chemistry, being a philosophy of sustainable chemistry applies to different branches of chemistry such as organic chemistry, inorganic chemistry, analytical chemistry, biochemistry and physical chemistry<sup>63</sup>. Since in industrial scale, huge

quantities and numerous varieties of small starting molecules, reagents, solvents, acid, base etc., are involved for production of different products and these chemical processes produces a large quantity of hazardous and undesired by-products in addition to the desired products which in turn pollute the environment and public health<sup>64</sup>. Therefore, the pressing need of the chemist is to minimize the chemical waste and in order to address the current environmental pollution due to hazardous chemicals, Prof. Anastas and Warner<sup>58</sup> coined a set of twelve principles of green chemistry. These principles are: -

1. **Waste Prevention:** It is better to prevent waste than to treat or clean up waste after it has been created.
2. **Atom Economy or Efficiency:** Synthetic Methods should be designed in such a way so as to maximize the incorporation of all materials used in the process into the final product. The concept of atom economy was introduced by Trost<sup>65</sup> and it represents how much of the reactant end up in the final product. The percentage atom economy was introduced by Sheldon<sup>66</sup> as follows:

$$\text{Atom economy} = \frac{\text{Molecular weight of the desired products}}{\text{Molecular weight of all products}} \times 100\%$$

Among synthetic chemists, the concept of atom economy is most widely used measure of the green chemistry.

3. **Less Hazardous Chemical Synthesis:** Wherever practicable, synthetic methods should be designed to use and generate substances that possess little or no toxicity to human health and the environment.
4. **Designing Safer Chemicals:** Chemical products should be designed to preserve efficacy of function while minimizing their toxicity.
5. **Safer Solvents and Auxiliaries:** The use of auxiliary substances should be made unnecessary wherever possible and innocuous when used.
6. **Design for Energy Efficiency:** Energy requirements of chemical processes should be recognized for their environmental and economic impacts should be minimized.
7. **Use of Renewable Feed stocks:** A raw material or feed stock should be renewable rather than depleting whenever technically and economically practicable.
8. **Reduce Derivatives:** Unnecessary derivatization should be minimized or avoided, if possible, because such steps require additional reagents and can generate waste.
9. **Catalysis:** Catalytic reagents are superior to stoichiometric reagents.
10. **Design for Degradation of Chemical Products:** Chemical products should be designed so that at the end of their function they break down into innocuous degradation products and do not persist in the environment.

11. **Real-time Analysis for Pollution Prevention:** Analytical methodologies need to be further developed to allow for real-time, in-process monitoring and control prior to the formation of hazardous substances.
12. **Inherently safer Chemistry for Accident Prevention:** Substances and the form of a substance used in a chemical process should be chosen to minimize the potential for chemical accidents, including releases, explosions and fires.

After the introduction of the new philosophical concept of Green chemistry or Sustainable chemistry, a vast number of literature is available with many interesting examples where the principles of green chemistry has been implemented for the development and designing of the different chemical reactions/processes in industrial as well as in laboratory scale<sup>67</sup>. Still, greater effort is being undertaken to develop and design an ideal chemical processes/reaction that begins from non-polluting starting materials, leads to no secondary by-products and requires no harmful solvents to carry out the chemical conversion or to isolate and purify the final product<sup>68</sup>. Many new analytical techniques which utilize the green chemistry principles have also been documented<sup>69</sup>. There are numerous approaches of green chemistry such as Microwave technology<sup>70</sup>, Ultrasonication<sup>71</sup>, Solvent-free synthesis or use of Green Solvents<sup>72</sup>, Photo catalysis<sup>73</sup>, Hydrothermal Synthesis<sup>74</sup>, Magnetic-field assisted synthesis<sup>75</sup>, Grinding technique<sup>76</sup>, Ball milling technique<sup>77</sup> to carry out organic synthesis. In this research work, we focused on the synthesis of some N-containing heterocyclic compounds under solvent free condition as solvent free reactions are gaining more importance now a days due to its efficiency, economic, short reaction time and high product yield.

### 1.2.1 Solvent free synthesis

“No Coopora nisi Fluida”, a famous statement given by the ancient Greek philosopher Aristotle, meaning “No reaction occurs in the absence of solvent” had a paramount influence on the advancement of the modern sciences and has provided one of the prominent reasons why organic reactions are carried out in solvents<sup>72</sup>. This statement is no longer valid as a large number of chemical reactions occur in solid state without solvent. Such solvent free or solid-state reactions have many advantages such as simple to handle, reduced pollution, comparatively cheaper to operate than the reactions carried out in solvents<sup>78</sup>. Interestingly, organic reaction in solid state is more efficient and more selective than those carried out in a solvent medium and they are largely green and therefore industrially useful<sup>79</sup>. Among the various proposed green procedure for the organic reaction, solvent-free or solid-state synthesis holds a leading position and therefore, a generalized concept is that **“the best solvent is no solvent”**<sup>80</sup>.

Solvent free synthesis or solid-state reactions have many advantages over the reaction carried out in solvent medium. Since, solvent is omitted from the reaction, therefore, from the prospect of economy one saves money on the solvent and it is environmentally friendly<sup>81</sup>. Solid state reaction or solvent free reaction is not a new



concept, in fact, Wohler's synthesis of urea (44) in 1828 is a historically significant organic reaction<sup>82</sup> (Fig.1.8)

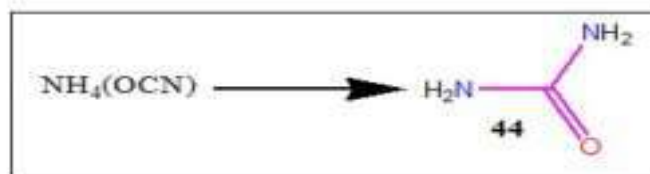


Fig. 1.8. Wohler's Synthesis of ammonia.

Examples of organic reactions carried out under solvent free conditions are numerous in the literature. For example, Baeyer-Villiger oxidations of ketones with *m*-chloroperbenzoic acid and it was found that this reaction proceeds much faster in the solid state than in solution at room temperature<sup>83</sup> (Fig.1.9).

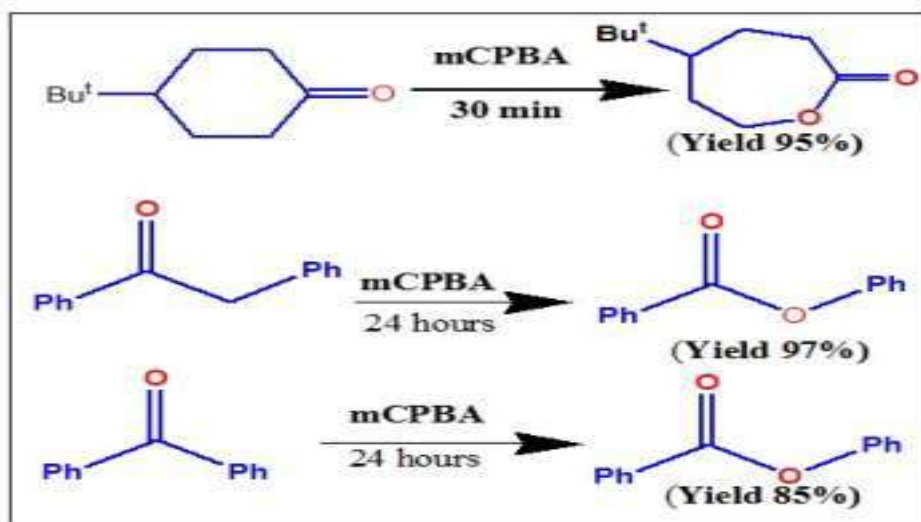


Fig. 1.9. Bayer-Villiger oxidation of ketones with mCPBA

Claisen rearrangement of allyl phenol to *o*-allylphenol (45) is another early record of organic synthesis carried out in solvent free condition<sup>84</sup> (Fig. 1.10).

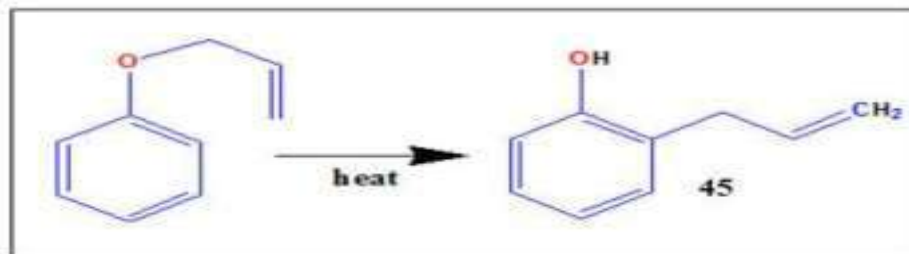


Fig. 1.10. Claisen rearrangement

Many other important organic reactions such as Michael addition<sup>85</sup>(46), Aldol condensation<sup>86</sup>(47), Stobbe condensation<sup>87</sup>(48), Thorpe reaction<sup>88</sup>(49), Tischenko reaction<sup>89</sup>(50) and Heck reaction<sup>90</sup>(51) etc., are also found to proceed efficiently in solvent free reaction conditions in contrast to the reaction carried out in solvent medium (Fig. 1.11). Furthermore, these reactions under solvent free conditions are highly atom and energy efficient and are highly chemo selective<sup>91</sup>.

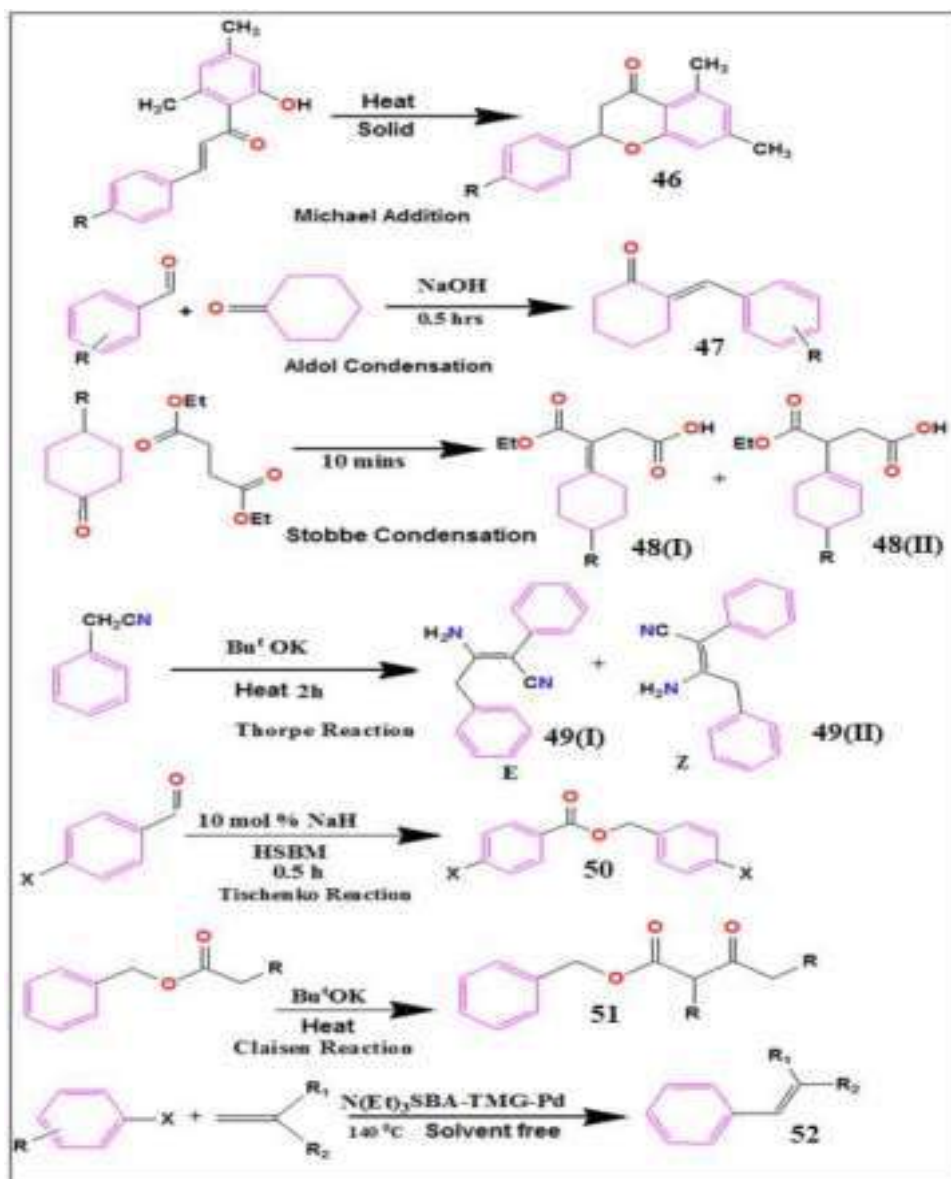
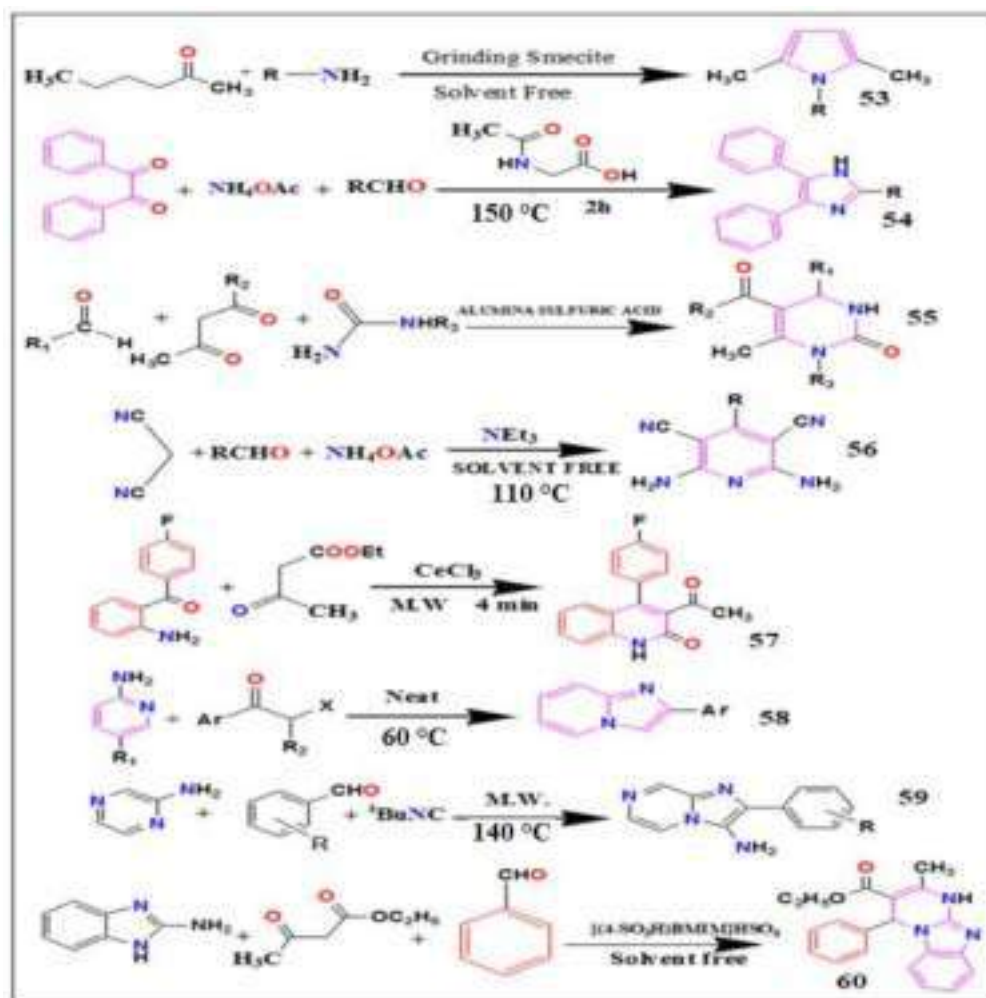


Fig. 1.11. Important organic reactions in solvent free condition.

Solvent free reactions are operationally simple; reduce pollution, comparatively economical and especially important in industries and therefore, various new methodologies and techniques have been developed to make the solvent free reaction more economical, more efficient and with less pollution<sup>92,93</sup>. Microwave<sup>70</sup>, Ultrasonication<sup>71</sup>, Grinding<sup>76</sup> and Ball milling<sup>77</sup> techniques are highly developed methodologies for the solvent free synthesis of industrially and clinically important organic molecules. Unfortunately, it has been observed that solid state reactions do not completely meet the meaning of no solvent since significant amount of solvent is still essential for adsorption of reactants and elution of products at the pre and post reaction stages respectively<sup>94</sup>. Since, our research work is focused on the synthesis of N-containing heterocyclic compounds under green reaction condition and therefore we are restricting our discussion with the solvent free synthesis of N-containing heterocyclic compounds only. During the past few decades, a vast number of works are documented towards the solvent free synthesis of different N-containing heterocyclic compounds under green reaction conditions<sup>95-98</sup>. The N-containing heterocyclic compound possesses distinct characteristics and therefore has gained immense importance in the rapidly growing fields of organic, medicinal chemistry and the pharmaceutical industry<sup>99</sup>. A number of solventless reaction protocols for the synthesis of different N-heterocyclic compounds such as pyrrole<sup>100</sup>(53), substituted imidazole<sup>101</sup>(54), dihydropyrimidinones<sup>102</sup>(55), substituted pyridines<sup>103</sup>(56), substituted quinolones<sup>104</sup>(57), imidazo[1,2-a]pyridines<sup>105</sup>(58), imidazo[1,2-a]pyrazines<sup>106</sup>(59) and imidazo[1,2-a]pyrimidines<sup>107</sup>(60) etc., have been developed during the past decades (Fig. 1.12). Since, green chemistry being a terminal goal for synthetic organic chemists, which requires chemical processes with high chemoselectivities and facile reaction systems and apparently, solvent free reaction condition meet the most of the criteria of the green chemistry. Therefore, solvent free synthesis is gaining a lot of interest in view of designing and development of new materials, processes, systems, and products that are benign to human health and the sustainable environment<sup>108</sup>. Though, we may not be able to avoid organic solvents during the synthesis of fine chemicals, nevertheless, continuous attempts have been made to devise and explore synthetic methods in the area of green chemistry. Thus, one way to achieve this goal is to adopt solvent free reaction condition as it will save environment and cuts cost of production by elimination of the use of expensive and hazardous solvents<sup>72</sup>.



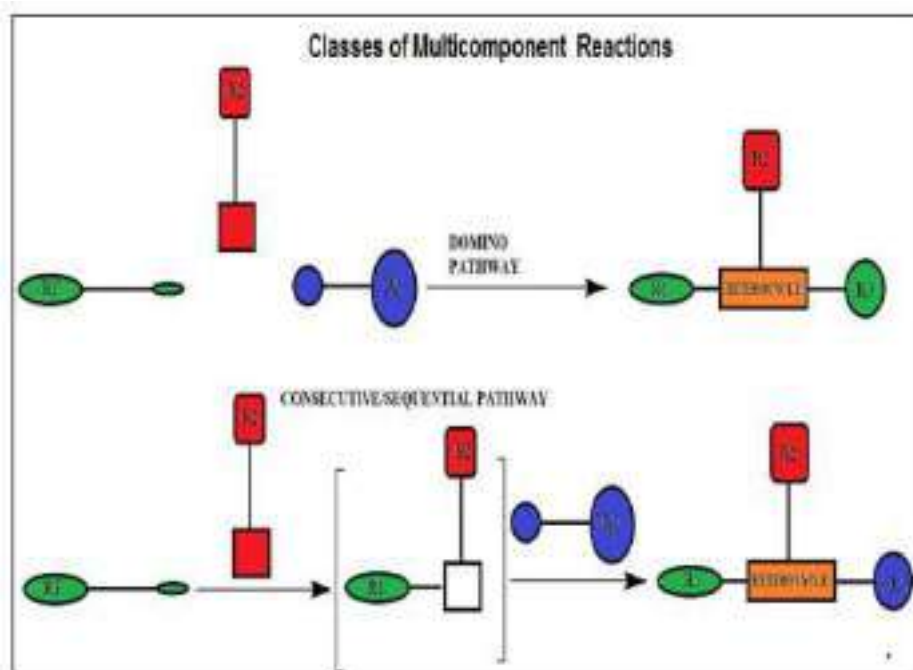
**Fig. 1.12.** Solventless reaction protocols for synthesis of some N-containing Heterocyclic compounds.

### 1.2.2 Multicomponent Reactions

In earlier days, the efficiency of the reaction for synthetic chemist was in terms of yield of the product, selectivity and number of steps involved in the synthesis. However, after the introduction of the concept of green chemistry and its underlying 12 principles, a broader concept for the design of chemical reactions evolved which includes criteria for waste generation, use of reagents and solvents, use of hazardous chemicals, energy intensity and general safety<sup>109</sup>. The main objective of green chemistry is to redesign the process in an economical and efficient protocol for the synthesis of valuable chemicals and it does not necessarily focus on the development of novel methods, but rather provides alternative sustainable variant to existing ones and most importantly, different synthetic strategies to include environmental considerations as early as in the process design stage<sup>110</sup>. In this context, Multicomponent Reactions (MCRs), where more than two reactants combine in a

sequential manner to give highly selective products that retain majority of the atoms of the starting material serves as a good example to meet the most of the requirements of the green chemistry<sup>111</sup>. Thus, Multicomponent Reactions (MCRs) are gaining lot of interest during these days for the synthetic chemist in view of the fact that this reaction condition is highly efficient and economical<sup>112-114</sup>. Multicomponent reactions (MCRs) find a prominent position in the organic synthesis as this method provides an option to bring together three or more reagents in one-pot, incorporating most of the atoms from the reagents in the final structure and decreases the time of the reaction<sup>115</sup>. A Multicomponent Reaction is in general a domino process, where a sequence of elementary steps of the chemical transformation is collaged to a single step. The domino reaction is also sometimes referred to as tandem reaction as this type of reaction has many advantages over conventional methods such as high atom economy, shorter reaction time, environmentally friendly, low cost and easy work up procedure<sup>116</sup>. Since, MCRs are one pot reactions; therefore, one can rapidly access large libraries of organic compounds with varied substitution in a single step by eliminating rigorous multistep syntheses<sup>117</sup>.

According to J. Zhu, MCRs may be appropriately defined as “*process involving sequential reactions among three or more reactant components that co-exist in same reaction mixture*”. Most interestingly, MCRs rely on the reactant components that are compatible with each other and do not undergo alternative reaction to form other products or by-products apart from the desired product<sup>118</sup>. Moreover, MCRs have many advantages such as simple experimental setup, high yield, atom economy, short reaction time, eco-friendly etc. over the classical approach for the synthesis of important organic motifs<sup>119</sup>. Thus, due to above underlying advantages, multicomponent reactions (MCRs) are considered to be pertinent methodological arsenal in synthetic and medicinal chemistry and these reactions have been advantageously employed in diverse synthetic transformations over classical methods which usually involve many steps with tedious procedures<sup>120</sup>. The MCRs can be divided into three distinct categories; i) the domino pathway in which the solvent, catalyst and the reagents are present in same reaction vessel at the start of the reaction, ii) sequential pathway is the second class of MCRs in which the reaction condition remains the same during the whole sequence but reactant components are added in well-defined sequential order from step to step and iii) The consecutive MCRs is the last class in which the components are added stepwise (as in sequential MCRs), but the reaction conditions may be altered with each reaction step<sup>121</sup>(Scheme 1.1).

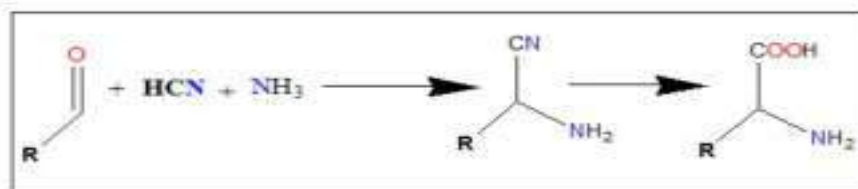


**Scheme. 1.1.** Graphical illustration of the classes of MCRs

Thus, designing and development of Multicomponent Reaction strategies incorporating the principle of green chemistry and using renewable and recyclable materials, using solvent-free conditions, green solvents, and green or reusable catalyst, using nonclassical conditions such as microwave technologies, ultrasonic irradiations is becoming a hotspot in the synthetic research field<sup>122</sup>.

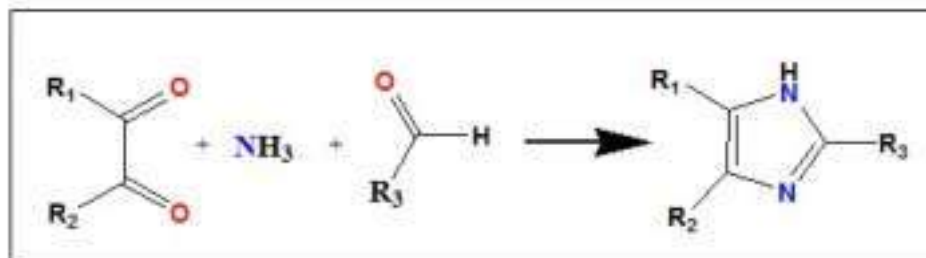
### 1.2.2.1 Historical development of Multicomponent Reactions

The historical development of Multicomponent Reactions can be traced back to the year 1850 where Adolf Strecker synthesized  $\alpha$ -amino acid through one pot multicomponent condensation of aldehydes, HCN and  $\text{NH}_3$ . The three-component condensation of the above reagents leads to the formation of  $\alpha$ -amino nitriles which is the main intermediate of the Strecker's synthesis. Subsequent hydrolysis of the  $\alpha$ -aminonitrile results in to the formation of  $\alpha$ -amino acid. Thus, historically Strecker's reaction may be regarded as a first multicomponent reaction and this reaction represents one of the most straightforward and economically viable multicomponent reaction<sup>123</sup>(Scheme 1.2).



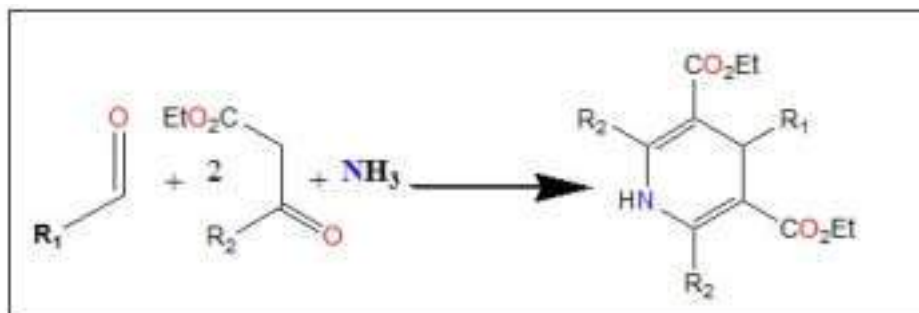
**Scheme. 1.2.** Strecker's Reaction

The Debus-Radziszewski imidazole synthesis was another step in the field of multicomponent reaction which was coined by Heinrich Debus in 1858<sup>124</sup> and later developed by Bronislaw Leonard Radziszewski in 1882<sup>125,126</sup>. In this multicomponent reaction, an imidazole scaffold was prepared by cyclocondensation of diketone, aldehyde and ammonia (Scheme 1.3).



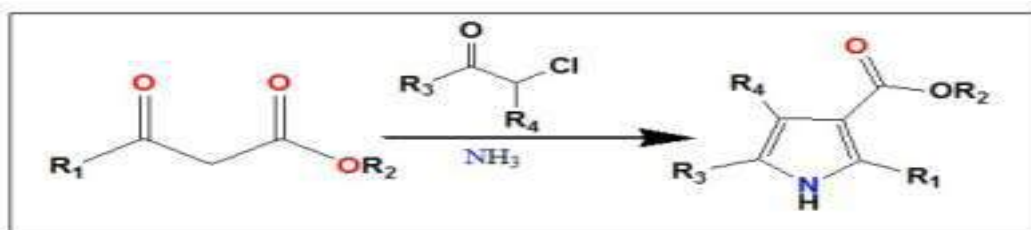
**Scheme. 1.3.** Debus-Radziszewski Synthesis.

Further progress in multicomponent synthetic chemistry was realized when Hantzsch (1881) synthesized symmetrically substituted dihydropyridines from one pot cyclocondensation of  $\text{NH}_3$ , aldehydes and two equivalent of  $\beta$ -ketoesters<sup>127</sup>(Scheme 1.4).



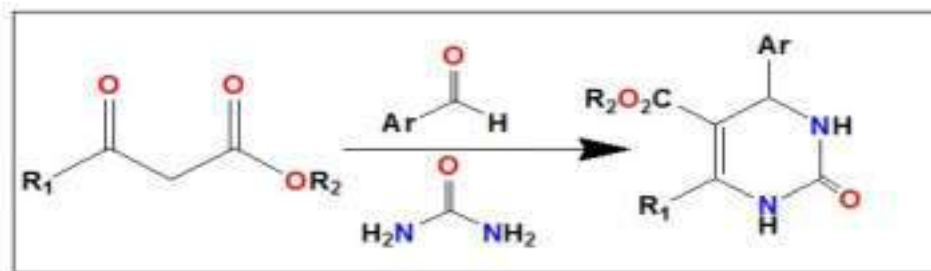
**Scheme. 1.4.** Hantzsch Synthesis of substituted dihydropyridines

The Hantzsch synthesis of pyrrole involving ammonia (or primary amine),  $\beta$ -ketoester and  $\alpha$ -haloketones is another contribution towards the development of multicomponent reaction<sup>128</sup> (Scheme 1.5).



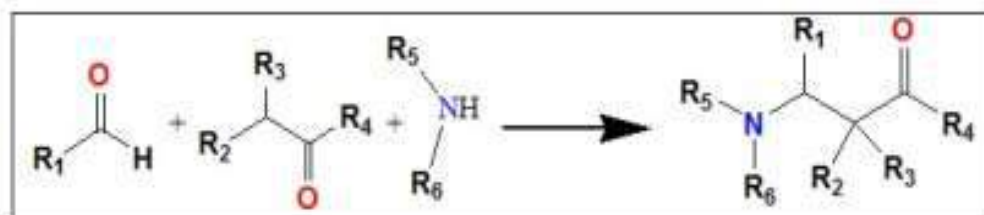
**Scheme. 1.5:** Hantzch Synthesis of pyrrole.

Another development in the field of Multicomponent Reaction can be visualized through the work of an Italian Chemist Pietro Bigenelli in the year 1891 wherein he adopted a three-component acid catalyzed cyclocondensation of  $\beta$ -ketoester, aromatic aldehydes and Urea to synthesized substituted Dihydropyrimidinones<sup>129</sup> (Scheme 1.6).



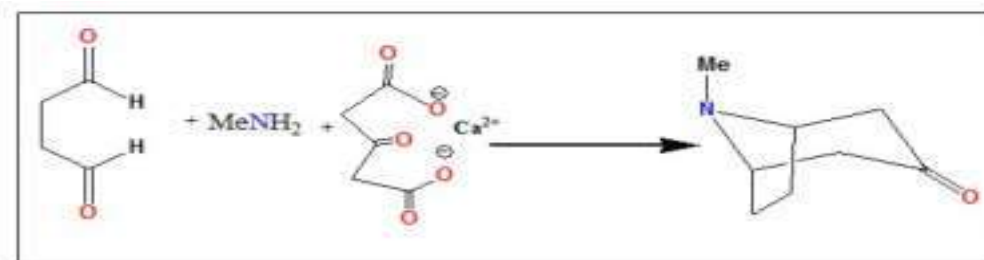
**Scheme. 1.6.** Bigenelli synthesis of dihydropyrimidinones

In the year 1912, Carl Mannich discovered a one-pot Multicomponent Reaction for the synthesis of optically active  $\beta$ -aminocarbonyl compounds through the condensation of amine derivatives, enolizable carbonyl compounds and non-enolizable aldehyde. This reaction is known as the famous Mannich reaction and the optically active compound serves as a valuable building block for the asymmetric synthesis of various pharmaceutical scaffolds and natural products<sup>130</sup> (Scheme 1.7).



**Scheme. 1.7.** Mannich Reaction

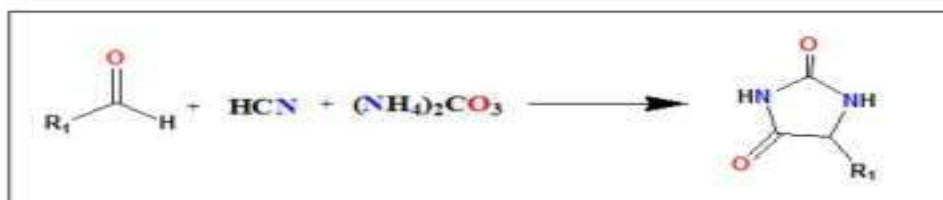
Moreover, Robinson synthesis of bioactive alkaloid Tropinone in 1917 can be taken as the first important application of MCRs in natural product synthesis<sup>131</sup>. The one-pot cyclocondensation of succinic di-aldehyde, methylamine and calcium salt of acetonedicarboxylic acid yielded biologically active Tropinone (Scheme 1.8).



**Scheme. 1.8.** Robinson's synthesis of bioactive alkaloid

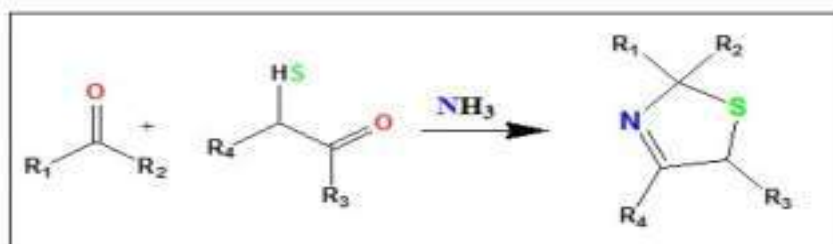


Bucherer and Bergs, in 1934 successfully synthesized hydantoin derivatives utilizing four component one pot condensation of HCN, aldehydes, ammonia and CO<sub>2</sub><sup>132</sup>. This reaction is very important as the hydantoin derivatives on hydrolysis transformed into  $\alpha$ -amino acid (Scheme 1.9)



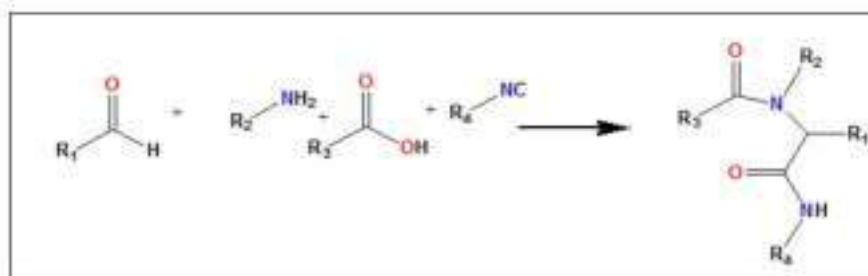
**Scheme. 1.9.** Bucherer and Bergs synthesis.

A-4CR reaction i.e., Asinger-4 component reaction was reported by Friedrich Asinger (1956) is an important four component reaction where  $\alpha$ -halogenated carbonyl compounds, Thiols and ammonia undergo cyclocondensation to afford thiazolines. An interesting feature of Asinger reaction is that the sodium hydrogen sulphide is generated in-situ from the thiols and subsequently the sodium hydrogen sulphide reacts with carbonyl compounds and ammonia to give thiazolines<sup>133</sup> (Scheme 1.10).



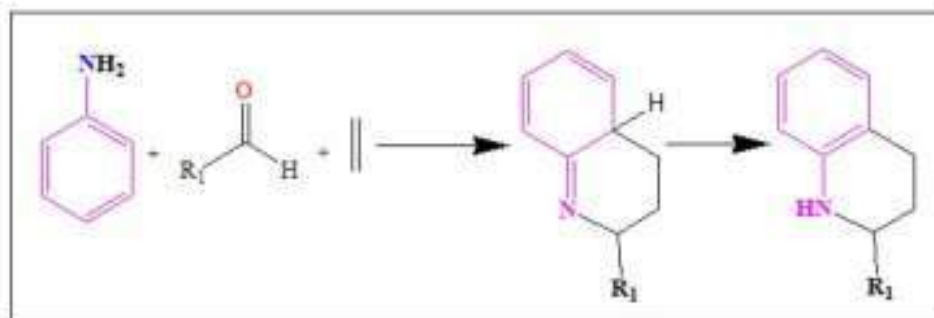
**Scheme. 1.10.** Asinger Reaction

Ugi reaction, a four-component reaction for the synthesis of  $\alpha$ -acylaminoamides by reacting aldehydes, primary amines, carboxylic acid and isocyanides discovered by Ivar Ugi (1959) is one of the most important and highly utilized multicomponent reaction in organic synthesis<sup>134</sup> (Scheme 1.11).



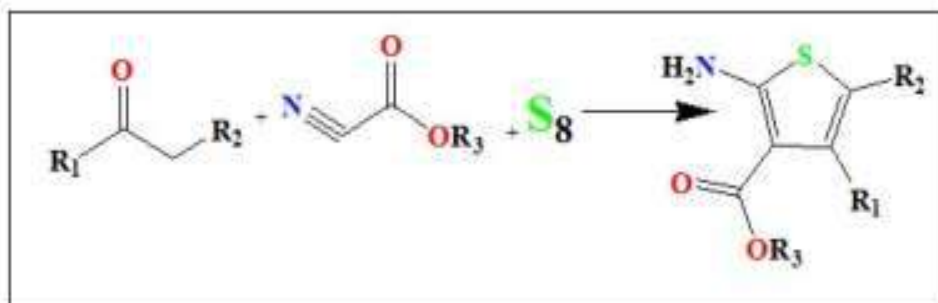
**Scheme. 1.11.** Ugi Reaction

Similarly, Povarov's (1965) acid catalysed three component cyclocondensation reaction where N-aryl imine produced in situ by the reaction between aromatic amine and aromatic aldehyde undergo cyclocondensation with alkene to afford substituted quinolines is an excellent example of Multicomponent reaction<sup>135</sup> (Scheme 1.12)



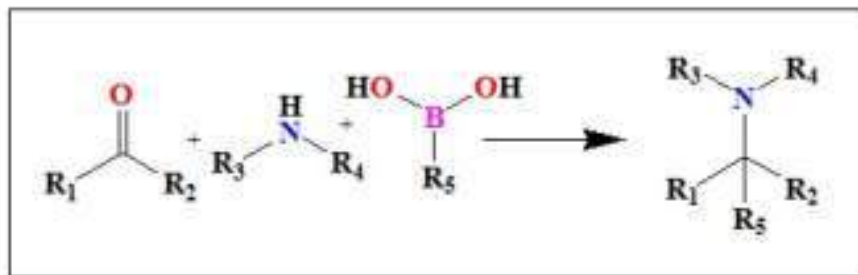
**Scheme. 1.12.** Povarov's reaction

The Gewald's synthesis (1966) of substituted thiophene at room temperature via one-pot multicomponent condensation between aldehydes, ketones or 1, 3-dicarbonyl compounds with activated nitriles and sulfur in presence of amine is another milestone in the development of Multicomponent Reactions<sup>136</sup> (Scheme 1.13).



**Scheme. 1.13.** Gewald's Synthesis

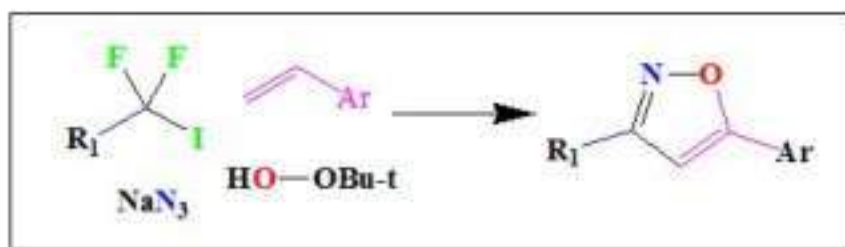
Though the Multicomponent Reactions (MCRs) have been known for over 100 years; however, MCRs gained importance in the early 1990s after the introduction of combinatorial chemistry and related library-synthesis strategies<sup>137</sup>. Petasis Multicomponent Reaction, coined by N. A. Petasis in 1993 may be viewed as a powerful synthetic strategy developed in the last decade for the preparation of amine derivatives from the condensation of amines, carbonyl derivatives and aryl- or vinyl boronic acid<sup>138</sup> (Scheme 1.14).



**Scheme. 1.14.** Petasis Multicomponent Reaction

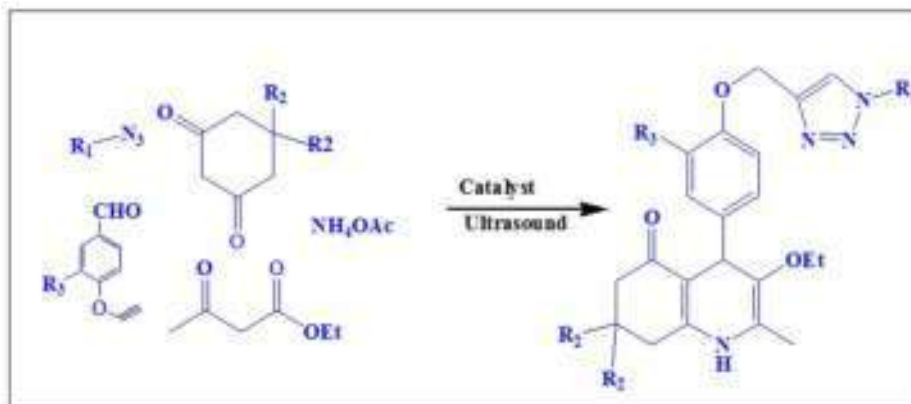
Many new MCRs have been documented during the past few decades and many new variants of synthetic strategies have been developed for the synthesis of libraries of different fine chemicals<sup>139</sup>. Over the years, the advancement of multicomponent reaction has taken a rapid pace and now a days, MCRs of different types involving 3, 4, 5, 6, 7 and even 8 reactant components in a single reaction mixture have been developed.

For example, Z. Li *et.al.*, have developed a four component one-pot synthesis of isoxazole skeleton and they have successfully developed the procedure for the synthesis of perfluoroalkyl isoxazoles by using simple perfluoroalkyl reagents<sup>140</sup> (Scheme 1.15).



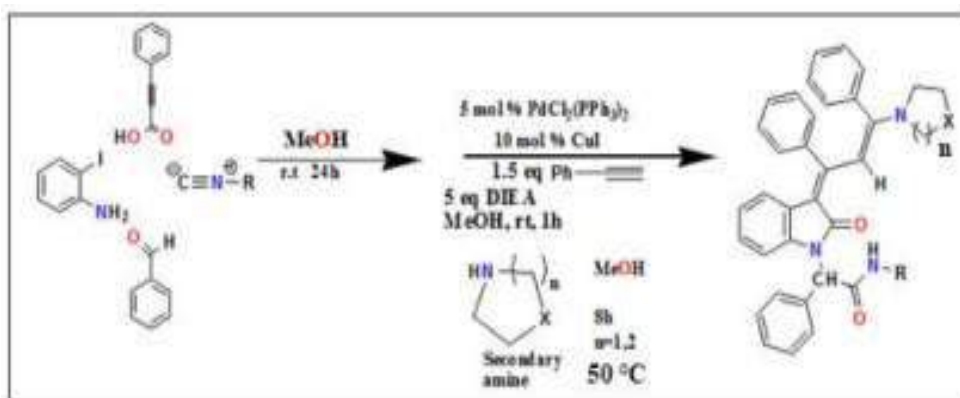
**Scheme. 1.15.** Synthesis of perfluoroalkyl isoxazoles by using perfluoroalkyl reagents.

Khurana *et.al.* have developed a simple and efficient one-pot five component reaction for the synthesis of 1,2,3-triazole linked 1,4-dihydropyridines under green condition using PEG-400 as a solvent medium<sup>141</sup> (Scheme 1.16).



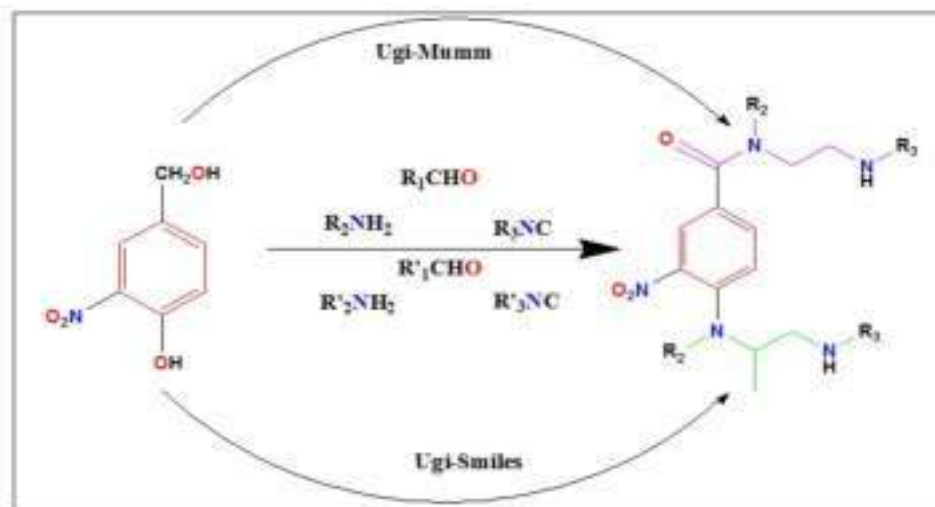
**Scheme. 1.16.** Synthesis of 1,4-dihydropyridines under green condition using PEG-400

S. Balalaie *et.al.* successfully utilized a Sequential One-Pot Ugi/Heck Carbocyclization/Sonogashira/Nucleophilic Addition reaction for the synthesis of 3-Arylidene-2-oxindoles and it serves as a good example of a six-component condensation reaction<sup>142</sup> (Scheme 1.17).



**Scheme. 1.17.** Sequential One-Pot Ugi/Heck Carbocyclization/Sonogashira/Nucleophilic Addition reaction.

As a seven-component reaction, Bernhard Westermann *et.al.* have utilized different chemoselectivities of the Ugi–Mumm and the Ugi–Smiles reaction in a sequential multicomponent reaction to afford highly diverse peptide and glycopeptides motifs<sup>143</sup>(Scheme 1.18)



**Scheme. 1.18.** Ugi-Mumm and Ugi Smiles Reaction.

Romano V. A. Orru *et.al.*, have developed a one-pot eight component reaction by utilizing union of Multicomponent Reactions to achieve a one-pot 8CR that involves nine new bond formations and eleven points of diversity<sup>144</sup>.

By virtue of considerable economic and ecological interest, Multicomponent Reactions have emerged as important tools for the rapid generation of molecular complexity and diversity with predefined functionality in the field of drug discovery<sup>145</sup>. Thus, the overall historical development of Multicomponent Reactions is shown in Fig 1.13

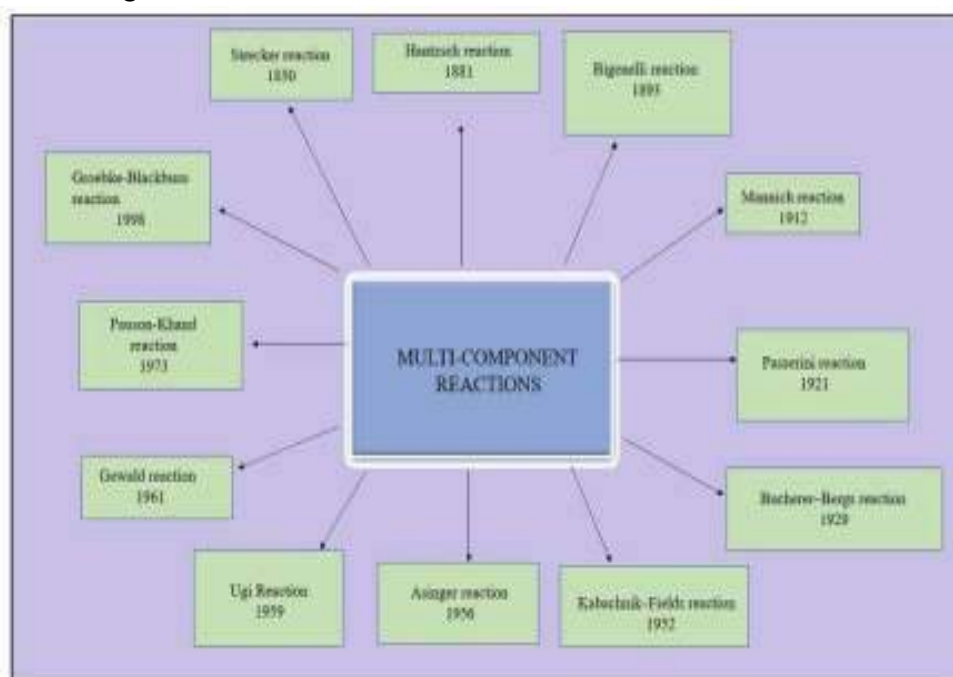


**Fig. 1.13.** Historical Development of Multi Component Reactions

Moreover, the present-day organic synthesis demands the designing of an operationally simple, useful and practical strategy which is cost effective and has less detrimental impact on the environment. A rational design strategy in Multicomponent Reactions (MCRs) are playing a chief role in current scenario because of the convergent nature, higher atom economy, and easy experimental procedures in the production of target compounds by the introduction of several diversity elements in a single operation, minimization of waste, labor, time, and cost, and thus, much work has been done to extend the scope of the well known classical Multicomponent Reactions to newer systems<sup>146</sup>.

Interestingly, Multicomponent Reactions carried under solvent free conditions are gaining much attention during last decades as because these reactions are finding much application in diversity Oriented Synthesis (DOS)<sup>147</sup>. Since, the demand for both clean and efficient chemical syntheses is becoming more urgent, the MCRs carried out under solvent free conditions compensate this demand as because solvent-free methods open up many possibilities to modernize classical procedures by making them cleaner, safer, and easier to perform<sup>148</sup>. Several solvent free reaction protocols have been developed for almost all the classical Multicomponent Reactions namely, Strecker<sup>149</sup>, Bigenelli<sup>150</sup>, Passerini<sup>151</sup>, Mannich<sup>152</sup>, Hantzsch<sup>153</sup>, Ugi<sup>154</sup>, Gewald<sup>155</sup>, Petasis<sup>156</sup>, Radziwinski<sup>157</sup> etc. Moreover, the solvent free organic reactions have aroused the attention of organic as well as medicinal chemists during the last few decades and will add more modern techniques and procedure for chemo-, regio-, Stereoselective synthesis of high-value chemicals and synthesis of libraries of small molecules under solvent free condition in near future<sup>146</sup>.

Therefore, all these factors prompted us to undertake the research work in the field of development of eco-friendly synthetic methodology for the synthesis of some important N-containing heterocyclic compounds using inexpensive transition metal borates as a catalyst under solvent free condition. In this research work, we focused our study on the Multicomponent green synthesis of some selected N-heterocyclic compounds such as 2,4,5-triarylimidazole, 3,4-dihydropyrimidin-2(1*H*)-one, 1-hydroxyimidazole-3-oxide and 1,2-disubstituted benzimidazole derivatives using inexpensive transition metal borate catalysts under solvent free conditions. Furthermore, we extended our research work towards the detailed theoretical (DFT), ADME and molecular docking study of the synthesized products in order to gain an insight into the potential application of the synthesized products in different scientific fields. The molecular structures of the studied N-heterocyclic scaffolds (as 2, 4, 5-triarylimidazole (61), 3, 4-dihydropyrimidin-2(1*H*)-one (62), 1-hydroxyimidazole 3-oxide (63) and 1,2-disubstituted benzimidazoles (64)) are given in Fig. 1.4.

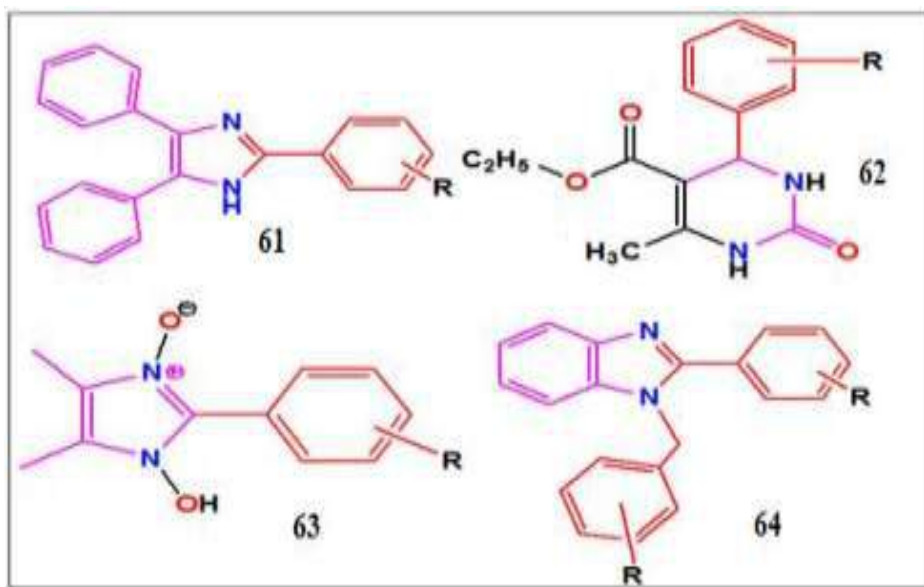


**Fig. 1.4.** Molecular structure of 2,4,5-triarylimidazole, 3,4-dihydropyrimidin-2(1*H*)-one, 1-hydroxyimidazole 3-oxide and 1,2-disubstituted benzimidazoles.

### 1.3 Brief information about the studied N-heterocyclic scaffolds

#### 1.3.1 2,4,5-triarylimidazole

Among many N-containing heterocyclic compounds, imidazole, a five-membered nitrogenous scaffold occupies a unique position due to its wide range of pharmacological and biological properties<sup>158</sup>. Imidazole and its derivatives, has the unique ability to form strong hydrogen bonds with biological targets as well as it has high affinity for the metals present in active site of many proteins<sup>159</sup>. Furthermore, by virtue of the ability of forming hydrogen bonds with important biological targets, imidazole possesses diverse biological properties such as antimicrobial<sup>160</sup>, anticancer<sup>161</sup>, antihistamatic<sup>162</sup>, anti-inflammatory<sup>163</sup> and antiviral<sup>164</sup> etc. Interestingly, imidazole scaffold is found to present in many drugs such as clotrimazole<sup>165</sup>(33), ketoconazole<sup>166</sup> (65), omeprazole<sup>167</sup>(66), Losartan<sup>168</sup>(67), Eprosartan<sup>169</sup>(68), and Trifenagrel<sup>170</sup>(69) etc. (Fig. 1.15).

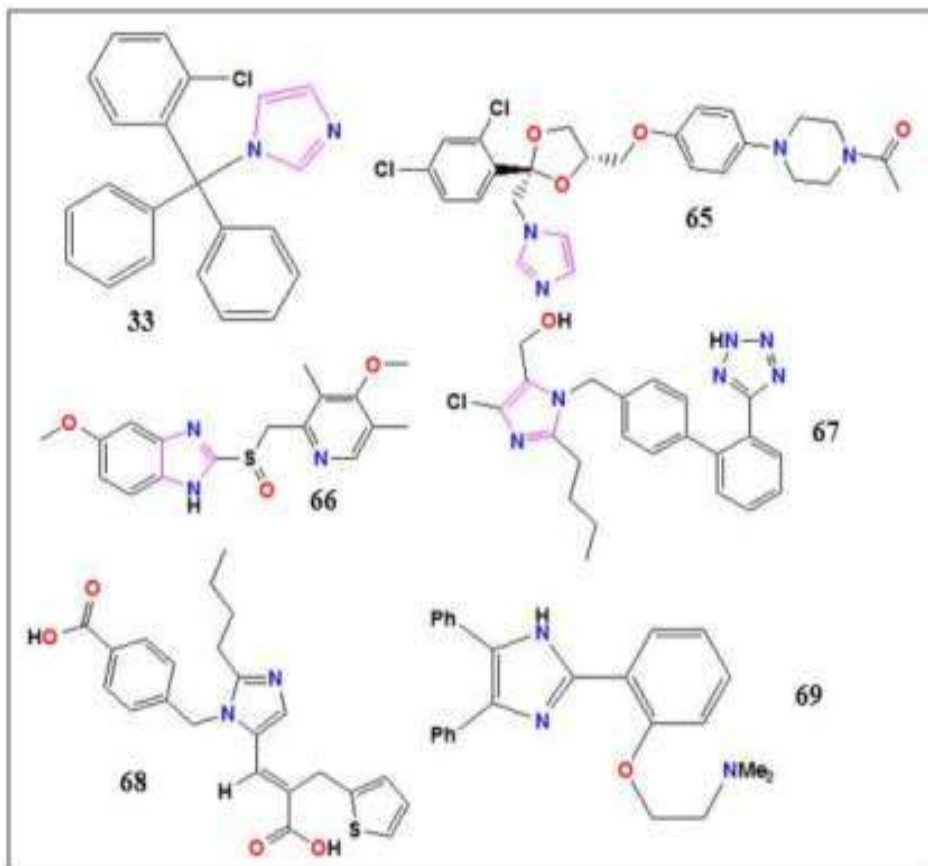


**Fig. 1.15.** Structures of few drugs containing imidazole scaffold.

It is also found in many naturally occurring biomolecules like histidine<sup>171</sup>(27), histamine<sup>172</sup> (70) and biotin<sup>173</sup>(71) (Fig. 1.16).

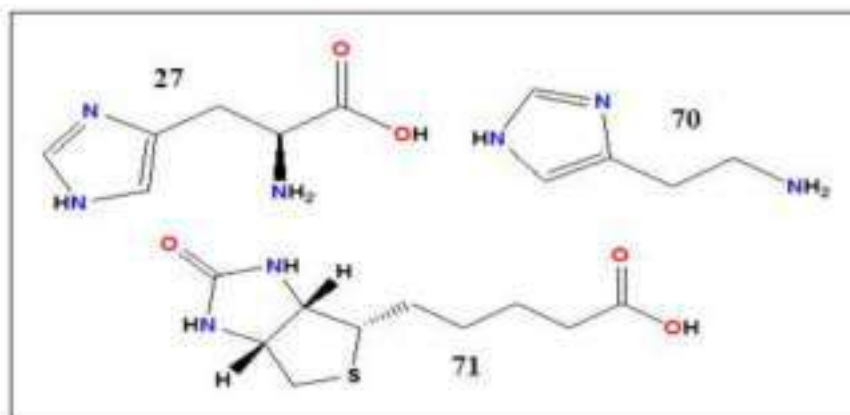


**Fig. 1.16.** Structures of few naturally occurring biomolecules

Substituted imidazole derivatives fall on the category of important class of N-heterocycles due to their wide range of pharmacological and biological properties and that are a subject of intensive current research<sup>58</sup>. Among several imidazole-based



scaffolds that have been known so far, 2,4,5-trisubstituted imidazoles occupy a special place in the area of natural, pharmaceutical and synthetic organic chemistry owing to their numerous biological and pharmacological properties<sup>174-176</sup>. Some substituted triarylimidazole derivatives have been found to exhibit selective antagonists of glucagon receptor<sup>177</sup>(72), inhibitors of Interleukin 1 (IL-1) biosynthesis<sup>178</sup> and P38MAP kinase inhibitor<sup>179</sup>(74) (Fig. 1.17). In recent years, much attention has been focused to the substituted imidazole derivatives due to their diversified therapeutic activities such as antibacterial<sup>180</sup>, antifungal<sup>181,182</sup>, antiviral<sup>183-185</sup>, antitubercular<sup>186</sup>, antidepressant<sup>187</sup>, antitumor<sup>188</sup>, herbicide<sup>189</sup> and plant growth regulators<sup>190</sup>. Apart from the biological activities, substituted imidazole derivatives finds extensive applications in various fields such as fluorescence labeling agents<sup>191</sup>, biological imaging agents<sup>192</sup>, non-linear optics<sup>193</sup>, cosmetics<sup>194</sup>, polymer chemistry<sup>195</sup>, agro chemicals<sup>196</sup>, material science (OLEDS, optical electronics, dye sensitized solar cells)<sup>197</sup>, photosensitive compounds in photography<sup>198</sup> and corrosion inhibitors<sup>199</sup>. Highly substituted imidazoles such as clemizole (antihistaminic agent)<sup>200</sup>(75), nocodazole (antinematodal)<sup>201</sup>(76), azathioprine (anti-rheumatoid arthritis)<sup>202</sup>(77), dacarbazine (anticancer)<sup>203,204</sup>(78) are commercially available drugs for the treatment of different diseases (Fig.1.18).

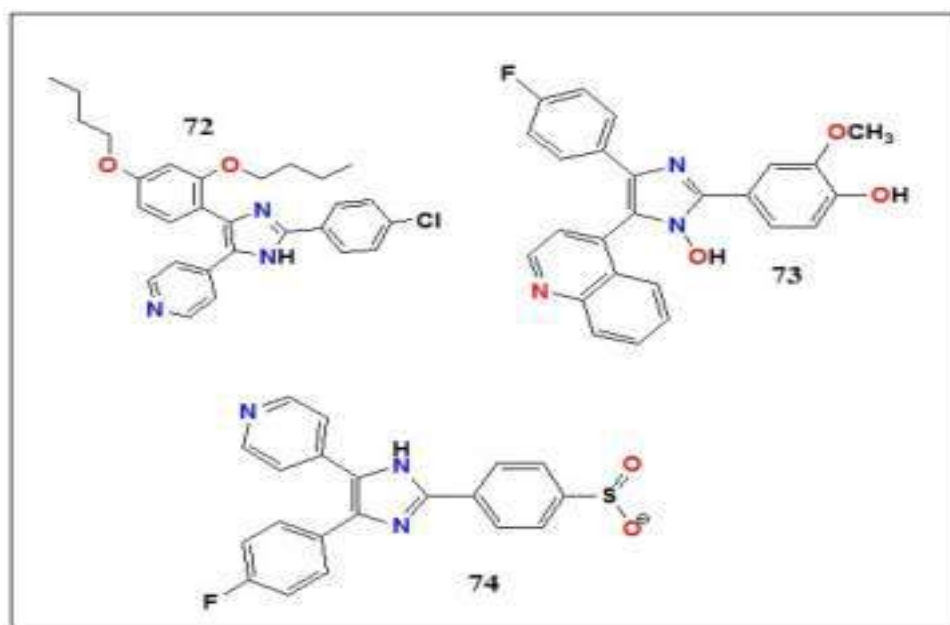


**Fig. 1.17.** Structures of some biologically important substituted imidazoles.

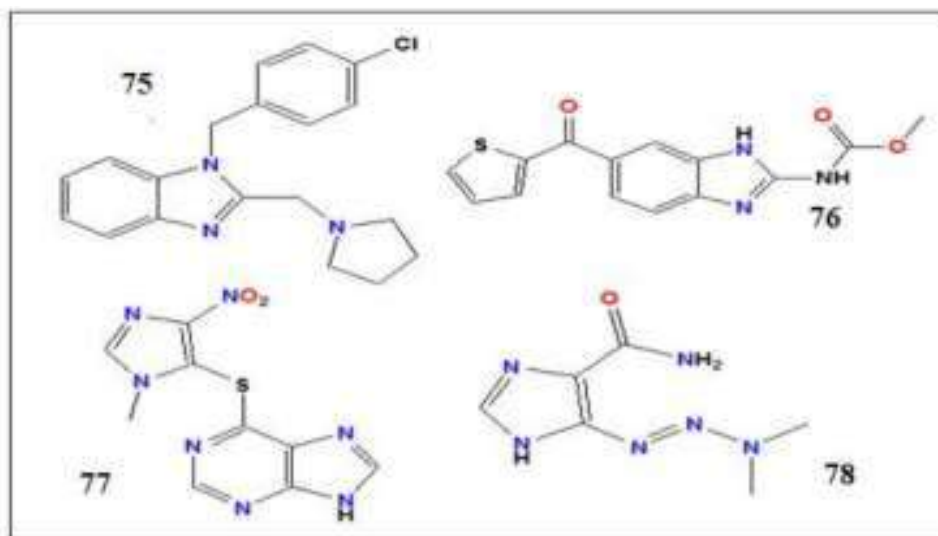


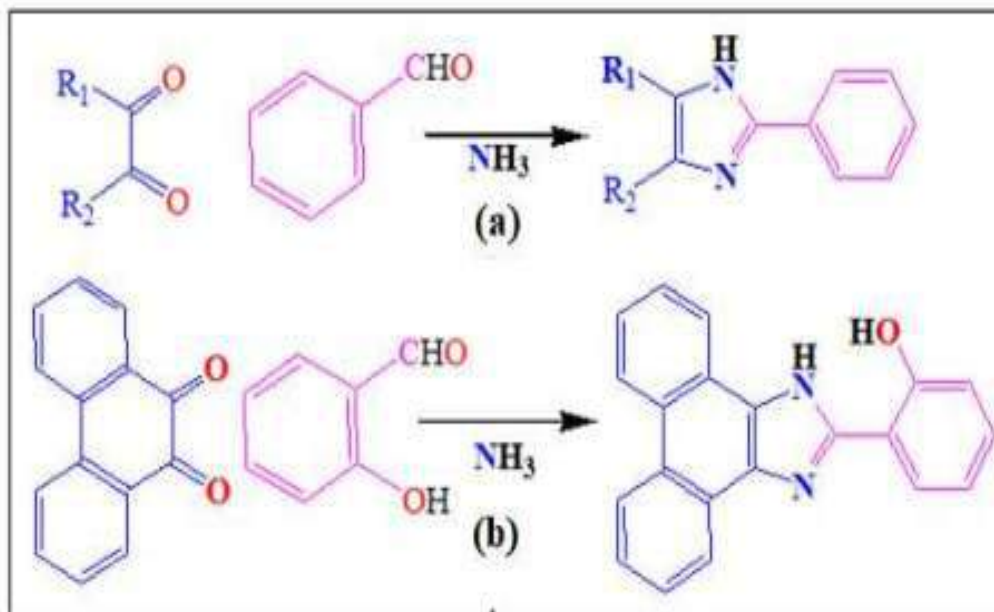
**Fig. 1.18.** Structures of few drugs having Imidazole Scaffold.

Thus, looking at the importance of the imidazole scaffold in different fields, various synthetic methodologies have been developed during the last few decades and numerous new synthetic methods are developing on daily basis<sup>205</sup>.

## 1.3.1.1 Various synthetic routes for the synthesis of 2, 4, 5-triarylimidazole

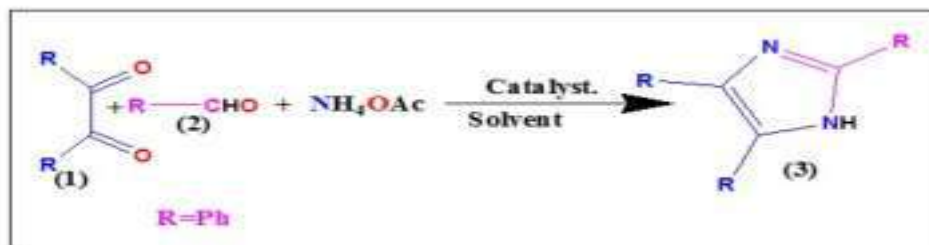
## 1.3.1.2 Classical method

In 1882, Radziszewski and Japp independently reported the first synthesis of 2,4,5-triarylimidazole by cyclo-condensation of 1, 2-dicarbonyl compound with an aldehyde in presence of ammonia as a nitrogen source in acidic medium<sup>125,206</sup> (Scheme 1.19 a-b).



**Scheme. 1.19.** a) Radziszewski and b) Japp imidazole synthesis

After the successful synthesis of triaryl imidazoles by Radziszewski and Japp, various synthetic modifications have been made in this approach. The most common modification that has been made is the use of ammonium acetate in place of ammonia as a nitrogen source. Till date, even after more than 150 years of discovery, the imidazole scaffold is attracting many researchers due to their potential applications in different fields. Therefore, recent developments in the area of synthesis of 2,4,5-triarylimidazole are discussed herein and a general scheme is shown in Scheme 1.20.



**Scheme. 1.20.** Modern synthetic route for the synthesis of 2, 4, 5-triarylimidazole derivatives.

Current literature review revealed that numerous synthetic procedures have been documented using various catalysts under the classical conditions.

Li-Min Wang *et.al.* developed an operationally simple method for the synthesis of 2,4,5-triaryimidazole (3) by condensation of 1,2-diketone (1) and aldehyde (2) in presence of Ammonium acetate using  $\text{Yb}(\text{OTf})_3$  catalyst. The Key feature of this method was the reusability of the catalyst and high yield of the products<sup>207</sup>.

Mazaahir Kidwai *et.al.* used molecular iodine as a catalyst for an efficient synthesis of (3) using in ethanol solvent. The key features of this reaction were: i. reaction was easy to carry out, ii. Inexpensive and non-toxic reagents were used, iii. High yield of products<sup>208</sup>.

Majid M. Heravi *et.al.* used  $\text{NiCl}_2 \cdot 6\text{H}_2\text{O}$ - a lewis acid supported on acidic alumina as a catalyst for the synthesis of (3) in ethanol medium. The reaction proceeded in short time under milder conditions using cheap  $\text{NiCl}_2 \cdot 6\text{H}_2\text{O}$  catalyst<sup>209</sup>.

A.F. Mohammed *et.al.* developed a facile method for the synthesis of tri substituted imidazoles under ethanol-water mixture using sulphanic acid as an organo catalyst<sup>210</sup>.

In another development, Jaiprakash Sangshetti *et.al.* used cheaply available Ceric Ammonium Nitrate as an efficient catalyst for the preparation of (3) in ethanol-water solvent<sup>211</sup>.

Lakshman. S. Gadekar *et.al.* used solecite as a heterogenous catalyst for the synthesis of (3) via a three-component reaction in ethanol solvent<sup>212</sup>.

A. Yasodha *et.al.* reported the synthesis and biological activities of various substituted triphenyl imidazoles in acetic acid medium<sup>213</sup>.

Babasaheb. P. Bandgar *et.al.* developed an efficient one pot synthesis of (3) using zinc oxide ( $\text{ZnO}$ ) as a catalyst in acetonitrile at room temperature to form the desired 2,4,5-triaryimidazole in excellent yield<sup>214</sup>.

J-T. Li. *et.al.* and Swati D. Burungale *et.al.* independently reported the synthesis of (3) in acetic acid medium<sup>215,216</sup>.

Paul.D. Sanasi *et.al.* have used nano copper and cobalt ferrite catalysts for the synthesis of (3) in ethanol solvent<sup>217</sup>.

J. Madhavi *et.al.* developed an efficient and environmentally benign method for the synthesis of (3) using  $ZrO_2$  catalyst for the first time in methanol and chloroform medium<sup>218</sup>.

Nora Chouha *et.al.* used citric acid as an organo catalyst for a three-component reaction for the synthesis of (3) in refluxing ethanol<sup>219</sup>.

Vishvanath. D. Patil *et.al.* reported  $PbCl_2$  and  $Pb(OAc)_2$  as an efficient catalyst for the synthesis of (3) in ethanol solvent<sup>220-221</sup>.

### 1.3.1.3 Green method

Apart from the above cited conventional classical methods for the synthesis of 2,4,5-triarylimidazole derivatives (3), during the past, numerous methodologies such as solvent free, ultrasound mediated and microwave irradiation under green reaction conditions have been reported.

#### 1.3.1.3.1 Solvent free synthesis

It has been an interesting observation that the reactions carried out in conventional organic solvents has many disadvantages and therefore synthetic chemists are paying more attention to the development of new methodologies based on solvent-free conditions<sup>146</sup>. Current literature review revealed that there are numerous reports on the solvent free synthesis of 2,4,5-triarylimidazole derivatives (Scheme 1.21).



**Scheme. 1.21.** Synthesis of 2,4,5-triarylimidazole derivatives under solvent free conditions.

Arshia Parveen *et.al.* reported an efficient method for the synthesis of triaryl imidazoles (3) using molecular  $I_2$  as a catalyst under solvent free conditions and the reaction was processed by grinding the contents in a mortar and pestle with excellent yield of products<sup>222</sup>.

In another solvent free synthesis of triarylimidazole, Runxia Wang *et.al.* reported Yttrium (III) trifluoroacetate as an excellent catalyst for the synthesis of triaryl imidazoles (3) under solvent free and neat conditions. It was observed that for aldehydes having electron donating or electron withdrawing groups at ortho and para positions the reaction was gave very good results<sup>223</sup>.

Bahador Karami *et.al.* reported  $Fe_3O_4$  nanoparticles as an efficient catalyst for the synthesis of triaryl imidazoles under heating conditions without any solvent<sup>224</sup>.

Bibi Fatemeh Mirjalilli *et al.* used trichloromelamine as an efficient catalyst for the synthesis of triaryl imidazoles under solvent free conditions in a short reaction time and with high yield of products<sup>225</sup>.

Behrooz Maleki *et al.* reported the use of sulfuric acid immobilized on silica gel as a catalyst for the synthesis of triaryl imidazoles (3) under solvent free conditions<sup>226</sup>.

B.F. Mirjalili *et al.* used nano SnCl<sub>4</sub> for the one pot synthesis of triaryl imidazoles (3) under solvent free conditions<sup>227</sup>.

Janardhan Banothu *et al.* reported a one pot three component synthesis of triaryl imidazoles (3) using an ionic liquid (4-sulfobutyl) tris(4-sulfophenyl) phosphonium hydrogen sulfate(4-SB) T(4-SPh) PHSO<sub>4</sub> as a catalyst<sup>228</sup>.

Goutam Brahmachari *et al.* utilized titanium dioxide as an effective and clean catalyst for the synthesis of Triaryl imidazoles (3) under solvent free conditions and the main advantage of this reaction was the easy recyclability of the catalyst and high yield of the products<sup>229</sup>.

Adel A. Marzouk *et al.* reported the use of diethyl hydrogen phosphate as a catalyst for the synthesis of triarylimidazole (3)<sup>230</sup>.

P.V. Maske *et al.* used papain as a catalyst with water as a solvent for the preparation of triaryl imidazoles (3)<sup>231</sup>.

K. Nikoofar *et al.* used ZnO nanorods as catalysts for their efficiency, reusability, and their mild reaction conditions for the synthesis of triaryl imidazoles (3) with water as a solvent<sup>232</sup>.

M. Vosoughi *et al.* used ZSM-5-SO<sub>3</sub>H as an efficient catalyst for the synthesis of triaryl imidazoles (3) under solvent free conditions<sup>233</sup>.

Ghodsii Mohammadi Ziarani *et al.* used sulfonic acid functionalized SBA-15 nanoporous material as a solid catalyst for the synthesis of tri aryl imidazoles under solvent free conditions<sup>234</sup>.

Mohammad Alikarami *et al.* used benzyltriphenylphosphonium chloride (BTPPC) as an inexpensive and an efficient catalyst for the synthesis of tri aryl imidazoles (3) under solvent free conditions<sup>235</sup>.

### 1.3.1.3.2 Microwave irradiation

In early 1990's various chemical transformations were achieved by adopting microwave irradiation as a heating source by various laboratories to synthesize the desired products in short reaction time since it was realized that microwave irradiation could be used as an alternate energy source to carry out chemical transformation in minutes instead of hours or even days<sup>236</sup>. In Microwave assisted organic synthesis, the rate of the reaction can be accelerated and the product can be synthesized selectively<sup>237</sup>. Therefore, solvent free microwave assisted organic synthesis provides an added advantage such as short reaction time, rapid heating, high temperature and selective heating for chemical transformation as compared to conventional heating method<sup>238</sup>. Thus, Microwave Assisted Organic Synthesis (MAOS) has become an important tool for the rapid and efficient synthesis of

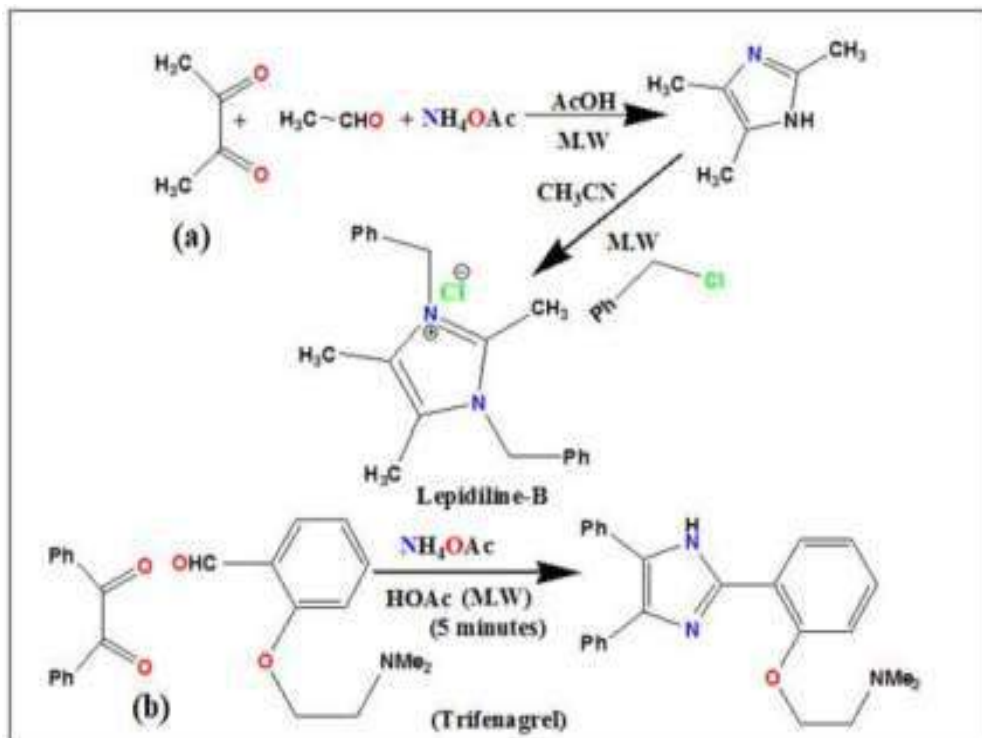
biologically active heterocyclic scaffolds<sup>239</sup>. Current literature review revealed that numerous synthetic protocols for the synthesis of triaryl imidazoles under microwave irradiation have been reported by various research groups (Scheme 1.22).



**Scheme. 1.22.** Synthesis of 2,4,5-triaryl imidazoles under microwave irradiation.

Saeed Balalaie *et.al.* used Zeolite HY and silica gel for the synthesis of (3) using (1) and (2) under microwave irradiation and under solvent free condition<sup>240</sup>.

In another report Scott E. Wolkenberg *et.al.* utilized microwave technique for the synthesis of triaryl imidazoles from (1) and (2) in presence of ammonium acetate and Acetic acid and they extended this protocol further to synthesize Lepidiline-B and Trifenagrel as shown in (Scheme 1.23a and 1.23b)<sup>241</sup>.



**Scheme. 1.23.** (a) Synthesis of Lepidiline, (b) Synthesis of Trifenagrel

K. Shelke *et.al.* reported a microwave induced one pot synthesis of triaryl imidazoles (3) with glyoxylic acid as a catalyst. The reaction was done in solvent free condition. The main advantages of this reaction were faster reaction time, cheaper and available catalyst and higher yield of the products<sup>242</sup>.

In another development for the Microwave induced synthesis of triarylimidazole derivatives (3), Santosh V. Nalage *et.al.* reported polyethylene glycol as an efficient catalyst and claimed to be a cleaner approach towards imidazole synthesis<sup>243</sup>.

In a similar instance, Javad Safari *et.al.* utilized  $(\text{NH}_4)_6\text{Mo}_7\text{O}_{24}\cdot 4\text{H}_2\text{O}$  as an efficient catalyst for the synthesis of triaryl imidazoles (3) by a one component, three pot condensation reaction under solvent free conditions and microwave irradiation<sup>244</sup>.

Kiran F. Shelke *et.al.* reported cellulose sulfuric acid as a solid-state catalyst under microwave irradiation for the synthesis of triaryl imidazoles (3) under solvent free conditions and the key feature of this reaction was easy preparation of the catalyst, recyclability of the catalyst and high yield of the products<sup>245</sup>.

Edouard Chauveau *et.al.*, reported a highly efficient catalyst free method for the synthesis of triaryl imidazoles (3) in water under microwave irradiation<sup>246</sup>.

Zinat Gordi *et.al.*, utilized Zeolite as an efficient catalyst under Microwave irradiation for the synthesis of triaryl imidazoles in solvent free condition<sup>247</sup>.

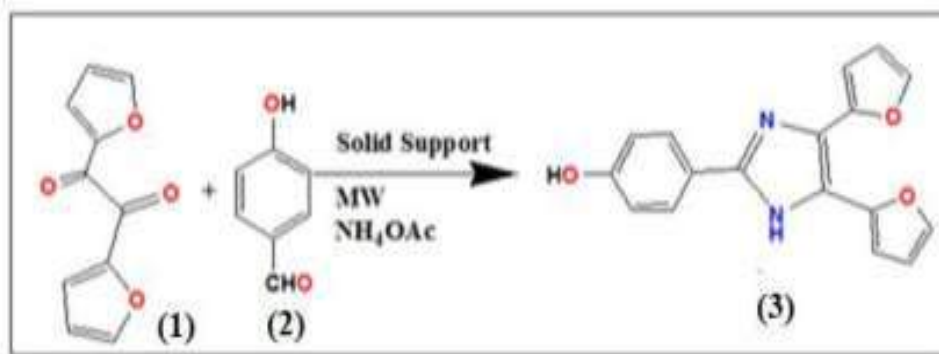
Alternatively, Andrew P. Combs *et.al.* reported an efficient procedure for the synthesis of 2,4,5-Triaryl-imidazoles (3) directly from the keto-oxime (1) and an aldehyde (2) in moderate to good yields via cyclization to the N-hydroxyimidazole and they have reported an unprecedented in situ thermal reduction of the N–O bond upon microwave irradiation at 200 °C for 20 min (Scheme 1.24)<sup>248</sup>.



**Scheme. 1.24:** Synthesis of substituted tri-aryl imidazole from keto-oxime

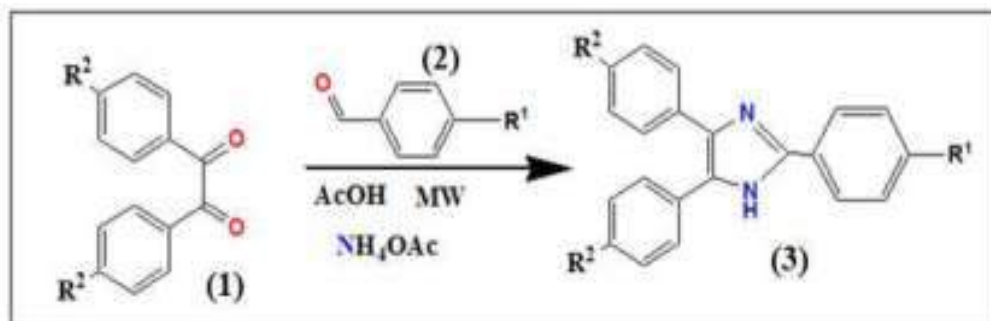
Similarly, S.C. Hu, reported a solvent-free microwave-assisted method for the synthesis of 2-substituted-4,5-di(2-furyl)-1H-imidazole (3) in moderate to good yield by condensation of furil (2) with aldehydes over acidic alumina impregnated with ammonium acetate<sup>249</sup> (Scheme 1.25).





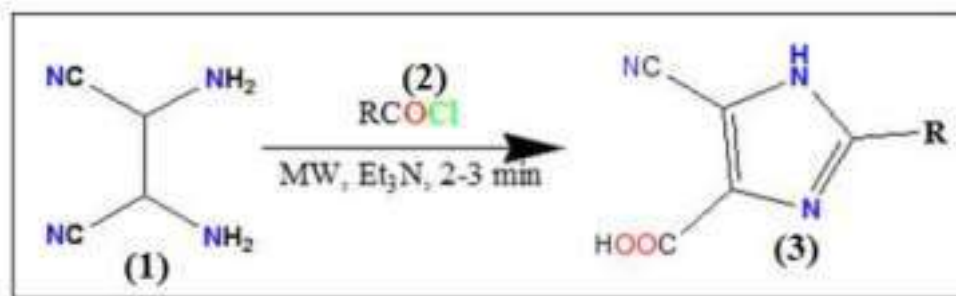
**Scheme. 1.25.** Microwave assisted synthesis of 2-substituted-4,5-di(2-furyl)-1H-imidazole.

In another study, Zhou *et.al.* have reported the synthesis of 2,4,5-triaryl imidazoles (3) by the cyclocondensation of substituted benzil (1) with the differently substituted aromatic aldehydes (2) and NH<sub>4</sub>OAc under catalyst-free, solvent-free and microwave irradiation conditions<sup>250</sup>(Scheme 1.26).



**Scheme. 1.26.** Microwave assisted, solvent and catalyst free synthesis of tri-aryl imidazoles.

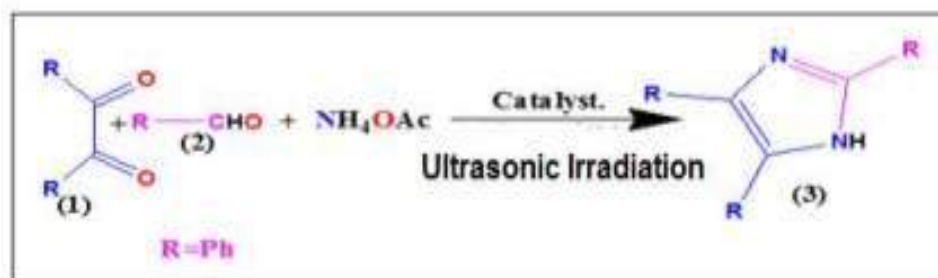
K. M. E. Shaieb alternatively synthesized tri-substituted imidazole derivatives (3) containing carboxamido and cyano groups at position 4 and 5 respectively by condensing diaminomaleonitrile (1) with acid chloride (2) in the presence of catalytic amount of NEt<sub>3</sub> under microwave conditions<sup>251</sup> (Scheme 1.27).



**Scheme. 1.27.** Synthesis of tri-substituted imidazoles containing carboxamido and cyano groups.

### 1.3.1.3.3 Ultrasonic method

During the past few decades, many chemical transformations have been performed with the aid of ultrasonic irradiation. The ultrasonic irradiation has been used to accelerate various catalytic reaction including both homogenous and heterogeneous reaction systems. The use of ultrasonic irradiation to accelerate chemical reactions has been termed as sonochemistry<sup>252</sup>. In 1917, Langevin made the first commercial application of ultrasonics and Richards and Loomis first utilized the effect of ultrasonic energy in chemical reaction in 1927<sup>252</sup>. There are numerous reports on the synthesis of triarylimidazole using ultrasonic irradiation as an energy source and we are discussing some of the reported procedure of synthesis of triarylimidazoles (3) under ultrasonic irradiation (Scheme 1.28).



**Scheme1.28.** Synthesis of 2,4,5-triaryl imidazoles under Ultrasound irradiation

Kiran F. Shelke *et.al.* synthesized triaryl imidazole (3) under Ultrasonic irradiation using boric acid as a catalyst in aqueous media<sup>253</sup>.

In another report, Kiran F. Shelke *et.al.* reported the Ultrasound assisted synthesis of triaryl imidazoles (3) in aqueous media using Ceric Ammonium Nitrate as a catalyst and the key feature of this reaction was the non-toxic nature of Ceric Ammonium Nitrate<sup>254</sup>.

Similarly, Hongjun Zang *et.al.* synthesized the triaryl imidazole derivatives (3) using an efficient ionic liquid catalyst 1-ethyl-3-methylimidazole acetate ([EMIM]OAc under Ultrasonic irradiation<sup>255</sup>.

Deepak Nagargoje *et.al.* used diethyl bromophosphate as an oxidant for the one pot synthesis of triaryl imidazoles (3) in acetonitrile as a solvent and ultrasound irradiation<sup>256</sup>.

J. Safari *et.al.* utilized sulfamic acid functionalized Fe<sub>3</sub>O<sub>4</sub> nano particles as an effective catalyst for the synthesis of triaryl imidazoles (3) under Ultrasound radiation in ethanol medium<sup>257</sup>.

Paul D. Sanasi *et.al.* reported an ultrasound assisted one-pot synthesis of triaryl imidazoles (3) using spinel nano copper ferrite as a heterogeneous catalyst in ethanol medium<sup>258</sup>.

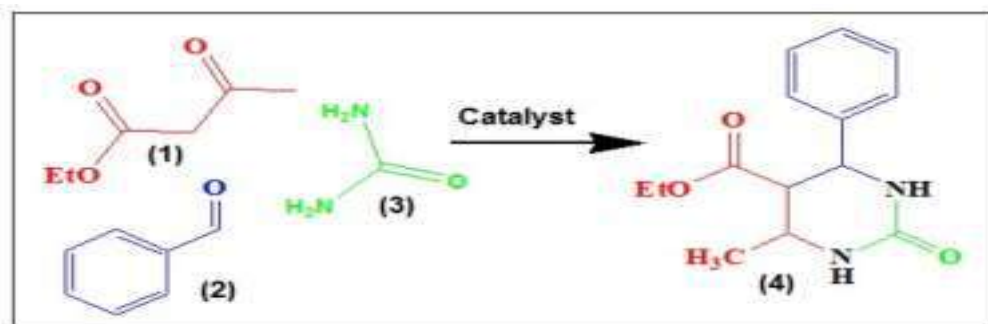
In another report, Mohsen Esmailipour *et.al.* utilized a green protocol for the synthesis of triaryl imidazole (3) under Ultrasound irradiation by using Dendrimer-PWA<sup>n</sup> nanoparticles as a catalyst under solvent free conditions<sup>259</sup>.

Esmail Eidi *et.al.* developed a one pot sonochemical reaction for the synthesis of triaryl imidazoles (3) using CoFe<sub>2</sub>O<sub>4</sub> nanoparticles as an efficient catalyst in ethanol medium<sup>260</sup>.

Balaji S. Londhe *et.al.* devised a green reaction for the synthesis of triaryl imidazoles (3) under Ultrasound radiation in methanol using Baker's yeast as a catalyst<sup>261</sup>.

### 1.3.2 Various synthetic routes for the preparation of 3,4-dihydropyrimidine-2-(1H)-ones

The Bigenelli reaction is a one pot three-component reaction in which 3,4-dihydropyrimidin-2(1H)-ones (4) are produced by the cyclocondensation of β-dicarbonyl compounds (1), aryl aldehyde (2), Urea (3) and this reaction was coined by Pietro Bigenelli in 1891<sup>129</sup> (Scheme 1.29).



**Scheme. 1.29.** Synthesis of 3,4-dihydropyrimidine-2-(1H)-ones

The Bigenelli compounds, 3,4-dihydropyrimidin-2(1H)-ones (79) are somewhat similar to dihydropyridines also known as Hantzsch pyridines as the preparation of these compounds also require the same reactants as required for

preparation of Bigenelli compounds. The reaction can also be carried out by replacing urea by thio-urea to yield 3,4-dihydropyrimidine-2-(1H)-thiones (80) (Fig. 1.19)

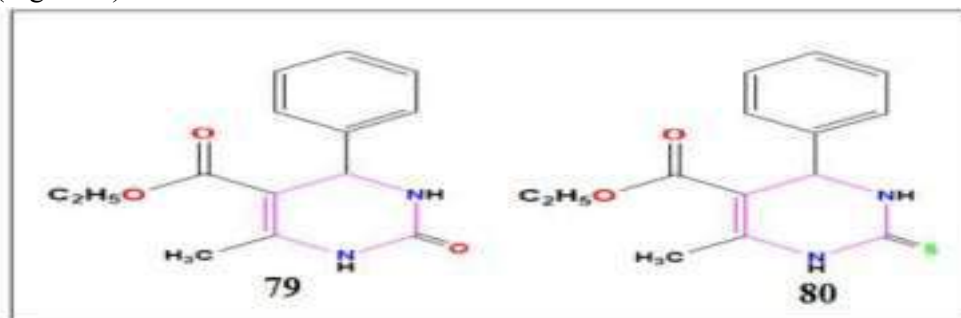


**Fig. 1.19.** Structures of 3,4-dihydropyrimidin-2(1H)-ones and 3,4-dihydropyrimidine-2-(1H)-thiones

In recent years, Dihydropyrimidinones (DHPMs) have attracted a lot of interest of chemists owing to their biological and therapeutic uses<sup>262</sup>. This compound serves as one among the five classes of Calcium Channel blocking drugs<sup>263</sup>. They also have anti-viral<sup>264</sup>, anti-inflammatory<sup>265</sup>, anti-bacterial<sup>266</sup>,  $\alpha$ -1a-adrenergic antagonist<sup>267</sup>, anti-cancer<sup>268</sup> and anti-hypersensitive properties<sup>269</sup>. In fact, Monastrol was the first Bigenelli compound that exhibited anti-cancer activity<sup>270</sup>. Due to the diverse biological activities of the Bigenelli products, the Bigenelli reactions have been considered as one of the most important Multi-component Reactions (MCRs)<sup>271</sup>. Some representative Bigenelli Compounds having Calcium Channel Blocking (81 a, b), Anti-tumor (82 a, b) and Anti-inflammatory (83 a, b) properties are depicted in Fig. 1.20.

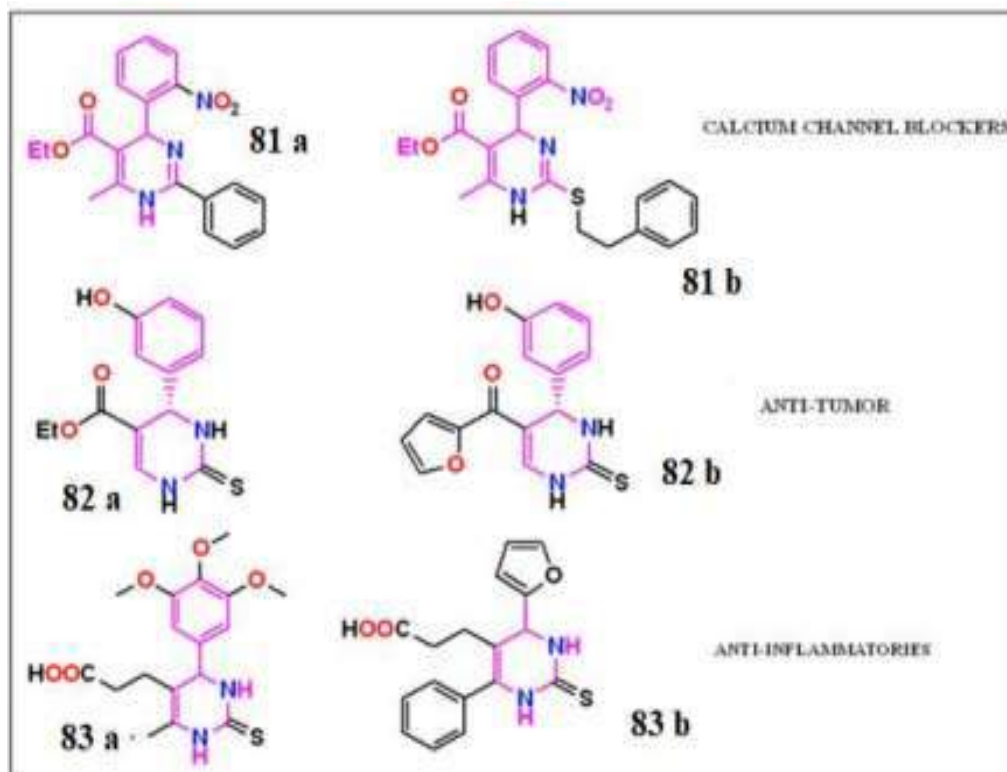
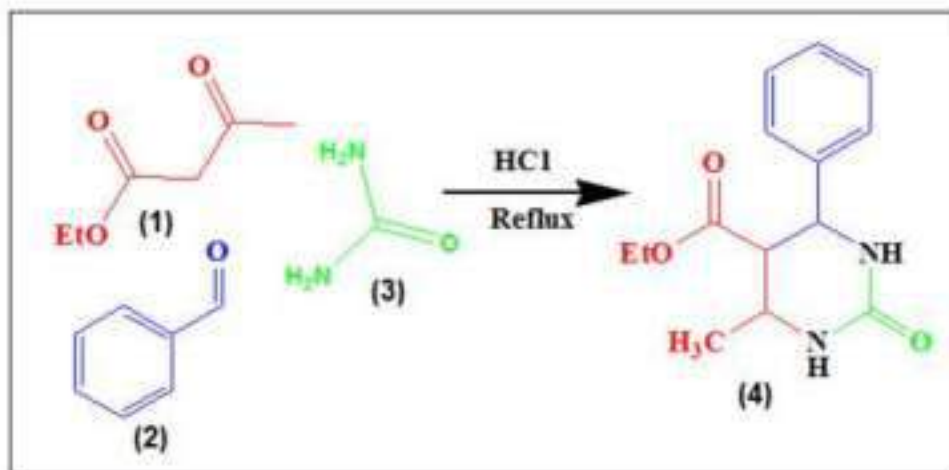


**Fig. 1.20.** Some biologically important Bigenelli Compounds

During the last few decades, Dihydropyrimidinones (DHPMs or Bigenelli compounds) have gained a lot of interest to organic as well as medicinal chemist as this class of compounds exhibit wide varieties of interesting therapeutic and pharmacological activities<sup>272</sup>. Thus, looking at the importance of the dihydropyrimidones scaffold in different fields, various synthetic procedures have been developed during the last few decades and numerous new synthetic methods are developing on daily basis for the synthesis of simple dihydropyrimidones to multi-functionalized dihydropyrimidones<sup>273</sup>.

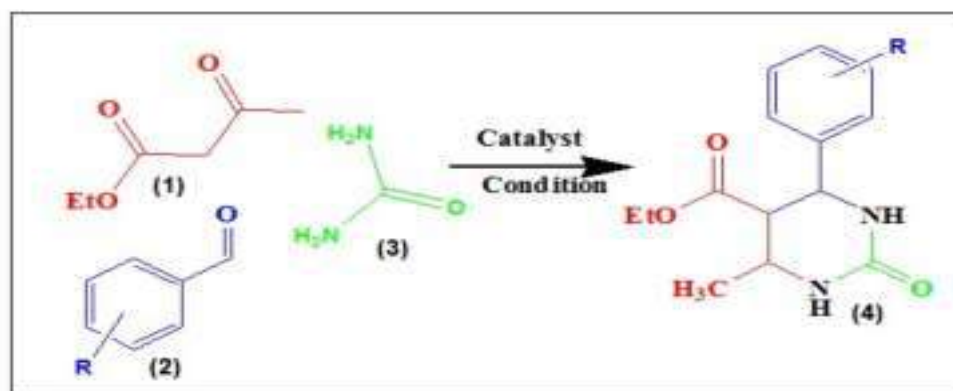
### 1.3.2.1 Classical method

It was the Italian chemist Pietro Bigenelli for the first time who synthesized 3, 4-dihydropyrimidin-2(1*H*)-one (4) by an acid catalysed condensation of ethyl acetoacetate (1), benzaldehyde (2) and urea (3) in ethanol solvent<sup>129</sup> (Scheme 1.29).



**Scheme 1.29.** Classical method for the synthesis of 3, 4-dihydropyrimidin-2(1*H*)-one

The conventional Bigenelli reaction suffers from a lot of drawbacks but the most important and worth mentioning drawback is the low yield of the products. Hence various modifications were employed to overcome the drawbacks of the conventional procedure<sup>274</sup> (Scheme 1.31).



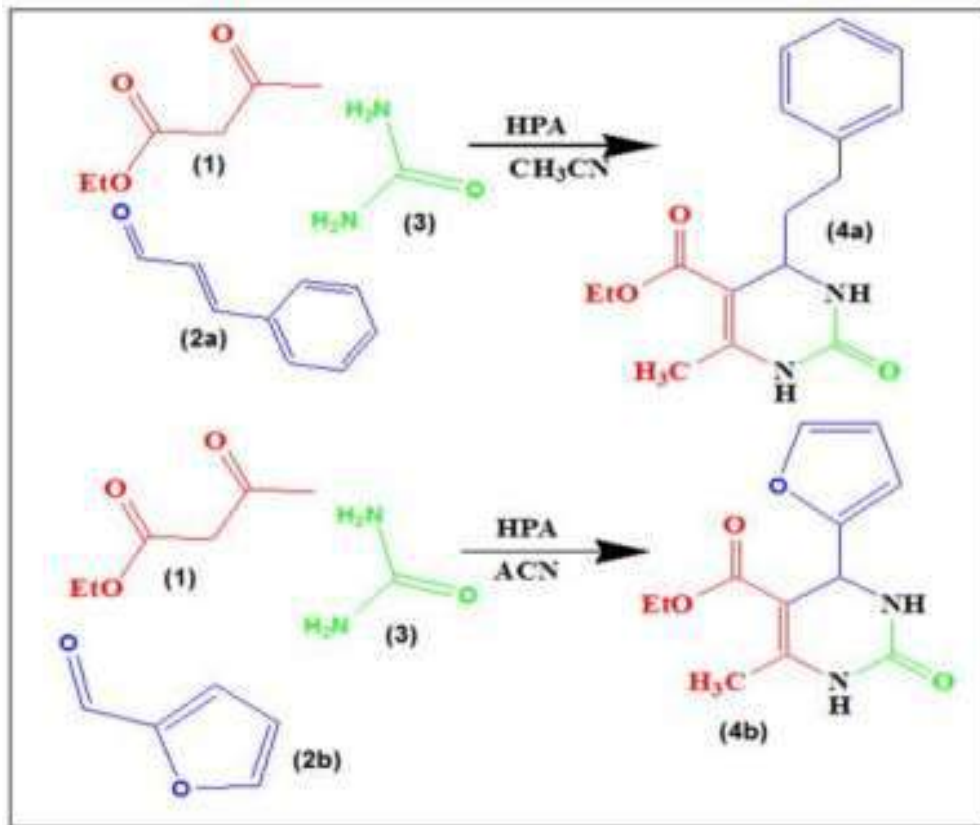
**Scheme. 1.31.** Synthesis of 3, 4-dihydropyrimidin-2(1*H*)-one

B. C. Ranu *et.al.* used Indium (III)chloride as a lewis catalyst for the synthesis of substituted 3,4-dihydropyrimidin-2(1*H*)-one (4) using  $\beta$ - dicarbonyl compounds (1), aryl aldehyde (2), urea (3) in THF solvent<sup>275</sup>.

R. S. Bhosale *et.al.* reported a simple procedure for the synthesis of (4) using iodine as a catalyst in toluene<sup>276</sup>.

In another development, E. Rafiee *et. al.* reported a multi component synthesis of (4) using Keggin-type hetero poly acids (HPA) such as  $H_3PW_{12}O_{40}$  (PW),  $H_3PMo_{12}O_{40}$  (PMo) and  $H_4SiW_{12}O_{40}$  (SiW) as catalysts in acetonitrile solvent and they reported that even acid sensitive aldehydes like cinnamaldehyde

(2a) and furfural (2b) gave excellent yield of the products (4a and 4b) respectively<sup>277</sup> (Scheme 1.32).



**Scheme. 1.32.** Synthesis of 3,4-dihydropyrimidin-2(1H)-one from Cinnamaldehyde and Furfural.

R. Gupta *et.al.* used covalently anchored sulfonic acid onto silica as an efficient catalyst for the synthesis of (4) in acetonitrile solvent<sup>278</sup>.

Similarly, Suresh *et.al.* reported Lactic acid as an organo catalyst for the synthesis of (4) in Ethanol solvent medium<sup>279</sup>.

Hossein Eshghi *et.al.* used Preyssler heteropolyacid supported on silica coated NiFe<sub>2</sub>O<sub>4</sub> nanoparticles (NFS-PRS) as a catalyst for the synthesis of (4) in ethanol medium<sup>280</sup>.

Zakaria Benzekri *et.al.* reported a method for the synthesis of (4) employing dicalcium phosphate dihydrate (DCPD) as an efficient and reusable catalyst in ethanol medium<sup>281</sup>.

Shanmugam Prakash *et.al.* used CuO nano particles as a catalyst for the synthesis of (4) in ethanol Solvent<sup>282</sup>.

S. Kaul *et.al.* used Montmorillonite-KSF as an efficient catalyst for one-pot green synthesis using dihydropyrimidinones (4) and they evaluate their cytotoxic activity<sup>283</sup>.

Chen-Jiang Liu *et.al.* used Copper (II) Sulfamate as an efficient catalyst for the synthesis of (4) in acetic acid solvent<sup>284</sup>.

S. K. Prajapati *et.al.* reported tris(pentafluorophenyl)borane as an efficient catalyst for the synthesis of (4) in ethanol medium<sup>285</sup>.

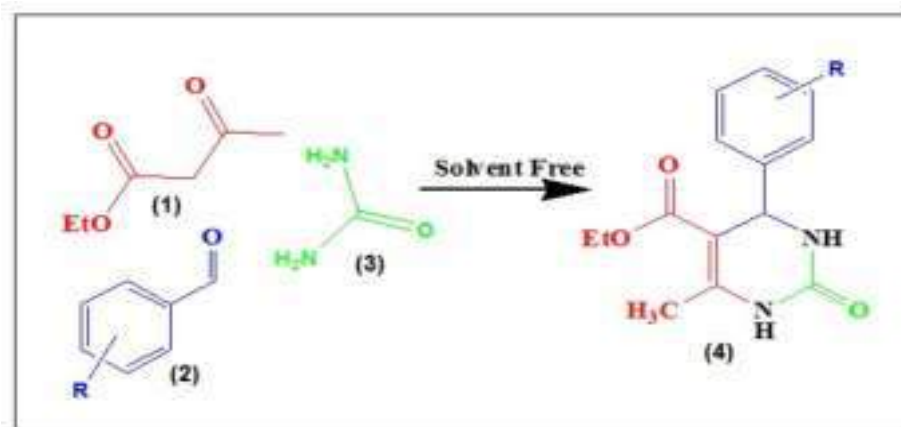
### 1.3.2.2 Green method

Among the various Multi-Component Reactions, Bigenelli reaction being a three-component reaction is usually employed for the direct synthesis of 3, 4-dihydropyrimidinone derivatives and finds a significant importance in organic synthesis<sup>286</sup>. The 3, 4-dihydropyrimidinone and its derivatives generally show diverse pharmacological and biological properties<sup>287</sup>. The current literature review revealed that there are numerous reports on the synthesis of Bigenelli products by classical methods but these documented procedures suffer from many drawbacks such as use of toxic reagent, low yield of the product, environmental hazards, cost, use of expensive catalyst, use of acid, high reaction temperature etc<sup>288-290</sup>. Thus, the development of highly efficient methods for the synthesis of these valuable products in economical and eco-friendly way is highly demanding and presents a great challenge for the scientific community<sup>291-293</sup>. During the past few decades, several improvements were made towards the synthesis of Bigenelli products such as good reaction conditions, use of catalysts/reagents, transition metal-based reagents, ionic liquids, polymer-immobilized reagents etc, but above all, the green chemical approach such as solvent free synthesis<sup>293</sup>, microwave assisted<sup>294</sup>, and ultrasound irradiation<sup>295</sup> are the best suited methods for the green synthesis of Bigenelli products. Many new improvements have been recently reported for the synthesis of the Bigenelli compounds.

#### 1.3.2.2.1 Solvent free synthesis

Owing to important pharmacological and medicinal properties exhibited by Bigenelli products, there has been a growing interest in the improvement of the synthesis of DHPMs by Bigenelli reaction<sup>296</sup>. In recent years, solvent free synthesis is gaining a lot of interest by virtue of the fact that it is operationally simple, efficient, green, and cost-effective<sup>297</sup>. There are lots of works on the solvent free synthesis of 3, 4-dihydropyrimidinone (4) and its derivatives that has been documented during the past few years<sup>298</sup> (Scheme 1.33).





**Scheme. 1.33.** Solvent free synthesis of 3, 4-dihydropyrimidin-2(1H)-one derivatives

Hadi Adibi *et.al.* employed Iron (III) trifluoroacetate [ $\text{Fe}(\text{CF}_3\text{CO}_2)_3$ ] and trifluoromethanesulfonate [ $\text{Fe}(\text{CF}_3\text{SO}_3)_3$ ] as an efficient catalyst for the synthesis of (4) under solvent free condition<sup>299</sup>.

In another development, B. C. Ranu *et.al.* reported a catalyst free synthesis of (4) in solvent free condition<sup>300</sup>.

Fang Dong *et.al.* reported a one pot synthesis of (4) using  $\text{SO}_3\text{H}$ -functional Brønsted-acidic halogen-free task-specific room-temperature ionic liquids (TSILs) under solvent free conditions<sup>301</sup>.

S. L. Jain *et.al.* reported a catalyst free and polyethylene glycol assisted synthesis of (4) under green condition<sup>302</sup>.

Sanny Verma *et.al.* employed PEG-embedded thiourea dioxide (PEG.TUD) as an efficient catalyst for the synthesis of (4) under solvent free condition<sup>303</sup>.

Suresh Patil *et.al.* developed a clean and green procedure for the synthesis of (4) by using lemon juice at room temperature under solvent free condition<sup>304</sup>.

In another work, Suresh Patil *et. al.* reported the synthesized (4) utilizing pineapple juice at room temperature under solvent free condition<sup>305</sup>.

Jaggi Lal *et.al.* reported a green method for the synthesis of (4) using Mg–Al– $\text{CO}_3$  hydrotalcite as a reusable catalyst under solvent free conditions<sup>306</sup>.

Najmaddin Azizi *et.al.* used a simple deep eutectic solvent based on tin (II) chloride (tin (II) chloride-choline chloride) as a catalyst as well as a solvent for the synthesis of (4)<sup>307</sup>.

H. Sachdeva *et al.* used lithium-acetate and phosphoric acid as a catalyst for the synthesis of (4) under solvent free conditions<sup>308</sup>.

A. Borse *et.al.* synthesized (4) using a mixture of phosphorus pentoxide ( $\text{P}_2\text{O}_5$ ) and methane sulfonic Acid ( $\text{MeSO}_3\text{H}$ ) as a catalyst under solvent free conditions<sup>309</sup>.

M. Dewan *et.al.* used copper nanoparticles (Cu-NPS) as an efficient catalyst for the synthesis of (4) under solvent free condition<sup>310</sup>.

Z. Karimi-Jaberi used trichloroacetic acid as a catalyst for the synthesis of (4) under solvent free conditions<sup>311</sup>.

B. B. Fatemeh Mirjalili *et.al.* used nano-TiCl<sub>4</sub>.SiO<sub>2</sub> as an efficient catalyst for the synthesis of (4) in solvent free conditions<sup>312</sup>.

Y. Zhang *et.al.* reported the use of brønsted acidic ionic liquid [Btto][*p*-TSA] as an efficient catalyst for the synthesis of (4) under solvent free conditions<sup>313</sup>.

Vijay V. Dabholkar *et.al.* reported an efficient and green synthesis of (4) using calcined Mg/Fe hydrotalcite catalyst under solvent free conditions<sup>314</sup>.

Mahbube Taii *et.al.* reported an efficient procedure for the synthesis of (4) using aluminate sulfonic acid nano particles (ASA-NPS) under solvent free conditions<sup>315</sup>.

Fe<sup>+3</sup> montmorillonite-K10 was used a catalyst for the synthesis of (4) by Leila Zare Fekri *et.al.* under solvent free conditions and they adopted a grinding method for the synthesis of 3, 4-dihydropyrimidinone derivatives<sup>316</sup>.

H. Yuan *et.al.* used gallium (III) chloride as an efficient and reusable catalyst for the synthesis of (4) under solvent free conditions<sup>317</sup>.

T. S. Choudhare *et.al.* used dioxane-HCl complex as a catalyst for the synthesis of (7) under solvent free conditions<sup>318</sup>.

### 1.3.2.2.2 Microwave irradiation

Microwave assisted synthesis of 3, 4-dihydropyrimidinone are gaining lot of interest these days since microwave energy is an unconventional energy source and they have uniform heating rate for all the reactant molecules<sup>319</sup>. A vast number of literatures are available for the synthesis of 3, 4-dihydropyrimidinone derivatives utilizing microwave irradiation techniques.

Misra *et.al.* employed calcium chloride (CaCl<sub>2</sub>) as an inexpensive catalyst for the synthesis of 3, 4-dihydropyrimidinone derivatives (4) under microwave irradiation and solvent free condition<sup>320</sup>.

Polystyrenesulfonic acid (PSSA) has been used as a catalyst for the synthesis of (4) by R. S. Varma *et.al.* under microwave irradiation<sup>321</sup>.

H. R. Shaterian *et.al.* employed alumina sulfuric acid (Al<sub>2</sub>O<sub>3</sub>-SO<sub>3</sub>H) as an efficient and recyclable catalyst for the microwave assisted synthesis of (4) under solvent free conditions<sup>322</sup>.

In another work, H. W. Zhan *et.al.* documented a procedure for the synthesis of (4) under microwave irradiation without any solvent and catalyst<sup>323</sup>.

D. Kumar *et.al.* employed aluminium chloride (AlCl<sub>3</sub>.H<sub>2</sub>O) as a green and efficient catalyst for the synthesis of (3) under microwave irradiation in solvent free conditions<sup>324</sup>.

K. K. Pasunooti *et.al.* utilized an inexpensive and efficient Cu (OTf)<sub>2</sub> salt as a novel catalyst for the synthesis of (4) under microwave assisted synthesis in ethanolic medium<sup>325</sup>.

A. Kuraitheerthakumaran *et al.* reported an efficient method for the synthesis of (4) using lanthanum oxide ( $\text{La}_2\text{O}_3$ ) as a catalyst under solvent free conditions<sup>326</sup>.

R.K. Sharma and co-workers used silica immobilized nickel complex as an efficient, inexpensive and highly recyclable catalyst for the synthesis of (4) under solvent free and microwave irradiation<sup>327</sup>.

Interestingly, V. Srivastava reported an efficient and green synthetic method for the preparation of (4) using ionic liquid  $[\text{Hmim}][\text{Tfa}]$  as a catalyst under microwave irradiation<sup>328</sup>.

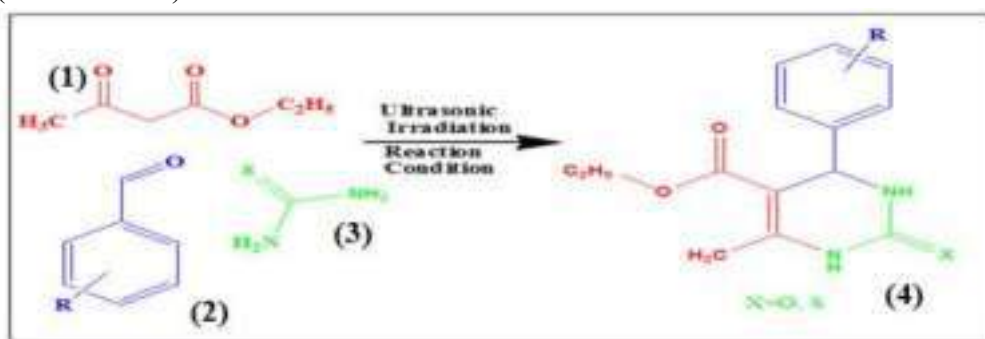
Similarly, M. Shingare reported the synthesis of (4) using ionic liquid N-(4-sulfonic acid) butyl triethyl ammonium hydrogen sulphate  $[\text{TEBSA}][\text{HSO}_4]$  as an efficient catalyst for under microwave condition<sup>329</sup>.

S. K. Padan *et al.* reported the use of fruit juice (Apple, Pomegranate and grape) as a catalyst for the synthesis of (4) under microwave irradiation<sup>330</sup>.

Moradi *et al.* reported  $\text{Fe}_3\text{O}_4$ @meglumine sulfonic acid ( $\text{Fe}_3\text{O}_4$ @MSA) as an efficient and green catalyst for the synthesis of (4) under microwave irradiation<sup>331</sup>.

### 1.3.2.2.3 Ultrasonic irradiation

Nowadays, chemical reactions are accelerated using ultrasound irradiation and form an interesting strategy in organic synthesis<sup>332</sup>. Ultrasonication not only speeds up the chemical reactions but also decreases the number of steps for chemical reaction and the cruder reagents can be used and reactions can be initiated without any additives. The phenomenon of acoustic cavitations of ultrasound is responsible for chemical effects and the primary chemical reactions result from a transient state of higher temperatures and pressures<sup>333</sup>. Current literature review revealed that numerous ultrasound-mediated Bigenelli synthesis of 3,4-dihydropyrimidinones has been reported in the presence various catalyst under green reaction condition (Schemes 1.34).



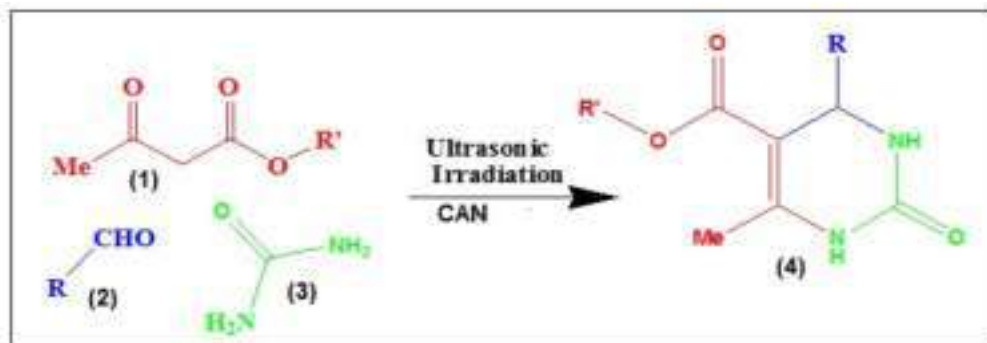
**Scheme. 1.34.** Ultrasound assisted synthesis of 3, 4-dihydropyrimidin-2(1H)-one derivatives

Zhidovinova *et al.* reported that the classical Bigenelli reaction for the synthesis of 3,4-dihydropyrimidinone (thione) (4) derivatives when carried out in

(EtOH and HCl) under microwave irradiation is accelerated by a factor of more than 40 times<sup>334</sup>.

In another development, Li *et. al.* reported the synthesis of 3, 4-dihydropyrimidinones (4) under ultrasonic condition using aminosulfonic acid as a catalyst<sup>335</sup>.

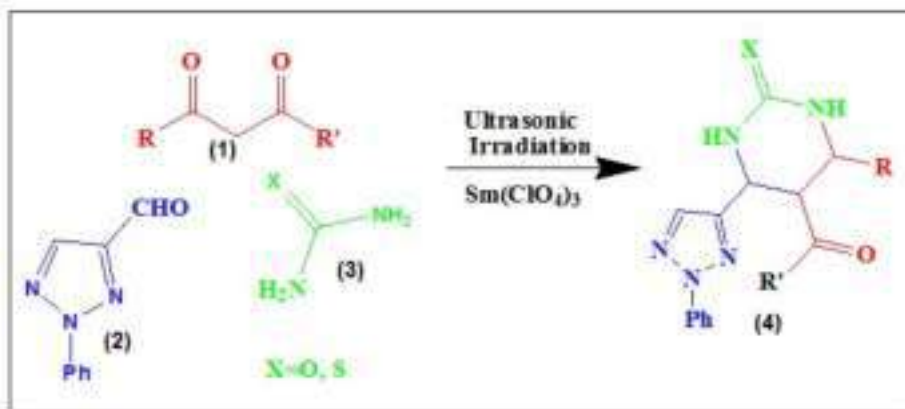
In another report, Yadav *et al.* employed ceric ammonium nitrate (CAN) as a catalyst in ultrasound promoted Bigenelli reaction in methanolic medium<sup>336</sup> (Scheme 1.35). They varied the substrate scope such as Heteroaryl, aromatic (electron-poor or electron-rich), aliphatic, and  $\alpha$ ,  $\beta$ -unsaturated aldehydes and, in all cases, they obtained the desired 3, 4-dihydropyrimidinones (4) compounds in good yields and with high purity.



**Scheme. 1.35.** Ultrasound assisted synthesis of 3, 4-dihydropyrimidin-2(1H)-one derivatives using CAN catalyst.

Similarly, C. W. Nogueira, reported the synthesis of 3, 4-dihydropyrimidinone (4) derivatives under ultrasonic irradiation using inexpensive ammonium chloride as a catalyst in methanol solvent<sup>337</sup>.

Wang *et. al.* reported an efficient synthesis of novel 4-(2-phenyl-1,2,3-triazol-4-yl)-3,4-dihydropyrimidin-2(1H) -(thio) ones (4) from 1,3-dicarbonyl compounds (1) 2-phenyl-1,2,3- triazole-4-carbaldehyde (2), and urea (3) or thiourea (3) under US irradiation using Samarium perchlorate as an efficient catalyst and the main advantages of this methodology are milder reaction conditions, shorter reaction times, and excellent yield<sup>338</sup> (Scheme 1.36).



**Scheme. 1.36.** Synthesis of novel 4-(2-phenyl-1,2,3-triazol-4-yl)-3,4-dihydropyrimidin-2(1H)-(thio)ones

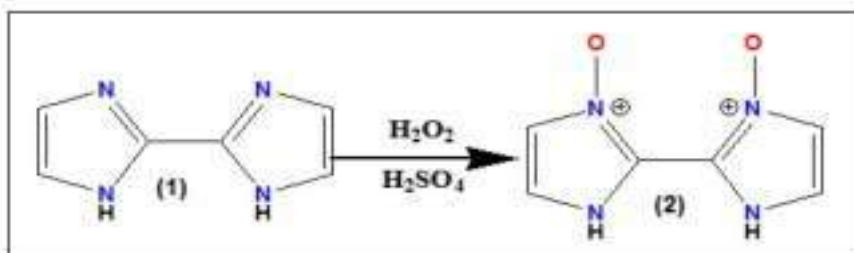
L. Zhi-Ping *et al.* reported iodine catalyzed One-Pot Synthesis of 3,4-Dihydropyrimidin-2(1H)-ones Under Ultrasound Irradiation<sup>339</sup>.

M. A. Pasha *et al.* reported silica iodide as an efficient catalyst for the one pot three component synthesis of 3,4-dihydropyrimidine-2-(1H) ones/thiones under ultrasound irradiation<sup>340</sup>.

### 1.3.3 Various synthetic routes for the preparation of Imidazole N-oxide

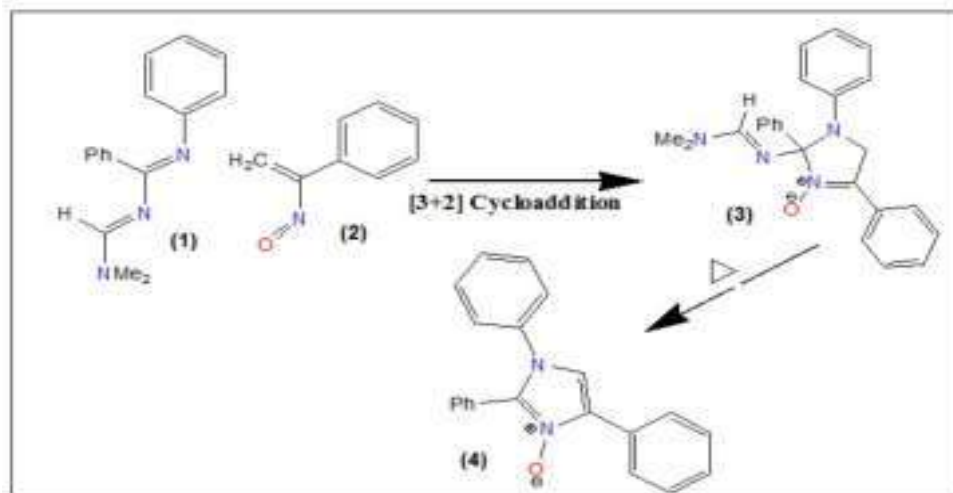
Imidazole derivatives play a crucial role in different biological processes and they exhibit wide range of biological activities<sup>341</sup>. Among many known imidazole derivatives, Imidazole N-oxide are interesting compounds and they are the key building blocks in advance heterocyclic chemistry<sup>342</sup>, natural product synthesis<sup>343</sup>, co-ordination chemistry<sup>344</sup> and catalysis<sup>345</sup>. Thus, among many heterocyclic N-oxide compounds, imidazole N-oxides constitute a practically valuable class of five-membered aromatic N-heterocycles<sup>346</sup>. Because of the diverse application of the imidazole N-oxide, various synthetic methods have been reported during the past few decades.

R. Kuhn *et al.* in 1958 prepared imidazole-N-oxide (2) by using 2,2'-diimidazolyl (1) with dilute hydrogen peroxide in acidic medium<sup>347</sup> (Scheme 1.37).



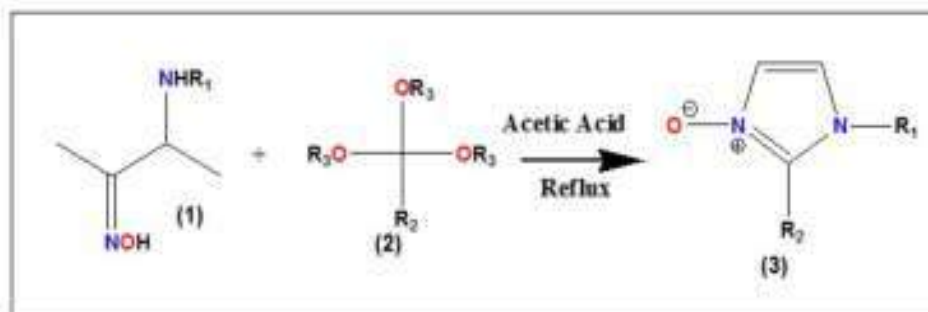
**Scheme. 1.37.** Synthesis of Imidazole-N-oxide by using 2,2'-diimidazolyl

Arun.K. Sharma *et. al.* reported (3+2) Cycloaddition 1-aryl-4-dimethylamino-1,3-diaza-1, 3-butadienes (1) with  $\alpha$ -nitrosostyrenes (2) to give corresponding nitrone (3) derivatives which on subsequent heating resulted in corresponding N-oxide derivative (4)<sup>348</sup> (Scheme 1.38).



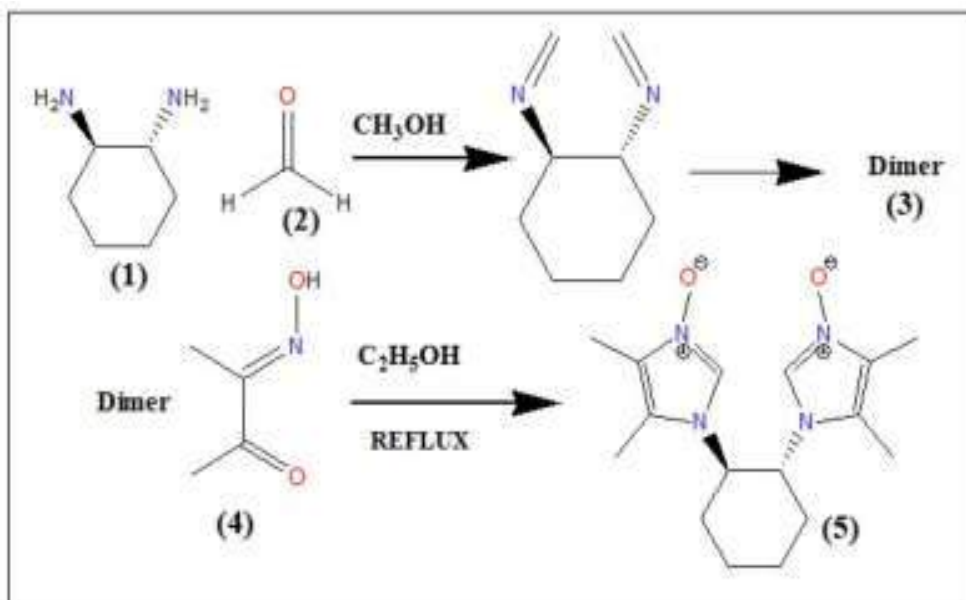
**Scheme. 1.38.** Synthesis of Imidazole-N-oxide from 1-aryl-4-dimethylamino-1,3-diaza-1, 3-butadienes

Hugo Cercetto *et.al.* successfully synthesized imidazole-N-oxides (3) by cyclocondensation of  $\alpha$ -amino oximes (1) with triethyl orthoformate (2) in refluxing acetic acid medium<sup>349</sup> (Scheme1.39).



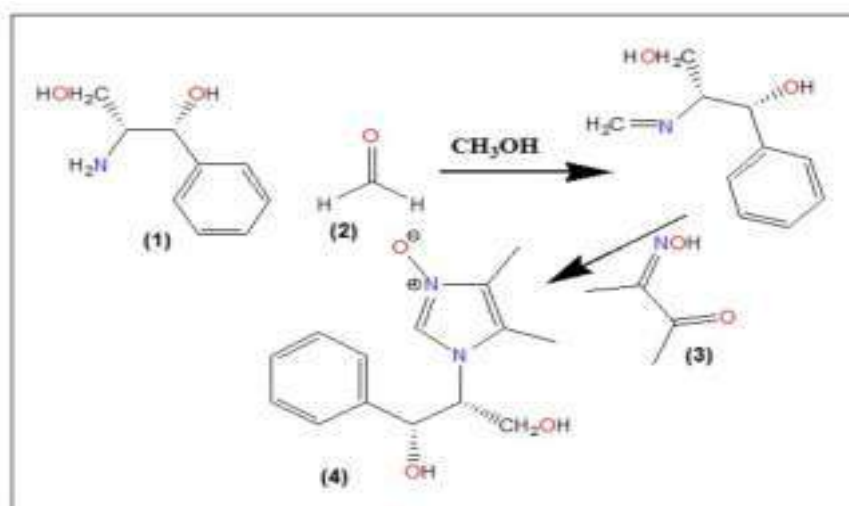
**Scheme. 1.39.** Synthesis of imidazole-N-oxides from  $\alpha$ -amino oximes and triethyl orthoformate

Paulina Mucha *et.al.* synthesized enantiomerically pure imidazole-N-Oxide (5) from trans-1,2-diaminocyclohexane (1) by using diacetyl monoxime (4) under reflux conditions<sup>350</sup> (Scheme 1.40). They first prepared the dimer of imine of the diaminocyclohexane (1) and formaldehyde (2) and subsequent reaction of dimer (3) with diacetylmonoxime yielded the product (5).



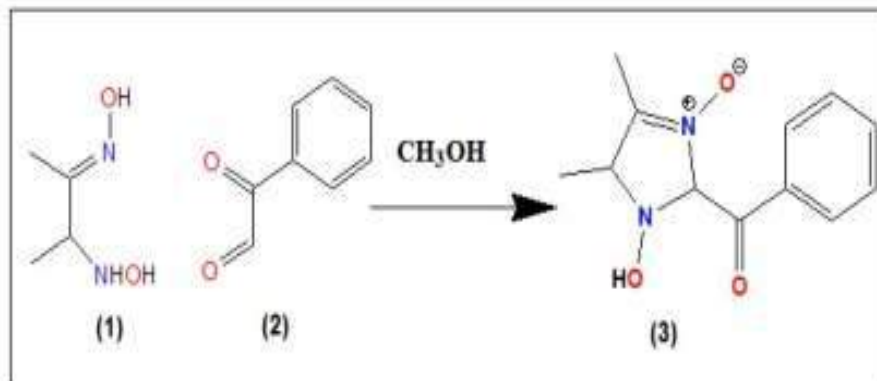
**Scheme. 1.40.** Synthesis of enantiomerically pure imidazole-N-oxide

Paulina Mucha *et.al.* also devised another method for the synthesis of enantiomerically pure imidazole-N-oxide (4) using 1-phenylethylamine (1) with formaldehyde (2) and diacetyl monoxime (3)<sup>351</sup> (Scheme 1.41).



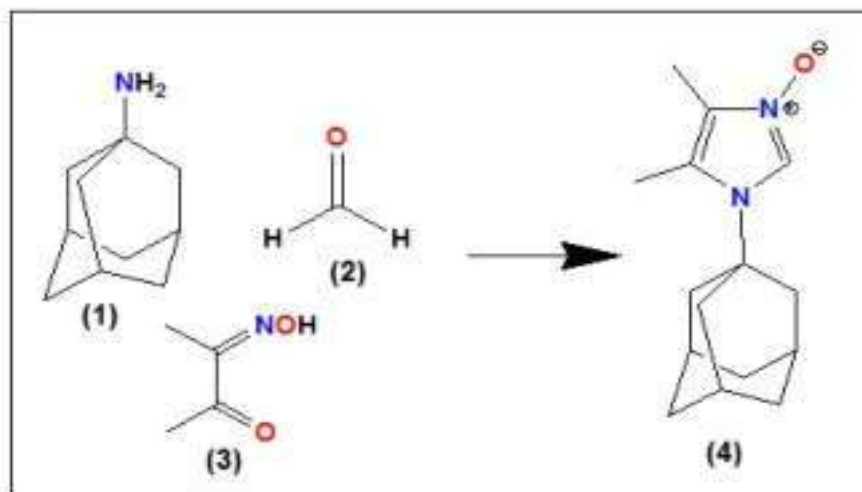
**Scheme. 1.41.** Synthesis of enantiomerically pure imidazole-N-oxide

S. A. Amitina *et.al.* successfully synthesized imidazole-N-oxide (3) derivative by condensing 3-hydroxyamino-2-butanone oxime (1) with phenyl glyoxal (2) at room temperature in methanol solvent medium<sup>352</sup> (Scheme 1.42)



**Scheme. 1.42.** Synthesis of imidazole-N-oxide from 3-hydroxyamino-2-butanone oxime.

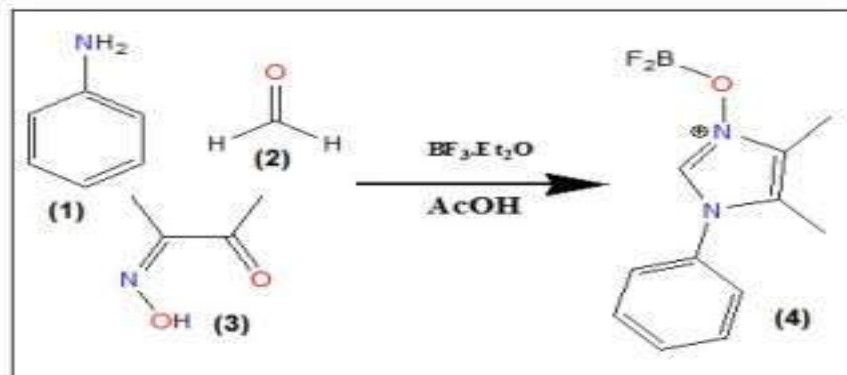
M Jasinski *et. al.* reported a synthetic method for the preparation of a bulky imidazole-N-oxide (4) using 1-amino adamantane (1) with formaldehyde (2) and diacetyl monoxime (3) in Acetic acid medium<sup>353</sup> (Scheme 1.43).



**Scheme. 1.43.** Synthesis of bulky bulky imidazole-N-oxide using 1-amino adamantane

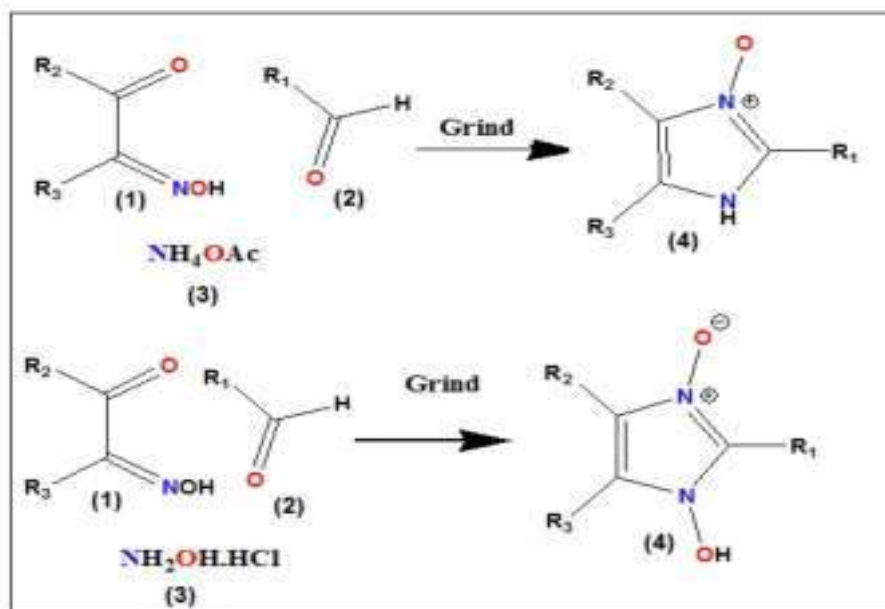
V. S. Mityanov *et.al.* devised a method for the synthesis of aryl imidazole-N-oxides (4) which was stabilized as a Boron trifluoride derivative using Boron trifluoride etherate in acetic acid<sup>354</sup>(Scheme 1.44)





**Scheme. 1.44.** Synthesis of aryl imidazole-N-oxides

K. Pradhan *et.al.* have reported a solvent free, self catalysed reaction for the synthesis of N-substituted imidazole-3-oxides (4) using an aldehyde (1), diacetylmonoxime (2) and ammonium acetate (3). The same group also reported the synthesis of 1-hydroxy-imidazole-3-oxides (4) using hydroxyl amine hydrochloride (3) instead of ammonium acetate (3)<sup>355</sup> (Scheme 1.45).



**Scheme. 1.45.** Solvent free, self catalysed reaction for the synthesis of N-substituted imidazole-3-oxides

Imidazole derivatives finds an extensive application in many fields and current literature review revealed that there are limited reports on the synthesis of imidazole N-oxide under green condition and therefore, these factors prompted us to carry out the solvent free synthesis of imidazole N-oxide derivatives.

### 1.3.4 Various synthetic routes for the preparation of 1,2-substituted benzimidazole

Benzimidazole (84) is a bicyclic aromatic heterocyclic compound having a benzene ring fused to the imidazole ring<sup>356</sup>. Owing to the numerous significant properties such as therapeutics, benzimidazole scaffold have occupied a prominent place in medicinal chemistry<sup>357</sup>. Benzimidazole scaffold, a small nitrogen containing heterocycle is a versatile pharmacophore having a diverse range of biological activities such as antiulcer<sup>358</sup>, antifungal<sup>359</sup>, antimicrobial<sup>360</sup>, antiasthmatic<sup>361</sup>, anti-inflammatory and analgesic<sup>362</sup>, antidiabetic<sup>363</sup>, antitubecular<sup>364</sup>, antiviral and antiprotozoal<sup>365</sup> and anticancer<sup>366</sup> etc. Among many N-containing heterocyclic scaffolds, benzimidazole nucleus serves as a fundamental building block that is incorporated in many natural and synthetic molecules displaying wide range of biological activities<sup>367,368</sup> (Fig 1.21).

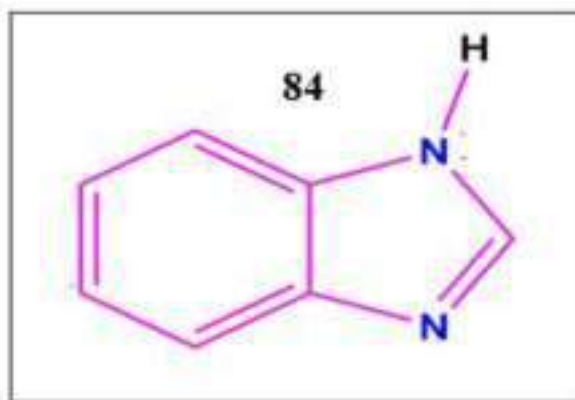


**Fig. 1.21.** Structure of Benzimidazole

Among the various type of benzimidazole derivatives, 1, 2-substituted benzimidazoles have gained a lot of interest because this class of compounds exhibit diverse type of biological activities such as antitumor activity<sup>369</sup>(85), AT1 receptor antagonists<sup>370</sup> (86), antileukemia agent<sup>371</sup>(87), ischemia-reperfusion injury<sup>372</sup>(88), hypertension<sup>373</sup>(89) and obesity<sup>374</sup>(90) (Fig.1.22).

In recent years, 1, 2-disubstituted benzimidazole scaffold have attracted great attention due to their wide applications in new drugs such as antihypertensive drugs<sup>375</sup>(91), GABA<sub>A</sub> receptor agonists<sup>376</sup>(92) and the hepatitis C virus (HCV) NS5B polymerase inhibitors<sup>377</sup>(93) (Fig.1.23).

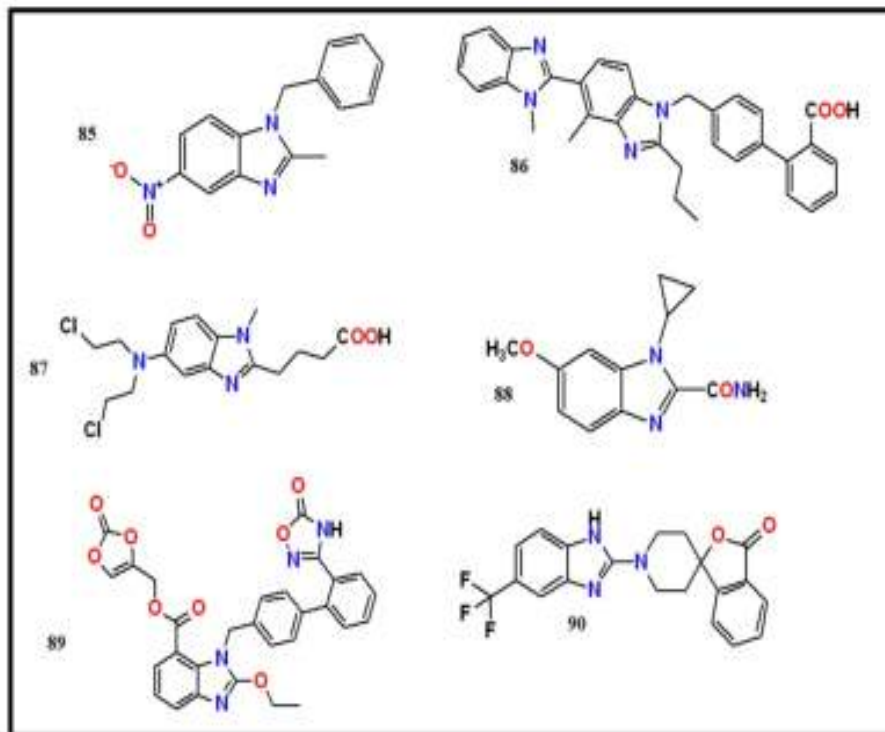


Fig. 1.22. Some of the biologically important Benzimidazole derivatives

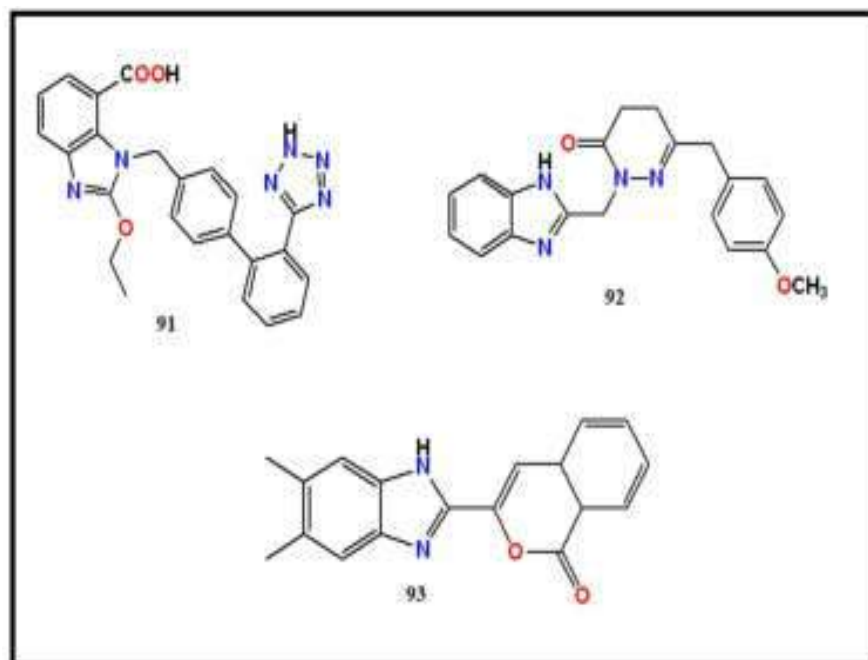
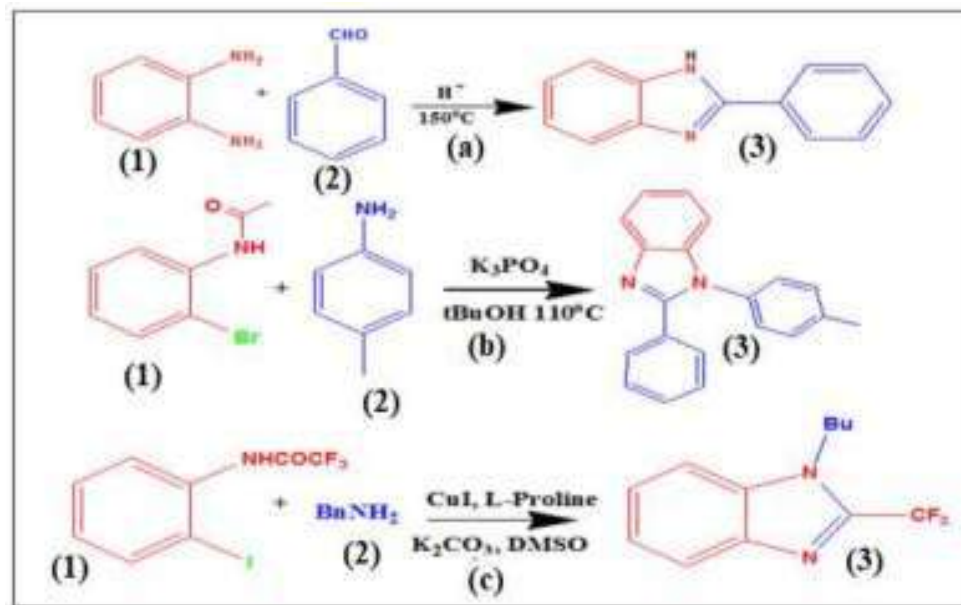


Fig. 1.23. Some of the important drugs containing benzimidazole nucleus

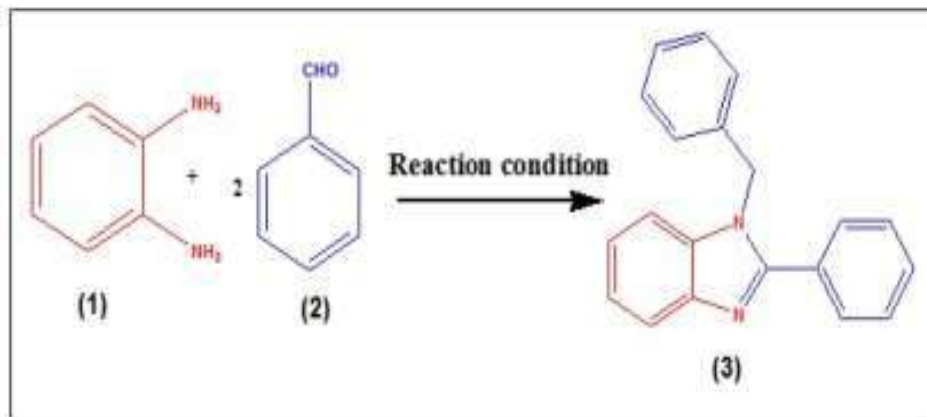
The synthesis of benzimidazoles involves the construction of C–N bond, which is an important category of transformation in organic synthesis<sup>378</sup>. A numerous method for the synthesis of 1,2-disubstituted benzimidazoles (3) such as condensation of anilines (1) with aldehydes (2) under relatively harsh conditions, direct oxidative coupling of amines to imines, and transition metal-catalyzed intramolecular cyclization have been reported during the past<sup>379–381</sup>(scheme 1.46).



**Scheme. 1.46.** Numerous methods for the synthesis of disubstituted benzimidazoles

However, the above cited methods have some serious drawbacks such as harsh and strict reaction conditions, expensive catalysts, longer reaction time and environmental hazards and considering such harsh conditions there could be a possibility of decomposition of substrates or products thus, it is noteworthy to find and explore milder conditions for the synthesis of 1,2-disubstituted benzimidazoles<sup>382</sup>.

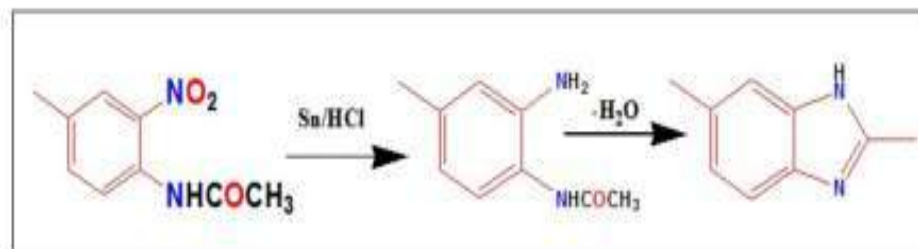
A considerable number of literature report is available for the synthesis of 1,2-disubstituted benzimidazole derivatives under different reaction conditions. A simple method for the synthesis of 1, 2-disubstituted benzimidazole (3) involves the cyclocondensation of *o*-phenylenediamine (1) with aldehyde (2) in 1:2 molar ratio<sup>383</sup> (Scheme 1.47).



**Scheme. 1.47.** Synthesis of 1,2-disubstituted Benzimidazole

### 1.3.4.1 Classical and non-classical approach

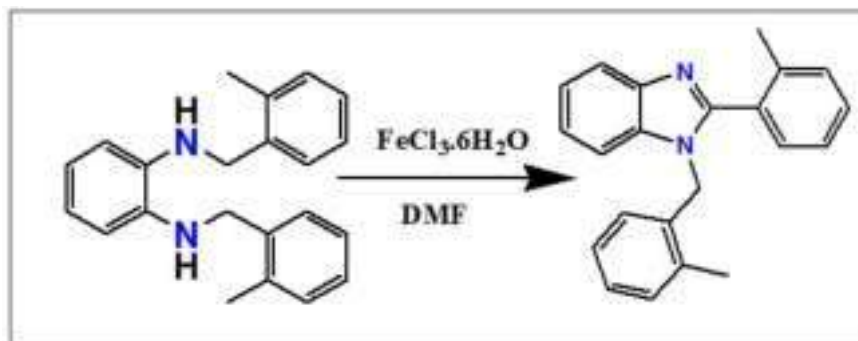
The first benzimidazole, 2,5-dimethylbenzimidazole (2) was synthesized by Hoebrecker [11], by reduction and dehydration of 2-nitro-4-methylacetanilide (1) in 1872.<sup>384</sup> (Scheme 1.48)



**Scheme. 1.48.** Hoebrecker's synthesis of Benzimidazole

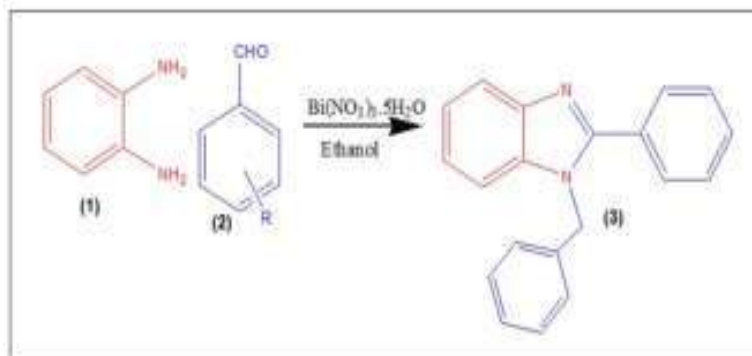
Various methods for the synthesis of benzimidazole have been developed by the condensation of *o*-phenylenediamine with aldehydes, carboxylic acids, or their derivatives (nitriles, amidates, orthoesters etc).<sup>385</sup>

Pawan Thapa *et.al.* employed FeCl<sub>3</sub>.6H<sub>2</sub>O as an efficient catalyst for the synthesis of 1,2 disubstituted imidazoles (2) using *N, N'*-disubstituted-*o*-phenylenediamine (1) in DMF<sup>386</sup>(Scheme 1.49).



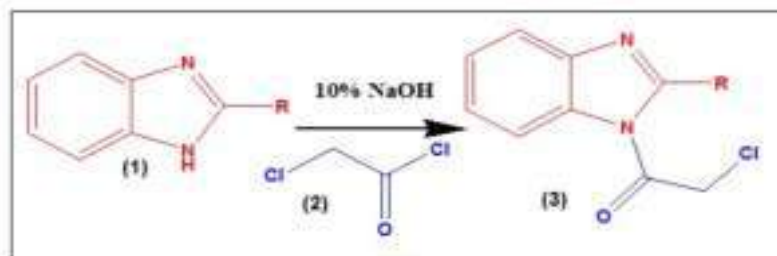
**Scheme. 1.49.** Synthesis of 1,2 disubstituted imidazoles using *N, N'*-disubstituted-*o*-phenylenediamine.

P. P. Mahulikar *et.al.* used bismuth nitrate as a catalyst for the synthesis of (3) using (1) and (2) in ethanolic medium<sup>387</sup> (Scheme 1.50).



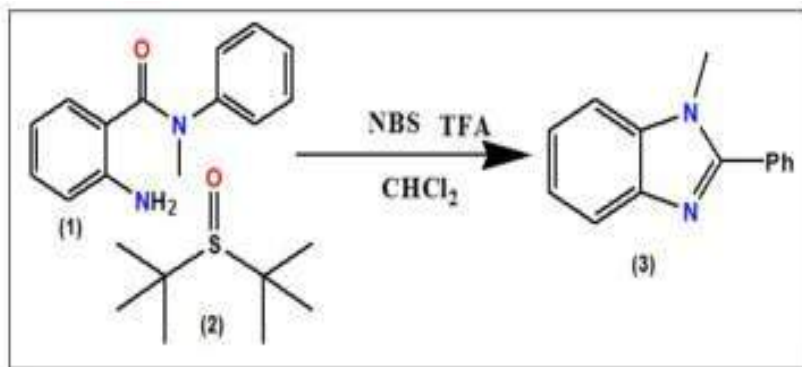
**Scheme. 1.50.** Synthesis of 1,2 disubstituted benzimidazole using Bismuth nitrate as catalyst

Praneetha V developed a method for the synthesis of (3) using 2-substituted benzimidazole derivatives (1), NaOH and chloroacetyl chloride (2)<sup>388</sup> (Scheme 1.51).



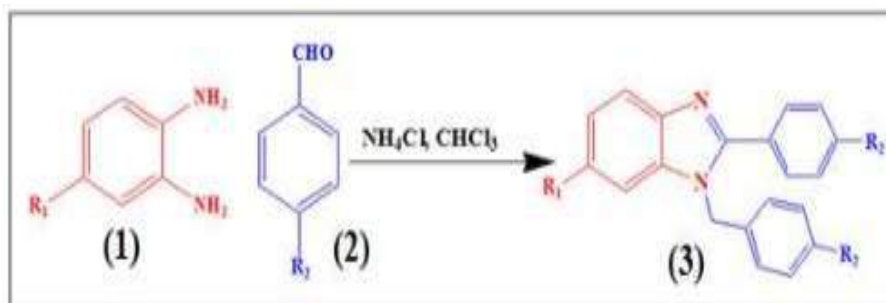
**Scheme. 1.51.** Synthesis of benzimidazole derivatives from chloroacetyl chloride

Z. Sun *et. al.* reported a method for the synthesis of (3) utilizing an aza-wittig equivalent process from a derivative of o-phenylene diamine (1), tertiary butane sulfoxide (2) and NBS under acidic conditions<sup>382</sup>(Scheme 1.52).



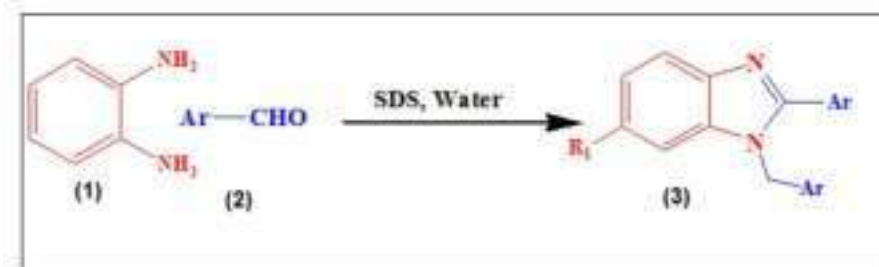
**Scheme. 1.52.** Synthesis of benzimidazole derivatives from tertiary butane sulfoxide

S. M. Abdur Rahman *et. al.* have reported the synthesis of 1, 2-disubstituted benzimidazoles (3) by cyclocondensation ortho-phenylene derivatives (1) and aromatic aldehyde (2) utilizing ammonium chloride as an inexpensive catalyst in chloroform solvent<sup>389</sup>(Scheme 1.53).



**Scheme. 1.53.** Synthesis of benzimidazole derivatives using Ammonium chloride catalyst

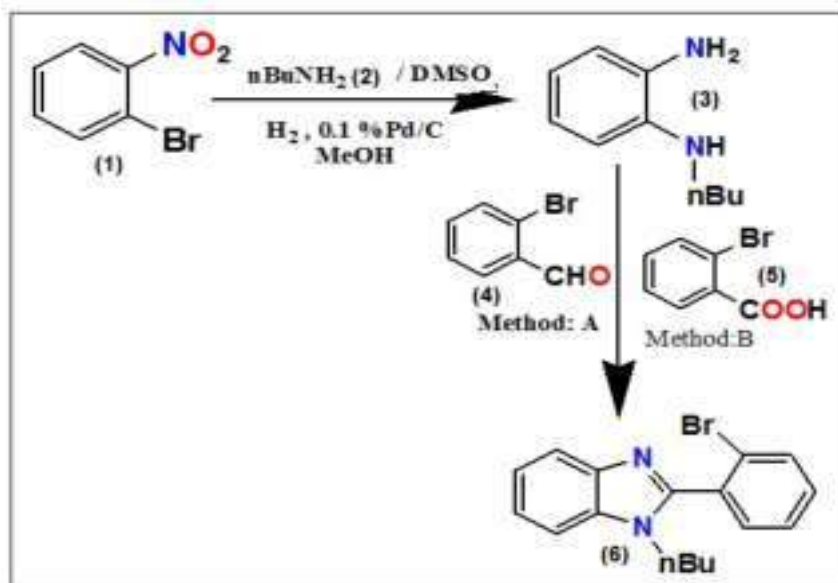
In another report, A. Nejati *et.al.* synthesized 1,2-disubstituted benzimidazoles (3) by the cyclocondensation of 1,2-phenylenediamine (1) and aryl aldehydes (2) in aqueous micellar media, using sodium dodecylsulfate (SDS) as a catalyst and surfactant to stabilize organic substrate<sup>390</sup> (Scheme 1.54).



**Scheme 1.54.** Synthesis of benzimidazole derivatives using SDS catalyst

Z.B. Song *et.al.* have reported the synthesis of 1, 2-disubstituted benzimidazole derivatives (3) by cyclocondensation reaction of 1, 2-phenylenediamine (1) and aryl aldehydes (2) in lactic acid medium without adding any additives<sup>391</sup>.

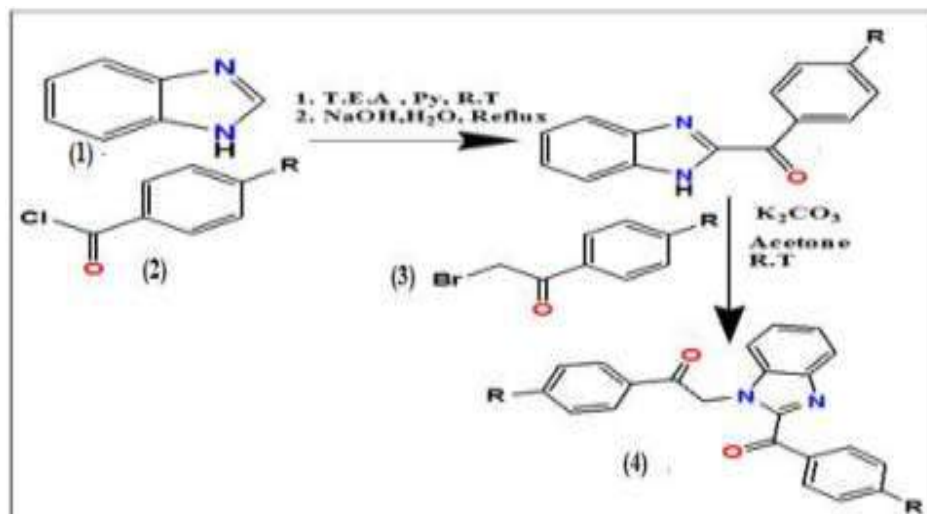
A.J. Blatch *et. al.* reported the synthesis of 1, 2-disubstituted benzimidazole (6) by subsequent reduction of Ortho-bromo nitrobenzene (1) with t-Bu-NH<sub>2</sub> (2) in DMSO solvent and cyclization of reduced product (3) with ortho bromo benzaldehyde (4) and ortho bromo benzoic acid (5) in two separate synthetic procedures<sup>392</sup> (Scheme 1.55).



**Scheme 1.55.** Two separate procedures for synthesis of benzimidazole derivatives

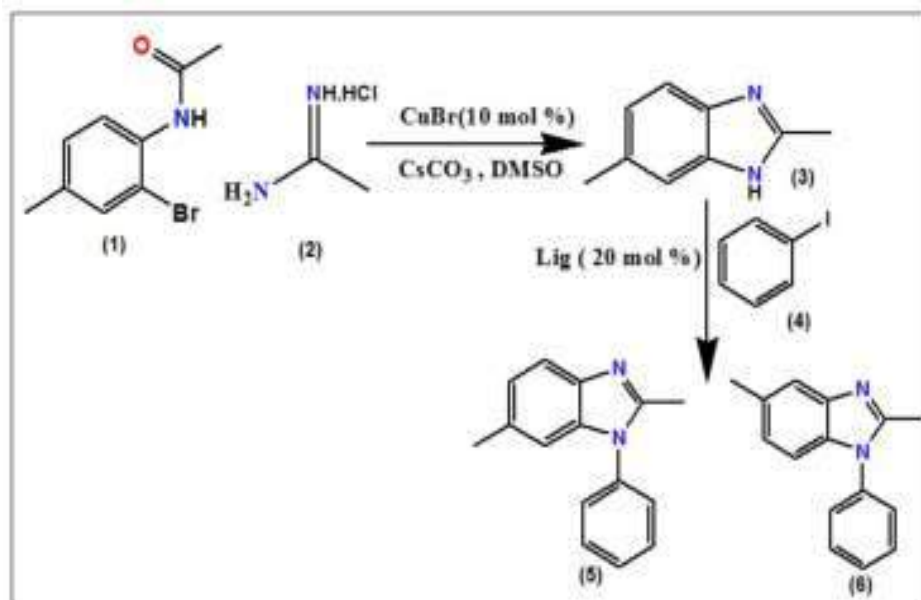
S. Demirayak *et.al.* developed a method for the synthesis of 1-(2-aryl-2-oxoethyl)-2-aryloylbenzimidazoles (4) using benzimidazoles (1), acyl chlorides (2), and 2-bromoacetophenones (3) under various solvents<sup>393</sup> (Scheme 1.56)





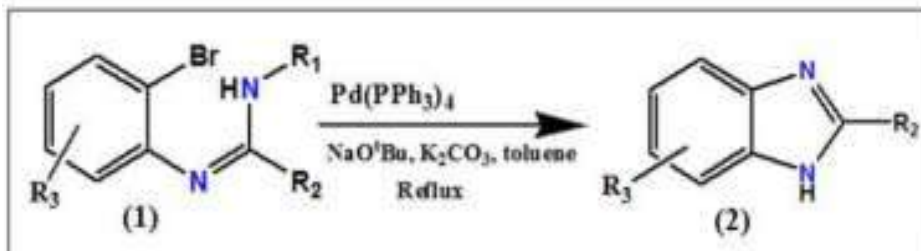
**Scheme. 1.56.** Synthesis of 1-(2-aryl-2-oxoethyl)-2-aryloylbenzimidazoles

Zhao *et.al.* reported a one pot method for the synthesis of two regioisomers of 1,2 disubstituted benzimidazoles (5 and 6). They first prepared 2- substituted-1H-benzimidazole (3) from N-(2-bromo-4-methylphenyl) acetamide (1) and amidine hydrochloride (2) in the presence of CuBr and CsCO<sub>3</sub> and then by using a combination 3,4,7,8-tetramethyl-1,10-phenonthraline ligand with aryl iodide (4) they converted 2- substituted-1H-benzimidazole to two regio isomers of 1,2-Disubstituted benzimidazoles (5 and 6)<sup>394</sup> (Scheme 1.57).



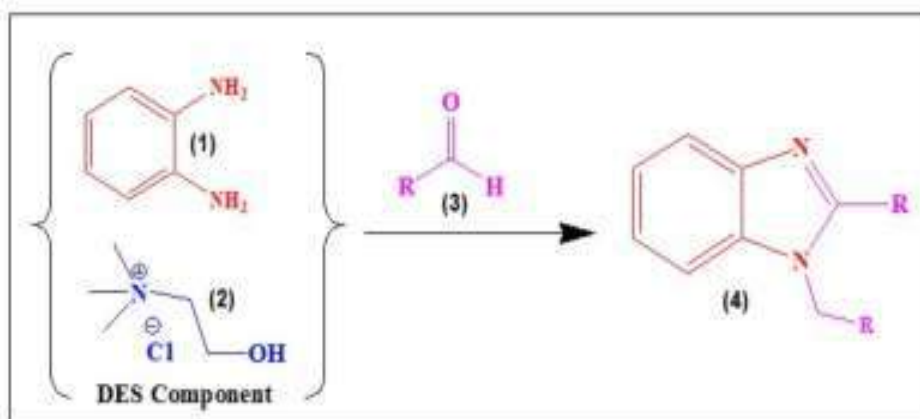
**Scheme. 1.57.** Synthesis of two regio isomers of 1,2-Disubstituted benzimidazoles

C.T. Brain *et al.* employed Palladium based catalyst for the synthesis of 1,2-Disubstituted benzimidazoles (2) using amidines (1), NaO<sup>t</sup>Bu, K<sub>2</sub>CO<sub>3</sub> in toluene solvent and under refluxing conditions<sup>395</sup> (Scheme 1.58).



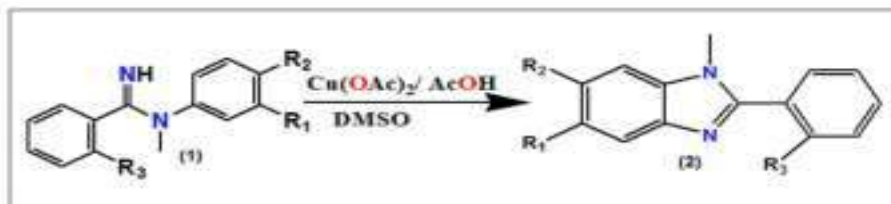
**Scheme. 1.58.** Synthesis of Benzimidazoles using Palladium based catalyst

M. Loredana *et al.* reported the synthesis of privileged benzimidazole (4) scaffolds by condensing aldehyde (3) and (1:1) mixture of orthophenylenediamine (1) and choline chloride (2) as an active deep eutectic solvent<sup>396</sup> (Scheme 1.59).



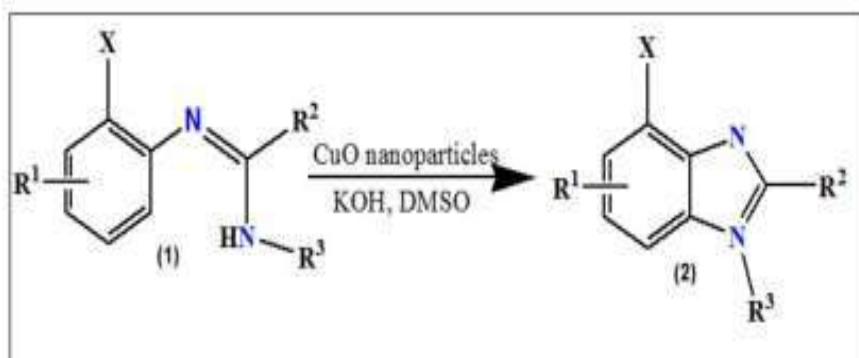
**Scheme. 1.59.** Synthesis of benzimidazole scaffold by using an active deep eutectic solvent.

Buchwald *et al.* employed copper acetate as an efficient catalyst for the preparation of N-methylated benzimidazoles (2) from amidines (1) in DMSO solvent<sup>397</sup> (Scheme 1.60).



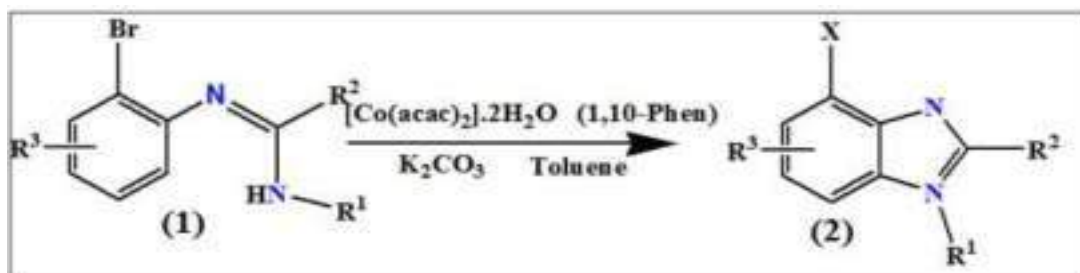
**Scheme. 1.60.** Synthesis of Benzimidazoles from amidine.

T. Punniyamurthy *et.al.* devised an efficient method for the synthesis of substituted benzimidazoles (2) by using CuO nanoparticles as a catalyst by using ortho-halo-aryl amidines (1) in DMSO solvent<sup>398</sup> (Scheme 1.61).



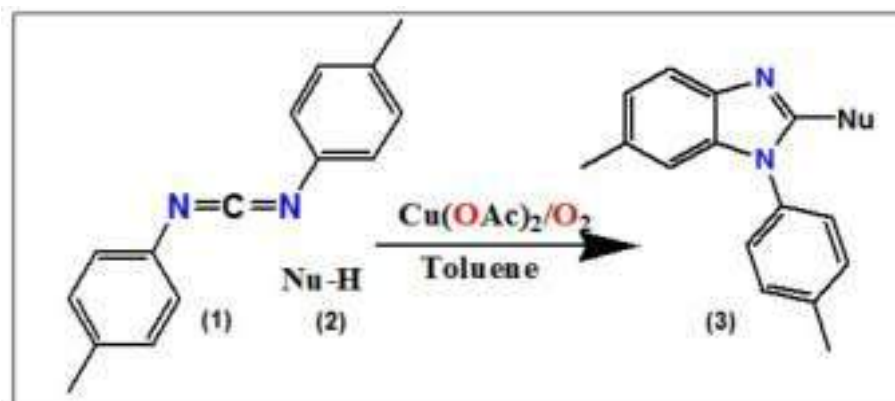
**Scheme. 1.61.** Synthesis of benzimidazoles by using CuO nanoparticle as catalyst.

The same group once again reported a method for the synthesis of benzimidazoles (2) using ortho-bromo-amidines (1) using a combination of Co(acac)<sub>2</sub>·2H<sub>2</sub>O and 1,10 phenanthroline as a catalyst in presence of K<sub>2</sub>CO<sub>3</sub> in Toluene solvent<sup>399</sup> (Scheme 1.62).



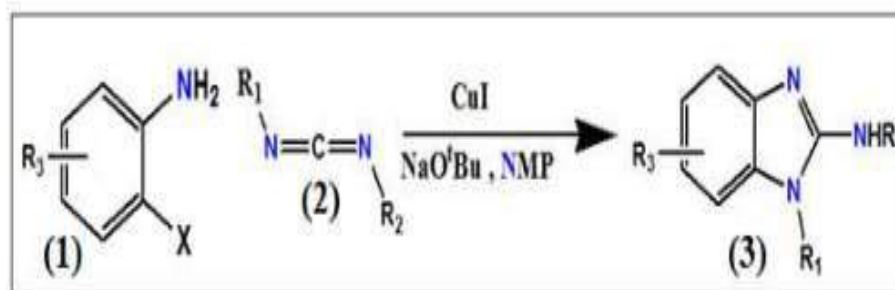
**Scheme. 1.62.** Synthesis of benzimidazoles using ortho-bromo-amidines.

Bao *et.al.* employed Cu (OAc)<sub>2</sub> as a catalyst for the synthesis of substituted benzimidazole (3) derivatives using diarylcarbodiimides (1) and various nucleophiles (2) in toluene solvent<sup>400</sup>(Scheme 1.63).



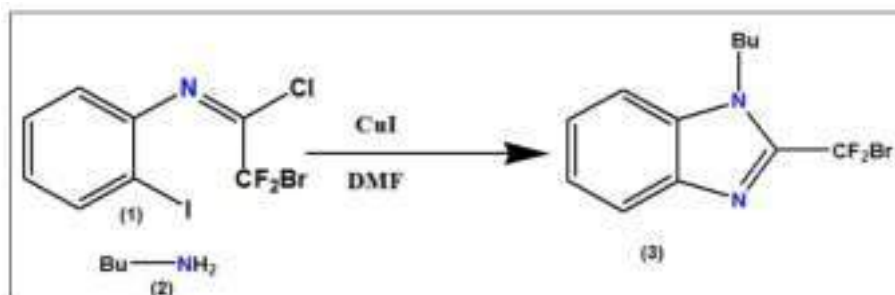
**Scheme. 1.63.** Synthesis of benzimidazole derivatives using diarylcarbodiimides

S. Cai *et al.* used copper iodide as an efficient catalyst for the synthesis of a variety of substituted benzimidazoles (3) from ortho-halo anilines (1) and carbodiimides (2) in presence of  $\text{NaO}^t\text{Bu}$  and N-methyl-2-pyrrolidone (NMP) as a solvent<sup>401</sup> (Scheme 1.64).



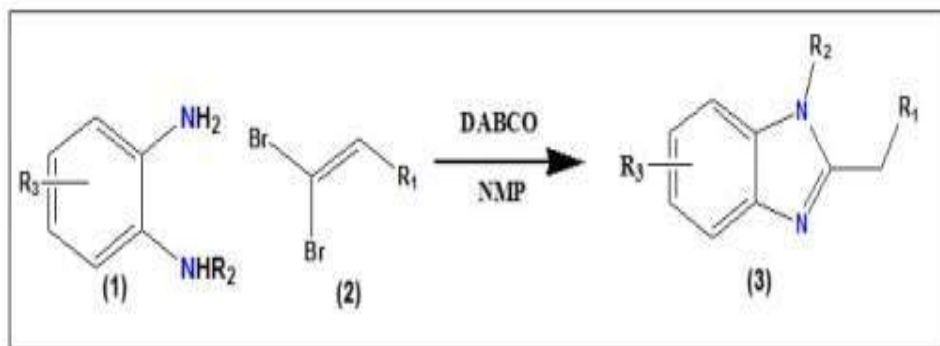
**Scheme. 1.64.** Synthesis of benzimidazole from ortho-halo anilines

Y. Wu *et al.* reported the synthesis of 2-fluoroalkylbenzimidazoles (3) from N-aryl bromodifluoroacetimidoylchlorides (1) and primary amines (2) using copper iodide as a catalyst in DMF solvent<sup>402</sup> (Scheme 1.65)



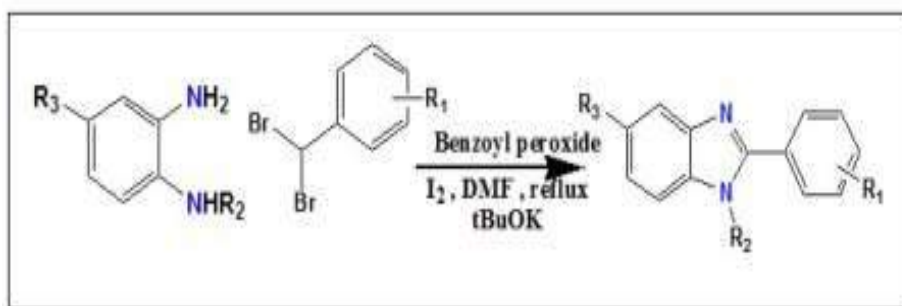
**Scheme. 1.65.** Synthesis of 2 fluoroalkylbenzimidazoles

Schmidt *et.al.* employed 1,4-diazabicyclo [2.2.2]octane (DABCO) as an efficient catalyst for the synthesis of substituted benzimidazoles (3) from 1,1 dibromoethene (2) and ortho-diamino benzene (1) using NMP as a solvent<sup>403</sup> (Scheme 1.66)



**Scheme. 1.66.** Synthesis of substituted benzimidazoles using DABCO as a catalyst.

Siddapa *et.al.* employed benzoyl peroxide as a catalyst for the synthesis of substituted benzimidazoles (2) from substituted orthophenylene diamine (1) and dibromomethylarenes (2) in presence of  $KO^tBu$  and molecular iodine under reflux conditions and DMF as a solvent<sup>404</sup> (Scheme 1.67).



**Scheme. 1.67.** Synthesis of substituted benzimidazoles from dibromomethylarenes.

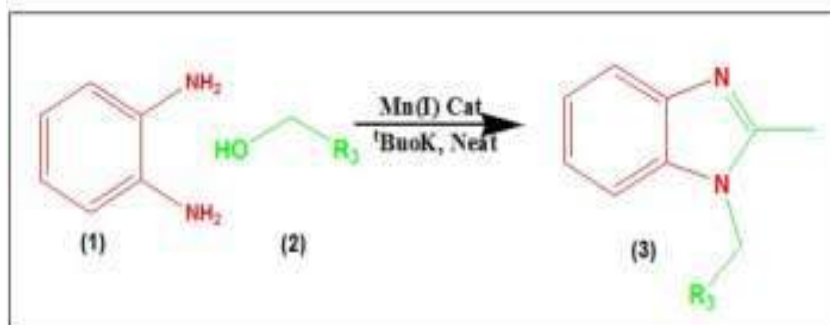
### 1.3.4.2 Green Method

There are numerous classical and nonclassical methods reported during the past for the synthesis of 1, 2-disubstituted benzimidazole derivatives. However, the reported procedure suffers from some serious drawbacks such as use of hazardous solvents, harsh reaction condition, expensive catalyst, environmental hazards, and long reaction time etc<sup>405</sup>. Therefore, by looking at the importance of this heterocyclic scaffolds, numerous green reaction methodologies for the synthesis of 1, 2-disubstituted benzimidazole derivatives have been developed for the past few decades<sup>406</sup>. A number of modifications in the synthetic approach such as the use of environmentally friendly solvents<sup>378</sup>, solvent free reaction conditions<sup>407</sup>, Microwave assisted synthesis<sup>408</sup>, Ultrasound irradiation<sup>409</sup> etc has been reported. These modifications largely contribute to the sustainability of the entire production system by greatly reducing industrial waste<sup>410</sup>.

#### 1.3.4.2.1 Solvent free synthesis

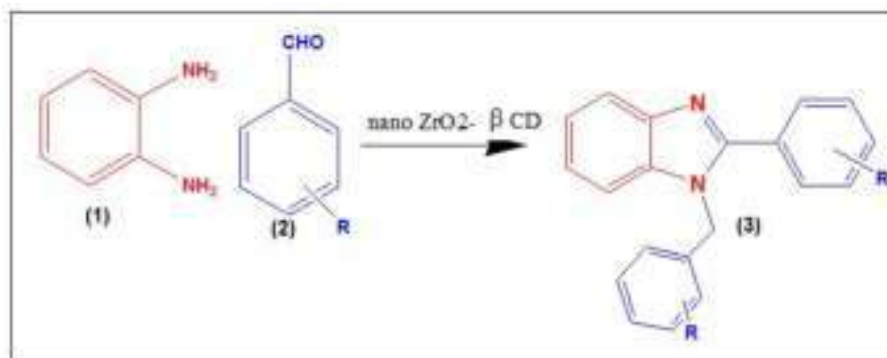
Solvent free synthesis is gaining a lot of interest these days as this technique has numerous advantages such as reduced pollution, low costs, and simplicity in process and handling and these factors have significance important in chemical industry<sup>91</sup>. Current literature review revealed that a variety of literatures are available for the solvent free synthesis of 1,2-disubstituted benzimidazole derivatives.

D. Srimani *et. al.* have reported an efficient protocol for the solvent free synthesis of 1, 2-disubstituted benzimidazole (3) derivatives by acceptor less dehydrogenative coupling of aromatic diamine (1) with primary alcohols (2) using phosphine free tridentate Mn(I) complex as a catalyst<sup>411</sup> (Scheme 1.68).



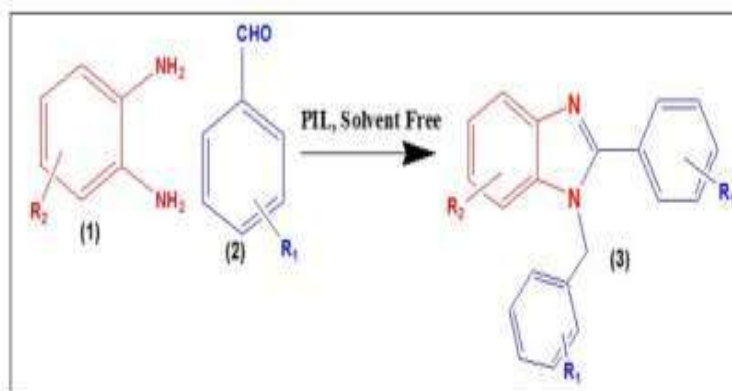
**Scheme. 1.68.** Synthesis of 1,2 disubstituted benzimidazole by dehydrogenative coupling.

S. Shashikanth *et.al.* have utilized ZrO<sub>2</sub>-supported-β-cyclodextrin (ZrO<sub>2</sub>-β-CD) as an efficient catalyst for the solvent free synthesis of 1, 2-disubstituted benzimidazole derivatives (3) by condensation of orthophenylene diamine (1) and aromatic aldehydes (2)<sup>412</sup> (Scheme 1.69)



**Scheme. 1.69.** Synthesis of bezimidazole derivatives using (ZrO<sub>2</sub>-β-CD) catalyst

D. K. Maiti *et al.* have reported the green synthesis of 1,2-disubstituted and 2-substituted benzimidazoles with outstanding selectivity using protic ionic liquid (PIL)-substrate as a catalyst utilizing grind stone chemistry under solvent free condition<sup>413</sup> (Scheme 1.70).



**Scheme. 1.70.** Synthesis of 1,2-disubstituted benzimidazole using PIL.

R. Nongkhlaw *et al.* utilized the grind stone technique to synthesize 1, 2-disubstituted benzimidazole derivatives (3) by condensation of ortho phenylenediamine (1) and various substituted aldehydes (2) using p-toluenesulfonic acid as a catalyst under solvent free condition<sup>414</sup>.

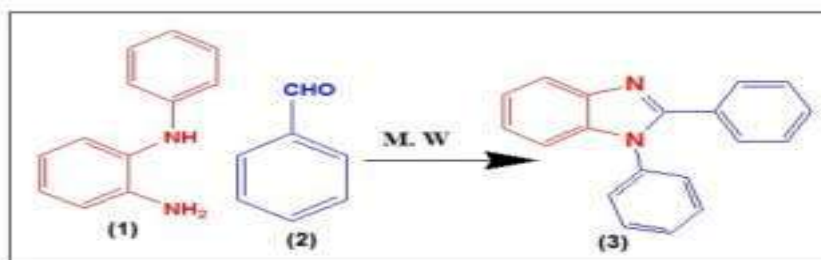
M. Barcellos *et al.* have reported the use of Nb<sub>2</sub>O<sub>5</sub>.5H<sub>2</sub>O as an efficient catalyst for the solvent free synthesis of 1, 2-disubstituted benzimidazole derivatives (3) by condensation of ortho phenylenediamine (1) and various substituted aliphatic and aromatic aldehydes<sup>415</sup>.

Similarly, D. O. Jang *et al.* reported the synergetic catalytic effect of ionic liquid and ZnO nanoparticle for the selective synthesis of 1, 2-disubstituted benzimidazoles (3) under solvent free condition utilizing ball-milling techniques<sup>383</sup>.

### 1.3.4.2.2 Microwave assisted synthesis

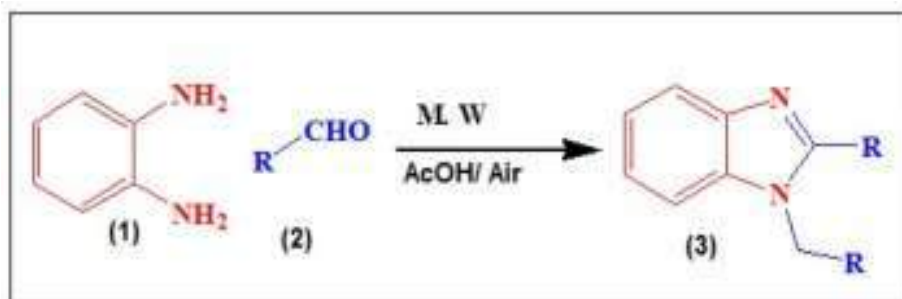
Microwave heating now a days has been used as an alternative power source for the chemical transformation reaction. Since the microwave assisted organic synthesis has many advantages such as instantaneous heating, high temperature, selectivity etc. over the conventional techniques<sup>416</sup>. A number of literature reports are available for the microwave assisted synthesis of 1, 2-disubstituted benzimidazole derivatives.

M. Nardi *et. al.* reported a highly efficient protocol for the synthesis of 1,2-disubstituted benzimidazoles (3) by the cyclization of N-phenyl-o-phenylenediamine (1) and aromatic aldehyde (2) using microwave irradiation employing  $\text{Er}(\text{OTf})_3$  as a catalyst<sup>417</sup> (Scheme 1.71).



**Scheme. 1.71.** Synthesis of 1,2-disubstituted benzimidazole using microwave irradiation

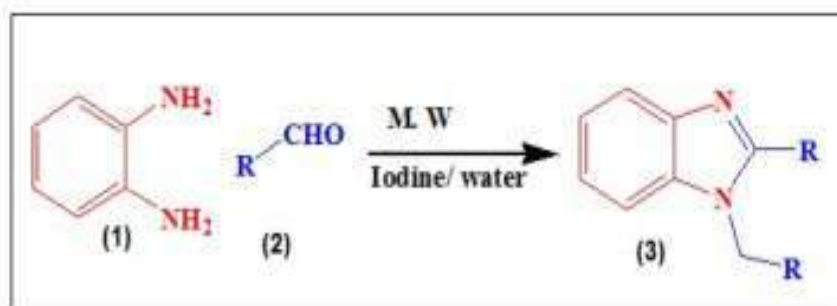
D. Azarifar *et. al.* reported acetic acid-promoted condensation of orthophenylenediamine (1) and aldehyde (2) under microwave irradiation to produce 1, 2-disubstituted benzimidazole (3)<sup>418</sup> (Scheme 1.72).



**Scheme. 1.72.** Synthesis of 1, 2-disubstituted benzimidazole derivatives from orthophenylene diammine



P. Aniket *et. al.* reported microwave assisted synthesis of 1, 2-disubstituted benzimidazole (3) by condensation of *o*-phenylenediamine (1) and aldehydes (2) catalysed by molecular Iodine in aqueous media<sup>419</sup> (Scheme 1.73).



**Scheme. 1.73.** Synthesis of 1, 2-disubstituted benzimidazole by using molecular I<sub>2</sub> as catalyst

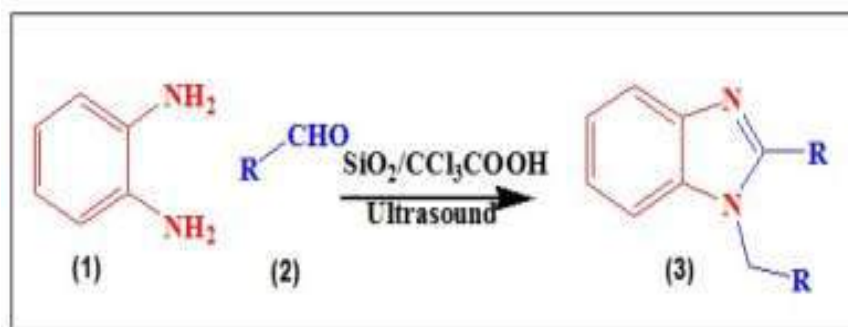
R. G. Jacob *et. al.* reported an easy and versatile method for the synthesis of 1,2-disubstituted benzimidazoles (3) using SiO<sub>2</sub>/ZnCl<sub>2</sub> and solvent-free conditions and Microwave irradiation<sup>420</sup>.

P. Bandyopadhyay *et. al.* developed an efficient catalytic method for the synthesis of 1, 2-disubstituted benzimidazole (3) using mesoporous mixed metal oxide nanocrystals of Al<sub>2</sub>O<sub>3</sub>-Fe<sub>2</sub>O<sub>3</sub>, Al<sub>2</sub>O<sub>3</sub>-V<sub>2</sub>O<sub>5</sub> and Al<sub>2</sub>O<sub>3</sub>-CuO as a catalyst under microwave irradiation<sup>421</sup>.

### 1.3.4.2.3 Ultrasound irradiation

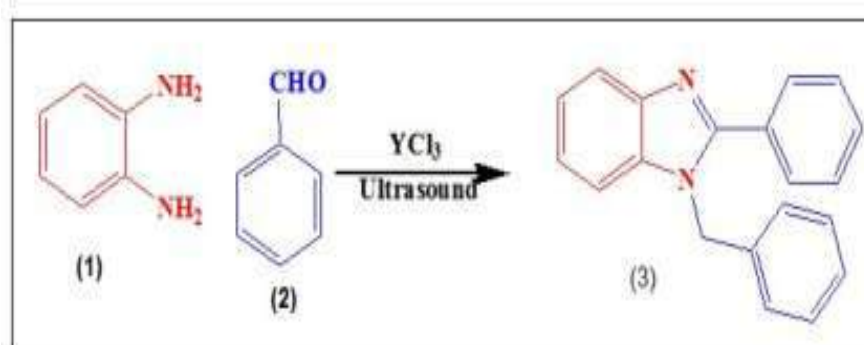
During the past few decades, several synthetic protocols have been developed for the synthesis of 1,2-disubstituted benzimidazole derivatives. However, the classical approach for the synthesis of above said compound has some serious drawbacks such as harsh reaction condition, expensive catalyst, environmental hazard, use of toxic solvents and long reaction time. Again, a major limitation of the classical method for the synthesis of 1,2-disubstituted imidazole is the poor selectivity in terms of N-1 substitution, which results in the formation of two compounds, i.e., 2-substituted benzimidazole along with 1, 2-disubstituted benzimidazole as a mixture. Several modifications in the synthesis of 1, 2-disubstituted benzimidazole derivatives have been documented during the past. Ultrasonic assisted synthesis is one of the most important and significant modification towards the goal for making the synthetic pathway environmentally friendly. Ultrasound-promoted synthesis of 1, 2-disubstituted benzimidazole of suitably functionalized substrates, allows the regioselective as well as provides milder and selective reaction conditions. A number of literatures are available for the ultrasonic assisted synthesis of 1, 2-disubstituted benzimidazole derivatives.

B. Kumar *et al.* reported the synthesis of 1, 2-disubstituted benzimidazole derivatives (3) under ultrasound irradiation by condensing o-phenylenediamine (1) with aldehydes (2) using  $\text{SiO}_2/\text{CCl}_3\text{COOH}$  catalyst<sup>422</sup> (Scheme 1.74).



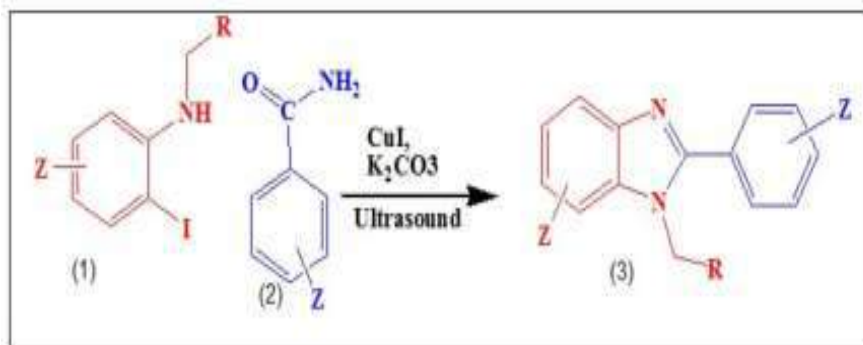
**Scheme. 1.74.** Synthesis of 1, 2-disubstituted benzimidazole derivatives under Ultrasound irradiation.

S.W. Wang *et al.* devised a method for the synthesis of 1, 2-disubstituted benzimidazole (3) derivatives using rare-earth metal chlorides as efficient Catalysts under Ultrasound irradiation<sup>423</sup> (Scheme 1.75).



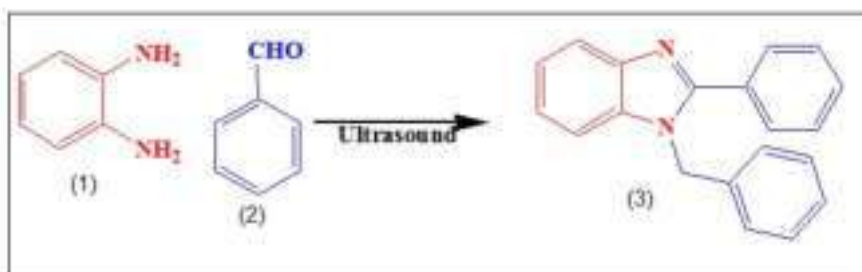
**Scheme. 1.75.** Synthesis of 1, 2-disubstituted benzimidazoles using  $\text{YCl}_3$

M. Pal *et al.* have reported the ultrasound assisted synthesis of 1, 2-disubstituted benzimidazole (3) derivatives utilizing  $\text{CuI}$  as an efficient catalyst under ultrasound irradiation by cyclocondensation of N-substituted 2-iodoanilines (1) and Benzamide derivatives (2)<sup>424</sup>(Scheme 1.76)



**Scheme. 1.76.** Synthesis of 1, 2-disubstituted benzimidazole derivatives using CuI as an efficient catalyst.

R. S. Salunkhe *et. al.* reported Ultrasound promoted synthesis of 1, 2-disubstituted benzimidazoles (3) using aqueous hydrotropic solution by condensing o-phenylenediamine (1) with aldehydes (2)<sup>425</sup> (Scheme 1.77).



**Scheme. 1.77.** Synthesis of 1, 2-disubstituted benzimidazoles using aqueous hydrotropic solution.

Similarly, S. W. Park *et. al.* developed a method for the synthesis of 1, 2-disubstituted benzimidazole (3) utilizing Amberlite IR-120 as a catalyst under Ultrasound irradiation<sup>426</sup>.

C. Wang *et. al.* reported the synthesis of 2-Aryl-1-arylmethyl-1H-benzimidazoles (3) catalyzed by bronsted acidic ionic liquid under ultrasonic irradiation<sup>427</sup>.

In another report, C. G. R. Nallagondur *et. al.* documented natural dolomitic limestone-catalyzed synthesis of 1, 2 disubstituted benzimidazoles (3), dihydropyrimidinones, and highly substituted pyridines under ultrasound irradiation<sup>428-429</sup>.

## 1.4 Brief information about the Transition Metal Borates

The chemistry of Transition metal borates is one of the vast and interesting fields of chemistry. The pioneers of borate chemistry were scientists like Hawthorne, Grimes and Braunschweig who have done tremendous work in this field<sup>429-432</sup>. The chemistry of borates is very similar to the chemistry of phosphates and silicates. Transition metal borates finds tremendous applications in the glass industries due to their channel like structure morphology<sup>433-434</sup> and “Boron Anomaly” in which these borates have been found to alter their structures with changing conditions<sup>435-436</sup>. Borates containing transition metals have interesting properties like humidity resistant and are luminescent<sup>437</sup>, bright visible colours give rise to different optical transitions<sup>438</sup>, use in glass electrodes<sup>439</sup>, nonlinear optical device materials<sup>433</sup>, lithium-ion batteries<sup>440,441</sup>. As a matter of fact, it is the transition metal which plays an important role in developing the properties of these borates<sup>442</sup>. These borates are also used in laser luminescent solar energy concentrators (LSCS) and optical communication devices<sup>443</sup>. In the past few decades, the research on borate materials has been rapidly expanding mainly because of their rich structural chemistry and potential applications in mineralogy and industry<sup>444-445</sup>. Current literature revealed that only a few reports are documented for the catalytic activity of borate salts during past few years.

J. Liu *et. al.* utilized Transition Metal Borides and Borates as an electrocatalyst for oxygen evolution reaction<sup>446</sup>.

S. Ghosh *et. al.* reported the Hydroboration reactions using transition metal borane and borate complexes<sup>447</sup>.

In another report, Y. Liu *et. al.* employed Ni-Fe-Boride as a catalyst for oxygen evolution reaction<sup>448</sup>.

Thus, it was thought worthwhile to explore the catalytic efficiency of few transition metal borates for the one-pot multicomponent synthesis of some N-containing heterocyclic compounds under green reaction conditions.

### 1.5 Objectives of the research work

The main aim of this work is to explore the catalytic activity of transition metal borates and to develop the novel, efficient, convenient, selective and environmentally benign synthetic methods for the synthesis of Nitrogen containing heterocyclic compounds. However the objective of the current research focuses on the following:

- To explore the catalytic efficiency of some transition metal borates in the green synthesis of Nitrogen containing heterocyclic compounds in order to search for a novel mild and efficient procedure.
- To develop an efficient, operationally simple, environmentally benign, and straight forward general method for the synthesis of Nitrogen containing heterocyclic compounds.
- To carry out detailed analytical and spectroscopic characterization of synthesized heterocyclic compounds.
- Theoretical Studies involving DFT, analysis of Non-Linear Optical properties (NLO), Pharmacokinetic analysis and molecular docking study of some selected synthesized derivatives.

## 1.6 References

- (1) X. Zhang, A. S. Shetty, S. A. Jenekhe., *Macromolecules*, **1999**, 32 (22), 7422–7429.
- (2) X. Wu, M. Li, Y. Qu, W. Tang, Y. Zheng, J. Lian, M. Ji, L. Xu., *Bioorganic & Medicinal Chemistry*, **2010**, 18 (11), 3812–3822.
- (3) I. M. El-Deeb, S. H. Lee., *Bioorganic & Medicinal Chemistry*, **2010**, 18 (11), 3860–3874.
- (4) O. O. Ajani, C. A. Obafemi, O. C. Nwinyi, D. A. Akinpelu., *Bioorganic & Medicinal Chemistry*, **2010**, 18 (1), 214–221.
- (5) M. M. Heravi, V. Zadsirjan., *RSC Advances*, **2020**, 10 (72), 44247–44311.
- (6) P. M. T. Ferreira, H. L. S. Maia, L. S. Monteiro., *Tetrahedron Letters*, **2002**, 43 (25), 4491–4493.
- (7) G. Daidone, B. Maggio, D. Schillaci., *Pharmazie*, **1990**, 45 (14), 441–442.
- (8) L. Gylbert., *Acta Crystallographica Section B Structural Crystallography and Crystal Chemistry*, **1973**, 29 (8), 1630–1635.
- (9) M. E. Prommer., *Journal of Opioid Management*, **2011**, 7 (5), 401–406.
- (10) H. Hotti, H. Rischer., *Molecules*, **2017**, 22 (11), 1962.
- (11) D. J. Sutor., *Acta Crystallographica*, **1958**, 11 (7), 453–458.
- (12) M. v. Djordjevic, K. D. Brunnemann, D. Hoffmann., *Carcinogenesis*, **1989**, 10 (9), 1725–1731.
- (13) M. Srivastava, J. Singh, S. B. Singh, K. Tiwari, V. K. Pathak, J. Singh., *Green Chemistry*, **2012**, 14 (4), 901–905.
- (14) D. Yang, B. An, W. Wei, L. Tian, B. Huang, H. Wang., *ACS Combinatorial Science*, **2015**, 17 (2), 113–119.
- (15) S. Shoja Shafti, M. Gilanipoor., *Schizophrenia Research and Treatment*, **2014**, 2014 (1), 1–5.
- (16) C. P. Tătaru, V. L. Purcărea., *J Med Life*, **2012**, 5 (3), 247–251.
- (17) C. le Tourneau, E. Raymond, S. Faivre., *Therapeutics and Clinical Risk Management*, **2007**, 3 (2), 341–348.
- (18) L. R. Wiseman, J. C. Adkins., *Drugs & Aging*, **1998**, 13 (4), 321–332.
- (19) J. W. Wheless, B. Vazquez., *Epilepsy Currents*, **2010**, 10 (1), 1–6.

- (20) N. Kerru, L. Gummidi, S. Maddila, K. K. Gangu, S. B. Jonnalagadda., *Molecules*, **2020**, 25 (8), 1909.
- (21) R. Kaur, S. Chaudhary, K. Kumar, M. K. Gupta, R. K. Rawal., *European Journal of Medicinal Chemistry*, **2017**, 132, 108–134.
- (22) E. Vitaku, D. T. Smith, J. T. Njardarson., *Journal of Medicinal Chemistry*, **2014**, 57 (24), 10257–10274.
- (23) W.-Y. Fang, L. Ravindar, K. P. Rakesh, H. M. Manukumar, C. S. Shantharam, N. S. Alharbi, H.-L. Qin., *European Journal of Medicinal Chemistry*, **2019**, 173, 117–153.
- (24) N. Kerru, A. Singh-Pillay, P. Awolade, P. Singh., *European Journal of Medicinal Chemistry*, **2018**, 152, 436–488.
- (25) B. R. Smith, C. M. Eastman, J. T. Njardarson., *Journal of Medicinal Chemistry*, **2014**, 57 (23), 9764–9773.
- (26) S. A. Jenekhe, L. Lu, M. M. Alam., *Macromolecules*, **2001**, 34 (21), 7315–7324.
- (27) M. Balasubramanian, JG. Keay., *Comprehensive Heterocyclic Chemistry II*, 1st ed.; Oxford : New York [Pergamon Press], **1996**; Vol. 5.
- (28) J. P. Michael., *Natural Product Reports*, **1997**, 14 (6), 605–618.
- (29) G.-W. Wang, C.-S. Jia, Y.-W. Dong., *Tetrahedron Letters*, **2006**, 47 (7), 1059–1063.
- (30) A. R. Katritzky., *Handbook of Heterocyclic Chemistry*, 1st ed.; Oxford [Oxfordshire]: New York [Pergamon Press], **1985**.
- (31) C. T. Walsh., *Tetrahedron Letters*, **2015**, 56 (23), 3075–3081.
- (32) B. Zhang, A. Studer., *Chemical Society Reviews*, **2015**, 44 (11), 3505–3521.
- (33) R. Gaynes., *Emerging Infectious Diseases*, **2017**, 23 (5), 849–853.
- (34) N. Das, J. Madhavan, A. Selvi, D. Das., *3 Biotech*, **2019**, 9 (6), 231.
- (35) R. Aviner., *Comput Struct Biotechnol J*, **2020**, 18, 1074–1083.
- (36) M. S. Saini, A. Kumar, J. Dwivedi, R. Singh., *International Journal of Pharma Sciences and Research*, **2013**, 4 (3), 66–77.
- (37) E. M. Flefel, W. I. El-Sofany, R. A. K. Al-Harbi, M. El-Shahat., *Molecules*, **2019**, 24 (13), 2511.
- (38) A. K. Dhingra, B. Chopra, J. S. Dua, D. N. Prasad., *Anti-Inflammatory & Anti-Allergy Agents in Medicinal Chemistry*, **2017**, 16 (3), 136–152.
- (39) N. Siddiqui, Andalip, S. Bawa, R. Ali, O. Afzal, M. Akhtar, B. Azad, R. Kumar., *Journal of Pharmacy And Bioallied Sciences*, **2011**, 3 (2), 194–212.

- (40) D. K. Lang, R. Kaur, R. Arora, B. Saini, S. Arora., *Anticancer Agents Med Chem*, **2020**, *20* (18), 2150–2168.
- (41) P. N. Kalaria, S. C. Karad, D. K. Raval., *Eur J Med Chem*, **2018**, *158*, 917–936.
- (42) T. K. Venkatachalam, E. A. Sudbeck, C. Mao, F. M. Uckun., *Bioorganic & Medicinal Chemistry Letters*, **2001**, *11* (4), 523–528.
- (43) A. H. M. Hussein, A. B. A. El-Adasy, A. M. El-Saghier, M. Olish, A. H. Abdelmonsef., *RSC Advances*, **2022**, *12* (20), 12607–12621.
- (44) N. B. Patel, H. R. Patel., *Indian Journal of Pharmaceutical Sciences*, **2010**, *72* (5), 620.
- (45) A. De, S. Sarkar, A. Majee., *Chem Heterocycl Compd (N Y)*, **2021**, *57* (4), 410–416.
- (46) D. Ma, Y. Yin, Y. L. Chen, Y. T. Yan, J. Wu., *RSC Advances*, **2021**, *11* (25), 15380–15386.
- (47) E. A. Ghareeb, N. F. H. Mahmoud, E. A. El-Bordany, E. A. E. El-Helw., *Bioorganic Chemistry*, **2021**, *112*.
- (48) A. P. Taylor, R. P. Robinson, Y. M. Fobian, D. C. Blakemore, L. H. Jones, O. Fadeyi., *Organic & Biomolecular Chemistry*, **2016**, *14* (28), 6611–6637.
- (49) W. Guo, M. Zhao, W. Tan, L. Zheng, K. Tao, X. Fan., *Organic Chemistry Frontiers*, **2019**, *6* (13), 2120–2141.
- (50) X. Chen, H. Yang, M. J. Hülsey, N. Yan., *ACS Sustainable Chemistry and Engineering*, **2017**, *5* (11), 11096–11104.
- (51) L. A. Aronica, G. Albano., *Catalysts*, **2022**, *12* (1), 68.
- (52) M. Henary, C. Kananda, L. Rotolo, B. Savino, E. A. Owens, G. Cravotto., *RSC Advances*, **2020**, *10* (24), 14170–14197.
- (53) I. K. Moiseev, M. N. Zemtsova, N. V. Makarova., *Chemistry of Heterocyclic Compounds*, **1994**, *30* (7), 745–761.
- (54) E. Chainikova, R. Safiullin, L. Spirikhin, A. Erastov., *Tetrahedron Letters*, **2013**, *54* (17), 2140–2142.
- (55) B. Lai, M. Ye, P. Liu, M. Li, R. Bai, Y. Gu., *Beilstein Journal of Organic Chemistry* *16:238*, **2020**, *16* (1), 2888–2902.
- (56) R. Hili, A. K. Yudin., *Nat Chem Biol*, **2006**, *2* (6), 284–287.
- (57) J. Bariwal, E. van der Eycken., *Chemical Society Reviews*, **2013**, *42* (24), 9283–9303.



- (58) P. T. Anastas, J. C. Warner., *Green Chemistry: Theory and Practice*, 1st ed.; Oxford University Press, **1998**.
- (59) J. C. Warner, A. S. Cannon, K. M. Dye., *Environmental Impact Assessment Review*, **2004**, *24* (7–8), 775–799.
- (60) P. Anastas, N. Eghbali., *Chemical Society Reviews*, **2009**, *39* (1), 301–312.
- (61) P. T. Anastas., *Critical Reviews in Analytical Chemistry*, **2010**, *29* (3), 167–175.
- (62) A. M. Sanseverino., *Química Nova (New Chem.)*, **2000**, *23* (1), 102–107.
- (63) M. de La Guardia, S. Armenta., *Analytical and Bioanalytical Chemistry*, **2012**, *404* (3), 625–626.
- (64) E. J. Lenardão, R. A. Freitag, M. J. Dabdoub, A. C. Ferreira Batista, C. da Cruz Silveira., *Química Nova (New Chem.)*, **2003**, *26* (1), 123–129.
- (65) B. M. Trost., *Angewandte Chemie International Edition in English*, **1995**, *34* (3), 259–281.
- (66) R. A. Sheldon., *Pure and Applied Chemistry*, **2000**, *72* (7), 1233–1246.
- (67) P. Poehlauer, J. Manley, R. Broxterman, B. Gregertsen, M. Ridemark., *Organic Process Research and Development*, **2012**, *16* (10), 1586–1590.
- (68) M. Poliakoff, P. Licence., *Nature*, **2007**, *450* (7171), 810–812.
- (69) F. R. Nolasco, G. A. Tavares, J. A. Bendassolli., *Engenharia Sanitaria e Ambiental (Sanitary and Environmental Engineering)*, **2006**, *11* (2), 118–124.
- (70) A. de La Hoz, A. Díaz-Ortiz, P. Prieto., *Alternative Energy Sources for Green Chemistry. Chapter 1 - Microwave-Assisted Green Organic Synthesis*; pp. 1-33; The Royal Society of Chemistry, **2016**.
- (71) S. Tagliapietra, E. Calcio Gaudino, G. Cravotto., *Power Ultrasonics. Chapter 33 - The Use of Power Ultrasound for Organic Synthesis in Green Chemistry*; pp. 997–1022; Woodhead Publishing: Oxford, **2015**.
- (72) K. Tanaka, F. Toda., *Chemical Reviews*, **2000**, *100* (3), 1025–1074.
- (73) D. Friedmann, A. Hakki, H. Kim, W. Choi, D. Bahnemann., *Green Chemistry*, **2016**, *18* (20), 5391–5411.
- (74) Udayabhanu, H. Nagabhushana, D. Suresh, H. Rajanaika, S. C. Sharma, G. Nagaraju., *Materials Today: Proceedings*, **2017**, *4* (11), 11888–11893.
- (75) R. S. Varma., *ACS Sustainable Chemistry and Engineering*, **2016**, *4* (11), 5866–5878.

- (76) M. Jug, P. A. Mura., *Pharmaceutics*, **2018**, *10* (4), 189.
- (77) C. C. Piras, S. Fernández-Prieto, W. M. de Borggraeve., *Nanoscale Advances*, **2019**, *1* (3), 937–947.
- (78) A. Pettignano, A. Charlot, E. Fleury., *Polymers (Basel)*, **2019**, *11* (7), 1227.
- (79) G. K. Verma, K. Raghuvanshi, R. K. Verma, P. Dwivedi, M. S. Singh., *Tetrahedron*, **2011**, *67* (20), 3698–3704.
- (80) K. Tanaka., *Organic Process Research & Development*, **2003**, *7* (4), 612–612.
- (81) G. R. Desiraju., *Organic Solid State Chemistry*; Elsevier: Amsterdam; New York, **1987**; Vol. 32.
- (82) F. Wöhler., *Ann Phys*, **1828**, *88* (2), 253–256.
- (83) F. Toda, M. Yagi, K. Kiyoshige., *Journal of the Chemical Society, Chemical Communications*, **1988**, *14*, 958–959.
- (84) L. Claisen., *Berichte der deutschen chemischen Gesellschaft*, **1912**, *45* (3), 3157–3166.
- (85) B. S. Goud, K. Panneerselvam, D. E. Zacharias, G. R. Desiraju., *Journal of the Chemical Society, Perkin Transactions 2*, **1995**, No. 2, 325–330.
- (86) C. L. Raston, J. L. Scott., *Green Chemistry*, **2000**, *2* (2), 49–52.
- (87) K. Tanaka, T. Sugino, F. Toda., *Green Chemistry*, **2000**, *2* (6), 303–304.
- (88) K. Yoshizawa, S. Toyota, F. Toda., *Green Chemistry*, **2002**, *4* (1), 68–70.
- (89) D. C. Waddell, J. Mack., *Green Chemistry*, **2009**, *11* (1), 79–82.
- (90) X. Ma, Y. Zhou, J. Zhang, A. Zhu, T. Jiang, B. Han., *Green Chemistry*, **2008**, *10* (1), 59–66.
- (91) F. Toda, K. Tanaka, K. Hamai., *Journal of the Chemical Society, Perkin Transactions 1*, **1990**, No. 11, 3207–3209.
- (92) S. B. Zangade, S. S. Mokle, A. T. Shinde, Y. B. Vibhute., *Green Chemistry Letters and Reviews*, **2013**, *6* (2), 123–127.
- (93) J. M. Thomas, W. J. Thomas., *Principles and Practice of Heterogeneous Catalysis*, 1st ed.; Wiley-VCH: Weinheim, **1996**.
- (94) G. Nagendrappa., *Resonance*, **2002**, *7* (10), 59–68.
- (95) Z. Kibou, N. Cheikh, N. Choukchou-Braham, B. Mostefa-Kara, M. Benabdellah, D. Villemin., *Scientific Study & Research - Chemistry & Chemical Engineering, Biotechnology, Food Industry*, **2011**, *12* (2), 121–126.

- (96) S. Tu, B. Jiang, Y. Zhang, R. Jia, J. Zhang, C. Yao, F. Shi., *Organic & Biomolecular Chemistry*, **2007**, 5 (2), 355–359.
- (97) M. S Al-Ajely, A. M. Noori., *Biomedical Journal of Scientific & Technical Research*, **2020**, 29 (3), 22510–22516.
- (98) R. R. Wani, H. K. Chaudhari, B. S. Takale., *Journal of Heterocyclic Chemistry*, **2019**, 56 (4), 1337–1340.
- (99) V. Bhardwaj, D. Gumber, V. Abbot, S. Dhiman, P. Sharma., *RSC Advances*, **2015**, 5 (20), 15233–15266.
- (100) P. N. Rakendu, T. Aneeja, G. Anilkumar., *Asian Journal of Organic Chemistry*, **2021**, 10 (9), 2318–2333.
- (101) C. K. Belwal, J. Patel., *Asian Journal of Green Chemistry*, **2019**, 3 (4), 483–491.
- (102) Y. L. N. Murthy, A. Rajack, K. Yuvaraj., *Arabian Journal of Chemistry*, **2016**, 9, S1740–S1746.
- (103) S. Yan, Y. Chen, L. Liu, N. He, J. Lin., *Green Chemistry*, **2010**, 12 (11), 2043–2052.
- (104) C. S. Jia, Y. W. Dong, S. J. Tu, G. W. Wang., *Tetrahedron*, **2007**, 63 (4), 892–897.
- (105) D. Kong, X. Wang, Z. Shi, M. Wu, Q. Lin, X. Wang., *Journal of Chemical Research*, **2016**, 40 (9), 529–531.
- (106) S. Martínez González, A. I. Hernández, C. Varela, S. Rodríguez-Arístegui, R. M. Alvarez, A. B. García, M. Lorenzo, V. Rivero, J. Oyarzabal, O. Rabal, J. R. Bischoff, M. Albarrán, A. Cebriá, P. Alfonso, W. Link, J. Fominaya, J. Pastor., *Bioorganic & Medicinal Chemistry Letters*, **2012**, 22 (5), 1874–1878.
- (107) P. H. Tran, T. P. Thi Bui, X. Q. Bach Lam, X. T. Thi Nguyen., *RSC Advances*, **2018**, 8 (63), 36392–36399.
- (108) E. A. Tiong, D. Rivalti, B. M. Williams, J. L. Gleason, E. A. Tiong, D. Rivalti, B. M. Williams, J. L. Gleason., *Angewandte Chemie International Edition*, **2013**, 52 (12), 3442–3445.
- (109) P. T. Anastas, J. B. Zimmerman., *Environmental Science & Technology*, **2003**, 37 (5), 94A-101A.
- (110) P. T. Anastas, E. S. Beach., *Green Chemistry Letters and Reviews*, **2008**, 1 (1), 9–24.
- (111) R. W. Armstrong, A. P. Combs, P. A. Tempest, S. D. Brown, T. A. Keating., *Accounts of Chemical Research*, **1996**, 29 (3), 123–131.
- (112) H. A. Younus, M. Al-Rashida, A. Hameed, M. Uroos, U. Salar, S. Rana, K. M. Khan., *Expert Opinion on Therapeutic Patents*, **2020**, 31 (3), 267–289.

- (113) B. A. D. Neto, R. O. Rocha, M. O. Rodrigues., *Molecules* , **2022**, 27 (1), 132.
- (114) Y. Volkova, S. Baranin, I. Zavarzin., *Advanced Synthesis & Catalysis*, **2021**, 363 (1), 40–61.
- (115) S. Siahrostami, S. J. Villegas, A. H. Bagherzadeh Mostaghimi, S. Back, A. B. Farimani, H. Wang, K. A. Persson, J. Montoya., *ACS Catalysis*, **2020**, 10 (14), 7495–7511.
- (116) L. Biesen, T. J. J. Müller., *Advanced Synthesis & Catalysis*, **2021**, 363 (4), 980–1006.
- (117) B. B. Touré, D. G. Hall., *Chemical Reviews*, **2009**, 109 (9), 4439–4486.
- (118) J. Zhu, H. Bienaymé., *Multicomponent Reactions*, 1st ed.; Wiley-VCH: Weinheim, Germany, **2005**.
- (119) L. F. Tietze., *Chemical Reviews*, **1996**, 96 (1), 115–136.
- (120) S. E. John, S. Gulati, N. Shankaraiah., *Organic Chemistry Frontiers*, **2021**, 8 (15), 4237–4287.
- (121) L. Biesen, T. J. J. Müller., *Advanced Synthesis & Catalysis*, **2021**, 363 (4), 980–1006.
- (122) M. Mamaghani, R. Hossein Nia., *Polycyclic Aromatic Compounds*, **2021**, 41 (2), 223–291.
- (123) A. Strecker., *Justus Liebigs Ann Chem*, **1850**, 75 (1), 27–45.
- (124) H. Debus., *Justus Liebigs Ann Chem*, **1858**, 107 (2), 199–208.
- (125) B. Radziszewski., *Berichte der deutschen chemischen Gesellschaft*, **1882**, 15 (2), 1493–1496.
- (126) B. Radziszewski., *Berichte der deutschen chemischen Gesellschaft*, **1882**, 15 (2), 2706–2708.
- (127) A. Hantzsch., *Berichte der deutschen chemischen Gesellschaft*, **1881**, 14 (2), 1637–1638.
- (128) A. Hantzsch., *Berichte der deutschen chemischen Gesellschaft*, **1890**, 23 (1), 1474–1476.
- (129) P. Bigenelli., *Berichte der deutschen chemischen Gesellschaft*, **1891**, 24 (2), 2962–2967.
- (130) C. Mannich, W. Krösche., *Arch Pharm (Weinheim)*, **1912**, 250 (1), 647–667.

- (131) R. Robinson., *Journal of the Chemical Society, Transactions*, **1917**, 111 (0), 762–768.
- (132) H. T. Bucherer, H. T. Fischbeck., *J. Prakt. Chem*, **1934**, 140, 69–89.
- (133) F. Asinger., *Angewandte Chemie*, **1956**, 68 (12), 413–413.
- (134) I. Ugi, C. Steinbrückner., *Angewandte Chemie*, **1960**, 72 (7–8), 267–268.
- (135) L. S. Povarov., *Russian Chemical Reviews*, **1965**, 34 (9), 639–656.
- (136) K. Gewald, E. Schinke, H. Böttcher., *Chem Ber*, **1966**, 99 (1), 94–100.
- (137) “The academic pursuit of screening”, *Nature Chemical Biology*, **2007**, 3 (8), 433–433.
- (138) N. A. Petasis, I. Akritopoulou., *Tetrahedron Letters*, **1993**, 34 (4), 583–586.
- (139) J. E. Biggs-Houck, A. Younai, J. T. Shaw., *Curr Opin Chem Biol*, **2010**, 14 (3), 371–382.
- (140) Y. Chen, L. Li, X. He, Z. Li., *ACS Catalysis*, **2019**, 9 (10), 9098–9102.
- (141) H. Singh, J. Sindhu, J. M. Khurana, C. Sharma, K. R. Aneja, H. Singh, J. Sindhu, J. M. Khurana, C. Sharma, K. R. Aneja., *Australian Journal of Chemistry*, **2013**, 66 (9), 1088–1096.
- (142) M. Bararjanian, S. Balalaie, F. Rominger, B. Movassagh, H. R. Bijanzadeh., *The Journal of Organic Chemistry*, **2010**, 75 (9), 2806–2812.
- (143) S. Brauch, L. Gabriel, B. Westermann., *Chemical Communications*, **2010**, 46 (19), 3387–3389.
- (144) N. Elders, D. van der Born, L. J. D. Hendrickx, B. J. I. Timmer, A. Krause, E. Janssen, F. J. J. de Kanter, E. Ruijter, R. V. A. Orru., *Angewandte Chemie. International Edition*, **2009**, 48 (32), 5856–5859.
- (145) A. Dondoni, A. Massi., *Accounts of Chemical Research*, **2006**, 39 (7), 451–463.
- (146) M. S. Singh, S. Chowdhury., *RSC Advances*, **2012**, 2 (11), 4547–4592.
- (147) H. Eckert., *Molecules 2012, Vol. 17, Pages 1074-1102*, **2012**, 17 (1), 1074–1102.
- (148) A. Corma, H. García., *Chemical Reviews*, **2003**, 103 (11), 4307–4365.
- (149) B. Karimi, D. Zareyee., *Journal of Materials Chemistry*, **2009**, 19 (45), 8665–8670.
- (150) F. Bigi, S. Carloni, B. Frullanti, R. Maggi, G. Sartori., *Tetrahedron Letters*, **1999**, 40 (17), 3465–3468.

- (151) D. Koszelewski, W. Szymanski, J. Krysiak, R. Ostaszewski., *Synthetic Communications*, **2008**, 38 (7), 1120–1127.
- (152) L. el Kaïm, L. Gautier, L. Grimaud, L. M. Harwood, V. Michaut., *Green Chemistry*, **2003**, 5 (4), 477–479.
- (153) M. A. Zolfigol, E. Kolvari, A. Abdoli, M. Shiri., *Molecular Diversity*, **2010**, 14 (4), 809–813.
- (154) L. el Kaïm, L. Grimaud, S. Hadrot., *Tetrahedron Letters*, **2006**, 47 (23), 3945–3947.
- (155) K. Wang, D. Kim, A. Dömling., *Journal of Combinatorial Chemistry*, **2010**, 12 (1), 111–118.
- (156) P. Nun, J. Martinez, F. Lamaty., *Synthesis (Stuttg)*, **2010**, 2010 (12), 2063–2068.
- (157) J. Zimmermann, B. Ondruschka, A. Stark., *Organic Process Research and Development*, **2010**, 14 (5), 1102–1109.
- (158) J. G. Lombardino, E. H. Wiseman., *J Med Chem*, **1974**, 17 (11), 1182–1188.
- (159) A. R. Phillips, H. L. White, S. Rosen., European Patent Application EP 58 8901; Chemical Abstracts, 98, 53894z; **1982**.
- (160) G. Şerban Andrei, B. F. Andrei, P. R. Roxana., *Mini-Reviews in Medicinal Chemistry*, **2021**, 21 (11), 1380–1392.
- (161) P. Sharma, C. Larosa, J. Antwi, R. Govindarajan, K. A. Werbovetz., *Molecules*, **2021**, 26 (14), 4213.
- (162) L. Zhang, X. M. Peng, G. L. V. Damu, R. X. Geng, C. H. Zhou., *Med Res Rev*, **2014**, 34 (2), 340–437.
- (163) H. C. Steel, G. R. Tintinger, R. Anderson., *Chemical Biology & Drug Design*, **2008**, 72 (3), 225–228.
- (164) T. G. Edwards, C. Fisher., *Antiviral Research*, **2018**, 152, 68–75.
- (165) P. R. Sawyer, R. N. Brogden, K. M. Pinder, T. M. Speight, G. S. Avery., *Drugs*, **1975**, 9 (6), 424–447.
- (166) R. C. Heel, R. N. Brogden, A. Carmine, P. A. Morley, T. M. Speight, G. S. Avery., *Drugs*, **1982**, 23 (1–2), 1–36.
- (167) D. S. Strand, D. Kim, D. A. Peura., *Gut and Liver*, **2017**, 11 (1), 27–37.
- (168) Y. Chen, S. Cui, H. Lin, Z. Xu, W. Zhu, L. Shi, R. Yang, R. Wang, Y. Dai., *International Journal of Impotence Research*, **2012**, 24 (6), 217–220.

- (169) P. Blankestijn, H. Rupp., *Cardiovascular & Hematological Agents in Medicinal Chemistry*, **2008**, 6 (4), 253–257.
- (170) S. L. Abrahams, R. J. Hazen, A. G. Batson, A. P. Phillips., *Journal of Pharmacology and Experimental Therapeutics*, **1989**, 249 (2), 359–365.
- (171) M. Holeček., *Nutrients* , **2020**, 12 (3), 848.
- (172) L. Maintz, N. Novak., *The American Journal of Clinical Nutrition*, **2007**, 85 (5), 1185–1196.
- (173) D. P. Patel, S. M. Swink, L. Castelo-Soccio., *Skin Appendage Disorders*, **2017**, 3 (3), 166–169.
- (174) Z. Haghighijoo, O. Firuzi, S. Meili, N. Edraki, M. Khoshneviszadeh, R. Miri., *Iranian Journal of Pharmaceutical Research*, **2020**, 19 (1), 181–191.
- (175) F. Mostaghni, H. Shafiekhani, N. Madadi Mahani., *Acta Chimica Slovenica*, **2022**, 69 (1), 91–97.
- (176) L. H. Al-Wahaibi, B. G. M. Youssif, E. S. Taher, A. H. Abdelazeem, A. A. Abdelhamid, A. A. Marzouk., *Molecules*, **2021**, 26 (16), 4718.
- (177) L. L. Chang, K. L. Sidler, M. A. Cascieri, S. de Laszlo, G. Koch, B. Li, M. MacCoss, N. Mantlo, S. O’Keefe, M. Pang, A. Rolando, W. K. Hagmann., *Bioorg Med Chem Lett*, **2001**, 11 (18), 2549–2553.
- (178) T. F. Gallagher, S. M. Fier-Thompson, R. S. Garigipati, M. E. Sorenson, J. M. Smietana, D. Lee, P. E. Bender, J. C. Lee, J. T. Laydon, D. E. Griswold, M. C. Chabot-Fletcher, J. J. Breton, J. L. Adams., *Bioorganic & Medicinal Chemistry Letters*, **1995**, 5 (11), 1171–1176.
- (179) J. C. Lee, J. T. Laydon, P. C. McDonnell, T. F. Gallagher, S. Kumar, D. Green, D. McNulty, M. J. Blumenthal, J. R. Keys, S. W. Land Vatter, J. E. Strickler, M. M. McLaughlin, I. R. Siemens, S. M. Fisher, G. P. Livi, J. R. White, J. L. Adams, P. R. Young., *Nature*, **1994**, 372 (6508), 739–746.
- (180) M. S. Khan, S. A. Siddiqui, M. S. R. A. Siddiqui, U. Goswami, K. V. Srinivasan, M. I. Khan., *Chemical Biology & Drug Design*, **2008**, 72 (3), 197–204.
- (181) M. K. Kathiravan, A. B. Salake, A. S. Chothe, P. B. Dudhe, R. P. Watode, M. S. Mukta, S. Gadhwe., *Bioorganic & Medicinal Chemistry*, **2012**, 20 (19), 5678–5698.
- (182) T. Hussain, H. L. Siddiqui, M. Zia-ur-Rehman, M. Masoom Yasinzai, M. Parvez., *European Journal of Medicinal Chemistry*, **2009**, 44 (11), 4654–4660.
- (183) M. Tonelli, G. Paglietti, V. Boido, F. Sparatore, F. Marongiu, E. Marongiu, P. la Colla, R. Loddo., *Chemistry & Biodiversity*, **2008**, 5 (11), 2386–2401.

- (184) M. Tonelli, M. Simone, B. Tasso, F. Novelli, V. Boido, F. Sparatore, G. Paglietti, S. Pricl, G. Giliberti, S. Blois, C. Ibba, G. Sanna, R. Loddo, P. la Colla., *Bioorganic & Medicinal Chemistry*, **2010**, *18* (8), 2937–2953.
- (185) M. Tonelli, F. Novelli, B. Tasso, I. Vazzana, A. Sparatore, V. Boido, F. Sparatore, P. la Colla, G. Sanna, G. Giliberti, B. Busonera, P. Farci, C. Ibba, R. Loddo., *Bioorganic & Medicinal Chemistry*, **2014**, *22* (17), 4893–4909.
- (186) R. v. Shingalapur, K. M. Hosamani, R. S. Keri., *European Journal of Medicinal Chemistry*, **2009**, *44* (10), 4244–4248.
- (187) M. P. Wentland, D. M. Bailey, E. J. Alexander, M. J. Castaldi, R. A. Ferrari, M. H. Perrone, D. A. Luttinger, D. R. Haubrich., *Journal of Medicinal Chemistry*, **1987**, *30* (8), 1482–1489.
- (188) H. M. Refaat., *European Journal of Medicinal Chemistry*, **2010**, *45* (7), 2949–2956.
- (189) A. Leone-Bay, P. E. Timony, L. Green, L. Glaser., *Journal of Agricultural and Food Chemistry*, **1986**, *34* (4), 733–736.
- (190) H. Takemura, J. H. Choi, N. Matsuzaki, Y. Taniguchi, J. Wu, H. Hirai, R. Motohashi, T. Asakawa, K. Ikeuchi, M. Inai, T. Kan, H. Kawagishi., *Scientific Reports*, **2019**, *9* (1), 1–8.
- (191) H. J. Zhu, J. S. Wang, K. S. Patrick, J. L. Donovan, C. L. DeVane, J. S. Markowitz., *Journal of Chromatography B: Anal. Technol. Biomed. Life Sci.*, **2007**, *858* (1–2), 91–95.
- (192) Y. F. Sun, W. Huang, C. G. Lu, Y. P. Cui., *Dyes and Pigments*, **2009**, *81* (1), 10–17.
- (193) M. Stähelin, D. M. Burland, M. Ebert, R. D. Miller, B. A. Smith, R. J. Twieg, W. Volksen, C. A. Walsh., *Applied Physics Letters*, **1992**, *61* (14), 1628.
- (194) M. A. Babizhayev., *Life Sciences*, **2006**, *78* (20), 2343–2357.
- (195) J. v. Olsson, D. Hult, Y. Cai, S. García-Gallego, M. Malkoch., *Polymer Chemistry*, **2014**, *5* (23), 6651–6655.
- (196) L. Chen, B. Zhao, Z. Fan, X. Liu, Q. Wu, H. Li, H. Wang., *Journal of Agricultural and Food Chemistry*, **2018**, *66* (28), 7319–7327.
- (197) Z. Wang, P. Lu, S. Chen, Z. Gao, F. Shen, W. Zhang, Y. Xu, H. S. Kwok, Y. Ma., *Journal of Materials Chemistry*, **2011**, *21* (14), 5451–5456.
- (198) K. Mutoh, J. Abe., *Journal of Physical Chemistry A*, **2011**, *115* (18), 4650–4656.
- (199) M. M. Antonijevic, M. B. Petrovic., *International Journal of Electrochemical Science*, **2008**, *3* (1), 1–28.



- (200) A. Griffin, K. R. Hamling, K. Knupp, S. G. Hong, L. P. Lee, S. C. Baraban., *Brain*, **2017**, *140* (3), 669–683.
- (201) U. Eilers, J. Klumperman, H. P. Hauri., *Journal of Cell Biology*, **1989**, *108* (1), 13–22.
- (202) M. E. Suarez-Almazor, C. Spooner, E. Belseck., *Cochrane Database of Systematic Reviews*; (4):*CD001461*, **2000**, 2010 (1).
- (203) C. Li, X. Han., *Nanoscale Research Letters*, **2020**, *15* (1), 1–10.
- (204) W. Xiong, Z. Guo, B. Zeng, T. Wang, X. Zeng, W. Cao, D. Lian., *Frontiers in Bioengineering and Biotechnology*, **2022**, *10*, 136.
- (205) J. Jayram, V. Jeena., *RSC Advances*, **2018**, *8* (66), 37557–37563.
- (206) F. R. Japp, H. H. Robinson., *Berichte der deutschen chemischen Gesellschaft*, **1882**, *15* (1), 1268–1270.
- (207) L. M. Wang, Y. H. Wang, H. Tian, Y. F. Yao, J. H. Shao, B. Liu., *Journal of Fluorine Chemistry*, **2006**, *127* (12), 1570–1573.
- (208) M. Kidwai, P. Mothra, V. Bansal, R. K. Somvanshi, A. S. Ethayathulla, S. Dey, T. P. Singh., *Journal of Molecular Catalysis A: Chemical*, **2007**, *265* (1–2), 177–182.
- (209) M. M. Heravi, K. Bakhtiari, H. A. Oskooie, S. Taheri., *Journal of Molecular Catalysis A: Chemical*, **2007**, *263* (1–2), 279–281.
- (210) A. F. Mohammed, N. D. Kokare, J. N. Sangshetti, D. B. Shinde., *Journal of the Korean Chemical Society*, **2007**, *51* (5), 418–422.
- (211) J. N. Sangshetti, N. D. Kokare, S. A. Kotharkara, D. B. Shinde., *Journal of Chemical Sciences*, **2008**, *120* (5), 463–467.
- (212) L. S. Gadekar, S. R. Mane, S. S. Katkar, B. R. Arbad, M. K. Lande., *Central European Journal of Chemistry*, **2009**, *7* (3), 550–554.
- (213) A. Yasodha, A. Sivakumar, G. Arunachalam, A. Puratchikody., *Journal of Pharmaceutical Science and Research*, **2009**, *1* (4), 127–130.
- (214) B. P. Bandgar, B. S. Hote, B. L. Korbad, S. A. Patil., *E-Journal of Chemistry*, **2011**, *8* (3), 1339–1345.
- (215) J.-T. Li, B.-H. Chen, Y.-W. Li, X.-L. Sun., *International Journal of Advances in Pharmacy, Biology and Chemistry (IJAPBC)*, **2012**, *1* (3), 287–292.
- (216) S. D. Burungale, M. J. Bhitre., *International Journal of Pharmaceutical Sciences and Research (IJPSR)*, **2013**, *4* (10), 4051–4057.

- (217) P. D. Sanasi, D. Santhipriya, Y. Ramesh, M. R. Kumar, B. Swathi, K. J. Rao., *Journal of Chemical Sciences*, **2014**, 126 (6), 1715–1720.
- (218) J. Madhavi, S. Anita, M. Suresh, P. U. Rani., *Indian Journal of Research in Pharmacy and Biotechnology*, **2015**, 3 (2), 157–160.
- (219) N. Chouha, T. Boumoud, I. Tebabel, B. Boumoud, A. Debache., *Der Pharma Chemica*, **2018**, 8 (4), 202–206.
- (220) V. D. Patil, N. R. Sutar, K. P. Patil., *Journal of Chemical and Pharmaceutical Research*, **2016**, 8 (7), 728–732.
- (221) V. D. Patil, N. R. Sutar, K. P. Patil, P. Giddh., *Der ChemicaSinica*, **2016**, 7 (2), 23–28.
- (222) A. Parveen, M. R. S. Ahmed, K. A. Shaikh, S. P. Deshmukh, R. P. Pawar., *ARKIVOC*, **2007**, 2007 (16), 12–18.
- (223) R. Wang, C. Liu, G. Luo., *Green Chemistry Letters and Reviews*, **2010**, 3 (2), 101–104.
- (224) B. Karami, K. Eskandari, A. Ghasemi., *Turkish Journal of Chemistry*, **2012**, 36 (4), 601–613.
- (225) B. F. Mirjalili, A. Bamoniri, N. Mohaghegh., *Current Chemistry Letters*, **2013**, 2 (1), 35–42.
- (226) B. Maleki, H. K. Shirvan, F. Taimazi, E. Akbarzadeh, B. Maleki, H. K. Shirvan, F. Taimazi, E. Akbarzadeh., *International Journal of Organic Chemistry*, **2012**, 2 (1), 93–99.
- (227) B. F. Mirjalili, A. Bamoniri, M. A. Mirhoseini., *Scientia Iranica*, **2013**, 20 (3), 587–591.
- (228) J. Banothu, R. Gali, R. Velpula, R. Bavantula., *Arabian Journal of Chemistry*, **2017**, 10 (2), S2754–S2761.
- (229) G. Brahmachari, S. Das., *Indian Journal of Chemistry*, **2013**, 52 (B), 387–393.
- (230) A. A. Marzouk, S. Kamel Mohamed, V. M. Abbasov, A. H. Talybov., *World Journal of Organic Chemistry*, **2013**, 1 (1), 6–10.
- (231) P. v Maske, S. J. Makhija., *Asian Journal of Biomedical and Pharmaceutical Sciences*, **2013**, 3 (20), 63–65.
- (232) K. Nikoofar, M. Haghghi, M. Lashanizadegan, Z. Ahmadvand., *Journal of Taibah University for Science*, **2015**, 9 (4), 570–578.
- (233) M. Vosoughi, F. Mohebali, A. Pesaran, S. Bonakdar, H. A. Lordegani, A. R. Massah., *Bulgarian Chemical Communications*, **2015**, 47 (2), 607–612.

- (234) G. Mohammadi Ziarani, A. Badiei, N. Lashgari, Z. Farahani., *Journal of Saudi Chemical Society*, **2016**, 20 (4), 419–427.
- (235) M. Alikarami, M. Amozad., *Bull Chem Soc Ethiop*, **2017**, 31 (1), 177–184.
- (236) B. Alimenla, A. Kumar, L. Jamir, D. Sinha, U. B. Sinha., *Radiation Effects and Defects in Solids*, **2007**, 161 (12), 687–693.
- (237) C. R. Strauss, R. W. Trainor., *Australian Journal of Chemistry*, **1995**, 48 (10), 1665–1692.
- (238) J. L. Krstenansky, I. Cotterill., *Curr Opin Drug Discov Devel*, **2000**, 3 (4), 454–461.
- (239) A. Lew, P. O. Krutzik, M. E. Hart, A. R. Chamberlin., *Journal of Combinatorial Chemistry*, **2002**, 4 (2), 95–105.
- (240) S. Balalaie, A. Arabanian, M. S. Hashtroudi., *Monatshefte für Chemie*, **2000**, 131 (9), 945–948.
- (241) S. E. Wolkenberg, D. D. Wisnoski, W. H. Leister, Y. Wang, Z. Zhao, C. W. Lindsley., *Organic Letters*, **2004**, 6 (9), 1453–1456.
- (242) K. Shelke, G. Kakade, B. Shingate, M. Shingare., *Rasayan Journal of Chemistry*, **2008**, 1 (3), 489–494.
- (243) S. v. Nalage, M. B. Kalyankar, V. S. Patil, S. v. Bhosale, S. U. Deshmukh, R. P. Pawar., *Open Catalysis Journal*, **2010**, 3 (1), 58–61.
- (244) J. Safari, S. D. Khalili, S. H. Banitaba., *Journal of Chemical Sciences*, **2010**, 122 (3), 437–441.
- (245) K. F. Shelke, S. B. Sapkal, G. K. Kakade, B. B. Shingate, M. S. Shingare., *Green Chemistry Letters and Reviews*, **2010**, 3 (1), 27–32.
- (246) E. Chauveau, C. Marestin, F. Schiets, R. Mercier., *Green Chemistry*, **2010**, 12 (6), 1018–1022.
- (247) Z. Gordi, M. Vazan., *Journal of Particle Science & Technology*, **2015**, 1 (4), 253–263.
- (248) R. B. Sparks, A. P. Combs., *Organic Letters*, **2004**, 6 (14), 2473–2475.
- (249) J. Zhang, T. Q. Zhao, Y. Chen, X. D. Chen, H. K. Chang, Y. M. Zhang, S. C. Hua., *Chemical Papers*, **2017**, 69 (2), 325–338.
- (250) J. F. Zhou, Y. Z. Song, Y. L. Yang, Y. L. Zhu, S. J. Tu., *Synthetic Communications*, **2006**, 35 (10), 1369–1373.
- (251) K. M. El-Shaieb., *Heteroatom Chemistry*, **2006**, 17 (5), 365–368.

- (252) S. Puri, B. Kaur, A. Parmar, H. Kumar., *Current Organic Chemistry*, **2013**, *17* (16), 1790–1828.
- (253) K. F. Shelke, S. B. Sapkal, S. S. Sonar, B. R. Madje, B. B. Shingate, M. S. Shingare., *Bull Korean Chem Soc*, **2009**, *30* (5), 1057–1060.
- (254) K. F. Shelke, S. B. Sapkal, M. S. Shingare., *Chinese Chemical Letters*, **2009**, *20* (3), 283–287.
- (255) H. Zang, Q. Su, Y. Mo, B. W. Cheng, S. Jun., *Ultrasonics Sonochemistry*, **2010**, *17* (5), 749–751.
- (256) D. Nagargoje, P. Mandhane, S. Shingote, P. Badadhe, C. Gill., *Ultrasonics Sonochemistry*, **2012**, *19* (1), 94–96.
- (257) J. Safari, Z. Zarnegar., *Ultrasonics Sonochemistry*, **2013**, *20* (2), 740–746.
- (258) P. D. Sanasi, R. K. Majji, S. Bandaru, S. Bassa, S. Pinninti, S. Vasamsetty, R. B. Korupolu, P. D. Sanasi, R. K. Majji, S. Bandaru, S. Bassa, S. Pinninti, S. Vasamsetty, R. B. Korupolu., *Modern Research in Catalysis*, **2016**, *5* (1), 31–44.
- (259) M. Esmaeilpour, J. Javidi, F. Dehghani, S. Zahmatkesh., *Research on Chemical Intermediates*, **2017**, *43* (1), 163–185.
- (260) E. Eidi, M. Z. Kassae, Z. Nasresfahani., *Applied Organometallic Chemistry*, **2016**, *30* (7), 561–565.
- (261) B. S. Londhe, S. L. Khillare, A. M. Nalawade, R. A. Mane., *International Journal of Research in Engineering and Science (IJRES)*, **2021**, *9* (1), 79–84.
- (262) C. O. Kappe., *European Journal of Medicinal Chemistry*, **2000**, *35* (12), 1043–1052.
- (263) H. Cernecka, L. Veizerova, L. Mensikova, J. Svetlik, P. Krenek., *Journal of Pharmacy and Pharmacology*, **2012**, *64* (5), 735–741.
- (264) D. Kumarasamy, B. G. Roy, J. Rocha-Pereira, J. Neyts, S. Nanjappan, S. Maity, M. Mookerjee, L. Naesens., *Bioorganic & Medicinal Chemistry Letters*, **2017**, *27* (2), 139–142.
- (265) R. Kaur, S. Chaudhary, K. Kumar, M. K. Gupta, R. K. Rawal., *European Journal of Medicinal Chemistry*, **2017**, *132*, 108–134.
- (266) M. Marinescu., *Molecules*, **2021**, *26* (19), 6022.
- (267) J. M. Wetzel, S. W. Miao, C. Forray, L. A. Borden, T. A. Brancheck, C. Gluchowski., *Journal of Medicinal Chemistry*, **1995**, *38* (10), 1579–1581.
- (268) P. A. Halim, R. A. Hassan, K. O. Mohamed, S. O. Hassanin, M. G. Khalil, A. M. Abdou, E. O. Osman., *Journal of Enzyme Inhibition and Medicinal Chemistry*, **2022**, *37* (1), 189–201.

- (269) M. Salmón, R. Osnaya, L. Gómez, G. Arroyo, F. Delgado, R. Miranda., *Revista de la Sociedad Química de México*, **2001**, 45 (4), 206–207.
- (270) S. A. Haque, T. P. Hasaka, A. D. Brooks, P. v. Lobanov, P. W. Baas., *Cell Motility and the Cytoskeleton*, **2004**, 58 (1), 10–16.
- (271) C. Pothiraj, A. S. Velan, J. Joseph, N. Raman., *Mycobiology*, **2008**, 36 (1), 69.
- (272) K. S. Atwal, B. N. Swanson, S. E. Unger, D. M. Floyd, S. Moreland, A. Hedberg, B. C. O'Reilly., *Journal of Medicinal Chemistry*, **1991**, 34 (2), 806–811.
- (273) E. Ramu, V. Kotra, N. Bansal, R. Varala, S. R. Adapa., *Rasayan Journal of Chemistry*, **2008**, 1 (1), 188–194.
- (274) F. Cohen, L. E. Overman, S. K. Ly Sakata., *Organic Letters*, **1999**, 1 (13), 2169–2172.
- (275) B. C. Ranu, A. Hajra, U. Jana., *Journal of Organic Chemistry*, **2000**, 65 (19), 6270–6272.
- (276) R. S. Bhosale, S. v. Bhosale, S. v. Bhosale, T. Wang, P. K. Zubaidha., *Tetrahedron Letters*, **2004**, 45 (49), 9111–9113.
- (277) E. Rafiee, H. Jafari., *Bioorganic & Medicinal Chemistry Letters*, **2006**, 16 (9), 2463–2466.
- (278) R. Gupta, S. Paul, R. Gupta., *Journal of Molecular Catalysis A: Chemical*, **2007**, 266 (1–2), 50–54.
- (279) Suresh, A. Saini, D. Kumar, J. S. Sandhu., *Green Chemistry Letters and Reviews*, **2009**, 2 (1), 29–33.
- (280) H. Eshghi, A. Javid, A. Khojastehnezhad, F. Moeinpour, F. F. Bamoharram, M. Bakavoli, M. Mirzaei., *Chinese Journal of Catalysis*, **2015**, 36 (3), 299–307.
- (281) Z. Benzekri, R. Benhdidou, S. Hamia, H. Serrar, S. Boukhris, B. Sallek, A. Hassikou, A. Souizi., *J Mex Chem Soc*, **2017**, 61 (3), 217–221.
- (282) S. Prakash, N. Elavarasan, A. Venkatesan, K. Subashini, M. Sowndharya, V. Sujatha., *Advanced Powder Technology*, **2018**, 29 (12), 3315–3326.
- (283) S. Farooq, F. A. Alharthi, A. Alsalme, A. Hussain, B. A. Dar, A. Hamid, S. Koul., *RSC Advances*, **2020**, 10 (69), 42221–42234.
- (284) C. J. Liu, J. de Wang., *Molecules*, **2009**, 14 (2), 763–770.
- (285) S. K. Prajapati, K. K. Gupta, B. N. Babu., *Journal of Chemical Sciences*, **2015**, 127 (6), 1047–1052.
- (286) P. Bigenelli., *Gazzetta Chimica Italiana*, **1893**, 23 (1), 360–413.

- (287) T. U. Mayer, T. M. Kapoor, S. J. Haggarty, R. W. King, S. L. Schreiber, T. J. Mitchison., *Science (1979)*, **1999**, 286 (5441), 971–974.
- (288) K. Folkers, H. J. Harwood, B. J. Treat., *J Am Chem Soc*, **1932**, 54 (9), 3751–3758.
- (289) Z. L. Shen, X. P. Xu, S. J. Ji., *Journal of Organic Chemistry*, **2010**, 75 (4), 1162–1167.
- (290) K.-Y. Lee, K.-Y. Ko., *Bull Korean Chem Soc*, **2004**, 25 (12), 1929–1931.
- (291) M. Kamal Raj, H. S. P. Rao, S. G. Manjunatha, R. Sridharan, S. Nambiar, J. Keshwan, J. Rappai, S. Bhagat, B. S. Shwetha, D. Hegde, U. Santhosh., *Tetrahedron Letters*, **2011**, 52 (28), 3605–3609.
- (292) A. Debache, M. Amimour, A. Belfaitah, S. Rhouati, B. Carboni., *Tetrahedron Letters*, **2008**, 49 (42), 6119–6121.
- (293) M. Kamali, A. Shockravi, M. S. Doost, S. E. Hooshmand., *Cogent Chemistry*, **2015**, 1 (1), 1081667.
- (294) B. S. Surendra, K. S. Prasad, T. R. S. Shekhar, A. A. Jahagirdar, S. C. Prashantha, N. Raghavendra, K. Gurushantha, N. Basavaraju, K. Rudresha., *Journal of Photochemistry and Photobiology*, **2021**, 8, 100063.
- (295) M. Mittersteiner, F. F. S. Farias, H. G. Bonacorso, M. A. P. Martins, N. Zanatta., *Ultrasonics Sonochemistry*, **2021**, 79, 105683.
- (296) K. S. Atwal, B. N. Swanson, S. E. Unger, D. M. Floyd, S. Moreland, A. Hedberg, B. C. O'Reilly., *Journal of Medicinal Chemistry*, **1991**, 34 (2), 806–811.
- (297) J. C. Barrow, P. G. Nantermet, H. G. Selnick, K. L. Glass, K. E. Rittle, K. F. Gilbert, T. G. Steele, C. F. Homnick, R. M. Freidinger, R. W. Ransom, P. Kling, D. Reiss, T. P. Broten, T. W. Schorn, R. S. L. Chang, S. S. O'Malley, T. v. Olah, J. D. Ellis, A. Barrish, K. Kassahun, P. Leppert, D. Nagarathnam, C. Forray., *Journal of Medicinal Chemistry*, **2000**, 43 (14), 2703–2718.
- (298) A. Shahid, N. S. Ahmed, T. S. Saleh, S. A. Al-Thabaiti, S. N. Basahel, W. Schwieger, M. Mokhtar., *Catalysts*, **2017**, 7 (3), 84.
- (299) H. Adibi, H. A. Samimi, M. Beygzadeh., *Catalysis Communications*, **2007**, 8 (12), 2119–2124.
- (300) B. C. Ranu, A. Hajra, S. S. Dey., *Organic Process Research and Development*, **2002**, 6 (6), 817–818.
- (301) F. Dong, L. Jun, Z. Xinli, Y. Zhiwen, L. Zuliang., *Journal of Molecular Catalysis A: Chemical*, **2007**, 274 (1–2), 208–211.
- (302) S. L. Jain, S. Singhal, B. Sain., *Green Chemistry*, **2007**, 9 (7), 740–741.

- (303) S. Verma, S. L. Jain, B. Sain., *Tetrahedron Letters*, **2010**, 51 (52), 6897–6900.
- (304) S. Patil, S. D. Jadhav, M. B. Deshmukh., *Archives of Applied Science Research*, **2011**, 3 (1), 203–208.
- (305) S. Patil, S. D. Jadhav, S. Y. Mane., *International Journal of Organic Chemistry*, **2011**, 1 (3), 125–131.
- (306) J. Lal, M. Sharma, S. Gupta, P. Parashar, P. Sahu, D. D. Agarwal., *Journal of Molecular Catalysis A: Chemical*, **2012**, 352, 31–37.
- (307) N. Azizi, S. Dezfuli, M. M. Hahsemi., *The Scientific World Journal*, **2012**, 2012 (Article ID 908702), 1–6.
- (308) H. Sachdeva, D. Dwivedi., *The Scientific World Journal*, **2012**, 2012 (Article ID 109432), 1–9.
- (309) A. Borse, M. Patil, N. Patil, R. Shinde., *ISRN Organic Chemistry*, **2012**, 2012 (Article ID 415645), 1–6.
- (310) M. Dewan, A. Kumar, A. Saxena, A. De, S. Mozumdar., *PLOS ONE*, **2012**, 7 (8), 1–8.
- (311) Z. Karimi-Jaberi, M. S. Moaddeli., *ISRN Organic Chemistry*, **2012**, 2012 (Article ID 474626), 1–4.
- (312) B. Mirjalili, L. Zamani., *South African Journal of Chemistry*, **2015**, 67 (1), 21–26.
- (313) Y. Zhang, B. Wang, X. Zhang, J. Huang, C. Liu., *Molecules*, **2015**, 20 (3), 3811–3820.
- (314) V. v Dabholkar, K. S. Badhe, S. K. Kurade., *Current Chemistry Letters*, **2017**, 6, 77–90.
- (315) M. Nasr-Esfahani, M. Taci., *RSC Advances*, **2015**, 5 (56), 44978–44989.
- (316) L. Z. Fekri, M. Nikpassand, M. Movaghari., *Bull Chem Soc Ethiop*, **2017**, 31 (2), 313–321.
- (317) H. Yuan, K. Zhang, J. Xia, X. Hu, S. Yuan., *Cogent Chemistry*, **2017**, 3 (1), 1318692.
- (318) T. S. Choudhare, D. S. Wagare, V. T. Kadam, A. A. Kharpe, P. D. Netankar., *Polycyclic Aromatic Compounds*, **2021**, 0:0, 1–8.
- (319) C. Simon, T. Constantieux, J. Rodriguez., *European Journal of Organic Chemistry*, **2004**, 2004 (24), 4957–4980.
- (320) A. K. Misra, G. Agnihotri, S. K. Madhusudan., *ChemInform*, **2005**, 36 (2).
- (321) V. Polshettiwar, R. S. Varma., *Tetrahedron Letters*, **2007**, 48 (41), 7343–7346.

- (322) H. R. Shaterian, A. Hosseinian, M. Ghashang, F. Khorami, N. Karimpoor., *Phosphorus, Sulphur, and Silicon and the Related Elements*, **2009**, *184* (9), 2333–2338.
- (323) H. W. Zhan, J. X. Wang, X. T. Wang., *Chinese Chemical Letters*, **2008**, *19* (10), 1183–1185.
- (324) D. Kumar, S. Suresh, J. S. Sandhu., *ChemInform*, **2010**, *41* (30).
- (325) K. K. Pasunooti, H. Chai, C. N. Jensen, B. K. Gorityala, S. Wang, X. W. Liu., *Tetrahedron Letters*, **2011**, *52* (1), 80–84.
- (326) A. Kuraitheerthakumaran, S. Pazhamalai, M. Gopalakrishnan., *Arabian Journal of Chemistry*, **2016**, *9* (Supplement 1), S461–S465.
- (327) R. K. Sharma, D. Rawat., *Inorganic Chemistry Communications*, **2012**, *17*, 58–63.
- (328) V. Srivastava., *Green and Sustainable Chemistry*, **2013**, *3* (2A), 38–40.
- (329) M. Shingare, S. Dhanmane., *Chemistry and Materials Research*, **2015**, *7* (3), 27–31.
- (330) T. Pramanik, S. K. Padan., *International Journal of Pharmacy and Pharmaceutical Sciences*, **2016**, *8* (3), 396–398.
- (331) L. Moradi, M. Tadayon., *Journal of Saudi Chemical Society*, **2018**, *22* (1), 66–75.
- (332) T. J. Mason, J. Phillip. Lorimer., *Applied Sonochemistry: The Uses of Power Ultrasound in Chemistry and Processing*; Wiley-VCH: New York, **2003**.
- (333) A. Kotronarou, G. Mills, M. R. Hoffmann., *Journal of Physical Chemistry*, **1991**, *95* (9), 3630–3638.
- (334) M. S. Zhidovinova, O. v. Fedorova, G. L. Rusinov, I. G. Ovchinnikova., *Russian Chemical Bulletin*, **2003**, *52* (11), 2527–2528.
- (335) J. T. Li, J. F. Han, J. H. Yang, T. S. Li., *Ultrasonics Sonochemistry*, **2003**, *10* (3), 119–122.
- (336) J. S. Yadav, B. V. S. Reddy, K. B. Reddy, K. S. Raj, A. R. Prasad., *Journal of the Chemical Society, Perkin Transactions 1*, **2001**, *Issue 16*, 1939–1941.
- (337) H. A. Stefani, C. B. Oliveira, R. B. Almeida, C. M. P. Pereira, R. C. Braga, R. Cella, V. C. Borges, L. Savegnago, C. W. Nogueira., *European Journal of Medicinal Chemistry*, **2006**, *41* (4), 513–518.
- (338) C. J. Liu, J. de Wang., *Molecules*, **2010**, *15* (4), 2087–2095.
- (339) Z.-P. Lin, J.-S. Wang, J.-T. Li., *Letters in Organic Chemistry*, **2006**, *3* (7), 523–525.



- (340) A. Khanum, R.-R. Khan, M. M. M. A. Pasha., *Universal Journal of Pharmaceutical Research*, **2021**, 6 (5), 46–51.
- (341) V. S. Mityanov, A. v. Kutasevich, M. M. Krayushkin, B. v. Lichitsky, A. A. Dudinov, A. N. Komogortsev, T. Y. Koldaeva, V. P. Perevalov., *Tetrahedron*, **2017**, 73 (47), 6669–6675.
- (342) N. Xi, Q. Huang, L. Liu., In *Comprehensive Heterocyclic Chemistry III (Chap. 4.02 - Imidazoles)*; Katritzky, A. R., Ramsden, C. A., Scriven, E. F. V., Taylor, R. J. K., Eds.; Elsevier Science: New York, **2008**; Vol. 4, pp 143–364.
- (343) G. V. Nikitina, M. S. Pevzner., *Chemistry of Heterocyclic Compounds*, **1993**, 29 (2), 127–151.
- (344) T. R. Jensen, C. P. Schaller, M. A. Hillmyer, W. B. Tolman., *Journal of Organometallic Chemistry*, **2005**, 690 (24–25), 5881–5891.
- (345) G. Mloston, M. Celeda, M. Jasinski, K. Urbaniak, P. J. Boratynski, P. R. Schreiner, H. Heimgartner., *Molecules*, **2019**, 24 (23), 4398.
- (346) Y. Wang, L. Zhang., *Synthesis (Stuttg)*, **2015**, 47 (03), 289–305.
- (347) R. Kuhn, W. Blau., *Justus Liebigs Ann Chem*, **1958**, 615 (1), 99–107.
- (348) A. K. Sharma, S. N. Mazumdar, M. P. Mahajan., *Tetrahedron Letters*, **1993**, 34 (49), 7961–7964.
- (349) H. Cerecetto, A. Gerpe, M. González, Y. Fernández Sainz, O. E. Piro, E. E. Castellano., *Synthesis (Stuttg)*, **2004**, 2004 (16), 2678–2684.
- (350) P. Mucha, G. Mlostoń, M. Jasiński, A. Linden, H. Heimgartner., *Tetrahedron: Asymmetry*, **2008**, 19 (13), 1600–1607.
- (351) G. Mlostoń, P. Mucha, K. Urbaniak, K. Broda, H. Heimgartner., *Helvetica Chimica Acta*, **2008**, 91 (2), 232–238.
- (352) S. A. Amitina, A. Y. Tikhonov, I. A. Grigor'Ev, Y. V. Gatilov, B. A. Selivanov., *Chemistry of Heterocyclic Compounds*, **2009**, 45 (6), 691–697.
- (353) G. Mlostoń, M. Jasiński., *ARKIVOC*, **2010**, 2011 (6), 162–175.
- (354) V. S. Mityanov, V. P. Perevalov, I. I. Tkach., *Chemistry of Heterocyclic Compounds*, **2013**, 48 (12), 1793–1800.
- (355) K. Pradhan, B. K. Tiwary, M. Hossain, R. Chakraborty, A. K. Nanda., *RSC Advances*, **2016**, 6 (13), 10743–10749.
- (356) M. Gaba, S. Singh, C. Mohan., *European Journal of Medicinal Chemistry*, **2014**, 76, 494–505.

- (357) Y. Bansal, O. Silakari., *Bioorganic & Medicinal Chemistry*, **2012**, 20 (21), 6208–6236.
- (358) J. B. Bariwal, A. K. Shah, M. K. Kathiravan, R. S. Somani, J. R. Jagtap, K. S. Jain., *Indian Journal of Pharmaceutical Education and Research*, **2008**, 42 (3), 225–231.
- (359) C. Kuş, N. Altanlar., *Turkish Journal of Chemistry*, **2003**, 27 (1), 35–40.
- (360) Y. S. Chhonker, B. Veenu, S. R. Hasim, N. Kaushik, D. Kumar, P. Kumar., *E-Journal of Chemistry*, **2009**, 6 (Suppl. 1, Article ID 604203), S342.
- (361) R. Vinodkumar, S. D. Vaidya, B. V. Siva Kumar, U. N. Bhise, S. B. Bhirud, U. C. Mashelkar., *European Journal of Medicinal Chemistry*, **2008**, 43 (5), 986–995.
- (362) B. G. Mohamed, M. A.-A. Abdel-Alim, M. A. Hussein., *Acta Pharmaceutica*, **2006**, 56 (1), 31–48.
- (363) B. Dik, D. Coşkun, E. Bahçivan, K. Üney., *Turkish Journal of Medical Sciences*, **2021**, 51 (3), 1585.
- (364) M. S. Yar, M. M. Abdullah, J. Majeed., *World Academy of Science, Engineering and Technology*, **2009**, 55, 593–599.
- (365) Z. Kazimierczuk, J. A. Upcroft, P. Upcroft, A. Górska, B. Starościak, A. Laudy., *Acta Biochimica Polonica*, **2002**, 49 (1), 185–195.
- (366) Ş. Demirayak, U. Abu Mohsen, A. Çağrı Karaburun., *European Journal of Medicinal Chemistry*, **2002**, 37 (3), 255–260.
- (367) M. Faheem, A. Rathaur, A. Pandey, V. Kumar Singh, A. K. Tiwari., *ChemistrySelect*, **2020**, 5 (13), 3981–3994.
- (368) V. A. S. Pardeshi, N. S. Chundawat, S. I. Pathan, P. Sukhwal, T. P. S. Chundawat, G. P. Singh., *Synthetic Communications*, **2021**, 51 (4), 485–513.
- (369) M. M. Ramla, M. A. Omar, A. M. M. El-Khamry, H. I. El-Diwani., *Bioorganic & Medicinal Chemistry*, **2006**, 14 (21), 7324–7332.
- (370) R. Pedro Rothlin, H. Miguel Vetulli, M. Duarte, F. Germán Pelorosso., *Drug Development Research*, **2020**, 81 (7), 768–770.
- (371) H. Mostafavi, M. R. Islami, E. Ghonchepour, A. M. Tikdari., *Chemical Papers*, **2018**, 72 (12), 2973–2978.
- (372) D. Chianelli, N. Nikolaides., WO 2001058878 A1. **2002**.
- (373) S. Vasiliou., *Drugs of Today (Barcelona, Spain : 1998)*, **2011**, 47 (9), 647–651.
- (374) A. K. Petersen, P. H. Olesen, L. B. Christiansen, H. C. Hansen, F. E. Nielsen., US 7915299 B2. **2008**.

- (375) Y. Li, M. Kataoka, M. Tatsuta, K. Yasoshima, T. Yura, K. Urbahns, A. Kiba, N. Yamamoto, J. B. Gupta, K. Hashimoto., *Bioorganic & Medicinal Chemistry Letters*, **2005**, *15* (3), 805–807.
- (376) T. Ishida, T. Suzuki, S. Hirashima, K. Mizutani, A. Yoshida, I. Ando, S. Ikeda, T. Adachi, H. Hashimoto., *Bioorganic & Medicinal Chemistry Letters*, **2006**, *16* (7), 1859–1863.
- (377) H. Zarrinmayeh, A. M. Nunes, P. L. Ornstein, D. M. Zimmerman, M. B. Arnold, D. A. Schober, S. L. Gackenheimer, R. F. Bruns, P. A. Hippskind, T. C. Britton, B. E. Cantrell, D. R. Gehlert., *Journal of Medicinal Chemistry*, **1998**, *41* (15), 2709–2719.
- (378) D. N. Kommi, P. S. Jadhavar, D. Kumar, A. K. Chakraborti., *Green Chemistry*, **2013**, *15* (3), 798–810.
- (379) T. B. Nguyen, L. Ermolenko, A. Al-Mourabit., *Green Chemistry*, **2013**, *15* (10), 2713–2717.
- (380) J. E. R. Sadig, R. Foster, F. Wakenhut, M. C. Willis., *Journal of Organic Chemistry*, **2012**, *77* (21), 9473–9486.
- (381) F. Fache, E. Schulz, M. L. Tommasino, M. Lemaire., *Chemical Reviews*, **2000**, *100* (6), 2159–2231.
- (382) Y. Chen, F. Xu, Z. Sun., *RSC Advances*, **2017**, *7* (70), 44421–44425.
- (383) H. Sharma, N. Kaur, N. Singh, D. O. Jang., *Green Chemistry*, **2015**, *17* (8), 4263–4270.
- (384) J. B. Wright., *Chemical Reviews*, **1951**, *48* (3), 397–541.
- (385) R. Wang, X. xia Lu, X. qi Yu, L. Shi, Y. Sun., *Journal of Molecular Catalysis A: Chemical*, **2007**, *266* (1–2), 198–201.
- (386) P. Thapa, P. M. Palacios, T. Tran, B. S. Pierce, F. W. Foss., *J Org Chem*, **2020**, *85* (4), 1991–2009.
- (387) V. N. Mahire, P. P. Mahulikar., *Chinese Chemical Letters*, **2015**, *26* (8), 983–987.
- (388) V. Praneetha, S. U. Rani, K. Srinivas., *Asian Journal of Research in Chemistry*, **2016**, *9* (10), 468.
- (389) P. Saha, S. R. Brishty, S. M. A. Rahman., *Indian Journal of Pharmaceutical Sciences*, **2020**, *82* (2), 222–229.
- (390) K. Bahrami, M. M. Khodaei, A. Nejati., *Green Chemistry*, **2010**, *12* (7), 1237–1241.
- (391) Z. Y. Yu, J. Zhou, Q. S. Fang, L. Chen, Z. bin Song., *Chemical Papers*, **2016**, *70* (9), 1293–1298.

- (392) A. J. Blatch, O. v. Chetina, J. A. K. Howard, L. G. F. Patrick, C. A. Smethurst, A. Whiting., *Organic & Biomolecular Chemistry*, **2006**, 4 (17), 3297–3302.
- (393) S. Demirayak, I. Kayagil, L. Yurttas., *European Journal of Medicinal Chemistry*, **2011**, 46 (1), 411–416.
- (394) D. Yang, H. Fu, L. Hu, Y. Jiang, Y. Zhao., *Journal of Organic Chemistry*, **2008**, 73 (19), 7841–7844.
- (395) C. T. Brain, S. A. Brunton., *Tetrahedron Letters*, **2002**, 43 (10), 1893–1895.
- (396) M. L. di Gioia, R. Cassano, P. Costanzo, N. H. Cano, L. Maiuolo, M. Nardi, F. P. Nicoletta, M. Oliverio, A. Procopio., *Molecules*, **2019**, 24 (16), 2885.
- (397) G. Brasche, S. L. Buchwald., *Angewandte Chemie International Edition*, **2008**, 47 (10), 1932–1934.
- (398) P. Saha, T. Ramana, N. Purkait, M. A. Ali, R. Paul, T. Punniyamurthy., *Journal of Organic Chemistry*, **2009**, 74 (22), 8719–8725.
- (399) P. Saha, M. A. Ali, P. Ghosh, T. Punniyamurthy., *Organic & Biomolecular Chemistry*, **2010**, 8 (24), 5692–5699.
- (400) H. F. He, Z. J. Wang, W. Bao., *Advanced Synthesis & Catalysis*, **2010**, 352 (17), 2905–2912.
- (401) F. Wang, S. Cai, Q. Liao, C. Xi., *Journal of Organic Chemistry*, **2011**, 76 (9), 3174–3180.
- (402) J. Zhu, H. Xie, Z. Chen, S. Li, Y. Wu., *Chemical Communications*, **2009**, 17, 2338–2340.
- (403) W. Shen, T. Kohn, Z. Fu, X. Jiao, S. Lai, M. Schmitt., *Tetrahedron Letters*, **2008**, 49 (51), 7284–7286.
- (404) C. Siddappa, V. Kambappa, A. K. C. Siddegowda, K. S. Rangappa., *Tetrahedron Letters*, **2010**, 51 (50), 6493–6497.
- (405) K. Bahrami, M. Mehdi Khodaei, F. Naali., *Journal of Organic Chemistry*, **2008**, 73 (17), 6835–6837.
- (406) C. Chen, C. Chen, B. Li, J. Tao, J. Peng., *Molecules*, **2012**, 17 (11), 12506–12520.
- (407) S. Bonacci, G. Iriti, S. Mancuso, P. Novelli, R. Paonessa, S. Tallarico, M. Nardi., *Catalysts*, **2020**, 10 (8), 845.
- (408) A. Procopio, C. Celia, M. Nardi, M. Oliverio, D. Paolino, G. Sindona., *Journal of Natural Products*, **2011**, 74 (11), 2377–2381.

- (409) T. J. Mason., *Philosophical Transactions of the Royal Society of London. Series A: Mathematical, Physical and Engineering Sciences*, **1999**, 357 (1751), 355–369.
- (410) M. S. Estevão, C. A. M. Afonso., *Tetrahedron Letters*, **2017**, 58 (4), 302–304.
- (411) K. Das, A. Mondal, D. Srimani., *Journal of Organic Chemistry*, **2018**, 83 (16), 9553–9560.
- (412) Y. R. Girish, K. S. Sharath Kumar, K. N. Thimmaiah, K. S. Rangappa, S. Shashikanth., *RSC Advances*, **2015**, 5 (92), 75533–75546.
- (413) S. Majumdar, M. Chakraborty, N. Pramanik, D. K. Maiti., *RSC Advances*, **2015**, 5 (63), 51012–51018.
- (414) C. Kathing, N. G. Singh, J. World Star Rani, R. Nongrum, R. Nongkhlaw., *Russian Journal of Organic Chemistry*, **2020**, 56 (9), 1628–1634.
- (415) B. Vieira, A. Barcellos, R. Schumacher, E. Lenardao, D. Alves., *Current Green Chemistry*, **2014**, 1 (2), 136–144.
- (416) A. de la Hoz, À. Díaz-Ortiz, A. Moreno., *Chemical Society Reviews*, **2005**, 34 (2), 164–178.
- (417) M. Nardi, S. Bonacci, N. H. Cano, M. Oliverio, A. Procopio., *Molecules*, **2022**, 27 (5), 1751.
- (418) D. Azarifar, M. Pirhayati, B. Maleki, M. Sanginabadi, R. N. Yami., *Journal of the Serbian Chemical Society*, **2010**, 75 (9), 1181–1189.
- (419) A. P. Sarkate, S. D. Shinde, A. O. Barde, A. P. Sarkate., *International Journal of ChemTech Research*, **2015**, 8 (2), 496–500.
- (420) R. G. Jacob, L. G. Dutra, C. S. Radatz, S. R. Mendes, G. Perin, E. J. Lenardão., *Tetrahedron Letters*, **2009**, 50 (13), 1495–1497.
- (421) P. Bandyopadhyay, M. Sathe, G. K. Prasad, P. Sharma, M. P. Kaushik., *Journal of Molecular Catalysis A: Chemical*, **2011**, 341 (1–2), 77–82.
- (422) B. Kumar, K. Smita, L. Cumbal., *Journal of Chemical Sciences*, **2014**, 126 (6), 1831–1840.
- (423) L. J. Zhang, J. Xia, Y. Q. Zhou, H. Wang, S. W. Wang., *Synthetic Communications*, **2012**, 42 (3), 328–336.
- (424) V. M. Rao, A. S. Rao, S. S. Rani, S. Yaraswi, M. Pal., *Mini Reviews in Medicinal Chemistry*, **2018**, 18 (14), 1233–1239.
- (425) A. A. Patil, S. B. Kamble, G. S. Rashinkar, R. S. Salunkhe., *Chemical Science Review and Letters*, **2014**, 3 (10), 214–220.

- (426) S. H. Nile, B. Kumar, S. W. Park., *Arabian Journal of Chemistry*, **2015**, 8 (5), 685–691.
- (427) W. Liu, S. Gao, Ph. Zhang, X. Zhou, C. Wang., *Asian Journal of Chemistry*, **2014**, 26 (7), 1980–1982.
- (428) K. Godugu, V. D. Sri Yadala, M. K. Mohinuddin Pinjari, T. R. Gundala, L. R. Sanapareddy, C. G. Reddy Nallagondu., *Beilstein Journal of Organic Chemistry*, **2020**, 16 (1), 1881–1900.
- (429) P. C. Keller, M. A. Banks, S. K. Boocock, J. R. Wermer, S. H. Lawrence, S. G. Shore., *Inorganic Chemistry*, **1986**, 25 (3), 367–372.
- (430) N. N. Greenwood, J. D. Kennedy., *Pure and Applied Chemistry*, **1991**, 63 (3), 317–326.
- (431) R. N. Grimes, A. P. E. York, P. E. Rakita, B. J. Coe, C. Nataro, M. A. Ferguson, K. M. Bocage, B. J. Hess, V. J. Ross, D. T. Swarr, K. Chwee, D. Tan, K. Goh, L. S. Chia, D. F. Treagust, J. E. Mcgrady, R. J. P. Williams, J. J. R. Fraústo Da Silva., *Journal of Chemical Education*, **2004**, 81 (5), 657–672.
- (432) H. Braunschweig, C. Kollann, D. Rais., *Angewandte Chemie International Edition*, **2006**, 45 (32), 5254–5274.
- (433) P. Becker., *Advanced Materials*, **1998**, 10 (13), 979–992.
- (434) Q. Li, F. Xue, T. C. W. Mak., *Inorganic Chemistry*, **1999**, 38 (18), 4142–4145.
- (435) H. Doweidar., *Journal of Materials Science*, **1990**, 25 (1), 253–258.
- (436) W. Vogel., *Glass Chemistry*; Springer-Verlag: Berlin Heidelberg, **1994**.
- (437) A. Thulasiramudu, S. Buddhudu., *Journal of Quantitative Spectroscopy and Radiative Transfer*, **2006**, 102 (2), 212–227.
- (438) B. H. Rudramadevi, S. Buddhudu., *Ferroelectrics Letters Section*, **2009**, 36 (3–4), 82–91.
- (439) V. Naresh, S. Buddhudu., *Ferroelectrics*, **2012**, 437 (1), 110–125.
- (440) X. X. Shi, X. J. Liu, L. J. Yuan., *Advanced Materials Research*, **2011**, Vol. 236-238, 876–879.
- (441) S. Li, L. Xu, Y. Zhai, H. Yu., *RSC Advances*, **2014**, 4 (16), 8245–8249.
- (442) P. Pascuta, R. Lungu, I. Ardelean., *Journal of Materials Science: Materials in Electronics*, **2010**, 21 (6), 548–553.
- (443) N. J. Kreidl., *Journal of Non-Crystalline Solids*, **1990**, 123 (1–3), 377–384.

- (444) C. L. Christ, J. R. Clark., *Physics and Chemistry of Minerals*, **1977**, 2 (1), 59–87.
- (445) P. C. Burns, J. D. Grice, F. C. Hawthorne., **1995**, 33, 1131–1151.
- (446) L. Cui, W. Zhang, R. Zheng, J. Liu., *Chemistry – A European Journal*, **2020**, 26 (51), 11661–11672.
- (447) K. Saha, S. Ghosh., *Dalton Transactions*, **2022**, 51 (7), 2631–2640.
- (448) N. Wang, A. Xu, P. Ou, S. F. Hung, A. Ozden, Y. R. Lu, J. Abed, Z. Wang, Y. Yan, M. J. Sun, Y. Xia, M. Han, J. Han, K. Yao, F. Y. Wu, P. H. Chen, A. Vomiero, A. Seifitokaldani, X. Sun, D. Sinton, Y. Liu, E. H. Sargent, H. Liang., *Nature Communications*, **2021**, 12 : 6089, 1–9.

## CHAPTER-II

### Experimental Section

#### **2.1 General Remarks**

The commercially available chemicals/reagents have been used without further purification and purification of some of the chemicals/reagents were performed only under specific requirements. The reagents required for the proposed work has been procured from the various chemical companies and suppliers such as Acros, Merck, Sigma Aldrich, Thomas Baker, Lab India, Avra etc. The glassware employed for all the works has been cleaned thoroughly and dried in an oven prior to the use.

#### **2.2 General procedure for the synthesis of different N-containing heterocyclic derivatives.**

We followed the green methodology for the synthesis of some selected N-containing heterocyclic compounds viz. 2,4,5-triaryl imidazole, 3, 4-dihydropyrimidin-2(1*H*)-one, 1-hydroxyimidazole 3-oxide and 1,2-disubstituted benzimidazoles utilizing the solvent free approach. In a typical solvent free reaction, the specific reactants and the catalyst were pulverized thoroughly in an agate mortar and pestle to make a homogenous mixture. The reaction mixture was then transferred into a test tube (20mL, Borosil glass) and heated thoroughly in an oil bath maintained at specific temperature with the help of magnetic stirrer with heating control (Fig 2.1). The progress of the reaction was monitored by TLC using aluminum sheet pre-coated with TLC silica gel 60 F<sub>254</sub> (Merck, Germany) and (20:80%) of Petroleum ether : Ethyl acetate mixture as an eluent. After completion of the reaction as indicated from TLC, the reaction mixture was extracted with specific solvents as per requirement for different reaction. The crude product was then purified by recrystallization from different solvents.



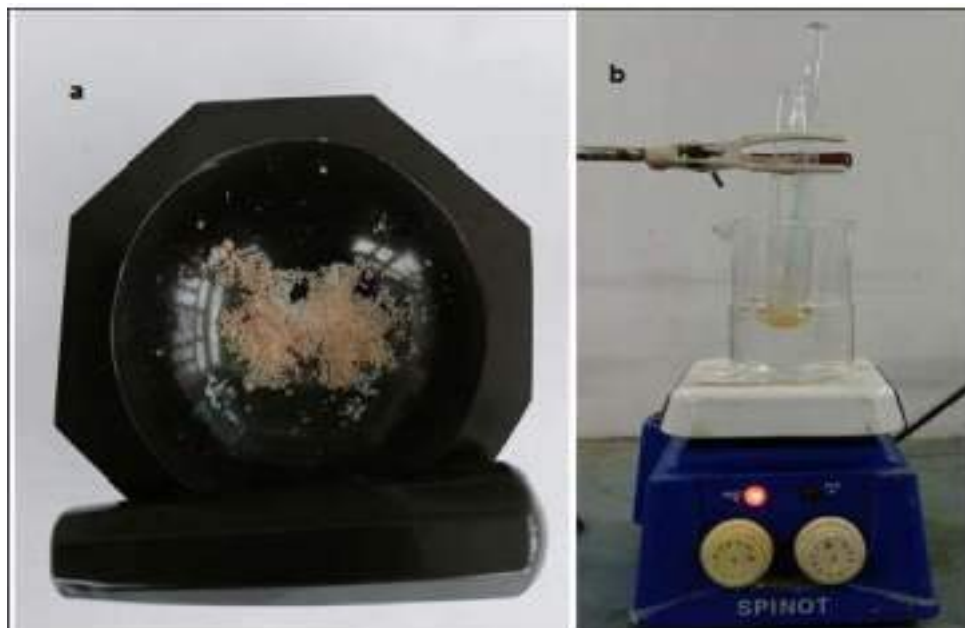


**Fig. 2.1.** a) Pulverization of reactant and catalyst in agate mortar and pestle and  
b) Heating the reaction mixture in oil bath.

Provenance and purity of different chemicals used during the synthesis of N-containing heterocyclic compounds are listed in Table 2.1.

**Table 2.1.** Provenance and purity of Chemicals

Entry	Reagents	Vendor	CAS number	Purity(%)
<b>Aldehydes</b>				
1	4-Cyano-benzaldehyde	AVRA	105-07-7	98
2	Indole-3-carboxaldehyde	AVRA	487-89-8	99
3	2,5-Dimethoxy benzaldehyde	AVRA	93-02-7	98
4	3,4,5-Trimethoxy benzaldehyde	AVRA	86-81-7	98
5	4-Nitro benzaldehyde	AVRA	555-16-8	95
6	3,5-Dibromo benzaldehyde	AVRA	56990-02-4	98
7	2,4- Dimethyl benzaldehyde	AVRA	15764-16-6	90
8	2-Chloro benzaldehyde	AVRA	89-98-5	98
9	3-Bromo benzaldehyde	AVRA	3132-99-8	95
10	3-Fluoro benzaldehyde	AVRA	456-48-4	98
11	5-Chloro 2-Hydroxybenzaldehyde	AVRA	635-93-8	97
12	4-hydroxy3,5-dimethoxy benzaldehyde	AVRA	134-96-3	98
13	3-Nitro benzaldehyde	Loba Chemie	99-61-6	98
14	2-Nitro benzaldehyde	Loba Chemie	552-89-6	99
15	2-Hydroxybenzaldehyde	Merck	90-02-8	99
16	Benzaldehyde	Sigma-	100-52-7	99

17	4-Chloro benzaldehyde	Aldrich Sigma- Aldrich	104-88-1	97
18	3-Hydroxy benzaldehyde	Sigma- Aldrich	100-83-4	99
19	5-bromo 2- Hydroxybenzaldehyde	Sigma- Aldrich	1761-61-1	98
20	5- Nitro 2- Hydroxybenzaldehyde	Sigma- Aldrich	97-51-8	98
21	2-Hydroxy 3-methoxy benzaldehyde	Sigma- Aldrich	148-53-8	99
22	4-hydroxy 3-methoxy benzaldehyde	Sigma- Aldrich	121-33-5	99
23	2,4-Dihydroxy benzaldehyde	Sigma- Aldrich	202-383-1	98
24	10-Chloro-9-anthranaldehyde	Sigma- Aldrich	10527-16-9	97
25	Cinnamaldehyde	Sigma- Aldrich	14371-10-9	99
<b>Other chemicals</b>				
1	Ortho-phenylene diammine	AVRA	98-54-5	98
2	Ammonium acetate	Sigma- Aldrich	631-61-8	97
3	Diacetyl monoxime	Sigma- Aldrich	57-71-6	98
4	Hydroxylamine hydrochloride	Sigma- Aldrich	5470-11-1	98
5	Ethyl acetoacetate	Sigma- Aldrich	141-97-9	99
6	Benzil	Sigma- Aldrich	134-81-6	98
7	Urea	SRL	57-13-6	99
8	KBr (FT-IR Grade)	Spectrochem	2/3/7758	FT-IR Grade

### 2.2.1 Brief information about the catalyst

In this research work, we mainly studied the efficacy of three transition metal borate salts namely Copper tetraborate ( $\text{CuB}_4\text{O}_7$ ), Iron (III) borate ( $\text{FeBO}_3$ ) and Nickel borate ( $(\text{NiB}_2\text{O}_4).x\text{H}_2\text{O}$ ) as a catalyst for the synthesis of N-containing heterocyclic compounds under solvent free condition and the particulars of the studied borate salts are given in Table 2.2.

**Table 2.2.** Particulars of the catalyst

Entry	Name	Molecular formula	CAS Number	Purity
1	Copper tetra borate	$\text{CuB}_4\text{O}_7$	39290-85-2	99
2	Iron(III) borate	$\text{FeBO}_3$	20542- 97-6	99
3	Nickel Borate hydrate	$(\text{NiB}_2\text{O}_4).x\text{H}_2\text{O}$	51142-85-9	99

### 2.2.2 Purification of the N-containing heterocyclic compounds.

Since we have carried out the synthesis of some selected N-containing heterocyclic compounds under green reaction condition employing solvent free methods but sometimes we needed some organic solvents for the purification and recrystallization of the desired compounds in small amounts. We also took care of using as minimum as possible amount of solvents to keep our synthetic methodology under green chemical context. The provenance and purity of the solvents used for the purification and recrystallization of the synthesized compounds are listed in table 2.3.

**Table. 2.3.** Provenance and purity of the solvent used

Entry	Solvent	Provenance	CAS number	Purity(%)
1	Ethanol	Merck	64-17-5	99
2	Methanol	SRL	67-56-1	99
3	Acetone	SRL	67-64-1	99.5
4	N,N-Dimethyl formamide	SRL	68-12-2	99
5	Ethyl acetate	SRL	141-78-6	99.5
6	Petroleum ether	Thermo Scientific	8032-32-4	HPLC grade

We generally carried out the purification of the desired product by recrystallization procedure and we excluded the tedious chromatographic techniques for the purification of the product. We monitored the progress of the reaction by Thin Layer Chromatography (TLC) using aluminum sheet pre-coated with TLC silica gel 60 F<sub>254</sub> (Merck, Germany) and (20:80%) of Petroleum ether: Ethyl acetate mixture for the development of chromatogram.

### 2.2.3 Characterization of the synthesized products using different Analytical and Spectroscopic Techniques.

The synthesized N-containing heterocyclic compounds have been characterized by employing different analytical and spectroscopic techniques and we compare the result with the literature published elsewhere.

#### 2.2.3.1 Melting point

The melting point of the synthesized compounds was determined by open capillary method using acid bath<sup>1</sup> (Fig. 2.2) and the melting point of the corresponding derivatives were compared with the literature value given elsewhere.



**Fig. 2.2.** Determination of melting point by open capillary method

### 2.2.3.2 FT-IR Spectroscopy

FT-IR spectra of the synthesized compounds were recorded on Bruker Alpha-II spectrophotometer (Ettlingen, Germany) (Fig. 2.3) using KBr pellets in the wave number range  $4000-400\text{ cm}^{-1}$  and only the characteristics bands are reported after comparing with literature value. The KBr obtained from the commercial source have been dried in an oven and kept over anhydrous  $\text{CaCl}_2$  in a vacuum desiccator before use. The abbreviations used are: s = strong, m = medium, w = weak, b = broad.



**Fig. 2.3.** Bruker Alpha-II FT-IR spectrophotometer

### 2.2.3.3 FT-NMR Spectroscopy

$^1\text{H}$ -NMR spectra of the synthesized compounds were recorded at room temperature on a Bruker Advance neo-FT-NMR spectrometer operating at 400 MHz frequency (Fig. 2.4) by using  $\text{DMSO-}d_6$  as solvents and chemical shifts are quoted in ppm downfield of internal standard tetramethylsilane (TMS  $\delta$  0.00ppm). The coupling patterns are described by the following abbreviations: s (singlet), d (doublet), t (triplet), q (quartet), m (multiplet).



Fig. 2.4. Bruker Advance neo-FT-NMR spectrometer

### 2.2.3.4 X-ray crystallography

X-ray single crystal diffraction study of some of the synthesized derivatives were performed on Bruker SMART-APEX CCD diffractometer and XtaLab Synergy, Dualflex Atlas S2 diffractometer and the Diffraction data was collected using monochromatic  $\text{Mo K}\alpha$  ( $\lambda = 0.71073 \text{ \AA}$ ) and  $\text{Cu K}\alpha$  ( $\lambda = 1.5406 \text{ \AA}$ ) radiation with the  $\omega$  and  $\phi$  scan technique (CrysAlis PRO, Rigaku OD, 2017 and 2018) as per the requirement. The unit cell was determined using Bruker SMART<sup>2</sup>, the diffraction data were integrated with Bruker SAINT System<sup>2</sup> and the data were corrected for absorption using SADABS<sup>2</sup>. The structure was solved by direct method and was refined by full matrix least squares based on  $F^2$  using SHELXL 97<sup>3</sup>. All non-hydrogen atoms were refined anisotropically until convergence was reached and all the H atoms were localized from the difference electron-density map and refined isotropically. ORTEP plot and packing diagram were generated

with ORTEP-3 for Windows<sup>4</sup> and PLATON<sup>5</sup>. WinGX<sup>6,7</sup> was used to prepare the material for publication.

### 2.3. Theoretical Study of some selected N-heterocyclic compounds

#### 2.3.1 Quantum Mechanical Calculations:

All Quantum Mechanical calculations were carried out on a hp-Z640 desktop P.C. with an Intel Xeon processor (Specifications: E5-2630 V4 @ 220GHz) using Gaussian 16 W package<sup>8</sup>. Density functional theory (DFT) with Becke's (B)<sup>9</sup> three parameter hybrid model, Lee, Yang and Parr's (LYP) correlation functional<sup>10</sup> under Pople's 6-31 G + (d,2p) basis set has been employed to optimize the geometry of the synthesized compounds.

A set of theoretical calculations of selected compounds was performed with Gaussian 16W (Gaussian 16, Revision A.03) programme package using B3LYP/6-31 G + (d, 2p) basis sets to optimize geometry and minimize energy for faster and accurate calculations<sup>8</sup>. With the optimized geometry, theoretical Raman and IR spectra were also calculated from the so chosen basis set. For analyzing the result of the theoretical calculations, a visual representation was obtained by Gauss View 6.0 program<sup>11</sup>. Some of the important parameters such as (i) optimized geometry, (ii) Raman and IR spectra<sup>12</sup>, (iii) Energies of HOMO and LUMO<sup>13</sup>, (iv) chemical potential ( $\mu$ )<sup>14</sup>, (v) Global hardness ( $\eta$ )<sup>15</sup>, (vi) global electrophilicity power ( $\omega$ )<sup>16</sup>, (vii) Mulliken charge<sup>17</sup> and MESP<sup>18</sup> were also determined for some selected compounds.

As Frontier Molecular Orbitals (HOMO and LUMO) are capable of qualitatively predicting the excitation properties and electron transport in a system, they can provide a reasonable estimate of molecular reactivity. From the values of the energy of HOMO and LUMO, it is possible to calculate the Ionization Energy (I) ( $I = -E_{\text{HOMO}}$ ), Electron Affinity ( $A = -E_{\text{LUMO}}$ ), Chemical potential ( $\mu = (E_{\text{HOMO}} + E_{\text{LUMO}})/2$ ), Global hardness ( $\eta = (E_{\text{HOMO}} - E_{\text{LUMO}})/2$ ) and Global electrophilicity power ( $\omega = \mu^2/2\eta$ ).

The Non-Linear Optical property has also been calculated taking urea as a reference NLO material<sup>19</sup>. Study of Nonlinear Optics (NLO) is based on the interaction between intense coherent light (like lasers) and matter that displays nonlinear response to light. Materials with nonlinear optical properties (NLOs) have become very important in the field of photonics<sup>20</sup> including sensor protectors<sup>21</sup>, optical information processing<sup>21</sup>, and data storage<sup>21</sup>. NLO response for some organic compounds is several times greater than that for widely known inorganic materials<sup>22-23</sup>. Amino acids (except glycine) have gained a lot of popularity in this field due the presence of a chiral carbon and their ability to crystallize in a non-centrosymmetric fashion in terms of point groups<sup>24-25</sup>. An advantage of making NLO materials from amino acids is that they don't absorb in the UV-Vis region<sup>25</sup>.

NLO materials are divided into different classes depending on the order "n" of the non-linear susceptibility  $\chi^{(n)}$ . This helps in describing the response

of the material, as affected by the electric field associated with the incident light radiation. There are majorly two types of NLO materials:

1.  $\chi^{(2)}$  materials are used for 2<sup>nd</sup> Harmonic generation, they must have an asymmetrical structure. Their refractive index can be controlled by an external electric field called as electro-optic effect.
2.  $\chi^{(3)}$  materials' properties similarly can be affected by light and can be controlled by light. They are applied to optical switches but are less efficient and not used majorly in devices due to their higher order of non-linearity.

Second Harmonic Generation is probably the most extensively studied NLO phenomenon. Second Harmonic generation is the conversion of an input light of a given frequency to an output light of double the frequency due to a process called as Two photon Resonance<sup>26</sup>. This process occurs in a material having NLO properties, usually a solid or a crystal. An example of this is the production of green light (532 nm) from a Nd-YAG laser operating at 1064 nm. (YAG= Ytterbium-Aluminum-Garnet)<sup>27</sup>.

The NLO response to polymers and organic materials has been intensively studied in recent years compared with that of inorganic materials as organic NLO materials have ultra-fast response and High nonlinearities<sup>28</sup>.

Quantum chemical assessment of the polarizability ( $\alpha$ ) and the hyperpolarizability ( $\beta$ ) and their structure property relationship is an intensive area of research<sup>29</sup>. This has often helped in the design of new NLO material, easily bringing different structural units together and helping in the development of high performance NLO materials.

The Finite Field (FF) method is used in this regard. The compound is incorporated in a static field (F) and the resulting energy is shown by equation<sup>30</sup> (1)

$$E = E^0 - \mu_i F_i - \frac{1}{2} \alpha_{ij} F_i F_j F_k - \frac{1}{24} \gamma_{ijkl} F_i F_j F_k F_l \dots \dots \dots (1)$$

Where,  $E^0$ = molecular energy in the absence of an electric field

Polarizability  $\langle \alpha \rangle$ , first ( $\beta_{\text{tot}}$ ) and second hyperpolarizability  $\langle \gamma \rangle$  tensors are calculated in the x,y and z directions by the following equations:

$$\langle \alpha \rangle = \frac{1}{3} (\alpha_{xx} + \alpha_{yy} + \alpha_{zz}) \dots \dots \dots (2)$$

$$B_{\text{tot}} = (\beta_x^2 + \beta_y^2 + \beta_z^2)^{1/2} \dots \dots \dots (3)$$

$$B_{\text{tot}} = [(\beta_{xxx} + \beta_{xyy} + \beta_{xzz})^2 + (\beta_{yyy} + \beta_{yzz} + \beta_{yxx})^2 + (\beta_{zzz} + \beta_{zxx} + \beta_{zyz})^2]^{1/2} \dots \dots \dots (4)$$

$$\langle \gamma \rangle = 1/5 [\gamma_{xxxx} + \gamma_{yyyy} + \gamma_{zzz} + 2(\gamma_{xxyy} + \gamma_{yyzz} + \gamma_{xxzz})] \dots \dots \dots (5)$$



The anisotropy of polarizability is given by:

$$\Delta \alpha = [(\alpha_{xx} - \alpha_{yy})^2 + (\alpha_{yy} - \alpha_{zz})^2 + (\alpha_{zz} - \alpha_{xx})^2 + 6(\alpha_{xy}^2 + \alpha_{xz}^2 + \alpha_{yz}^2)]^{1/2} \times (1/2)^{1/2} \dots \dots (6)$$

The different values can therefore be calculated with the help of the above given equations to elucidate the Non-Linear optical properties of the studied compounds.

### 2.3.2 Hirshfeld surface analysis

Hirshfeld surface analysis provides a quantitative way to examine the intermolecular interactions of the molecules in a crystal structure. Moreover, it helps in predicting the overall packing behavior of the crystal<sup>31</sup>. The Hirshfeld surfaces and fingerprint plots were mapped with Crystal Explorer 3.1 software<sup>32</sup>. Hirshfeld surface analysis can be utilized to visualize and compute different non-covalent interactions that stabilize the crystal packing<sup>33</sup>.

Hirshfeld surface can be mapped with different properties such as  $d_{norm}$ , electrostatic potential, shape index and curvature. The normalized contact distance  $d_{norm}$  is a symmetric function of distances to the surface between nuclei inside ( $d_i$ ) and outside ( $d_e$ ) of the Hirshfeld surface relative to their respective van der Waals radii (vdW) as represented by equation (7) enables identification of the regions of particular importance to intermolecular interactions<sup>34</sup>.

$$d_{norm} = \frac{d_i - r_i^{vdw}}{r_i^{vdw}} + \frac{d_e - r_e^{vdw}}{r_e} \dots \dots \dots (7)$$

Where  $d_e$  is the distance from the Hirshfeld surface to the nearest nucleus outside the surface,  $d_i$  is the corresponding distance to the nearest nucleus inside the surface, and  $r_i^{vdw}$  is the van der Waals radius of the atom<sup>35</sup>. The  $d_{norm}$  parameter exhibits a surface with a red-white blue color scheme<sup>31</sup>. Bright red spots show the intermolecular contacts less than their vdW radii, while the blue spots show intermolecular contacts longer than their vdW radii. White spots are the sum of their vdW radii.

### 2.3.3 Molecular docking study

The molecular docking study for selected synthesized compounds were carried out in the AutoDock Vina programme 1.1.2 developed by Scripps Research institute<sup>36</sup> and the corresponding result were analyzed using BIOVIA Discovery Studio 2020 (DS), version 20.1.0.0 (Dassault Systèmes BIOVIA, Discovery Studio Modeling Environment, Release 2017, San Diego: Dassault Systèmes, 2016) and Edu pymol version 1.7.4.4<sup>37,38</sup>. The three-dimensional (3D) affinity (grid) maps, electrostatic grid boxes and grid center (X, Y, Z) of specific dimension with a spacing of 1.00 Å generated by AutoGrid auxiliary program for each of the receptor protein for blind docking were generated to

cover the entire active site of the receptor protein in order to eliminate any biasness arising during the docking simulation<sup>39</sup>. For docking simulation, Lamarckian genetic algorithm and a standard protocol with default setting of other run parameters have been used. For each docking, several runs were performed by the program with one predicted binding mode with each run and the best binding mode with RMSD value 0 have been used to discuss the docking result. All the torsions were allowed to rotate freely. The predicted inhibitory constant ( $pK_i$ ) has been calculated using the following standardized equations (8).

$$pK_i = 10^{\frac{\text{Binding Energy Score}}{1.336}} \dots\dots\dots (8)$$

The following combination of ligands and proteins has been used for the molecular docking study embodied in this thesis.

1. Protein : 1IR3 (Insulin receptor kinase)  
Ligands: Selected ligands of the synthesized 2, 4, 5-triarylimidazole (IM-1 to IM-6)
2. Protein : 3DH4 (vSGLT (SGLT2, sodium-dependent glucose transporter) inhibition for Diabetes Mellitus type-1 treatment)  
Ligands : selected ligands of the synthesized 3, 4 dihydropyrimidin-2-(1H)-one (DP-1 to DP-3)
3. Protein: 3ERT (Breast cancer protein estrogen receptor)  
Ligands: selected ligands of the synthesized 1-hydroxy-2-arylimidazole-3-oxide derivatives (IMO-1 to IMO-6).

## 2.4 References

- (1) Organic Laboratory Techniques  
<http://www.chem.ucalgary.ca/courses/351/laboratory/meltingpoint.pdf> (accessed 2022 -07 -09).
- (2) *SADABS, SMART and SAINT*; Bruker AXS Inc., Madison, Wisconsin, USA, **2000**.
- (3) G. M. Sheldrick., *SHELXS-97 and SHELXL-97, Program for Crystal Structure Solution and Refinement*; University of Gottingen, Gottingen, **1997**.
- (4) L. J. Farrugia., *Journal of Applied Crystallography*, **1997**, 30 (5), 565–565.
- (5) A. L. Spek., *Acta Crystallographica*, **2009**, D65 (2), 148–155.
- (6) L. J. Farrugia., *Journal of Applied Crystallography*, **1999**, 32 (4), 837–838.
- (7) L. J. Farrugia., *Journal of Applied Crystallography*, **2012**, 45 (4), 849–854.
- (8) M. J. Frisch, G. W. Trucks, H. B. Schlegel, G. E. Scuseria, M. A. Robb, J. R. Cheeseman, G. Scalmani, V. Barone, G. A. Petersson, H. Nakatsuji, X. Li, M. Caricato, A. v Marenich, J. Bloino, B. G. Janesko, R. Gomperts, B. Mennucci, H. P. Hratchian, J. v Ortiz, A. F. Izmaylov, J. L. Sonnenberg, D. Williams-Young, F. Ding, F. Lipparini, F. Egidi, J. Goings, B. Peng, A. Petrone, T. Henderson, D. Ranasinghe, V. G. Zakrzewski, J. Gao, N. Rega, G. Zheng, W. Liang, M. Hada, M. Ehara, K. Toyota, R. Fukuda, J. Hasegawa, M. Ishida, T. Nakajima, Y. Honda, O. Kitao, H. Nakai, T. Vreven, K. Throssell, J. A. Montgomery Jr., J. E. Peralta, F. Ogliaro, M. J. Bearpark, J. J. Heyd, E. N. Brothers, K. N. Kudin, V. N. Staroverov, T. A. Keith, R. Kobayashi, J. Normand, K. Raghavachari, A. P. Rendell, J. C. Burant, S. S. Iyengar, J. Tomasi, M. Cossi, J. M. Millam, M. Klene, C. Adamo, R. Cammi, J. W. Ochterski, R. L. Martin, K. Morokuma, O. Farkas, J. B. Foresman, D. J. Fox., *Gaussian, Inc., Wallingford CT*, **2016**.
- (9) A. D. Becke., *Physical Review A*, **1988**, 38 (6), 3098–3100.
- (10) C. Lee, W. Yang, R. G. Parr., *Physical Review B*, **1988**, 37 (2), 789.
- (11) R. Dennington, T. A. Keith, J. M. Millam., *GaussView Version 6, Semichem Inc., Shawnee Mission, KS*, **2016**.
- (12) C. F. Leybold, M. Reiher, G. Brehm, M. O. Schmitt, S. Schneider, P. Matousek, M. Towrie., *Physical Chemistry Chemical Physics*, **2003**, 5 (6), 1149–1157.
- (13) C. Khantha, T. Yakhanthip, C. M. Macneill, P. Pornprasit, V. Kruefu, N. Kungwan, R. C. Coffin, S. Phanichphant, D. L. Carroll., *Molecular Crystal and Liquid Crystals*, **2013**, 578 (1), 37–43.

- (14) P. Geerlings, F. de Proft, W. Langenaeker., *Chemical Reviews*, **2003**, *103* (5), 1793–1873.
- (15) R. G. Pearson., *Journal of Chemical Sciences*, **2005**, *117* (5), 369–377.
- (16) L. R. Domingo, M. Ríos-Gutiérrez, P. Pérez., *Molecules*, **2016**, *21* (6), 748.
- (17) A. B. Marahatta., *International Journal of Progressive Sciences and Technologies*, **2019**, *16* (1), 51–65.
- (18) M. Drissi, N. Benhalima, Y. Megrouss, R. Rachida, A. Chouaih, F. Hamzaoui., *Molecules*, **2015**, *20* (3), 4042–4054.
- (19) S. J. Luo, J. T. Yang, W. F. Du, A. Laref., *Journal of Physical Chemistry A*, **2011**, *115* (20), 5192–5200.
- (20) J. W. You, S. R. Bongu, Q. Bao, N. C. Panoiu., *Nanophotonics*, **2019**, *8* (1), 63–97.
- (21) Z. Miao, Y. Chu, L. Wang, W. Zhu, D. Wang., *Polymers (Basel)*, **2022**, *14* (8), 1516.
- (22) N. V. Kamanina, A. I. Plekhanov., *Optics and Spectroscopy*, **2002**, *93* (3), 408–415.
- (23) N. V. Kamanina, S. v. Serov, N. A. Shurpo, S. v. Likhomanova, D. N. Timonin, P. v. Kuzhakov, N. N. Rozhkova, I. v. Kityk, K. J. Plucinski, D. P. Uskokovic., *Journal of Materials Science: Materials in Electronics*, **2012**, *23* (8), 1538–1542.
- (24) L. Misoguti, A. T. Varela, F. D. Nunes, V. S. Bagnato, F. E. A. Melo, J. Mendes Filho, S. C. Zilio., *Opt Mater (Amst)*, **1996**, *6* (3), 147–152.
- (25) M. Fleck, A. M. Petrosyan., *Salts of Amino Acids: Crystallization, Structure and Properties*; Springer International Publishing: Switzerland, **2014**.
- (26) V. Kumar, N. Coluccelli, D. Polli., In *Molecular and Laser Spectroscopy (Chap 5-Coherent Optical Spectroscopy/Microscopy and Applications)*; Gupta, V. P., Ed.; Elsevier, **2018**; pp 87–115.
- (27) T. I. Kaya, U. Guvenc., *Dermatologic Therapy*, **2019**, *32* (3), e12907.
- (28) F. Liu, H. Xiao, H. Xu, S. Bo, C. Hu, Y. He, J. Liu, Z. Zhen, X. Liu, L. Qiu., *Dyes and Pigments*, **2017**, *136*, 182–190.
- (29) Y. Sheng, Y. Jiang., *Journal of the Chemical Society, Faraday Transactions*, **1998**, *94* (13), 1829–1833.
- (30) A. H. G. Patel, A. A. K. Mohammed, P. A. Limacher, P. W. Ayers., *Journal of Physical Chemistry A*, **2017**, *121* (28), 5313–5323.
- (31) M. A. Spackman, D. Jayatilaka., *CrystEngComm*, **2009**, *11* (1), 19–32.

- (32) P. R. Spackman, M. J. Turner, J. J. McKinnon, S. K. Wolff, D. J. Grimwood, D. Jayatilaka, M. A. Spackman., *Journal of Applied Crystallography*, **2021**, 54 (3), 1006–1011.
- (33) S. L. Tan, M. M. Jotani, E. R. T. Tiekink., *Acta Crystallographica*, **2019**, E75 (3), 308–318.
- (34) S. K. Seth, N. C. Saha, S. Ghosh, T. Kar., *Chemical Physics Letters*, **2011**, 506 (4–6), 309–314.
- (35) N. E. Eltayeb, F. Şen, J. Lasri, M. A. Hussien, S. E. Elsilik, B. A. Babgi, H. Gökce, Y. Sert., *Journal of Molecular Structure*, **2020**, 1202, pp 127315.
- (36) R. Huey, G. M. Morris., *Using AutoDock 4 with AutoDocktools: A Tutorial.*; The Scripps Research Institute, Molecular Graphics Laboratory, pp. 54-56: La Jolla, CA, USA, **2008**.
- (37) J. Eberhardt, D. Santos-Martins, A. F. Tillack, S. Forli., *Journal of Chemical Information and Modeling*, **2021**, 61 (8), 3891–3898.
- (38) O. Trott, A. J. Olson., *Journal of Computational Chemistry*, **2010**, 31 (2), 455–461.
- (39) G. M. Morris, D. S. Goodsell, R. S. Halliday, R. Huey, W. E. Hart, R. K. Belew, A. J. Olson., *Journal of Computational Chemistry*, **1998**, 19 (14), 1639–1662.

## **CHAPTER-III**

### **Section A**

#### **Copper Borate (CuB<sub>4</sub>O<sub>7</sub>) catalyzed multi-component green synthesis of 2,4,5 Tri-aryl imidazole derivatives**

##### **3.A.1 Background of the present investigation**

Recent trend in synthetic organic chemistry research focuses on the design and development of the reaction methodology in an environmentally benign greener and sustainable way to reduce the use of the hazardous chemicals and to explore the alternative reaction conditions or reaction media to bring about the desired chemical transformations by minimizing the by-products or waste and exclusion of the conventional organic solvents<sup>1-10</sup>. Multi-Component Reactions (MCRs) serve as a good example to meet the requirements for the green chemical processes and it may be viewed as an art of performing efficient chemical transformation by coupling three or more reactants in a single pot in single operation avoiding toxic reagents, solvents and expensive purification techniques. MCRs also have an advantage in the development of novel and cost-effective approaches in synthetic chemistry research leading to environmental protection and have emerged as powerful tools for drug discovery<sup>11-15</sup>. The Multi-Component Reaction technique has gained special attention and drawn great interest in modern synthetic chemistry and pharmaceutical chemistry because one pot Multi-Component Reactions (MCRs) has many advantages such as high atom-economy, high selectivity, operational simplicity, structural diversity, short reaction time, low cost, low energy consumption, high yield and easy purification process<sup>16-20</sup>. Among many Nitrogen containing heterocyclic compounds, imidazole scaffold is an important heterocyclic scaffold due to their richness in various natural products and their widespread use in the medicinal field<sup>21-22</sup>. Imidazole ring system possesses variety of pharmaceutical properties and plays a fundamental role in numerous biochemical processes<sup>23</sup>. Over the past few years, highly substituted imidazole has gained a lot of interest due to their biological relevance in many natural products and their extensive applications in the area of material science<sup>24</sup> and their potential use as herbicide<sup>25</sup>, fungicide<sup>26</sup>, inhibitors of P38 MAP kinase<sup>27</sup>, B-Rafkinase<sup>28</sup>, anti-inflammatory<sup>29</sup>, anti-tumor<sup>30</sup>, and anti-thrombotic<sup>31</sup>agents. In addition, some of the highly substituted imidazole compounds serve as a photosensitive material in photography<sup>32</sup>. Highly substituted imidazoles such as clemizole (antihistaminic agent)<sup>33</sup> (94), nocodazole (antinematodal)<sup>34</sup> (95), azathioprine (anti-rheumatoid arthritis)<sup>35</sup> (96), dacarbazine (anticancer)<sup>36-37</sup> (97) are commercially available drugs for the treatment of different diseases (Fig.3.1).

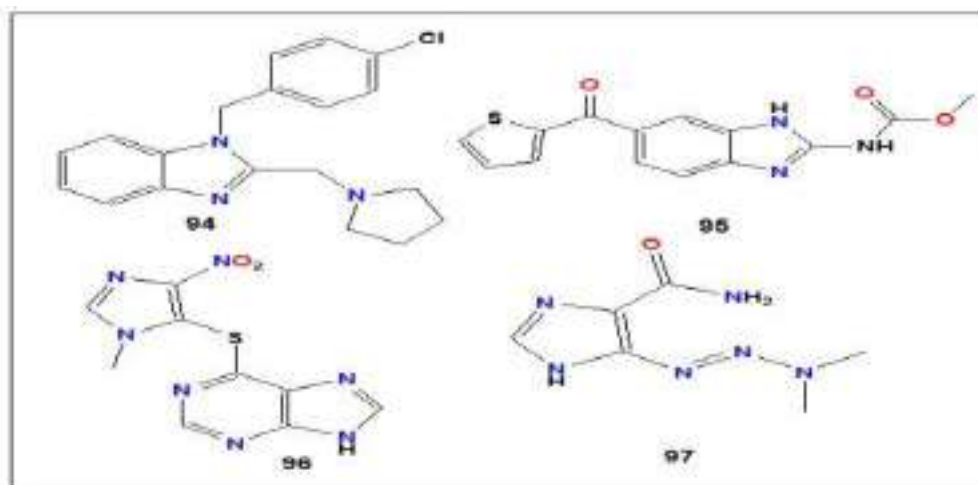


**Fig. 3.A.1.** Structures of commercially available drugs containing imidazole core

In view of the diverse properties and applications of imidazole core, numerous synthetic methodologies have been formulated using various catalytic systems under different reaction conditions for the efficient and rapid synthesis of substituted imidazole derivatives by three-component cyclocondensation of a 1,2-diketone,  $\alpha$ -hydroxyketone or  $\alpha$ -ketonoxime with an aldehyde and ammonium acetate<sup>38-50</sup> (Scheme 3.A.1A). Apart from the conventional use of 1, 2-diketone,  $\alpha$ -hydroxyketone or  $\alpha$ -ketonoxime, several reports on the synthesis of substituted imidazoles have been documented using  $\alpha$ -methylene ketone<sup>51-52</sup> (Scheme 3.A.1B).

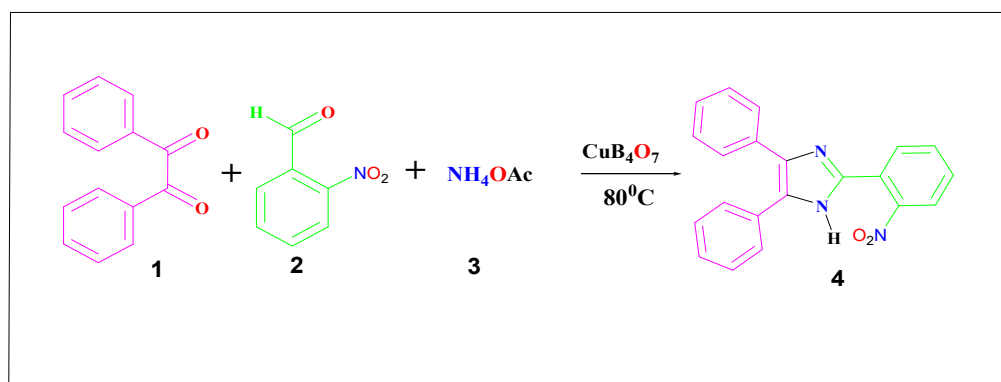


**Scheme. 3.A.1A.** Debus-Radiszewski imidazole synthesis and **Scheme. 3.A.1B.** Synthesis of tri-substituted imidazole using  $\alpha$ -hydroxyketone.

Although, these documented procedures offer several beneficial features, yet most of them have serious drawbacks such as use of expensive catalyst, lower yield, use of the toxic solvent, harsh reaction condition, longer reaction time and tedious work-up procedures<sup>53-56</sup>. All these facts have encouraged us to find an eco-friendly, environmentally benign greener and sustainable method for the synthesis of substituted imidazole and stimulated us to employ copper (II)borate ( $\text{CuB}_4\text{O}_7$ ) as a catalyst for the one-pot three-component synthesis of 2, 4, 5 triarylimidazole derivatives by condensation of benzil,  $\text{NH}_4\text{OAc}$  and aromatic aldehydes in solvent free condition.

### 3.A.2 Results and discussion

Interestingly, there are several reports on the synthesis of 2, 4, 5 tri-substituted imidazole using different copper salts as a catalyst<sup>57-61</sup> but there are no reports on the study of catalytic activities of copper borate ( $\text{CuB}_4\text{O}_7$ ) so far. While going through the literature review for the organic transformation reactions catalyzed by transition metal salts, our research group encountered that there are no reports on the catalytic activities of transition metal borates for such reactions. Therefore, it was thought worthwhile to explore the catalytic efficiency of copper (II) borate salt ( $\text{CuB}_4\text{O}_7$ ) for the green synthesis of 2, 4, 5- triaryl imidazole derivatives. Initially, for a model reaction, we screened Benzil (1), 2 Nitrobenzaldehyde (2) and  $\text{NH}_4\text{OAc}$  (3) as model compounds in different environmentally friendly conditions at  $80^\circ\text{C}$  (Scheme 3.A.2) for 2 hours using different mol % (0.5, 1.0, 1.5, 2.0, 2.5, 3.0) of copper borate catalyst to synthesize 2, 4, 5 tri-substituted imidazole (4).



**Scheme. 3.A.2.** Model reaction for the synthesis of 2,4,5 triaryl imidazole, Benzil (1) 1mmol, 2-Nitrobenzaldehyde (2) 1mmol and  $\text{NH}_4\text{OAc}$  (3) 2.5 mmol.

We screened the catalytic efficiency of the studied catalyst with the model reactants in different solvents under different reaction conditions and the result is summarized in table 3.1. We found that in more polar solvents like alcohol and DMF, the yield of the products were good (Table 3.A.1, entry 1, 2, 3) but the



reaction needed more time (2 hour) to go for completion. Due to this drawback, we focused our study on the solid phase synthesis using silica gel as a reaction medium but in this case also we encountered problems during work-up of the desired product.

**Table 3.A.1.** Screening of the solvent for model reaction

Entry	Solvent <sup>a</sup>	Yield % <sup>b</sup>
1	<b>Ethanol</b>	<b>84</b>
2	<b>Methanol</b>	<b>80</b>
3	<b>DMF</b>	<b>88</b>
4	DMSO	82
5	Water	32
6	Silica gel	85
7	Neat	96

<sup>a</sup>The reaction was performed with benzil 1 (1mmol), 2-nitrobenzaldehyde 2 (1mmol) and ammonium acetate 3 (2.5mmol) and a catalyst under different solvent. <sup>b</sup> isolated yields

Therefore, these drawbacks prompted us to carry out the desired reaction in neat condition without using any organic solvents. The results of the model reaction for different mol% of catalyst loading under optimized condition are summarized in Table 3.A.2. Encouragingly, the desired product 2, 4, 5 triaryl imidazole (4) was obtained in satisfactory yield in less time (8-10 minutes) at 80 °C and the maximum yield was obtained for 2 mol% of the catalyst loading (Table 3.A.2, entry 5).

**Table 3.A.2.** Screening of the amount of the catalyst for the model reaction

Entry	Catalyst mol % <sup>a</sup>	Temperature (°C)	Time (Mins)	Yield <sup>b</sup> (%)
1	0	80	10	20
2	0.5	80	10	70
3	1.0	80	10	76
4	1.5	80	10	85
<b>5</b>	<b>2</b>	<b>80</b>	<b>10</b>	<b>96</b>
6	2.5	80	10	96
7	3.0	80	10	95

<sup>a</sup>The reaction was performed with benzil 1 (1mmol), 2-nitrobenzaldehyde 2 (1mmol) and ammonium acetate 3 (2.5mmol) and a catalyst under different solvent at 80 °C with different mol% of the catalyst. <sup>b</sup> isolated yields.

Also, we observed that the yield of the product is maximum when the ratio of amount of NH<sub>4</sub>OAc is 2.5 mmol with respect to other substrate and with decrease or increase in the amount of NH<sub>4</sub>OAc, the yield of the product (4) decreases. A control experiment without catalyst has showed a low overall yield of products (Table 3.A.2 entry 1). Moreover, having recognized the optimized reaction condition, we subsequently, examined the catalytic efficiency and applicability of this protocol by extending this protocol to other substituted benzaldehydes and other aromatic aldehydes to prepare 2, 4, 5-triaryl imidazole derivatives (Fig 3.A.2) and we observed that all the reactions proceeded smoothly in very short reaction time to afford the desired imidazoles (4a-4w) in good to excellent yields (88-98%) (Table 3.A.3).

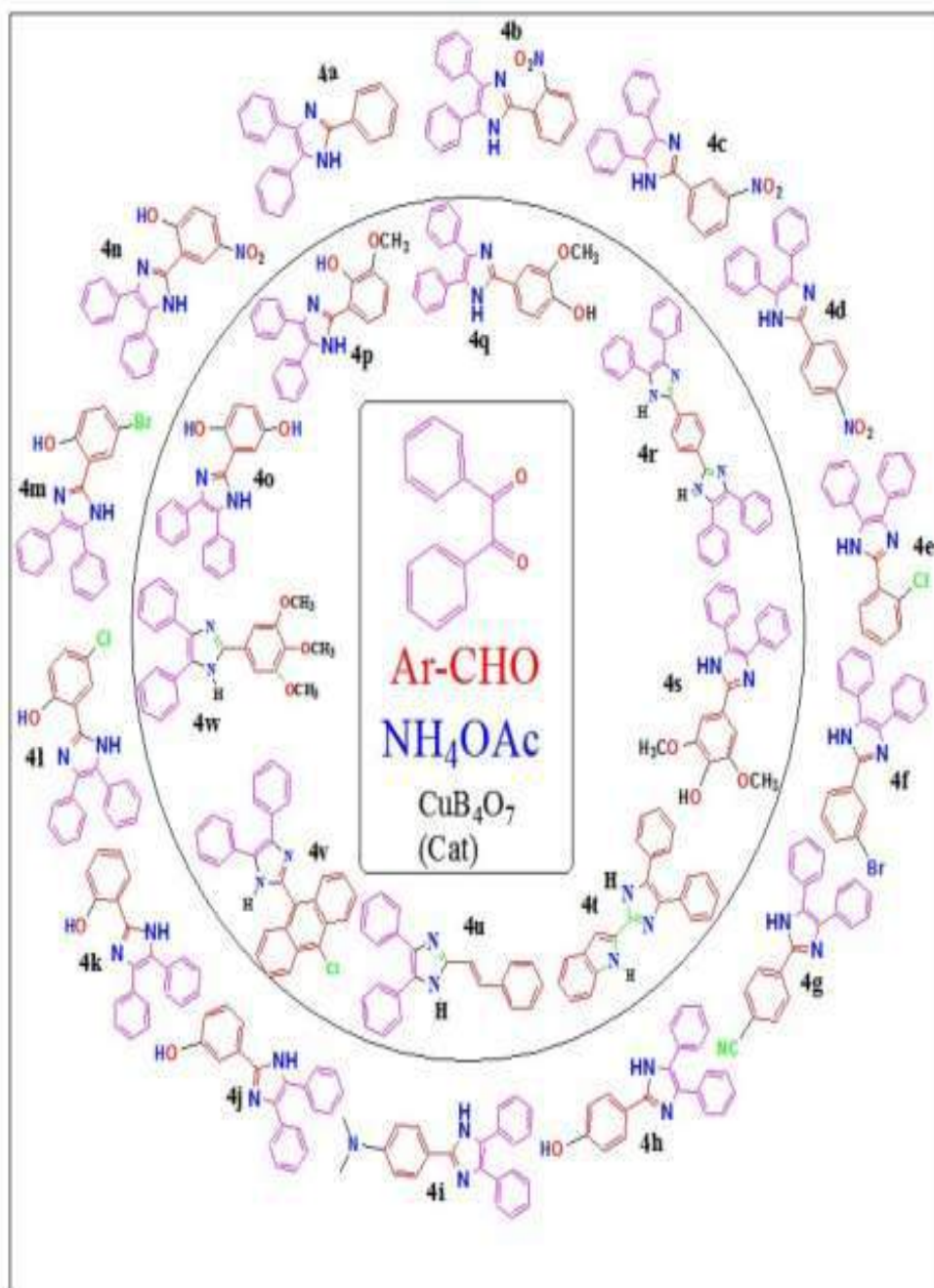


Fig. 3.A.2. 2, 4, 5 triaryl imidazole derivatives (4a-4w)

**Table. 3.A.3.** CuB<sub>4</sub>O<sub>7</sub> catalyzed solvent free synthesis of 2,4,5-triarylimidazole derivatives (4a-4w)

Entry	1,2 diketone	Aldehyde substrate	product	Yield(%) <sup>b</sup>
1	Benzil	Benzaldehyde	4a	98
2	Benzil	2-nitrobenzaldehyde	4b	96
3	Benzil	3-nitrobenzaldehyde	4c	95
4	Benzil	4-nitrobenzaldehyde	4d	97
5	Benzil	2-Chlorobenzaldehyde	4e	96
6	Benzil	3-bromobenzaldehyde	4f	93
7	Benzil	4-cyanobenzaldehyde	4g	95
8	Benzil	4-hydroxybenzaldehyde	4h	89
9	Benzil	4-N, N-dimethylbenzaldehyde	4i	97
10	Benzil	3-hydroxybenzaldehyde	4j	98
11	Benzil	2-hydroxybenzaldehyde	4k	97
12	Benzil	5-chloro 2-hydroxybenzaldehyde	4l	94
13	Benzil	5-bromo 2-hydroxybenzaldehyde	4m	96
14	Benzil	5-nitro 2-hydroxybenzaldehyde	4n	96
15	Benzil	2,4-dihydroxybenzaldehyde	4o	97
16	Benzil	2-hydroxy-3-methoxybenzaldehyde	4p	95
17	Benzil	4-Hydroxy-3-methoxybenzaldehyde	4q	94
18	Benzil	Benzene-1,4-dicarboxaldehyde	4r	86
19	Benzil	4-Hydroxy-3,5- dimethoxybenzaldehyde	4s	94
20	Benzil	Indole-2-carboxaldehyde	4t	96
21	Benzil	Cinnamaldehyde	4u	92
22	Benzil	10-Chloro-9-anthraldehyde	4v	93
23	Benzil	3,4,5-trimethoxybenzaldehyde	4w	98

<sup>b</sup>isolated yield

It was observed that para substituted benzaldehyde with electron withdrawing group successfully afforded the corresponding imidazoles in excellent yield under optimized condition compared to the Para substituent benzaldehyde with electron releasing group. Ortho substituent benzaldehyde and other aromatic aldehydes also afforded the corresponding imidazoles in good yield but they

**Table. 3.A.4.** Comparison of Catalytic efficacy of CuB<sub>4</sub>O<sub>7</sub> with other reported Catalysts:

Entry	Catalyst	Solvent <sup>a</sup>	Temperature	Time	Yield (%) <sup>b</sup>
1	L-Proline	MeOH	60 °C	9 Hours	90 [lit <sup>62</sup> ]
2	Zeolite ZSM-11	Neat	Reflux	60 Minutes	80 [lit <sup>63</sup> ]
3	Zr(acac) <sub>4</sub>	EtOH	Reflux	2.5 Hours	90 [lit <sup>64</sup> ]
4	Yb(OTf) <sub>3</sub>	OHAc	70 °C	2 Hours	92 [lit <sup>65</sup> ]
5	ZnO Nano rod	H <sub>2</sub> O	Reflux	1.45 Hours	83 [lit <sup>66</sup> ]
6	I <sub>2</sub>	Neat	RT	15 Minutes	90 [lit <sup>67</sup> ]
7	Fe <sub>3</sub> O <sub>4</sub> nano particle	Neat	80 °C	20 Minutes	96 [lit <sup>68</sup> ]
8	Nano TiCl <sub>4</sub> .SiO <sub>2</sub>	Neat	110 °C	1 Hour	90 [lit <sup>69</sup> ]
9	Nano MgO	Neat	100 °C	0.6 Hours	94 [lit <sup>70</sup> ]
10	InF <sub>3</sub>	Neat	60 °C	0.3 Hours	90 [lit <sup>50</sup> ]
11	CoFe <sub>2</sub> O <sub>4</sub> Nps	EtOH	40 °C	20 Minutes	95 [lit <sup>71</sup> ]
12	Y(TFA) <sub>3</sub>	Neat	100 °C	3 Hours	97 [lit <sup>72</sup> ]
13	Boric Acid	H <sub>2</sub> O	Ultrasound	30 Minutes	98 [lit <sup>73</sup> ]
14	ZSM-5-SO <sub>3</sub> H	Neat	110 °C	90 Minutes	90 [lit <sup>74</sup> ]
15	Trichloro melamine	Neat	110 °C	1 Hour	92 [lit <sup>75</sup> ]
16	TiO <sub>2</sub>	Neat	120 °C	2.5 Hours	92 [lit <sup>76</sup> ]
17	H <sub>2</sub> SO <sub>4</sub> .SiO <sub>2</sub>	Neat	110 °C	60 Minutes	94 [lit <sup>77</sup> ]
18	Copper Nano particles	Neat	RT	60 Minutes	94 [lit <sup>78</sup> ]
19	HMDS	Neat	120 °C	3 Hours	96 [lit <sup>79</sup> ]

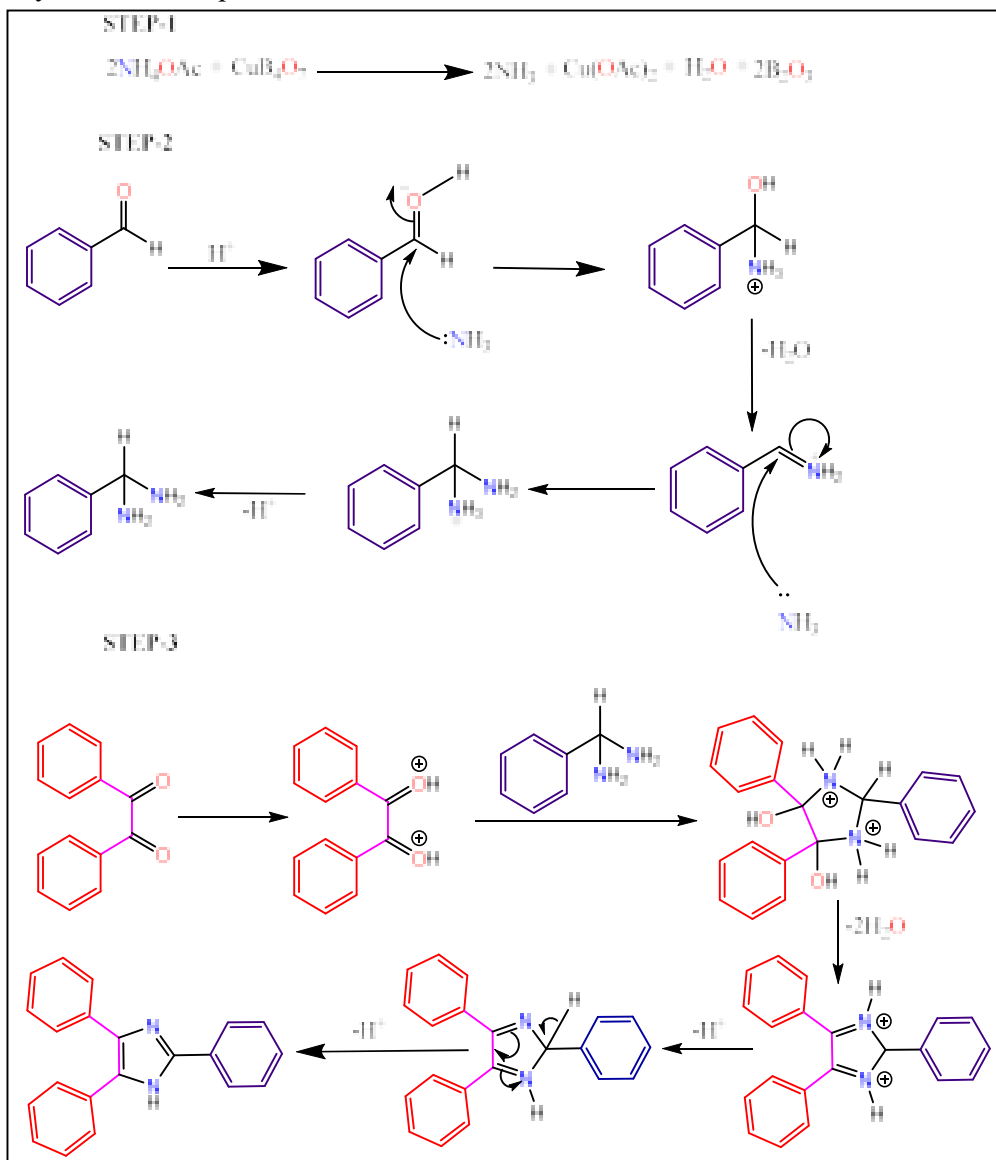
20	KMnO <sub>4</sub> /CuSO <sub>4</sub>	EtOH	Reflux	70 Minutes	85 [lit <sup>57</sup> ]
21	SiO <sub>2</sub> -NaHSO <sub>4</sub>	Neat	120 °C	30 Minutes	95 [lit <sup>80</sup> ]
22	Zeolite HY/ Silica Gel	Neat	M.W	6 Minutes	89 [lit <sup>81</sup> ]
23	<b>CuB<sub>4</sub>O<sub>7</sub> [this work]</b>	<b>Neat</b>	<b>80 °C</b>	<b>10 minutes</b>	<b>98</b>

<sup>a</sup>Comparison of catalytic efficacy of CuB<sub>4</sub>O<sub>7</sub> with other reported catalyst for the synthesis of 2,4,5-triaryl-imidazole derivatives using benzil, aromatic aldehyde and ammonium acetate under different reaction conditions. <sup>b</sup> isolated yields.

required more time for the reaction to complete. Also, we compared the catalytic efficiency of CuB<sub>4</sub>O<sub>7</sub> for the synthesis of 2,4,5-triarylimidazole derivatives with other reported catalyst and we observed that CuB<sub>4</sub>O<sub>7</sub> has high catalytic efficiency and need less reaction time for the reaction to go for completion. The comparative data of CuB<sub>4</sub>O<sub>7</sub> with other reported catalyst is listed in Table 3.A.3.

### 3.A.3 Plausible Mechanism

A proposed mechanism for the synthesis of 2,4,5-triarylimidazole catalyzed by  $\text{CuB}_4\text{O}_7$  is depicted below in Scheme 3.A.3.



Scheme. 3.A.3. Proposed mechanism for the synthesis of 2,4,5 - triarylimidazole

### 3.A.4 Experimental section:

#### 3.A.4.1 Materials:

All starting materials of high-purity for the aforementioned synthesis were purchased commercially and were used as received. The FT-IR spectra of the prepared compound were recorded in Bruker Alpha III spectrophotometer operating in the wave number region 4000 to 400  $\text{cm}^{-1}$  in dry KBr. The melting point of the synthesized compounds was determined by open capillary method.  $^1\text{H}$ -NMR spectra of the synthesized tri-aryl imidazole derivatives were recorded at room temperature on a FT-NMR (Bruker Advance-II 400 MHz) spectrometer by using  $\text{DMSO-}d_6$  as solvents and chemical shifts are quoted in ppm downfield of internal standard tetramethylsilane (TMS).

#### 3.A.4.2 General procedure for synthesis of 2, 4, 5-tri-aryl imidazole:

In a typical procedure a mixture of benzil (1.0 mmol), substituted benzaldehyde (1.0 mmol), ammonium acetate (2.5 mmol), copper borate (2 mol %) thoroughly ground and mixed in a mortar and pestle to make a homogenous mixture. The mixture was then transferred to a test tube. The reaction was heated at  $80^\circ\text{C}$  for 10 minutes. The progress of the reaction was monitored by TLC using hexane/ethyl acetate (80:20) solvent. After completion of the reaction, the reaction mixture was dissolved in methanol and filtered. The filtrate was evaporated under vacuum and subsequently dried to afford desired product. All the synthesized compounds (4a-4w) were recrystallized from ethanol and have been characterized by their analytical (yield and melting point) and spectroscopic data (FT-IR and  $^1\text{H}$  NMR) and compared with the literature value.

### 3.A.5 Conclusion

Herein, we have successfully developed a simple, environmentally benign and efficient green methodology for a synthesis of 2, 4, 5-triarylimidazole derivatives using unconventional  $\text{CuB}_4\text{O}_7$  as a catalyst utilizing one pot three component reaction. This environmentally green approach provides access to substituted imidazole derivatives in good to excellent yield using an unconventional and inexpensive  $\text{CuB}_4\text{O}_7$  catalyst. The developed catalytic procedure was found to be operative for a wide range of the aromatic aldehyde substrates.



**3.A.6 Analytical and Spectroscopic data:**

**3.A.6.1** 2,4,5-triphenyl-1H-imidazole (4a): White solid, yield=98%, melting point found (°C)=273-275, IR (KBr,  $\text{cm}^{-1}$ )  $\nu_{\text{max}}$ : 3453 (NH), 1636 (C=C), 1503(C=N),  $^1\text{H}$  NMR (400 MHz, DMSO- $d_6$ ):  $\delta_{\text{ppm}}$  = 12.69 (s,1H, NH), 7.22 -7.55 (m, Ar H, 13H), 8.09 (d, 2H)  $J$  = 7.2 Hz.

**3.A.6.2** 2-(2-nitrophenyl)-4,5-diphenyl-1H-imidazole (4b): pale yellow solid, yield=96%, melting point (°C)=231-233, IR (KBr,  $\text{cm}^{-1}$ )  $\nu_{\text{max}}$ : 3444(NH), 1619(C=C), 1602(C=N),  $^1\text{H}$  NMR (400 MHz, DMSO- $d_6$ ):  $\delta_{\text{ppm}}$  = 12.98 (s,1H, NH), 7.21 -7.97 (m, Ar H, 12H), 8.01 (d, 2H)  $J$  = 8.0 Hz.

**3.A.6.3** 2-(3-nitrophenyl)-4,5-diphenyl-1H-imidazole (4c): pale yellow solid, yield=95%, melting point (°C)=316-318, IR (KBr,  $\text{cm}^{-1}$ )  $\nu_{\text{max}}$ =3443(NH), 3056-3026 (Aromatic C-H) 1660(C=C), 1598(C=N),  $^1\text{H}$  NMR (400 MHz, DMSO- $d_6$ ):  $\delta_{\text{ppm}}$  = 12.56 (s,1H, NH), 7.61 -8.37 (m, , 12H, Ar H), 8.62-8.68 (d, 2H, Ar H).

**3.A.6.4** 2-(4-nitrophenyl)-4,5-diphenyl-1H-imidazole (4d): yellow solid, yield: 97%, melting point (°C)= 235-237, IR (KBr,  $\text{cm}^{-1}$ )  $\nu_{\text{max}}$ =3422 (NH), 3057 (Aromatic C-H),1660 (C=C), 1600 (C=N),  $^1\text{H}$  NMR (400 MHz, DMSO- $d_6$ ):  $\delta_{\text{ppm}}$  = 12.60 (s,1H, NH), 7.24- 8.45 (m, Ar H, 14H).

**3.A.6.5** 2-(2-chlorophenyl)-4,5-diphenyl-1H-imidazole (4e): off white solid, yield: 96%, melting point (°C)= 194-196, IR (KBr,  $\text{cm}^{-1}$ )  $\nu_{\text{max}}$ =3426(NH), 3060(Aromatic C-H), 1665 (C=C), 1602(C=N),  $^1\text{H}$  NMR (400 MHz, DMSO- $d_6$ ):  $\delta_{\text{ppm}}$  = 12.66 (s,1H, NH), 7.21 -7.93 (m, Ar H, 14H).

**3.A.6.6** 2-(3-bromophenyl)-4,5-diphenyl-1H-imidazole (4f): Off white solid, yield=93%, melting point (°C)= 290-293, IR (KBr,  $\text{cm}^{-1}$ )  $\nu_{\text{max}}$ =3451(NH), 3062, 3027 (Aromatic C-H),1694 (C=C), 1601(C=N),  $^1\text{H}$  NMR (400 MHz, DMSO- $d_6$ ):  $\delta_{\text{ppm}}$  = 12.83 (s,1H, NH), 8.30 (s, Ar H, 1H), 7.24-8.10 (m, Ar H, 13H)

**3.A.6.7** 4-(4,5-diphenyl-1H-imidazol-2-yl)benzotrile(4g): White solid, yield: 95%, melting point (°C)=186-188, IR (KBr,  $\text{cm}^{-1}$ )  $\nu_{\text{max}}$ =3449 (NH), 3081, 3053 (Aromatic C-H), 1636 (C=C), 1610(C=N),  $^1\text{H}$  NMR (400 MHz, DMSO- $d_6$ ):  $\delta_{\text{ppm}}$  = 13.03 (s,1H, NH), 7.23-7.96 (m, Ar H, 12H), 8.26 (d, 2H,  $J$  = 8.2 Hz).

**3.A.6.8** 4-(4,5-diphenyl-1H-imidazol-2-yl)phenol (4h): White solid, yield=89%, melting point (°C)= 232-234, IR (KBr,  $\text{cm}^{-1}$ )  $\nu_{\text{max}}$ =3448(NH), 3178 (Aromatic C-H), 1641, (C=C), 1612(C=N),  $^1\text{H}$  NMR (400 MHz, DMSO- $d_6$ ):  $\delta_{\text{ppm}}$  = 12.41 (s,1H, NH), 9.73 (s, 1H, OH), 6.86-8.31 (m, Ar H, 14H).

**3.A.6.9** 4-(4,5-diphenyl-1H-imidazol-2-yl)-N,N-dimethylaniline (4i): Brown solid, yield=97%, melting point (°C)= 257-260, IR (KBr,  $\text{cm}^{-1}$ )  $\nu_{\text{max}}$ = 3427(NH),3060 (Aromatic C-H),1615(C=C), 1552(C=N),  $^1\text{H}$  NMR (400 MHz, DMSO- $d_6$ ):  $\delta_{\text{ppm}}$  = 13.03(s,1H, NH), 8.26 (d, 2H), 7.96 (d, 2H), 7.25-7.56) (m,

Ar H, 10H).

**3.A.6.10** 3-(4,5-diphenyl-1H-imidazol-2-yl)phenol (4j): White solid, yield =98%, melting point (°C)= 270-274, IR (KBr,  $\text{cm}^{-1}$ )  $\nu_{\text{max}}$ =3423(NH), 3061(Aromatic C-H), 1593(C=N),  $^1\text{H}$  NMR (400 MHz, DMSO- $d_6$ ):  $\delta_{\text{ppm}}$  =13.51 (s,1H, NH), 9.75 (s, 1H, OH), 6.87 (d, 2H, Ar-H), 7.30-7.93 (m, Ar H, 12H).

**3.A.6.11** 2-(4,5-diphenyl-1H-imidazol-2-yl)phenol (4k): White solid, yield=97%, melting point(°C)= 205-207, IR (KBr,  $\text{cm}^{-1}$ )  $\nu_{\text{max}}$ =3443(NH), 3060 (Aromatic C-H), 1621(C=C), 1603(C=N),  $^1\text{H}$  NMR (400 MHz, DMSO- $d_6$ ):  $\delta_{\text{ppm}}$  = 12.97(s,1H, NH), 12.7(s,1H,OH), 6.95-8.13 (m, Ar H, 14H).

**3.A.6.12** 4-chloro-2-(4,5-diphenyl-1H-imidazol-2-yl)phenol (4l): White solid, yield=94%, melting point (°C)= >300, IR (KBr,  $\text{cm}^{-1}$ )  $\nu_{\text{max}}$ = 3443(NH), 3060 (Aromatic C-H), 1644(C=C), 1595(C=N),  $^1\text{H}$  NMR (400 MHz, DMSO- $d_6$ ):  $\delta_{\text{ppm}}$  = 13.13(s,1H, NH), 10.27(s,1H,OH), 6.95-8.23(m, Ar H, 13H).

**3.A.6.13** 4-bromo-2-(4,5-diphenyl-1H-imidazol-2-yl)phenol (4m): White solid, yield=96%, melting point (°C)=179-181, IR (KBr,  $\text{cm}^{-1}$ )  $\nu_{\text{max}}$ =3449(NH), 3053 (Aromatic C-H), 1636(C=C), 1610(C=N),  $^1\text{H}$  NMR (400 MHz, DMSO- $d_6$ ):  $\delta_{\text{ppm}}$  = 13.15(s,1H, NH), 13.09(s,1H,OH), 6.91-8.31(m, Ar H, 13H).

**3.A.6.14** 2-(4,5-diphenyl-1H-imidazol-2-yl)-4-nitrophenol (4n): yellow solid, yield=96%, melting point (°C)= 262-264, IR (KBr,  $\text{cm}^{-1}$ )  $\nu_{\text{max}}$ =3443(NH), 2958, 1633(C=C),(C=N),  $^1\text{H}$  NMR (400 MHz, DMSO- $d_6$ ):  $\delta_{\text{ppm}}$  = 13.3(s,1H, NH), 8.6 (s,1H,OH), 7.20-7.50(m, Ar H, 13H).

**3.A.6.15** 4-(4,5-diphenyl-1H-imidazol-2-yl)benzene-1,3-diol (4o): Black solid, yield=97%, melting point (°C)= 270-273, IR KBr, ( $\text{cm}^{-1}$ )  $\nu_{\text{max}}$ =3443(NH), 3063 (Aromatic C-H), 1619(C=C), 1606(C=N),  $^1\text{H}$  NMR (400 MHz, DMSO- $d_6$ ):  $\delta_{\text{ppm}}$  = 12.943(s,1H, NH), 9.73(s,1H, OH), 6.18-8.11(m, Ar H, 13H), 4.049 (s,1H, OH).

**3.A.6.16** 2-methoxy-6-(4,5-diphenyl-1H-imidazol-2-yl)phenol (4p): White solid, yield=95%, melting point (°C)=168-172, IR (KBr,  $\text{cm}^{-1}$ )  $\nu_{\text{max}}$ =3464(NH), 3050, 1632(C=C), 1604(C=N),  $^1\text{H}$  NMR (400 MHz, DMSO- $d_6$ ):  $\delta_{\text{ppm}}$  = 12.97(s,1H, NH), 6.86-7.67(m, Ar H, 13H), 4.28(s,1H, OH),3.87(s,3H, OCH<sub>3</sub>).

**3.A.6.17** 4-(4,5-diphenyl-1H-imidazol-2-yl)-2-methoxyphenol (4q): White solid, yield= 94%, melting point (°C)=258-262, IR (KBr,  $\text{cm}^{-1}$ )  $\nu_{\text{max}}$ =3447(NH), 2970 Aromatic C-H), 1647(C=C), 1606(C=N),  $^1\text{H}$  NMR (400 MHz, DMSO- $d_6$ ):  $\delta_{\text{ppm}}$  = 12.41(s,1H, NH), 6.83-7.67(m, Ar H, 13H), 4.03 (s,1H, OH),3.90(s,3H, OCH<sub>3</sub>).

**3.A.6.18** 2-(4-(4,5-diphenyl-1H-imidazol-2-yl)phenyl)-5,6-diphenyl-1H-benzo[d]imidazole (4r): yellow solid, yield=86%, melting point (°C)=210-212, IR (KBr,  $\text{cm}^{-1}$ )  $\nu_{\text{max}}$ =3443, 3424(NH), 3048 (Aromatic C-H), 1654(C=C), 1605, 1531(C=N),  $^1\text{H}$  NMR (400 MHz, DMSO- $d_6$ ):  $\delta_{\text{ppm}}$  = 12.72(s,1H, NH), 8.21 (d,

2H),7.25-7.55(m, Ar H, 14H).

**3.A.6.19** 4-(4,5-diphenyl-1H-imidazol-2-yl)-2,6-dimethoxyphenol (4s): white solid, yield: 94%, melting point (°C)=190-192, IR (KBr,  $\text{cm}^{-1}$ )  $\nu_{\text{max}}$ =3511(NH), 3027 (Aromatic C-H), 1615(C=C), 1543(C=N),  $^1\text{H}$  NMR (400 MHz, DMSO-d<sub>6</sub>):  $\delta_{\text{ppm}}$  = 13.97(s,1H, NH), 9.15(s,1H, OH), 7.19-8.18(m, Ar H, 12H), 3.36 (s, OCH<sub>3</sub>, 6H).

**3.A.6.20** 2-(4,5-diphenyl-1H-imidazol-2-yl)-1H-indole (4t):yellow solid, yield=96%, melting point (°C)= 306-308, IR (KBr,  $\text{cm}^{-1}$ )  $\nu_{\text{max}}$ =3413(NH), 3056 (Aromatic C-H), 1622(C=C), 1598(C=N),  $^1\text{H}$  NMR (400 MHz, DMSO-d<sub>6</sub>):  $\delta_{\text{ppm}}$  = 12.31(s,1H, NH), 11.40(s,1H, NH), 7.13-8.50(m, Ar H, 15H).

**3.A.6.21** 4,5-diphenyl-2-styryl-1H-imidazole (4u): White solid, yield=92%, melting point (°C)=140-143, IR (KBr,  $\text{cm}^{-1}$ )  $\nu_{\text{max}}$  =3449(NH), 3060 (Aromatic C-H), 1646(C=C), 1600(C=N),  $^1\text{H}$  NMR (400 MHz, DMSO-d<sub>6</sub>):  $\delta_{\text{ppm}}$  = 12.6(s,1H, NH), 7.58-7.92(m, Ar H, 15H), 6.52(d,2H, CH=CH).

**3.A.6.22** 2-(10-chloroanthracen-9-yl)-4,5-diphenyl-1H-imidazole (4v): yellow solid, yield= 93%, melting point (°C)>300, IR (KBr,  $\text{cm}^{-1}$ )  $\nu_{\text{max}}$ = 3465(NH), 3428(Ar C-H stretch), 3048, 1654(C=C), 1605(C=N),  $^1\text{H}$  NMR (400 MHz, DMSO-d<sub>6</sub>):  $\delta_{\text{ppm}}$  = 13.07(s,1H, NH), 8.56 (d 2H Ar-H J=8.0 Hz), 7.29-8.51(m, Ar H, 16H).

**3.A.6.23** 4,5-diphenyl-2-(3,4,5-trimethoxyphenyl)-1H-imidazole (4w): white solid, yield=98%, melting point (°C)= 162-166, IR (KBr,  $\text{cm}^{-1}$ )  $\nu_{\text{max}}$ =3354(NH), 2930 (Aromatic C-H), 1625(C=C), 1590(C=N),  $^1\text{H}$  NMR (400 MHz, DMSO-d<sub>6</sub>):  $\delta_{\text{ppm}}$  = 12.3(s,1H, NH),7.20-7.62(m, Ar H, 12H), 3.89(s,9H,OCH<sub>3</sub>).

## 3.A.7 Supporting spectra:

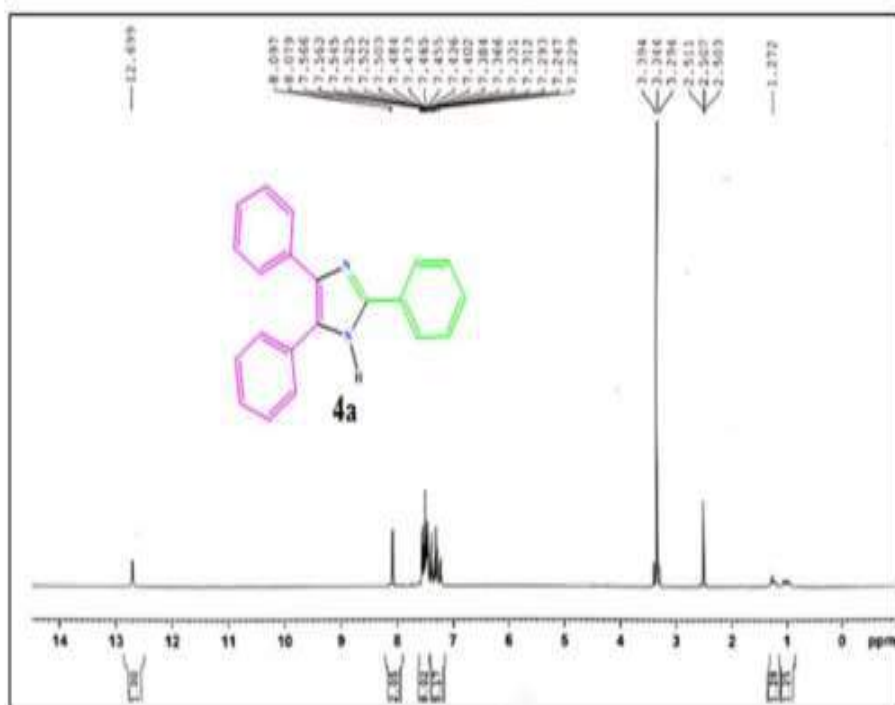
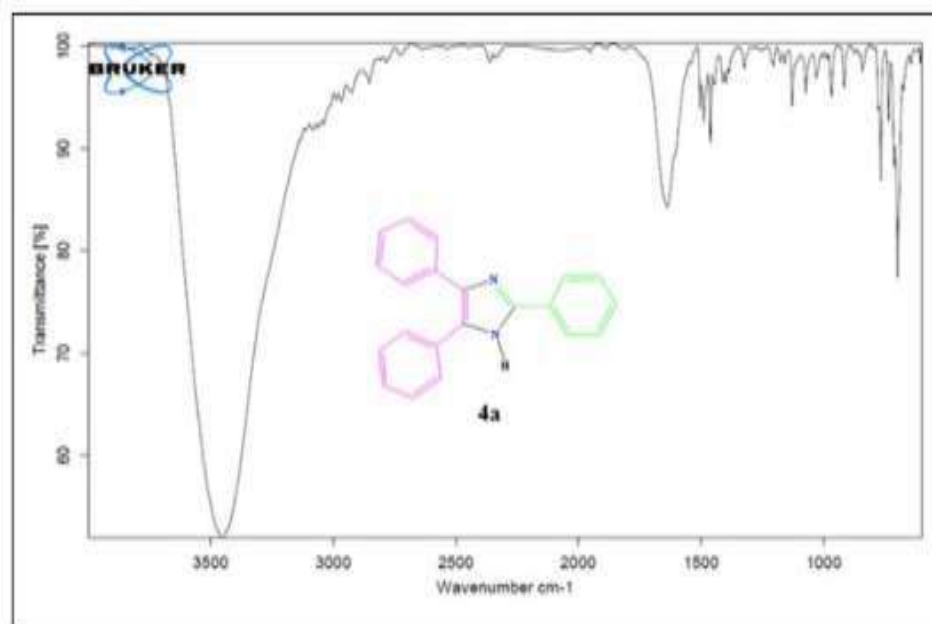
Fig. 3.A.7.1.  $^1\text{H}$  NMR spectra of 2,4,5-triphenyl-1H-imidazole (4a)

Fig. 3.A.7.2. FT-IR spectra of 2,4,5-triphenyl-1H-imidazole (4a)

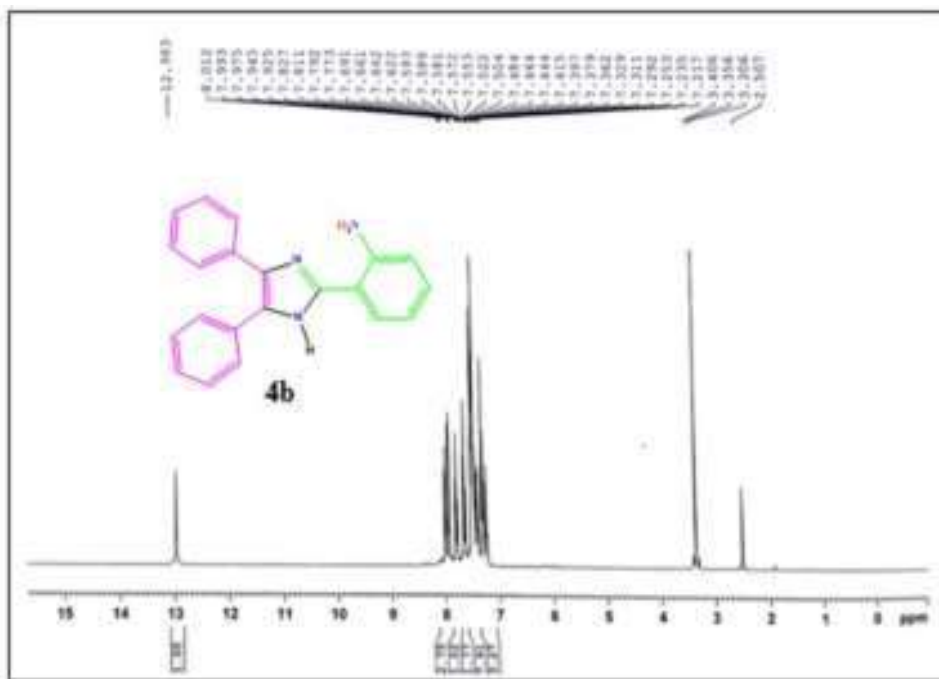


Fig. 3.A.7.3.  $^1\text{H}$  NMR spectra of 2-(2-nitrophenyl)-4,5-diphenyl-1H-imidazole (4b)

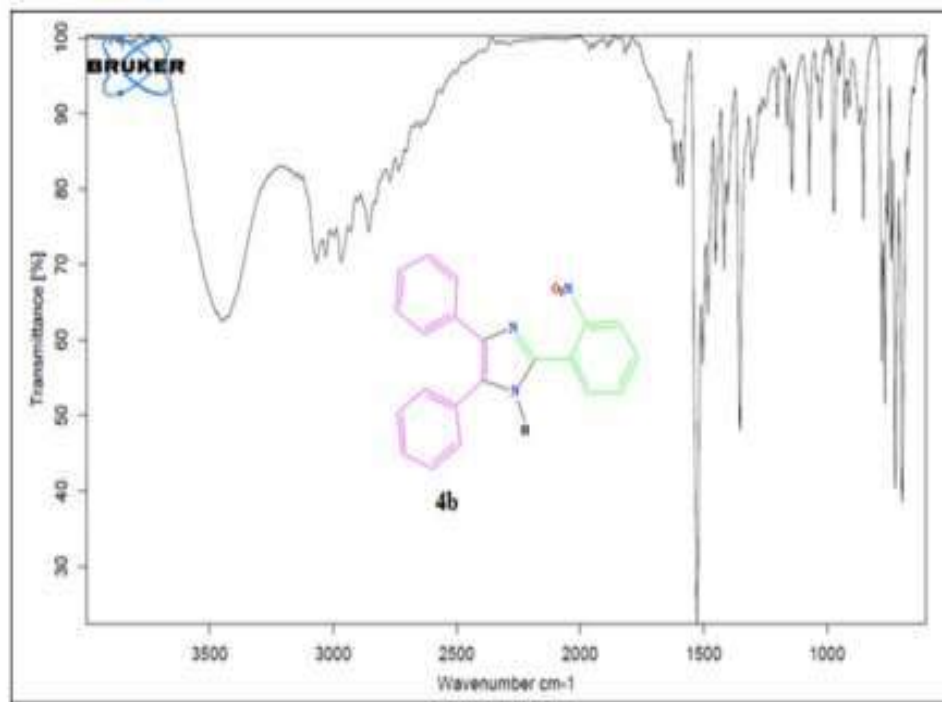


Fig. 3.A.7.4. FT-IR spectra of 2-(2-nitrophenyl)-4,5-diphenyl-1H-imidazole (4b)

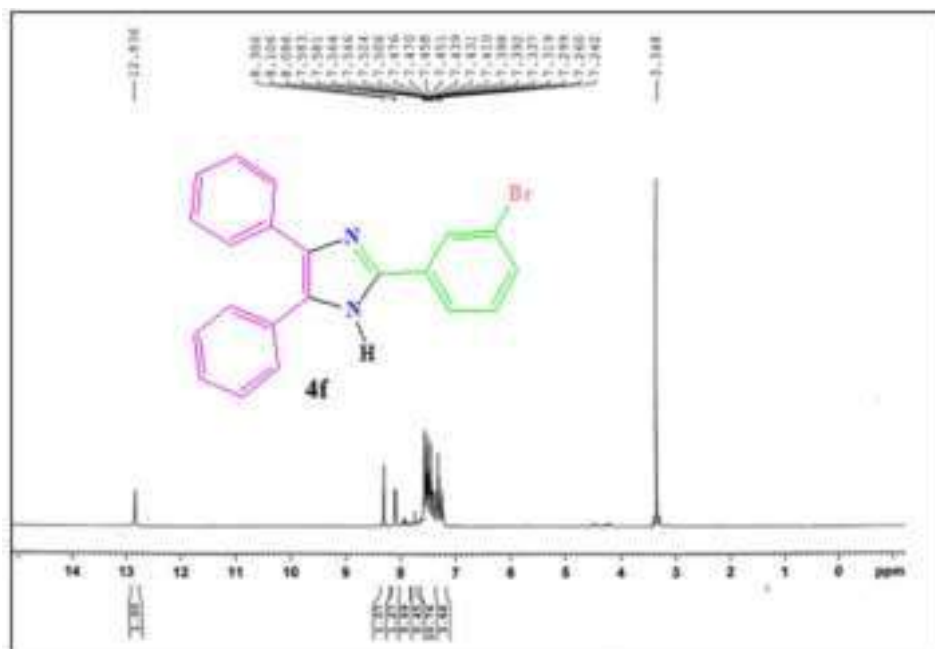


Fig. 3.A.7.5.  $^1\text{H}$  NMR of 2-(3-bromophenyl)-4,5-diphenyl-1H-imidazole(4f)

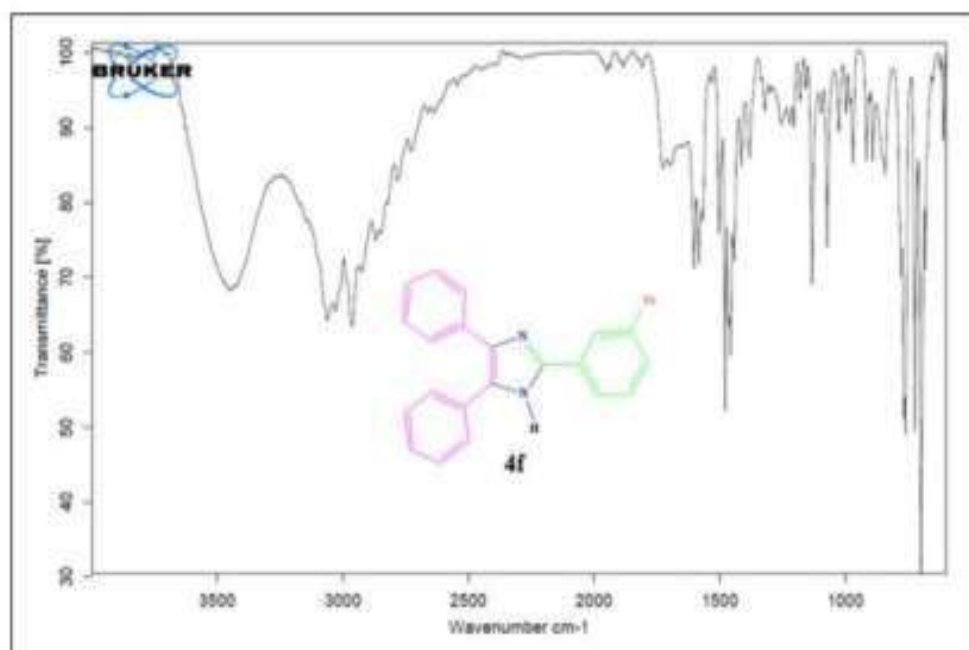


Fig. 3.A.7.6. FT-IR spectra of 2-(3-bromophenyl)-4,5-diphenyl-1H-imidazole (4f)

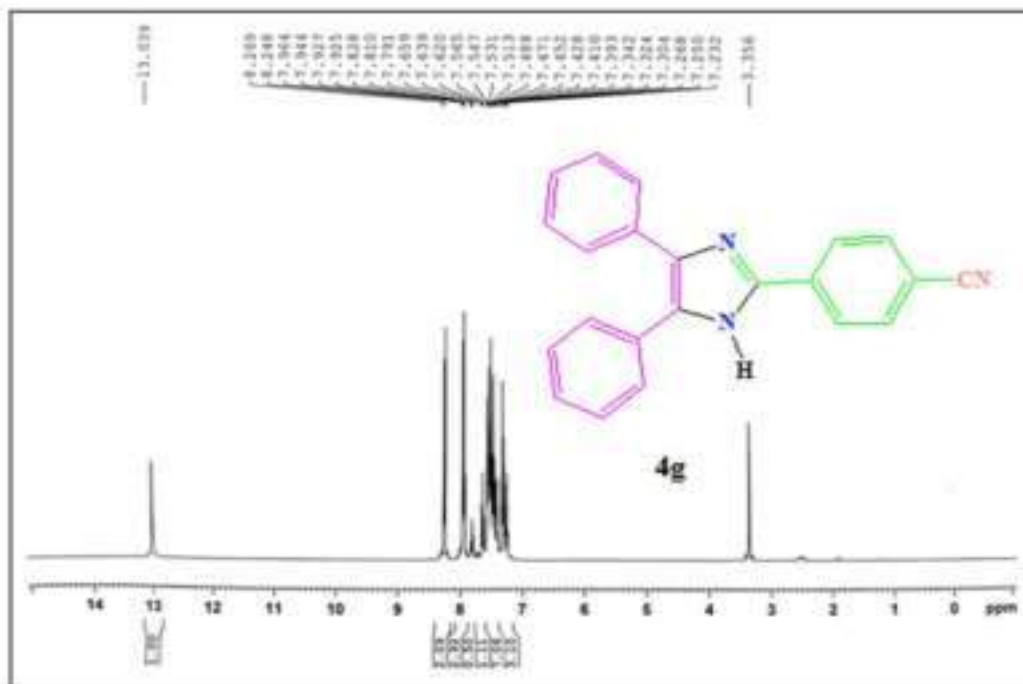


Fig. 3.A.7.7.  $^1\text{H}$  NMR of 4-(4,5-diphenyl-1H-imidazol-2-yl)benzonitrile(4g)

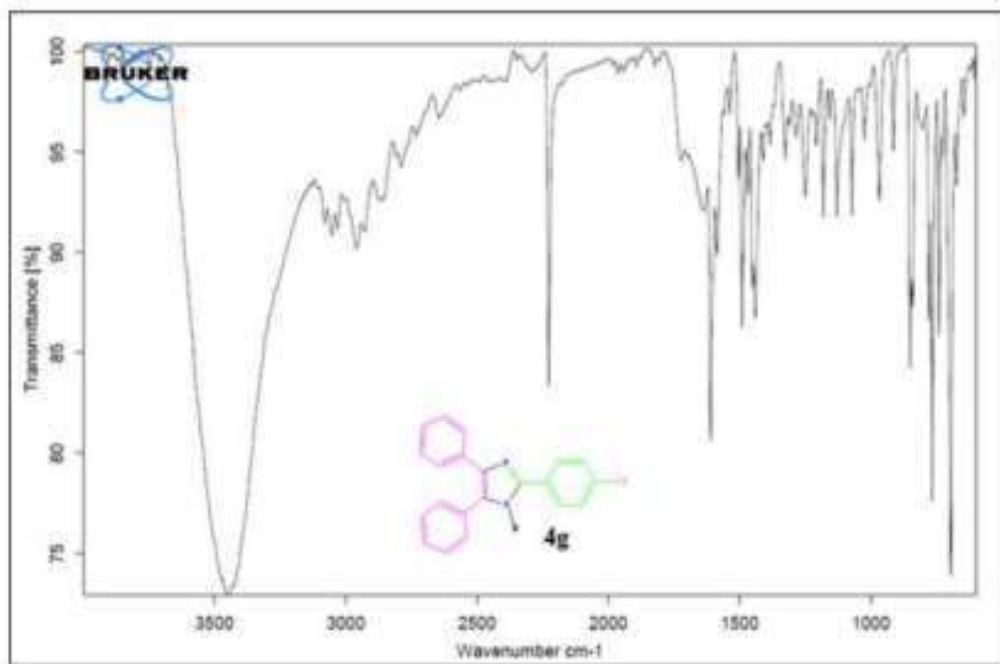


Fig. 3.A.7.8 FT-IR spectra of 4-(4,5-diphenyl-1H-imidazol-2-yl)benzonitrile(4g)

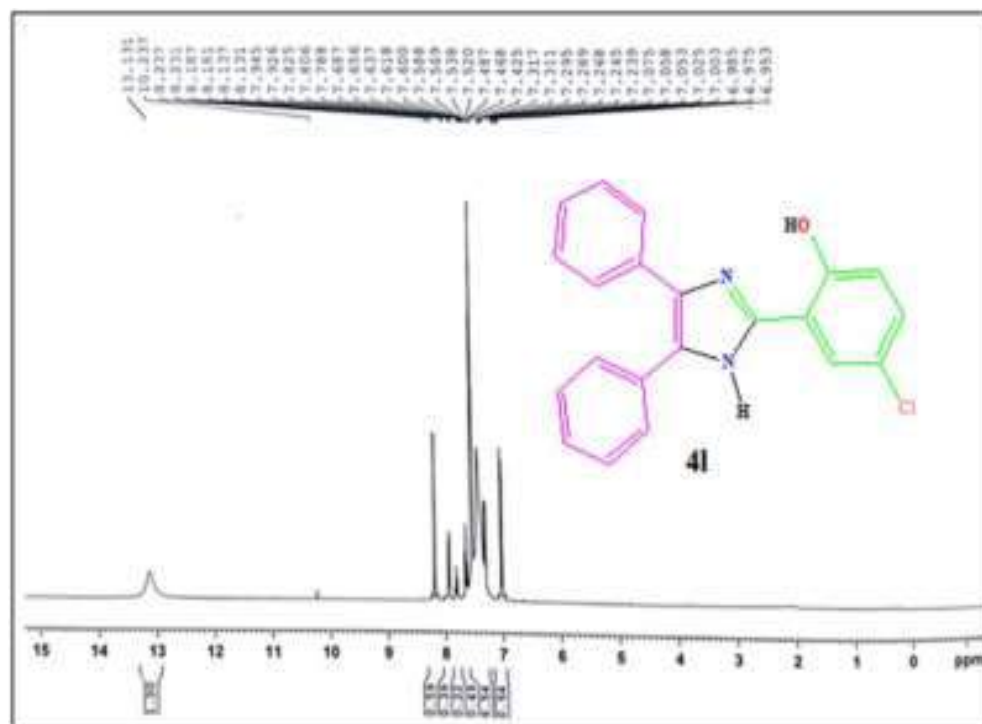


Fig. 3.A.7.9.  $^1\text{H}$  NMR of 4-chloro-2-(4,5-diphenyl-1H-imidazol-2-yl)phenol (4I)

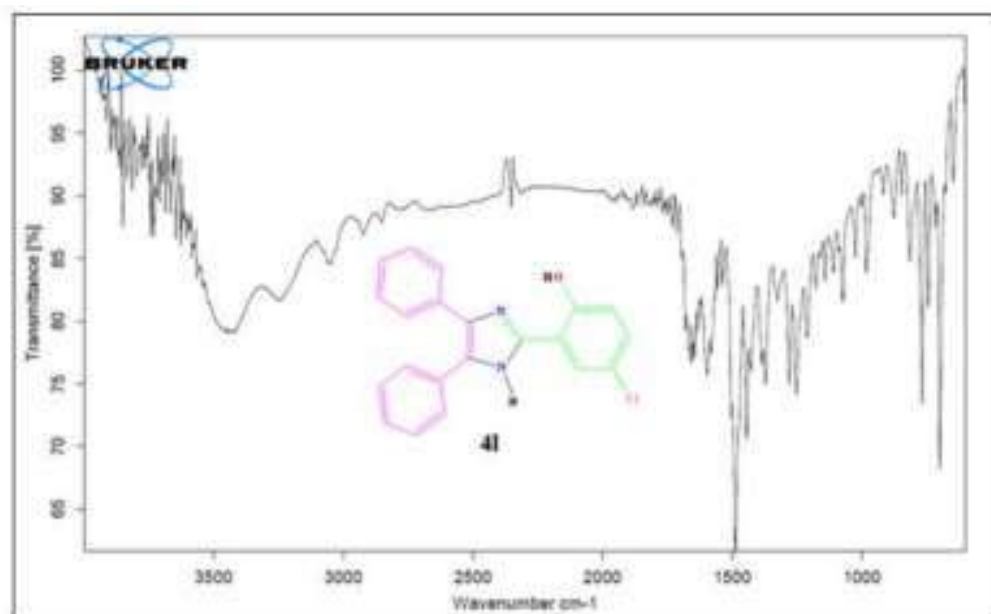


Fig. 3.A.7.10. FT-IR spectra of 4-chloro-2-(4,5-diphenyl-1H-imidazol-2-yl)phenol (4I)

**\*\*Rest of the spectras are given in Appendix-I\*\***



## 3.A.8 References

- (1) P. T. Anastas, T. C. Williamson., *Green Chemistry : Frontiers in Benign Chemical Syntheses and Processes*; Oxford Science Publications: New York, **1998**.
- (2) M. Poliakoff, P. Anastas., *Nature*, **2001**, *413* (6853).
- (3) J. M. DeSimone., *Science (1979)*, **2002**, *297* (5582), 799–803.
- (4) R. A. Sheldon., *Green Chemistry*, **2016**, *18* (11), 3180–3183.
- (5) R. A. Sheldon., *Green Chemistry*, **2017**, *19* (1), 18–43.
- (6) P. Gupta, A. Mahajan., *RSC Advances*, **2015**, *5* (34), 26686–26705.
- (7) R. R. Magar, S. S. Choudhare, S. V. Padghan., *International Journal of Multidisciplinary Research (Epitome Journals)*, **2015**, *1* (7), 1–9.
- (8) E. Ezzatzadeh, F. Z. Hargalani, F. Shafaei., *Polycyclic Aromatic Compounds*, **2021**, *0* (0), 1–16.
- (9) T. Welton., *Green Chemistry*, **2011**, *13* (2), 225.
- (10) G. Centi, S. Perathoner., *Catalysis Today*, **2003**, *77* (4), 287–297.
- (11) P. T. Anastas, M. M. Kirchhoff, T. C. Williamson., *Applied Catalysis A: General*, **2001**, *221* (1–2), 3–13.
- (12) A. Dömling, U. Ivar., *Angewandte Chemie International Edition*, **2000**, *39* (18), 3168–3210.
- (13) J. E. Biggs-Houck, A. Younai, J. T. Shaw., *Current Opinion in Chemical Biology*, **2010**, *14* (3), 371–382.
- (14) B. Jiang, T. Rajale, W. Wever, S. J. Tu, G. Li., *Chemistry – An Asian Journal*, **2010**, *5* (11), 2318–2335.
- (15) S. Brauch, S. S. van Berkel, B. Westermann., *Chemical Society Reviews*, **2013**, *42* (12), 4948–4962.
- (16) C. de Graaff, E. Ruijter, R. V. A. Orru., *Chemical Society Reviews*, **2012**, *41* (10), 3969–4009.
- (17) M. C. Pirrung, K. das Sarma., *Tetrahedron*, **2005**, *61* (48), 11456–11472.
- (18) C. G. Neochoritis, T. Zarganes-Tzitzikas, K. Katsampoxaki-Hodgetts, A. Dömling., *Journal of Chemical Education*, **2020**, *97* (10), 3739–3745.
- (19) S. Garbarino, D. Ravelli, S. Protti, A. Basso., *Angewandte Chemie International Edition*, **2016**, *55* (50), 15476–15484.

- (20) G. van der Heijden, E. Ruijter, R. V. A. Orru., *Synlett*, **2013**, 24 (6), 666–685.
- (21) D. Insuasty, J. Castillo, D. Becerra, H. Rojas, R. Abonia., *Molecules*, **2020**, 25 (3), 576.
- (22) J. G. Lombardino, E. H. Wiseman., *Journal of Medicinal Chemistry*, **1974**, 17 (11), 1182–1188.
- (23) A. Chawla, A. Sharma, A. Kumar Sharma., *Der Pharma Chemica*, **2012**, 4 (1), 116–140.
- (24) R. Breslow., *Accounts of Chemical Research*, **1995**, 28 (3), 146–153.
- (25) A. P. Kulkarni, C. J. Tonzola, A. Babel, S. A. Jenekhe., *Chemistry of Materials*, **2004**, 16 (23), 4556–4573.
- (26) L. Streit, M. Moreau, J. Gaudin, E. Ebert, H. vanden Bossche., *Pesticide Biochemistry and Physiology*, **1991**, 40 (2), 162–168.
- (27) A. Husain, S. Drabu, N. Kumar, M. M. Alam, S. Bawa., *Journal of Pharmacy And Bioallied Sciences*, **2013**, 5 (2), 161.
- (28) T. Scior, D. M. Domeyer, K. Cuanalo-Contreras, S. A. Laufer., *Current Medicinal Chemistry*, **2011**, 18 (10), 1526–1539.
- (29) A. K. Takle, M. J. B. Brown, S. Davies, D. K. Dean, G. Francis, A. Gaiba, A. W. Hird, F. D. King, P. J. Lovell, A. Naylor, A. D. Reith, J. G. Steadman, D. M. Wilson., *Bioorganic & Medicinal Chemistry Letters*, **2006**, 16 (2), 378–381.
- (30) L. Wang, K. W. Woods, Q. Li, K. J. Barr, R. W. McCroskey, S. M. Hannick, L. Gherke, R. B. Credo, Y. H. Hui, K. Marsh, R. Warner, J. Y. Lee, N. Zielinski-Mozng, D. Frost, S. H. Rosenberg, H. L. Sham., *J Med Chem*, **2002**, 45 (8), 1697–1711.
- (31) A. R. Phillips, H. L. White, S. Rosen., European Patent Application EP 58 8901; Chemical Abstracts, 98, 53894z; **1982**.
- (32) R. A. Turner, C. F. Huebner, C. R. Scholz., *J Am Chem Soc*, **1949**, 71 (8), 2801–2803.
- (33) J. Miller., *Annals of Allergy*, **1963**, 21, 692–697.
- (34) A. Goyal, J. Singh, D. P. Pathak., *Journal of Pharmaceutical Technology, Research and Management*, **2013**, 1 (1), 69–79.
- (35) K. Gaffney, D. G. I. Scott., *British Journal of Rheumatology*, **1998**, 37 (8), 824–836.
- (36) J. Baharara, E. Amini, N. Nikdel, F. Salek-Abdollahi., *Avicenna Journal of Medical Biotechnology*, **2016**, 8 (3), 119.

- (37) J.-B. Tagne, S. Kakumanu, R. J. Nicolosi., *Molecular Pharmaceutics*, **2008**, 5 (6), 1055–1063.
- (38) R. S. Joshi, P. G. Mandhane, M. U. Shaikh, R. P. Kale, C. H. Gill., *Chinese Chemical Letters*, **2010**, 21 (4), 429–432.
- (39) C. Yu, M. Lei, W. Su, Y. Xie., *Synthetic Communications*, **2007**, 37 (19), 3301–3309.
- (40) S. D. Sharma, P. Hazarika, D. Konwar., *Tetrahedron Letters*, **2008**, 49 (14), 2216–2220.
- (41) J. N. Sangshetti, N. D. Kokare, S. A. Kotharkara, D. B. Shinde., *Journal of Chemical Sciences*, **2008**, 120 (5), 463–467.
- (42) S. N. Murthy, B. Madhav, Y. V. D. Nageswar., *Tetrahedron Letters*, **2010**, 51 (40), 5252–5257.
- (43) S. Samai, G. C. Nandi, P. Singh, M. S. Singh., *Tetrahedron*, **2009**, 65 (49), 10155–10161.
- (44) A. R. Khosropour., *Ultrasonics Sonochemistry*, **2008**, 15 (5), 659–664.
- (45) R. K. Sharma, C. Sharma., *Catalysis Communications*, **2011**, 12 (5), 327–331.
- (46) M. Kidwai, P. Mothra, V. Bansal, R. K. Somvanshi, A. S. Ethayathulla, S. Dey, T. P. Singh., *Journal of Molecular Catalysis A: Chemical*, **2007**, 265 (1–2), 177–182.
- (47) G. H. Mahdavinia, A. M. Amani, H. Sepehrian., *Chinese Journal of Chemistry*, **2012**, 30 (3), 703–708.
- (48) H. Zang, Q. Su, Y. Mo, B. W. Cheng, S. Jun., *Ultrasonics Sonochemistry*, **2010**, 17 (5), 749–751.
- (49) M. Xia, Y. dong Lu., *Journal of Molecular Catalysis A: Chemical*, **2007**, 265 (1–2), 205–208.
- (50) M. Veerananarayana Reddy, Y. T. Jeong., *Journal of Fluorine Chemistry*, **2012**, 142, 45–51.
- (51) J. Jayram, V. Jeena., *Green Chemistry*, **2017**, 19 (24), 5841–5845.
- (52) J. Jayram, V. Jeena., *RSC Advances*, **2018**, 8 (66), 37557–37563.
- (53) K. Nikoofar, M. Haghghi, M. Lashanizadegan, Z. Ahmadvand., *Journal of Taibah University for Science*, **2015**, 9 (4), 570–578.
- (54) M. Kalhor, Z. Zarnegar., *RSC Advances*, **2019**, 9 (34), 19333–19346.

- (55) M. Kalhor, N. Khodaparast., *Research on Chemical Intermediates*, **2015**, 41 (5), 3235–3242.
- (56) A. Bamoniri, B. B. Fatemeh Mirjalili, S. Saleh., *RSC Advances*, **2018**, 8 (11), 6178–6182.
- (57) A. Khorramabadi-zad, M. Azadmanesh, S. Mohammadi., *South African Journal of Chemistry*, **2013**, 66 (1), 244–247.
- (58) N. V. Gandhare, R. G. Chaudhary, V. P. Meshram, J. A. Tanna, S. Lade, M. P. Gharpure, H. D. Juneja., *Journal of the Chinese Advanced Materials Society*, **2015**, 3 (4), 270–279.
- (59) Z. Varzi, M. S. Esmacili, R. Taheri-Ledari, A. Maleki., *Inorganic Chemistry Communications*, **2021**, 125, 108465.
- (60) D. Kumar, D. N. Kommi, N. Bollineni, A. R. Patel, A. K. Chakraborti., *Green Chemistry*, **2012**, 14 (7), 2038–2049.
- (61) K. Sivakumar, A. Kathirvel, A. Lalitha., *Tetrahedron Letters*, **2010**, 51 (22), 3018–3021.
- (62) N. V. Shitole, K. F. Shelke, S. S. Sonar, S. A. Sadaphal, B. B. Shingate, M. S. Shingare., *Bull Korean Chem Soc*, **2009**, 30 (9), 1963–1966.
- (63) S. S. Dipake, M. K. Lande, A. S. Rajbhoj, S. T. Gaikwad., *Research on Chemical Intermediates*, **2021**, 47 (6), 2245–2261.
- (64) A. R. Khosropour., *Ultrasonics Sonochemistry*, **2008**, 15 (5), 659–664.
- (65) L. M. Wang, Y. H. Wang, H. Tian, Y. F. Yao, J. H. Shao, B. Liu., *Journal of Fluorine Chemistry*, **2006**, 127 (12), 1570–1573.
- (66) K. Nikoofar, M. Haghighi, M. Lashanizadegan, Z. Ahmadvand., *Journal of Taibah University for Science*, **2015**, 9 (4), 570–578.
- (67) M. Kidwai, P. Mothsra, V. Bansal, R. Goyal., *Monatshefte für Chemie / Chemical Monthly*, **2006**, 137 (9), 1189–1194.
- (68) M. Banazadeh, S. Amirnejat, S. Javanshir., *Frontiers in Chemistry*, **2020**, 8 (Article 596029), 1–15.
- (69) J. Safari, S. D. Khalili, S. H. Banitaba., *Synthetic Communications*, **2011**, 41 (16), 2359–2373.
- (70) J. Safari, S. D. Khalili, M. Rezaei, S. H. Banitaba, F. Meshkani., *Monatshefte für Chemie - Chemical Monthly*, **2010**, 141 (12), 1339–1345.
- (71) E. Eidi, M. Z. Kassae, Z. Nasresfahani., *Applied Organometallic Chemistry*, **2016**, 30 (7), 561–565.

- (72) R. Wang, C. Liu, G. Luo., *Green Chemistry Letters and Reviews*, **2010**, 3 (2), 101–104.
- (73) K. F. Shelke, S. B. Sapkal, S. S. Sonar, B. R. Madje, B. B. Shingate, M. S. Shingare., *Bull Korean Chem Soc*, **2009**, 30 (5), 1057–1060.
- (74) M. Vosoughi, F. Mohebbali, A. P. S. Bonakdar, H. A. Lordegani, A. R. Massah., *Bulgarian Chemical Communications*, **2015**, 47 (2), 607–612.
- (75) B. F. Mirjalili, A. Bamoniri, N. Mohaghegh., *Current Chemistry Letters*, **2013**, 2 (1), 35–42.
- (76) G. Brahmachari, S. Das., *Indian Journal of Chemistry - Section B*, **2013**, 52B, 387–393.
- (77) B. Maleki, H. K. Shirvan, F. Taimazi, E. Akbarzadeh., *International Journal of Organic Chemistry*, **2012**, 2 (1), 93–99.
- (78) N. V. Gandhare, R. G. Chaudhary, V. P. Meshram, J. A. Tanna, S. Lade, M. P. Gharpure, H. D. Juneja., *Journal of the Chinese Advanced Materials Society*, **2015**, 3 (4), 270–279.
- (79) A. Sedrpoushan, Z. Joshani, L. Fatollahi., *Letters in Organic Chemistry*, **2014**, 11 (4), 287–292.
- (80) F. Hatamjafari, H. Khojastehkouhi., *Oriental Journal of Chemistry*, **2014**, 30 (1), 329–331.
- (81) S. Balalaie, A. Arabanian, M. S. Hashtroudi., *Monatshefte für Chemie/Chemical Monthly*, **2000**, 131 (9), 945–948.

## CHAPTER-III

### Section B

**Bis[2-(4,5-diphenyl-1H-imizol-2-yl)-4-nitro-phenolato] copper (II) dihydrate complex: Synthesis, Hirshfeld surface analysis, Catalytic activity and Evidence of *in-situ* conversion of  $\text{CuB}_4\text{O}_7$  into  $\text{Cu}(\text{OAc})_2 \cdot 2\text{H}_2\text{O}$  in presence of  $\text{NH}_4\text{OAc}$ \***

#### **3.B.1 Background of the present investigation**

Among many transition metal ions, Copper (II) ion have been studied extensively owing to their versatile coordination geometries, exquisite colors, and numerous applications in the field such as medicine, biochemistry, spectroscopy and fluorescent chemo sensors<sup>1-3</sup>. Copper ion draws significant consideration due to its very important role in fundamental biochemical processes in living organisms and also serves as a catalytic cofactor for a variety of metalloenzymes taking advantage of its redox and catalytic properties<sup>4-6</sup>. Interestingly, Imidazole motif being a five-membered nitrogen heterocyclic compound is ubiquitous in wide range of naturally occurring organic molecules and it serves as an important scaffold in various metalloenzymes and non-natural metal complexes<sup>7-10</sup>. Moreover, imidazole scaffold is present in the side chain of amino acid histidine which is present in many proteins, enzymes and metalloenzymes and plays an important role in numerous biochemical processes<sup>11</sup>. A remarkable and interesting biological activity is observed when copper ion combines with the imidazole motif and one such example is plastocyanin in which  $\text{Cu}(\text{II})$  binds to histidine residue<sup>12</sup> (Fig. 3.B.1).

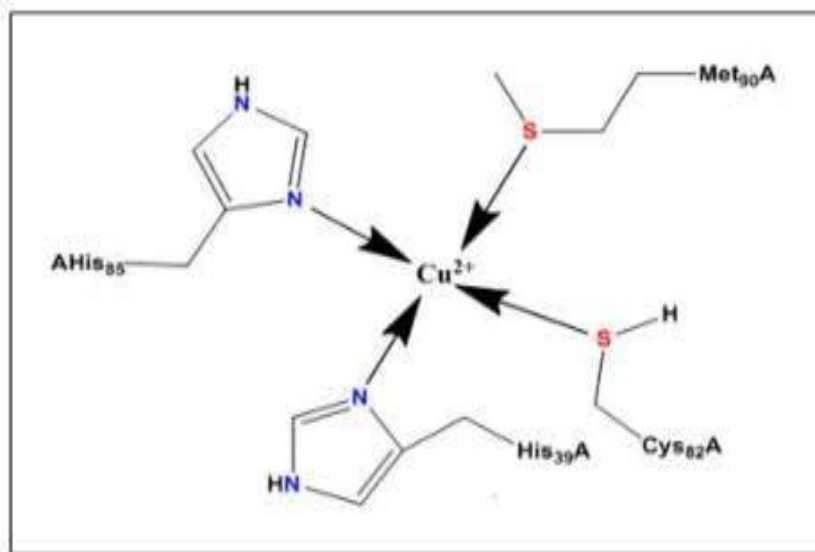


**Fig. 3.B.1.** Structure of plastocyanin

**\*Published in Acta Cryst. (2019). E75, 1664–1671**

Apart from the naturally occurring copper-imidazole complex, there is a vast literature on the synthetic copper complex with imidazole ligand<sup>13,14</sup>. Over the past few decades, synthesis of copper (II) coordination complexes with imidazole and substituted imidazole ligand has been rapidly developing owing to their widespread range of potential applications such as catalysis, gas absorption, photocatalysis, electrocatalytic, magnetic, perovskite solar cell<sup>7</sup>, luminescence, etc and structural diversity<sup>15-20</sup>.

Interestingly, during our ongoing research for the development of efficient catalyst for the synthesis of 2,4,5-triarylimidazole derivatives under green condition by utilizing copper borate as a catalyst, we encountered an *in-situ* formation of copper (II) complex with synthesized 2,4,5-triarylimidazole ligand and we also observed that during the reaction copper borate was converted into copper acetate in presence of ammonium acetate. Hence, in this chapter we will discuss about the *in-situ* formation of copper complex with synthesized 2,4,5-triarylimidazole and conversion of copper borate and other copper salts to copper acetate in presence of ammonium acetate.

### 3.B.2 Results and discussion

#### 3.B.2.1 *In-situ* formation of Bis[2-(4,5-diphenyl-1H-imidazol-2-yl)-4-nitrophenolato] copper (II) dihydrate (1)

In chapter III section A, we reported the catalytic efficacy of CuB<sub>4</sub>O<sub>7</sub> for the green synthesis of 2,4,5-triarylimidazole derivatives under solvent free condition and during the reaction, interestingly, we encountered that the catalyst could not be recovered after final work up of the product. Since, the catalyst copper borate was insoluble in most of the solvents and also, we carried out the reaction under neat condition and therefore, we were hopeful to recover the catalyst in fair amount but surprisingly, we found that during the addition of catalyst to the reaction mixture, the reaction mixture turned blue and after the work-up of the product, unfortunately the desired catalyst could not be recovered. Therefore, we focused our research to find out the actual reason for non-recovery of the catalyst. Moreover, the catalyst efficiently afforded the desired 2,4,5-triarylimidazole derivatives in good to excellent yield yet still there were some doubts for the non-recyclability of the catalyst. Fortunately, when we used aromatic aldehyde as 2-OH-benzaldehyde derivatives, we encountered that there was formation of some blue colored product in the reaction mixture along with the desired product. We then carefully recrystallized the blue colored compound in N,N-dimethylformamide (DMF) solvent and after 5 days a blue colored crystal suitable for X-ray single crystal diffraction was isolated for the reaction where we used 2-OH-5-NO<sub>2</sub>benzaldehyde. After successful X-ray single crystal diffraction study, it was revealed that the desired imidazole product was formed during the reaction but the product itself acted as a bidentate chelating ligand for the copper (II) ion in the reaction mixture thereby forming Bis [2-(4, 5-diphenyl-1H-imidazol-2-

yl)-4-nitro-phenolato] copper (II) dihydrate complex (1)<sup>21</sup>, (Fig. 3.B.2a and Fig. 3B.2b).

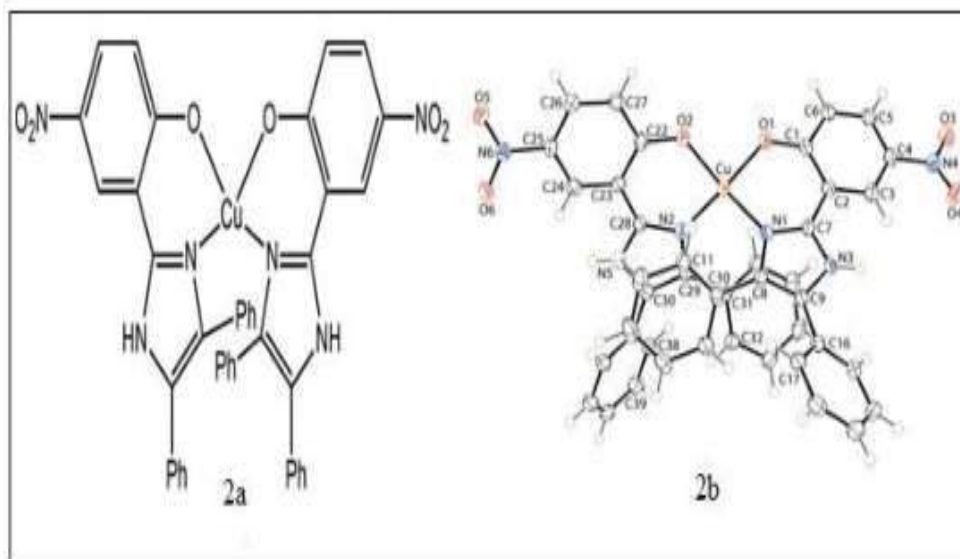


**Fig. 3.B.2a-b** . 2a) Molecular structure of complex (1) and 2b) Crystal structure of the complex molecule (1), showing the atom-labeling scheme and with displacement ellipsoids drawn at the 70% probability level (1).

### 3.B.2.2 Detailed study of the formation of Copper complex (1) and (2)

In order to understand the actual reason of *in-situ* formation of complex (1) we carried out the detailed study of transformation of copper borate into other intermediate in the reaction mixture under given condition separately.

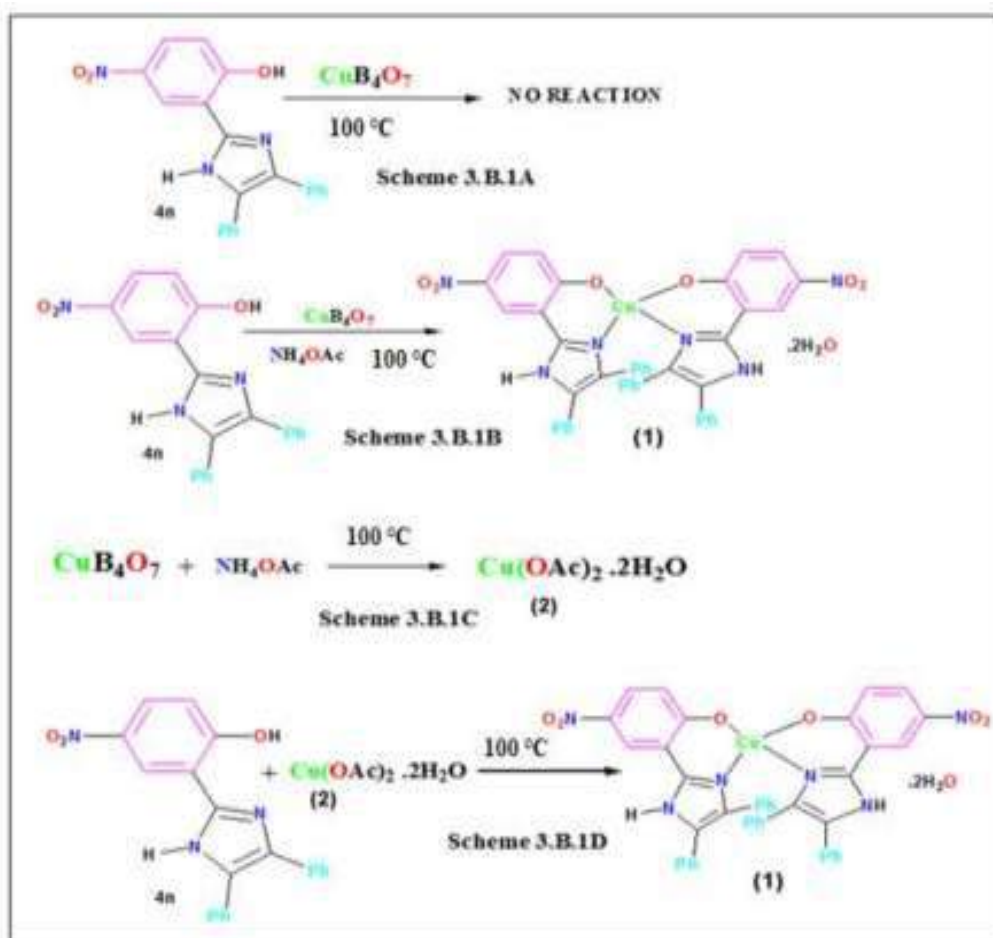
Firstly, we synthesized 2-(4,5-diphenyl-1H-imidazol-2-yl)-4-nitrophenol (**4n**) ligand and subsequently reacted with  $\text{CuB}_4\text{O}_7$  in neat condition at  $100^\circ\text{C}$  for 8-10 hours but we failed to get the desired product (1) (Scheme 3.B.1a) but when we added stoichiometric amount of  $\text{NH}_4\text{OAc}$  to the same reaction, the reaction mixture instantaneously turned blue and after reacting for 4 hours, the compound was extracted with DMF and the filtrate was kept for 5-8 days for slow evaporation at room temperature. Surprisingly, we got the same blue colored copper (II) complex (**1**) in excellent yield (60%) (Scheme 3.B.1b).

Secondly, in order to understand the role of  $\text{NH}_4\text{OAc}$ , a separate reaction was set up in which 1mmol of  $\text{CuB}_4\text{O}_7$  was directly added to 50 ml of water containing 3mmol of  $\text{NH}_4\text{OAc}$  in 100 ml round bottomed flask (Scheme 3.B.1c) and the reaction mixture was allowed to stir at room temperature for 8 hours. It was seen that  $\text{CuB}_4\text{O}_7$  slowly discharged into the  $\text{NH}_4\text{OAc}$  solution and with the passage of time entire  $\text{CuB}_4\text{O}_7$  dissolved in the reaction mixture. The reaction mixture was



allowed to evaporate at room temperature and finally after 14 days blue colored single crystal suitable for X-ray single crystal diffraction study was appeared in the solution. After successful X-ray single crystal diffraction of the compound, it was appeared that the blue colored complex was Copper (II) acetate dihydrate<sup>22</sup> (2) (Molecular formula  $\text{Cu}_2\text{C}_8\text{H}_{16}\text{O}_{10}$ ) with monoclinic crystal system and (C 2/c) space group having paddle wheel type of structure.

Thus, it was evident from the above reaction that  $\text{CuB}_4\text{O}_7$  in presence of  $\text{NH}_4\text{OAc}$  is converted to intermediate  $\text{Cu}(\text{OAc})_2 \cdot 2\text{H}_2\text{O}$  in the reaction mixture and undergo metallation with the ligand (4n) to give the complex (1) under the given reaction condition. We again set up a reaction directly with the compound 4n employing  $\text{Cu}(\text{OAc})_2 \cdot 2\text{H}_2\text{O}$  under the same reaction conditions and we obtained the same compound (1) (Scheme 3.B.1d).



(Scheme. 3.B.1a-3.B.1d). **3.B.1a)** Reaction between ligand 4n and  $\text{CuB}_4\text{O}_7$ , **3.B.1b)** Reaction between ligand 4n and  $\text{CuB}_4\text{O}_7$  in presence of  $\text{NH}_4\text{OAc}$  for the synthesis of (1), **3.B.1c)** Reaction between  $\text{CuB}_4\text{O}_7$  and  $\text{NH}_4\text{OAc}$  to for compound (2) and **3.B.1d)** Reaction between ligand 4n and compound (2) to form compound (1).

Again, this finding prompted us to examine whether other copper salts such as  $\text{CuO}$ ,  $\text{CuSO}_4$  and  $\text{CuCl}_2$  gets converted to copper acetate dihydrate or not in presence of ammonium acetate during the synthesis of 2, 4, 5-triarylimidazole derivatives and therefore we subsequently carried out the reaction of other copper salts with ammonium acetate under the same reaction condition separately. Interestingly it was observed that all the studied copper salts were converted to copper acetate dihydrate in presence of ammonium acetate as evident from the comparisons of FT-IR spectra of the reaction mixtures with that of the commercially available copper acetate dihydrate (Fig. 3.B.3).

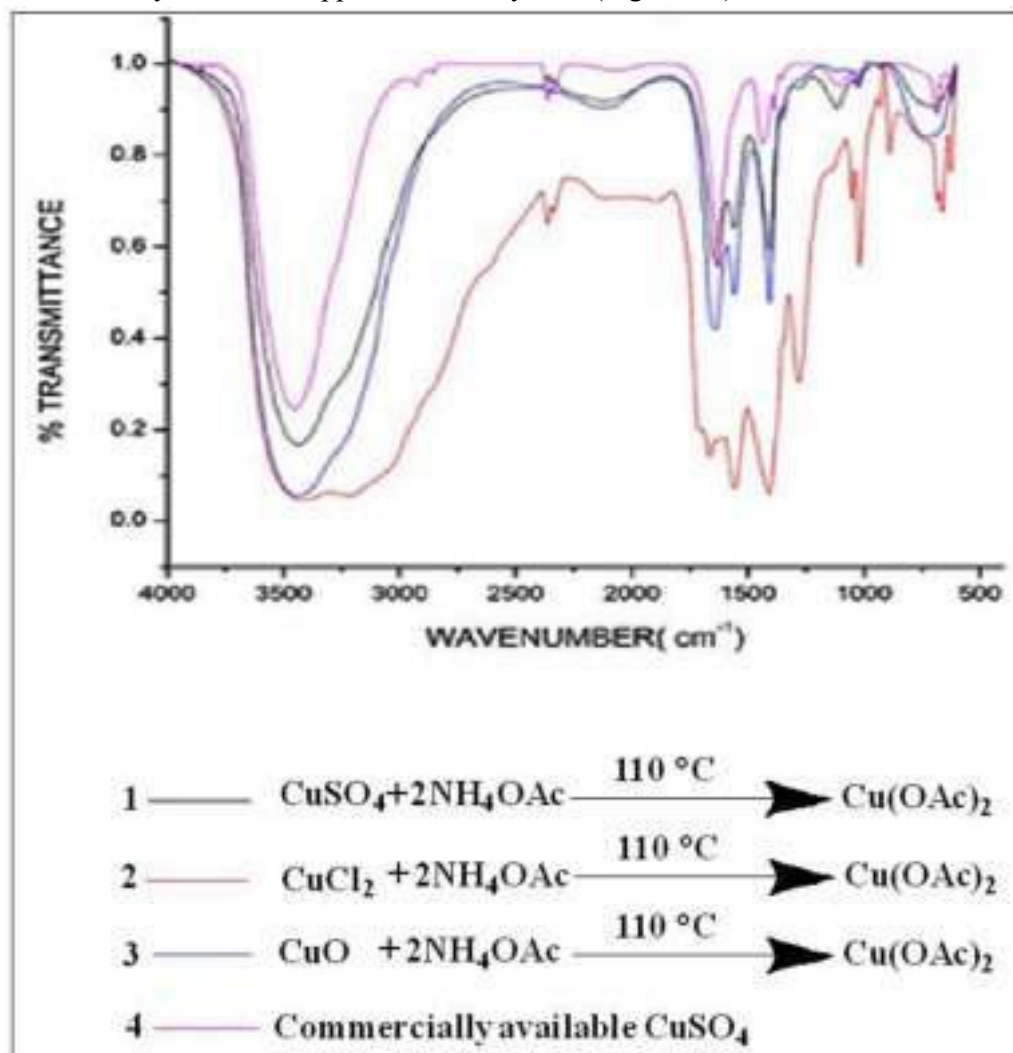


**Fig. 3.B.3.** (1) FT-IR spectra of the reaction mixture of  $\text{CuSO}_4$  and  $\text{NH}_4\text{OAc}$ , (2) FT-IR spectra of the reaction mixture of  $\text{CuCl}_2$  and  $\text{NH}_4\text{OAc}$  (3) FT-IR spectra of the reaction mixture of  $\text{CuO}$  and  $\text{NH}_4\text{OAc}$  and (4) FT-IR spectra of commercially available  $\text{Cu}(\text{OAc})_2 \cdot 2\text{H}_2\text{O}$

Thus, it is evident from the above findings that whenever we use Copper (II) salt as a catalyst for the synthesis of 2,4,5-triarylimidazole derivatives in presence of ammonium acetate, these salts are readily converted into copper acetate dihydrate in the reaction mixture. Hence an interesting feature of this finding is that we have been able to trap the acetate ion liberated from ammonium acetate as copper acetate dihydrate.

### **3.B.2.3 Description of crystal structure of copper complex (1) and (2)**

#### **3.B.2.3.1 Bis [2-(4, 5-diphenyl-1H-imidazol-2-yl)-4-nitro-phenolato] copper (II) dihydrate complex (1)**

The title copper (II) complex, (1), was isolated during an ongoing research programme on the catalytic activity of copper borate ( $\text{CuB}_4\text{O}_7$ ) for the synthesis of 2,4,5-triarylimidazole derivatives. Complex (1) was formed during the attempted synthesis of a triaryl imidazole derivative using benzil and 2-hydroxy 5-nitrobenzaldehyde with copper borate, using ammonium acetate as a nitrogen source. The single-crystal analysis of the synthesized product revealed that in the copper (II) complex, the triaryl imidazole moiety acts as a bidentate ligand for the copper atom. During the successful synthesis of the triaryl imidazole, the desired product formed in good yield at a temperature in the range 80-100°C. However, when the reaction was conducted at 100°C and above, the title copper (II) complex formed instead of the targeted triarylimidazole. The crystal and molecular structures of (1) are described herein, along with a detailed analysis of the molecular packing (Fig.3.B.2a-b). The crystallographic asymmetric unit of (1) comprises a complex molecule and two water molecules of crystallization. The crystallographic parameters and selected geometric parameters of the complex (1) are given in Table 3.B.1 and Table 3.B.2 respectively.

**Table 3.B.1.** Crystallographic parameters of complex (1)

Crystal data	
Chemical formula	[Cu(C <sub>21</sub> H <sub>14</sub> N <sub>3</sub> O <sub>3</sub> ) <sub>2</sub> ].2H <sub>2</sub> O141
M <sub>r</sub>	812.27
Crystal system, space group	Monoclinic, P2 <sub>1</sub> /c
Temperature (K)	100
a, b, c (Å)	13.2752 (2), 25.1602 (4), 11.1166 (2)
β(°)	141
V (Å <sup>3</sup> )	3598.68 (10)
Z	4
Radiation type	Cu Kα
μ (mm <sup>-1</sup> )	1.42
Crystal size(mm)	0.14X 0.11X0.07
Data collection diffractometer	XtaLAB Synergy, Dualflex, AtlasS2
Absorption correction	Gaussian (CrysAlis PRO; Rigaku OD, 2018)
Tmin, Tmax	0.757, 1.000
No. Of measured, independent and observed [I > 2σ(I)] reflections	46023, 7490, 6420
R <sub>int</sub>	0.058
(sin θ/λ) <sub>max</sub> (Å <sup>-1</sup> )	0.631
Refinement	
R[F <sup>2</sup> >2σ(F <sup>2</sup> )], wR(F <sup>2</sup> ), S	0.047, 0.128, 1.05
No. Of reflections	7490
No. Of parameters	532
No. Of restraints	8
H-atom treatment	H atoms treated by a mixture of independent and constrained refinement
Δ ρ <sub>max</sub> , Δ ρ <sub>min</sub> (e Å <sup>-3</sup> )	0.61, -0.74

Computer programs: CrysAlis PRO (Rigaku OD, 2018), SHELXS (Sheldrick, 2015a), SHELXL2014 (Sheldrick, 2015b), ORTEP-3 for Windows (Farrugia, 2012), DIAMOND (Brandenburg, 2006) and publCIF (Westrip, 2010).

The copper (II) centre in (1) is bis-N,O-chelated by two 2-(4,5-diphenyl-1H-imidazol-2-yl)-4-nitrophenolate monoanions. The resulting N<sub>2</sub>O<sub>2</sub> donor set defines highly distorted coordination geometry, as seen in the angles included in Table 3.B.2 and Fig.3.B.4.

**Table. 3.B.2.** Selected geometric parameters of complex (1)

Selected geometric parameters (Å, °) of complex (1)			
Cu—O1	1.9291 (17)	Cu—N1	1.9586 (19)
Cu—O2	1.9304 (17)	Cu—N2	1.957 (2)
O1—Cu—O2	89.36 (7)	O2—Cu—N1	144.41 (8)
O1—Cu—N2	147.34 (8)	O2—Cu—N2	93.56 (7)
O1—Cu—N1	92.83 (8)	N1—Cu—N2	103.14 (8)

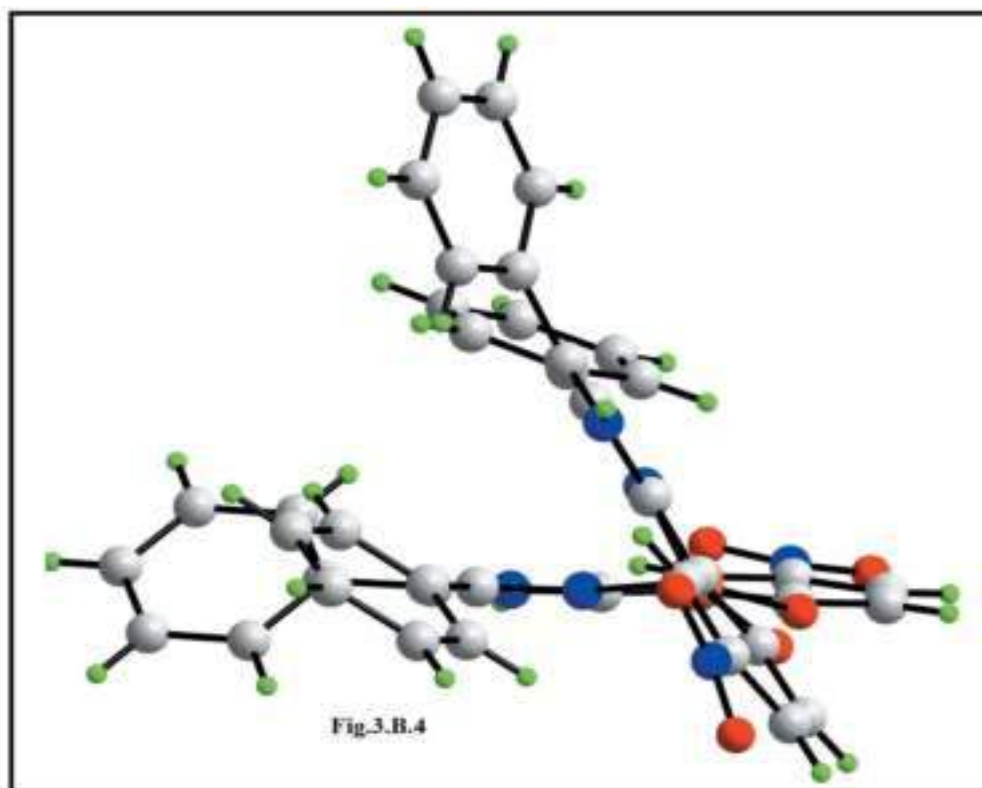


**Fig. 3.B.4.** A view of the molecular structure of the complex molecule in (1), highlighting the distorted coordination geometry about the copper (II) atom.

The angles range from a narrow 89.36 (7), for O1—Cu—O2, to a wide 147.34 (8), for O1—Cu—N2. The distortion is highlighted in the dihedral angle

between the best planes through the two chelate rings of 49.82 (7). The value of  $\tau_4$  is a geometric measure of the distortion of four-coordinate geometry<sup>23</sup>. For (1), the value computes as 0.48 which is almost exactly intermediate between the values of  $\tau_4 = 0$  for an ideal tetrahedron and  $\tau_4 = 1.0$  for an ideal square-planar geometry. In fact, the six-membered chelate rings are not planar, each adopting an envelope conformation with the Cu atom being the flap atom. In this description, the r.m.s. deviation for the least-squares plane through the O1/N1/C1/C2 atoms is 0.036 Å with the Cu atom lying 0.410 (3) Å out of the plane. The comparable parameters for the O2-chelate ring are 0.033 and 0.354 (3) Å, respectively. The dihedral angle formed between the two planar regions of the chelate rings is 49.38 (8). The dihedral angles between the best plane through the O1- chelate ring and each of the fused six- and five-membered rings are 9.18 (12)° and 5.54 (14)°, respectively; the equivalent angles for the O2-chelate rings are 8.44 (8) and 2.71 (9)°, respectively. The N1-imidazol-2-yl ring forms dihedral angles of 41.20 (11) and 37.46 (10)° with the C10- and C16-phenyl substituents, respectively, and the dihedral angle between the 143 phenyl rings is 59.92 (8)°, i.e., all indicating splayed relationships. A similar situation pertains to the N2-imidazol-2-yl ring, where the comparable dihedral angles formed with the C31- and C37-phenyl rings are 38.29 (10)°, 48.5 (9)° and 50.84 (7)°, respectively. Finally, the nitro groups are not strictly coplanar with the benzene rings to which they are connected, as seen in the dihedral angles of 14.2 (4)° for C1–C6/N4/O3/O4 and 5.9(3) for C22–C27/N6/O5/O6.

### 3. B.2.3.2 Supramolecular features of complex (1)

As each component of the asymmetric unit has hydrogen bonding functionality, conventional hydrogen bonds are found in the crystal of (1); the geometric parameters characterizing the identified intermolecular interactions operating in the crystal of (1) are collated in Table 3.B.3. Each of the imidazolylamine- N—H atoms forms a donor interaction to a water molecule to generate a three-molecule aggregate. The O1W water molecule forms donor interactions to the coordinated O2 atom and to a symmetry-related O2W water molecule. The O2W water molecule connects to the coordinated O1 atom as well as to a nitro-O3 atom. Hence, the O2W water molecule is involved in four hydrogen-bonding interactions. The fourth contact involving the O1W water molecule, a C—H...O acceptor contact, is provided by the nitrobenzene ring. There is also a phenyl-C—H...O (nitro) contact of note, Table 3.B.3. The aforementioned interactions combine to stabilize a supramolecular layer lying parallel to (101), as shown in Fig. 3.B.4a. There are also  $\pi$ - $\pi$  stacking and C—H...O interactions in the crystal, Fig. 3.B.4b. Within layers, there are  $\pi$ - $\pi$  interactions occurring between the imidazolyl and nitrobenzene rings [inter-centroid distances: Cg(N1/N3/C7–C9)...Cg(C1–C6) = 3.7452 (14) Å and angle of inclination = 9.70 (13)° for symmetry operation (-x + 2, -y + 1, -z + 1); Cg(N2/N5/C28–C30)...Cg(C22–C27) = 3.6647 (13) Å and angle of inclination = 8.15 (12)° for (-x + 1, -y + 1, -z + 1)]. The connections between layers along [010]

are of the type nitrobenzene-C—H...O (nitro) and phenyl-C—H.....(phenyl), as detailed in Table 3.B.3.

**Table. 3.B.3.** Hydrogen Bond geometry for complex (1)

Hydrogen bond geometry (Å, °)				
Cg1 is the ring centroid of the C16-C21 ring				
D-H...A144	D-H	H...A	D...A	D-H...A
N3—H3N...O1W <sup>i</sup>	0.89 (2)	1.91 (2)	2.790 (3)	173 (3)
N5—H5N...O2W144	0.88 (2)	1.95 (2)	2.822 (3)	172 (3)
O1W—H1W...O2144	0.85 (2)	1.92 (2)	2.745 (2)	164 (2)
O1W— H2W...O2W <sup>ii</sup> 144	0.85 (2)	2.21 (2)	2.868 (2)	134 (2)
O2W—H3W...O1 <sup>iii</sup> 144	0.84 (2)	2.01 (2)	2.841 (2)	172 (2)
O2W—H4W...O3 <sup>iiii</sup> 144	0.84 (2)	2.27 (2)	2.938 (2)	136 (2)
C3—H3...O1W <sup>i</sup> 144	0.95	2.57	3.435 (3)	151
C33—H33...O5 <sup>iv</sup>	0.95	2.48	3.345 (3)	151
C5—H5...O6 <sup>v</sup> 144	0.95	2.50	3.361(3)	151
C34—H34...Cg1 <sup>vi</sup> 144	0.95	2.49	3.426(3)	168

**Symmetry codes:** (i)  $-x + 2; -y + 1; -z + 1$ ; (ii)  $-x + 1; -y + 1; -z + 1$ ; (iii)  $x - 1, y, z - 1$ ; (iv)  $-x + 1, y + 1/2; -z + 1/2$ ; (v)  $x + 1; y, z + 1$  (vi)  $x, -y + 1/2; z - 1/2$ .

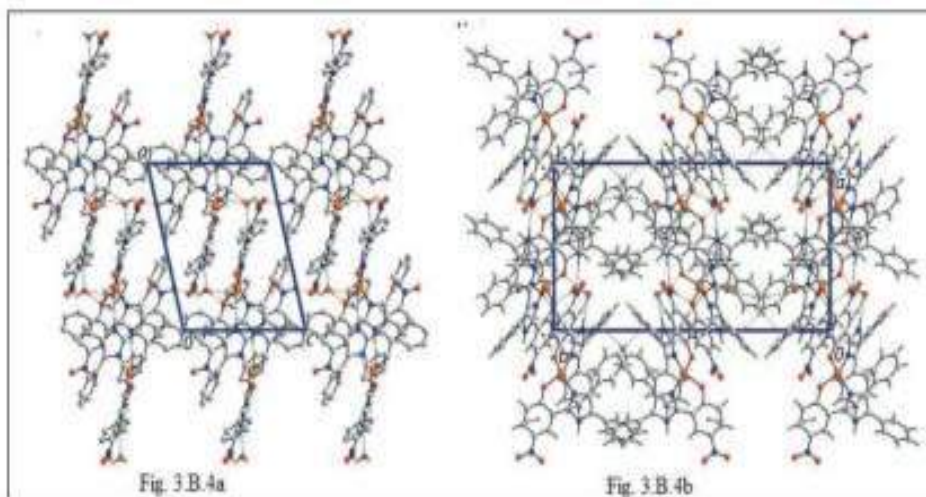


**Fig. (3.B.4a-4b).** The molecular packing in the crystal of (1): (3.B.4a) a supramolecular layer parallel to (101) sustained by O—H...O, N—H...O and C—H...O interactions shown as orange, blue and green dashed lines, respectively, and (3.B.4b) a view of the unit-cell contents in projection down the c axis, with  $\pi$ - $\pi$  and C—H... $\pi$  interactions shown as purple and pink dashed lines, respectively.

## 3.B.2.3.3 Hirshfeld surface analysis of complex (1)

The Hirshfeld surface calculations for (1) were performed with CrystalExplorer17 and published protocols<sup>24</sup> and serve to indicate the significant role of the two water molecules in the supramolecular association in the crystal. The involvement of both the water molecules in hydrogen bonds, Table 3.B.3, is evident as bright-red spots near the respective atoms on the Hirshfeld surfaces mapped over dnorm for the O1W-, Fig. 3B.5a, and O2W-water, Fig. 3B.5b, molecules. In addition, the presence of faint-red spots near the O1W, O2W and H1W atoms in Fig. 3B.5a and Fig. 3B.5b are indicative of the other contacts of these atoms with those of the Cu<sup>II</sup> complex molecule (Table 3.B.3). The donors and acceptors of the hydrogen bonds involving atoms of the complex molecule are also apparent as bright-red spots near the participating atoms in the views of the Hirshfeld surfaces calculated for the complex molecule shown in Figs. 3B.(5c–5d). The presence of a short interatomic C...C contact between atoms C22 and C28 (Table 3.B.4) arises from  $\pi$ - $\pi$  stacking between symmetry-related imidazole and nitrobenzene rings, and is observable as the faint-red spots near these atoms on the dnorm-mapped Hirshfeld surface in Fig.3.B.5c.

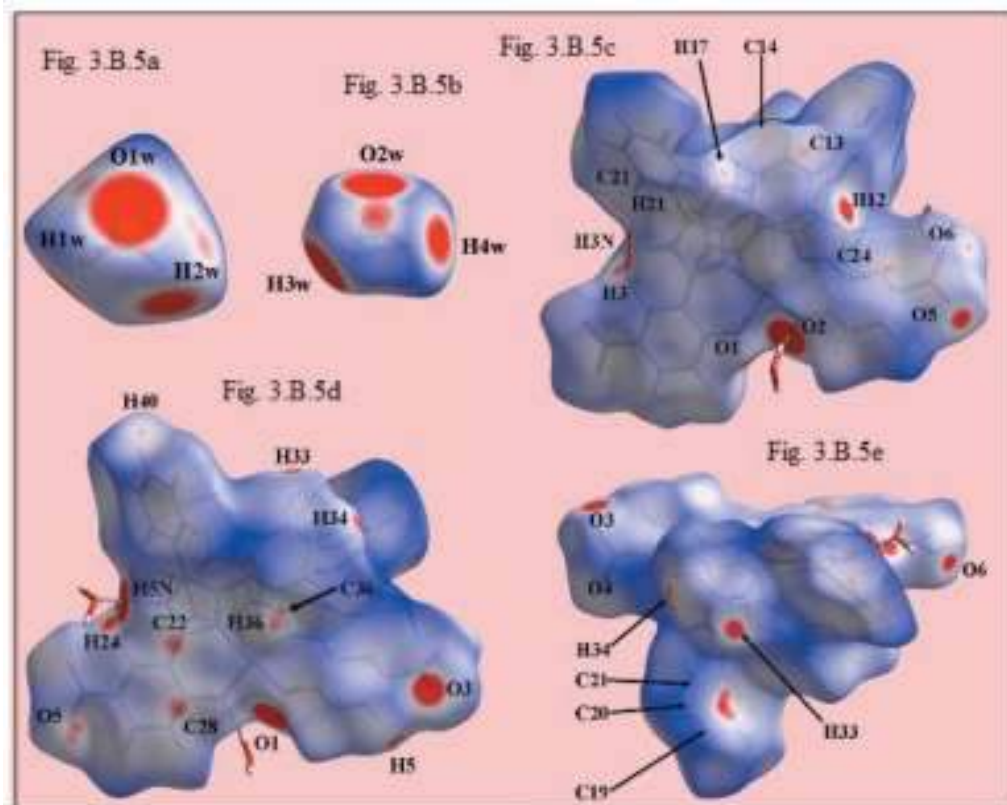


**Fig. 3.B.5a-e.** Different views of the Hirshfeld surfaces for the constituents of (I) mapped over dnorm for the (5a) water-O1W molecule [in the range -0.2369 to +1.2173 arbitrary units (au)], (5b) water-O2W molecule (-0.2114 to + 0.7500 au) and 5(c)–5(e) complex molecule (-0.1170 to + 1.6287 au).



**Table 3.B.4.** Summary of short interatomic contacts (Å) in complex (1)<sup>a</sup>

Contact	Distance	Symmetry operation
H12...H12	1.92	-x+1, -y+1, -z+1
H1W...H3N	2.22	-x+2, -y+1, -z+1
H2W...H3N	2.26	-x+2, -y+1, -z+1
O4...H4O	2.54	x+1, -y+3/2, z+1/2
C1...H3W	2.74	-x+1, -y+1, -z+1
C6...O6	3.206(3)	-x+1, -y+1, -z+1
C12...H12	2.55	-x+1, -y+1, -z
C13...C25	3.347(3)	-x+1, -y+1, -z
C14...O5	3.197(3)	-x+1, -y+1, -z
H17...O6	2.55	-x+1, -y+1, -z
C19...H34	2.68	x, -y+3/2, z-1/2
C20...H34	2.60	x, -y+3/2, z-1/2
C21...H34	2.67	x, -y+3/2, z-1/2
C21...H2W	2.64	-x+2, -y+1, -z+1
C21...O1W	3.161(3)	-x+2, -y+1, -z+1
C22...C28	3.267(3)	-x+1, -y+1, -z+1
C36...O5	3.146(3)	-x+1, -y+1, -z+1
H36...O5	2.49	-x+1, -y+1, -z+1
C41...H20	2.76	-x+1, y, z

Notes: (a) the interatomic distances are calculated in CrystalExplorer17 whereby the X-H bond lengths are adjusted to their neutron values.

The pair of faint-red spots appearing near the phenyl-C36 and H36 atoms, and also near the nitro-O5 atom on the surface indicating short interatomic contacts that characterize the weak C—H...O interaction, (Table 3.B.4). The influence of the C—H... $\pi$  contact on the molecular packing is recognized from the three faint-red spots in the phenyl-(C16–C21) ring and another near atom H34 in Fig.3.B.5e. The donors and acceptors of this interaction are also evident as the blue bump and a bright orange spot enclosed within the black circle on the Hirshfeld surface mapped with the shape-index property in Fig. 3.B.6a. The bright-orange region enclosed within a black circle in Fig.3.B.6b is also an indication of the O2W—H4W...Cg(C16–C21) contact. The Hirshfeld surfaces mapped over the calculated electrostatic potential for the water and complex molecules in Fig.3.B.7a-7c also illustrate the donors and acceptors of intermolecular interactions through blue and red regions corresponding to positive and negative electrostatic potentials, respectively. The  $\pi$ – $\pi$  stacking between symmetry-related imidazolyl and nitrobenzene rings are viewed as the flat regions enclosing them on the Hirshfeld surfaces mapped over curvedness in Fig.3.B.8a-8b.

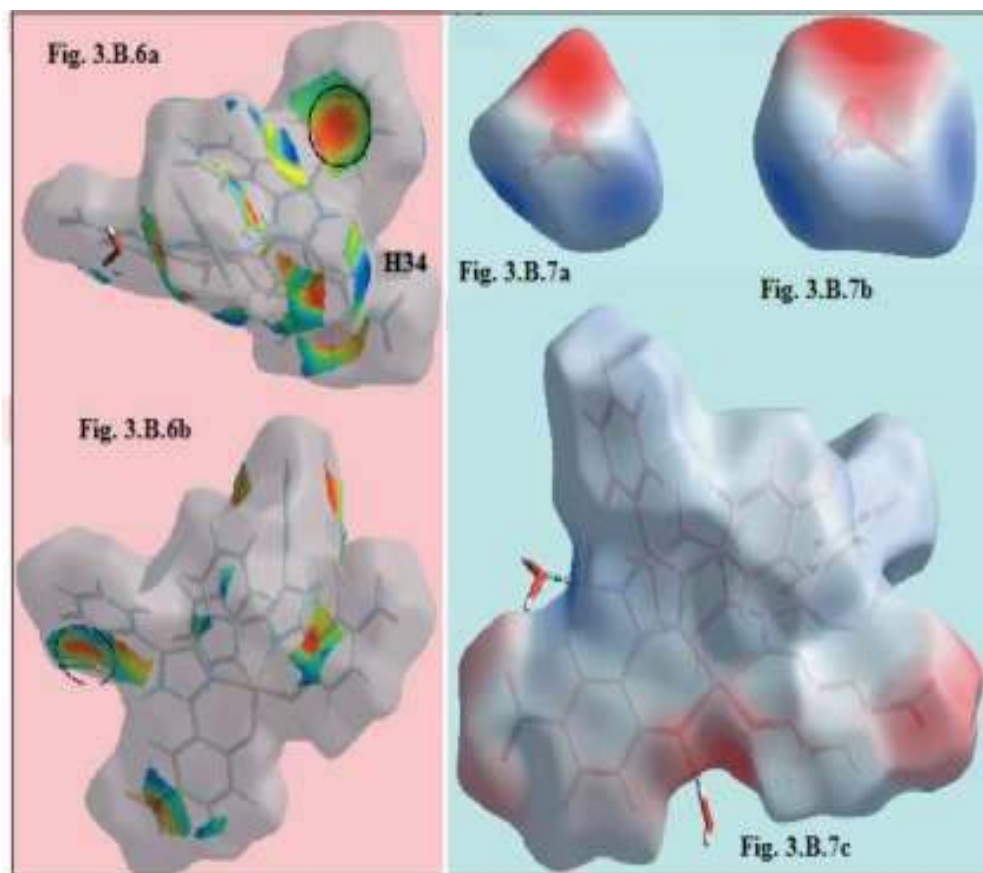


**Fig. 3.B.6a-b.** Two views of the Hirshfeld surface mapped with the shape-index property for the complex molecule in (1) from  $-1.0$  to  $+1.0$  arbitrary units highlighting (a) the donor and acceptor atoms of the C—H... $\pi$  interaction through a blue bump near the H34 atom and bright-orange curvature, enclosed within the black circle, and (b) the O2W—H4W... $\pi$  interaction by the bright-orange region enclosed within the black circle.

**Fig. 3.B.7a-c.** Different views of the Hirshfeld surfaces for the constituents of (1) mapped over the electrostatic potential (the red and blue regions represent negative and positive electrostatic potentials, respectively) for the (a) water-O1W molecule [in the range  $-0.1001$  to  $+0.1943$  atomic units (a.u.)], (b) water-O2W molecule ( $-0.1013$  to  $+0.1751$  a.u.) and (c) complex molecule ( $-0.1209$  to  $+0.2076$  a.u.). The hydrogen bonds involving water molecules in (c) are indicated by green dashed lines.

On the Hirshfeld surfaces mapped over  $d_{\text{norm}}$  illustrated in Figs. 3.B.5c–5e, faint-red spots also appear near other atoms indicating their involvement in other short interatomic contacts, as summarized in (Table 3.B.4). The Hirshfeld surfaces also provide an insight into the distortion in the coordination geometry

formed by the  $N_2O_4$  donor set about the copper(II) centre in the complex molecule. This is performed by considering the Hirshfeld surface about the metal centre alone<sup>25</sup>. The distortion in the coordination geometry is observed on the Hirshfeld surface mapped with the shape-index property as the bright orange patches of irregular shape covering a major region for the Cu—O bonds in Fig. 3.B.9a and the small orange regions on the surface relatively far from the Cu—N bonds in Fig. 3.B.9b. The different curvature of the Hirshfeld surfaces coordinated by the  $N_2O_4$  donor set in Figs. 3.B.9c and 3.B.9d also support this observation.

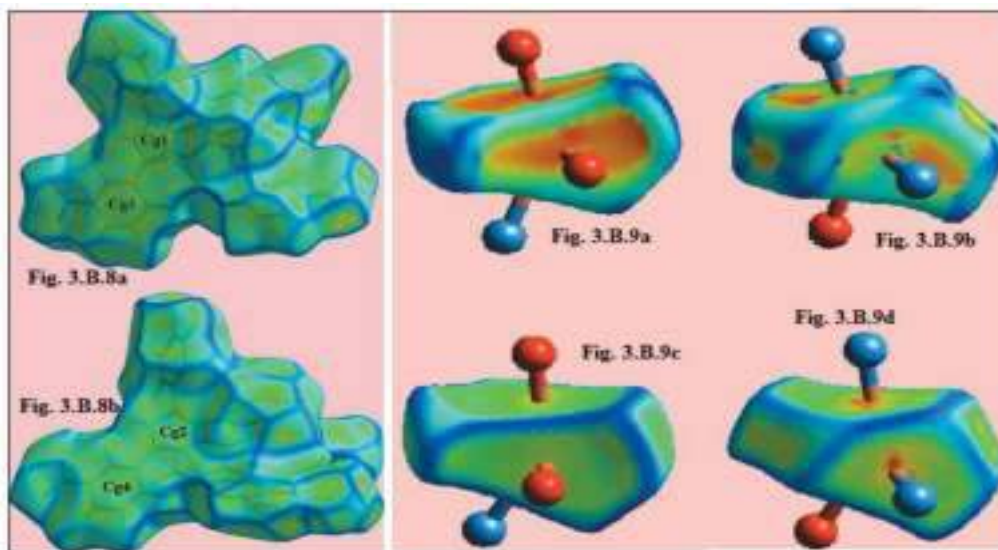


**Fig. 3.B.8a-b.** Two views of the Hirshfeld surface mapped over curvedness for the complex molecule in (1), highlighting flat regions enclosing symmetry related imidazole and nitrobenzene rings involved in  $\pi$ - $\pi$  stacking, labelled Cg1 and Cg3 for one pair of rings in (a), and Cg2 and Cg4 for the other pair in (b).

**Fig. 3.B.9a-d:** Different views of the Hirshfeld surfaces calculated for the copper(II) centre in (I) highlighting the coordination by the  $N_2O_4$  donor set mapped over (a)/(b) shape-index in the range -1.0 to +1.0 arbitrary units and (c)/(d) curvedness in the range -4.0 to +0.4 arbitrary units.

The Cu—O and Cu—N bonds are rationalized in the two-dimensional fingerprint plot taking into account only the Hirshfeld surface for the copper atom shown in **Fig. 3.B.10**. The distribution of points in the fingerprint plot through the pair of aligned red points at different inclinations from  $d_e + d_i \approx 2.0 \text{ \AA}$  for the Cu—N bonds (upper region) and the Cu—O bonds (lower region) are indicative of the distorted geometry.

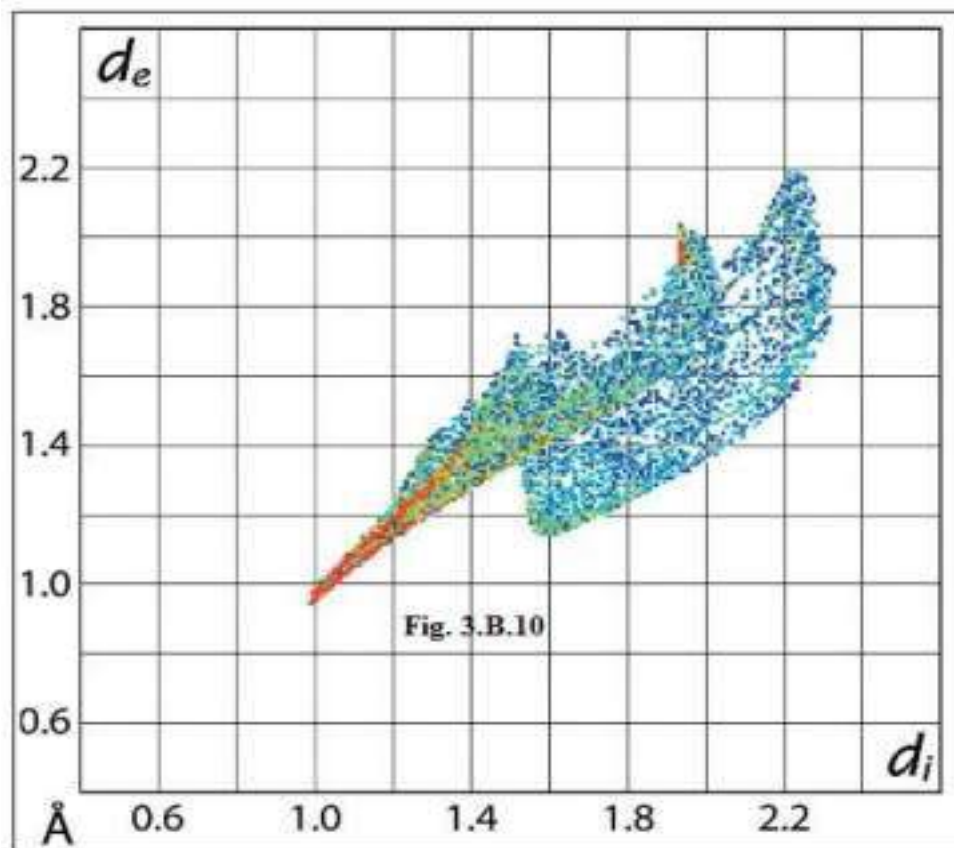


**Fig. 3.B.10.** The two-dimensional fingerprint plot taking into account only the Hirshfeld surface calculated about the copper(II) atom.

The overall two-dimensional fingerprint plot for (1), i.e. the entire asymmetric unit, Fig.3.B.11(a), and those delineated into H...H, O...H/H...O, C...H/H...C, C...C and C...O/O...C contacts are illustrated in Figs.3.B.11(b)–(f), respectively. The percentage contributions from different interatomic contacts to the Hirshfeld surfaces of the complex molecule and for overall (1) are summarized in Table 3.B.5. The presence of water molecules in the crystal of (1) increases the percentage contribution from O...H/H...O contacts (**Table 3.B.5**) to the Hirshfeld surface of the asymmetric unit compared with the complex molecule alone.

**Table 3.B.5.** Percentage contributions of interatomic contacts to the Hirschfeld surface for the complex in (I) and overall (II)

Contact	Percentage contribution	
	Complex molecule	(I)
H...H	41.3	41.0
O...H/H...O	25.6	27.1
C...H/H...C	19.8	19.6
C...C	3.5	3.3
C...O/O...C	3.4	3.2
C...N/N...C	2.8	2.7
N...H/H...N	2.2	2.1
O...O	0.6	0.5
N...O/O...N	0.2	0.2
Cu...O/O...Cu	0.0	0.3
Cu...C/C...Cu	0.3	0.0

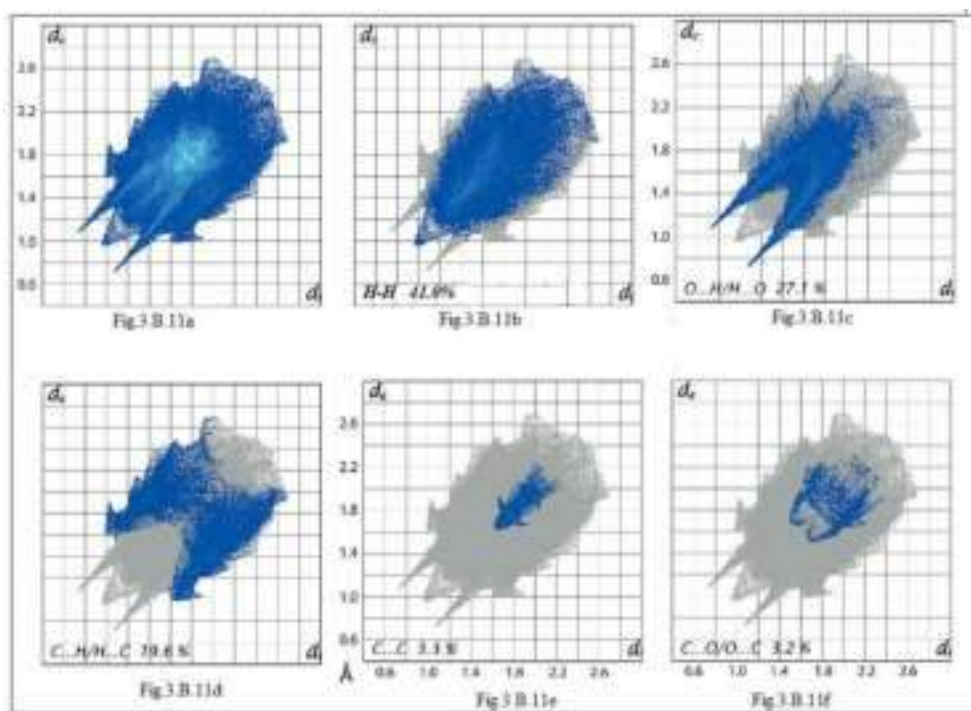


**Fig. 3.B.11a-f.** (a) A comparison of the full two-dimensional fingerprint plot for (I) and those delineated into (b) H...H, (c) O...H/H...O, (d) C...H/H...C, (e) C...C and (f) C...O/O...C contacts.

This results in slight decreases in the percentage contributions from other interatomic contacts for (1) (Table 3.B.5). A single conical tip at  $d_e + d_i \approx 1.9 \text{ \AA}$  in the fingerprint plot delineated into H...H contacts shown in Fig.3.B.11 (b) is the result of the involvement of the H12 atom in a short interatomic H...H contact, Table 3.B.4. The points due to short interatomic contacts between amine hydrogen-H3N and water hydrogen atoms, H1W and H2W, Table 3.B.4 are merged within the plot. Although the molecular packing of (1) is influenced by several intermolecular O—H...O and C—H...O interactions, the presence of a pair of long spikes at  $d_e + d_i \approx 1.8 \text{ \AA}$  in the plot delineated into O...H/H...O contacts, Fig.3.B.11(c), arise from the N—H...O hydrogen bond, while the merged points correspond to other interactions at greater interatomic distances. The significant contribution from interatomic C...H/H...C contacts (Table 3.B.5) to the Hirshfeld surface of (1) reflect the combined influence of intermolecular C—H... $\pi$  interactions (Table 3.B.4) and the short interatomic C...H/H...C contacts, summarized in Table 3.B.4, and viewed as the distribution of points in the form of characteristic wings in Fig.3.B.11d. The presence of short interatomic C...C contacts are evident as the points near a rocket shape tip at  $d_e + d_i \approx 3.2 \text{ \AA}$  in the respective delineated fingerprint plot, Fig.3.B.11e, while the points corresponding  $\pi$ - $\pi$  stacking between the imidazole and nitrobenzene rings are distributed about  $d_e = d_i = 1.7 \text{ \AA}$  in the plot. The small, i.e. 2.7%, contribution from C... N/N...C contacts to the surface is also due to these  $\pi$ - $\pi$  stacking interactions (delineated plot not shown). The contribution of 3.2% from C...O/O...C contacts is due to the presence of short interatomic contacts involving nitro-O atoms, Table 3.B.4, and are apparent as the pair of parabolic tips at  $d_e + d_i \approx 3.2 \text{ \AA}$  in the delineated plot of Fig.3.B.11f. The contribution from other interatomic contacts to the surface summarized in Table 3.B.5 has negligible influence on the molecular packing.

### 3. B.2.3.2 Crystal structure of Copper acetate monohydrate ( $\text{Cu}_2\text{C}_8\text{H}_{16}\text{O}_{10}$ ) (2)

The compound copper acetate monohydrate (2) was obtained as a by-product of the reaction between the catalyst  $\text{CuB}_4\text{O}_7$  and  $\text{NH}_4\text{OAc}$  during the synthesis of 2,4,5-triarylimidazole derivatives under the solvent free condition. After successful single crystal diffraction study, its structure has been compared with the reported structure<sup>22</sup>. A detail of crystallographic data (crystal parameters, data collection and refinements) of the Compound (2) is given in Table 3.B.6. The atomic numbering scheme along with the atom connectivity for compound (2) is shown in Fig.3.B.12a-12b. Single crystal X-ray analysis revealed that the compound (2) crystallizes in the monoclinic crystal system with space group  $C2/c$  and the crystallographic parameters are  $a=13.0799(8) \text{ \AA}$ ,  $[13.167 (4) \text{ \AA}]^{22}$ ,  $b=8.5056(4)\text{\AA}$ ,  $[8.563 (2) \text{ \AA}]^{22}$ ,  $c=13.7429(7)\text{\AA}$ ,  $[13.862 (7) \text{ \AA}]^{22}$ ,  $\beta=116.887(7)^\circ$ ,  $[117.019 (2)^\circ]^{22}$   $\alpha=\gamma=90^\circ$  and  $Z = 4$ .

**Table. 3.B.6.** Crystal data collection and structure refinement for compound (2)

<b>Crystal data</b>	
Moiety formula, Chemical formula	Cu <sub>2</sub> C <sub>8</sub> H <sub>16</sub> O <sub>10</sub> , Cu <sub>2</sub> (O <sub>2</sub> CCH <sub>3</sub> ) <sub>4</sub> . 2H <sub>2</sub> O
Formula weight	399.31
Crystal system, Space group	Monoclinic, C 2/c
Colour, Size, mm	Blue, 0.24 × 0.22 × 0.20
Unit cell dimensions	
a, b, c	13.0799 (8) Å, 8.5056(4) Å, 13.7429(7) Å
α, β, γ	90°, 116.887(7)°, 90°
Volume Å <sup>3</sup> , Z	1363.65(13), 4
Density (calculated), Mg/m <sup>3</sup>	1.945
Absorption coefficient, mm <sup>-1</sup>	3.164
F(000)	808
Data collection	
Temperature, K	119.98(10)
Theta range for data collection	2.96° to 29.01°
Index ranges	-17 ≤ h ≤ 17, -11 ≤ k ≤ 10, -18 ≤ l ≤ 17
Reflections collected	8716
Unique reflections	1660
Observed reflections (>2σ(I))	1438
R <sub>int</sub>	0.0387
Completeness to θ, %	29.01°, 91.1
Absorption correction	Multi-scan (Rigaku Oxford Diffraction, 2017)
	T <sub>min</sub> = 0.473, T <sub>max</sub> = 0.531
Refinement	
Refinement method	Full-matrix least-squares on F <sup>2</sup>
Data / restraints / parameters	1660 / 0 / 101
Goodness-of-fit on F <sup>2</sup>	1.052
Final R indices [ I > 2σ(I) ]	R <sub>1</sub> = 0.0266, wR <sub>2</sub> = 0.0582
R indices (all data)	R <sub>1</sub> = 0.0328, wR <sub>2</sub> = 0.0603
Largest diff. peak and hole	0.532 and -0.566 e.Å <sup>-3</sup>

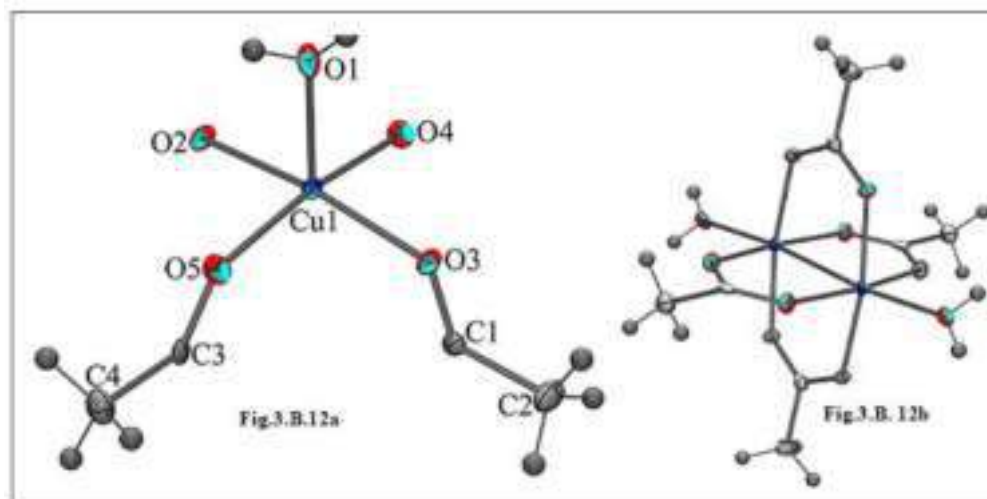


**Fig. 3.B.12a-b.** a) Asymmetric unit of compound (2) and b) ortep diagram of (2) with 50% probability

As evident from Fig.3.B.12b, The two copper ions are bridged symmetrically by four acetates in a centrosymmetric dimeric unit and two waters coordinate along the Cu-Cu axis and assumes paddle wheel structure in which the Cu-Cu distance is about 2.6118 (5) Å (Cu-Cu distance in metallic copper, 2.556Å). The selected bond lengths (Å) and bond angles (°) for compound (2) is listed in Table 3.B.7.

**Table. 3.B.7.** The selected bond lengths (Å) and bond angles (°) for compound (2)

<b>Bond lengths (Å)</b>			
Cu(1)-Cu(1) <sup>i</sup>	2.6118(5)	Cu(1)-O(3)	1.9847(15)
Cu(1)-O(1)	2.1411(17)	Cu(1)-O(4)	1.9415(15)
Cu(1)-O(2)	1.9907(15)	Cu(1)-O(5)	1.9559(15)
<i>Symmetry Code: (i) -x+1, -y+1, -z+1</i>			
<b>Bond angles (°)</b>			
O(2)-Cu(1)-O(1)	92.58(7)	O(4)-Cu(1)-O(2)	90.29(6)
O(3)-Cu(1)-O(1)	98.35(7)	O(5)-Cu(1)-O(2)	89.42(6)
O(4)-Cu(1)-O(1)	97.28(7)	O(4)-Cu(1)-O(3)	87.20(6)
O(5)-Cu(1)-O(1)	93.52(7)	O(5)-Cu(1)-O(3)	91.06(6)



The Cu(1)-O(1) and Cu(1)-O(2) bond distances in the complex (2) are 2.1411 (17) Å and 1.9907(15) Å respectively. Similarly, Cu(1)-O(3), Cu(1)-O(4) and Cu(1)-O(5) bond distances are 1.9847(15), 1.9415(15) and 1.9559(15) respectively. Hydrogen bonding pattern and hydrogen bonding geometrical parameters in compound (2) is shown in Fig.3.B.13 and Table 3.B.8 respectively.

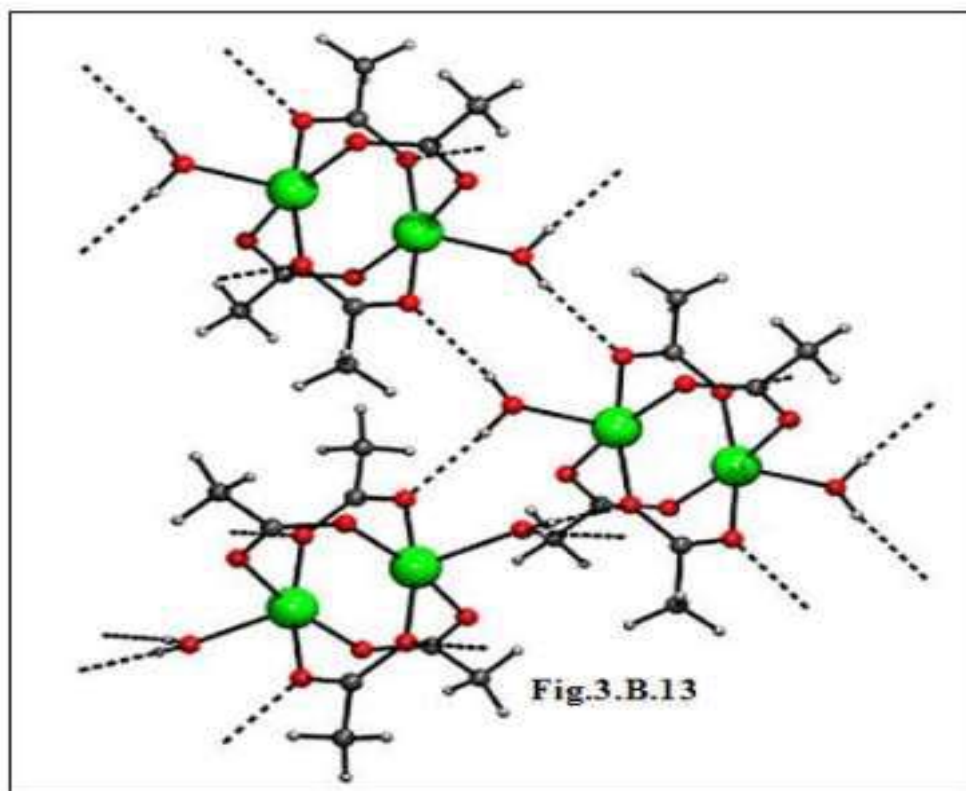


Fig. 3.B.13. Hydrogen bonding pattern in compound (2)

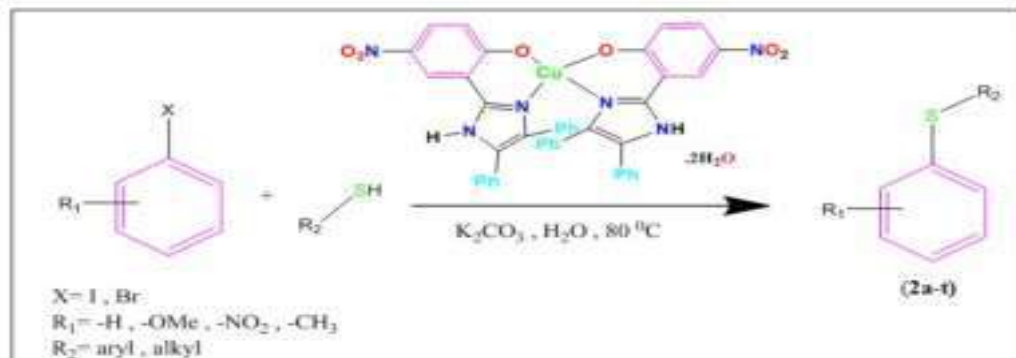
Table 3.B.8. Hydrogen bonded geometries in compound (2)

Bond	D - H	H···A	D···A	D - H···A
O(1)–H(1A)···O(3) <sup>iii</sup>	0.73(3)	2.16(3)	2.892(3)	171(3)
O(1)–H(1B)···O(2) <sup>iv</sup>	0.77(3)	2.02(3)	2.786(2)	175(4)
C(4)–H(4A)···O(5) <sup>v</sup>	0.96	2.58	3.522(3)	168

*Symmetry Code: (iii) -1/2-x, 1/2-y, -z; (iv) -x, y, 1/2-z; (v) 1/2+x, 1/2+y, z*

### 3.B.2.4 Catalytic activity of Bis[2-(4,5-diphenyl-1H-imizol-2-yl)-4-nitrophenolato] copper (II) dihydrate (1) towards C–S cross coupling reaction

We employed the complex (1) to study the efficacy for the C–S cross coupling reaction under the green condition as because C–S cross-coupling reaction is one of the most promising approaches for the synthesis of valuable pharmaceutical as well as industrially important compounds<sup>26,27</sup>. Thus, we designed our reaction by employing aryl halides and aryl thiols under green condition using water as a reaction medium and complex (1) as a catalyst to synthesize C–S cross-coupled products (2a-t)<sup>28</sup>(Scheme 3.B.2).



**Scheme. 3.B.2.** C-S cross-coupling between aryl halide and aryl thiols using complex (1) as a catalyst.

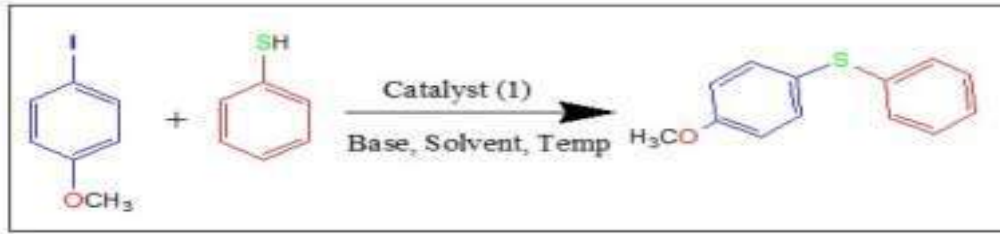
Initially, in order to explore the catalytic efficacy of newly synthesized complex (1), we set up a model reaction for C-S coupling by employing 4-iodoanisole (1mmol), thiophenol (1mmol), K<sub>2</sub>CO<sub>3</sub> (1.2mmol) with different amount (mg) of catalyst (1) in different solvent medium under refluxing condition. The optimized result of the catalyst loading and selection of solvent for the model reaction is summarized in Table 3.B.9 and Table 3.B.10 respectively.

**Table 3.B.9.** Optimization of catalyst loading<sup>a</sup>

Entry	Catalyst (mg)	Yield (%) <sup>b</sup>
1	2	60
2	4	65
3	6	72
4	8	85
<b>5</b>	<b>10</b>	<b>96</b>
6	12	97

<sup>a</sup>reaction condition: 4-iodoanisole (1mmol), thiophenol (1mmol), K<sub>2</sub>CO<sub>3</sub> (1.2mmol) at 80°C.

<sup>b</sup>yield.

**Table.3.B.10.** Optimization of reaction parameters for the C-S coupling reaction<sup>a</sup>


Entry <sup>a</sup>	Catalyst(mg)	Time (h)	Solvent (5ml)	Base	Temperature (°C)	Yield <sup>b</sup> (%)
1	10	10	DMF	K <sub>2</sub> CO <sub>3</sub>	80	90
2	10	10	DMSO	K <sub>2</sub> CO <sub>3</sub>	80	87
3	10	10	CH <sub>3</sub> CN	K <sub>2</sub> CO <sub>3</sub>	80	90
4	10	10	Toulene	K <sub>2</sub> CO <sub>3</sub>	80	92
5	10	10	Ethanol	K <sub>2</sub> CO <sub>3</sub>	80	91
<b>6</b>	<b>10</b>	<b>10</b>	<b>H<sub>2</sub>O</b>	<b>K<sub>2</sub>CO<sub>3</sub></b>	<b>80</b>	<b>96</b>
7	10	10	H <sub>2</sub> O	K <sub>2</sub> CO <sub>3</sub>	100	97
8	10	10	H <sub>2</sub> O	K <sub>2</sub> CO <sub>3</sub>	60	40
9	10	10	H <sub>2</sub> O	K <sub>2</sub> CO <sub>3</sub>	RT	Nil
<b>10</b>	<b>Nil</b>	<b>24</b>	<b>H<sub>2</sub>O</b>	<b>K<sub>2</sub>CO<sub>3</sub></b>	<b>80</b>	<b>Nil</b>
11	10	10	H <sub>2</sub> O	Cs <sub>2</sub> CO <sub>3</sub>	80	97
12	10	10	H <sub>2</sub> O	KO <sup>t</sup> Bu	80	60
13	10	10	H <sub>2</sub> O	Et <sub>3</sub> N	80	62
14	10	10	H <sub>2</sub> O	KOH	80	70

<sup>a</sup>reaction condition: 4-iodoanisole (1mmol), thiophenol (1mmol), K<sub>2</sub>CO<sub>3</sub> (1.2mmol) at 80°C,

<sup>b</sup>yield, **Nil** stands for in absence of catalyst as well as no yield of the desired product.

From the optimized model reaction, it was evident that C-S coupled product formed efficiently (96%) when the amount of catalyst loading is 10 mg (0.09 mol %) in aqueous medium (Table 3.B.10, entry 6). Also, we carried out the control reaction under the same condition without catalyst and we observed that the C-S coupled product did not form in absence of the catalyst (Table 3.B.10,

entry 10). Therefore, it may be concluded that the reaction did not proceed in absence of the catalyst.

To check the generality and efficacy of catalyst (1) for C–S cross-coupling reaction, we extended this protocol with a variety of haloarenes and aliphatic as well as aromatic thiols and interestingly, we found that the C-S coupled product (2a-t) formed in excellent yield under the optimized reaction condition and it is depicted in Fig.3.B.13.

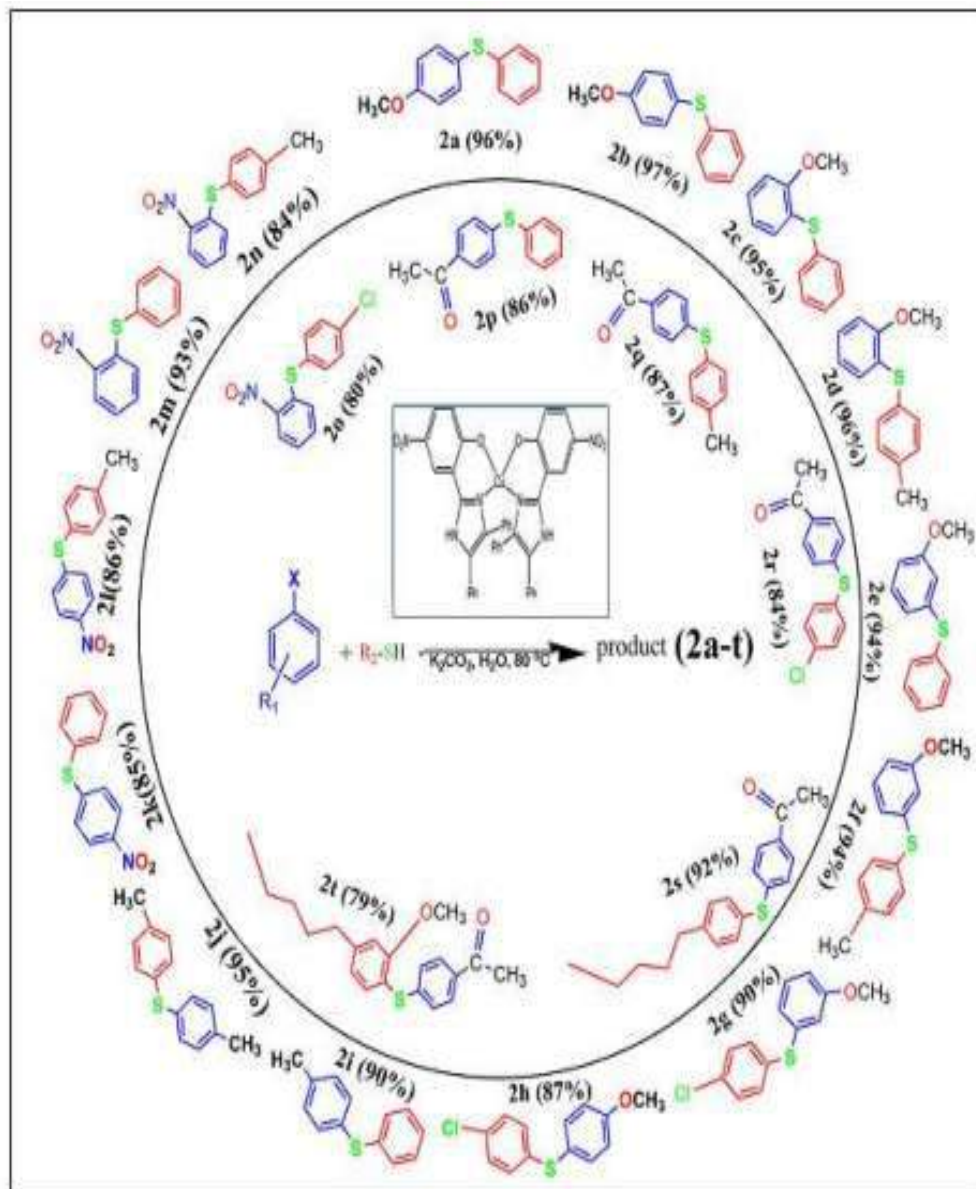


Fig. 3.B.14. C-S coupled product (2a-t)

Thus, from the present investigation, it was evident that the complex (1), Bis[2-(4,5-diphenyl-1H-imizol-2-yl)-4-nitro-phenolato] copper(II) dihydrate has shown excellent catalytic efficiency for the synthesis of C-S cross-coupled reaction under green reaction condition and therefore, giving an excellent yield of the desired C-S coupled product in water.

### 3. B.3. Experimental section

#### 3. B.3.1 Materials and methods:

All the starting chemicals of high purity for the present investigation were procured commercially and were used as received. The FT-IR spectra of the synthesized products were recorded in Bruker Alpha III spectrophotometer operating in the wave number region 4000 to 400  $\text{cm}^{-1}$  in dry KBr. Single crystal X-ray diffraction study was carried out with XtaLAB Synergy, Dualflex AtlasS2 diffractometre and Diffraction data was collected using monochromatic Cu  $K\alpha$  radiation for complex (1) and Mo  $K\alpha$  radiation for compound (2) respectively with the  $\omega$  and  $\phi$  scan technique (CrysAlis PRO, Rigaku OD, 2017 & 2018). The structure was solved by direct method and was refined by full matrix least squares based on  $F^2$  using SHELXL 2014 & SHELXL 97<sup>29,30</sup>. All the H atoms were localized from the difference electron-density map and refined isotropically. ORTEP-plot and packing diagram were generated with ORTEP-3 for Windows<sup>31</sup> and PLATON<sup>32</sup>. The Hirshfeld surface calculations for complex (1) were performed with *CrystalExplorer17*<sup>33</sup>.

#### 3.B.3.2 Synthesis of Bis[2-(4,5-diphenyl-1H-imizol-2-yl)-4-nitro-phenolato] copper(II) dihydrate (1)

In a typical procedure, benzil (0.3 g, 1 mmol), ammonium acetate (0.19 g, 2.5 mmol), 2-hydroxy-5-nitrobenzaldehyde (0.167 g, 1 mmol) and copper (II) borate (0.218 mg, 1 mmol) were ground in an agate mortar with a pestle and the reaction mixture was ground again for 30 min. The whole reaction mixture was then transferred to a 100 ml round-bottomed flask and heated at 100°C with constant stirring for 4 h. The reaction mixture was then extracted with dry acetone and dried over  $\text{MgSO}_4$ . After a few days, a dark-brown solid was obtained. The product was recrystallized from dry dimethylformamide and, after 5 d, light-blue crystals of (I) were obtained (yield 60%; m.p. >300°C). IR ( $\text{cm}^{-1}$ )  $\nu_{\text{max}}$  =3430 (O-H Stretching of  $\text{H}_2\text{O}$ ), 3065 (N-H Stretching), 1578 (C=N Stretching), 1487, 1135 (C-H Stretching), 466 (Cu-N Stretching).

### 3.B.4 Conclusion

The title copper (II) complex, Bis[2-(4,5-diphenyl-1H-imidazol-2-yl)-4-nitrophenolato] copper (II) dihydrate (1) was isolated during an ongoing research programme on the catalytic activity of copper borate ( $\text{CuB}_4\text{O}_7$ ) for C—N heterocyclic bond formation reactions. Complex (1) was formed during the attempted synthesis of a triarylimidazole derivative using benzil and the respective aromatic aldehyde with copper borate, using ammonium acetate as a nitrogen source. The single-crystal analysis of the synthesized product revealed that in the copper (II) complex, the triarylimidazole moiety acts as a bidentate ligand for the copper atom. During the successful synthesis of the triarylimidazole, the desired product formed in good yield at a temperature in the range 80°C. However, when the reaction was conducted at and above 100 °C the title copper (II) complex formed instead of the targeted triarylimidazole. The crystal and molecular structures of (1) are described herein, along with a detailed analysis of the molecular packing via an analysis of the calculated Hirshfeld surfaces. Again, the transformation of catalyst  $\text{CuB}_4\text{O}_7$  into the Copper acetate monohydrate in the presence of  $\text{NH}_4\text{OAc}$  during the synthesis of 2,4,5-triarylimidazole has been explored and this fact is supported from the single crystal x-ray analysis of the compound (2). Also, the catalytic efficiency of the complex (1) has been explored for the C-S coupling reaction using aryl halide and aryl thio compounds under green reaction condition.

## 3.B.5 References

- (1) B. Valeur, I. Leray., *Coordination Chemistry Reviews*, **2000**, 205 (1), 3–40.
- (2) Y. Gabe, Y. Urano, K. Kikuchi, H. Kojima, T. Nagano., *J Am Chem Soc*, **2004**, 126 (10), 3357–3367.
- (3) S. L. Wiskur, H. Ait-Haddou, J. J. Lavigne, E. v. Anslyn., *Accounts of Chemical Research*, **2001**, 34 (12), 963–972.
- (4) E. L. Que, D. W. Domaille, C. J. Chang., *Chemical Reviews*, **2008**, 108 (5), 1517–1549.
- (5) E. L. Que, D. W. Domaille, C. J. Chang., *Chemical Reviews*, **2008**, 108 (10), 4328.
- (6) B. Sarkar., In *Metal Ions in Biological Systems Vol. 12 (Chap. 6 - Transport of Copper)*; Siegel, H., Siegel, A., Dekker, M., Eds.; New York, **1981**; pp 233–281.
- (7) F. M. Raymo., *Advanced Materials*, **2021**, 14 (6), 401–414.
- (8) D. J. Faulkner., *Natural Product Reports*, **2000**, 17 (1), 7–55.
- (9) J. Z. Ho, R. M. Mohareb, J. H. Ahn, T. B. Sim, H. Rapoport., *Journal of Organic Chemistry*, **2003**, 68 (1), 109–114.
- (10) A. R. Katritzky, C. W. Rees, E. F. V. Scriven., In *Comprehensive Heterocyclic Chemistry II, Vol. 2 (Chap 4.02 - Imidazoles)*; Katritzky, A. R., Rees, C. W., Scriven, E. F. V., Eds.; Oxford: New York, Pergamom, **1996**; pp 77–220.
- (11) L. de Luca., *Current Medicinal Chemistry*, **2006**, 13 (1), 1–23.
- (12) P. M. Colman, H. C. Freeman, J. M. Guss, M. Murata, V. A. Norris, J. A. M. Ramshaw, M. P. Venkatappa., *Nature*, **1978**, 272 (5651), 319–324.
- (13) E. I. Solomon, D. E. Heppner, E. M. Johnston, J. W. Ginsbach, J. Cirera, M. Qayyum, M. T. Kieber-Emmons, C. H. Kjaergaard, R. G. Hadt, L. Tian., *Chemical Reviews*, **2014**, 114 (7), 3659–3853.
- (14) M. Andersson, J. Hedin, P. Johansson, J. Nordström, M. Nydén., *Journal of Physical Chemistry A*, **2010**, 114 (50), 13146–13153.
- (15) V. Pascanu, G. González Miera, A. K. Inge, B. Martín-Matute., *J Am Chem Soc*, **2019**, 141 (18), 7223–7234.
- (16) Y. Li, R. T. Yang., *Langmuir*, **2007**, 23 (26), 12937–12944.
- (17) Q. Wang, Q. Gao, A. M. Al-Enizi, A. Nafady, S. Ma., *Inorganic Chemistry Frontiers*, **2020**, 7 (2), 300–339.

- (18) C. Chen, W. Zhang, J. Cong, M. Cheng, B. Zhang, H. Chen, P. Liu, R. Li, M. Safdari, L. Kloo, L. Sun., *ACS Energy Letters*, **2017**, 2 (2), 497–503.
- (19) S. S. Nadar, V. K. Rathod., *International Journal of Biological Macromolecules*, **2018**, 120 (Part B), 2293–2302.
- (20) S. Charoensuk, J. Tan, M. Sain, H. Manuspiya., *Nanomaterials*, **2021**, 11 (9), 2281.
- (21) S. Chettri, D. Brahman, B. Sinha, M. M. Jotani, E. R. T. Tiekink., *Acta Crystallographica*, **2019**, E75 (11), 1664–1671.
- (22) G. M. Brown, R. Chidambaram., *Acta Crystallographica*, **1973**, B29 (11), 2393–2403.
- (23) L. Yang, D. R. Powell, R. P. Houser., *Dalton Transactions*, **2007**, Issue 9, 955–964.
- (24) S. L. Tan, M. M. Jotani, E. R. T. Tiekink., *Acta Crystallographica*, **2019**, E75 (3), 308–318.
- (25) C. B. Pinto, L. H. R. dos Santos, B. L. Rodrigues., *Acta Crystallographica*, **2019**, C75 (Part 6), 707–716.
- (26) D. Das., *ChemistrySelect*, **2016**, 1 (9), 1959–1980.
- (27) S. V. Ley, A. W. Thomas., *Angewandte Chemie International Edition*, **2003**, 42 (44), 5400–5449.
- (28) R. Singha, S. Chettri, D. Brahman, B. Sinha, P. Ghosh., *Molecular Diversity*, **2022**, 26 (1), 505–511.
- (29) G. M. Sheldrick., *Acta Crystallographica*, **2015**, C71 (1), 3–8.
- (30) G. M. Sheldrick., *SHELXS-97 and SHELXL-97, Program for Crystal Structure Solution and Refinement*; University of Gottingen, Gottingen, **1997**.
- (31) L. J. Farrugia., *Journal of Applied Crystallography*, **1997**, 30 (5), 565–565.
- (32) A. L. Spek., *Acta Crystallographica*, **2009**, D65 (2), 148–155.
- (33) P. R. Spackman, M. J. Turner, J. J. McKinnon, S. K. Wolff, D. J. Grimwood, D. Jayatilaka, M. A. Spackman., *Journal of Applied Crystallography*, **2021**, 54 (3), 1006–1011.



## **CHAPTER-III**

### **Section-C**

#### **DFT, Molecular Docking and Pharmacokinetic study of some selected 2, 4, 5-triarylimidazole derivatives**

##### **3.C.1 Background of the present investigation**

Imidazole scaffold, an important heterocyclic compound is ubiquitous in nature and found in many natural products<sup>1</sup>. Among a large variety of organic compounds containing imidazole core, 2, 4, 5-triarylimidazole occupies a special position as these scaffolds are recognized to show a diverse range of biological and pharmacological properties<sup>2</sup>. These five membered organic heterocyclic scaffolds not only find application in biological and medicinal field but also finds many applications in analytical and industrial fields<sup>3</sup>. Substituted imidazole derivatives have good binding affinity with different metals present in various biological active sites and also found to exhibit good inhibitory activity against glucagon receptor antagonists<sup>4</sup>, inhibitors of P38 MAP kinase<sup>5</sup>, B-Raf kinase<sup>6</sup> etc. Apart from the biological activities, substituted imidazole derivatives found to possess several other applications such as corrosion inhibitors<sup>7</sup>, optoelectric<sup>8</sup>, metal sensing<sup>9</sup>, fluorescent probe<sup>10</sup> and biological imaging<sup>11</sup>. Because of the wide application of substituted imidazole derivatives, it has drawn a considerable attention of the synthetic, medicinal and theoretical chemist during the past few decades<sup>12</sup>. Moreover, computational study now a days has reached a stage whereby new scientific information about the target molecule could be easily generated and may enable the researcher to explore the new properties of the compounds under investigation<sup>13</sup>. Interestingly, Density functional Theory (DFT) helps in analyzing and predicting the structures, dipole moment, vibration frequencies, optical properties and thermodynamic properties of organic compounds with high accuracy<sup>14</sup>. On the other hand, computer aided drug design process (Molecular docking and Molecular dynamics) may enable the chemist to determine the desired properties in the drug molecule for making the process and discovery of new therapeutic agents more efficient and economical<sup>15,16</sup>. Basically, structure-based drug design and ligand-based drug design approaches are the two fundamental categories of Computer Aided Drug Design process and both approaches have been widely employed in the modern drug discovery processes for the identification of suitable and specific target drug molecules. Thus, Computer Aided Drug Design enables the researchers to understand the different types of interaction prevailing between the ligand and the active site of the protein<sup>17</sup>. Furthermore, Diabetes mellitus or hyperglycemia is a chronic metabolic disorder caused by either insulin deficiency or insulin resistance is a global concern now a days<sup>18</sup>. A numerous synthetic therapeutic measures are available for the treatment or management of diabetes yet they are not the permanent measure to cure the

diabetes as they have unwanted side effects<sup>19</sup>. Therefore, finding an excellent therapeutic agent for the treatment and cure of above mention disorder is a challenging task and during the past few decades researchers are engaged in testifying different therapeutic agents to cure for diabetes<sup>20</sup>. In modern day drug designing, Molecular docking study is helpful in obtaining the information about different types of interactions prevailing between ligand and the receptor protein and therefore facilitating the process of drug discovery easier and economical<sup>21</sup>. Here, in this chapter a detailed theoretical study of some selected 2, 4, 5-triarylimidazole (Fig. 3.C.1) has been carried out using Density Functional Theory.

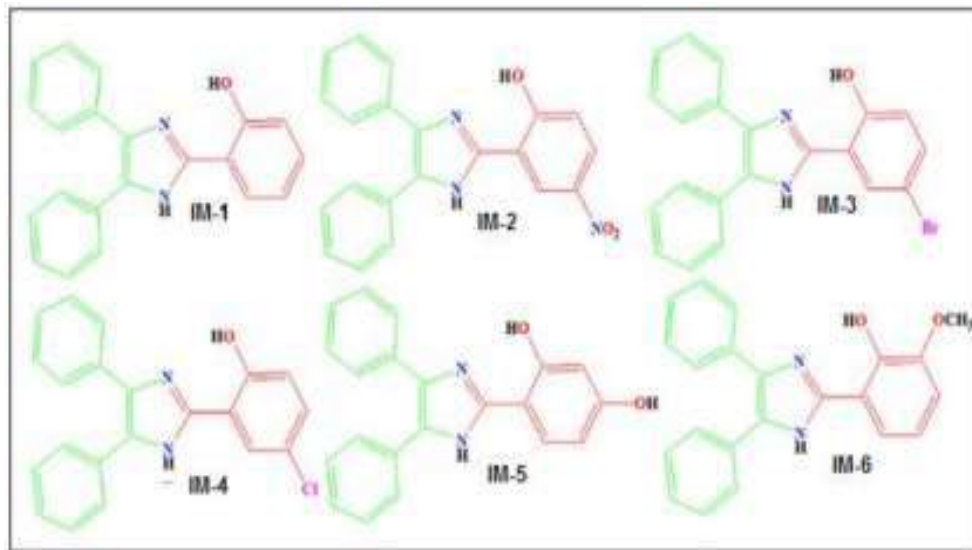


**Fig. 3.C.1.** Molecular structure of 2, 4, 5-triarylimidazole derivatives (IM-1 to IM-6)

The optimized molecular geometry, vibrational analysis (FT-IR and Raman), molecular orbital (HOMO, LUMO), nonlinear optical property, Global chemical descriptors and Molecular Electrostatic Potential (MEP) of the 2, 4, 5-triarylimidazole derivatives (IM-1 to IM-6) have been reported in this section. Also, an attempt has been made to recognize the inhibitory potential of these derivatives against the Diabetes mellitus protein (PDB ID: 1IR3) by employing molecular docking study and pharmacokinetic properties (ADME) have also been studied.

### 3.C.2 Results and discussion

#### 3.C.2.1 Computational Study

The molecular geometry, molecular orbital (HOMO, LUMO), Nonlinear Optical property (NLO), Global chemical descriptors and Molecular Electrostatic Potential (MEP) of the selected 2, 4, 5-triarylimidazole derivatives namely, 2-(4,5-diphenyl-1H-imidazol-2-yl)phenol (IM-1), 2-(4,5-diphenyl-1H-imidazol-2-yl)-4-nitrophenol (IM-2), 4-bromo-2-(4,5-diphenyl-1H-imidazol-2-yl)phenol (IM-3), 4-chloro-2-(4,5-diphenyl-1H-imidazol-2-yl)phenol (IM-4), 4-(4,5-diphenyl-1H-imidazol-2-yl)benzene-1,3-diol (IM-5) and 2-methoxy-6-(4,5-diphenyl-1H-imidazol-2-yl)phenol (IM-6) has been optimized by Density Functional Theory (DFT) using Becke's three-parameter hybrid method (B3) with the Lee, Yang and Parr correlation functional methods (LYP) with B3LYP/6-31G+ (d, 2p) level of basis set<sup>22,23</sup>. All the computational calculations were calculated by Gaussian 16, Revision A.03 programme package<sup>24</sup> and the results were visualized using GAUSSVIEW 6.0 software<sup>25</sup> on a hp-Z640 desktop P.C. with an Intel Xeon processor (Specifications: E5-2630 V4 @ 220GHz).

##### 3.C.2.1.1 Optimization of Molecular geometry

To the best of our knowledge, the x-ray single crystal structure of the studied compounds (IM-1 to IM-6) have not been reported so far and therefore structure optimization using DFT method serves as a good alternative to ascertain the different geometrical parameters. Thus, the geometrical parameters of the studied compounds (IM-1 to IM-6) were calculated by DFT assay using B3LYP/6-31G+ (d, 2p) level of basis set. The optimized gas phase molecular geometry of the compounds (IM-1 to IM-6) with atom labelling scheme is shown in Fig. 3.C.2 and the structural parameters (bond lengths, bond angle and dihedral angle) are listed in Table 3.C.1. From the Table 3.C.1, the dihedral angles C23-C18-C17-N4, C19-C18-C17-N2 is close to 180° and C19-C18-C17-N4 and C23-C18-C17-N2 is close to 0° except IM-5 for the phenyl ring (2) and this suggest that the phenyl ring (2) is almost planar with the imidazole ring (Fig. 3. C.3.). However, it is evident from the table 3.C.1 that the dihedral angle of other phenyl rings (4 and 5) are far less than the dihedral angle for planar molecule and thus from this, we can infer that the phenyl ring 4 and 5 are not planar with the imidazole ring. Also, for the compound IM-5 all the phenyl rings are not planar to imidazole ring. From Table 3.C.1, it is clearly seen that the C-N bond lengths of imidazole ring in all the studied compounds (IM-1 to IM6) are in the range C1-N2=1.374 Å-1.389 Å, C3-N4=1.380 Å-1.390 Å, N4-C17=1.358 Å to 1.369Å and N2-C17=1.325 Å to 1.330 Å respectively. The shortening of the C-N bond lengths reveals the effect of resonance in this part of the molecule and this can be attributed to the difference in hybridization state of different carbon atoms in the imidazole ring<sup>26</sup>.

**Table. 3.C.1.** Structural parameters (bond lengths, bond angle and dihedral angle) of the studied compounds (IM-1 to IM-6)

<b>C-C bond length (Å)</b>					
<b>IM-1</b>		<b>IM-2</b>		<b>IM-3</b>	
C6-C5	1.406	C6-C5	1.407	C6-C5	1.408
C7-C6	1.395	C7-C6	1.396	C7-C6	1.396
C8-C7	1.397	C8-C7	1.397	C8-C7	1.396
C9-C8	1.397	C9-C8	1.398	C9-C8	1.398
C10-C9	1.395	C10-C9	1.394	C10-C9	1.394
C10-C5	1.407	C10-C5	1.407	C10-C5	1.406
C12-C11	1.407	C12-C11	1.405	C12-C11	1.405
C13-C12	1.394	C13-C12	1.395	C13-C12	1.395
C14-C13	1.398	C14-C13	1.397	C14-C13	1.397
C15-C14	1.396	C15-C14	1.398	C15-C14	1.398
C16-C15	1.396	C16-C15	1.395	C16-C15	1.395
C16-C11	1.406	C16-C11	1.406	C16-C11	1.408
C19-C18	1.421	C19-C18	1.412	C19-C18	1.410
C20-C19	1.403	C20-C19	1.310	C20-C19	1.395
C21-C20	1.390	C21-C20	1.388	C21-C20	1.393
C22-C21	1.402	C22-C21	1.396	C22-C21	1.395
C23-C22	1.390	C23-C22	1.389	C23-C22	1.387
C23-C18	1.404	C23-C18	1.404	C23-C18	1.408
<b>IM-4</b>		<b>IM-5</b>		<b>IM-6</b>	
C6-C5	1.408	C6-C5	1.408	C6-C5	1.408
C7-C6	1.396	C7-C6	1.396	C7-C6	1.396
C8-C7	1.397	C8-C7	1.396	C8-C7	1.397
C9-C8	1.398	C9-C8	1.398	C9-C8	1.398
C10-C9	1.394	C10-C9	1.394	C10-C9	1.394
C10-C5	1.407	C10-C5	1.408	C10-C5	1.408
C12-C11	1.405	C12-C11	1.405	C12-C11	1.406
C13-C12	1.395	C13-C12	1.395	C13-C12	1.395
C14-C13	1.397	C14-C13	1.397	C14-C13	1.397
C15-C14	1.398	C15-C14	1.398	C15-C14	1.398
C16-C15	1.395	C16-C15	1.395	C16-C15	1.395
C16-C11	1.406	C16-C11	1.406	C16-C11	1.406
C19-C18	1.410	C19-C18	1.410	C19-C18	1.401
C20-C19	1.395	C20-C19	1.395	C20-C19	1.407
C21-C20	1.393	C21-C20	1.395	C21-C20	1.390
C22-C21	1.395	C22-C21	1.401	C22-C21	1.403
C23-C22	1.388	C23-C22	1.387	C23-C22	1.386
C23-C18	1.407	C23-C18	1.408	C23-C18	1.412
<b>C-H, C-O, N-H, C-Cl, C-Br and O-H bond distances (Å)</b>					
<b>IM-1 (Å)</b>		<b>IM-2 (Å)</b>		<b>IM-3 (Å)</b>	
C6-H26	1.084	C6-H31	1.085	C6-H31	1.085
C7-H27	1.085	C7-H35	1.085	C7-H35	1.085
C8-H28	1.085	C8-H34	1.084	C8-H34	1.084
C9-H29	1.085	C9-H33	1.085	C9-H33	1.085
C10-H30	1.084	C10-H32	1.083	C10-H32	1.083
C12-H31	1.083	C12-H29	1.084	C12-H39	1.084

C13-H32	1.085	C13-H28	1.085	C13-H28	1.085
C14-H33	1.084	C14-H27	1.085	C14-H27	1.085
C15-H34	1.085	C15-H26	1.085	C15-H26	1.085
C16-H35	1.086	C16-H25	1.083	C16-H25	1.083
C20-H36	1.084	C20-H38	1.086	C20-H38	1.082
C21-H37	1.085	C21-H36	1.081	C21-H36	1.082
C22-H38	1.084				
C23-H39	1.086	C23-H39	1.081	C23-H39	1.082
C24-H37		C24-H37	0.965	C24-H37	0.965
C19-O24	1.347	C19-O24	1.372	C19-O24	1.380
N2-H25	1.007	N4-H30	1.009	N4-H30	1.009
O24-H40	0.994	O24-H37	0.966	O24-H37	0.965
				C22- Br40	1.906
IM-4 (Å)		IM-5 (Å)		IM-6 (Å)	
C6-H31	1.085	C6-H31	1.085	C6-H33	1.086
C7-H35	1.085	C7-H35	1.085	C7-H37	1.085
C8-H34	1.084	C8-H34	1.084	C8-H36	1.085
C9-H33	1.085	C9-H33	1.085	C9-H35	1.085
C10-H32	1.083	C10-H32	1.083	C10-H34	1.084
C12-H29	1.084	C12-H29	1.084	C12-H31	1.084
C13-H28	1.085	C13-H28	1.085	C13-H30	1.086
C14-H37	1.085	C14-H27	1.085	C14-H29	1.085
C15-H26	1.085	C15-H26	1.085	C15-H28	1.086
C16-H25	1.084	C16-H25	1.083	C16-H27	1.084
C20-H38	1.086	C20-H38	1.085	C21-H40	1.083
C21-H36	1.082	C22-H40	1.083	C22-H39	1.084
C23-H39	1.082	C23-H39	1.083	C23-H38	1.083
C24-H37	0.965	C19-O24	1.375	C19-O24	1.375
C19-O24	1.380	C21- O36	1.367	C20-O25	1.377
N4-H30	1.009	N4-H30	1.010	N4-H32	1.010
O24-H37	0.965	O24-H37	0.967	O24-H44	0.970
Cl40-C22	1.759	O36-H41	0.965	O36-H41	0.965
Bond Angle (°)					
IM-1		IM-2		IM-3	
C3-C1-N2	104.87	C1-C3-N2	109.73	C3-C1- N2	109.78
N4-C3-C1	109.19	N4-C3-C1	104.63	N4-C3- C1	104.58
C5-C3-C1	130.35	C5-C3-C1	134.54	C5-C3-C1	134.56
C6-C5-C3	119.66	C6-C5-C3	120.55	C6-C5-C3	120.54
C7-C6-C5	120.70	C7-C6-C5	120.80	C7-C6-C5	120.84
C8-C7-C6	120.29	C8-C7-C6	120.19	C8-C7-C6	120.21
C9-C8-C7	119.47	C9-C8-C7	119.50	C9-C8-C7	119.46
C10-C9- C8	120.32	C10-C9-C8	120.43	C10-C9- C8	120.45
C11-C1- N2	120.70	C11-C1-N2	120.14	C11-C1- N2	120.06
C12-C11- C1	121.00	C12-C11- C1	122.04	C12-C11- C1	122.09

C13-C12-C11	120.60	C13-C12-C11	120.68	C13-C12-C11	120.71
C14-C13-C12	120.44	C14-C13-C12	120.32	C14-C13-C12	120.33
C15-C14-C13	119.51	C15-C14-C13	119.45	C15-C14-C13	119.42
C16-C15-C14	120.18	C16-C15-C14	120.31	C16-C15-C14	120.32
C17-N4-C3	107.58	C17-N2-C1	106.79	C17-N2-C1	106.76
C18-C17-N4	124.52	C18-C17-N2	124.14	C18-C17-N2	124.47
C19-C18-C17	119.19	C19-C18-C17	124.05	C19-C18-C18	123.84
C20-C19-C18	119.51	C20-C19-C18	121.23	C20-C19-C18	120.71
C21-C20-C19	120.64	C21-C20-C19	120.63	C21-C20-C19	120.70
C22-C21-C20	120.43	C22-C21-C20	118.17	C22-C21-C20	118.78
C23-C22-C21	119.26	C23-C22-C21	121.97	C23-C22-C21	121.07
O24-C19-C18	122.50	O24-C19-C18	118.03	O24-C19-C18	118.34
H25-N2-C1	124.46	H25-C16-C15	120.39	H25-C16-C15	120.42
H26-C6-C5	119.15	H26-C15-C14	120.07	H26-C15-C14	120.04
H27-C7-C6	119.61	H27-C14-C13	120.24	H27-C14-C13	120.26
H28-C8-C7	120.27	H28-C13-C12	119.58	H28-C13-C12	119.57
H29-C9-C8	120.08	H29-C12-C11	119.81	H29-C12-C11	119.76
H30-C10-C9	119.59	H30-N4-C3	126.48	H30-N4-C3	126.78
H31-C12-C11	119.43	H31-C6-C5	119.67	H31-C6-C5	119.66
H32-C13-C12	119.51	H32-C10-C9	119.94	H32-C10-C9	119.92
H33-C14-C13	120.24	H33-C9-C8	120.04	H33-C9-C8	120.03
H34-C15-C14	120.15	H34-C8-C7	120.24	H34-C8-C7	120.26
H35-C16-C15	119.44	H35-C7-C6	119.65	H35-C7-C6	119.64
H36-C20-C19	117.92	H36-C21-C20	121.62	H36-C21-C20	120.32
H37-C21-C20	119.54	H37-C24-C19	110.05	H37-C24-C19	109.66

H38-C22-C21	120.57	H38-C20-C19	119.42	H38-C20-C19	119.58
H39-C23-C22	118.68	H39-C23-C22	120.56	H39-C23-C22	121.32
H40-O24-C19	108.35	N40-C22-C21	118.86	Br40-C22-C21	119.33
		O41-N40-C22	117.57		
		O42-N40-C22	118.01		
<b>IM-4</b>		<b>IM-5</b>		<b>IM-6</b>	
C3-C1-N2	109.78	C3-C1-N2	109.99	C3-C1-N2	109.85
N4-C3-C1	104.58	N4-C3-C1	104.57	N4-C3-C1	104.54
C5-C3-C1	134.55	C5-C3-C1	134.86	C5-C3-C1	134.58
C6-C5-C3	120.55	C6-C5-C3	120.67	C6-C5-C3	120.55
C7-C6-C5	120.84	C7-C6-C5	120.87	C7-C6-C5	120.87
C8-C7-C6	120.21	C8-C7-C6	120.20	C8-C7-C6	120.23
C9-C8-C7	119.47	C9-C8-C7	119.45	C9-C8-C7	119.43
C10-C9-C8	120.44	C10-C9-C8	120.47	C10-C9-C8	120.46
C11-C1-N2	120.10	C11-C1-N2	119.81	C11-C1-N2	120.01
C12-C11-C1	122.07	C12-C11-C1	122.12	C12-C11-C1	122.13
C13-C12-C11	120.71	C13-C12-C11	120.75	C13-C12-C11	120.75
C14-C13-C12	120.33	C14-C13-C12	120.33	C14-C13-C12	120.34
C15-C14-C13	119.42	C15-C14-C13	119.42	C15-C14-C13	119.39
C16-C15-C14	120.31	C16-C15-C14	120.32	C16-C15-C14	120.33
C17-N2-C1	106.76	C17-N2-C1	106.91	C17-N2-C1	106.69
C18-C17-N2	124.49	C18-C17-N2	125.92	C18-C17-N2	124.85
C19-C18-C17	123.91	C19-C18-C17	122.83	C19-C18-C17	122.93
C20-C19-C18	120.77	C20-C19-C18	121.03	C20-C19-C18	120.78
C21-C20-C19	120.76	C21-C20-C19	119.80	C21-C20-C19	120.60
C22-C21-C20	118.69	C22-C21-C20	120.35	C22-C21-C20	118.83
C23-C22-C21	121.07	C23-C22-C21	119.14	C23-C22-C21	120.76
O24-C19-C18	118.29	O24-C19-C18	122.70	O24-C19-C18	120.66

H25-C16-C15	120.42	H25-C16-C15	120.41	O25-C20-C19	113.36
H26-C15-C14	120.05	H26-C15-C14	120.04	C26-O25-C20	118.41
H27-C14-C13	120.26	H27-C14-C13	120.25	H27-C16-C15	120.45
H28-C13-C12	119.57	H28-C13-C12	119.58	H28-C15-C14	120.03
H29-C12-C11	119.76	H29-C12-C11	119.78	H29-C14-C13	120.27
H30-N4-C3	126.78	H30-N4-C3	123.78	H30-C13-C12	119.57
H31-C6-C5	119.64	H31-C6-C5	119.72	H31-C12-C11	119.72
H32-C10-C9	119.92	H32-C10-C9	119.92	H32-N4-C3	126.98
H33-C9-C8	120.03	H33-C9-C8	120.02	H33-C16-C5	119.63
H34-C8-C7	120.26	H34-C8-C7	120.26	H34-C10-C9	119.90
H35-C7-C6	119.64			H35-C9-C8	120.03
H36-C21-C20	120.61			H36-C8-C7	120.28
H37-C24-C19	109.72			H37-C7-C6	119.62
H38-C20-C19	119.54			H38-C23-C22	121.14
H39-C23-C22	121.02			H39-C22-C21	119.33
C140-C22-C21	119.37			H40-C21-C20	120.91
<b>Selected dihedral angle (°)</b>					
<b>IM-1</b>		<b>IM-2</b>		<b>IM-3</b>	
C23-C18-C17-N4	179.82	C23-C18-C17-N4	-179.26	C23-C18-C17-N4	-179.15
C19-C18-C17-N2	179.40	C19-C18-C17-N2	-179.19	C19-C18-C17-N2	-179.29
C19-C18-C17-N4	-0.13	C19-C18-C17-N4	0.98	C19-C18-C17-N4	0.95
C23-C18-C17-N2	-0.63	C23-C18-C17-N2	0.55	C23-C18-C17-N2	0.60
C10-C5-C3-N4	143.72	C10-C5-C3-N4	-136.48	C10-C5-C3-N4	-137.70
C12-11-C1-N2	136.82	C12-11-C1-N2	-145.75	C12-11-C1-N2	-145.51
C6-C5-C3-N4	-34.50	C6-C5-C3-N4	41.46	C6-C5-C3-N4	40.27
C16-C11-C1-N2	-41.19	C16-C11-C1-N2	32.26	C16-C11-C1-N2	32.45



C6-C5-C3- C1	147.34	C6-C5-C3- C1	-141.20	C6-C5-C3- C1	-142.26
C16-C11- C1-C3	141.25	C16-C11- C1-C3	-149.64	C16-C11- C1-C3	-149.45
C12-C11- C1-C3	-40.72	C12-C11- C1-C3	32.34	C12-C11- C1-C3	32.57
C10-C5-C3- C1	-34.42	C10-C5-C3- C1	40.83	C10-C5- C3-C1	39.75
<b>IM-4</b>		<b>IM-5</b>		<b>IM-6</b>	
C23-C18- C17-N4	-178.77	C23-C18- C17-N4	147.23	C23-C18- C17-N4	179.63
C19-C18- C17-N2	-178.14	C19-C18- C17-N2	147.76	C19-C18- C17-N2	179.99
C19-C18- C17-N4	1.46	C19-C18- C17-N4	-33.45	C19-C18- C17-N4	0.02
C23-C18- C17-N2	1.02	C23-C18- C17-N2	-31.54	C23-C18- C17-N2	-0.39
C10-C5-C3- N4	-137.16	C10-C5-C3- N4	60.73	C10-C5- C3-N4	143.49
C12-11-C1- N2	-145.31	C12-11-C1- N2	-145.86	C12-11- C1-N2	-136.97
C6-C5-C3- N4	40.80	C6-C5-C3- N4	39.14	C6-C5-C3- N4	-34.72
C16-C11- C1-N2	32.69	C16-C11- C1-N2	32.14	C16-C11- C1-N2	-41.66
C6-C5-C3- C1	-141.84	C6-C5-C3- C1	-143.52	C6-C5-C3- C1	-142.57
C16-C11- C1-C3	-149.25	C16-C11- C1-C3	-150.71	C16-C11- C1-C3	-149.20
C12-C11- C1-C3	32.73	C12-C11- C1-C3	31.26	C12-C11- C1-C3	32.83
C10-C5-C3- C1	40.18	C10-C5-C3- C1	38.85	C10-C5- C3-C1	39.46

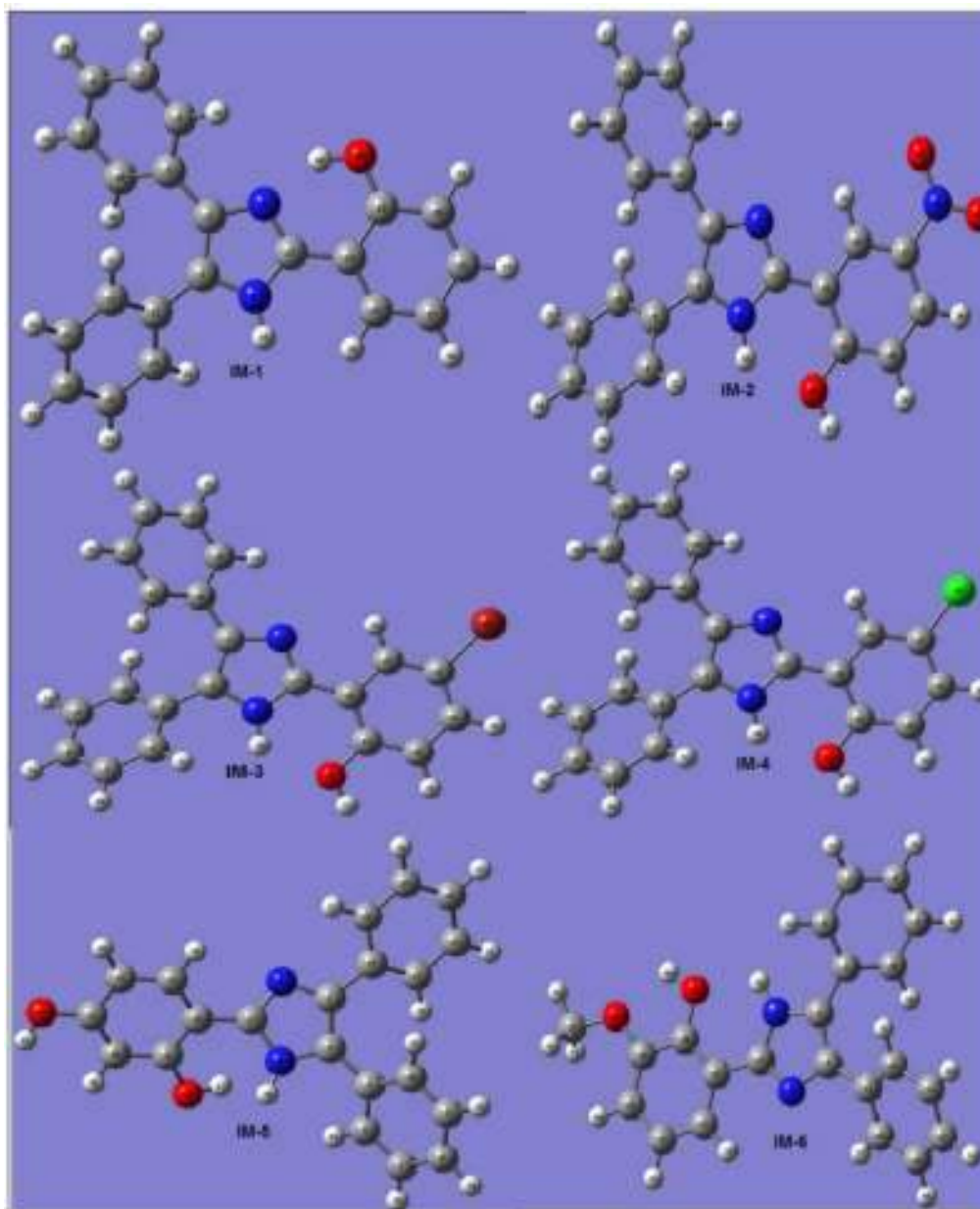


**Fig. 3.C.2.** Optimized gas phase molecular geometry of the compounds (IM-1 to IM-6) with atom labelling scheme

Again, from the optimized geometry, it is evident that the C-C bond distance of all the aryl groups (IM-1 to IM-6) are in the range 1.390 Å to 1.421 Å which suggests that the carbon atoms are highly conjugated and electrons are delocalized through resonance<sup>27</sup>.

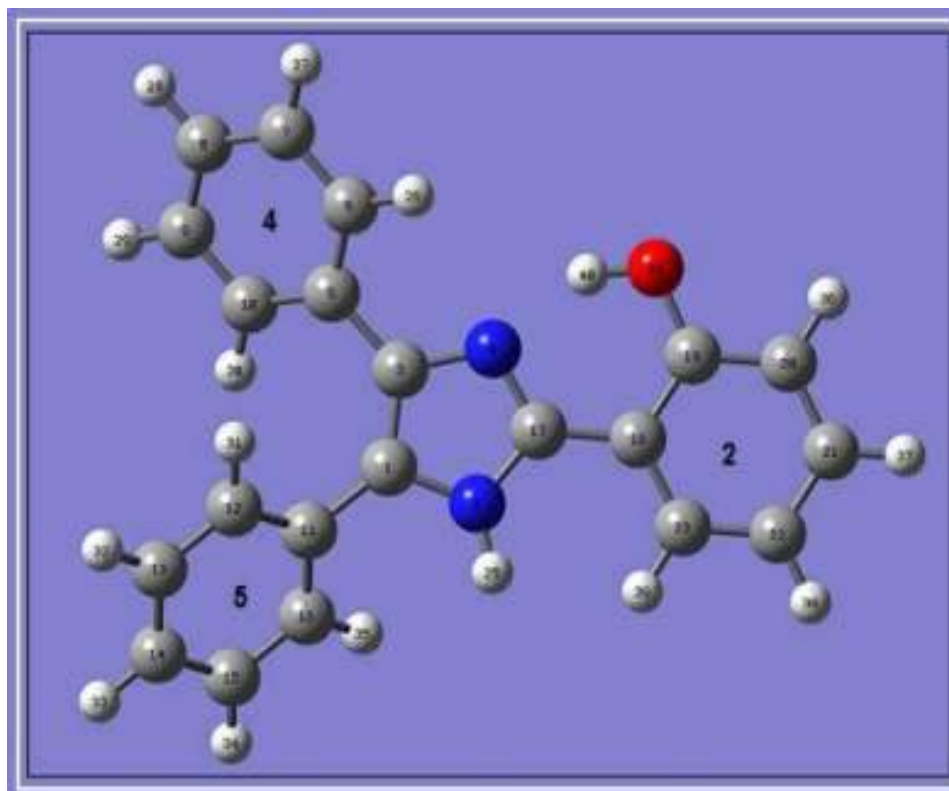


**Fig. 3.C.3.** Labelling of different phenyl ring attached to imidazole ring

The aromatic C-H, aliphatic C-H, C-O, O-H and N-H and C-halogen bond distances for the studied compounds are in the range 1.081 Å-1.095 Å, 1.089 Å-1.095 Å, 1.348 Å-1.380 Å, 0.960 Å-0.990 Å, 1.008 Å-1.011 Å and 1.795 Å-1.907 Å respectively.

### 3.C.2.1.2 Frontier Molecular Orbitals

The Highest Occupied Molecular Orbital (HOMO) and the Lowest Unoccupied Molecular Orbital (LUMO) constitutes the frontier molecular orbitals and the HOMO and LUMO are very important quantum mechanical parameter which determines the molecular reactivity. The frontier molecular orbital helps in predicting the excitation properties as well as electron transport quantitatively<sup>28,29</sup>. Since HOMO is the higher energy orbital containing the outermost electron and therefore it acts as an electron donor whereas, LUMO is the lowest energy orbital that has vacant space to accept the electrons and thus it acts as an electron acceptor<sup>30</sup>. The energies of HOMO and LUMO orbitals of the studied compounds (IM-1 to IM-6) are calculated using DFT/B3LYP method using 6-31G+ (d, 2p) level of basis set and shown in Fig. 3. C.4. The energy of HOMO and LUMO orbitals of the studied compounds (IM-1 to IM-6) are listed in Table 3.C.2

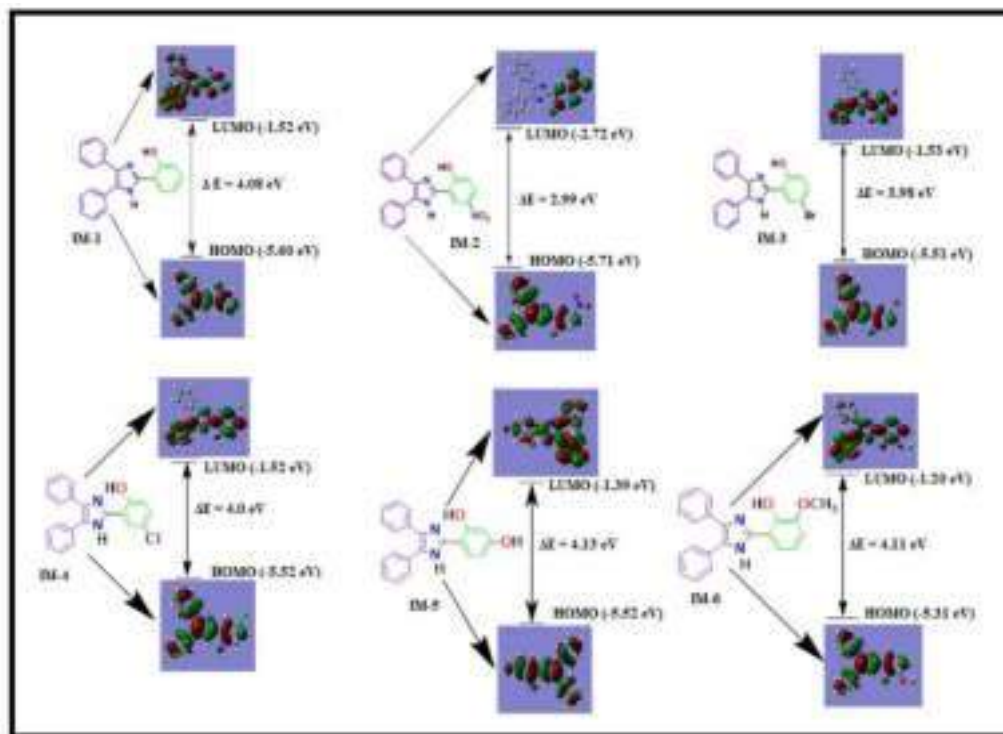


**Fig. 3.C.4.** Energies of HOMO and LUMO orbitals of the studied compounds (IM-1 to IM-6)

From the Table3.C.2 it is evident that the energy of HOMO and LUMO orbitals for all the compounds are negative and this infers that the compounds (IM-1 to IM-6) under investigation are relatively stable<sup>31</sup> and the energy of HOMO and LUMO orbitals of the compounds -5.60 eV (IM-1), -5.71 eV (IM-2), -5.51 eV (IM-3), -5.52 eV (IM-4), -5.52 eV (IM-5) and -5.31 eV (IM-6) and -1.52 eV (IM-1), -2.72 eV (IM-2), -1.53 eV (IM-3), -1.52 eV (IM-4), -1.39 eV (IM-5), and -1.2 eV (IM-6), respectively. Interestingly, by employing HOMO-LUMO energy, it is possible to calculate the global chemical descriptors like chemical potential, global hardness and global electrophilicity which in turn are very much helpful in understanding the structure of molecule and their reactivity. Thus, these new chemical descriptors could help in understanding the various aspects of pharmacological properties of the molecule for the process of drug design<sup>32</sup>. The ionization energy (I) and electron affinity (A) can be express in terms of HOMO and LUMO orbital energies as follows;

$$I = -E_{\text{HOMO}} \quad \text{and} \quad A = -E_{\text{LUMO}}$$

The chemical reactivity descriptors such as chemical potential ( $\mu$ ), Electronegativity ( $\chi$ ), Global hardness ( $\eta$ ) and global electrophilicity power ( $\omega$ ) can be calculated with the help of following relation;

$$\text{Chemical potential } (\mu) = (E_{\text{HOMO}} + E_{\text{LUMO}})/2 = -(I+A)/2$$

$$\text{Electronegativity } (\chi) = (I+A)/2$$

$$\text{Global Hardness } (\eta) = (-E_{\text{HOMO}} + E_{\text{LUMO}})/2 = (I-A)/2$$

$$\text{electrophilicity power } (\omega) = \mu^2/2 \eta$$

Where I and A are the first ionization potential and electron affinity of the chemical species<sup>33-35</sup>. The ionization energy (I), electron affinity (A), Chemical potential ( $\mu$ ), Electronegativity ( $\chi$ ), Global hardness ( $\eta$ ) and Global electrophilicity power ( $\omega$ ) of the studied compounds (IM-1 to IM-6) are listed in Table 3.C.

**Table. 3.C.2.** Energies of HOMO and LUMO orbitals, ionization energy (I), electron affinity (A), Chemical potential ( $\mu$ ), Electronegativity ( $\chi$ ), Global hardness ( $\eta$ ) and Global electrophilicity power ( $\omega$ ) of the studied compounds (IM-1 to IM-6)

Parameters (eV)	IM-1	IM-2	IM-3	IM-4	IM-5	IM-6
$E_{\text{HOMO}}$	-5.60	-5.71	-5.51	-5.52	-5.52	-5.31
$E_{\text{LUMO}}$	-1.52	-2.72	-1.53	-1.52	-1.39	-1.2
$\Delta E$	4.08	2.99	3.98	4.0	4.13	4.11
Ionization Energy (I)	5.60	5.71	5.51	5.52	5.52	5.31
Electron Affinity (A)	1.52	2.72	1.53	1.52	1.39	1.2
Chemical potential ( $\mu$ )	-3.56	-4.21	-3.52	-3.52	-3.40	-3.25
Electronegativity ( $\chi$ )	3.56	4.21	3.52	3.52	3.40	3.25
Global hardness ( $\eta$ )	2.04	1.49	1.99	2.0	2.06	2.05
Electrophilicity power ( $\omega$ )	3.10	5.96	3.11	3.09	2.80	2.57

It is seen that the chemical potential of all the studied molecules are negative and it suggest that they do not decompose spontaneously into its elements they are made up of.

Apparently, it is seen that the hard molecule has large HOMO-LUMO gap and soft molecule has small HOMO-LUMO gap<sup>36</sup>. Thus, from the Table 3.C.2 it is evident that the hardness of the studied molecule follows the order IM-5 > IM-6 > IM-1 > IM-4 > IM-3 > IM-2. Moreover, the hardness signifies the resistance towards the deformation of electron cloud of chemical systems under small perturbation that occur during the chemical reaction. Thus, hard system is less polarisable than soft system<sup>237</sup>. Again, a large value of electrophilicity is assigned for good electrophile whereas nucleophile is described by low value of nucleophilicity<sup>38</sup>.

## 3.C.2.1.3 FT-IR analysis

Study of the molecular vibrations of organic compounds has become an important area of interest for both the experimental and theoretical chemist. DFT method provides an avenue for the theoretical calculation of molecular vibrations of the studied system and therefore, it is possible to correlate the experimental and theoretical FT-IR spectra of the studied compounds to ascertain the different type of structural features in the molecules. Thus, we calculated the theoretical vibrational spectra of 2, 4, 5-triarylimidazole derivative (IM-1 to IM-6) using DFT at the B3LYP/6-31G+ (d, 2p) level of theory on optimized geometry of the molecules in the gas phase. The experimental and theoretical vibrational frequencies of the compounds (IM-1 to IM-6) are given in Table 3.C.3 with the proper assignment of the observed peaks.

**Table. 3.C.3.** Experimental and theoretical vibrational frequencies of compounds (IM-1 to IM-6) (with B3LYP/6-31G+(d,2p)) with proposed assignments.

<b>IM-1</b>				
Unscaled frequency (cm <sup>-1</sup> ) (theoretical)	IR <sub>i</sub>	R <sub>A</sub>	IR Frequency (cm <sup>-1</sup> ) (Experimental)	Assignments
3658	48.42	41.924		νNH stretch
3232	788.36	41.92	3474	νOH, Ar-H stretch
3210.38	12.79	412.3	3242	ν(s)Ar-H stretch
3210.13	10.63	173.5		ν(s)Ar-H stretch
3207	5.99	252.96		ν(s)Ar-H stretch
3203	15.59	10.53		ν(as)Ar-H stretch
3202.69	18.27	127.8		ν(as)Ar-H stretch
3202.38	25.25	191.27		ν(as)Ar-H stretch
3195	28.92	119.46		ν(as)Ar-H stretch
3190	14.55	115.89		ν(as)Ar-H stretch
3184	11.35	84.24		ν(as)Ar-H stretch
3183	5.81	145.3		ν(as)Ar-H stretch
3181	0.03	82.33		ν(as)Ar-H stretch
3174	1.35	37.83		ν(as)Ar-H stretch
3171	6.61	27.66		ν(as)Ar-H stretch
3165	7.91	23.38	3060	ν(as)Ar-H stretch
1667	40.73	1053.19		νAr C-C stretch
1651	11.3085	485.91		νAr C-C stretch
1649	24.92	911.16		νAr C-C stretch
1620	3.78	20.55	1622	νAr C-C stretch
1600	22.71	297.28	1604	νC-N stretch
1566	95	599.49	1540	νC-N stretch
<b>IM-2</b>				
3641.38	96.29	58.99	3472	νNH Stretch
3818.57	103.21	149.09		νOH Stretch
3245.02	10.7009	15.8316		νAr-H Stretch
3242.89	9.6	77.38		νAr-H Stretch

## Chapter-III C

3210.27	5.55	194.82		vAr-H, Stretching
3209.76	6.88	181.62		vAr-H, Stretching
3204.4	11.18	74.42		vAr-H, Stretching
3201.73	24.08	209.41		v(s)Ar-H stretch
3195.78	29.7	141.34		v(as)Ar-H stretch
3183.01	9.03	139.87		v(as)Ar-H stretch
3173.62	0.89	38.95		v(as)Ar-H stretch
3190.47	15.81	116.5		v(as)Ar-H stretch
3181.28	0.1676	85.0583		v(as)Ar-H stretch
3172.01	5.86	27.03	3114	v(as)Ar-H stretch
3172.56	11.23	173.41	3074	v(as)Ar-H stretch
1601.4	208.7869	690.64	1633	vAr C-C stretch
1589.21	87.99	491.21	1582	v(C-N)
1557.33	15.84	2333.06	1542	v(C-N)
1497.57	17.92	1378.67	1521	vAr C-C stretch
1489	14.61	11.26	1486	v(as)Ar C-C stretch
<b>IM-3</b>				
3827.08	86.96	136.75	3442	vOH stretch
3634.83	788.36	41.92	3291	vNH stretch
3231.07	4.2	21.86	3135	vAr-H stretch
3219.75	0.4123	123.25	3226	vAr-H stretch
3209.7	6.76	309.08	3076	vAr-H stretch
3209.56	5.4	54.34	3056	v(as)Ar-H stretch
3204.22	11.0532	64.22		v(as)Ar-H
1651.52	12.58	681.24	1644	vAr C-C stretch
1649.41	21.27	1360.38	1604	vAr C-C stretch
1646.76	41.32	1580.4		vAr C-C stretch
1630.5	20.72	5.08	1632	vAr C-C stretch
1622.25	0.0707	111.5005		vAr C-C stretch
1620.15	4.37	33.26		vAr C-C stretch
1590.39	11.6654	396.9559	1578	C-N stretch
1556.97	17.1555	2615.621	1567	C-N stretch
<b>IM-4</b>				
3827.32	85.7726	133.9766		vOH stretch
3634.43	106.0925	57.1155	3418	vNH stretch
3229.9	3.9093	26.2057	3251	vAr-H stretch
3220.4	0.2948	147.3086	3242	vAr-H stretch
3209.54	7.252	318.69		vAr-H stretch
3209.41	5.1044	50.3604	3209	v(as)Ar-H stretch
3203.97	11.3212	66.8154		v(as)Ar-H stretch
3201.19	25.63	219.486	3201	v(as)Ar-H stretch
3194.92	31.52	149.25	3114	v(as)Ar-H stretch
3189.81	17.09	110.6403		v(as)Ar-H stretch
3181.62	9.84	142.99		v(as)Ar-H stretch
3180.59	0.414	90.1		v(as)Ar-H stretch
3172.33	1.116	41.03		v(as)Ar-H stretch
3171.93	5.66	26.12		v(as)Ar-H stretch
3166.56	13.56	154.75	3061	v(as)Ar-H stretch
1651.54	11.81	718.24	1651	vAr C-C stretch
1649.53	17.79	1524.32		vAr C-C stretch

1647.47	48.77	1257.07	1644	vAr C-C stretch
1631.68	18.44	68.34	1634	vAr C-C stretch
1622.58	0.137	112.94	1622	vAr C-C stretch
1620.09	4.105	34.3	1614	vAr C-C stretch
1590.66	13.006	386.67	1595	v(C-N) stretch
1557.07	19.22	2502.51	1556	v(C-N) stretch

**IM-5**

3773.49	111.57	108.6881		vOH stretch
3619.13	47.1489	49.9262	3425	vNH stretch
3220.43	4.1185	152.5289		vAr-H stretch
3210.31	5.9372	204.4215		vAr-H stretch
3209.86	6.2675	170.2552		vAr-H, v(as)Ar-H
3206.14	1.3545	66.4073		v(as)Ar-H stretch
3204.36	10.288	69.6803		v(as)Ar-H stretch
3202	23.7868	211.9301		v(as)Ar-H stretch
3195.43	30.8886	150.7853		v(as)Ar-H stretch
3190.52	16.7916	106.2932		v(as)Ar-H stretch
3185.34	9.1487	153.3553		v(as)Ar-H stretch
3182.19	9.6808	143.7116		v(as)Ar-H stretch
3181.11	0.2736	85.9813		v(as)Ar-H stretch
3172.94	1.1981	41.401		v(as)Ar-H stretch
3172.28	6.8368	27.2422	3072	v(as)Ar-H stretch
1671.12	253.3	970.9654	1719	vAr C-C stretch
1651.49	17.3527	554.8251		vAr C-C stretch
1648.56	35.9852	860.9897		vAr C-C stretch
1632.65	55.6989	24.6022		vAr(as) C-C stretch
1624.93	7.7909	70.4983		vAr(as) C-C stretch
1619.8	4.8628	40.5719	1619	vAr(as) C-C stretch
1598.7	12.1418	348.9312	1606	v(C-N) stretch
1571.67	4.4461	2693.2735	1504	v(C-N) stretch

**IM-6**

3748.11	166.697	79.0223		vOH stretch
3625.93	116.3687	55.5652	3472	vNH stretch
3224.9	5.8139	105.2289		vAr-H stretch
3218.13	4.0713	123.0545		v(as)Ar-H stretch
3209.12	7.4102	309.2013		vAr-H stretch
3208.97	5.0436	54.2279		vAr-H stretch
3203.78	11.3706	61.8553		vAr-H stretch
3200.59	26.48	222.2055		v(as)Ar-H stretch
3194.17	34.5723	164.4011		v(as)Ar-H stretch
3193.13	8.8803	100.0075		v(as)Ar-H stretch
3189.17	18.3066	101.4483		v(as)Ar-H stretch
3180.41	10.6102	151.1789		v(as)Ar-H stretch
3179.8	1.1344	94.3466		v(as)Ar-H stretch
3171.75	5.3497	26.4064		v(as)Ar-H stretch
3171.08	1.3653	41.0078		v(as)Ar-H stretch
3151.36	17.9877	129.9481	3113	v(as)C-H stretch
3089.03	29.3834	70.125	3095	v(as)C-H stretch



3022.44	65.2015	202.1064	3057	v(as)C-H stretch
1665.15	44.6263	1988.7348		v Ar C-C stretch
1651	22.0456	535.5365		vAr C-C stretch
1648	34.9659	781.8783		vAr C-C stretch
1634	1.1624	16.2312	1632	vAr C-C stretch
1623	9.1141	56.3615		vAr C-C stretch
1619	2.9154	30.9688	1616	vAr C-C stretch
1592	47.7744	316.3398	1604	v(C-N) stretch
1561	34.8924	2702.0752	1539	v(C-N) stretch

### 3. C.2.1.3.1 C-H stretching vibration.

For the studied compounds (IM-1 to IM-6), C-H functional group is present at a number of positions. The characteristics region of C-H stretching vibration of aromatic ring falls in the range 3100-3000  $\text{cm}^{-1}$ <sup>39</sup>. In the present investigation, theoretically calculated bands in the range 3210-3165  $\text{cm}^{-1}$ , 3245-3172  $\text{cm}^{-1}$ , 3231-3204  $\text{cm}^{-1}$ , 3229-3166  $\text{cm}^{-1}$ , 3220-3172  $\text{cm}^{-1}$  and 3224-3151  $\text{cm}^{-1}$  were assigned to aromatic C-H stretching vibrations for compounds IM-1, IM-2, IM-3, IM-4, IM-5 and IM-6 respectively. Pure symmetric bands were calculated at 3210 and 3207  $\text{cm}^{-1}$  in IM-1, 3245, 3242, 3210, 3209, 3204 and 3201  $\text{cm}^{-1}$  in IM-2, 3231, 3219 and 3209  $\text{cm}^{-1}$  in IM-3, 3229, 3220 and 3209  $\text{cm}^{-1}$  in IM-4, 3220, 3210 and 3209  $\text{cm}^{-1}$  in IM-5 and 3224, 3209, 3208 and 3203  $\text{cm}^{-1}$  in IM-6 respectively. Experimentally, symmetric bands were observed at 3242  $\text{cm}^{-1}$  in IM-1, 3135 and 3126  $\text{cm}^{-1}$  in IM-3 and 3251 and 3242  $\text{cm}^{-1}$  in IM-4 respectively. Asymmetric vibrational bands were calculated with stretching frequencies 3203, 3202, 3195, 3190, 3184, 3183, 3181, 3174, 3171 and 3165  $\text{cm}^{-1}$  in IM-1, 3195, 3183, 3181, 3173, and 3172  $\text{cm}^{-1}$  in IM-2, 3209 and 3204  $\text{cm}^{-1}$  in IM-3, 3209, 3203, 3201, 3194, 3189, 3180, 3172 and 3166  $\text{cm}^{-1}$  in IM-4, 3206, 3204, 3202, 3195, 3190, 3185, 3182, 3181 and 3172  $\text{cm}^{-1}$  in IM-5 and 3194, 3193, 3189, 3180, 3179, 3151, 3089 and 3022  $\text{cm}^{-1}$  in IM-6 respectively. Experimentally, Asymmetric vibrational bands were observed at 3060  $\text{cm}^{-1}$  in IM-1, 3114 and 3074  $\text{cm}^{-1}$  in IM-2, 3056  $\text{cm}^{-1}$  in IM-3, 3201, 3114 and 3061  $\text{cm}^{-1}$  in IM-4, 3072  $\text{cm}^{-1}$  in IM-5 and 3113, 3095 and 3057  $\text{cm}^{-1}$  in IM-6 respectively (Table 3.C.3).

### 3. C.2.1.3.2 Aromatic C-C stretching vibrations

Generally, the bands observed in the range 1650-1400  $\text{cm}^{-1}$  are assigned to C-C stretching mode of aromatic derivatives<sup>40</sup>. In our present study, the range for theoretically calculated C-C stretching vibrational mode showing sharp bands are in the range 1667-1620  $\text{cm}^{-1}$ , 1497-1489  $\text{cm}^{-1}$ , 1651-1620  $\text{cm}^{-1}$ , 1651-1620  $\text{cm}^{-1}$ , 1671-1619  $\text{cm}^{-1}$  and 1665-1619  $\text{cm}^{-1}$  for IM-1, IM-2, IM-3, IM-4, IM-5 and IM-6 respectively (Table 3.C.3). Experimentally, the aromatic C-C stretching frequencies for the studied compounds observed in the range 1622-1540  $\text{cm}^{-1}$  in IM-1, 1521-1486  $\text{cm}^{-1}$  in IM-2, 1644-1632  $\text{cm}^{-1}$  in IM-3, 1651-1614  $\text{cm}^{-1}$  in IM-4, 1619  $\text{cm}^{-1}$  in IM-5 and 1632-1616  $\text{cm}^{-1}$  in IM-6 respectively.

### 3. C.2.1.3.3 C-N bond stretching vibrations

C-N stretching vibration is an important stretching vibration for the compounds containing N- atom in the ring structure. Since we are focusing our study on the 2, 4, 5-trisubstituted imidazole derivatives and therefore, C-N stretching vibration of such molecule is fundamentally important to ascertain their structure. Because of the integration of several bands, it is very difficult to detect the C-N stretching vibration in a molecule. Theoretically we observed the C-N stretching frequency of the studied compound at 1600 and 1566  $\text{cm}^{-1}$  in IM-1, 1589 and 1557  $\text{cm}^{-1}$  in IM-2, 1590 and 1556  $\text{cm}^{-1}$  in IM-3, 1590 and 1557  $\text{cm}^{-1}$  in IM-4, 1598 and 1571  $\text{cm}^{-1}$  in IM-5 and 1592 and 1561  $\text{cm}^{-1}$  in IM-6 respectively. 1604 and 1540  $\text{cm}^{-1}$  in IM-1, 1582 and 1542  $\text{cm}^{-1}$  in IM-2, 1578 and 1562  $\text{cm}^{-1}$  in IM-3, 1595 and 1556  $\text{cm}^{-1}$  in IM-4, 1606 and 1504  $\text{cm}^{-1}$  in IM-5 and 1604 and 1539  $\text{cm}^{-1}$  in IM-6 respectively.

Thus, from the above discussion it is evident that the theoretically calculated vibrational frequency matched well with the experimental results for the studied compounds (Fig. 3.C.5).

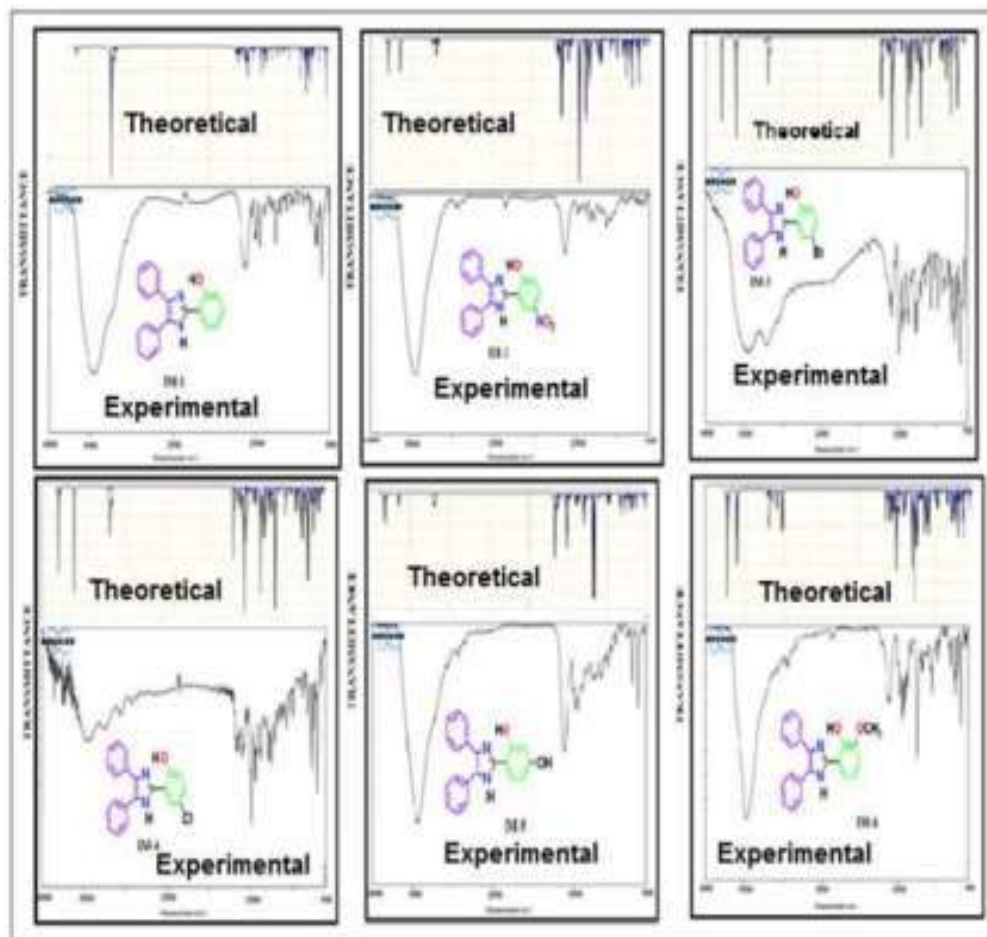


Fig. 3.C.5. Theoretical and experimental FT-IR spectra of IM-1 to IM-6

### 3.C.2.1.4 Molecular Electrostatic Potential (MEP)

A chemical system always creates an electrostatic potential around itself and Molecular electrostatic potential is an important parameter to ascertain and correlate between the molecular structure and the physicochemical properties of molecules<sup>41</sup>. MEP is also useful in understanding the sites for electrophilic and nucleophilic reactions along with the hydrogen bonding interactions<sup>42</sup>. To predict the reactive sites of electrophilic and nucleophilic attack for the investigated molecules (IM-1 to IM-6), MEP at B3LYP/6-31G+ (d, 2p) optimized geometry was calculated. The significance of MEP provides a visual method to understand the relative polarity of the given molecule and the different values of the electrostatic potential at the MEP surface are given by different colours such as red, blue and green. Red, blue and green colour represents the region of most negative, most positive and zero electrostatic potential respectively. Thus, the electrostatic potential increases in the order blue > green > yellow > orange > red. The most negative electrostatic potential (red, orange and yellow region) in the MEP surface is assigned for the electrophilic reaction sites and the positive (blue region) corresponds to nucleophilic reaction site<sup>43,44</sup>. The MEP surface of the studied compounds (IM-1 to IM-6) is depicted in Fig. 3.C.6.

A detailed description of the MEP surface indicating the region of negative/electrophilic reaction sites and positive/nucleophilic reaction site for the studied compounds (IM-1 to IM-6) are listed in Table 3.C.4.

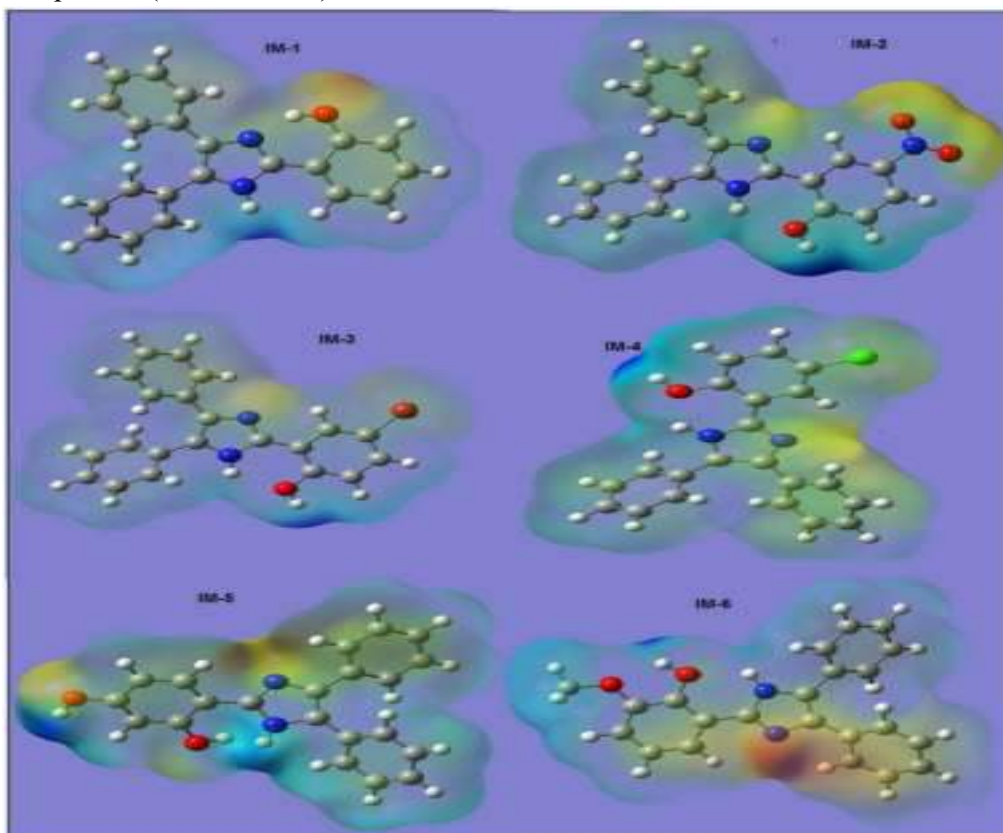
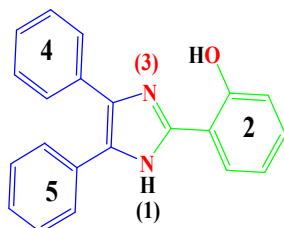


Fig. 3.C.6. MEP plot of studied compounds (IM-1 to IM-6)

**Table. 3.C.4.** Detailed description of MEP surface for compounds IM-1 to IM-6

Entry	Negative region (red, orange, yellow)/Electrophilic reaction site	Positive region (blue)/Nucleophilic reaction site
<b>IM-1</b>	-OH group of 2-phenyl ring and N(3) of imidazole core	NH(1) of imidazole ring and 5-phenyl ring
<b>IM-2</b>	NO <sub>2</sub> group of 2-phenyl ring and N(3) of imidazole core	-OH group of 2-phenyl ring and NH(1) region of imidazole core
<b>IM-3</b>	N(3) of imidazole ring and Br group of 2-phenyl ring	-OH group of 2-phenyl ring and NH (1) region of imidazole core
<b>IM-4</b>	N(3) of imidazole ring and Cl group of 2-phenyl ring	-OH group region of 2-phenyl ring and NH (1) region of imidazole core
<b>IM-5</b>	N(3) of imidazole ring and both the -OH group of 2-phenyl ring	NH (1) region of imidazole core and 5-phenyl ring
<b>IM-6</b>	N(3) of imidazole ring and 4-phenyl ring.	-OH and -OCH <sub>3</sub> group of 2-phenyl ring, NH (1) region of imidazole core and 5-phenyl ring.



### 3.C.2.1.5 NLO properties

Nonlinear optical phenomenon is generally associated with the generation of new electromagnetic fields, altered in wave number, phase or other physical properties by the interaction of various materials with the applied electromagnetic field<sup>45</sup>. Interestingly, organic molecules consisting of delocalized electron density with  $\pi$ - conjugation is known to exhibit relatively strong NLO properties<sup>46</sup>. Thus, the NLO properties of the organic molecules are due to the delocalization of electrons and the intra-molecular charge transfer from donor orbital to acceptor orbital through  $\pi$ -spacer<sup>47</sup>. Organic molecule based NLO materials are gaining lot of interest during last few decades because of their facile synthesis and structural modification. Structural modifications of such organic NLO materials could easily be achieved either by suitably positioning the donor-acceptor groups or simply by lengthening the chain of the  $\pi$ -spacer<sup>48</sup>. Thus, organic nonlinear optical materials are at the centre of attention because of its application in optical communications, optical computing, dynamic image processing, optical modulation and signal processing<sup>49</sup>. The second order nonlinear optical properties in the molecule arise due to the absence of centre of symmetry in the molecule and this phenomenon is largely exploited in the field of telecommunications and optical switches<sup>50</sup>. Theoretically, the NLO properties of the given compound is calculated by determining the parameters such as magnitude of dipole moment ( $\mu$ ), polarizability ( $\alpha$ ), anisotropy of polarizability ( $\Delta\alpha$ ), first hyperpolarizability ( $\beta$ ) and second order hyperpolarizability ( $\gamma$ ). The polarizability tensors are calculated using the following relations:<sup>51</sup>

$$\text{Dipole moment } \mu = (\mu_x^2 + \mu_y^2 + \mu_z^2)^{1/2} \dots\dots\dots (1)$$

$$\alpha(\text{total}) \text{ or } \langle \alpha \rangle = \frac{1}{3} (\alpha_{xx} + \alpha_{yy} + \alpha_{zz}) \dots\dots\dots (2)$$

$$\Delta\alpha = 1/\sqrt{2} [(\alpha_{xx} - \alpha_{yy})^2 + (\alpha_{yy} - \alpha_{zz})^2 + (\alpha_{zz} - \alpha_{xx})^2 + 6(\alpha_{xy}^2 + \alpha_{xz}^2 + \alpha_{yz}^2)]^{1/2} \dots\dots\dots (3)$$

$$\beta_x = \beta_{xxx} + \beta_{xyy} + \beta_{xzz} \dots\dots\dots (4)$$

$$\beta_y = \beta_{yyy} + \beta_{yzz} + \beta_{yxx} \dots\dots\dots (5)$$

$$\beta_z = \beta_{zzz} + \beta_{zxx} + \beta_{yyz} \dots\dots\dots (6)$$

$$\beta_{\text{total}} = (\beta_x^2 + \beta_y^2 + \beta_z^2)^{1/2} \dots\dots\dots (7)$$

$$\langle \gamma \rangle \text{ or } \gamma_{\text{total}} = 1/5 (\gamma_{xxxx} + \gamma_{yyyy} + \gamma_{zzzz} + 2(\gamma_{xxyy} + \gamma_{yyzz} + \gamma_{xxzz})) \dots\dots\dots (8)$$

**Table. 3.C.5.** Dipole moments, dipole polarizabilities, anisotropic polarizabilities and First order hyperpolarizabilities of the studied compounds (IM-1 to IM-6)

<b>Dipole moments, dipole polarizabilities and anisotropic polarizabilities</b>							
<b>Entry</b>	<b>IM-1</b>	<b>IM-2</b>	<b>IM-3</b>	<b>IM-4</b>	<b>IM-5</b>	<b>IM-6</b>	<b>Ref.</b>
$\mu_x$	-2.23	-3.40	-0.96	-0.40	0.47	-0.03	0
$\mu_y$	-3.82	-7.76	-5.33	-5.46	-3.22	3.83	-4.06
$\mu_z$	0.22	-0.27	-0.24	-0.26	0.06	-0.22	0.0018
$\mu$	4.43	8.48	5.42	5.48	3.25	3.84	4.06
$\alpha_{xx}$	-130.17	-168.1	-148.8	-141.5	-130.7	-122.2	-16.62
$\alpha_{yy}$	-129.16	-138.0	-134.4	-133.3	-138.1	-147.6	-24.64
$\alpha_{zz}$	-144.20	-157.7	-162.3	-156.1	-147.8	-155.6	-27.03
$\alpha_{xy}$	-5.86	-25.3	-9.28	-14.22	4.66	2.55	-0.0003
$\alpha_{xz}$	0.14	-0.63	-0.80	-0.62	3.74	0.89	-0.07
$\alpha_{yz}$	4.37	-4.16	-4.00	-4.06	5.21	4.40	0.01
$\alpha_{tot} \times 10^{-24}(\text{esu})$	-19.93	-22.91	-22.01	-21.29	-20.58	-21.01	-3.37
$\Delta\alpha \times 10^{-24}(\text{esu})$	2.86	7.66	4.42	4.82	2.99	4.67	1.39
<b>First order hyperpolarizabilities</b>							
$\beta_{xxx}$	9.65	-206.5	104.05	-12.63	-68.75	178.34	-0.0026
$\beta_{xyy}$	-29.5	5.42	81.60	26.13	19.42	-36.02	-0.0004
$\beta_{xzz}$	-10.0	22.01	56.70	4.90	-9.85	5.37	0.001
$\beta_{yyy}$	-15.4	-79.68	43.75	-58.45	-9.91	39.65	-16.94
$\beta_{xxy}$	-27.9	-152.5	-49.38	-88.01	-66.01	17.55	-0.63
$\beta_{yzz}$	1.60	-0.55	6.41	-4.14	-5.56	4.36	2.05
$\beta_{zzz}$	0.32	-0.72	-0.38	-0.60	-5.49	-0.57	-0.01
$\beta_{xxz}$	3.53	-4.61	-2.71	-4.87	-26.53	-4.12	-0.09
$\beta_{yyz}$	-1.46	1.04	1.31	0.37	8.19	-0.76	-0.03
$\beta_{xyz}$	1.65	3.03	5.15	2.68	-9.19	-0.34	0.05
$\beta_{total} \times 10^{-30}(\text{esu})$	0.44	2.53	2.22	1.31	0.89	1.38	0.13

Encouragingly, 2, 4, 5-triarylimidazole derivatives also consists of extended  $\pi$ -conjugated system carrying three phenyl rings in conjugation with imidazole core and therefore, it was thought worthwhile to study the NLO properties of this type molecules. The nonlinear optical properties such as dipole moments, dipole polarizabilities, first- and second order hyperpolarizabilities of the studied compounds (IM-1 to IM-6) were calculated by B3LYP/ 6-31G + (d, 2p) basis set and the computed results are listed in Table 3.C.5

A comparative study of the dipole moment in the studied system indicates that they have different charge distributions for different directions. The theoretically calculated dipole moments of the studied compounds are 4.433 D (IM-1), 8.485 D (IM-2), 5.426 D (IM-3), 5.485 D (IM-4), 3.257 D (IM-5) and

3.845 D (IM-6) respectively and the dipole moment increases in the order IM-2 > IM-4 > IM-3 > IM-1 > IM-6 > IM-5.

The compounds IM-2, IM-3 and IM-4 have dipole moment value greater than that of urea (4.06 D) whereas the compounds IM-1, IM-5 and IM-6 have dipole moment value less than that of urea reference. Also, the total dipole polarizabilities value of the studied compounds along all three directions is listed in Table 3.C.5. From the Table 3.C.5 it is evident that the dipole polarizability of the studied compounds follows the order IM-2 ( $-2.291 \times 10^{-25}$  esu) > IM-3 ( $-2.201 \times 10^{-25}$ ) > IM-4 ( $-2.129 \times 10^{-25}$ ) > IM-6 ( $-2.101 \times 10^{-25}$ ) > IM-5 ( $-2.058 \times 10^{-25}$ ) > IM-1 ( $-1.993 \times 10^{-25}$ ).

The theoretically computed first-order hyperpolarizabilities and their individual components for the studied compounds (IM-1 to IM-6) are listed in Table 3.C.5. From the table, it is evident that the first-order hyperpolarizability of the studied compounds are  $0.44 \times 10^{-30}$  esu,  $2.53 \times 10^{-30}$  esu,  $2.22 \times 10^{-30}$  esu,  $1.31 \times 10^{-30}$  esu,  $0.89 \times 10^{-30}$  esu and  $1.38 \times 10^{-30}$  esu for compounds IM-1, IM-2, IM-3, IM-4, IM-5 and IM-6 respectively. A comparison of the first-order hyperpolarizability value of the studied compounds with the standard reference urea ( $0.13 \times 10^{-30}$  esu) have shown that the studied compounds have far greater value of first-order hyperpolarizability value than urea. Thus, the order for the first-order hyperpolarizability of the studied compounds are IM-2 > IM-3 > IM-6 > IM-4 > IM-5 > IM-1 and the large value of first-order hyperpolarizability of compounds IM-2 and IM-3 may be attributed to the presence of on strongly activating -OH group and one weakly deactivating -NO<sub>2</sub> and -Br group on the same ring of IM-2 and IM-3 respectively. The smallest first-order hyperpolarizability of compound IM-1 is due to the presence of only one activating group (-OH) which in turn do not favour the long-range charge transfer.

The second order hyperpolarizabilities of the compounds IM-1 to IM-6 are given in Table. 3.C.6. The second order hyperpolarizability of the studied compounds are  $-2.09 \times 10^{-36}$  esu,  $2.90 \times 10^{-36}$  esu,  $2.81 \times 10^{-36}$  esu,  $2.58 \times 10^{-36}$  esu,  $2.35 \times 10^{-36}$  esu and  $2.54 \times 10^{-36}$  esu for IM-1, IM-2, IM-3, IM-4, IM-5 and IM-6 respectively and the order of second-hyperpolarizability of the studied compounds is given by IM-2 > IM-3 > IM-4 > IM-6 > IM-5 > IM-1. From the table it is evident that the second-hyperpolarizability of the studied compounds are much greater than the reference NLO material urea (Table 3.C.6).

**Table. 3.C.6.** Second order hyperpolarizabilities of studied compounds IM-1 to IM-6

Second order hyperpolarizabilities							
Entry	$\gamma_{xxxx}$	$\gamma_{yyyy}$	$\gamma_{zzzz}$	$\gamma_{xxyy}$	$\gamma_{yyzz}$	$\gamma_{xxzz}$	$\gamma_{total}$ (X $10^{-36}$ ) esu
IM-1	-7820.16	-3932.39	-390.80	-1949.79	-790.72	-1563.42	-2.09
IM-2	-13028.6	-4271.77	-391.77	-2623.38	-892.70	-2053.87	-2.90
IM-3	-11965.2	-4234.85	-402.27	-2554.67	-911.54	-2198.72	-2.81
IM-4	-10704.9	-4204.68	-395.87	-2314.38	-878.58	-1968.24	-2.58
IM-5	-9278.62	-3865.49	-529.51	-2209.55	-806.84	-1832.3	-2.35
IM-6	-9718.89	-4378.68	-408.31	-2470.13	-853.66	-2057.45	-2.54
Urea	-120.668	-117.90	-29.39	-44.0275	-28.019	-39.86	-0.049

From the above discussion, it is evident that the studied molecule IM-1 to IM-6 have shown greater value of nonlinear optical parameters than the reference urea molecule and we may infer that this set of molecules could act as a better nonlinear optical material.

### 3.C.2.2 Molecular Docking Study

Molecular docking now a day have become an essential technique in structure-based drug design and can be employed in facilitating and speed up the process of development of drugs<sup>52,53</sup>. Molecular docking provides a useful insight into the different types of interactions prevailing between the ligand and the target protein as well as helps in predicting the binding confirmations and affinities of any ligand to the target protein. Diabetes mellitus which is caused either by insulin deficiency or insulin resistance is a chronic metabolic disorder and have become a global concern now a day<sup>54</sup>. Since, insulin is an essential component in human body which maintain blood glucose and regulates carbohydrate mechanism. Any disruption in blood glucose level in human body leads to hyperglycemia and other metabolic abnormalities of the disease. Basically, there are two types of diabetes, type I usually associated with the autoimmune of beta cells of the pancreas which leads to insulin deficiency and type II which usually involves insulin resistance or decreased insulin secretion<sup>55</sup>. For the regulation of blood sugar level in our body, Tyrosine Kinase beta subunit gets activated by the conformational change of the receptor through the binding of insulin to the alpha subunit of insulin Receptor (IR) and helps in insulin signal pathway and this activation. In diabetes mellitus, Insulin



signaling including activation of IR tyrosine kinase activity is impaired. Several human proteins such as glucokinase, AMP-activated protein kinase, 11  $\beta$ -hydroxysteroid dehydrogenases (11  $\beta$ -HSD), insulin receptor substrate, interleukin1 beta, dipeptidyl peptidase IV, glutamine-fructose-6-phosphate amidotransferase (GFAT), peroxisome proliferator-activated receptor-gamma (PPAR-gamma), tyrosine phosphatases, tyrosine kinase insulin receptor, protein kinase B, and insulin receptor have been identified as key regulators in the development of diabetes. Interestingly, among the many types of tyrosine kinase receptor, protein kinase (PDB ID: 1IR3) is a protein receptor that are highly regulated enzyme<sup>56</sup>. Therefore, any compound or drugs which augment insulin receptor tyrosine kinase activity would be useful in the treatment of diabetes mellitus. The 1IR3 protein kinase receptor consists of two lobes, the N-terminal lobe and the C-terminal lobes that are connected to each other by hinge region and features a deep cleft bound by the two lobes. This cleft contains the ATP binding pocket in the protein kinase domain (Fig 3.C.7).

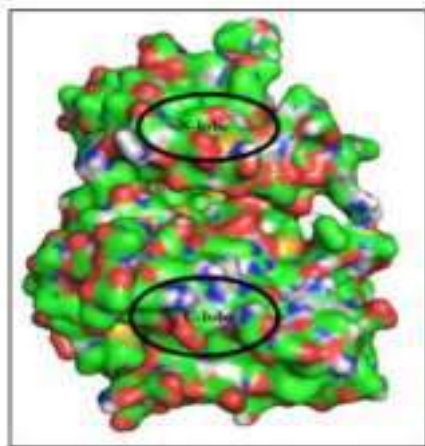


**Fig. 3.C.7.** The N-terminal and C-terminal lobe in the protein 1IR3.

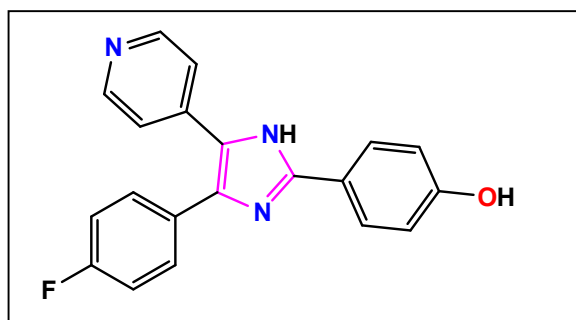


**Fig. 3.C.8.** Molecular structure of SB202190

A numerous therapeutic agents have been developed and reported to treat and manage diabetes, including dietary modifications, exercise, and anti-diabetic agents. However, many of the reported anti-diabetic agents are usually associated with severe side effects<sup>57</sup>. Moreover, tri-arylimidazole drug SB202190 or 4-(4-Fluorophenyl)-2-(4-hydroxyphenyl)-5-(4-pyridyl)-1H-imidazole (Fig.3.C.8) have been used as an inhibitor of MAP kinase P38<sup>2</sup> by SmithKline Beechman scientists and they found that this drug could block the cytokine production<sup>58</sup>. Therefore, we were interested to explore the inhibitory efficacy of some of the selected 2, 4, 5-triarylimidazole derivatives against the insulin receptor protein 1IR3. Interestingly, studies on the phosphorylate of tyrosine complex (1IR3) have shown that the Activation (A-) loop of the kinase goes through major conformational change due to the autophosphorylation of amino acid residues Tyr1158, Try1162 and Tyr1163<sup>59</sup>. Thus, in this section we are reporting the molecular docking study of the selected 2, 4, 5-triaryimidazole derivatives against the insulin receptor protein (PDB ID: 1IR3).

### 3.C.2.2.1 Visualization of the Docking result

Molecular docking study of the compounds (IM-1 to IM-6) against the insulin receptor protein (1IR3) has been carried out using GUI interface programme of Autodock Tools (MGL tool or Molecular Graphics Laboratory tool developed by Scripps research Institute<sup>60</sup>). The docking results have been visualized with the help of Biovia Discovery Studio 2020 (DS), version 21.1.0.20298 and Edu Pymol version 2.5.2.

After successful docking of the compounds (IM-1 to IM-6) with the protein 1IR3, the docking result showed different types of protein-ligand interactions with particular binding energies. For better understanding of fitting of the ligand into the binding pocket of the protein, ligands are shown as blue green stick. The hydrogen bonding interactions between ligands and protein are shown by green dash line, the Pi-sulfur interaction as yellow dash line,  $\pi$ -anion/ $\pi$ -cation interactions as orange dash line,  $\pi$ -sigma interactions as purple dash line,  $\pi$ - $\pi$  stacking/  $\pi$ - $\pi$  T-shaped interactions as dark pink dash line and  $\pi$ -alkyl interactions as light pink dash line respectively. The binding energy ( $\Delta G$ ) and the predicted inhibitory constant (**pKi**) of the studied compounds (IM-1 to IM-6) are found to be -8.7 Kcal/mole (IM-1), -8.4 Kcal/mole (IM-2), -8.8 Kcal/mole (IM-3), -8.0 Kcal/mole (IM-4), -8.9 Kcal/mole (IM-5) and -7.8 Kcal/mole (IM-6) respectively and 0.307  $\mu$ M, 0.515  $\mu$ M, 0.258  $\mu$ M, 1.027  $\mu$ M, 0.217  $\mu$ M and 1.451  $\mu$ M respectively (Table 3.C.7).

**Table. 3.C.7.** Summary of docking of the compound (IM-1 to IM-6) against insulin receptor protein IIR3 with corresponding binding energy ( $\Delta G$ ), predicted inhibitory constant (**pKi**), interacting amino acid residues and type of interactions.

Compounds	Binding Energy (kcal/mol)	Predicted inhibitory constant (pKi) $\mu M$	Amino Acid residues	Type of interactions
IM-1	-8.7	0.307	His1268, Asp1143 and Phe1144	$\pi$ - Cation, H-bonding and $\pi$ - $\pi$ stacked
IM-2	-8.4	0.515	His1057, His1058, Gln1111, Asp1143, His1268, Phe1144 and Met1112	H-bonding, Carbon H-bond, $\pi$ -donor H-bond, $\pi$ - $\pi$ stacked, $\pi$ - $\pi$ T-shaped, $\pi$ - $\pi$ stacked and $\pi$ - Alkyl
IM-3	-8.8	0.258	Glu1115 and His1268	H-bonding, $\pi$ - $\pi$ T-shaped and $\pi$ - Cation
IM-4	-8.0	1.027	Arg1092, Pro1103, Leu1205, Glu1207, Asp1232 and Thr1203	Alkyl, $\pi$ - Alkyl, $\pi$ -Sigma, Alkyl, $\pi$ - Alkyl $\pi$ - Anion, H-bonding and $\pi$ - Anion
IM-5	-8.9	0.217	His1268, Glu1115 and Gln1111	$\pi$ - Cation, Unfavorable Acceptor-Acceptor and H-bonding
IM-6	-7.8	1.451	Thr1145, Glu1115, Asp1143, Glu1108, Met1112, Ser1270, Phe1144, His1268, His1057 and Val1274	H-bonding, $\pi$ - Anion, $\pi$ -Sulphur, $\pi$ - Donor $\pi$ - $\pi$ stacked, Alkyl and $\pi$ - Alkyl

The visualization of the docking result of compound IM-1 against the protein IIR3 revealed that the ligand IM-1 fits in the vicinity of C-lobe inside a pocket region of the receptor protein. A detailed analysis of the docking result of IM-1 with protein IIR3 showed that the ligand IM-1 binds to the protein with binding energy ( $\Delta G$ ) -8.7 Kcal/mole and the predicted inhibitory constant (**pKi**) found to be 0.307  $\mu M$ . The important interactions prevailing between the ligand IM-1 and the protein IIR3 have been characterized by a conventional hydrogen bonding between carboxyl group (-COOH) of the amino acid residue Asp1143 and the H atom of -OH group of the ligand present at the 2-phenyl ring (Fig 3.C.9) at a distance 2.32 Å. Also, the amino acid residue Phe1144 interacts with the ligand IM-1 through  $\pi$ - $\pi$  stacked interactions between two phenyl ring of the Phe1144 and the 5-phenyl ring of the ligand at a distance 5.90 Å. Furthermore, the amino acid residue His1268 interacts with the ligand via  $\pi$ -cation interaction involving the  $\pi$ -

electron of the amino acid residue and 4-phenyl ring of the ligand at a distance 4.92 Å.

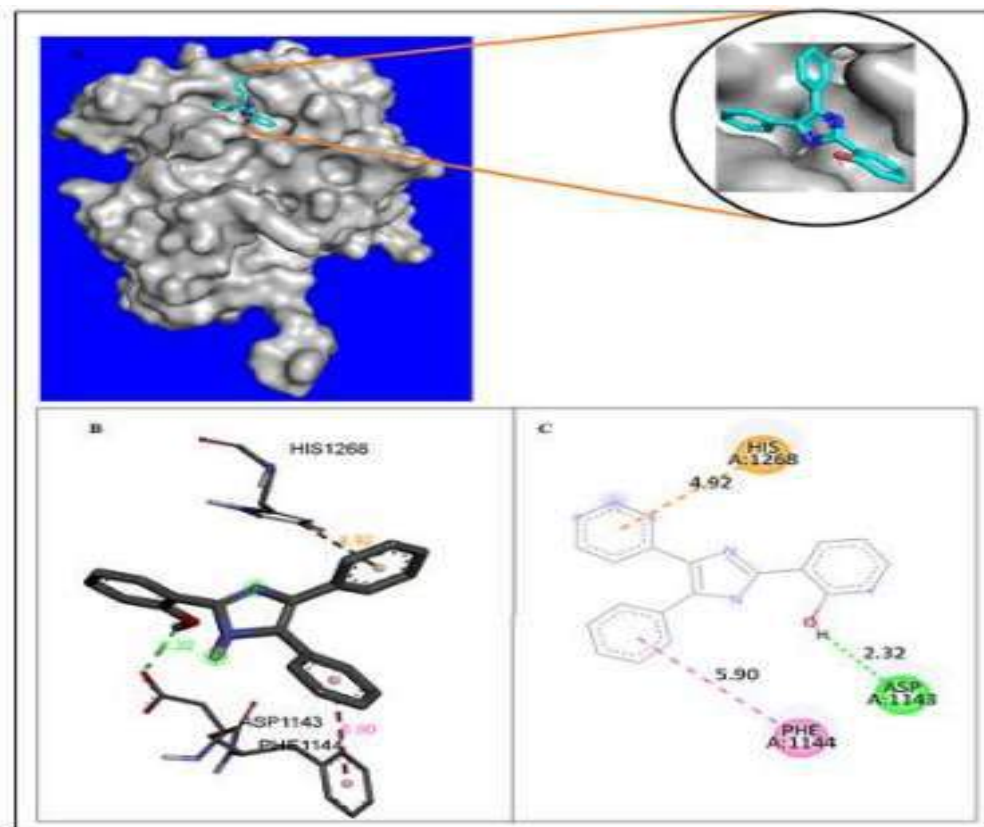


**Fig. 3.C.9.** Visualisation of docking results of ligand IM-1 within protein kinase 1IR3: (A) Optimal binding mode of the protein kinase with IM-1 ligand (Ligand IM-1 shown as blue and green stick model). (B) Amino acid residues involved in different interactions (green dash lines show H-bonding, pink lines show  $\pi$ - $\pi$  stacked interaction, and orange dash line shows  $\pi$ -cation interactions). (C) 2D representation of binding interaction of ligand IM-1 with different amino acid residues of the protein 1IR3.

A close visualization of the docking result of ligand IM-2 with the receptor protein 1IR3 revealed that the ligand also fits in the vicinity of C lobe of the protein with binding energy ( $\Delta G$ ) -8.4 Kcal/mole and predicted inhibitory constant (**pKi**) 0.515  $\mu$ M. The major interactions between the ligand IM-2 and the receptor protein 1IR3 have been characterized by five hydrogen bonding interactions namely, (i) first hydrogen bonding occurs between H atom of NH group of Imidazole ring of amino acid residue His 1057 and O atom of NO<sub>2</sub> group of ligand IM-2 at a distance 2.83Å, (ii) second H-bonding interaction exist between H atom of NH group of imidazole ring of amino acid residue His 1058 and O atom of NO<sub>2</sub> group of ligand IM-2 at a distance 1.89 Å, (iii) Third hydrogen bonding exist between the O atom of C=O group of amino acid residue Asp1143 and H atom of NH group of imidazole core of ligand IM-2 at a distance 1.89 Å and (iv) fourth and

fifth hydrogen bonding interactions occurs between both the H atom of NH<sub>2</sub> group of amino acid residue Gln 1111 and O atom of NO<sub>2</sub> group of ligand IM-2 at a distance 2.84 Å and 2.91 Å respectively (Fig 3.C.10). Apart from conventional hydrogen bonding interactions, other type of interactions between the ligand IM-2 and protein 1IR3 includes,  $\pi$ - $\pi$  stacking between the  $\pi$ -electrons of the 2-phenyl ring and 4-phenyl ring of ligand IM-2 and  $\pi$ -electron of imidazole ring of the amino acid residue His1268 at a distance 4.83 Å and 5.44 Å respectively.

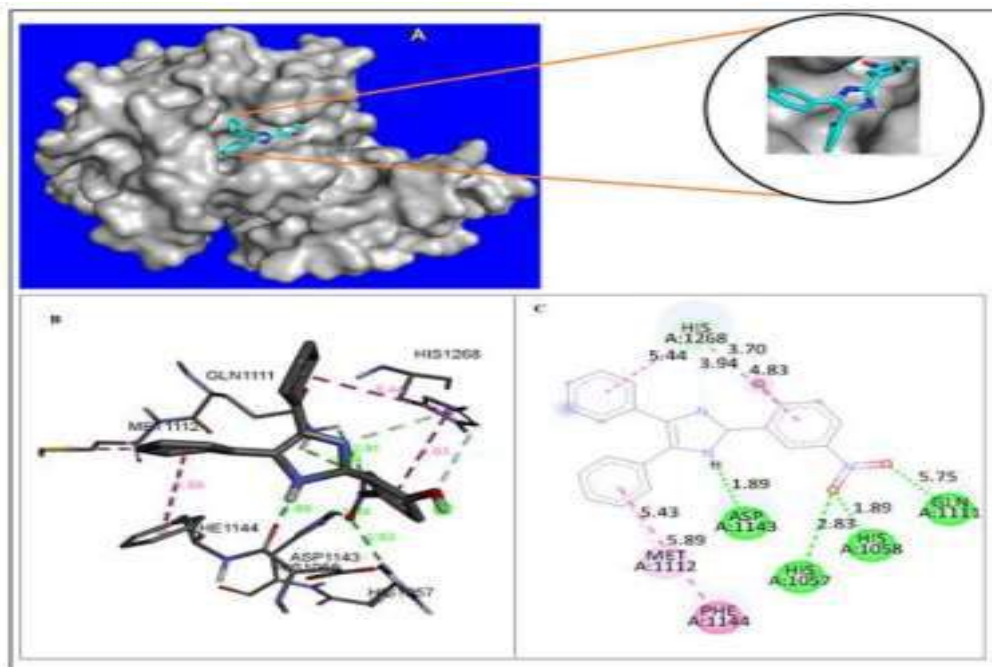


**Fig. 3.C.10.** Visualisation of docking results of ligand IM-2 with the protein kinase 1IR3: (A) Optimal binding mode of the protein kinase with IM-2 ligand (Ligand IM-2 shown as blue and green stick model). (B) Amino acid residues involved in different interactions (green dash lines show H-bonding, pink lines show  $\pi$ - $\pi$  stacked,  $\pi$ - $\pi$  T-shaped interactions and light-pink lines show  $\pi$ -alkyl interactions). (C) 2D representation of binding interaction of ligand IM-2 with different amino acid residues of the protein 1IR3

Another  $\pi$ - $\pi$  T shaped interaction occur between the  $\pi$ -electron of phenyl ring of amino acid residue Phe1144 and  $\pi$ -electron of 5-phenyl ring of ligand IM-2 at a distance 5.89 Å. Other interactions such as carbon-hydrogen bond (between CH group of imidazole moiety of amino acid residue His1268 and O-atom of OH group of ligand IM-2 at a distance 3.70 Å),  $\pi$ -alkyl interaction (between  $\pi$ -electron of 5-phenyl ring of ligand IM-2 and alkyl group of amino acid residue Met 1122 at a distance 5.43 Å) and  $\pi$ -donor hydrogen bond (between  $\pi$ -electron of imidazole ring of residue His 1268 and N atom of imidazole core of ligand IM-2 at a distance 3.94 Å) respectively have also been observed.

Docking of ligand IM-3 with protein 1IR3 revealed that the ligand IM-3 interacts with the protein through three major type of interactions namely

conventional hydrogen bonding,  $\pi$ - $\pi$  T-shaped and  $\pi$ -cation interactions respectively with binding energy ( $\Delta G$ ) -8.8 Kcal/mole and predicted inhibitory constant (**pKi**) 0.258  $\mu$ M. The conventional hydrogen bonding interaction occurs between the O atom of COOH group of amino acid residue Glu 1115 and H-atom of OH group present at 2-phenyl ring of ligand IM-3 at a distance 1.91 Å (Fig 3.C.11).  $\pi$ - $\pi$  T shaped interaction occurs between  $\pi$ -electron of imidazole ring of amino acid residue His 1268 and  $\pi$ -electron of imidazole core of the ligand IM-3 at a distance 5.03 Å. Also,  $\pi$ -cation interaction is exhibited between the NH group of imidazole moiety of amino acid residue His 1268 and  $\pi$ -electron of 4-phenyl ring of the ligand IM-3 at a distance 4.77 Å.

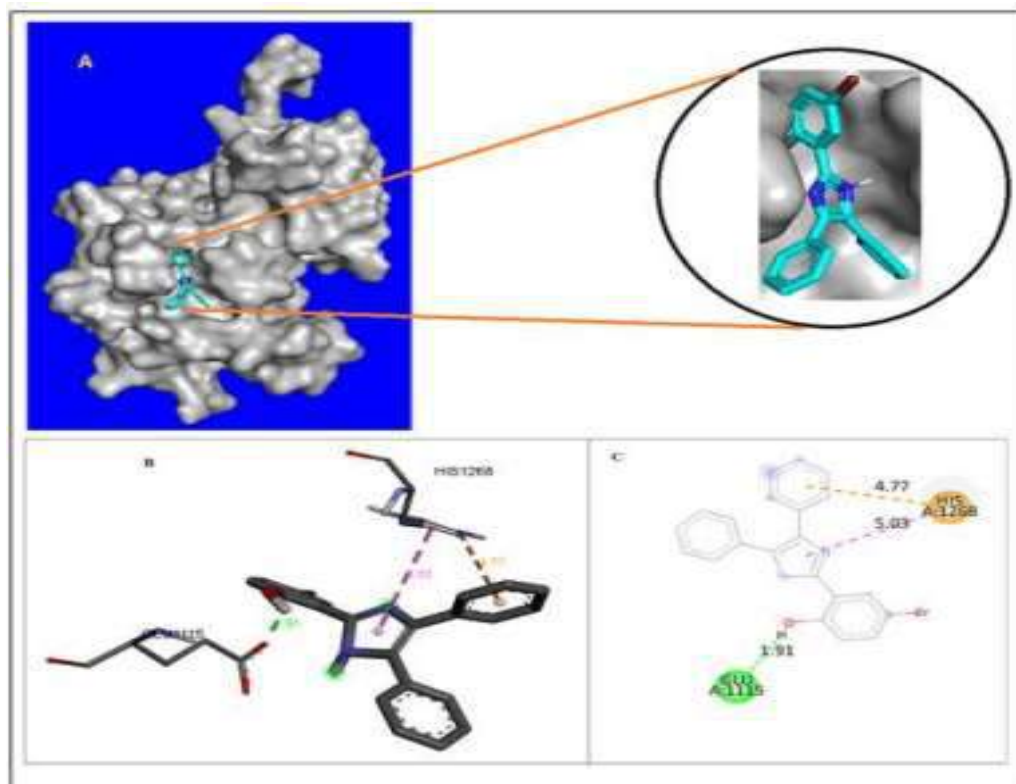


**Fig. 3.C.11.** Visualisation of docking results of ligand IM-3 with the protein kinase 1IR3: (A) Optimal binding mode of the protein kinase with IM-3 ligand (Ligand IM-3 shown as blue and green stick model). (B) Amino acid residues involved in different interactions (green dash lines show H-bonding, pink lines show  $\pi$ - $\pi$  T-shaped interactions and orange lines show  $\pi$ -cation interactions). (C) 2D representation of binding interaction of ligand IM-3 with different amino acid residues of the protein 1IR3.

The analysis of docking result of ligand IM-4 with the protein 1IR3 revealed that the ligand binds to the protein inside the pocket region present at the C-lobe with binding energy ( $\Delta G$ ) -8.0 Kcal/mole and predicted inhibitory constant (**pKi**) 1.027  $\mu$ M. The ligand IM-5 forms four major hydrogen bonding interactions with the protein 1IR3. Among the four hydrogen bonding interactions, two of the

hydrogen bonds are formed between the O atom of C=O group of amino acid residue Asp 1232 and H-atom of OH group present at 2-phenyl ring and H atom of NH group of imidazole core of ligand IM-4 at a distance 2.76 Å and 2.61 Å respectively. The other two hydrogen bonds are formed between O atom of C=O group of amino acid residue Thr 1203 and H atom of OH group present at 2-phenyl ring and H atom of NH group of imidazole core of ligand IM-4 at a distance 2.51 Å and 2.35 Å respectively (Fig 3.C.12). Other interactions are characterized as  $\pi$ -anion (between  $\pi$ -electron of 5-phenyl ring of ligand IM-4 and COO<sup>-</sup> group of amino acid residue Glu 1207 and Asp 1232 at a distance 4.56 Å and 3.79 Å respectively),  $\pi$ -sigma interaction (between  $\pi$  electron of 4 phenyl ring of ligand IM-4 and sigma electron of amino acid residue Leu 1205 at a distance 3.56 Å) and  $\pi$ -alkyl interaction (between  $\pi$ -electron of 4-phenyl ring of ligand IM-4 and alkyl group of amino acid residue Arg 1092 at a distance 4.60 Å).

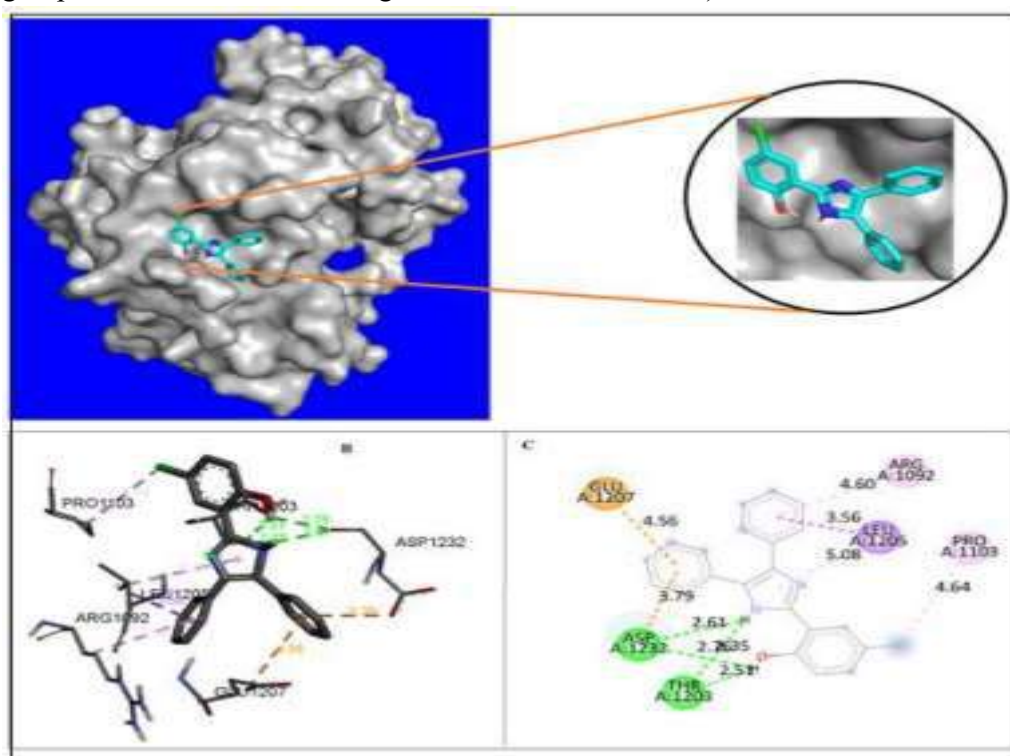


**Fig. 3.C.12.** Visualisation of docking results of ligand IM-4 with the protein kinase 11R3: (A) Optimal binding mode of the protein kinase with IM-4 ligand (Ligand IM-4 shown as blue and green stick model). (B) Amino acid residues involved in different interactions (green dash lines show H-bonding, pink lines show  $\pi$ -sigma interactions, light-pink lines show alkyl and  $\pi$ -alkyl interactions, and orange lines show  $\pi$ -anion interactions). (C) 2D representation of binding interaction of ligand IM-4 with different amino acid residues of the protein 11R3.

A close inspection of the docking result of ligand IM-5 with the protein IIR3 revealed that the ligand IM-5 displayed highest binding affinity among all the studied ligands (IM1-IM-6) with binding energy ( $\Delta G$ ) -8.9 Kcal/mole and predicted inhibitory constant (**pKi**) 0.217  $\mu\text{M}$ . The ligand IM-5 also fits in a similar pocket region present at the C-lobe of the protein. A conventional hydrogen bonding was found to exist between the H atom of amide group ( $\text{NH}_2\text{-C=O}$ ) of the amino acid residue Gln 1111 and the O atom of OH group present at 2-phenyl ring of the ligand IM-5 at a distance 2.21 Å. The other interaction is  $\pi$ -cation interaction which exist between NH group of imidazole ring of amino acid residue His 1268 and  $\pi$ -electron of 4-phenyl ring of ligand IM-5 at a distance 4.83 Å. An unfavourable acceptor-acceptor interaction has also been observed between O atom of COO- group of amino acid residue Glu1115 and O atom of OH group present at 2-phenyl ring of ligand IM-5 at a distance 2.72 Å (Fig 3.C.13).

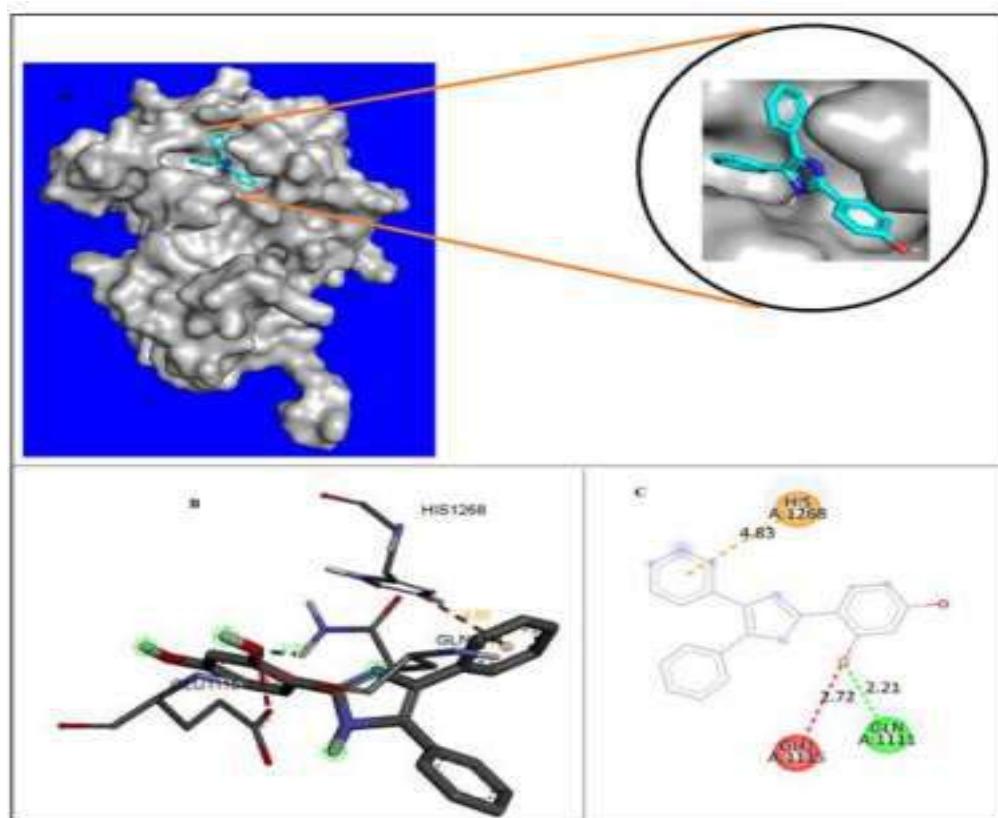


**Fig. 3.C.13.** Visualisation of docking results of ligand IM-5 with the protein kinase IIR3: (A) Optimal binding mode of the protein kinase with IM-5 ligand (Ligand TI5 shown as blue and green stick model). (B) Amino acid residues involved in different interactions (green dash lines show H-bonding, red lines show unfavourable acceptor-acceptor interactions, and orange lines show  $\pi$ -cation interactions). (C) 2D representation of binding interaction of ligand IM-5 with different amino acid residues of the protein IIR3.

The analysis of docking result of ligand IM-6 with the protein IIR3 showed that the ligand IM-6 binds with the protein at the same binding pocket present at



the C-lobe of the protein with binding affinity ( $\Delta G$ ) -7.8 Kcal/mole and predicted inhibitory constant (**pKi**) 1.45  $\mu\text{M}$ . The interactions between ligand IM-6 and the protein 1IR3 have been characterized by three major hydrogen bonding interactions. The first two hydrogen bonds occurs between the H atom of OH group present at 2-phenyl ring of ligand IM-6 and O atom of COO- group of amino acid residue Glu1115 and O atom of OH group of amino acid residue Thr 1145 at a distance 2.66 Å and 2.36 Å respectively. The other hydrogen bond exists between H atom of NH (imidazole core) of ligand IM-6 and O atom of C=O group of amino acid residue Asp 1143 at a distance 2.36 Å (Fig. 3.C.14).

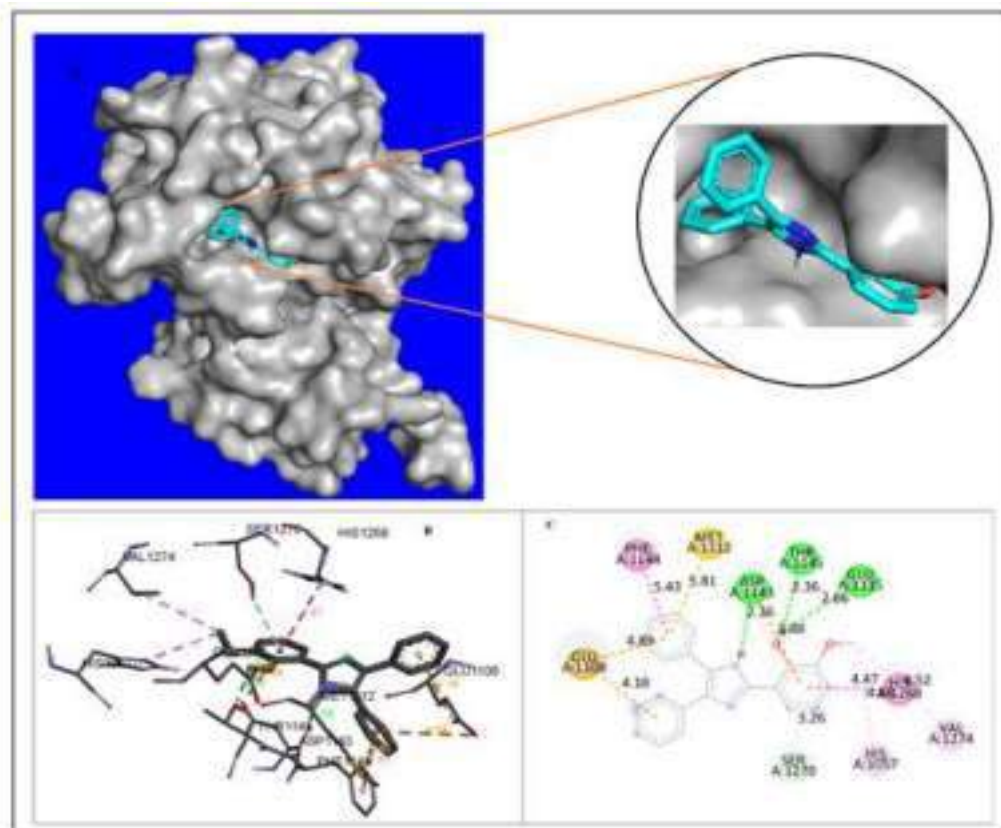


**Fig. 3.C.14** Visualisation of docking results of ligand IM-6 with the protein kinase 1IR3: (A) Optimal binding mode of the protein kinase with IM-6 ligand (Ligand TI6 shown as blue and green stick model). (B) Amino acid residues involved in different interactions (green dash lines show H-bonding, light-green lines show  $\pi$ -donor hydrogen bond, yellow lines show  $\pi$ -sulfur interactions, orange lines show  $\pi$ -anion interactions, pink lines show  $\pi$ - $\pi$  stacked interactions, and light-pink lines show alkyl and  $\pi$ -alkyl interactions). (C) 2D representation of binding interaction of ligand IM-6 with different amino acid residues of the protein 1IR3.

The other type of interactions between ligand IM-6 and protein have been characterized by  $\pi$ -anion (between  $\pi$  electron of 4 and 5-phenyl ring of ligand IM-6 and O atom of COO- group of amino acid residue Glu 1108 at a distance 4.18 Å and 4.89 Å respectively),  $\pi$ -donor hydrogen bond (between  $\pi$  electron of 2-phenyl ring of ligand IM-6 and H atom of OH group of amino acid residue Ser 1270 at a distance 3.26 Å),  $\pi$ -sulfur (between  $\pi$  electron of 5-phenyl ring of ligand IM-6 and S-atom of amino acid residue Met 1112 at a distance 5.81 Å),  $\pi$ - $\pi$  stacking (between  $\pi$  electron of 2-phenyl ring of ligand IM-6 and  $\pi$  electron of imidazole ring of amino acid residue His1268 at 4.47 Å and  $\pi$  electron of 5-phenyl ring of ligand IM-6 and  $\pi$  electron of phenyl ring of Phe1144 at 5.43 Å respectively) and  $\pi$ -alkyl interaction (between OCH<sub>3</sub> group of 2-phenyl ring of IM-6 and  $\pi$  electron of imidazole ring of amino acid residue His1057 at a distance 4.68 Å). Therefore, it is evident from the docking study that the studied molecules IM-1 to IM-6 could act as a potential inhibitor for the insulin receptor protein IIR3 and the binding affinity of the studied ligands towards the protein IIR3 follows the order IM-5 > IM-3 > IM-1 > IM-2 > IM-4 > IM-6.

### 3.C.2.3 In silico Pharmacokinetics analysis of IM-1 to IM-6

The pharmacokinetic properties like absorption, distribution, metabolism, excretion and toxicity (ADMET) are fundamental properties in determining the drug likeness of any compounds prior to its clinical and animal studies. Therefore, ADMET property of the studied compounds plays an important role in categorizing them as a drug candidate as well as their activity inside the body<sup>61</sup>. The ADMET parameters provide useful information about the concentrations of the drug in the different parts of the body with respect to time<sup>62</sup>. ADMET properties such as gastrointestinal absorption (GI), water soluble capability (Log s), lipophilicity (Log Po/W), CYP1A2 inhibitor and Blood-Brain Barrier (BBB) are fundamentally important for any studied compounds to be considered them as a drug candidate<sup>63</sup>. Therefore, the pharmacokinetic properties of the selected 2, 4, 5-triarylimidazole derivatives (IM-1 to IM-6) have been computed with the help of computer aided online SwissADME database (<http://www.swissadme.ch>) and the result of the pharmacokinetic properties along with the Lipinski's property are listed in Table 3.C.8.

From the Table 3.C.8 it is evident that all the studied compounds (IM-1 to IM-6) with bioavailability in the range 55 % have lipophilicity value (LogPo/W) in the range 3.48-4.82 and has high gastrointestinal absorption. The high and positive value of lipophilicity (LogPo/w) for the studied compounds indicated that the compounds are more lipophilic and these compounds could easily pass through the lipid bilayer of most cellular membrane. Except compound IM-2 and IM-3, all other compounds have shown promising Blood-Brain Barrier properties and therefore, these compounds could be test for the treatment of disease related to central nervous system as they have BBB crossing ability<sup>63</sup>. However, the solubility value (LogS) of the studied compounds falls in the range -5.09 to -6.14

and it indicates that the compounds are moderately and poorly soluble in water. Interestingly, all the studied compounds are found to be potential CYP1A2 inhibitors. Thus, the pharmacokinetic parameters suggest that the studied compounds (IM-1 to IM-6) could serve as a potential drug candidate with no violation of Lipinski's rule of five and hence the compounds qualify the criteria of drug likeness.

**Table. 3.C.8.** Lipinski's properties and pharmacokinetic properties (ADME) of 2, 4, 5-triarylimidazole derivatives (IM-1 to IM-6)

Compounds						
Properties	IM-1	IM-2	IM-3	IM-4	IM-5	IM-6
<b>Molecular weight (gm/mole)</b>	312.36	357.36	391.26	346.81	328.36	342.39
<b>Rotatable bonds</b>	3	4	3	3	3	4
<b>H-bond acceptor</b>	2	4	2	2	3	3
<b>H-bond donor</b>	2	2	2	2	3	2
<b>Violations</b>	0	0	0	0	0	0
<b>Log Po/W</b>	4.26	3.48	4.82	4.73	3.89	4.19
<b>Log S</b>	-5.24(MS)	-5.27(MS)	-6.14(PS)	-5.82(MS)	-5.09(MS)	-5.29(MS)
<b>GI</b>	High	High	High	High	High	High
<b>BBB</b>	Yes	No	No	Yes	Yes	Yes
<b>CYP1A2</b>	Yes	Yes	Yes	Yes	Yes	Yes
<b>Bioavailability Score</b>	0.55	0.55	0.55	0.55	0.55	0.55
<b>Topological Surface Area (A<sup>o2</sup>)</b>	48.91	94.73	48.91	48.91	69.14	58.14

\*MS: Moderately soluble, PS: Partially soluble, BBB: Blood-Brain Barrier, CYP: Cytochrome P450, GI: Gastrointestinal absorption

### 3.C.2.4 Computational details

#### 3.C.2.4.1 DFT study

All Quantum Mechanical calculations were carried out on a hp-Z640 desktop P.C. with an Intel Xeon processor (Specifications: E5-2630 V4 @ 220GHz) using Gaussian 16 W package. Density functional theory (DFT) with Becke's (B) three parameter hybrid model, Lee, Yang and Parr's (LYP) using 6-31 G +(d,2p) basis set has been employed to optimize the geometry of the 2, 4, 5-triarylimidazole derivatives (IM-1 to IM-6).

A set of theoretical calculations of selected compounds (IM-1 to IM-6) were performed with Gaussian 16W, Revision A.03 programme package using B3LYP/6-31 G +(d,2p) basis sets to optimize geometry and minimize energy for faster and accurate calculations. With the optimized geometry, theoretical Raman and IR spectra were also calculated from the so chosen basis set. From the optimized geometry, the energy of HOMO and LUMO molecular orbitals along with the energy of HOMO-LUMO gap has also been measured. For analyzing the results of the theoretical calculations, a visual representation was obtained by Gauss View program 6 and it has been used to construct the molecular electrostatic potential surface (MESP) as well as the shape of HOMO and LUMO molecular orbitals. Also, the nonlinear Optical property (NLO) of the selected 2, 4, 5-triarylimidazole have also been calculated taking urea as a reference NLO material.

#### 3.C.2.4.2 Preparation of Protein and ligand for docking Study

The X-ray crystallographic structures of phosphorylated insulin receptor tyrosine kinase protein (PDB ID 1IR3) has been downloaded from the Protein Data Bank (PDB) (<http://www.pdb.org>) database. Graphical User Interface program "Auto Dock Tools (ADT) 1.5.6" from Molecular Graphics Laboratory (MGL) developed by Scripps Research Institute has been used for the preparation of protein for docking study<sup>60</sup>. Input file of receptor protein for the blind docking study were created by taking specific chain (Chain A) of the protein (1IR3). In a typical receptor protein preparation, water molecules and hetero atoms along with the co-crystallised ligands in PDB crystal structure was removed and subsequently, the receptor. pdbqt file has been prepared by adding polar hydrogen atoms and Kollman united atom charges<sup>52-53</sup>. The three-dimensional (3D) structures of ligands (IM-1 to IM-6) were drawn using Chems sketch (ACD/Structure Elucidator, version 12.01, Advanced Chemistry Development, Inc., Toronto, Canada, 2014, <http://www.acdlabs.com>) and geometry optimization of the ligands (IM-1 to IM-6) were carried out using MM2 program incorporated in Chem. Draw Ultra 8.0 and further optimization of geometry of each molecule were carried out with the MOPAC 6 package using the semi-empirical AM1 Hamiltonian<sup>64</sup>. The input .pdbqt file of the ligands was generated using Auto Dock Tools (ADT). As the ligand molecules (IM-1 to IM-6) were non peptides, therefore, Gasteiger charge was assigned and then non-polar hydrogen was merged.

### 3.C.2.4.3 Molecular docking study using Autodock vina

All molecular docking calculations of the studied ligands (IM-1 to IM-6) with protein IIR3 were carried out in the AutoDock Vina programme 1.1.2 developed by Scripps Research institute<sup>65,66</sup> and the results of the docking study and the intermolecular interactions between receptors protein and the ligand molecules were analyzed using BIOVIA Discovery Studio 2020 (DS), version 20.1.0.0 (Dassault Systèmes BIOVIA, Discovery Studio Modeling Environment, Release 2017, San Diego: Dassault Systèmes, 2016) and Edu pymol version 1.7.4.4<sup>66</sup>. The three-dimensional (3D) affinity (grid) maps and electrostatic a grid boxes of 80×80×80 Å grid points and grid centre (X, Y, Z) of -24.099, 39.015, 11.431 with a spacing of 1.00 Å generated by AutoGrid auxiliary program for each of the receptor protein for blind docking were generated to cover the entire active site of the receptor protein in order to eliminate biasness arising during the docking simulation<sup>67</sup>. Lamarckian genetic algorithm and a standard protocol with default setting of other run parameters were used for docking simulation. For each docking experiments, several runs were performed by the program with one predicted binding mode with each run. All the torsions were allowed to rotate. The predicted inhibitory constant (**pK<sub>i</sub>**) has been calculated using the following standardized equation.<sup>68</sup>

$$pK_i = 10^{\frac{\text{Binding Energy Score}}{1.336}}$$

### 3.C.2.4.4 Pharmacokinetic study

The pharmacokinetic properties like like absorption, distribution, metabolism, excretion and toxicity (ADMET) of the compounds (IM-1 to IM-6) have been studied using the computer aided online SwissADME database (<http://www.swissadme.ch>).

**3.C.3 References**

- (1) M. Waheed, N. Ahmed, M. A Alsharif, M. I. Alahmdi, S. Mukhtar., *ChemistrySelect*, **2017**, 2 (26), 7946–7950.
- (2) T. S. Rajasekar, P. Navamani, K. Jayamoorthy, N. Srinivasan., *Journal of Inorganic and Organometallic Polymers and Materials*, **2017**, 27 (4), 962–967.
- (3) S. Chauhan, V. Verma, D. Kumar, A. Kumar., *Synthetic Communications*, **2019**, 49 (11), 1427–1435.
- (4) A. Z. al Munsur, H. N. Roy, M. K. Imon., *Arabian Journal of Chemistry*, **2020**, 13 (12), 8807–8814.
- (5) S. H. Gebre., *Synthetic Communications*, **2021**, 51 (11), 1669–1699.
- (6) M. A. Zayed, M. A. Abdallah., *Egyptian Journal of Chemistry*, **2019**, 62 (11), 2143–2162.
- (7) D. Gustinčič, A. Kokalj., *Physical Chemistry Chemical Physics*, **2015**, 17 (43), 28602–28615.
- (8) A. P. Kulkarni, C. J. Tonzola, A. Babel, S. A. Jenekhe., *Chemistry of Materials*, **2004**, 16 (23), 4556–4573.
- (9) L. Fabbrizzi, F. Foti, S. Patroni, P. Pallavicini, A. Taglietti., *Angewandte Chemie International Edition*, **2004**, 43 (38), 5073–5077.
- (10) Z. Li, X. Lou, H. Yu, Z. Li, J. Qin., *Macromolecules*, **2008**, 41 (20), 7433–7439.
- (11) Z. Song, W. Zhang, M. Jiang, H. H. Y. Sung, R. T. K. Kwok, H. Nie, I. D. Williams, B. Liu, B. Z. Tang., *Advanced Functional Materials*, **2016**, 26 (6), 824–832.
- (12) S. Suresh, N. Bhuvanesh, A. Raman, P. Sugumar, D. Padmanabhan, S. Easwaramoorthi, M. N. Ponnuswamy, S. Kavitha, R. Nandhakumar., *Journal of Photochemistry and Photobiology A: Chemistry*, **2019**, 385, 112092.
- (13) Y. H. Lam, Y. Abramov, R. S. Ananthula, J. M. Elward, L. R. Hilden, S. O. Nilsson Lill, P. O. Norrby, A. Ramirez, E. C. Sherer, J. Mustakis, G. J. Tanoury., *Organic Process Research and Development*, **2020**, 24 (8), 1496–1507.
- (14) M. Evecen, H. Tanak., *Materials Science- Poland*, **2016**, 34 (4), 886–904.
- (15) S. Gümüş, L. Türker., *Heterocyclic Communications*, **2012**, 18 (1), 11–16.
- (16) P. Lienard, J. Gavartin, G. Boccardi, M. Meunier., *Pharmaceutical Research*, **2015**, 32 (1), 300–310.

- (17) H. J. Huang, H. W. Yu, C. Y. Chen, C. H. Hsu, H. Y. Chen, K. J. Lee, F. J. Tsai, C. Y. C. Chen., *J Taiwan Inst Chem Eng*, **2010**, *41* (6), 623–635.
- (18) D. Giugliano, A. Ceriello, K. Esposito., *The American Journal of Clinical Nutrition*, **2008**, *87* (1), 217S-222S.
- (19) G. S. Mohiuddin, S. Palaian, P. R. Shankar, K. G. Sam, M. Kumar., *International Journal of Pharmaceutical Sciences and Research*, **2019**, *10* (9), 4145–4148.
- (20) J. Ganugapati, A. Baldwa, S. Lalani., *Bioinformation*, **2012**, *8* (5), 220.
- (21) N. Satheesha Rai, B. Kalluraya, B. Lingappa, S. Shenoy, V. G. Puranic., *European Journal of Medicinal Chemistry*, **2008**, *43* (8), 1715–1720.
- (22) A. D. Becke., *The Journal of Chemical Physics*, **1993**, *98* (7), 5652.
- (23) C. Lee, W. Yang, R. G. Parr., *Physical Review B*, **1988**, *37* (2), 789.
- (24) M. J. Frisch, G. W. Trucks, H. B. Schlegel, G. E. Scuseria, M. A. Robb, J. R. Cheeseman, G. Scalmani, V. Barone, G. A. Petersson, H. Nakatsuji, X. Li, M. Caricato, A. v Marenich, J. Bloino, B. G. Janesko, R. Gomperts, B. Mennucci, H. P. Hratchian, J. v Ortiz, A. F. Izmaylov, J. L. Sonnenberg, D. Williams-Young, F. Ding, F. Lipparini, F. Egidi, J. Goings, B. Peng, A. Petrone, T. Henderson, D. Ranasinghe, V. G. Zakrzewski, J. Gao, N. Rega, G. Zheng, W. Liang, M. Hada, M. Ehara, K. Toyota, R. Fukuda, J. Hasegawa, M. Ishida, T. Nakajima, Y. Honda, O. Kitao, H. Nakai, T. Vreven, K. Throssell, J. A. Montgomery Jr., J. E. Peralta, F. Ogliaro, M. J. Bearpark, J. J. Heyd, E. N. Brothers, K. N. Kudin, V. N. Staroverov, T. A. Keith, R. Kobayashi, J. Normand, K. Raghavachari, A. P. Rendell, J. C. Burant, S. S. Iyengar, J. Tomasi, M. Cossi, J. M. Millam, M. Klene, C. Adamo, R. Cammi, J. W. Ochterski, R. L. Martin, K. Morokuma, O. Farkas, J. B. Foresman, D. J. Fox., *Gaussian, Inc., Wallingford CT, Gaussian 16 Revision C.01*, **2016**.
- (25) R. Dennington, T. A. Keith, J. M. Millam., *GaussView Version 6, Semichem Inc., Shawnee Mission, KS*, **2016**.
- (26) G. Varvounis, V. Gkalpinos, P. Theodorakopoulou, E. Tsemperlidou., In *Comprehensive Heterocyclic Chemistry IV (Chap 4.02 - Imidazoles)*; Black, D. S., Cossy, J., Stevens, C. V., Eds.; Elsevier: Oxford, **2022**; Vol. 4, pp 113–307.
- (27) P. Sykes., *A Guidebook to Mechanism in Organic Chemistry*, 6th ed.; Pearson Education: New Delhi, India, **2004**.
- (28) M. Belletête, J. F. Morin, M. Leclerc, G. Durocher., *Journal of Physical Chemistry A*, **2005**, *109* (31), 6953–6959.
- (29) D. Zhenming, S. Heping, L. Yufang, L. Diansheng, L. Bo., *Spectrochimica Acta Part A: Molecular and Biomolecular Spectroscopy*, **2011**, *78* (3), 1143–1148.

- (30) K. B. Benzon, H. T. Varghese, C. Y. Panicker, K. Pradhan, B. K. Tiwary, A. K. Nanda, C. van Alsenoy., *Spectrochimica Acta Part A: Molecular and Biomolecular Spectroscopy*, **2015**, *151*, 965–979.
- (31) S. W. Xia, X. Xu, Y.-L. Sun, Y.-H. Fan, C.-F. Bi, D. M. Zhang, L.-R. Yang., *Chinese Journal of Structural Chemistry*, **2006**, *25* (2), 197–203.
- (32) M. Snehalatha, C. Ravikumar, I. Hubert Joe, N. Sekar, V. S. Jayakumar., *Spectrochimica Acta Part A: Molecular and Biomolecular Spectroscopy*, **2009**, *72* (3), 654–662.
- (33) T. A. Koopmans., *Physica*, **1934**, *1* (1–6), 104–113.
- (34) R. G. Parr, R. G. Pearson., *J Am Chem Soc*, **1983**, *105* (26), 7512–7516.
- (35) R. G. Parr, L. V. Szentpály, S. Liu., *J Am Chem Soc*, **1999**, *121* (9), 1922–1924.
- (36) R. G. Pearson., *Journal of Chemical Sciences*, **2005**, *117* (5), 369–377.
- (37) S. Mandal, D. K. Poria, D. K. Seth, P. S. Ray, P. Gupta., *Polyhedron*, **2014**, *73*, 12–21.
- (38) P. Jaramillo, P. Pérez, R. Contreras, W. Tiznado, P. Fuentealba., *Journal of Physical Chemistry A*, **2006**, *110* (26), 8181–8187.
- (39) N. P. G. Roeges., *A Guide to the Complete Interpretation of Infrared Spectra of Organic Structures*; John Wiley and Sons Inc.: New York, **1994**.
- (40) B. C. Smith., *Infrared Spectral Interpretation*, 1st ed.; CRC Press: Washington, DC, **1999**; Vol. 2.
- (41) P. Politzer, D. G. Truhlar., *Chemical Applications of Atomic and Molecular Electrostatic Potentials*; Plenum Press: New York, **1981**.
- (42) E. Scrocco, J. Tomasi., *Advances in Quantum Chemistry*, **1978**, *11* (C), 115–193.
- (43) P. Politzer, J. S. Murray., In *Theoretical Biochemistry and Molecular Biophysics: A Comprehensive Survey*; Beveridge, D. L., Lavery, R., Eds.; Adenine Press: Schenectady, New York.
- (44) E. Scrocco, J. Tomasi., *Topics in Current Chemistry* , **1973**, *42*, 95–170.
- (45) *Principles and Applications of Nonlinear Optical Materials*, 1st ed.; Munn, R. W., Ironside, C. N., Eds.; Springer Dordrecht: Netherlands, **1993**.
- (46) A. Migalska-Zalas, K. el Korchi, T. Chtouki., *Optical and Quantum Electronics*, **2018**, *50*(11) (Article no. 389), 1–10.



- (47) M. U. Khan, M. Khalid, S. Asim, Momina, R. Hussain, K. Mahmood, J. Iqbal, M. N. Akhtar, A. Hussain, M. Imran, A. Irfan, A. Ali, M. F. ur Rehman, Y. Jiang, C. Lu., *Frontiers in Materials*, **2021**, 8 (Article 719971), 287.
- (48) M. R. S. A. Janjua., *Journal of the Iranian Chemical Society*, **2017**, 14 (9), 2041–2054.
- (49) V. M. Geskin, C. Lambert, J. L. Brédas., *J Am Chem Soc*, **2003**, 125 (50), 15651–15658.
- (50) M. Beytur, F. Kardaş, O. Akyıldırım, A. Özkan, B. Bankoğlu, H. Yüksek, M. L. Yola, N. Atar., *Journal of Molecular Liquids*, **2018**, 251, 212–217.
- (51) S. Muthu, T. Rajamani, M. Karabacak, A. M. Asiri., *Spectrochimica Acta Part A: Molecular and Biomolecular Spectroscopy*, **2014**, 122, 1–14.
- (52) L. G. Ferreira, R. N. dos Santos, G. Oliva, A. D. Andricopulo., *Molecules*, **2015**, 20 (7), 13384–13421.
- (53) X.-Y. Meng, H.-X. Zhang, M. Mezei, M. Cui., *Current Computer-Aided Drug Design*, **2011**, 7 (2), 146–157.
- (54) A. T. Kharroubi, H. M. Darwish., *World J Diabetes*, **2015**, 6 (6), 867.
- (55) A. B. Olokoba, O. A. Obateru, L. B. Olokoba., *Oman Medical Journal*, **2012**, 27 (4), 269–273.
- (56) S. A. Ashraf, A. E. O. Elkhalfa, K. Mehmood, M. Adnan, M. A. Khan, N. E. Eltoun, A. Krishnan, M. S. Baig., *Molecules*, **2021**, 26 (19), 5957.
- (57) R. Chaturvedi, C. Desai, P. Patel, A. Shah, R. K. Dikshit., *Perspectives in Clinical Research*, **2018**, 9 (1), 15–22.
- (58) J. C. Lee, J. T. Laydon, P. C. McDonnell, T. F. Gallagher, S. Kumar, D. Green, D. McNulty, M. J. Blumenthal, J. R. Keys, S. W. Land Vatter, J. E. Strickler, M. M. McLaughlin, I. R. Siemens, S. M. Fisher, G. P. Livi, J. R. White, J. L. Adams, P. R. Young., *Nature*, **1994**, 372 (6508), 739–746.
- (59) K. L. Binns, P. P. Taylor, F. Sicheri, T. Pawson, S. J. Holland., *Molecular and Cellular Biology*, **2000**, 20 (13), 4791–4805.
- (60) R. Huey, G. M. Morris., *Using AutoDock 4 with AutoDocktools: A Tutorial.*; The Scripps Research Institute, Molecular Graphics Laboratory, pp. 54-56: La Jolla, CA, USA, **2008**.
- (61) S. Hari., *Journal of Applied Pharmaceutical Science*, **2019**, 9 (7), 18–26.
- (62) K. Boussery, F. M. Belpaire, J. van de Voorde., In *The Practice of Medicinal Chemistry*; Wermuth, C. G., Ed.; Elsevier Science, **2008**; pp 635–654.

- (63) F. Ntie-Kang, L. L. Lifongo, J. A. Mbah, L. C. Owono Owono, E. Megnassan, L. M. Mbaze, P. N. Judson, W. Sippl, S. M. N. Efange., *In Silico Pharmacology*, **2013**, *1(1)* (Article 12), 1–11.
- (64) K. Ohtawara, H. Teramae., *Chemical Physics Letters*, **2004**, *390* (1–3), 84–88.
- (65) J. Eberhardt, D. Santos-Martins, A. F. Tillack, S. Forli., *Journal of Chemical Information and Modeling*, **2021**, *61* (8), 3891–3898.
- (66) O. Trott, A. J. Olson., *Journal of Computational Chemistry*, **2010**, *31* (2), 455–461.
- (67) G. M. Morris, D. S. Goodsell, R. S. Halliday, R. Huey, W. E. Hart, R. K. Belew, A. J. Olson., *Journal of Computational Chemistry*, **1998**, *19* (14), 1639–1662.

## CHAPTER-IV

### Section A

#### **Green Synthesis of 3,4-dihydropyrimidine-2-(1H)-ones (DHPMs) using Iron Borate as an Efficient Catalyst**

##### **4.A.1 Background of the present investigation**

In synthetic organic chemistry, it is becoming increasingly important to develop clean and environmentally sound chemical processes that use less hazardous reaction conditions and covers the essential prospects of green chemistry principle. Solvent free reaction on one hand provides avenues for the requirement of green chemical condition as this reaction condition are highly significant from both the economic and environmental point of view<sup>1</sup>. Now a days, one-pot Multicomponent Reactions are gaining lot of interest for the synthesis of wide range of biologically active heterocyclic compounds<sup>2</sup>. Thus, the combination of solvent free reaction condition and one-pot Multicomponent reaction could serve as an optimal and efficient method for the synthesis of diverse class of heterocyclic compounds under green chemical conditions. Since this type of combination has many added advantages such as short reaction time, economical, environmentally benign, elimination of hazardous solvents and easy work up procedure over the classical synthetic methods<sup>3</sup>. Among the numerous Multicomponent reactions, Bigenelli reaction is used for the direct synthesis of 3,4-dihydropyrimidine-2-(1H)-one derivatives. The Bigenelli Reaction coined by Italian Chemist Pietro Bigenelli in 1893 is one of the most important and useful multicomponent condensation reaction involving an aldehyde, urea and  $\beta$ -dicarbonyl compounds to yield 3,4-dihydropyrimidine-2-(1H)-ones (Fig. 4.A.1a). These compounds are somewhat similar to dihydropyridines also known as Hantzsch pyridines as the preparation of these compounds also requires the same reactants as required for preparation of Bigenelli compounds<sup>4</sup>. The reaction can also be carried out by using thiourea in place of urea to yield 3,4-dihydropyrimidine-2-(1H)-thione (Fig. 4. A.1b)<sup>5</sup>. In recent times, DHPMs have gained a lot of attention of chemists because of their biological and therapeutic uses<sup>6</sup>. These compounds are one among the five classes of Calcium Channel blocking drugs<sup>7-8</sup>. They also have anti-viral<sup>9</sup>, anti-inflammatory, anti-bacterial<sup>10</sup>,  $\alpha$ -1a-adrenergic antagonist<sup>11</sup>, anti-tumor<sup>12</sup>, anti-cancer<sup>13</sup>, anti-HIV<sup>14</sup>, anti-inflammatory<sup>15</sup> properties. Apart from these properties, DHPMs also have shown other significant properties like anti-oxidant<sup>16</sup>, antimuscarinic<sup>17</sup>, antithyroid<sup>18</sup>, antiparasitic<sup>19</sup>, antidiabetic<sup>20</sup>, Urease Inhibition<sup>21</sup>, Carbonic anhydrase inhibition<sup>22</sup>, cardiac effects<sup>23</sup>. DHPMs are also present in some polyguanidine alkaloids like batzelladine that have found been found to be HIV gp-120-CD-4 inhibitors<sup>24</sup>. Few important drugs that contain the DHPM moiety are monastrol (99), riboflavin (100), 5-Fluoro uracil (101), aminophylline (102), idoxuridine (103) Fig.4. A.2.

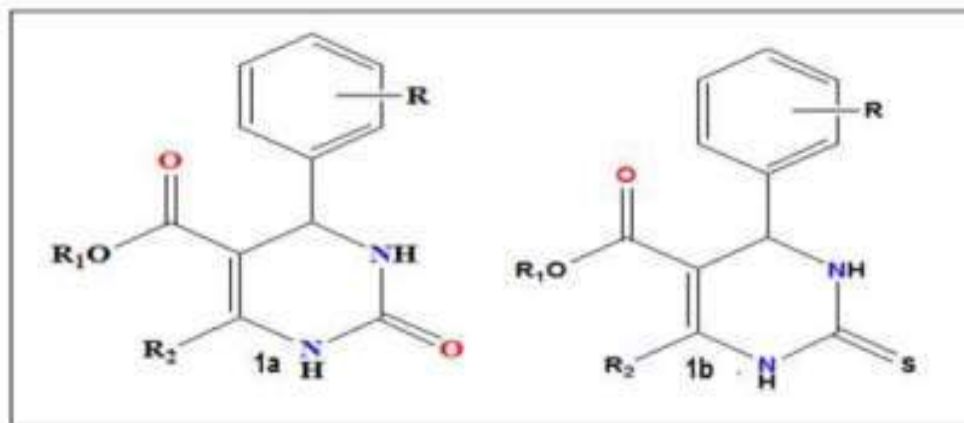


**Fig. 4.A.1a-1b.** 1a) Structure of yield 3,4-dihydropyrimidine-2-(1H)-one and 1b) 3,4-dihydropyrimidine-2-(1H)-thione

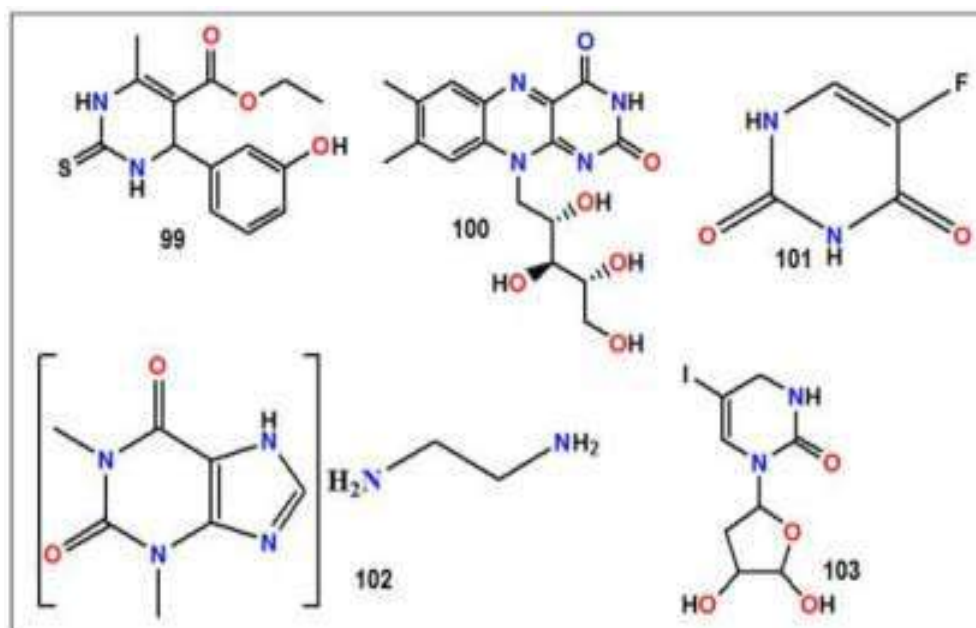


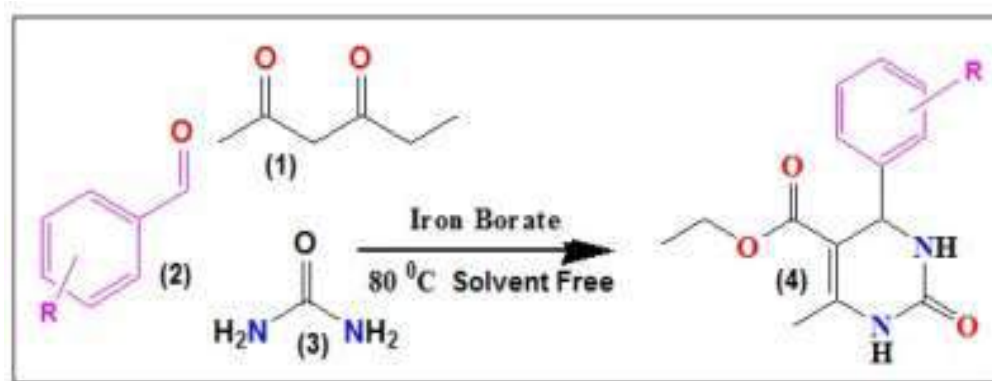
**Fig. 4.A.2.** Structures of few drugs that contain the DHPM moiety

In view of the diverse pharmacological, medicinal, biological and industrial properties associated with 3, 4-dihydropyrimidine derivatives, numerous synthetic methodologies have been developed during the past few decades under both classical and green chemical conditions<sup>25-26</sup>. However, these reported synthetic procedures found to contain one or more serious drawbacks such as use of expensive catalyst, non-recyclable catalyst, moisture sensitive metal salts, long reaction time, low yield, large amount of catalyst loading, use of hazardous solvent, tedious work-up procedure and environmental pollution<sup>27</sup>. Thus, the development of a clean, environmentally benign and economically cost-effective

protocol for the synthesis of 3, 4-dihydropyrimidine-2-(1H)-one derivatives is highly demanding and, in this context, synthetic chemists are devoting time to develop a protocol for solvent free synthesis, solid phase synthesis and even reaction in water medium. The prominent advantages of solvent free, solid phase or reaction in water medium is that it omits the use of the environmentally hazardous solvents which definitely reduce chemical pollution and at the same time reduce the cost of the work<sup>28</sup>. Therefore, in order to overcome these shortcomings and fulfilling the criteria of green chemistry principle and sustainable chemistry, in this chapter, we are reporting the synthesis of 3, 4-dihydropyrimidine-2-(1H)-one derivatives using inexpensive iron borate as a catalyst under solvent free condition.

### 4.A.2. Results and Discussions

The classical method for the synthesis of 3,4-dihydropyrimidine-2-ones (4) involves a one pot condensation of  $\beta$ -keto ester (1), aldehyde (2) and urea (3) under harsh acidic conditions with low yield of the products<sup>29</sup>. Thus, it has become inevitable that the synthesis of 3, 4-dihydropyrimidine-2-ones to be pursued in an environmentally friendly manner for its use in different fields<sup>30</sup>. Although a large variety of new catalytic / modified synthetic protocols such as microwave assisted, Ultrasound irradiation, use of ionic liquid, solvent free synthesis has been developed for the synthesis of 3, 4-dihydropyrimidine-2-one derivatives in an elegant manner during the past few decades yet these reported protocols encounter some serious limitations as discussed above<sup>31-40</sup>. These factors prompted us to find a new catalyst for the synthesis of Bigenelli derivatives under solvent free condition. A number of reports are available for the synthesis of 3, 4-dihydropyrimidine-2-one derivatives using different iron salts as a catalyst under different reaction condition but there is not a single report for the synthesis of the above mention derivatives using iron borate as a catalyst. Therefore, it was thought worthwhile to explore the catalytic efficacy of iron borate for the synthesis of 3, 4-dihydropyrimidine-2-one derivatives (4) by one-pot cyclo-condensation of  $\beta$ -dicarbonyl compound (1), Aldehyde (2) and Urea (3) under solvent free reaction condition following the green chemistry protocol (Scheme 4.A.1).



**Scheme. 4.A.1.** Schematic representation of Biginelli reaction catalyzed by Fe-borate catalyst

Initially, for the synthesis 3, 4-dihydropyrimidine-2-ones (4), we choose ethylacetoacetate (1), 2-nitrobenzaldehyde (2) and urea (3) as model compounds under different environmentally friendly reaction conditions at 80 °C for 3 hours using different mol% (0.5 to 4) of the catalyst iron borate. We choose the different solvent systems as well for screening the catalytic efficiency of the catalyst with model reactants under different conditions and the results are summarized in Table 4.A.1

**Table. 4.A.1.** Screening of the solvent for control reaction

Entry	Solvent <sup>a</sup>	Time (hours)	Yield <sup>b</sup>
1	Ethanol	3	86
2	Methanol	3	82
3	DMF	3	90
4	DMSO	3	80
5	Water	3	40
6	Silica Gel	1	86
7	<b>Neat</b>	<b>8 (mins)</b>	<b>97</b>

<sup>a</sup>The reaction was performed with Ethylacetoacetate 1(1 mmol), 2-nitro-Benzaldehyde 2 (1 mmol), and Urea 3 (1 mmol) with the catalyst using different solvents. <sup>b</sup>Isolated Yields.

We observed that the Biginelli reaction proceed well in more polar solvent like alcohol, DMF and DMSO (Table 4.A.1, entry 1, 2, 3, 4) but we observed that under this condition, the reaction needed more time to go for completion. Therefore, we focused our study towards the green protocol employing solid phase

synthesis using silica gel as a reaction medium but in this case also we found that under this condition, the work-up of the desired product needs more attention and rigorous techniques such as column chromatography to recover the final product (Table 4.A.1, entry 6).

Therefore, these limitations prompted us to investigate more suitable and environmentally friendly reaction condition for the synthesis of 3, 4-dihydropyrimidine-2-ones (4). As a part of the green chemical methodology, we were interested to carry out the above reaction under solvent free condition and encouragingly we encountered that the desired product formed with good yield and less reaction time (6-8 minutes) (Table 4.A.1, entry 7). The results of the model reaction for different mol% of the catalyst loading under optimized condition are listed in Table 4.A.2.

**Table 4.A.2.** Screening of the amount of the catalyst for the model reaction

Entry	Catalyst mol % <sup>a</sup>	Temperature ( <sup>o</sup> C)	Time (Minutes)	Yield <sup>b</sup> (%)
1	0	80	8	15
2	0.5	80	8	65
3	1.0	80	8	70
4	1.5	80	8	73
5	2.0	80	8	80
6	2.5	80	8	91
<b>7</b>	<b>3.0</b>	<b>80</b>	<b>8</b>	<b>97</b>
8	3.5	80	8	94
9	4.0	80	8	94

<sup>a</sup>The reaction was performed with Ethyl acetoacetate 1 (1 mmol) 2-nitrobenzaldehyde 2 (1 mmol), and Urea 3 (1 mmol) with the catalyst under solvent free condition. <sup>b</sup>Isolated Yields.

Interestingly, we observed that the reaction proceeds in much faster rate under solvent free condition in short reaction time (8 minutes) when the amount of catalyst loading is 3 mol% (Table 4.A.2, entry 7). A controlled reaction without catalyst leads to the formation of the product in negligible amount (Table 4.A.2, entry 1). Having recognized the optimal reaction condition, we subsequently examined the catalytic efficiency and applicability of this protocol by extending this protocol with differently substituted aldehydes (2) and keeping the component (1) and (3) fixed (Fig. tt). We examined that all the reactions proceeded well and smoothly in very short reaction time to afford the desired products, 3,4-

dihydropyrimidine-2-ones (4a-r) in good to excellent yields (90-98%) (Fig 4.A.3 and Table 4.A.3).

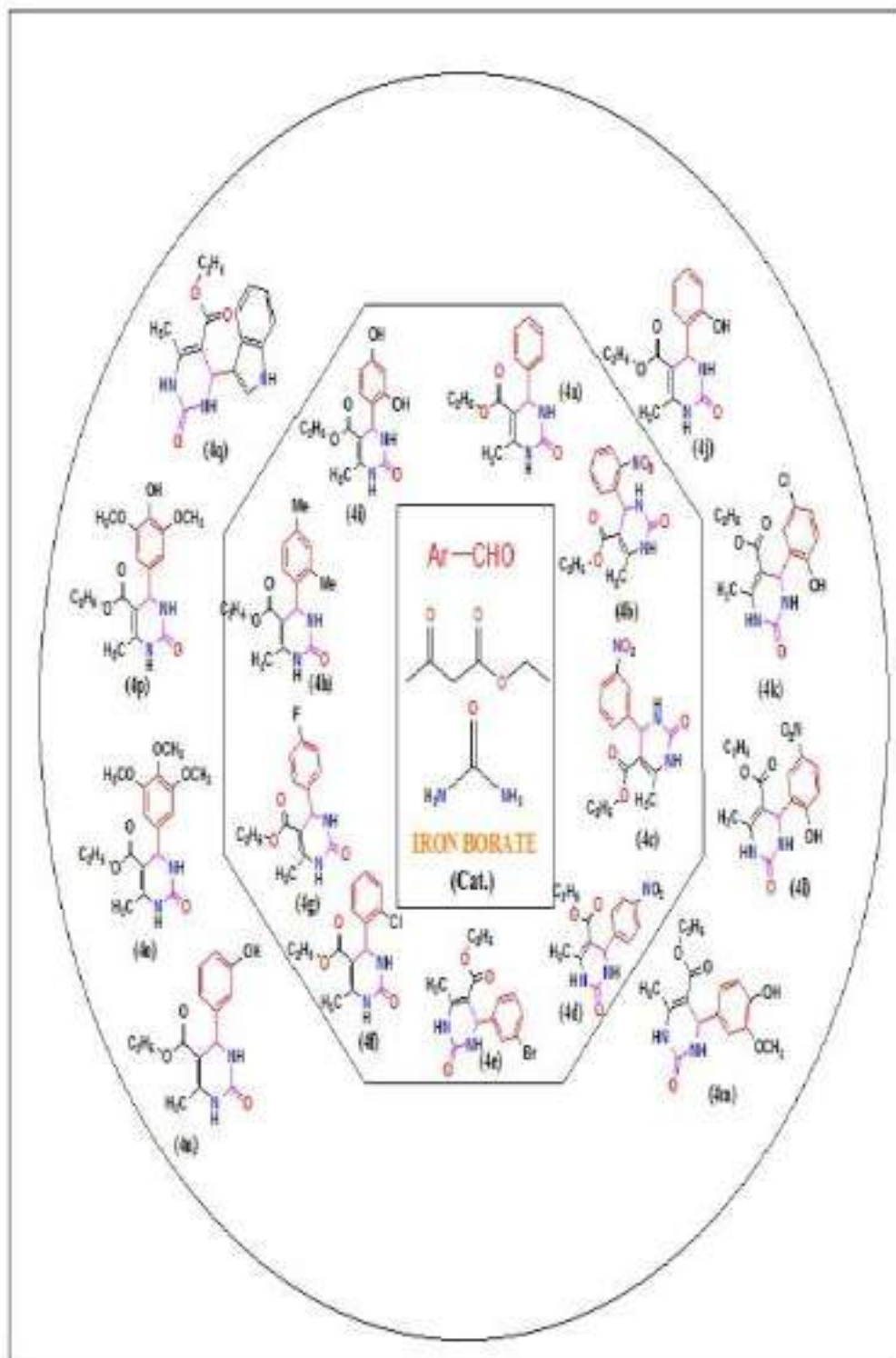


Fig. 4.A.3. Pictorial representation of the Biginelli products (4a-4q).



**Table. 4.A.3.** Iron Borate catalyzed solvent free neat synthesis of 3,4-dihydropyrimidine-2-one derivatives (4a-4q)

Entry	B-keto ester	Aldehyde substrate	Product	Yield <sup>b</sup> (%)
1	Ethylacetoacetate	Benzaldehyde	4a	97
2	Ethylacetoacetate	2-nitrobenzaldehyde	4b	98
3	Ethylacetoacetate	3-nitrobenzaldehyde	4c	97
4	Ethylacetoacetate	4-nitrobenzaldehyde	4d	96
5	Ethylacetoacetate	3-bromobenzaldehyde	4e	96
6	Ethylacetoacetate	2-chlorobenzaldehyde	4f	97
7	Ethylacetoacetate	4-fluorobenzaldehyde	4g	97
8	Ethylacetoacetate	2,4-dimethylbenzaldehyde	4h	93
9	Ethylacetoacetate	2,4-dihydroxybenzaldehyde	4i	92
10	Ethylacetoacetate	2-hydroxybenzaldehyde	4j	95
11	Ethylacetoacetate	5-chloro-2-hydroxybenzaldehyde	4k	96
12	Ethylacetoacetate	5-nitro-2-hydroxybenzaldehyde	4l	95
13	Ethylacetoacetate	4-hydroxy-3-methoxybenzaldehyde	4m	88
14	Ethylacetoacetate	3-hydroxybenzaldehyde	4n	90
15	Ethylacetoacetate	3,4,5-trimethoxybenzaldehyde	4o	88
16	Ethylacetoacetate	4-hydroxy-3, 5-dimethoxybenzaldehyde	4p	88
16	Ethylacetoacetate	Indole-3-carboxaldehyde	4q	90

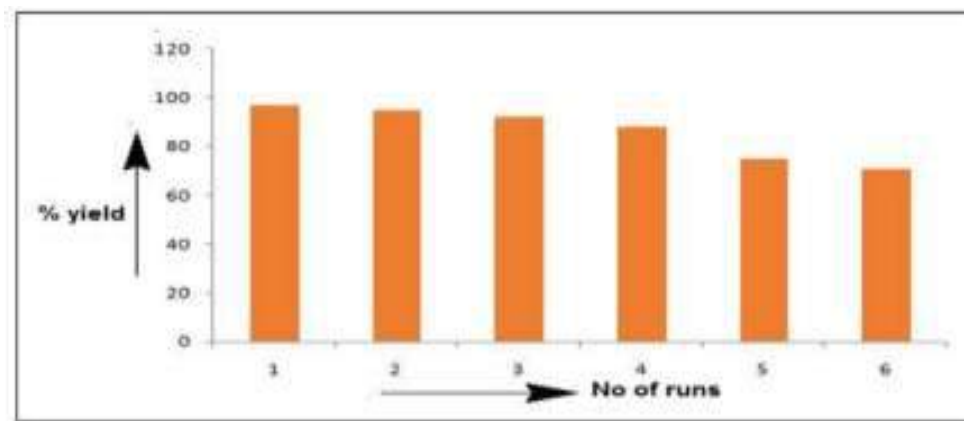
<sup>b</sup>Isolated yields

Moreover, it is interesting to note that para-substituted benzaldehyde with electron withdrawing group successfully afforded the corresponding product in excellent yield under optimized condition as compared to the electron releasing group present at the same position. Ortho and meta-substituted aldehydes also afforded the desired products in good yields but they required more time for reaction to complete.

We then compared the catalytic efficacy of the iron borate with different catalyst reported in the literature documented elsewhere and we found that iron borate has high catalytic efficiency and recyclability as compared to other catalyst and needs only few minutes for the completion of the reaction. Surprisingly, we could recover the catalyst after 4<sup>th</sup> run also and we observed that the catalyst lost its efficiency partially after 5<sup>th</sup> run of the reaction (Table 4.A.4).

**Table 4.A.4.** Study on the recyclability of the catalyst

Entry	No. of runs	Isolated yields (%)
1	1	97
2	2	95
3	3	92
4	4	88
5	5	75
6	6	71

**Fig. 4.A.4.** Recyclability of the catalyst

It was observed during the reaction that a variety of functional groups like acidic, nitro, methoxy, etc. remains un-affected during the reaction. Substituted benzaldehydes with either electron donating or electron withdrawing groups afforded good yield of the products, however it was also found that benzaldehyde with electron releasing groups gave a slight less yield of the products. We also compared the catalytic efficiency of Iron borate with other previously reported catalysts and found that Iron Borate has high catalytic efficiency and required less reaction time to go for completion Table 4.A.5.

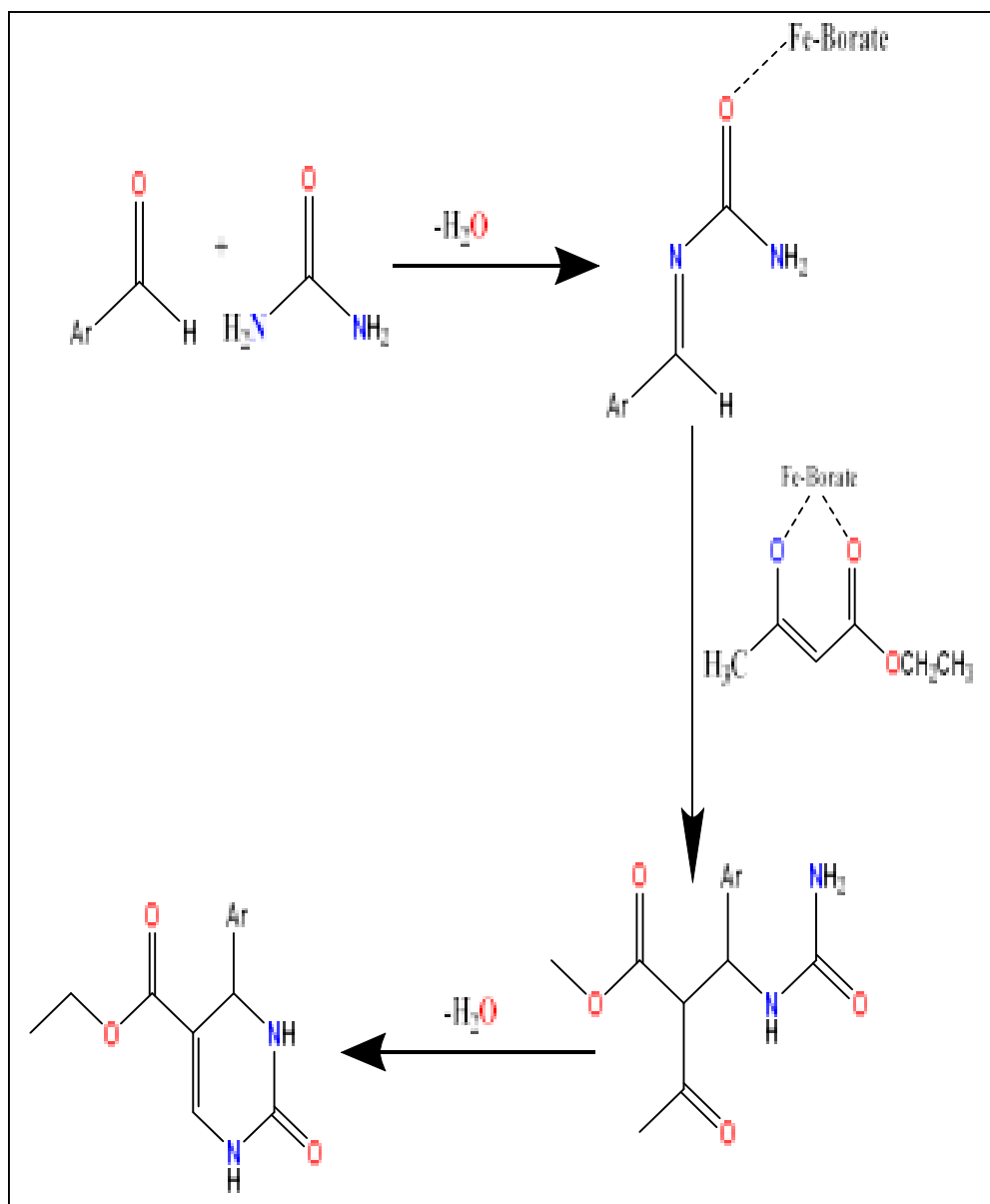
**Table. 4.A.5.** Comparison of Catalytic efficiency of Iron Borate with other reported catalysts for the synthesis of 3,4-dihydropyrimidine-2-one derivatives (4a-4q).

Entry	Catalyst	Solvent <sup>a</sup>	Temperature	Time	Yield (%) <sup>b</sup>
1	IL-OPPh <sub>2</sub>	Neat	100 °C	2.5 hours	91[lit <sup>41</sup> ]
2	TSIL	Water	Room Temperature	10 minutes	94[lit <sup>35</sup> ]
3	[Btto][p-TSA]	Neat	90 °C	30 minutes	96[lit <sup>42</sup> ]
4	L-Proline nitrate	MeCN	Room Temperature	50 minutes	92[lit <sup>43</sup> ]
5	Co-functionalised Na <sup>+</sup> montmocillonite	Neat	100 °C	10 minutes	92[lit <sup>44</sup> ]
6	BF <sub>3</sub> .OEt <sub>2</sub> /CuCl	THF	Reflux	18 hours	71[lit <sup>45</sup> ]
7	Cu(Otf) <sub>2</sub>	EtOH	M.W	1 hour	95[lit <sup>46</sup> ]
8	Chiral-phosphoric acid	DCM	25 °C	4 days	77[lit <sup>47</sup> ]
9	SnCl <sub>2</sub> -nano SiO <sub>2</sub>	EtOH	Reflux	40 minutes	92[lit <sup>48</sup> ]
10	CD-SO <sub>3</sub> H	Neat	80 °C	2 hours	89[lit <sup>49</sup> ]
11	Sulfated-Tungstate	Neat	80 °C	1 hour	92[lit <sup>50</sup> ]
12	IRMOF-3	Neat	Reflux	5 hours	89[lit <sup>51</sup> ]
13	CsF-Celite	Neat	80 °C	1 hour	95[lit <sup>52</sup> ]
14	Cuttlebone	Neat	90 °C	10 minutes	92[lit <sup>53</sup> ]
15	Co(NO <sub>3</sub> ) <sub>2</sub> .6H <sub>2</sub> O	Neat	80 °C	40 minutes	90[lit <sup>54</sup> ]
16	<b>Iron Borate</b>	<b>Neat</b>	<b>80 °C</b>	<b>8 minutes</b>	<b>97 [This work]</b>

<sup>a</sup>Comparison of catalytic efficiency of Iron Borate with other reported catalyst for the synthesis of 3,4-dihydropyrimidine-2-one derivatives using benzaldehyde, ethyl acetoacetate and Urea under different reaction conditions. <sup>b</sup>Isolated Yields.

## 4.A.3 Plausible Mechanism

The Biginelli reaction may proceed through acylimine intermediate (5) which is formed by the imine reaction between an aldehyde (2) and urea (3) catalyzed by iron borate. Further, addition of enolate of  $\beta$  keto-ester (1) to acylimine intermediate followed by dehydration and cyclization leads to the formation of corresponding dihydropyrimidinone derivative (4). A proposed mechanism for the synthesis of 3, 4-dihydropyrimidine-2-one catalyzed by Fe-borate is depicted below in Scheme 4.A.2.



**Scheme. 4.A.2.** Proposed mechanism for the synthesis of 3, 4-dihydropyrimidine-2-one catalyzed by Fe-borate

#### 4.A.4 Experimental Section

##### 4.A.4.1 Materials

All starting materials of high purity for the described synthesis were purchased commercially as received. The FT-IR spectra of the prepared compounds were recorded in Bruker Alpha III spectrophotometer operating in the wave number region 4000 to 400  $\text{cm}^{-1}$  in dry KBr. The melting points of the synthesized compounds were determined by open capillary method.  $^1\text{H-NMR}$  spectra of the synthesized 3,4-dihydropyrimidine-2-one derivatives (4a-4u) were recorded at room temperature on a FT-NMR (Bruker Advance-II 400 MHz) spectrometer by using  $\text{DMSO-d}_6$  as solvents and chemical shifts are quoted in ppm downfield of internal standard tetramethylsilane(TMS).

##### 4.A.4.2 General procedure for the synthesis of 3,4-dihydropyrimidine-2-ones:

In a typical procedure, a mixture of substituted benzaldehyde (1.0 mmol), ethylacetoacetate (1.0 mmol), urea (1.0 mmol) and Iron borate (3 mol %) thoroughly ground and mixed in a mortar and pestle to make a homogenous mixture. The mixture was then transferred to a test tube. The reaction was heated at  $80^\circ\text{C}$  for 8 minutes. The progress of the reaction was monitored by TLC using hexane/ethyl acetate (80:20) solvent. After completion of the reaction, the reaction mixture was dissolved in methanol and filtered. The filtrate was evaporated under vacuum and subsequently dried to afford desired product. All the synthesized compounds (4a-4q) were recrystallized from ethanol and have been characterized by their analytical (yield and melting point value) and spectroscopic data (FT-IR and  $^1\text{HNMR}$ ) and compared with the literature value.

##### 4.A.5. Conclusion

In this chapter, we described a simple, green and efficient procedure for the synthesis of 3,4- dihydropyrimidine-2-one derivatives using an unconventional Iron borate catalyst under solvent free condition. The reaction provides a method for the synthesis of a variety of 3, 4-dihydropyrimidine-2-ones with good to excellent yields and the catalyst has been versatile for a wide range of aromatic aldehydes.

#### 4.A.6. Analytical and Spectroscopic data

**4.A.6.1 Ethyl 1,2,3,4-tetrahydro-6-methyl-2-oxo-4-phenylpyrimidine-5-carboxylate (4a):** white solid, yield= 97 %, melting point found ( $^{\circ}\text{C}$ ) = 202-205, IR ( $\text{cm}^{-1}$ )  $\nu_{\text{max}}$ : IR ( $\text{cm}^{-1}$ )  $\nu_{\text{max}}$ : 3442, 3298, 3190, 2981, (N-H), 1685, 1651 (C=O),  $^1\text{H}$ NMR (400 MHz, DMSO  $d_6$ ):  $\delta_{\text{ppm}}$  = 9.36 (s, 1H, NH), 7.54 (s, 1H, NH), 7.31-7.43 (m, 3H, Ar-H), 5.66 (d, 1H), 3.46 (m, 2H,  $\text{CH}_2$ ), 2.50 (s, 3H,  $\text{CH}_3$ ), 1.07 (t, 3H,  $\text{CH}_3$ ).

**4.A.6.2 Ethyl 1,2,3,4-tetrahydro-6-methyl-4-(2-nitrophenyl)-2-oxopyrimidine-5-carboxylate (4b):** yellow powder, yield= 98 %, melting point found ( $^{\circ}\text{C}$ ) = 219-221, IR (KBr,  $\text{cm}^{-1}$ )  $\nu_{\text{max}}$ : 3443, 3369, 3235 (NH), 1685, 1636  $\text{cm}^{-1}$  (C=O),  $^1\text{H}$  NMR (400 MHz, DMSO- $d_6$ ):  $\delta_{\text{ppm}}$ = 9.92 (s, 1H, NH), 8.32 (s, 1H, NH), 7.51 (d, 1H, Ar-H), 7.23-7.27(m, 3H, Ar-H), 5.41 (s, 1H, CH), 4.51(q, 2H,  $\text{CH}_2$  of ethyl), 2.49(s, 3H,  $\text{CH}_3$ ), 1.31(t, 3H,  $\text{CH}_3$ ).

**4.A.6.3 Ethyl 1,2,3,4-tetrahydro-6-methyl-4-(3-nitrophenyl)-2-oxopyrimidine-5-carboxylate (4c):** yellow solid, yield= 97 %, melting point found ( $^{\circ}\text{C}$ ) = 226-229, IR ( $\text{cm}^{-1}$ )  $\nu_{\text{max}}$ : 3444, 3100, 2985 (NH), 1655, 1532 (C=O),  $^1\text{H}$ NMR (400 MHz, DMSO  $d_6$ ):  $\delta_{\text{ppm}}$  = 9.39 (s, 1H, NH), 8.38 (s, 1H, NH), 7.17-7.19 (m, 2H, Ar-H), 7.75-7.82 (m, 2H, Ar-H), 5.78 (s, 1H, CH), 4.25 (q, 2H,  $\text{CH}_2$ ), 2.84 (s, 3H,  $\text{CH}_3$ ), 1.18 (t, 3H,  $\text{CH}_3$ ).

**4.A.6.4 Ethyl 1,2,3,4-tetrahydro-6-methyl-4-(4-nitrophenyl)-2-oxopyrimidine-5-carboxylate (4d):** pale yellow solid, yield= 97 %, melting point found ( $^{\circ}\text{C}$ ) = 208-210, IR ( $\text{cm}^{-1}$ )  $\nu_{\text{max}}$ : 3455  $\text{cm}^{-1}$ , 2966  $\text{cm}^{-1}$  (N-H), 1659  $\text{cm}^{-1}$  (C=O),  $^1\text{H}$ NMR (400 MHz, DMSO  $d_6$ ):  $\delta_{\text{ppm}}$  = 9.29 (s, 1H, NH), 8.23 (d, 2H, Ar-H), 7.58 (d, 2H, Ar-H), 6.96 (s, 1H, Ar-H), 6.17(s, 1H, NH), 5.78 (d, 1H, CH), 3.38 (q, 2H,  $\text{CH}_2$ ), 2.50 (s, 3H,  $\text{CH}_3$ ), 1.08 (t, 3H,  $\text{CH}_3$ ).

**4.A.6.5 Ethyl 4-(3-bromophenyl)-1,2,3,4-tetrahydro-6-methyl-2-oxopyrimidine-5-carboxylate (4e):** White Crystals, yield= 96 %, melting point found ( $^{\circ}\text{C}$ ) = 189-191, , IR ( $\text{cm}^{-1}$ )  $\nu_{\text{max}}$ : 3448, 3240, 3112 (NH), 1672, 1621 (C=O),  $^1\text{H}$ NMR (400 MHz, DMSO  $d_6$ ):  $\delta_{\text{ppm}}$  = 9.98 (s, 1H, NH), 7.95 (s, 1H, NH), 7.30-7.73 (m, 4H, Ar-H), 5.43 (d, 1H, CH), 4.24 (q, 2H,  $\text{CH}_2$ ), 2.27 (s, 3H,  $\text{CH}_3$ ), 1.23 (t, 3H,  $\text{CH}_3$ ).

**4.A.6.6 Ethyl 4-(2-chlorophenyl)-1,2,3,4-tetrahydro-6-methyl-2-oxopyrimidine-5-carboxylate (4f):** White solid, yield= 97 %, melting point found ( $^{\circ}\text{C}$ ) = 221-225, IR ( $\text{cm}^{-1}$ )  $\nu_{\text{max}}$ : 3354  $\text{cm}^{-1}$ , 3235, 3111 (N-H), 1662, 1640  $\text{cm}^{-1}$  (C=O),  $^1\text{H}$ NMR (400 MHz, DMSO  $d_6$ ):  $\delta_{\text{ppm}}$  = 9.32 (s, 1H, NH), 7.70(s, 1H, NH), 7.21-7.40(m, 4H, Ar-H), 5.59 (s, 1H, C-H), 4.11 (q, 2H,  $\text{CH}_2$ ), 2.28 (s, 3H,  $\text{CH}_3$ ), 1.08(t, 3H,  $\text{CH}_3$ ).

**4.A.6.7 Ethyl 4-(4-fluorophenyl)-1,2,3,4-tetrahydro-6-methyl-2-oxopyrimidine-5-carboxylate (4g):** White Crystals, yield= 97 %, melting point found ( $^{\circ}\text{C}$ ) = 208-212, IR ( $\text{cm}^{-1}$ )  $\nu_{\text{max}}$ : 3326, 3200 ( $\text{N-H}$ ), 1695, 1625 ( $\text{C=O}$ ),  $^1\text{H}$  NMR (400 MHz, DMSO- $d_6$ ):  $\delta_{\text{ppm}}$ = 9.32(s, 1H, NH), 7.62(s, 1H, NH), 7.21-7.42(m, 4H, Ar-H), 5.22 (s, 1H, C-H), 3.85 (q, 2H,  $\text{CH}_2$  of ethyl), 2.24 (s, 3H,  $\text{CH}_3$ ), 1.12(t, 3H,  $\text{CH}_3$ ).

**4.A.6.8. Ethyl 1,2,3,4-tetrahydro-6-methyl-4-(2,4-dimethylphenyl)-2-oxopyrimidine-5-carboxylate (4h):** White Crystals, yield= 93 %, melting point found ( $^{\circ}\text{C}$ ) = 199-202, IR ( $\text{cm}^{-1}$ )  $\nu_{\text{max}}$ : 3234, 3313, 3171, 2933 ( $\text{N-H}$ ), 1700, 1648 ( $\text{C=O}$ ),  $^1\text{H}$  NMR (400 MHz, DMSO- $d_6$ ):  $\delta_{\text{ppm}}$ = 9.24 (s, 1H, NH), 7.58 (s, 1H, NH), 6.68-6.78(m, 3H, Ar-H), 5.18 (s, 1H, C-H), 4.08(q, 2H,  $\text{CH}_2$ ), 2.38(s, 3H,  $\text{CH}_3$ ), 1.05(t, 3H,  $\text{CH}_3$ ).

**4.A.6.9 Ethyl 1,2,3,4-tetrahydro-4-(2,4-dihydroxyphenyl)-6-methyl-2-oxopyrimidine-5-carboxylate (4i):** Pale brown Crystals, yield= 92 %, IR ( $\text{cm}^{-1}$ )  $\nu_{\text{max}}$ : 3449, 3234 ( $\text{N-H}$ ), 1664, 1626 ( $\text{C=O}$ ),  $^1\text{H}$ NMR (400 MHz, DMSO- $d_6$ ):  $\delta_{\text{ppm}}$  = 12.97(s, 1H, OH), 11.79(s, 1H, OH), 10.18(s, 1H, NH), 8.51(s, 1H, NH), 6.79-7.18(m, 3H, Ar-H), 5.42 (d, 1H, C-H), 4.02(q, 2H,  $\text{CH}_2$ ), 2.49 (s, 3H,  $\text{CH}_3$ ), 1.25(t, 3H,  $\text{CH}_3$ ).

**4. A.6.10 Ethyl 1,2,3,4-tetrahydro-4-(2-hydroxyphenyl)-6-methyl-2-oxopyrimidine-5-carboxylate (4j):** White solid, yield= 93 %, melting point found ( $^{\circ}\text{C}$ ) = 203-206, IR (KBr,  $\text{cm}^{-1}$ )  $\nu_{\text{max}}$ : 3348 ( $\text{O-H}$ ), 3244, 3082 ( $\text{N-H}$ ), 1686, 1638 ( $\text{C=O}$ ),  $^1\text{H}$ NMR (400 MHz, DMSO- $d_6$ ):  $\delta_{\text{ppm}}$ = 13.34(s, 1H, OH), 8.94(s, 1H, NH), 8.93(s, 1H, NH), 6.84-7.38 (m, 3H, Ar-H), 6.82 (s, 1H, C-H), 3.38 (q, 2H,  $\text{CH}_2$ ), 2.55(s, 3H,  $\text{CH}_3$ ), 1.913(t, 3H,  $\text{CH}_3$ ).

**4.A.6.11 Ethyl 4-(5-chloro-2-hydroxyphenyl)-1,2,3,4-tetrahydro-6-methyl-2-oxopyrimidine-5-carboxylate (4k):** Dirty white solid, melting point found ( $^{\circ}\text{C}$ ) = 208-211, IR (KBr,  $\text{cm}^{-1}$ )  $\nu_{\text{max}}$ : 3443 (OH), 3298, 2955 (NH), 1666, 1625 ( $\text{C=O}$ ),  $^1\text{H}$ NMR (400 MHz, DMSO- $d_6$ ):  $\delta_{\text{ppm}}$  = 9.36 (s, 1H, OH), 7.54(s, 1H, NH), 7.52(s, 1H, NH), 7.30-7.43(m, 3H, Ar-H), 5.48 (d, 1H, C-H), 3.45 (q, 2H,  $\text{CH}_2$ ), 2.45(s, 3H,  $\text{CH}_3$ ), 1.29(t, 3H,  $\text{CH}_3$ ).

**4. A.6.12 Ethyl 1,2,3,4-tetrahydro-4-(2-hydroxy-5-nitrophenyl)-6-methyl-2-oxopyrimidine-5-carboxylate (5l):** yellow solid, IR (KBr,  $\text{cm}^{-1}$ )  $\nu_{\text{max}}$ : 3442 (OH), 3125, 2954, 2924 (NH), 1731, 1681 ( $\text{C=O}$ ),  $^1\text{H}$ NMR (400 MHz, DMSO- $d_6$ ):  $\delta_{\text{ppm}}$  = 9.91(s, 1H, OH), 8.53(s, 1H, NH), 8.40(s, 1H, NH), 7.48-7.82(m, 2H, Ar-H), 6.91-6.89 (d, 1H, Ar-H), 5.43(d, 1H, CH), 3.40(m, 2H,  $\text{CH}_2$ ), 2.25(s, 3H,  $\text{CH}_3$ ), 2.51(t, 3H,  $\text{CH}_3$ ).

**4. A.6.13 Ethyl 1,2,3,4-tetrahydro-4-(4-hydroxy-3-methoxyphenyl)-6-methyl-2-oxopyrimidine-5-carboxylate (4m):** yellow solid, IR (KBr,  $\text{cm}^{-1}$ )  $\nu_{\text{max}}$ : 3425 (OH), 3348 3125, 2974, 2924 (NH), 1731, 1681 ( $\text{C=O}$ ),  $^1\text{H}$ NMR (400 MHz, DMSO- $d_6$ ):  $\delta$ = 9.12(s, 1H, OH), 8.51(s, 1H, NH), 7.63(s, 1H, NH), 6.51-6.79(m,

3H, Ar-H), 5.42(d, 1H, CH), 4.00 (s, 3H, OCH<sub>3</sub>), 3.72(m, 2H, CH<sub>2</sub>), 2.47(s, 3H, CH<sub>3</sub>), 1.16(t, 3H, CH<sub>3</sub>).

**4.A.6.14 Ethyl 1,2,3,4-tetrahydro-4-(3-hydroxyphenyl)-6-methyl-2-oxopyrimidine-5-carboxylate (4n):** Dirty white powder, yield= 88 %, melting point found (°C) = 258-261. IR (KBr, cm<sup>-1</sup>) v<sub>max</sub>:3443 (O-H), 3244, 3110, 2950(N-H), 1647, 1578(C=O), <sup>1</sup>HNMR (400 MHz, DMSO-d<sub>6</sub>): δppm= 9.97(s, 1H, OH), 9.35(s, 1H, NH),7.66(s, 1H, NH), 6.50-6.74(m, 3H, Ar-H), 5.62(s, 1H, -C-H), 3.37 (q, 2H, CH<sub>2</sub>), 2.22(s, 3H, CH<sub>3</sub>), 1.10 (t, 3H, CH<sub>3</sub>).

**4.A.6.15 Ethyl 1,2,3,4-tetrahydro-4-(3,4,5-trimethoxyphenyl)-6-methyl-2-oxopyrimidine-5-carboxylate (4o):** White solid , yield= 88 %, melting point found (°C) =202-206, IR (KBr, cm<sup>-1</sup>) v<sub>max</sub>: 3443 (O-H), 3364, 3302, 2971(N-H), 1660, 1595(C=O), <sup>1</sup>HNMR (400 MHz, DMSO-d<sub>6</sub>): δppm= 9.80(s, 1H, OH), 9.20(s, 1H, NH),7.25(s, 1H, NH), 6.87(s, 1H, Ar-H), 6.64 (s, 1H, Ar-H), 5.40(s, 1H, C-H), 3.85(q, 2H, CH<sub>2</sub>), 3.71(s, 3H, O-CH<sub>3</sub>),3.67(s, 3H, O-CH<sub>3</sub>), 3.62(s, 3H, O-CH<sub>3</sub>), 3.37(s, 3H, CH<sub>3</sub>), 1.27 (t, 3H, CH<sub>3</sub>).

**4.A.6.16 Ethyl 1,2,3,4-tetrahydro-4-(4-hydroxy-3,5-dimethoxyphenyl)-6-methyl-2-oxopyrimidine-5-carboxylate (4p):** Dirty white solid, yield=88 %, IR (KBr, cm<sup>-1</sup>) v<sub>max</sub>: 3433 (O-H), 3302, 2970, 2926(N-H), 1665, 1627 (C=O), <sup>1</sup>HNMR (400 MHz, DMSO-d<sub>6</sub>): δppm= 11.40 (s, 1H, OH), 9.77(s, 1H, NH), 8.31(s, 1H, NH), 7.20(s, 1H, Ar-H), 6.92 (s, 1H, Ar-H), 5.39(s, 1H, C-H), 3.88 (s, 6H, OCH<sub>3</sub>), 3.31(q, 2H, CH<sub>2</sub>), 2.49(s, 3H, CH<sub>3</sub>), 1.21 (t, 3H, CH<sub>3</sub>).

**4.A.6.17 Ethyl 1,2,3,4-tetrahydro-4-(1H-indol-3-yl)-6-methyl-2-oxopyrimidine-5-carboxylate (4q):** brown solid, IR (KBr, cm<sup>-1</sup>) v<sub>max</sub>: 3445, 2932 (N-H), 1662, 1632 (C=O), <sup>1</sup>HNMR (400 MHz, DMSO-d<sub>6</sub>): δppm= 12.14 (s, 1H, NH indole), 9.92(s, 1H, NH), 8.32(s, 1H, NH), 8.27 (m, 1H Ar-H indole), 7.18-7.51(m, 4H, Ar-H), 5.41(s, 1H, C-H), 3.33(q, 2H, CH<sub>2</sub>), 2.49(s, 3H, CH<sub>3</sub>), 1.81 (t, 3H, CH<sub>3</sub>).



## 4.A.7 Supporting spectra:

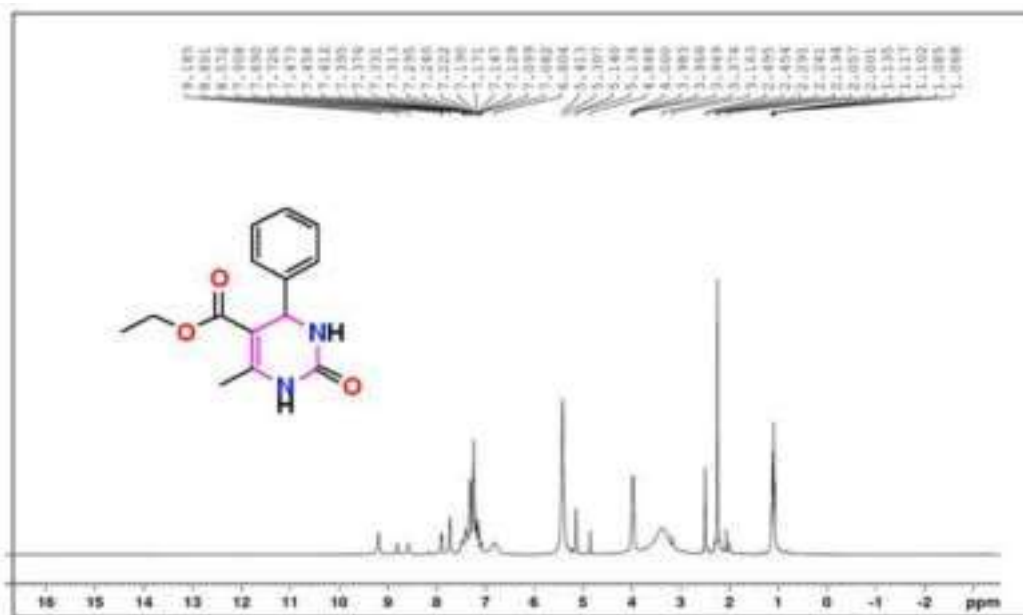


**Fig. 4.A.7.1.** <sup>1</sup>H NMR spectra of Ethyl 1,2,3,4-tetrahydro-6-methyl-2-oxo-4-phenylpyrimidine-5-carboxylate (4a)

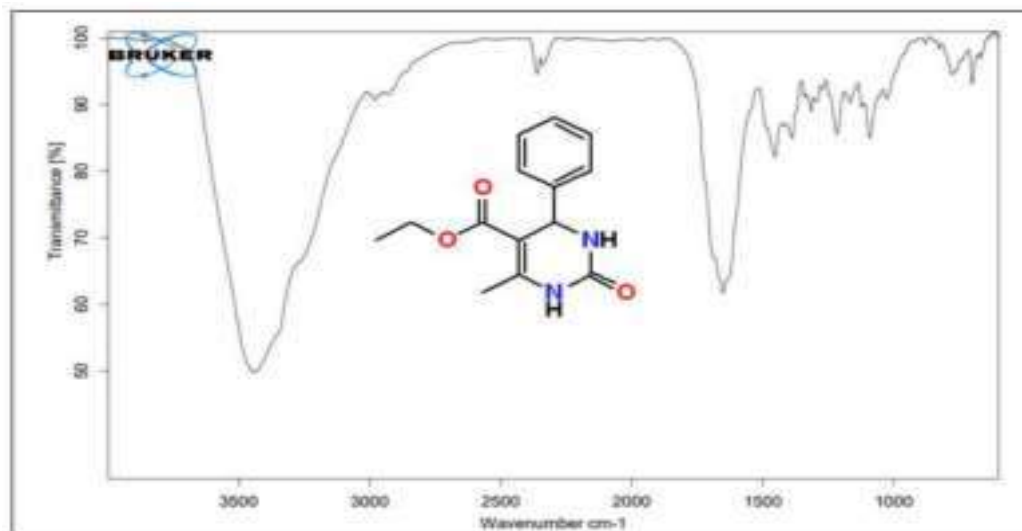


**Fig. 4.A.7.2.** FT-IR spectra of Ethyl 1,2,3,4-tetrahydro-6-methyl-2-oxo-4-phenylpyrimidine-5-carboxylate (4a)

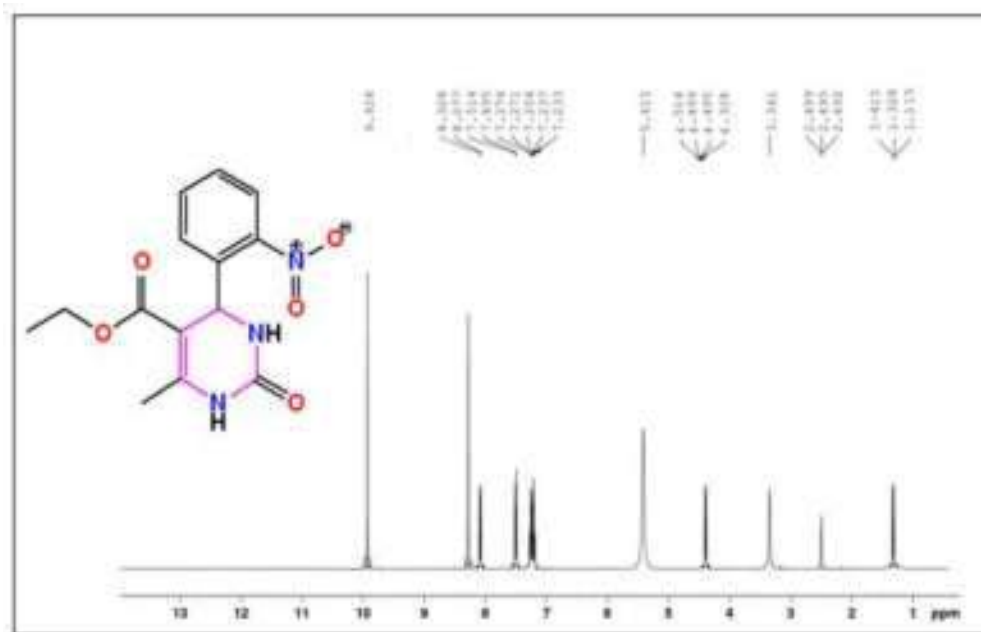


**Fig. 4.A.7.3.** <sup>1</sup>H NMR spectra of Ethyl 1,2,3,4-tetrahydro-6-methyl-4-(2-nitrophenyl)-2-oxopyrimidine-5-carboxylate (4b)

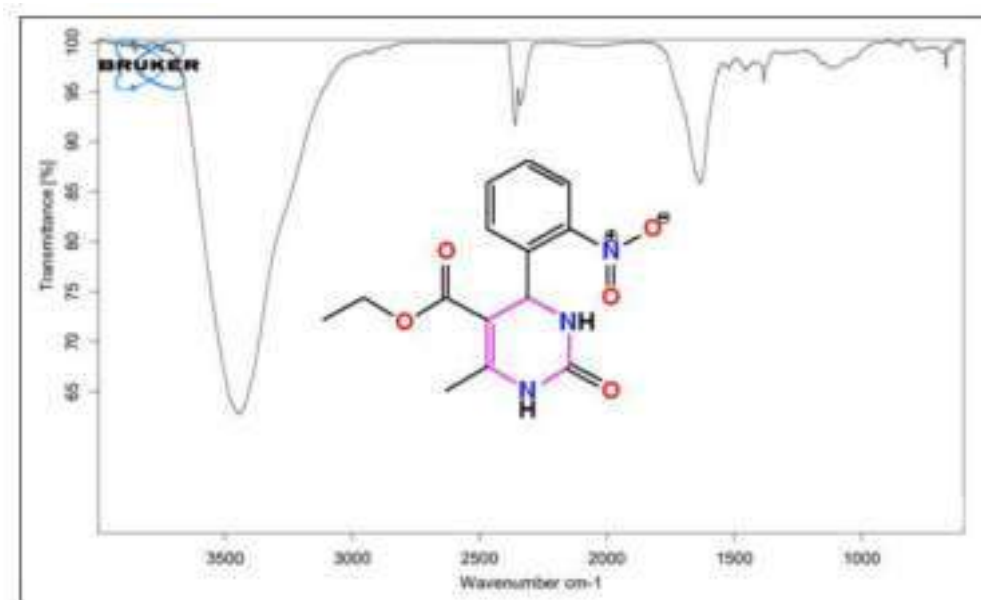


**Fig. 4.A.7.4.** FT-IR spectra of Ethyl 1,2,3,4-tetrahydro-6-methyl-4-(2-nitrophenyl)-2-oxopyrimidine-5-carboxylate (4b)

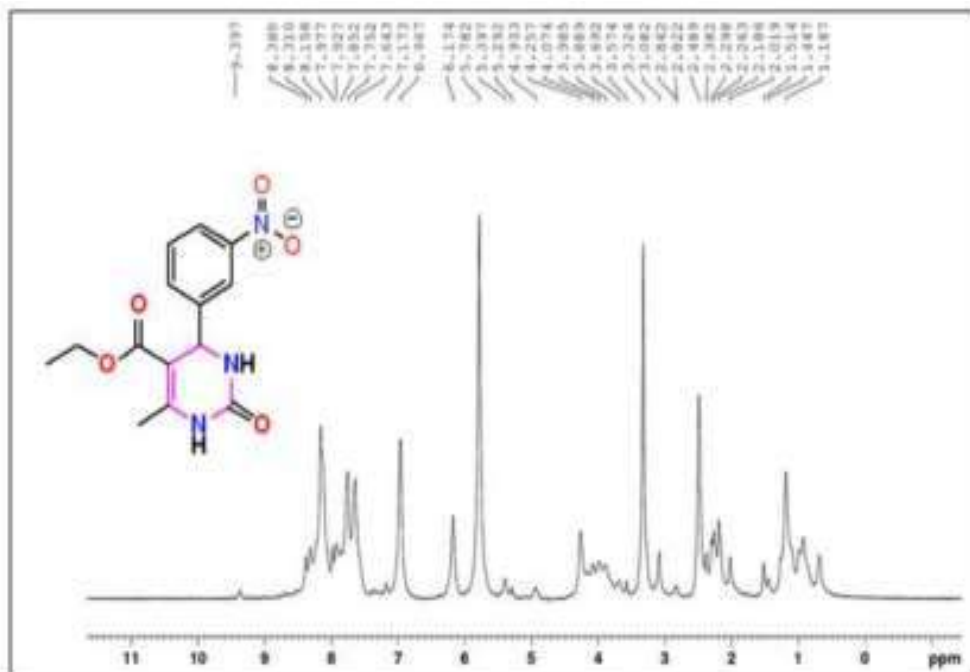


Fig. 4.A.7.5.  $^1\text{H}$  NMR spectra of Ethyl 1,2,3,4-tetrahydro-6-methyl-4-(3-nitrophenyl)-2-oxopyrimidine-5-carboxylate (4c).

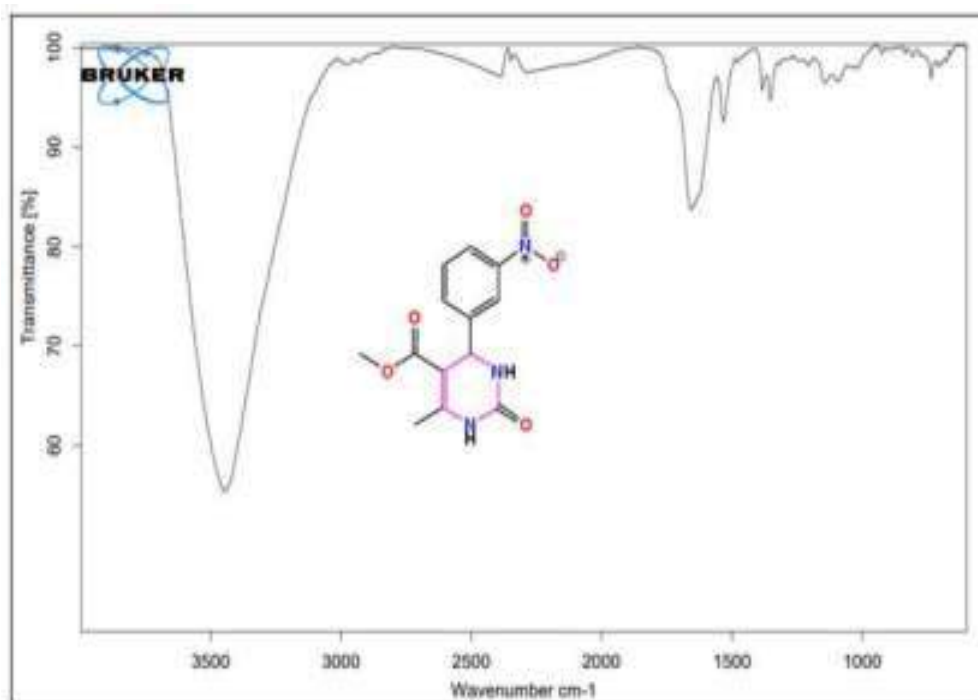
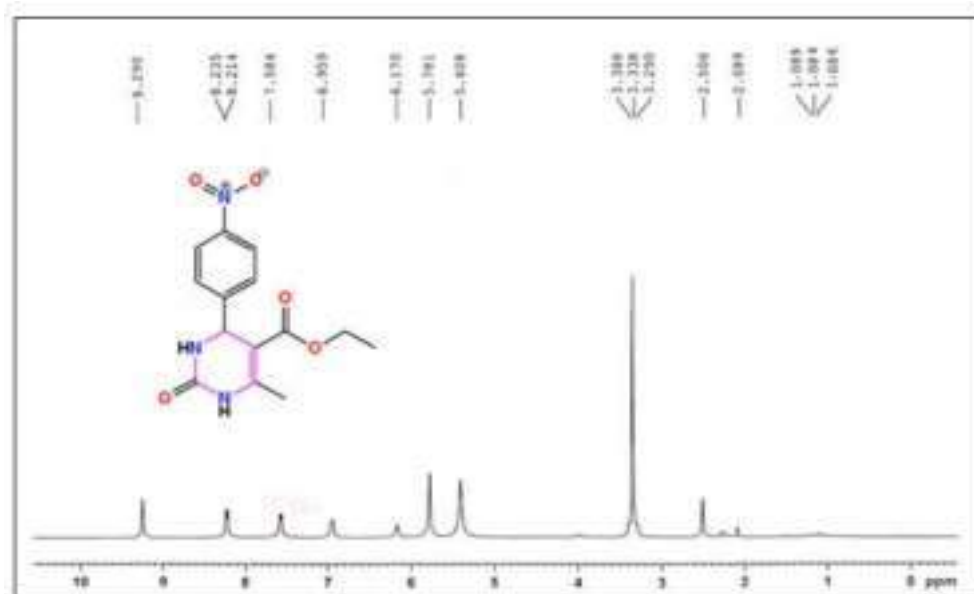
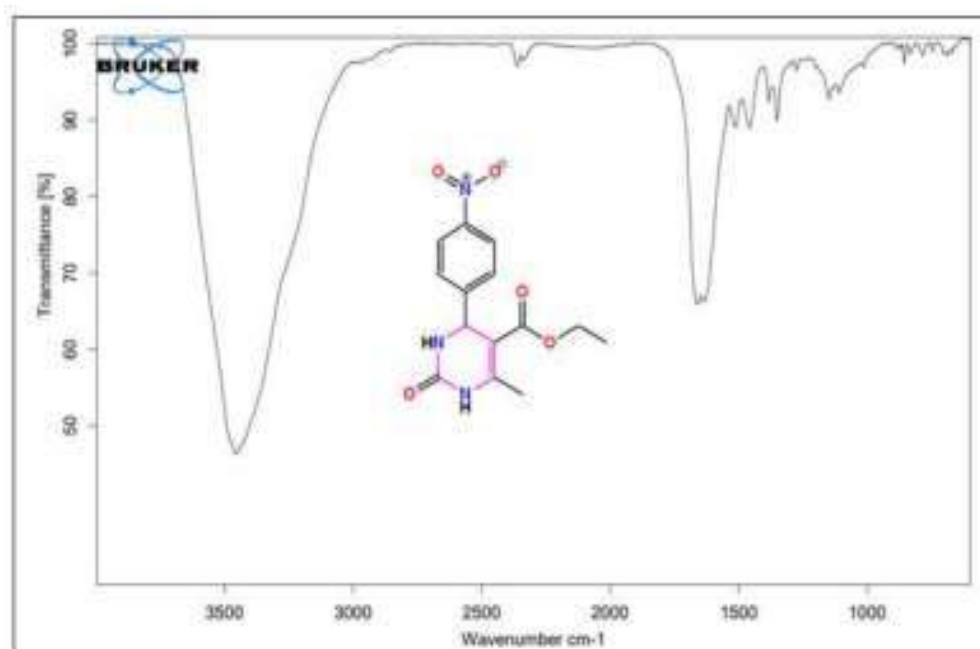


Fig. 4.A.7.6. FT-IR spectra of Ethyl 1,2,3,4-tetrahydro-6-methyl-4-(3-nitrophenyl)-2-oxopyrimidine-5-carboxylate (4c)



**Fig. 4.A.7.7.** <sup>1</sup>H NMR spectra of Ethyl 1,2,3,4-tetrahydro-6-methyl-4-(4-nitrophenyl)-2-oxopyrimidine-5-carboxylate (4d).



**Fig. 4.A.7.8.** FT-IR spectra of Ethyl 1,2,3,4-tetrahydro-6-methyl-4-(4-nitrophenyl)-2-oxopyrimidine-5-carboxylate (4d)

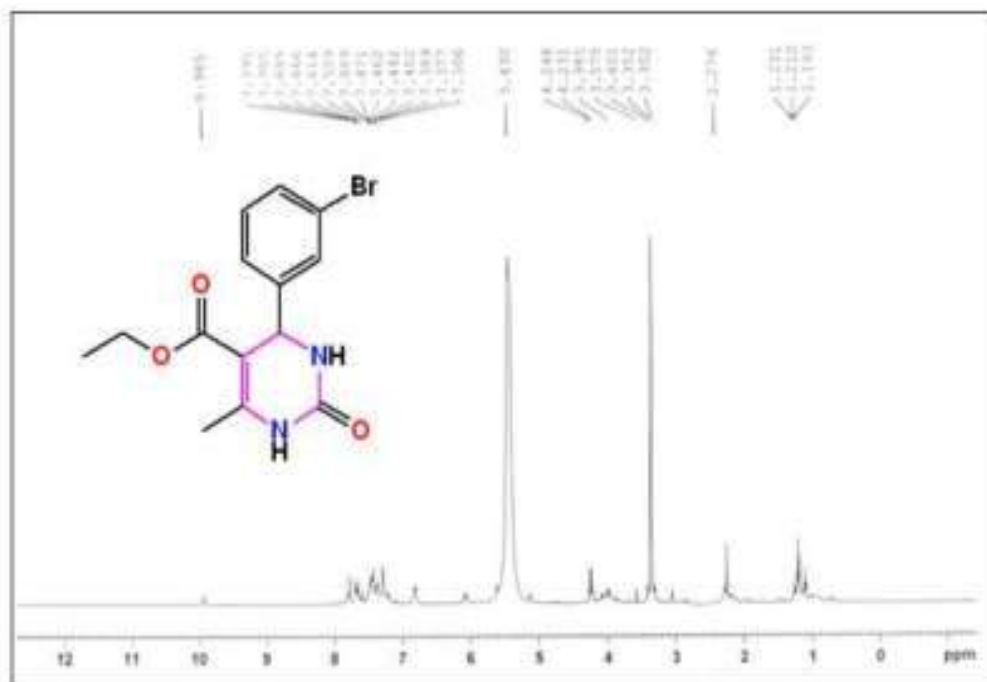


**Fig.4. A.7.9.**  $^1\text{H}$  NMR spectra of Ethyl 4-(3-bromophenyl)-1,2,3,4-tetrahydro-6-methyl-2-oxypyrimidine-5-carboxylate (4e).

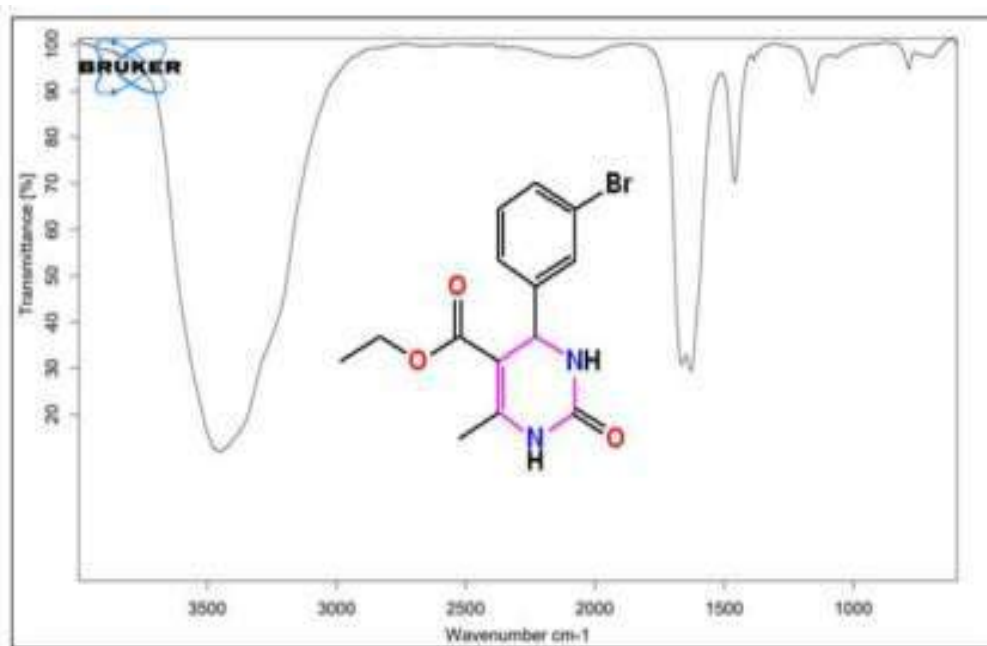


**Fig. 4.A.7.10.** FT-IR spectra of Ethyl 4-(3-bromophenyl)-1,2,3,4-tetrahydro-6-methyl-2-oxypyrimidine-5-carboxylate (4e).

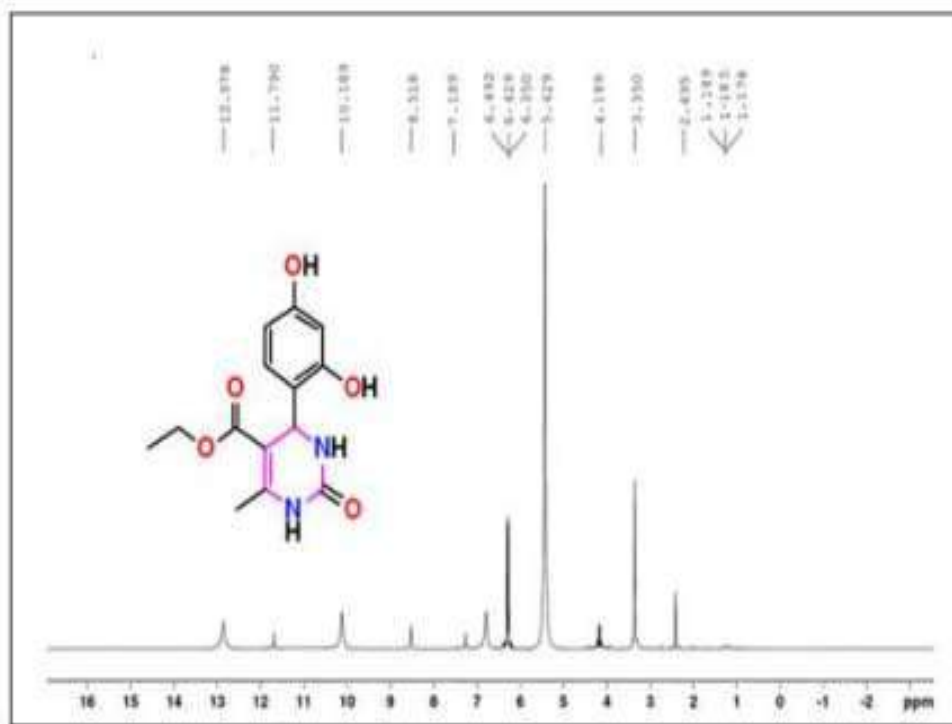


Fig. 4.A.7.11. <sup>1</sup>H NMR spectra of Ethyl 1,2,3,4-tetrahydro-4-(2,4-dihydroxyphenyl)-6-methyl-2-oxopyrimidine-5-carboxylate (4i).

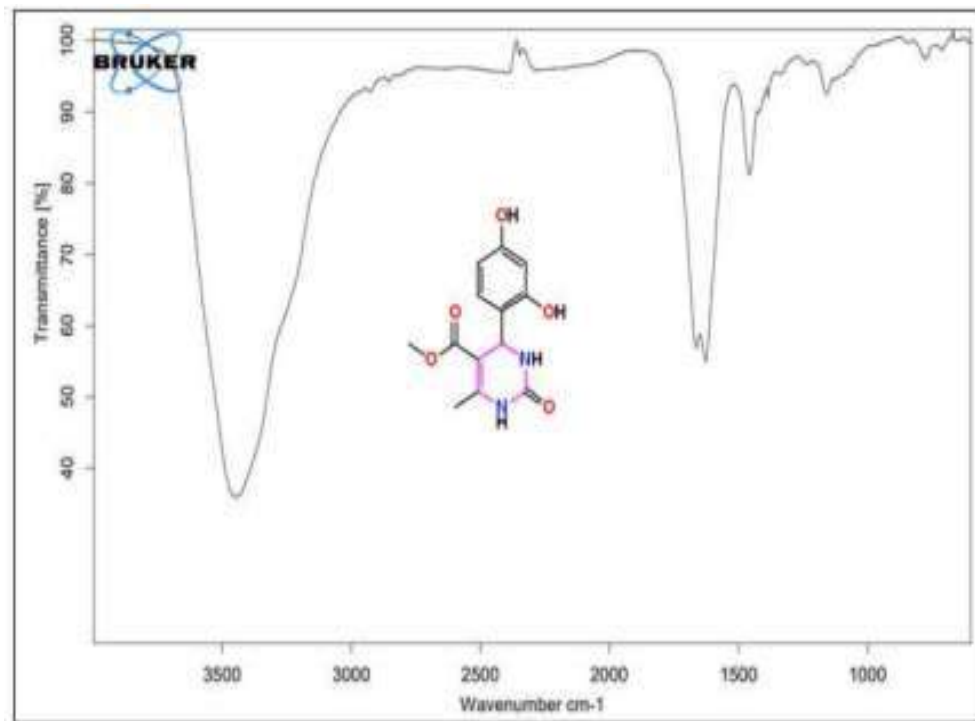


Fig. 4.A.7.12. FT-IR spectra of Ethyl 1,2,3,4-tetrahydro-4-(2,4-dihydroxyphenyl)-6-methyl-2-oxopyrimidine-5-carboxylate (4i).

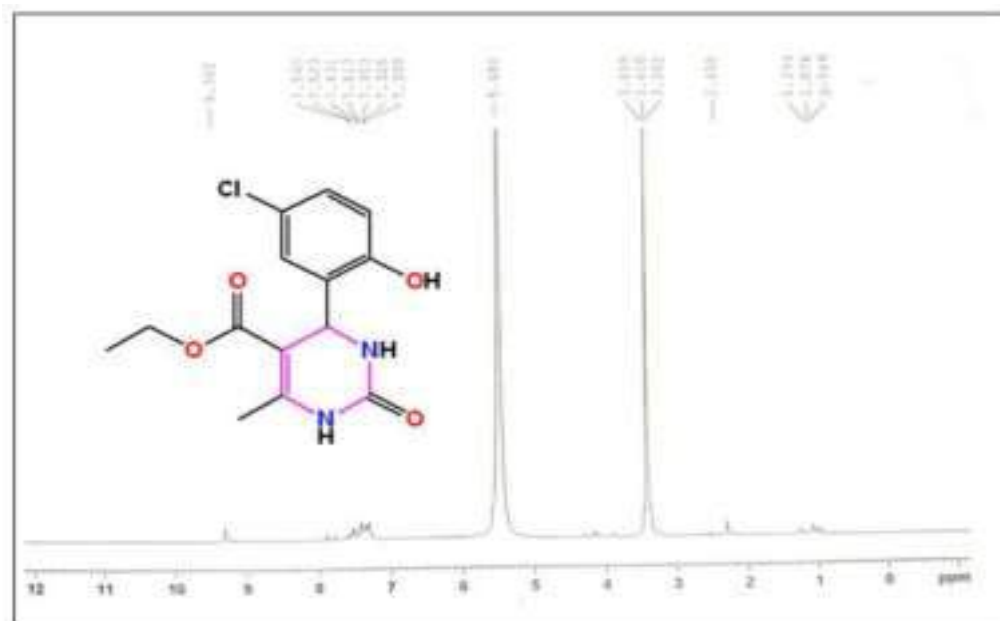


Fig. 4.A.7.13. <sup>1</sup>H NMR spectra of Ethyl 4-(5-chloro-2-hydroxyphenyl)-1,2,3,4-tetrahydro-6-methyl-2-oxypyrimidine-5-carboxylate (4k).

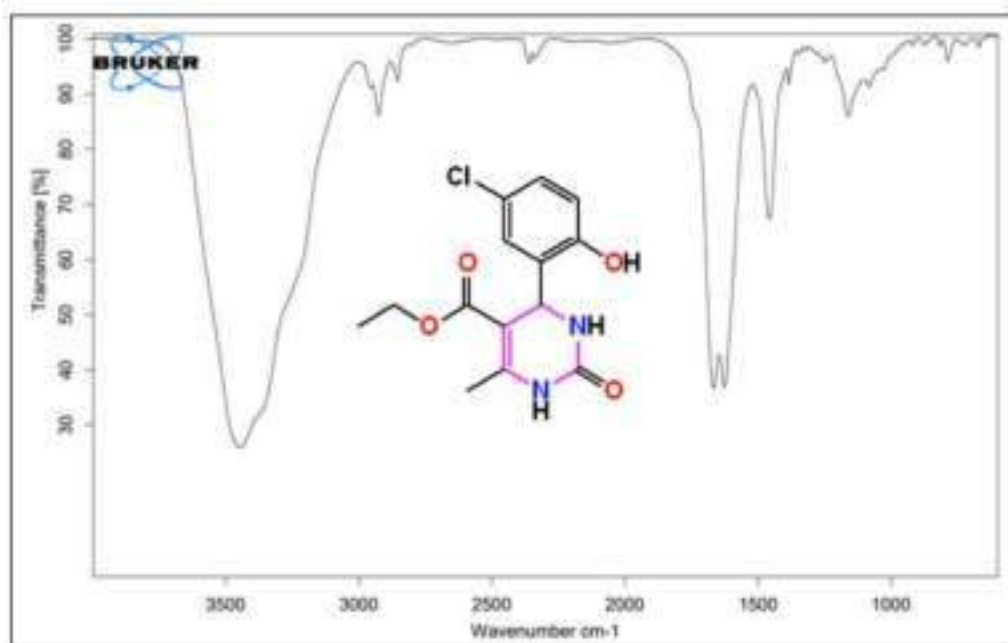
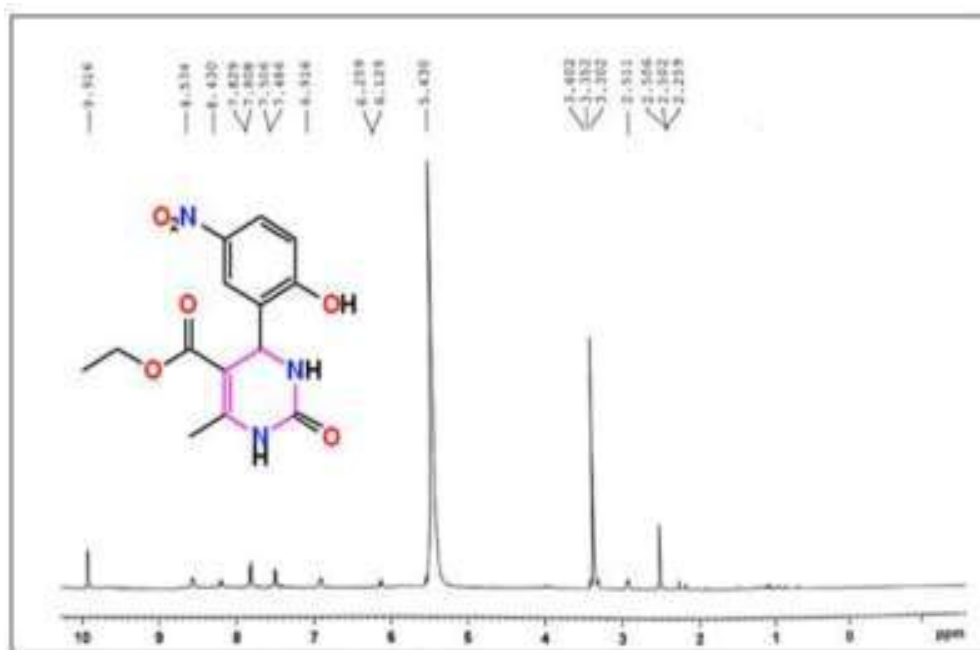
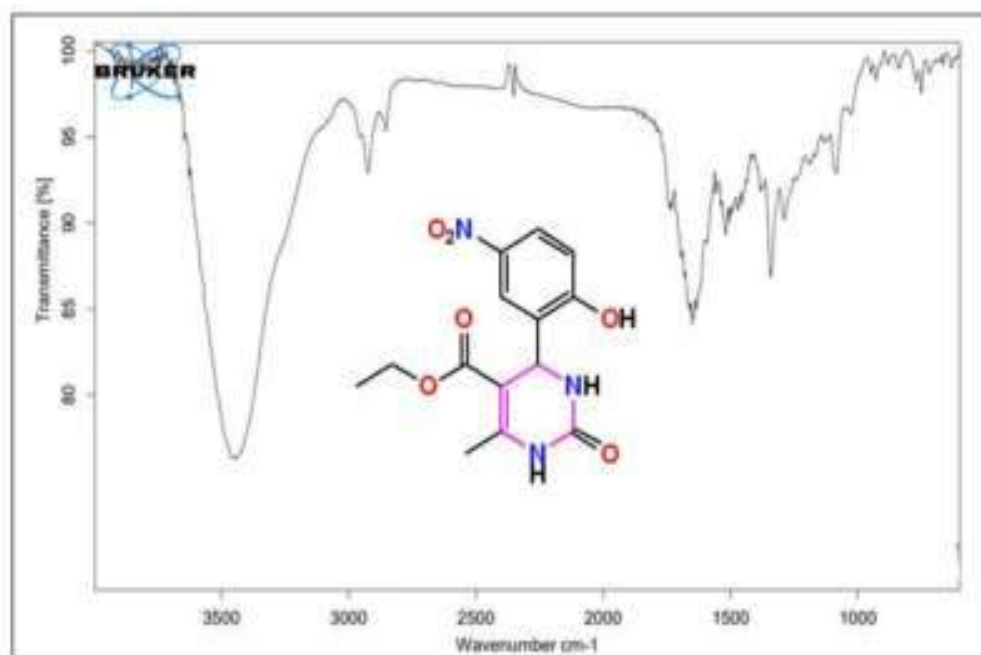


Fig. 4.A.7.14. FT-IR spectra of Ethyl 4-(5-chloro-2-hydroxyphenyl)-1,2,3,4-tetrahydro-6-methyl-2-oxypyrimidine-5-carboxylate (4k).



**Fig. 4.A.7.15.** <sup>1</sup>H NMR spectra of Ethyl 1,2,3,4-tetrahydro-4-(2-hydroxy-5-nitrophenyl)-6-methyl-2-oxopyrimidine-5-carboxylate (4l).



**Fig. 4.A.7.16.** FT-IR spectra of Ethyl 1,2,3,4-tetrahydro-4-(2-hydroxy-5-nitrophenyl)-6-methyl-2-oxopyrimidine-5-carboxylate (4l).



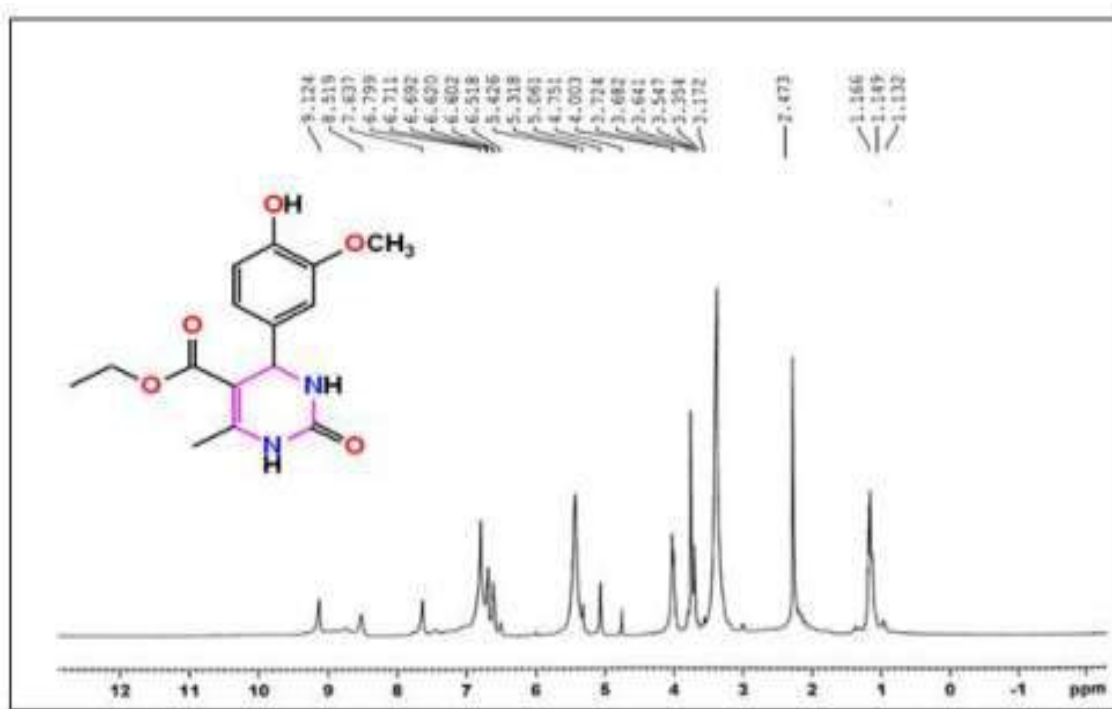


Fig. 4.A.7.17.  $^1\text{H}$  NMR spectra of Ethyl 1,2,3,4-tetrahydro-4-(4-hydroxy-3-methoxyphenyl)-6-methyl-2-oxopyrimidine-5-carboxylate (4m).

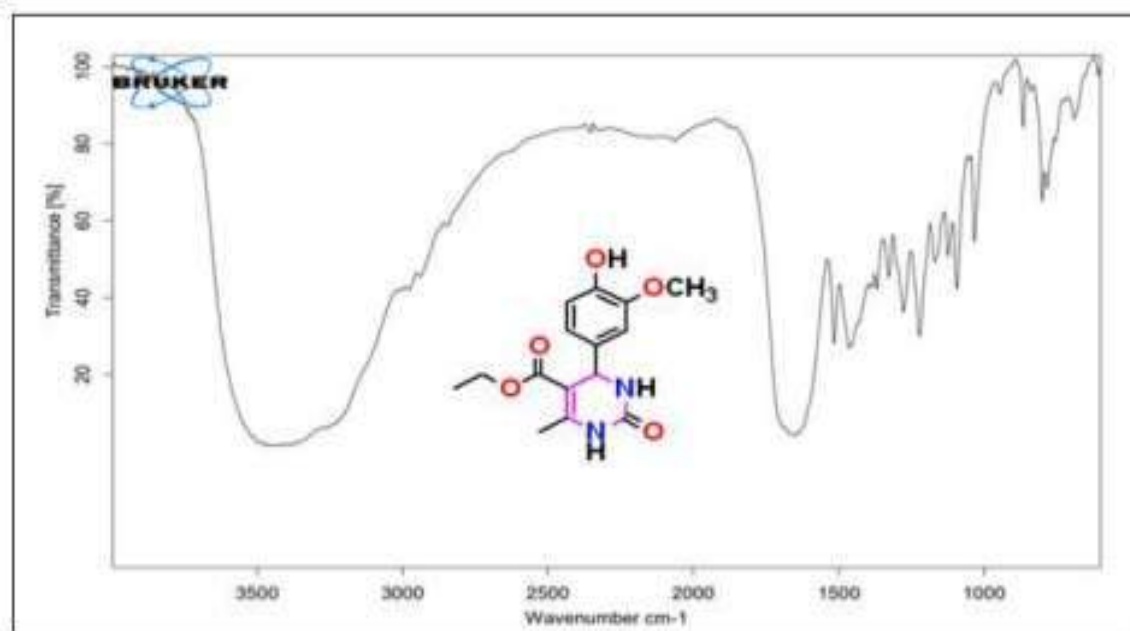
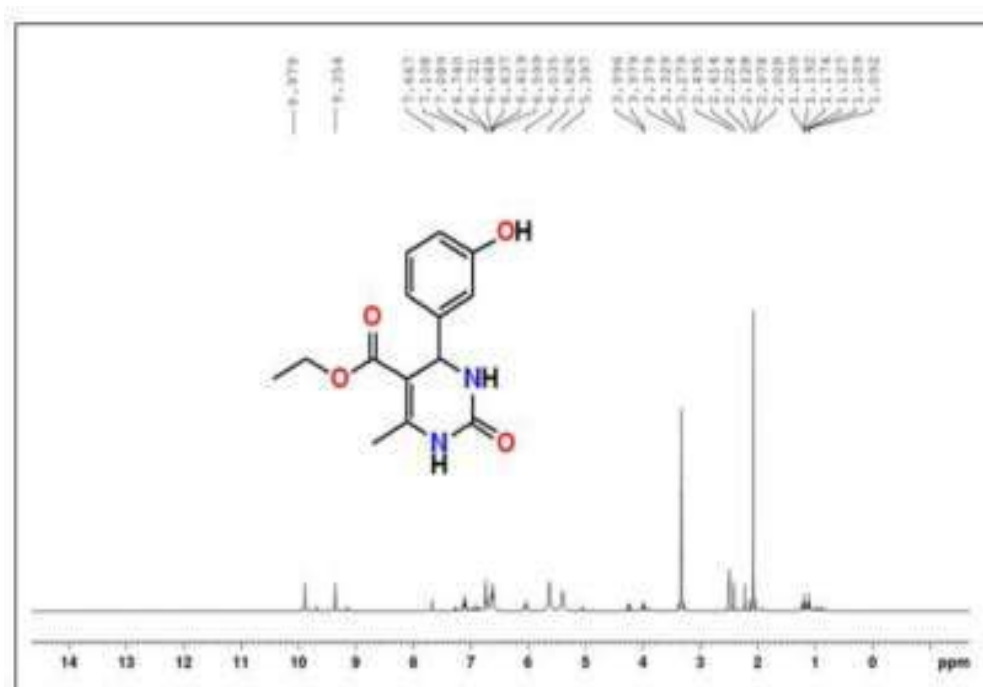
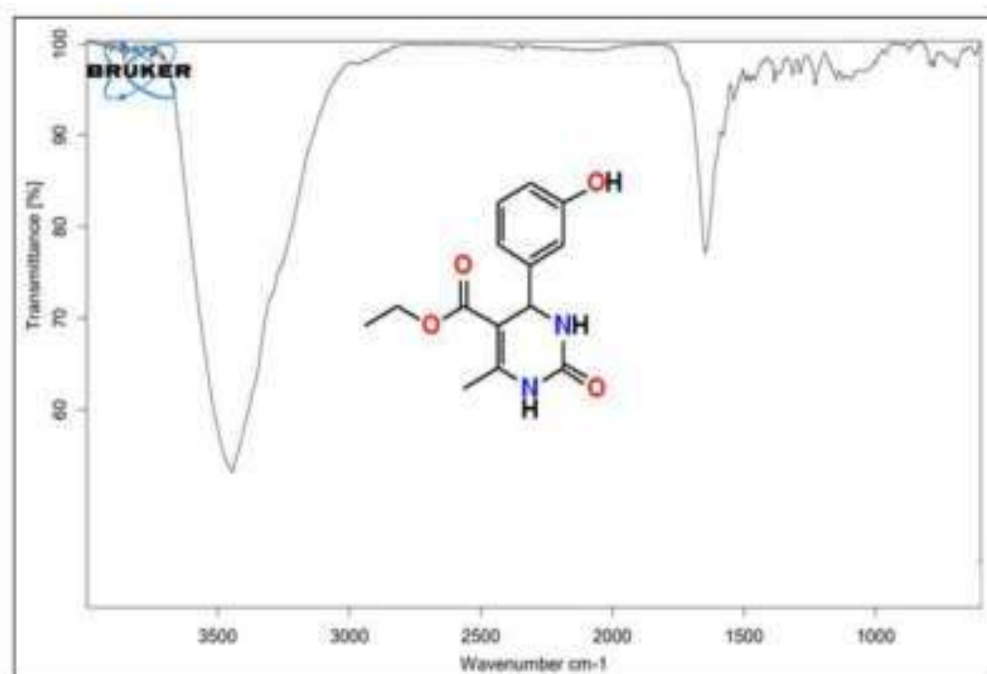


Fig. 4.A.7.18. FT-IR spectra of Ethyl 1,2,3,4-tetrahydro-4-(4-hydroxy-3-methoxyphenyl)-6-methyl-2-oxopyrimidine-5-carboxylate (4m).



**Fig. 4.A.7.19.**  $^1\text{H}$  NMR spectra of Ethyl 1,2,3,4-tetrahydro-4-(3-hydroxyphenyl)-6-methyl-2-oxopyrimidine-5-carboxylate (4n)



**Fig. 4.A.7.20.** FT-IR spectra of Ethyl 1,2,3,4-tetrahydro-4-(3-hydroxyphenyl)-6-methyl-2-oxopyrimidine-5-carboxylate (4n)

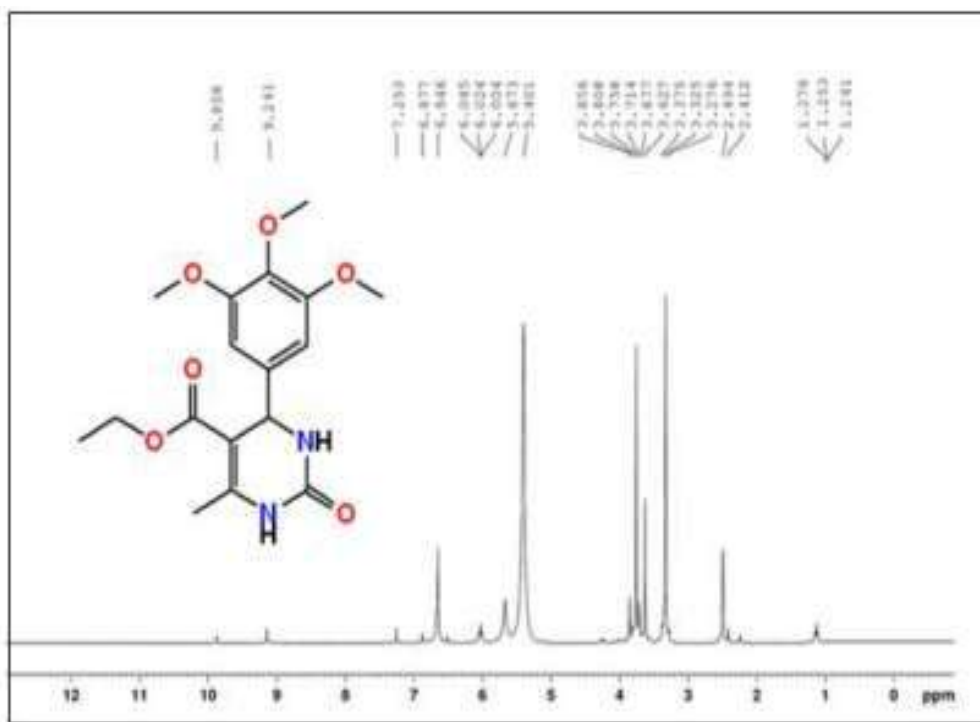


**Fig. 4.A.7.21.** <sup>1</sup>H NMR spectra of Ethyl 1,2,3,4-tetrahydro-4-(3,4,5-trimethoxyphenyl)-6-methyl-2-oxopyrimidine-5-carboxylate (4o).

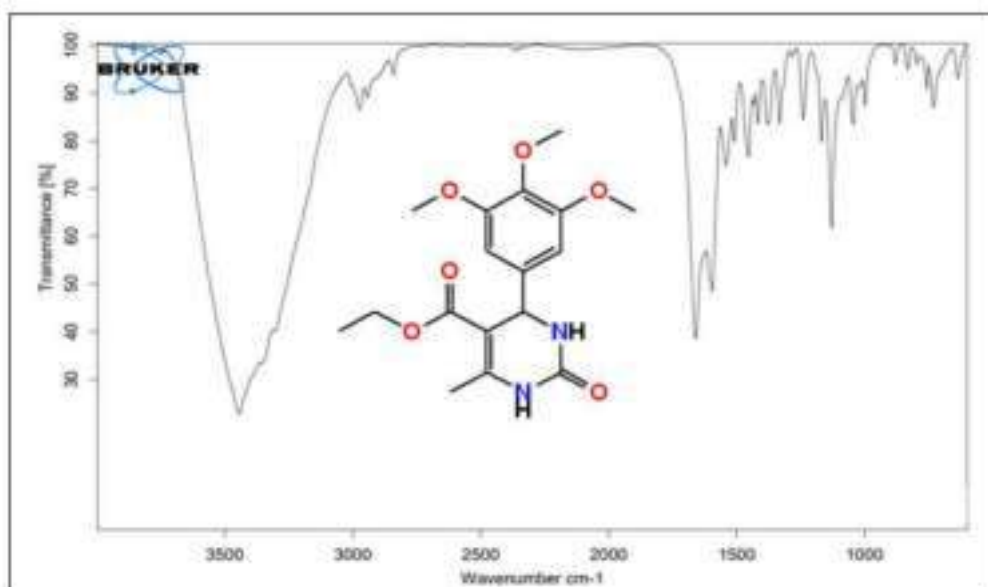


**Fig. 4.A.7.22.** FT-IR spectra of Ethyl 1,2,3,4-tetrahydro-4-(3,4,5-trimethoxyphenyl)-6-methyl-2-oxopyrimidine-5-carboxylate.

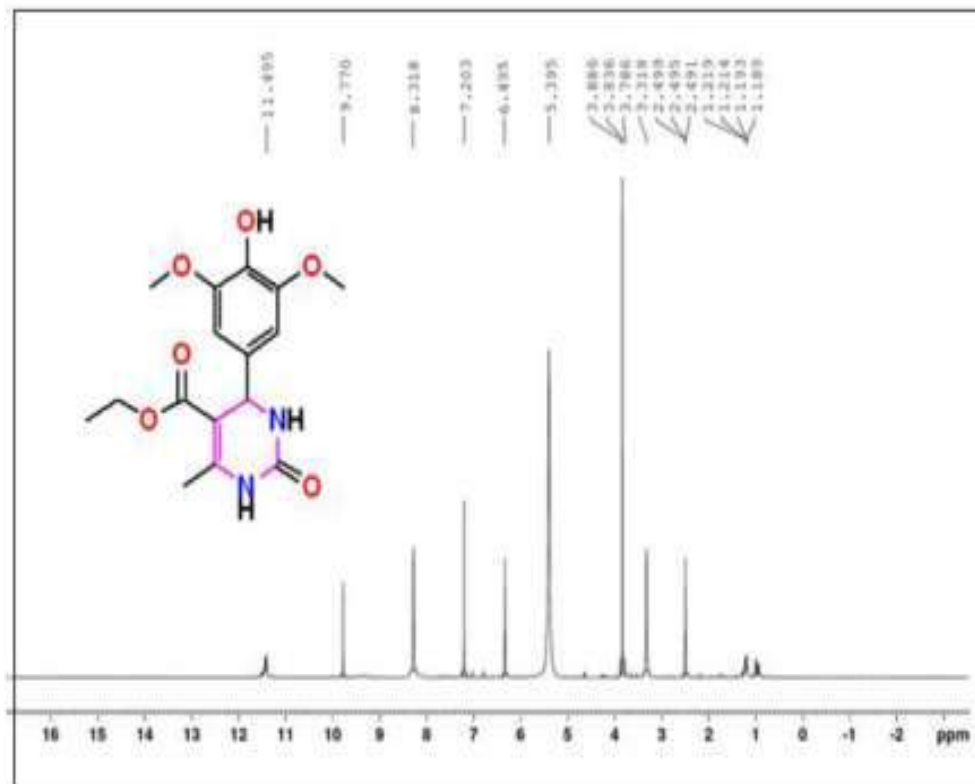


**Fig. 4.A.7.23.** <sup>1</sup>H NMR spectra of Ethyl 1,2,3,4-tetrahydro-4-(4-hydroxy-3,5-dimethoxyphenyl)-6-methyl-2-oxopyrimidine-5-carboxylate (4p)

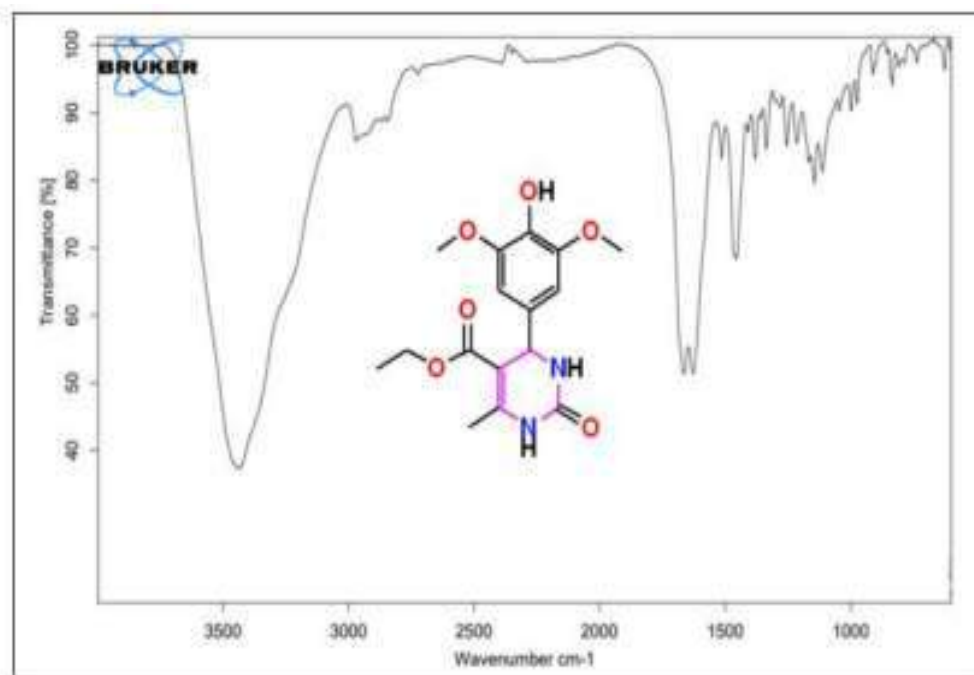


**Fig. 4.A.7.24.** FT-IR spectra of Ethyl 1,2,3,4-tetrahydro-4-(4-hydroxy-3,5-dimethoxyphenyl)-6-methyl-2-oxopyrimidine-5-carboxylate (4p)

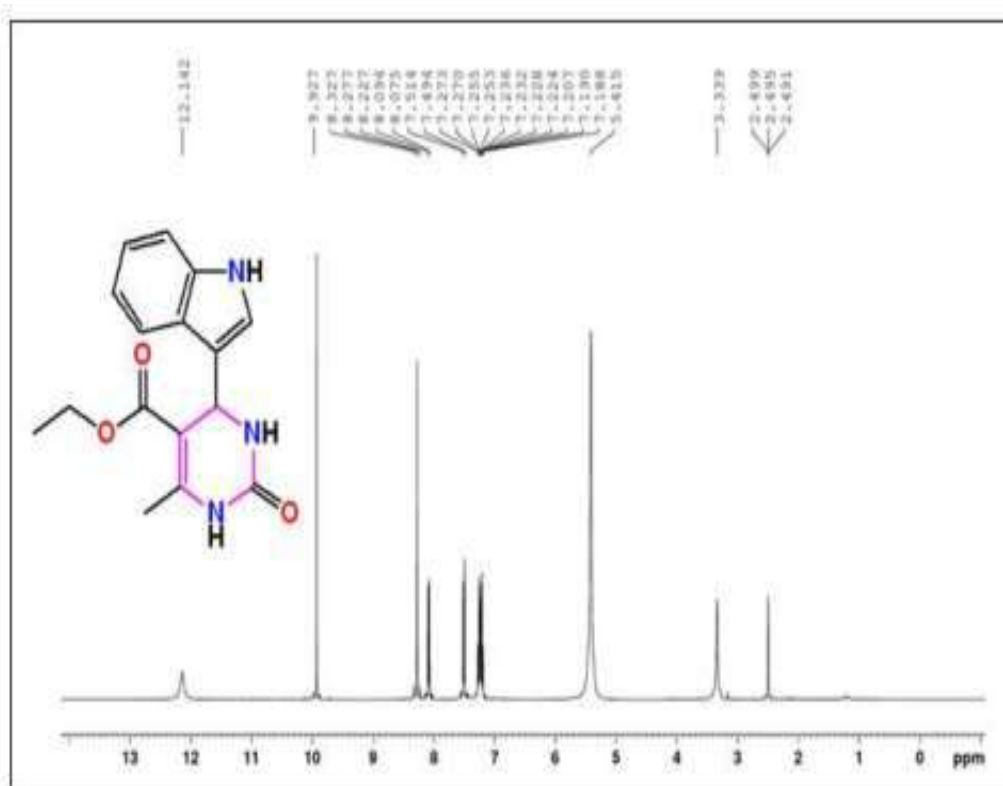


Fig. 4.A.7.25.  $^1\text{H}$  NMR spectra of Ethyl 1,2,3,4-tetrahydro-4-(1H-indol-3-yl)-6-methyl-2-oxypyrimidine-5-carboxylate (4q)

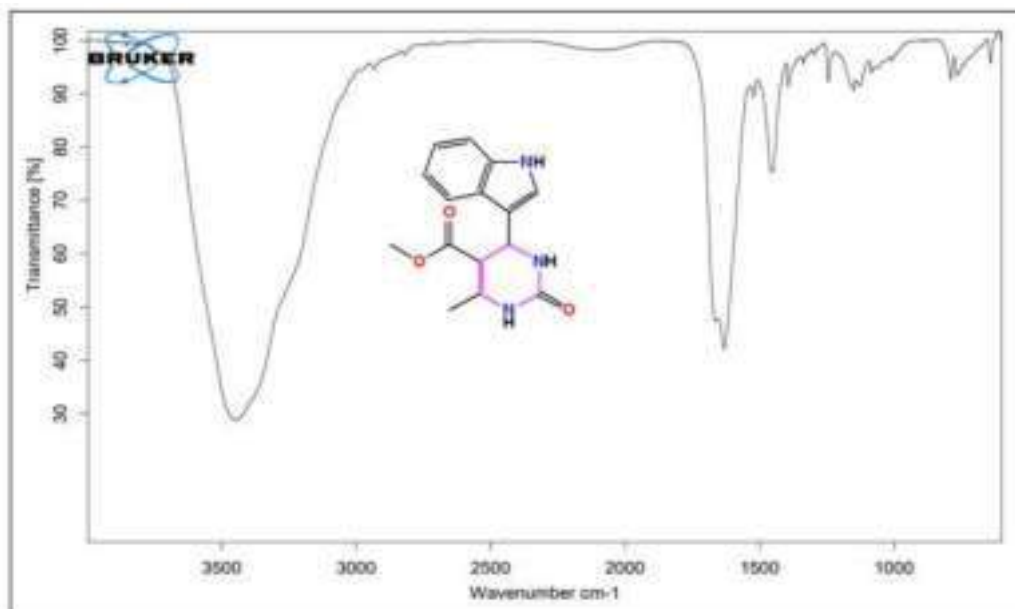


Fig. 4.A.7.26. FT-IR spectra of Ethyl 1,2,3,4-tetrahydro-4-(1H-indol-3-yl)-6-methyl-2-oxypyrimidine-5-carboxylate (4q)

## 4.A.8 References

- (1) S. Zangade, P. Patil., *Current Organic Chemistry*, **2019**, 23 (21), 2295–2318.
- (2) T. T. Nguyen, P. H. Tran., *RSC Advances*, **2020**, 10 (16), 9663–9671.
- (3) L. Biesen, T. J. J. Müller., *Advanced Synthesis & Catalysis*, **2021**, 363 (4), 980–1006.
- (4) B. M. Sahoo, B. V. V. R. Kumar, J. Panda, S. C. Dinda., *Journal of Nanoparticles*, **2013**, 2013 (Article ID 780786), 1–6.
- (5) P. Costanzo, M. Nardi, M. Oliverio., *European Journal of Organic Chemistry*, **2020**, 2020 (26), 3954–3964.
- (6) B. Mohammadi, F. K. Behbahani., *Molecular Diversity*, **2018**, 22 (2), 405–446.
- (7) R. Kaur, S. Chaudhary, K. Kumar, M. K. Gupta, R. K. Rawal., *European Journal of Medicinal Chemistry*, **2017**, 132, 108–134.
- (8) J. Lloyd, H. J. Finlay, K. Atwal, A. Kover, J. Prol, L. Yan, R. Bhandaru, W. Vaccaro, T. Huynh, C. S. Huang, M. L. Conder, T. Jenkins-West, H. Sun, D. Li, P. Levesque., *Bioorganic & Medicinal Chemistry Letters*, **2009**, 19 (18), 5469–5473.
- (9) J. Lloyd, H. J. Finlay, W. Vaccaro, T. Huynh, A. Kover, R. Bhandaru, L. Yan, K. Atwal, M. L. Conder, T. Jenkins-West, H. Shi, C. Huang, D. Li, H. Sun, P. Levesque., *Bioorganic & Medicinal Chemistry Letters*, **2010**, 20 (4), 1436–1439.
- (10) E. W. Hurst, R. Hull., *Journal of Medicinal Chemistry*, **1961**, 3 (2), 215–229.
- (11) C. O. Kappe., *European Journal of Medicinal Chemistry*, **2000**, 35 (12), 1043–1052.
- (12) L. M. Ramos, B. C. Guido, C. C. Nobrega, J. R. Corrêa, R. G. Silva, H. C. B. de Oliveira, A. F. Gomes, F. C. Gozzo, B. A. D. Neto., *Chemistry – A European Journal*, **2013**, 19 (13), 4156–4168.
- (13) R. Sharma, S. S. Jadav, S. Yasmin, S. Bhatia, H. Khalilullah, M. J. Ahsan., *Medicinal Chemistry Research*, **2015**, 24 (2), 636–644.
- (14) C. A. Bewley, S. Ray, F. Cohen, S. K. Collins, L. E. Overman., *Journal of Natural Products*, **2004**, 67 (8), 1319–1324.
- (15) S. Tcherniuk, R. van Lis, F. Kozielski, D. A. Skoufias., *Biochemical Pharmacology*, **2010**, 79 (6), 864–872.
- (16) G. Fitzharris., *Curr Biol*, **2012**, 22 (5), 437–444.
- (17) B. N. Acharya, G. B. D. Rao, D. Kumar, P. Kumar, M. P. Kaushik., *Medicinal Chemistry Research*, **2015**, 24 (4), 1763–1775.

- (18) P. Lacotte, D. A. Buisson, Y. Ambroise., *European Journal of Medicinal Chemistry*, **2013**, *62*, 722–727.
- (19) N. Singh, J. Kaur, P. Kumar, S. Gupta, N. Singh, A. Ghosal, A. Dutta, A. Kumar, R. Tripathi, M. I. Siddiqi, C. Mandal, A. Dube., *Parasitology Research*, **2009**, *105* (5), 1317–1325.
- (20) K. L. Dhumaskar, S. N. Meena, S. C. Ghadi, S. G. Tilve., *Bioorganic & Medicinal Chemistry Letters*, **2014**, *24* (13), 2897–2899.
- (21) A. Khan, J. Hashim, N. Arshad, I. Khan, N. Siddiqui, A. Wadood, M. Ali, F. Arshad, K. M. Khan, M. I. Choudhary., *Bioorganic Chemistry*, **2016**, *64*, 85–96.
- (22) F. Celik, M. Arslan, M. O. Kaya, E. Yavuz, N. Gencer, O. Arslan., *Artificial Cells, Nanomedicine and Biotechnology*, **2014**, *42* (1), 58–62.
- (23) A. O. Bryzgalov, M. P. Dolgikh, I. v. Sorokina, T. G. Tolstikova, V. F. Sedova, O. P. Shkurko., *Bioorganic & Medicinal Chemistry Letters*, **2006**, *16* (5), 1418–1420.
- (24) F. Cohen, L. E. Overman, S. K. Ly Sakata., *Organic Letters*, **1999**, *1* (13), 2169–2172.
- (25) S. Mondal, M. A. Mondal., *Journal of Heterocyclic Chemistry*, **2020**, *57* (12), 4175–4180.
- (26) M. Khashaei, L. Kafi-Ahmadi, S. Khademinia, A. Poursattar Marjani, E. Nozad., *Scientific Reports*, **2022**, *12* (1), 1–15.
- (27) Z. Karimi-Jaberi, M. S. Moaddeli., *ISRN Organic Chemistry*, **2012**, *2012* (Article ID 474626).
- (28) S. J. Kim, S. R. McAlpine., *Molecules*, **2013**, *18* (1), 1111–1121.
- (29) P. Biginelli., *Berichte der deutschen chemischen Gesellschaft*, **1891**, *24* (2), 2962–2967.
- (30) S. S. Panda, P. Khanna, L. Khanna., *Current Organic Chemistry*, **2012**, *16* (4), 507–520.
- (31) E. Kolvari, N. Koukabi, O. Armandpour., *Tetrahedron*, **2014**, *70* (6), 1383–1386.
- (32) B. K. Banik, A. T. Reddy, A. Datta, C. Mukhopadhyay., *Tetrahedron Letters*, **2007**, *48* (41), 7392–7394.
- (33) V. Polshettiwar, R. S. Varma., *Tetrahedron Letters*, **2007**, *48* (41), 7343–7346.
- (34) K. K. Pasunooti, H. Chai, C. N. Jensen, B. K. Gorityala, S. Wang, X. W. Liu., *Tetrahedron Letters*, **2011**, *52* (1), 80–84.

- (35) F. Dong, L. Jun, Z. Xinli, Y. Zhiwen, L. Zuliang., *Journal of Molecular Catalysis A: Chemical*, **2007**, 274 (1), 208–211.
- (36) A. Kuraitheerthakumaran, S. Pazhamalai, M. Gopalakrishnan., *Arabian Journal of Chemistry*, **2016**, 9 (Suppl. 1), S461–S465.
- (37) X. Chen, Y. Peng., *Catalysis Letters*, **2008**, 122 (3–4), 310–313.
- (38) S. L. Jain, J. K. Joseph, B. Sain., *Catalysis Letters*, **2007**, 115 (1–2), 52–55.
- (39) C. Ramalingan, S. J. Park, I. S. Lee, Y. W. Kwak., *Tetrahedron*, **2010**, 66 (16), 2987–2994.
- (40) F. Tamaddon, Z. Razmi, A. A. Jafari., *Tetrahedron Letters*, **2010**, 51 (8), 1187–1189.
- (41) H. Valizadeh, A. Shockravi., *Heteroatom Chemistry*, **2009**, 20 (5), 284–288.
- (42) Y. Zhang, B. Wang, X. Zhang, J. Huang, C. Liu., *Molecules*, **2015**, 20 (3), 3811–3820.
- (43) S. P. Bahekar, P. B. Sarode, M. P. Wadekar, H. S. Chandak., *Journal of Saudi Chemical Society*, **2017**, 21 (4), 415–419.
- (44) A. Khorshidi, K. Tabatabaieian, H. Azizi, M. Aghaei-Hashjin, E. Abbaspour-Gilandeh., *RSC Advances*, **2017**, 7 (29), 17732–17740.
- (45) M. M. Khodaei, A. R. Khosropour, M. Beygzadeh., *Synthetic Communications*, **2004**, 34 (9), 1551–1557.
- (46) S. Asghari, M. Tajbakhsh, B. J. Kenari, S. Khaksar., *Chinese Chemical Letters*, **2011**, 22 (2), 127–130.
- (47) X. H. Chen, X. Y. Xu, H. Liu, L. F. Cun, L. Z. Gong., *J Am Chem Soc*, **2006**, 128 (46), 14802–14803.
- (48) J. Safaei Ghomi, R. Teymuri, A. Ziarati., *Monatshefte fur Chemie*, **2013**, 144 (12), 1865–1870.
- (49) M. Zeinali-Dastmalbaf, A. Davoodnia, M. M. Heravi, N. Tavakoli-Hoseini, A. Khojastehnezhad, H. A. Zamani., *Bull Korean Chem Soc*, **2011**, 32 (2), 656–658.
- (50) S. D. Salim, K. G. Akamanchi., *Catalysis Communications*, **2011**, 12 (12), 1153–1156.
- (51) S. Rostamnia, A. Morsali., *RSC Advances*, **2014**, 4 (21), 10514–10518.
- (52) S. Chancharunee, P. Pinhom, M. Pohmakotr, P. Perlmutter., *Synthetic Communications*, **2009**, 39 (5), 880–886.



- (53) N. Firoozeh, S. Rezazadeh, C. Izanloo., *J Mex Chem Soc*, **2017**, *61* (3), 241–249.
- (54) M. Nasr-Esfahani, M. Montazerozohori, M. Aghel-Mirrezaee, H. Kashi., *Journal of the Chilean Chemical Society*, **2014**, *59* (1), 2311–2314.

## **CHAPTER-IV**

### **Section-B**

#### **DFT, Molecular Docking and Pharmacokinetic study of some selected 3, 4-dihydropyrimidin-2(1H)-one (DHPM) derivatives**

##### **4.B.1 Background of the present investigation**

Dihydropyrimidin-2(1H)-ones are a class of organic compounds which are synthesized using Bigenelli reaction and have significant biological activity<sup>1</sup>. Dihydropyrimidinones also called as Bigenelli compounds were first prepared by Pietro Bigenelli in the year 1893<sup>1</sup>. These classes of compounds have shown promising biological activities like calcium channel anragonists<sup>2-3</sup>, anti-cancer<sup>4-5</sup>, anti-hypertensive<sup>6</sup>, anti-bacterial<sup>7</sup>, anti-inflammatory<sup>8</sup>,  $\alpha_1\alpha$ adrenergic antagonists<sup>9</sup> and HIV-gp-120-CD4 inhibitors<sup>10</sup>. Apart from biological activities, DHPMs are also used as essential building blocks for a variety of other heterocyclic compounds<sup>11-17</sup>(Fig.4.B.1). Computational chemistry and theoretical calculations based on physicochemical and quantum mechanics involving organic molecules are gaining a lot interest these days as it helps in understanding the geometrical properties, reaction pathways and chemical mechanisms<sup>18-19</sup>. Also, these theoretical techniques provide information about the electronic properties of the reactants, intermediates and products which helps in inculcating new ideas for planning an organic synthesis<sup>20-21</sup>. Recently, Density Functional Theory (DFT) is mostly used for exploring the geometry and electronic properties of organic molecules along with some important properties like dipole moments, optical properties, vibration frequencies and thermodynamic properties<sup>22-24</sup>. The information obtained from theoretical calculations can be compared with the experimental finding which helps to gain a deep insight into the various properties of the compounds under study. With the advancement in computational chemistry, Computer Aided Drug Design (CADD) is an emerging field of research<sup>25</sup> and it helps to predict the different types of interaction prevailing between the ligand and active site of the protein<sup>26</sup>. Usually, the development of a new drug for a particular disease is a very long tedious and also a costly process<sup>27</sup> and therefore, CADD method is widely used for drug designing as it efficiently reduces the time and cost for drug discovery<sup>28</sup>.

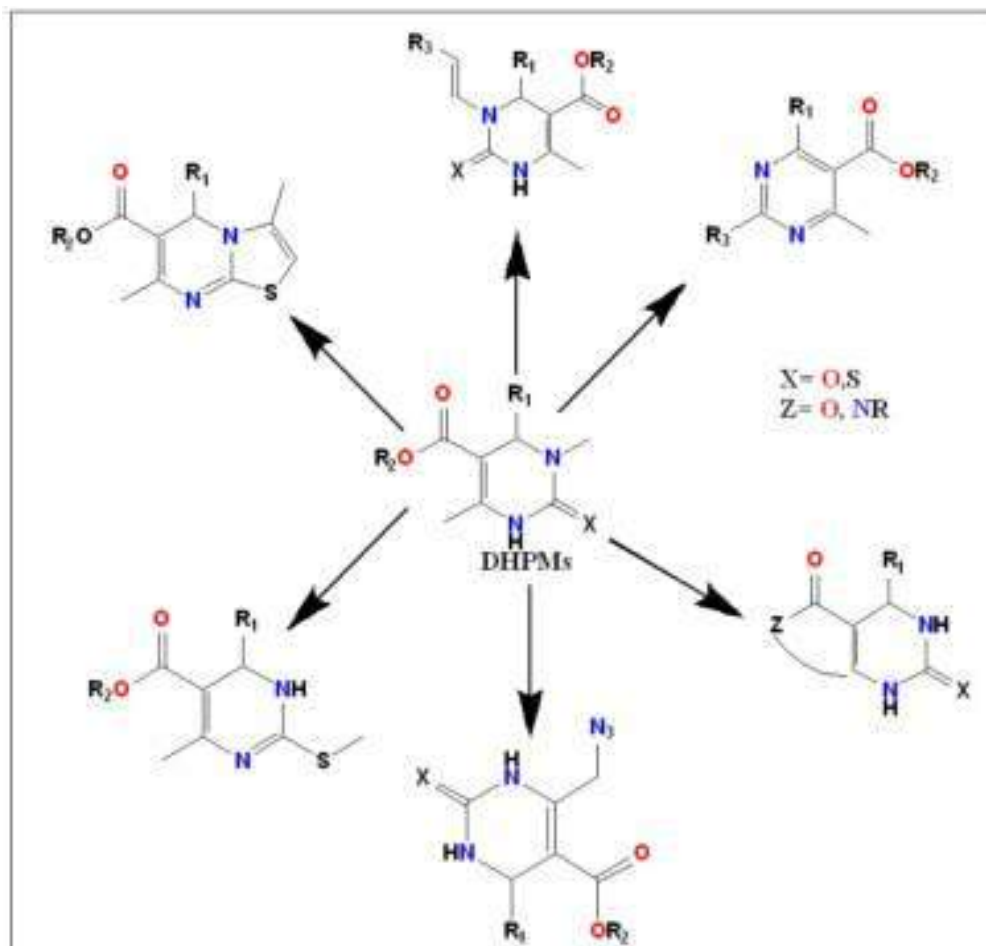


**Fig. 4.B.1.** DHPMs as essential building blocks.

Type 2 diabetes mellitus is a condition where regulation and use of glucose by the body is impaired leading to the increase of circulating blood sugar (when in the chronic stages). Eventually, disorders of the circulatory, immune and nervous systems. Type 2 diabetes is primarily the result of two correlated problems namely insulin resistance in cells in muscles, fat and liver causing reduced storage of glucose as glycogen, and the pancreas beta cells are unable to produce enough insulin to keep blood sugar levels in check<sup>29</sup>. It is mostly characterized by hyperglycemia, insulin resistance and relative insulin deficiency<sup>30</sup>. In the 2010s, inhibition of sodium-dependent glucose transporters (SGLTs) have been proposed as a new therapy for the treatment of type 2 diabetes mellitus<sup>31</sup>. SGLT2, the most prominent among all of the SGLTs, is expressed mainly in the kidney and is responsible for the reabsorption of a vast amount of the filtered glucose. Thus, SGLT2 plays a key role in the blood-glucose homeostasis and as such is a prominent target which has been clear from the results of pre-clinical and clinical studies. Any drug discovery project that focuses on promising SGLT2 inhibitors also has to factor in any significant selectivity towards SGLT1<sup>32</sup>. This is because though there are many therapeutic goals of SGLT2 inhibition like weight loss and

reduced plasma glucose levels, a few side effects may exist due to co-inhibition of SGLT1. SGLT1 being expressed in the intestine is responsible for glucose and galactose absorption from food sources, therefore, leading to galactose- and glucose malabsorption, diarrhoea and dehydration. This can be mediated through lack of selectivity towards SGLT1.

Selectivity of any drug or ligands towards SGLT2 thus needs to be offset by its lack of selectivity towards SGLT1. So, to describe selectivity with respect to structure, extensive use of molecular modelling techniques has been utilized as no x-ray structural data was available for either SGLT1 or SGLT2. Faham S. et al., thus, generated homology models for both transporters using the published x-ray structure from vSGLT (PDB 3DH4)<sup>33</sup>. Although there are numerous drugs available for the treatment of type-2 diabetes mellitus still these drugs have several side effects<sup>34</sup>. So, it is worthwhile to find an efficient drug for this disease with minimum or no side effect.

With the improvements in the field of drug designing, Molecular Docking studies are very popular in studying the different types of interactions between ligand and the receptor<sup>35-36</sup>.

Molecular docking is a virtual procedure which helps to find a ligand that fits exactly and efficiently in the binding site of the protein and is an important tool for accurate drug discovery<sup>37-38</sup>.

Furthermore, a variety of 2,4-dihydropyrimidin-2(1H)-ones using solvent free, green methodology have been prepared in excellent yields and its synthetic procedure, spectroscopic and analytical investigations have been discussed in section-A of chapter 4. In this chapter we are presenting the theoretical aspects of some selected Bigenelli compounds wherein HOMO-LUMO energies, bond lengths, bond angles, dihedral angles, global chemical descriptors and Molecular Electrostatic Potential (MEP) have been studied in detail using DFT. The inhibitory potential of these selected derivatives against the protein 3DH4 which is used in homology studies for the inhibition of Sodium-Dependent Glucose Transporters (SGLTs) have also been reported.

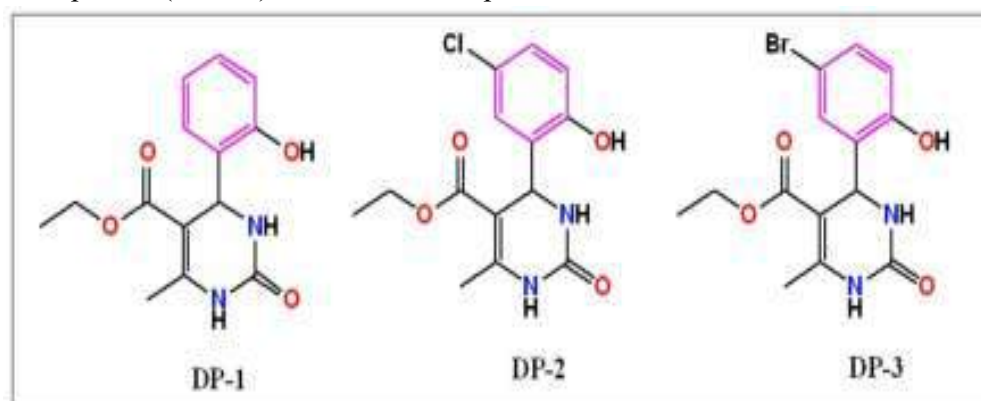


**Fig. 4.B.2.** Molecular Structures of selected 3, 4-dihydropyrimidin-(2H)-one derivatives (DP-1 to DP-3)

## 4.B.2 Results and Discussions

### 4.B.2.1 Computational Study

The molecular geometry, molecular orbital (HOMO,LUMO), Nonlinear Optical property (NLO), Global chemical descriptors and Molecular Electrostatic Potential (MEP) of the selected 3,4-dihydropyrimidin-(2H)-one derivatives namely, Ethyl 4-(2-hydroxyphenyl)-6-methyl-2-oxo-1,2,3,4-tetrahydropyrimidine-5-carboxylate (DP-1), Ethyl 4-(5-chloro-2-hydroxyphenyl)-6-methyl-2-oxo-1,2,3,4-tetrahydropyrimidine-5-carboxylate (DP-2) and Ethyl 4-(5-bromo-2-hydroxyphenyl)-6-methyl-2-oxo-1,2,3,4-tetrahydropyrimidine-5-carboxylate (DP-3) have been optimized by Density Functional Theory (DFT) using Becke's three-parameter hybrid method (B3) with Lee, Yang and Parr correlation functional methods (LYP) with B3LYP/631G+(d,2p) level of basis set<sup>39-40</sup>. All the computational calculations were calculated by Gaussian 16, Revision A.03 programme package<sup>41</sup> and the results were visualized using GAUSSVIEW 6.0 software<sup>42</sup> on ahp-Z640 desktop P.C. with an Intel Xeon processor (Specifications: E5-2630 V4 @ 220GHz).

#### 4.B.2.1.1 Optimization of Molecular Geometry

To the best of our knowledge, the X-Ray single crystal structure of the selected compounds (DP-1 to DP-3) have not been reported till now, therefore, structure optimization using DFT method serves as a good alternative to ascertain the different geometrical parameters. The geometrical parameters of the studied compounds (DP-1 to DP-3) were calculated by DFT assay using B3LYP/631G+(d,2p) level of basis set. The optimized gas phase molecular geometry of the compounds (DP-1 to DP-3) with atom labelling scheme is shown in Fig.4.B.3 and 4.B.4 and the structural parameters like bond lengths, bond angles and dihedral angles are listed in Table 4.B.1.

From the analysis of the dihedral angles as given in Table 4.B.1, it can be inferred that the phenyl ring is not in plane with the DHPM nucleus as the dihedral angles are nowhere close to 0° or 180°. The dihedral angle between the phenyl ring (2) and the DHPM nucleus (1) depends on the type of substituent present in the phenyl ring as evident from the fact that in DP-1, the dihedral angle between C17-C12-C6-C5 and between C17-C12-C6-C1 is 34.148° and -138.05° respectively whereas in DP-2 it is -146.31° and 26.00° respectively and in DP-3 it is found to be 147.425° and -26.54° respectively. From Table 4.B.1, it is clearly seen that the C-N bond lengths in the DHPM nucleus (1) of all the studied compounds (DP-1 to DP-3) are in the range C6-N5 = 1.407 Å - 1.413 Å, C4-N5 = 1.370 Å - 1.377 Å, C4-N3 = 1.382 Å - 1.392 Å, C2-N3 = 1.393 Å - 1.401 Å respectively. The C4-N5 and C4-N3 are shorter than C6-N5 and C2-N3 a bond length which suggests that the lone pairs on nitrogen are delocalized on atom C4 which is double bonded with oxygen atom O19. Also, from the optimized geometry, it was found that C=O bond length in all the studied compounds (DP-1

to DP-4) fall in the range  $C7=O8 = 1.210-1.219 \text{ \AA}$ ,  $C4=O19 = 1.224-1.225 \text{ \AA}$  respectively. The C-O bond lengths in these compounds (DP-1 to DP-3) are found to be in the range  $C7-O9 = 1.348-1.358 \text{ \AA}$ ,  $C10-O9 = 1.450-1.455 \text{ \AA}$  respectively.

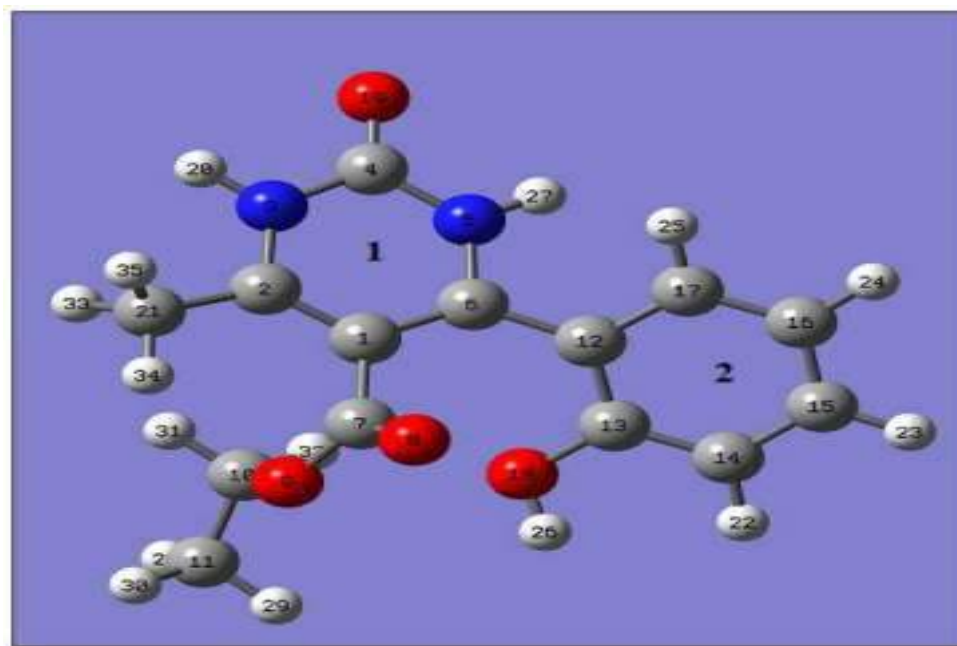


**Fig. 4.B.3.** Atom labelling of the DHPM nucleus (1) and the phenyl ring (2) in the studied compounds.

The C-C bond lengths of all the aryl groups present in the compounds (DP-1 to DP-3) are in the range  $1.386$  to  $1.417 \text{ \AA}$  which suggests that the carbon atoms are highly conjugated and electrons are involved in resonance<sup>43</sup>. Again, from the table 4.B.1, it is clearly seen that the N-H bond length of the DHPM nucleus (1) in all the studied compounds are almost equal and falls in the range of  $1.010-1.012 \text{ \AA}$ . The aromatic C-H, aliphatic C-H, O-H, and C-halogen bond distances of the studied compounds (DP-1 to DP-3) are in the range  $1.392-1.417 \text{ \AA}$ ,  $1.086-1.094 \text{ \AA}$ ,  $0.963-0.966 \text{ \AA}$ ,  $1.761-1.909 \text{ \AA}$  respectively.

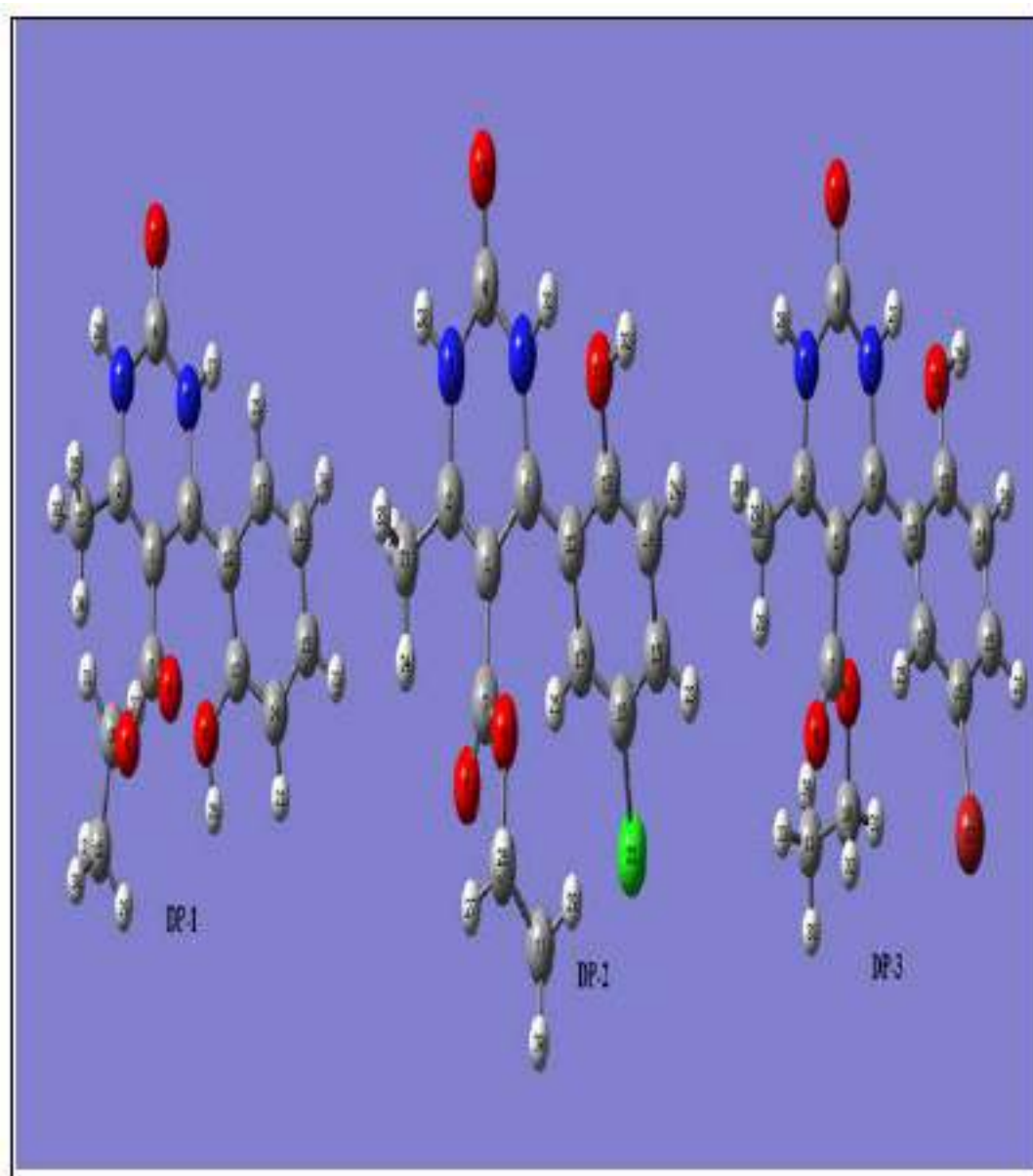


**Fig. 4.B.4.** Optimized gas phase molecular geometry of the compounds (DP-1 to DP-3) with atom labelling scheme.

**Table. 4.B.1.** Structural parameters (bond lengths, bond angles and dihedral angles) of the studied compounds (DP-1 to DP-3)

<b>C-C bond length (Å)</b>					
<b>DP-1</b>		<b>DP-2</b>		<b>DP-3</b>	
C2-C1	1.387	C2-C1	1.382	C2-C1	1.382
C6-C1	1.419	C6-C1	1.435	C6-C1	1.435
C6-C12	1.461	C6-C12	1.452	C6-C12	1.452
C7-C1	1.508	C7-C1	1.498	C7-C1	1.497
C11-C10	1.518	C11-C10	1.520	C11-C10	1.520
C12-C13	1.415	C12-C13	1.422	C12-C13	1.421
C12-C17	1.416	C12-C17	1.417	C12-C17	1.417
C13-C14	1.394	C13-C14	1.392	C13-C14	1.392
C14-C15	1.396	C14-C15	1.397	C14-C15	1.396
C15-C16	1.397	C15-C16	1.395	C15-C16	1.394
C16-C17	1.392	C16-C17	1.388	C16-C17	1.386
C2-C21	1.499	C2-C21	1.499	C2-C21	1.499
<b>C-H, C-O, N-H, C-Cl, C-Br and O-H bond distances (Å)</b>					
<b>DP-1</b>		<b>DP-2</b>		<b>DP-3</b>	
C10-H31	1.094	C10-H26	1.091	C10-H31	1.091
C10-H32	1.091	C10-H27	1.091	C10-H32	1.091
C11-H29	1.093	C11-H29	1.092	C11-H33	1.093
C11-H30	1.093	C11-H30	1.095	C11-H34	1.093
C11-H28	1.094	C11-H28	1.092	C11-H35	1.095
C14-H22	1.087	C14-H24	1.087	C14-H24	1.087
C15-H23	1.084	C15-H23	1.083	C15-H23	1.082
C16-H24	1.084	C17-H25	1.082	C17-H25	1.082
C17-H25	1.085	C21-H34	1.086	C21-H29	1.097
C21-H34	1.089	C21-H33	1.097	C21-H28	1.086
C21-H33	1.089	C31-H35	1.097	C21-H30	1.097
C21-H35	1.089	C4-O19	1.224	C7-O8	1.219
C7-O8	1.210	C7-O8	1.219	C7-O9	1.348
C10-O9	1.450	C10-O9	1.455	C10-O9	1.454
C7-O9	1.358	C7-O9	1.348	C4-O19	1.224
C13-O18	1.373	C13-O18	1.380	C13-O18	1.380
N3-H20	1.010	C16-Cl22	1.761	C16-Br22	1.909
N5-H27	1.010	N3-H20	1.010	N3-H20	1.010
		N5-H31	1.012	N5-H27	1.012
				O18-H26	0.965
<b>Bond Angle (°)</b>					
<b>DP-1</b>		<b>DP-2</b>		<b>DP-3</b>	
N3-C2-C1	118.536	N3-C2-C1	118.149	N3-C2-C1	118.168
C4-N3-C2	124.964	C4-N3-C2	124.805	C4-N3-C2	124.900
N5-C4-N3	113.609	N5-C4-N3	113.679	N5-C4-N3	113.724
C6-N5-C4	126.458	C6-N5-C4	125.653	C6-N5-C4	125.751
C7-C1-C2	117.987	C7-C1-C2	118.097	C7-C1-C2	118.307
O8-C7-C1	122.513	O8-C7-C1	124.954	O8-C7-C1	124.905
O9-C7-C1	118.270	O9-C7-C1	111.433	O9-C7-C1	111.501
C10-O9-C7	121.837	C10-O9-C7	117.416	C10-O9-C7	117.653
C11-C10-O9	107.199	C11-C10-O9	111.996	C11-C10-O9	110.810
C12-C6-N5	114.758	C12-C6-N5	118.386	C12-C6-N5	118.573
C13-C12-C6	123.601	C13-C12-C6	123.437	C13-C12-C6	123.612



C14-C13-C12	121.313	C14-C13-C12	121.406	C14-C13-C12	121.315
C15-C14-C13	120.635	C15-C14-C13	121.179	C15-C14-C13	121.185
C16-C15-C14	119.435	C16-C15-C14	118.164	C16-C15-C14	118.156
C17-C16-C15	119.776	C17-C16-C15	121.348	C17-C16-C15	121.344
O18-C13-C12	117.560	O18-C13-C12	117.857	O18-C13-C12	117.950
O19-C4-N3	122.986	O19-C4-N3	122.276	O19-C4-N3	122.260
H20-N3-C2	120.311	H20-N3-C2	119.635	H20-N3-C2	119.706
C21-C2-C1	127.084	C21-C2-C1	127.928	C21-C2-C10	127.915
H22-C14-C13	119.084	C122-C16-C15	119.316	Br22-C16-C1	119.423
H23-C15-C14	119.845	H23-C15-C14	120.889	H23-C15-C14	120.630
H24-C16-C15	120.450	H24-C14-C13	119.264	H24-C14-C13	119.247
H25-C17-C16	118.907	H25-C17-C16	118.859	H25-C17-C16	119.070
H26-O18-C13	109.471	H26-C10-O9	103.562	H26-O18-C13	109.820
H27-N5-C4	113.965	H27-C10-O9	108.559	H27-N5-C4	115.438
H28-C11-C10	109.660	H28-C11-C10	111.349	H28-C21-C2	111.974
H29-C11-C10	110.966	H29-C11-C10	111.087	H29-C21-C2	109.832
H30-C11-C10	110.980	H30-C11-C10	109.146	H30-C21-C2	110.311
H31-C10-O9	109.302	H31-N5-C4	115.525	H31-C10-O9	104.054
H32-C10-O9	109.177	H32-O18-C13	109.866	H32-C10-O9	108.843
H33-C21-C2	111.242	H33-C21-C2	109.785	H33-C11-C10	110.970
H34-C21-C2	112.093	H34-C21-C2	111.958	H34-C11-C10	110.911
H35-C21-C2	110.254	H35-C21-C2	110.351	H35-C11-C10	109.565
<b>Selected dihedral angles (°)</b>					
C17-C12-C6-C5	34.140	C17-C12-C6-C5	-146.301	C17-C12-C6-C5	147.420
C13-C12-C6-C1	45.550	C13-C12-C6-C1	-156.009	C13-C12-C6-C1	154.530
C13-C12-C6-C5	-144.240	C13-C12-C6-C5	31.570	C13-C12-C6-C5	-31.500
C1-C6-C12-C17	-138.050	C1-C6-C12-C17	26.000	C1-C6-C12-C17	-26.540
O8-C7-C1-C6	60.470	O8-C7-C1-C6	-138.601	O8-C7-C1-C6	138.760
C2-C1-C7-O8	-109.610	C2-C1-C7-O8	48.060	C2-C1-C7-O8	-46.580
H31-C10-C11-H29	179.310	H27-C10-C11-H29	177.980	H32-C10-C11-H33	56.640
H31-C10-C11-H30	-60.200	H27-C10-C11-H30	-62.680	H31-C10-C11-H33	179.400
O9-C10-C11-H30	58.910	O9-C10-C11-H30	175.450	O9-C10-C11-H33	-65.160

O9-C10-C11- H29	-61.510	O9-C10-C11- H29	56.130	O9-C10-C11- H35	179.500
C2-C1-C7- O9	66.010	C2-C1-C7-O9	-128.907	C2-C1-C7-O9	131.950

#### 4.B.2.1.2 Frontier Molecular Orbitals

The Highest occupied molecular orbital (HOMO) and the Lowest Unoccupied Molecular orbital (LUMO) constitutes the frontier molecular orbitals and they are very important in predicting the molecular reactivity. The electron donor ability of a molecule is determined by the energy of HOMO while the electron acceptor ability is determined by the energy of LUMO<sup>44</sup>. Several important properties like kinetic stability, reactivity and the polarizability of a molecule can be determined by analyzing the energy gap ( $\Delta E = E_{\text{LUMO}} - E_{\text{HOMO}}$ ) between the HOMO and the LUMO<sup>44</sup>. Also, a large and positive  $\Delta E$  value indicates that the molecule is less polarizable and is chemically stable<sup>45</sup>. In order to get into a deep insight into the electronic behavior of the studied compounds, the HOMO-LUMO energies have been calculated using B3LYP/631G+(d,2p) basis set and its pictorial representation is shown in Fig.4.B.5. and the energies of the HOMO-LUMO of the studied compounds are shown in Table 4.B.2.

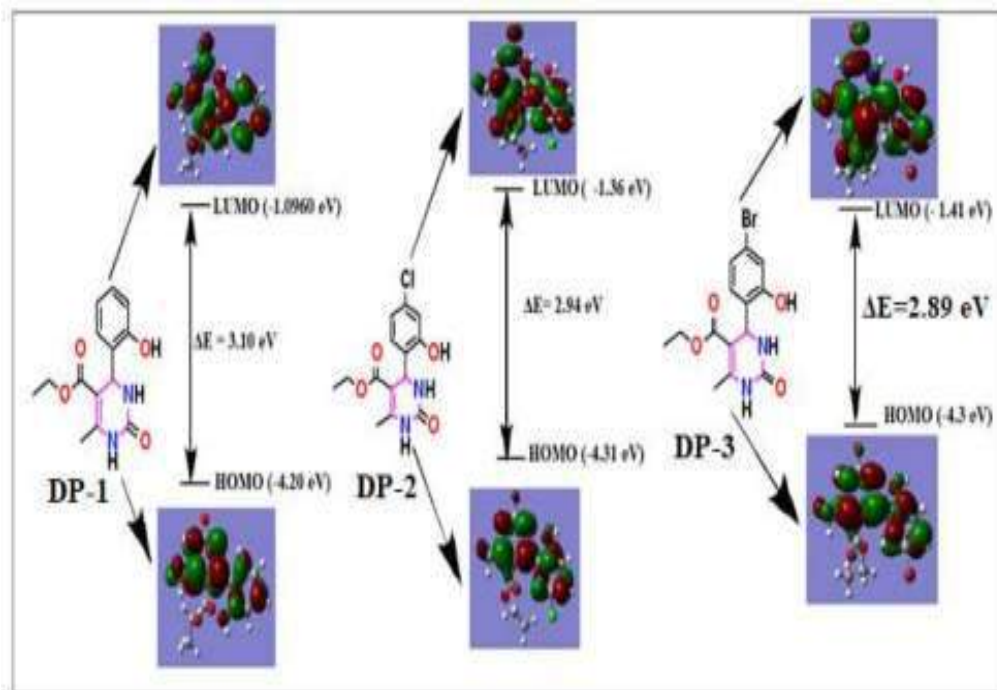


**Fig. 4.B.5.** Pictorial representation of the HOMO-LUMO of selected compounds (DP-1 to DP-3)

From the Table 4.B.2., It is evident that the energy of HOMO and LUMO orbitals are negative and this shows that the compounds under study (DP1 to DP-3) are relatively stable<sup>45</sup> and the energy of HOMO and LUMO orbitals of the compounds are -4.20 eV (DP-1), -4.31 eV (DP-2), -4.30 eV (DP-3) and -1.09 eV (DP-1), -1.36 eV (DP-2), -1.41 eV (DP-3) respectively. With the help of the energies of the HOMO and LUMO, global chemical descriptors like chemical potential, global hardness and global electrophilicity can be determined which is helpful for understanding the reactivity and the structure of the molecule which in turn is essential for determination of the various pharmacological properties of the molecule for the process of drug design<sup>46</sup>. The ionization energy (I) and electron affinity (A) can be expressed in terms of HOMO and LUMO orbital energies as follows

$$I = -E_{\text{HOMO}} \text{ and } A = -E_{\text{LUMO}}$$

The chemical reactivity descriptors such as chemical potential ( $\mu$ ), Electronegativity ( $\chi$ ), Global hardness ( $\eta$ ) and global electrophilicity power ( $\omega$ ) can be calculated with the help of following relation;

$$\text{Chemical potential } (\mu) = (E_{\text{HOMO}} + E_{\text{LUMO}})/2 = -(I+A)/2$$

$$\text{Electronegativity } (\chi) = (I+A)/2$$

$$\text{Global Hardness } (\eta) = (-E_{\text{HOMO}} - E_{\text{LUMO}})/2 = (I-A)/2$$

$$\text{Electrophilicity power } (\omega) = \mu^2/2 \eta$$

Where I and A are the first ionization potential and electron affinity of the chemical species<sup>47-49</sup>.

The ionization energy (I), electron affinity (A), Chemical potential ( $\mu$ ), Electronegativity ( $\chi$ ), Global hardness ( $\eta$ ) and Global electrophilicity power ( $\omega$ ) of the studied compounds (DP-1 to DP-3) are listed in Table 4.B.3.

**Table. 4.B.2.** Energies of HOMO and LUMO orbitals, ionization energy (I), electron affinity (A), Chemical potential ( $\mu$ ), Electronegativity ( $\chi$ ), Global hardness ( $\eta$ ) and Global electrophilicity power ( $\omega$ ) of the studied compounds (DP-1 to DP-3)

Parameters (eV)	DP-1	DP-2	DP-3
$E_{\text{HOMO}}$	-4.20	-4.31	-4.30
$E_{\text{LUMO}}$	-1.09	-1.36	-1.41
$\Delta E$	3.10	2.94	2.89
Ionization Energy (I)	4.20	4.31	4.30
Electron Affinity (A)	1.09	1.36	1.41
Chemical potential ( $\mu$ )	-2.64	-2.83	-2.85
Electronegativity ( $\chi$ )	2.64	2.83	2.85
Global hardness( $\eta$ )	1.55	1.47	1.44
Electrophilicity power( $\omega$ )	2.25	2.72	3.81

It is seen that the chemical potential of all the studied molecules are negative and this suggests that the compounds under investigation do not decompose spontaneously into its elements they are made up of.

Apparently, it is seen that the hard molecule has large HOMO-LUMO gap and soft molecule has small HOMO-LUMO gap<sup>50</sup>. Thus, from the Table 4.B.3, it is evident that the hardness of the studied molecule follows the order DP-1 > DP-2 > DP-3. Moreover, the hardness signifies the resistance towards the deformation of electron cloud of chemical systems under small perturbation that occur during the chemical reaction. Thus, hard system is less polarizable than soft system<sup>51</sup>. Again, a large value of electrophilicity is assigned for good electrophile whereas nucleophile is described by low value of nucleophilicity<sup>52</sup>.

#### 4.B.2.1.3 FT-IR analysis

Study of the molecular vibrations of organic compounds is an important area of research as it is possible to correlate the theoretical and experimental FT-IR spectra of the studied compounds to figure out the different structural features in the molecules.

The theoretical vibrational spectra of the studied compounds (DP-1 to DP-3) was calculated using B3LYP/631G+(d,2p) basis set on the optimized geometry of the molecules in the gas phase. The experimental and theoretical vibrational

frequencies of the studied compounds (DP-1 to DP-3) are given in Table 4.B.3 with proper assignment of the observed peaks.

**Table. 4.B.3. FT-IR analysis of studied compounds DP-1 to DP-3**

<b>DP-1</b>				
Unscaled frequency (cm-1) (theoretical)	IR <sub>i</sub>	R(A)	IR Frequency (cm-1) Experimental	Assignments
3821.74	69.7539	96.4066	3444	vOH stretch
3639.2	96.5826	232.3846	3009	vNH stretch
3626.02	40.3333	94.4064		vNH stretch
3209.13	14.3066	301.7885		v(s)Ar-H stretch
3195.6	9.456	75.1909		v(as)Ar-H stretch
3183.72	2.6979	58.8911		v(as)Ar-H stretch
3162.77	12.7405	107.6511		v(as)Ar-H stretch
3155.52	2.4726	43.1897		v(as)CH <sub>3</sub>
3133.24	25.3587	5.5061		v(as)C <sub>2</sub> H <sub>5</sub>
3115.21	23.2341	65.8397		v(as)C <sub>2</sub> H <sub>5</sub>
3110.33	1.6272	86.7641		v(as)C <sub>2</sub> H <sub>5</sub>
3058.58	22.7075	88.3833		v(as)C <sub>2</sub> H <sub>5</sub>
3045.41	7.9017	262.1293	2988	vC <sub>2</sub> H <sub>5</sub> ,v(as)CH 3
3045.06	32.4389	163.6919		vC <sub>2</sub> H <sub>5</sub> ,v(as)CH 3
3006.11	87.5886	680.6065		vCH <sub>3</sub>
1637	14.539	1000.461		vAr C=C stretch, 1
1615.03	31.014	67.1562	1629	vAr C=C stretch
1555.13	59.3641	259.6895	1531	vArC=C stretch
1790.21	1074.1713	36.4448	1666	v(C=O) stretch
<b>DP-2</b>				
3826.93	89.3908	147.631		vOH
3632.99	116.8733	247.8722	3444	vNH
3595.47	87.0333	115.2456		vNH
3223.96	0.1725	113.6372		vAr-H
3220.11	0.1289	14.8199		v(as)Ar-H
3188.08	0.7012	37.0334		v(as)CH <sub>3</sub>
3164.66	16.1413	162.2694		v(as)Ar-H
3145.92	17.4996	4.2482		v(as)C <sub>2</sub> H <sub>5</sub>
3124.08	3.3019	72.0917		v(as)C <sub>2</sub> H <sub>5</sub>
3114.24	31.4035	80.5211		v(as)C <sub>2</sub> H <sub>5</sub>
3079.04	29.1354	115.075		v(as)C <sub>2</sub> H <sub>5</sub>

3061.2	12.2927	219.1467		v(as)CH3
3047.06	14.3386	183.7124		vC2H5
3017.79	73.4512	739.7649	3004	vCH3
1622.84	1070.0928	1178.464		vArC=C stretch
		9		
1601.41	50.1923	258.3946	1625	vAr C=C stretch
1587.72	123.0225	301.1709		vAr C=C stretch
1790.76	1013.8192	42.7887	1667	vC=O stretch
<b>DP-3</b>				
3826.49	90.5042	152.7938	3473	vOH
3633.14	120.0181	261.1812	3455	vNH
3596.46	86.4332	124.2294		vNH
3223.38	0.6732	98.986		vAr-H
3220.45	0.3245	10.9341		v(as)Ar-H
3188.57	0.6232	37.27		v(as)CH3
3163.85	16.7887	168.0818		v(as)Ar-H
3144.92	13.6097	6.3731		v(as)C2H5
3119.59	9.7442	56.2076		v(as)C2H5
3111.15	20.7016	85.4523		v(as)C2H5
3060.74	12.4734	222.5195		v(as)CH3
3043.58	20.9182	168.1723		vC2H5
3017.63	74.5452	745.067	2969	vCH3
1621.72	106.7411	1271.234		vArC=C stretch
		5		
1599.92	61.0917	271.8334		vAr C=C stretch
1586.55	113.1961	310.4236	1474	vAr C=C stretch
1791.55	1035.7274	1791.55	1635	v(C=O) stretch

#### 4.B.2.1.3.1 C-H stretching vibration

For the studied compounds (DP-1 to DP-3), C-H functional group is present at various positions. The characteristic C-H stretching vibration of the aromatic ring falls in the range 3100-3000  $\text{cm}^{-1}$ <sup>53</sup>. In the present investigation, theoretically calculated bands in the range of 3209-3162  $\text{cm}^{-1}$ , 3223-3164  $\text{cm}^{-1}$  and 3220-3163  $\text{cm}^{-1}$  were assigned to aromatic C-H stretching vibrations for the compounds DP-1, DP-2 and DP-3 respectively. Pure symmetric bands were calculated at 3209  $\text{cm}^{-1}$  in DP-1, 3223  $\text{cm}^{-1}$  in DP-2 and 3223  $\text{cm}^{-1}$  in DP-3 respectively. Asymmetric vibrational bands were calculated with stretching frequencies 3195  $\text{cm}^{-1}$ , 3183  $\text{cm}^{-1}$  and 3162  $\text{cm}^{-1}$  for DP-1, 3220  $\text{cm}^{-1}$ , 3220  $\text{cm}^{-1}$ , 3164  $\text{cm}^{-1}$  for DP-2 and 3220  $\text{cm}^{-1}$ , 3163  $\text{cm}^{-1}$  for DP-3 respectively. Because of the integration of several bands in the molecules, it is very difficult to detect the aromatic C-H stretching in this type of systems.

The characteristic C-H stretching vibration for aliphatic systems like the C-H symmetric stretching vibration for CH<sub>3</sub> group is found at 3006 cm<sup>-1</sup> for DP-1, 3017 cm<sup>-1</sup> for DP-2 and 3017 cm<sup>-1</sup> for DP-3 respectively. The experimentally observed values for C-H symmetric stretching vibrations for CH<sub>3</sub> group lies in the range 2988 cm<sup>-1</sup> for DP-1, 3004 cm<sup>-1</sup> for DP-2 and 2969 cm<sup>-1</sup> for DP-3 respectively. Another important C-H stretching vibration found in BHPMs is the C-H symmetric stretching vibration for C<sub>2</sub>H<sub>5</sub> group. Theoretically, the C-H symmetric stretching vibration for C<sub>2</sub>H<sub>5</sub> group is found at 3045 cm<sup>-1</sup> for DP-1, 3047 cm<sup>-1</sup> for DP-2 and 3043 cm<sup>-1</sup> for DP-3 respectively.

#### 4.B.2.1.3.2 C-O stretching vibration

For the studied compounds, the C=O stretching frequency is an important stretching vibration. The C=O stretching vibration for the studied compounds were found at 1790.21 cm<sup>-1</sup> for DP-1, 1790.76 cm<sup>-1</sup> for DP-2 and 1791.55 cm<sup>-1</sup> for DP-3 respectively. The experimental C=O stretching vibration for these compounds were found at 1666 cm<sup>-1</sup> for DP-1, 1667 cm<sup>-1</sup> for DP-2 and 1635 cm<sup>-1</sup> for DP-3.

#### 4.B.2.1.3.3. N-H stretching vibration

N-H stretching vibration is an important stretching vibration for the studied compounds (DP-1 to DP-3). For the compound DP-1, the theoretical N-H stretching vibration was found at 3639 cm<sup>-1</sup>, for DP-2 it was found at 3632 cm<sup>-1</sup> and for DP-3 it was found at 3633 cm<sup>-1</sup>. The experimentally determined N-H stretching vibration for DP-1 was assigned at 3009 cm<sup>-1</sup>, for DP-2 it was found at 3444 cm<sup>-1</sup> and for DP-3 the N-H stretching vibration was found at 3455 cm<sup>-1</sup> respectively.

#### 4.B.2.1.3.4. Aromatic C-C stretching vibration

Generally, the bands observed in the range 1650-1400 cm<sup>-1</sup> are assigned to C-C stretching mode of aromatic derivatives<sup>54</sup>. In our present study, the range for theoretically calculated C-C stretching vibrational mode showing sharp bands are in the range 1637-1555 cm<sup>-1</sup>, 1622-1587cm<sup>-1</sup> and 1621-1586 cm<sup>-1</sup> for DP-1, DP-2 and DP-3 respectively (Table 4.B.3). Experimentally, the aromatic C-C stretching frequencies for the studied compounds observed in the range 1629-1531 cm<sup>-1</sup> in DP-1, 1625 cm<sup>-1</sup> in DP-2, and 1474 cm<sup>-1</sup> for DP-3 respectively.

Thus, from the above discussions, it is evident that the theoretically calculated vibrational frequency matched well with the experimental results for the studied compounds (Fig. 4.B.6).

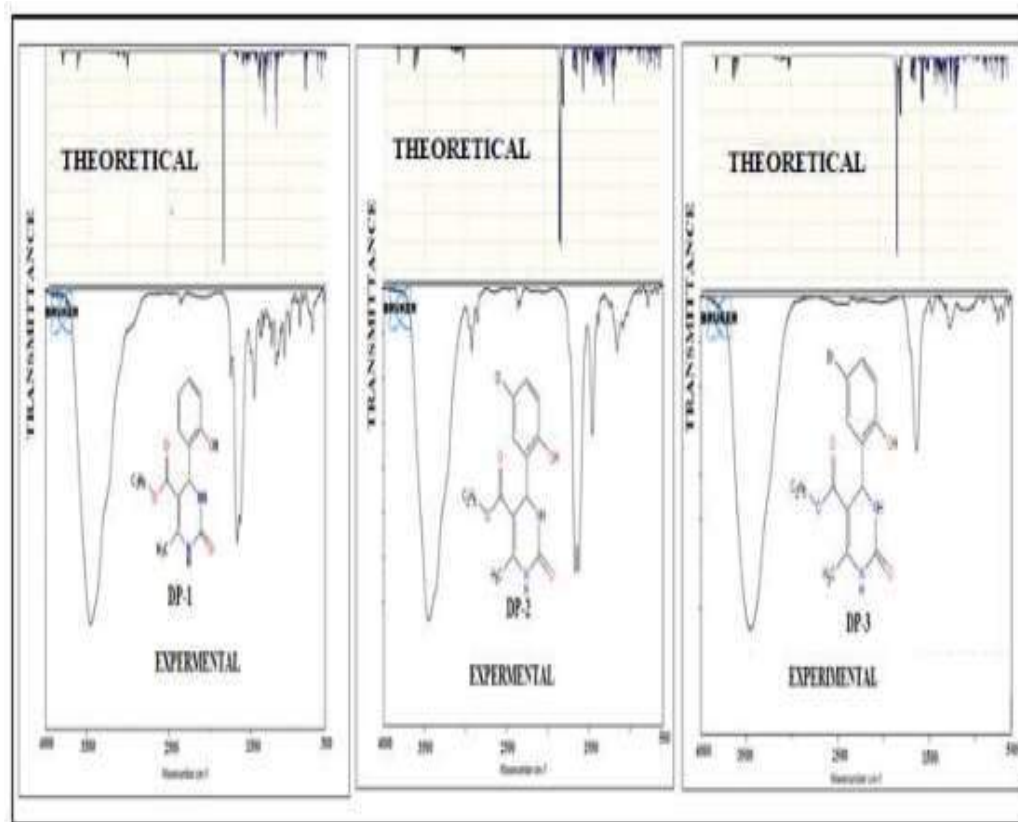
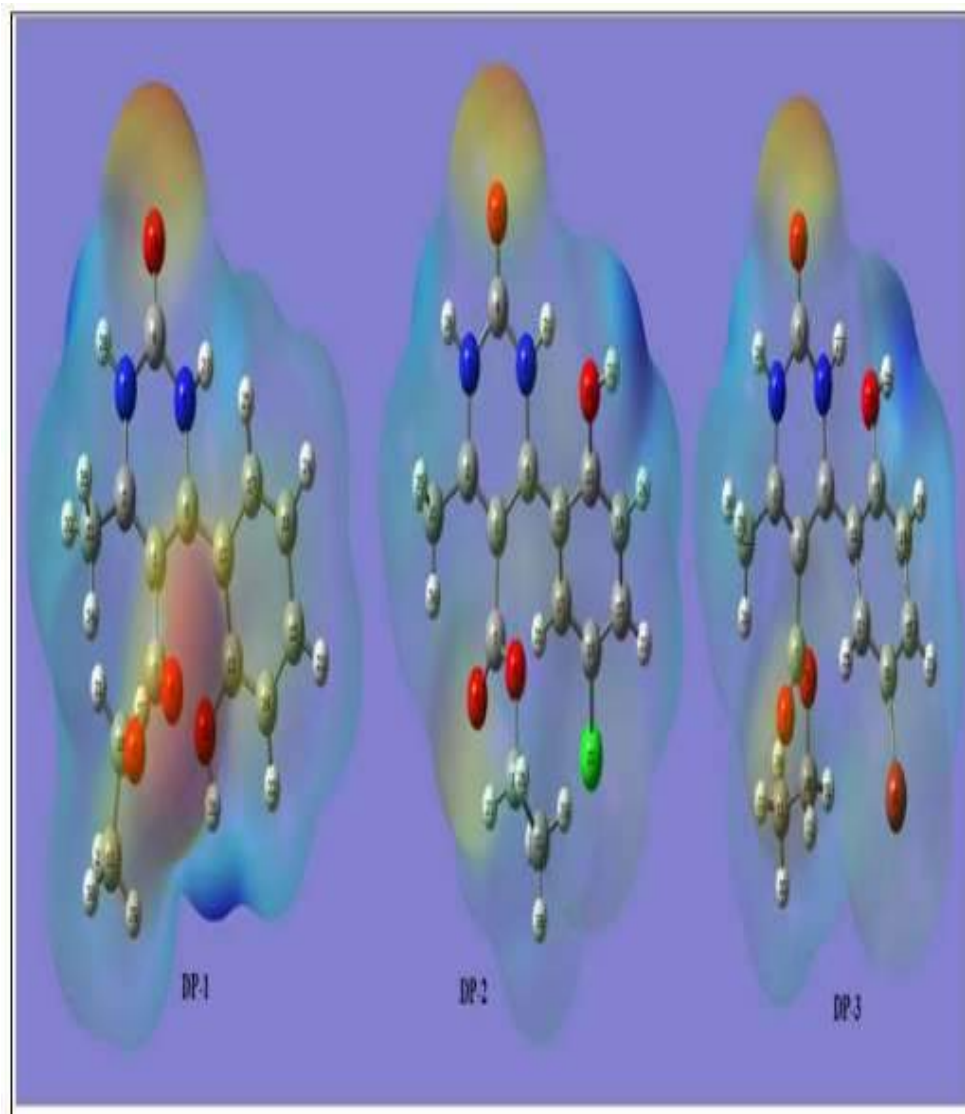


Fig. 4.B.6. Theoretical and experimental FTIR spectra of DP-1 to DP-3

#### 4. B.2.1.4 Molecular Electrostatic Potential (MEP)

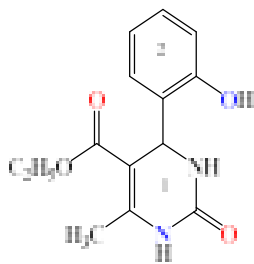
In chemical systems, the electrostatic potential around molecules is an important parameter for assessing and correlating the molecular structure and their physicochemical properties<sup>55</sup>. Moreover, MEP helps in understanding the sites of electrophilic and nucleophilic reactions, along with hydrogen bonding interactions<sup>56</sup>. To analyze the reactive sites of electrophilic and nucleophilic attack for the compounds under study (DP-1 to DP-3), Molecular Electrostatic Potentials at B3LYP/631G+ (d, 2p) was calculated. The electrostatic potentials at the MEP surfaces are given by different colors like red, blue and green. Red, blue and green colour represents the region of most negative, most positive and zero electrostatic potential respectively. Thus, the electrostatic potential increases in the order blue > green > yellow > orange > red. The most negative electrostatic potential (red, orange and yellow region) in the MEP surface is assigned for the electrophilic reaction sites and the positive (blue) region corresponds to nucleophilic reaction site<sup>57-58</sup>. The MEP surface of the studied compounds (DP-1 to DP-3) is depicted in Fig.4.B.7. A detailed description of the MEP surface indicating the region of negative/ electrophilic reaction sites and positive/nucleophilic reaction site for the studied compounds (DP-1 to DP-3) are listed in Table 4.B.4.





**Fig. 4.B.7.** MEP plots of studied compounds (DP-1 to DP-3)

**Table. 4.B.4.** Detailed description of MEP surface for compounds DP-1 to DP-3

Entry	Negative region (red, orange, yellow)/Electrophilic reaction site	Positive region (blue)/ Nucleophilic reaction site
	<b>DP-1</b> -OH group of 2-phenyl ring and O19,O8,O9 of the DHPM nucleus 1	N5-H27(1), N3-H20(1), H26 (2) and C21-H34,H35,H33 of the DHPM nucleus (1) and H26 of the phenyl ring 2
	<b>DP-2</b> O19, O8 of DHPM nucleus1	N5-H31(1), N3-H20(1), H32 of the O18-H32 group and C21-H34, H35,H33 of the DHPM nucleus (1)
	<b>DP-3</b> O19, O8 of DHPM nucleus1	N3-H20, C21-H28,H29,H30, of DHPM nucleus1 and -O18H25 group of phenyl ring2

#### 4.B.2.1.2.5 NLO properties

Nonlinear optical phenomenon is generally caused by the interaction of materials with electromagnetic fields, resulting in altered wave numbers, phases, or other physical properties of the electromagnetic field<sup>59</sup>. Organic molecules having extended  $\pi$ - conjugation with delocalized electrons and intra molecular charge transfer from donor to acceptor orbital through  $\pi$ -spacer generally show a rapid response to light and have strong NLO properties<sup>60</sup>. Organic molecules having good non-linear properties are widely used in the field of organic light emitting diodes, transistors and dye sensitized solar cells<sup>61</sup>

Theoretically, the NLO properties of the given compound is calculated by determining the parameters such as magnitude of dipole moment ( $\mu$ ), polarizability ( $\alpha$ ), anisotropy of polarizability ( $\Delta\alpha$ ), first hyperpolarizability ( $\beta$ ) and second order hyperpolarizability ( $\gamma$ ). The polarizability tensors are calculated using the following relations<sup>62</sup>

$$\text{Dipole moment } \mu = (\mu_x^2 + \mu_y^2 + \mu_z^2)^{1/2} \dots\dots\dots (1)$$

$$\alpha(\text{total}) \text{ or } \langle \alpha \rangle = \frac{1}{3} (\alpha_{xx} + \alpha_{yy} + \alpha_{zz}) \dots\dots\dots (2)$$

$$\Delta\alpha = 1/\sqrt{2} [(\alpha_{xx} - \alpha_{yy})^2 + (\alpha_{yy} - \alpha_{zz})^2 + (\alpha_{zz} - \alpha_{xx})^2 + 6(\alpha_{xy}^2 + \alpha_{xz}^2 + \alpha_{yz}^2) ]^{1/2} \dots\dots\dots (3)$$

$$\beta_x = \beta_{xxx} + \beta_{xyy} + \beta_{xzz} \dots\dots\dots (4)$$

$$\beta_y = \beta_{yyy} + \beta_{yzz} + \beta_{yxx} \dots\dots\dots (5)$$

$$\beta_z = \beta_{zzz} + \beta_{zxx} + \beta_{yyz} \dots\dots\dots (6)$$

$$\beta_{\text{total}} = (\beta_x^2 + \beta_y^2 + \beta_z^2)^{1/2} \dots\dots\dots (7)$$

$$\langle \gamma \rangle \text{ or } \gamma_{\text{total}} = 1/5 (\gamma_{xxxx} + \gamma_{yyyy} + \gamma_{zzzz} + 2(\gamma_{xxyy} + \gamma_{yyzz} + \gamma_{xxzz})) \dots\dots\dots (8)$$

The nonlinear optical properties such as dipole moments, dipole polarizabilities, first- and second order hyperpolarizabilities of the studied compounds (DP-1 to DP-3) were calculated by B3LYP/ 6-31G + (d, 2p) basis set and the computed results are listed in Table 4.B.5.

**Table. 4.B.5.** Computed Dipole moments, dipole polarizabilities and anisotropic Polarizabilities and first-order hyperpolarizabilities of compounds DP-1 to DP-3

<b>Dipole moments, dipole polarizabilities and anisotropic polarizabilities</b>				
<b>Entry</b>	<b>DP-1</b>	<b>DP-2</b>	<b>DP-3</b>	<b>Ref.</b>
$\mu_x$	-1.1327	-3.0611	0.2975	0
$\mu_y$	-2.6007	0.1471	2.6826	-4.06
$\mu_z$	-2.1905	-0.3033	-0.3464	0.0018
<b><math>\mu</math></b>	<b>3.5840</b>	<b>3.0796</b>	<b>2.7212</b>	<b>4.06</b>
$\alpha_{xx}$	-94.9715	-149.803	-159.27	-16.62
$\alpha_{yy}$	-126.959	-106.795	-109.169	-24.64
$\alpha_{zz}$	-127.257	-134.888	-140.665	-27.03
$\alpha_{xy}$	-1.4797	18.461	15.8639	-0.0003
$\alpha_{xz}$	-1.4248	0.4048	-0.0525	-0.07
$\alpha_{yz}$	15.2026	-1.4331	-1.5948	0.01
<b><math>\alpha_{tot} \times 10^{-24}(\text{esu})</math></b>	<b>-17.249</b>	<b>-19.266</b>	<b>-20.209</b>	<b>-3.37</b>
<b><math>\Delta\alpha \times 10^{-24} (\text{esu})</math></b>	<b>6.179</b>	<b>7.350</b>	<b>7.681</b>	<b>1.39</b>
<b>First order hyperpolarizabilities</b>				
$\beta_{xxx}$	-26.36	-68.10	-157.70	-0.002
$\beta_{xyy}$	25.66	-42.54	-48.73	-0.0004
$\beta_{xzz}$	-16.98	3.72	-28.344	0.001
$\beta_{yyy}$	-125.62	-77.15	-51.36	-16.94
$\beta_{xxy}$	3.44	73.77	98.76	-0.63
$\beta_{yzz}$	2.49	8.88	12.02	2.05
$\beta_{zzz}$	-14.93	-1.43	-4.43	-0.01
$\beta_{xxz}$	8.75	-4.99	-4.12	-0.09
$\beta_{yyz}$	7.03	-1.69	-1.51	-0.03
$\beta_{xyz}$	-10.75	4.48	2.97	0.05
<b><math>\beta_{total} \times 10^{-30}</math> (esu)</b>	<b>1.045</b>	<b>0.927</b>	<b>2.094</b>	<b>0.13</b>

A comparative study of the dipole moment in the studied system indicates that they have different charge distributions for different directions. The theoretically calculated dipole moments of the studied compounds are 3.58D (DP-1), 3.079D (DP-2), 2.721D (DP-3) respectively and the dipole moment follows the order DP-1 > DP-2 > DP-3.

The compounds DP-1, DP-2 and DP-3 have dipole moment value less than the dipole moment value of urea (4.06 D) reference. Also, the total dipole polarizabilities value of the studied compounds along all three directions is listed in Table 4.B.5. From the Table 4.B.5, it is evident that the dipole polarizability of the studied compounds follows the order DP-3( $-20.209 \times 10^{-24}$ ) > DP-2( $-19.266 \times 10^{-24}$ ) > DP-1( $-17.249 \times 10^{-24}$ ).

The theoretically computed first-order hyperpolarizabilities and their individual components for the studied compounds (DP-1 to DP-3) are listed in Table 4.B.6. From the Table 4.B.5, it is evident that the first-order hyperpolarizability of the studied compounds are  $1.045 \times 10^{-30}$  esu,  $0.927 \times 10^{-30}$  esu and  $2.094 \times 10^{-30}$  esu for compounds DP-1, DP-2 and DP-3 respectively. A comparison of the first-order hyperpolarizability value of the studied compounds with the standard reference urea ( $0.13 \times 10^{-30}$  esu) have shown that the studied compounds have far greater value of first-order hyperpolarizability value than urea. Thus, the order for the first-order hyperpolarizability of the studied compounds are DP-3 > DP-1 > DP-2.

The second order hyperpolarizabilities of the compounds DP-1 to DP-3 are given in Table 4.B.6. The second order hyperpolarizability of the studied compounds are  $-0.877 \times 10^{-36}$  esu,  $-1.129 \times 10^{-36}$  esu and  $-1.670 \times 10^{-36}$  esu for DP-1, DP-2 and DP-3 respectively.

**Table. 4.B.6.** Second order hyperpolarizabilities of studied compounds DP-1 to DP-3

Second order hyperpolarizabilities							
Entry	$\gamma_{xxxx}$	$\gamma_{yyyy}$	$\gamma_{zzzz}$	$\gamma_{xxyy}$	$\gamma_{yyzz}$	$\gamma_{xxzz}$	$\gamma_{total}$ (x $10^{-36}$ ) esu
DP-1	-3558.66	-3133.59	-635.75	-86.88	174.92	-779.3	-0.87
DP-2	-5633.49	-3064.38	-191.64	443.58	-680.33	-924.5	-1.12
DP-3	-6568.69	-3064.22	-201.93	-1639.22	-683.36	-1050	-1.67
Urea	-120.66	-117.90	-29.39	-44.02	-28.01	-39.86	-0.04

The order of second-hyperpolarizability of the studied compounds is given by DP-3 > DP-2 > DP-1 and from the Table 4.B.6, it is evident that the second-order

hyperpolarizability of the studied compounds are much greater than the reference NLO material urea.

From the above discussion, it is evident that the studied molecule DP-1 to DP-3 have shown greater value of nonlinear optical parameters than the reference urea molecule and we may infer that this set of molecules could act as a better nonlinear optical material.

#### 4.B.2.2 Molecular Docking Study

Type-2 diabetes mellitus is a condition where there is an elevation of glucose level in the blood (hyperglycemia) or an elevation in the insulin levels in the blood (hyperinsulinemia)<sup>63</sup>. Among various available therapies for type-2 diabetes mellitus, Sodium glucose co-transporter 2 (SGLT2) inhibitors are very popular class of drugs which is used to control hyperglycemia<sup>64</sup>

Molecular Docking studies now days have become an essential tool for drug design and provides helpful information about various interactions between the ligand and the protein in a faster and cost-effective way<sup>62,65</sup>. In this chapter, we have reported the molecular docking study of the selected 3,4 Dihydropyrimidine-2-[1H]-one derivatives against the protein 3DH4.

The protein 3DH4 structure has often been used in homology studies for the inhibition of sodium-dependent glucose transporters (SGLTs). The protein has an approximately 3.0 Å structure that contains 14 transmembrane helices in an inward facing conformation with a core structure of inverted repeats of 5 TM helices (TM2 – TM6 and TM7 – TM11). Galactose can be found bound to the center of the core, kept in place away from the outside by hydrophobic residues.

##### 4.B.2.2.1 Visualization of the Docking Result

Molecular docking study of the compounds (DP-1 to DP-3) against the protein 3DH4 has been carried out using GUI interface programme of Autodock Tools (MGL tool or Molecular Graphics Laboratory tool developed by Scripps research Institute<sup>66</sup>). The docking results have been visualized with the help of Biovia Discovery Studio 2020 (DS), version 21.1.0.20298 and Edu Pymol version 2.5.2.

After successful docking of the compounds (DP-1 to DP-3) with the protein 3DH4, the docking result showed different types of protein-ligand interactions with particular binding energies. For better understanding of fitting of the ligand into the binding pocket of the protein, ligands are shown as blue green stick. The hydrogen bonding interactions between ligands and protein are shown by green dash line, the  $\pi$ -sulfur interaction as yellow dash line,  $\pi$ -anion/ $\pi$ -cation interactions as orange dash line,  $\pi$ -sigma interactions as purple dash line,  $\pi$ - $\pi$  stacking/  $\pi$ - $\pi$  T-shaped interactions as dark pink dash line and  $\pi$ -alkyl interactions as light pink dash line respectively. The binding energy ( $\Delta G$ ) and the predicted inhibitory constant ( $pK_i$ ) of the studied compounds (DP-1 to DP-3) are found to be -6.9 Kcal/mole (DP-1), -

7.9 Kcal/mole (DP-2), -6.1 Kcal/mole (DP-3) respectively and 6.85  $\mu\text{M}$ , 1.23  $\mu\text{M}$ , and 27.22  $\mu\text{M}$  respectively (Table 4.B.7)

**Table. 4.B.7.** Summary of docking of the compound (IM-1 to IM-6) against insulin receptor protein IIR3 with corresponding binding energy ( $\Delta G$ ), predicted inhibitory constant ( $\text{pK}_i$ ), interacting amino acid residues and type of interactions.

Ligands	Binding Energy (kcal/mol)	Predicted inhibitory constant ( $\text{pK}_i$ ) $\mu\text{M}$	Amino Acid residues	Types of interactions
DP-1	-6.9	6.85	Phe133, Tyr430, Leu433, Ile464, Val434	$\pi$ - $\pi$ T-shaped, Alkyl, $\pi$ - Alkyl $\pi$ -Sigma
DP-2	-7.9	1.23	Phe479, Met244, Met477, Lys471	Conventional H-bonding, Unfavorable Acceptor-Acceptor, $\pi$ -Donor Hydrogen Bond, Carbon H-bond
DP-3	-6.1	27.22	Glu68, Gln69, Asn142, Asn267, Leu137, Tyr263	Conventional H-bonding, Alkyl, $\pi$ - Alkyl, Halogen (Cl, Br)

The visualization of the docking result of compound DP-1 with the protein 3DH4 showed that the ligand fits into a pocket region present in the outer regions of the protein surface (Fig. 4.B.7). A close analysis of the docking result revealed that the ligand interacts with the protein with binding energy ( $\Delta G$ ) value of -6.9 Kcal/mole and predicted inhibitory constant ( $\text{pK}_i$ ) 6.85 $\mu\text{M}$ . The main interactions between the ligand DP1 and the protein were characterized by different interactions between  $\pi$  – electron of the ligand and different amino acid residues. A  $\pi$ - $\pi$  T-shaped interaction is observed between the phenyl ring of the amino acid residue Phe133 and the phenyl ring of the ligand DP-1 at a distance of 5.00 Å. A  $\pi$ -sigma interaction occurs between the sigma electron of isopropyl group of amino acid residue Val434 and  $\pi$ -electron of the phenyl ring of the ligand DP-1 at a distance 3.80 Å. In addition, there are three  $\pi$ -alkyl interactions also observed between the ligand DP-1 and the protein. The first and second  $\pi$ -alkyl interactions exist between the  $\pi$ -electron of the phenyl ring of ligand DP-1 and alkyl group of amino acid residue Ile464 and Leu433 at 5.09 Å and 5.32 Å respectively. The third  $\pi$ -alkyl interaction was observed between the  $\text{CH}_3$  (6) group of the ligand DP-1 and the  $\pi$ -electron of phenyl ring of amino acid residue Tyr430 at 4.72 Å.

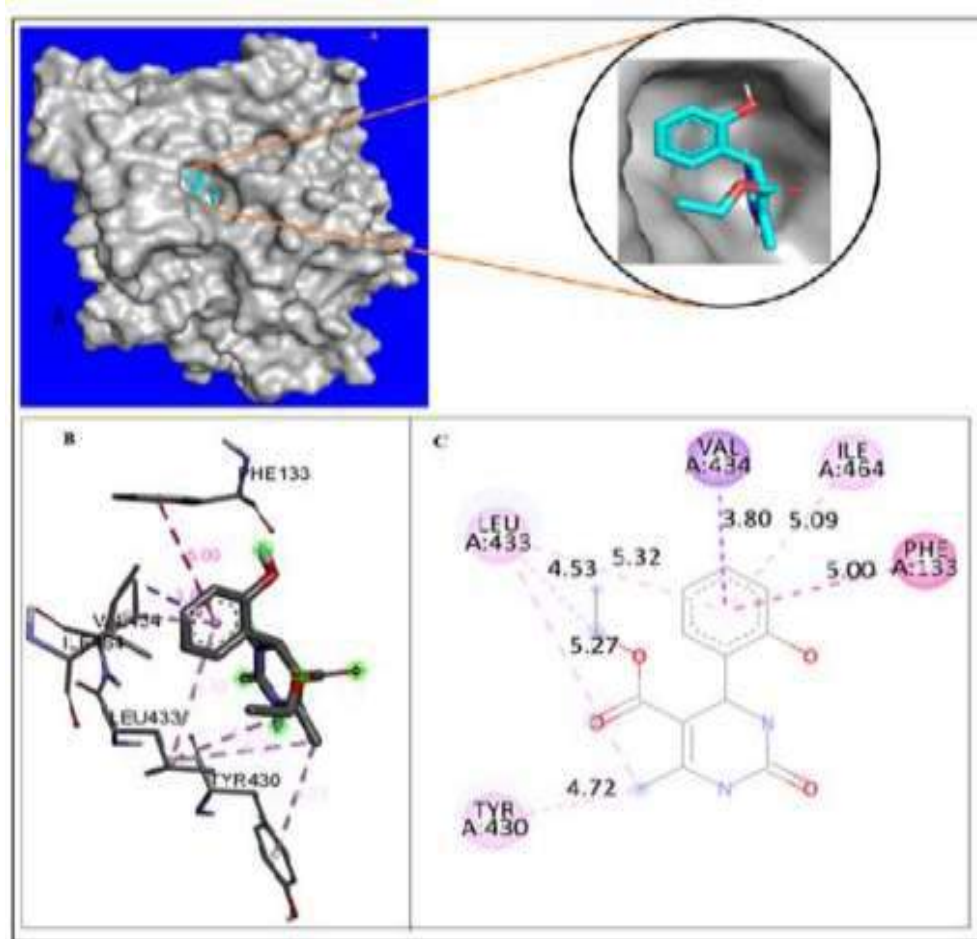


**Fig 4.B.8.** Visualisation of docking results of ligand DP-1 within a receptor site in the protein 3DH4: (A) Optimal binding mode of the protein with DP-1 ligand (Ligand DP-1 shown as blue and green stick model). (B) Amino acid residues involved in different interactions (purple dash lines show  $\pi$ -sigma interactions, dark pink lines show  $\pi$ - $\pi$  T-shaped interaction, and light pink dash lines show alkyl and  $\pi$ -alkyl interactions). (C) 2D representation of binding interaction of ligand DP-1 with different amino acid residues of the protein 3DH4.

Visualization of the docking results of the ligand DP-2 with the protein receptor 3DH4 revealed that the ligand fits into a pocket region present in the core region of the protein with the highest binding energy ( $\Delta G$ ) value of -7.9 kcal/mol and the predicted inhibitory constant ( $pK_i$ ) value of 1.23 $\mu$ M. The major interactions between the ligand DP-2 and the protein receptor are characterized by four major conventional hydrogen bonding. These hydrogen bonding are i) between C=O group of the amino residue Glu68 and the -NH group of the ligand DP-2 at a distance of 2.37 Å, ii) between the -NH<sub>2</sub> group present in the amino acid Gln68 and the C=O group of the of the DHPM nucleus of the ligand at a distance of 2.46Å, iii) between the -NH<sub>2</sub> group of the amino acid Asn142 and the carbonyl oxygen atom of the -COOEt group present on the DHPM nucleus at a distance of



2.80 Å, and iv) between the -NH<sub>2</sub> group of the residue Asn267 and the ethereal oxygen of the -COOEt group present on the DHPM nucleus at a distance of 2.95 Å respectively (Fig.4.B.8).  $\Pi$ -alkyl interaction was observed between the phenyl ring of the amino acid residue Leu137 and the methyl group (6) of the DHPM nucleus at a distance of 4.57 Å. A halogen induced interaction between the C=O group of the residue Tyr263 and the Cl atom of the ligand DP-2 was observed at a distance of 3.15 Å.

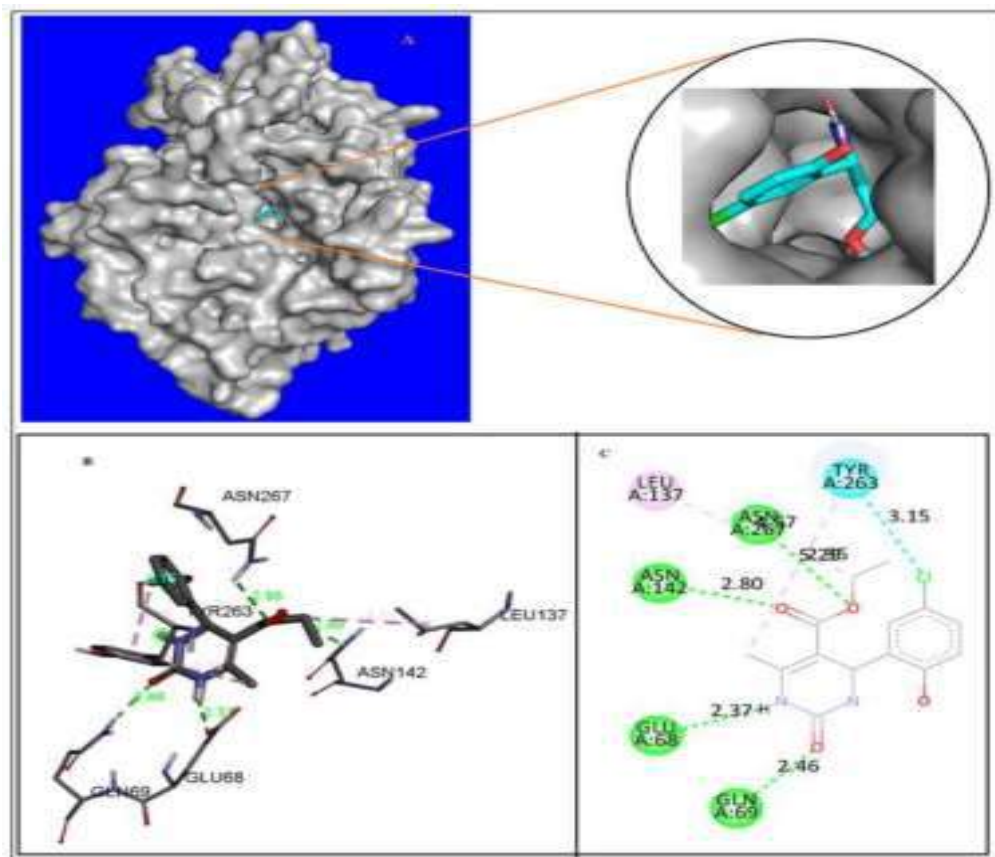


**Fig. 4.B.9.** Visualisation of docking results of ligand DP-2 with receptor protein 3DH4: (A) Optimal binding mode of the protein with DP-2 ligand (Ligand DP-2 shown as blue and green stick model). (B) Amino acid residues involved in different interactions (green dash lines show conventional hydrogen bonding interactions, light blue dash lines show halogen induced interactions, and light pink dash lines show alkyl and  $\pi$ -alkyl interactions). (C) 2D representation of binding interaction of ligand DP-2 with different amino acid residues of the protein 3DH4.

Analysis of the docking results of the ligand DP-3 with the protein receptor 3DH4 showed high interaction affinity whereby the ligand fits into a pocket region of the protein present in the outer regions of protein with a binding energy ( $\Delta G$ ) value of -6.1 kcal/mole and predicted inhibitory constant ( $pK_i$ ) of 27.22  $\mu$ M. The main interactions between the ligand DP-3 and the protein have been characterized

by two conventional hydrogen bonding between the -NH group of the residue Phe479 and the carbonyl group of the DHPM nucleus of the ligand at a distance of 2.21Å, and between the C=O group of the residue Met477 and the NH group of the ligand DP-3 at a distance of 2.25Å respectively (Fig.4.B.9). Two unfavorable acceptor-acceptor interaction was encountered between the C=O group of the residue Met244 and the carbonyl group of the ligand DP-3 at a distance of 3.00Å and between the C=O group of the residue Lys471 with the oxygen atom present in the phenyl ring of the ligand DP-3 at a distance of 2.89Å. In addition, a  $\pi$ -donor hydrogen bonding interaction was also observed between the -NH group of the residue Met477 and the  $\pi$ -electron of phenyl ring of the ligand DP-3 at a distance of 2.99Å.

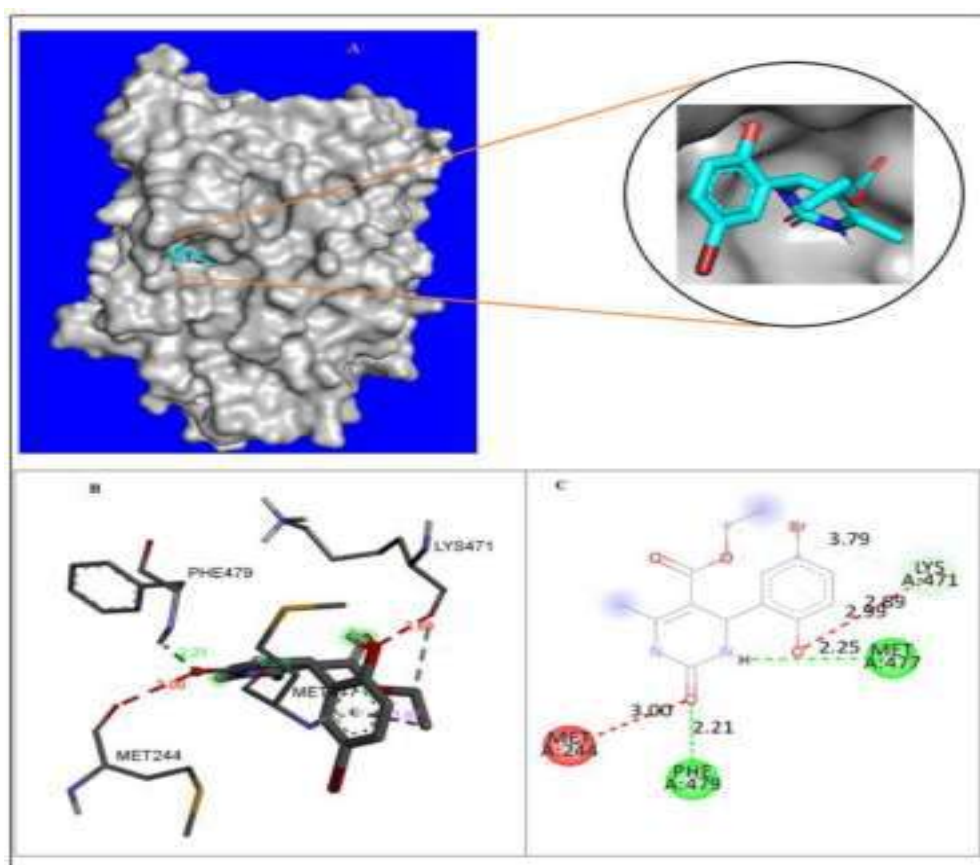


**Fig. 4.B.10.** Visualisation of docking results of ligand DP-3 within a receptor site in the protein 3DH4: (A) Optimal binding mode of the protein with DP-3 ligand (Ligand DP-3 shown as blue and green stick model). (B) Amino acid residues involved in different interactions (green dash lines show conventional hydrogen bonding interactions, light green dash lines depict carbon hydrogen bonding and  $\pi$ -donor hydrogen bonding interactions, and red dash lines show unfavourable acceptor-acceptor interactions). (C) 2D representation of binding interaction of ligand DP-3 with different amino acid residues of the protein 3DH4.

#### 4.B.2.3 In silico Pharmacokinetic analysis of DP-1 to DP-3

The pharmacokinetic properties like absorption, distribution, metabolism, excretion and toxicity (ADMET) are fundamental properties in determining the drug likeness of any compounds prior to its clinical and animal studies. Therefore, ADMET property of the studied compounds plays an important role in categorizing them as a drug candidate as well as their activity inside the body<sup>67</sup>. The ADMET parameters provide useful information about the concentrations of the drug in the different parts of the body with respect to time<sup>68</sup>. ADMET properties such as gastrointestinal absorption (GI), water solule capability (Log s), lipophilicity (Log Po/W), CYP1A2 inhibitor and Blood-Brain Barrier (BBB) are fundamentally important for any studied compounds to be considered them as a drug candidate<sup>69</sup>. Therefore, the pharmacokinetic properties of the selected 2, 4, 5-triarylimidazole derivatives (IM-1 to IM-6) have been computed with the help of computer aided online SwissADME database (<http://www.swissadme.ch>) and the result of the pharmacokinetic properties along with the Lipinski's property are listed in Table 4.B.8

From the table it is evident that all the studied compounds (DP-1 to DP-3) with bioavailability score in the range of 55% have lipophilicity value (Log Po/W) in the range 1.14-1.79 and has good gastrointestinal absorption. The high and positive value of lipophilicity (LogPo/w) for the studied compounds indicated that the compounds are more lipophilic and these compounds could easily pass through the lipid bilayer of most cellular membrane. From the solubility (Log S) values of the studied compounds which falls in the range of -2.15 to -3.07 it can be said that all the studied compounds are soluble in water. However, the studied compounds do not have any BBB and CYP1A2 properties. It can also be clearly seen that all these compounds have no violations of Lipinski's rule and can be qualified as a potential candidate for a drug.

**Table. 4.B.8.** Lipinski's properties and pharmacokinetic properties (ADME) of studied compounds DP-1 to DP-3

<b>COMPOUNDS</b>			
<b>Properties</b>	<b>DP-1</b>	<b>DP-2</b>	<b>DP-3</b>
<b>Molecular weight (gm/mole)</b>	276.29	310.73	355.18
<b>Rotatable bonds</b>	4	4	4
<b>H-bond acceptor</b>	4	4	4
<b>H-bond donor</b>	3	3	3
<b>Violations</b>	0	0	0
<b>Log Po/W</b>	1.14	1.71	1.79
<b>Log S</b>	-2.15(S)	-2.75(S)	-3.07
<b>GI</b>	High	High	High
<b>BBB</b>	No	No	No
<b>CYP1A2</b>	No	No	No
<b>Bioavailability Score</b>	0.55	0.55	0.55
<b>Topological Surface Area (A<sup>2</sup>)</b>	87.66	87.66	87.66

\*MS: Moderately soluble, PS: Partially soluble, BBB: Blood-Brain Barrier, CYP: Cytochrome P450, GI: Gastrointestinal absorption

#### 4. B.2.4 Computational details

##### 4.B.2.4.1 DFT study

All Quantum Mechanical calculations were carried out on a hp-Z640 desktop P.C. with an Intel Xeon processor (Specifications: E5-2630 V4 @ 220GHz) using Gaussian 16 W package. Density functional theory (DFT) with Becke's (B)three parameter hybrid model, Lee, Yang and Parr's (LYP) using 631G+(d,2p) basis set has been employed to optimize the geometry of the 3,4-dihydropyrimidin-(2H)-one derivatives (DP-1 to DP-3).

A set of theoretical calculations of selected compounds (DP-1 to DP-3) were performed with Gaussian 16W, Revision A.03 programme package using B3LYP/631G+(d,2p) basis sets to optimize geometry and minimize energy for faster and accurate calculations. With the optimized geometry, theoretical Raman and IR spectra were also calculated from the so chosen basis set. From the optimized geometry, the energy of HOMO and LUMO molecular orbitals along with the energy of HOMO-LUMO gap has also been measured. For analyzing the result of the theoretical calculations, a visual representation was obtained by Gauss View program6 and it has been used to construct the molecular electrostatic

potential surface (MESP) as well as the shape of HOMO and LUMO molecular orbitals. Also, nonlinear Optical property (NLO) of the selected 3,4-dihydropyrimidin-(2H)-one derivatives have also been calculated taking urea as a reference NLO material.

#### 4.B.2.4.2 Preparation of Protein and ligand for docking Study

The X-ray crystallographic structures of phosphorylated insulin receptor tyrosine kinase protein (PDB 3DH4) has been downloaded from the Protein Data Bank (PDB) (<http://www.pdb.org>) database. Graphical User Interface program “Auto Dock Tools (ADT) 1.5.6” from Molecular Graphics Laboratory (MGL) developed by Scripps Research Institute has been used for the preparation of protein for docking study<sup>66</sup>. Input file of receptor protein for the blind docking study were created by taking specific chain (Chain A) of the protein (3DH4). In a typical receptor protein preparation, water molecules and hetero atoms along with the co-crystallized ligands in PDB crystal structure was removed and subsequently, the receptor. pdbqt file has been prepared by adding polar hydrogen atoms and Kollman united atom charges<sup>62,65</sup>. The three-dimensional (3D) structures of ligands (DP-1 to DP-3) were drawn using Chemsketch (ACD/Structure Elucidator, version 12.01, Advanced Chemistry Development, Inc., Toronto, Canada, 2014, <http://www.acdlabs.com>) and geometry optimization of the ligands (DP-1 to DP-3) were carried out using MM2 program incorporated in Chem. Draw Ultra 8.0 and further optimization of geometry of each molecule were carried out with the MOPAC 6 package using the semi-empirical AM1 Hamiltonian<sup>70</sup>. The input .pdbqt file of the ligands was generated using Auto Dock Tools (ADT). As the ligand molecules (DP-1 to DP-3) were non peptides, therefore, Gasteiger charge was assigned and then non-polar hydrogen was merged.

#### 4.B.2.4.3 Molecular docking study using Autodock vina

All molecular docking calculations of the studied ligands (DP-1 to DP-3) with protein 3DH4 were carried out in the AutoDock Vina programme 1.1.2 developed by Scripps Research institute<sup>71-72</sup> and the results of the docking study and the intermolecular interactions between receptors protein and the ligand molecules were analyzed using BIOVIA Discovery Studio 2020 (DS), version 20.1.0.0 (Dassault Systèmes BIOVIA, Discovery Studio Modeling Environment, Release 2017, San Diego: Dassault Systèmes, 2016) and Edu pymol version 1.7.4.4<sup>72</sup>. The three-dimensional (3D) affinity (grid) maps and electrostatic a grid boxes of 80×80×80 Å grid points and grid centre (X, Y, Z) of 28.108, -43.008, 59.313 with a spacing of 1.00 Å generated by AutoGrid auxiliary program for each of the receptor protein for blind docking were generated to cover the entire active site of the receptor protein in order to eliminate biasness arising during the docking simulation<sup>73</sup>. Lamarckian genetic algorithm and a standard protocol with default setting of other run parameters were used for docking simulation. For each docking experiments, several runs were performed by the program with one predicted binding mode with each run. All the torsions were allowed to rotate. The predicted

inhibitory constant (**pK<sub>i</sub>**) has been calculated using the following standardized equation<sup>74</sup>

$$pK_i = 10^{\frac{\text{Binding Energy Score}}{1.336}}$$

#### **4.B.2.4.4 Pharmacokinetic study**

The pharmacokinetic properties like absorption, distribution, metabolism, excretion and toxicity (ADMET) of the compounds (IM-1 to IM-6) have been studied using the computer aided online SwissADME database (<http://www.swissadme.ch>)

## 4.B.3 References

- (1) P. Biginelli., *Gazzetta Chimica Italiana*, **1893**, 23 (1), 360–413.
- (2) I. S. Zorkun, S. Saraç, S. Çelebi, K. Erol., *Bioorganic & Medicinal Chemistry*, **2006**, 14 (24), 8582–8589.
- (3) K. S. Atwal, G. C. Rovnyak, B. C. O'Reilly, J. Schwartz., *Journal of Organic Chemistry*, **1989**, 54 (25), 5898–5907.
- (4) Z. Maliga, T. M. Kapoor, T. J. Mitchison., *Chemistry & Biology*, **2002**, 9 (9), 989–996.
- (5) S. DeBonis, J. P. Simorre, I. Crevel, L. Lebeau, D. A. Skoufias, A. Blanzzy, C. Ebel, P. Gans, R. Cross, D. D. Hackney, R. H. Wade, F. Kozielski., *Biochemistry*, **2003**, 42 (2), 338–349.
- (6) K. S. Atwal, B. N. Swanson, S. E. Unger, D. M. Floyd, S. Moreland, A. Hedberg, B. C. O'Reilly., *Journal of Medicinal Chemistry*, **1991**, 34 (2), 806–811.
- (7) M. Brands, R. Endermann, R. Gahlmann, J. Krüger, S. Raddatz., *Bioorganic & Medicinal Chemistry Letters*, **2003**, 13 (2), 241–245.
- (8) M. M. Ghorab, S. M. Abdel-Gawad, M. S. A. El-Gaby., *Il Farmaco*, **2000**, 55 (4), 249–255.
- (9) C. Oliver Kappe, W. M. F. Fabian, M. A. Semones., *Tetrahedron*, **1997**, 53 (8), 2803–2816.
- (10) A. D. Patil, N. V. Kumar, W. C. Kokke, M. F. Bean, A. J. Freyer, C. de Brosse, S. Mai, A. Trunch, D. J. Faulkner, B. Carte, A. L. Breen, R. P. Hertzberg, R. K. Johnson, J. W. Westley, B. C. M. Potts., *Journal of Organic Chemistry*, **1995**, 60 (5), 1182–1188.
- (11) S. K. Sam, S. C. Bo, H. L. Jae, K. L. Ki, H. L. Tae, H. K. Young, H. Shin., *Synlett*, **2009**, 2009 (4), 599–602.
- (12) K. Yamamoto, Y. G. Chen, F. G. Buono., *Organic Letters*, **2005**, 7 (21), 4673–4676.
- (13) X. Wang, Z. Quan, Z. Zhang., *Tetrahedron*, **2007**, 63 (34), 8227–8233.
- (14) X.-C. Wang, Z.-J. Quan, Z. Zhang, Y.-J. Liu, P.-Y. Ji., *Letters in Organic Chemistry*, **2007**, 4, 370–373.
- (15) R. Pérez, T. Beryozkina, O. I. Zbruyev, W. Haas, C. O. Kappe., *Journal of Combinatorial Chemistry*, **2002**, 4 (5), 501–510.
- (16) A. Lengar, C. O. Kappe., *Organic Letters*, **2004**, 6 (5), 771–774.

- (17) B. Khanetsky, D. Dallinger, C. O. Kappe., *Journal of Combinatorial Chemistry*, **2004**, 6 (6), 884–892.
- (18) A. D. Bochevarov, M. A. Watson, J. R. Greenwood, D. M. Philipp., *Journal of Chemical Theory and Computation*, **2016**, 12 (12), 6001–6019.
- (19) M. Mutailipu, Z. Xie, X. Su, M. Zhang, Y. Wang, Z. Yang, M. R. S. A. Janjua, S. Pan., *J Am Chem Soc*, **2017**, 139 (50), 18397–18405.
- (20) A. K. Sharma, W. M. C. Sameera, M. Jin, L. Adak, C. Okuzono, T. Iwamoto, M. Kato, M. Nakamura, K. Morokuma., *J Am Chem Soc*, **2017**, 139 (45), 16117–16125.
- (21) N. D. Yilmazer, M. Korth., *Journal of Physical Chemistry B*, **2013**, 117 (27), 8075–8084.
- (22) M. Evecen, H. Tanak., *Materials Science- Poland*, **2016**, 34 (4), 886–904.
- (23) X. Ma, D. Chang, C. Zhao, R. Li, X. Huang, Z. Zeng, X. Huang, Y. Jia., *Journal of Materials Chemistry C*, **2018**, 6 (48), 13241–13249.
- (24) S. Naseem, M. Khalid, M. N. Tahir, M. A. Halim, A. A. C. Braga, M. M. Naseer, Z. Shafiq., *Journal of Molecular Structure*, **2017**, 1143, 235–244.
- (25) M. Zheng, X. Liu, Y. Xu, H. Li, C. Luo, H. Jiang., *Trends in Pharmacological Sciences*, **2013**, 34 (10), 549–559.
- (26) H. J. Huang, H. W. Yu, C. Y. Chen, C. H. Hsu, H. Y. Chen, K. J. Lee, F. J. Tsai, C. Y. C. Chen., *J Taiwan Inst Chem Eng*, **2010**, 41 (6), 623–635.
- (27) A. Daina, M. C. Blatter, V. Baillie Gerritsen, P. M. Palagi, D. Marek, I. Xenarios, T. Schwede, O. Michielin, V. Zoete., *Journal of Chemical Education*, **2017**, 94 (3), 335–344.
- (28) M. Xiang, Y. Cao, W. Fan, L. Chen, Y. Mo., *Combinatorial Chemistry & High Throughput Screening*, **2012**, 15 (4), 328–337.
- (29) A. B. Olokoba, O. A. Obateru, L. B. Olokoba., *Oman Medical Journal*, **2012**, 27 (4), 269–273.
- (30) A. Maitra, A. K. Abbas., In *Robbins & Cotran Pathologic Basis of Disease (Chapter 24 - Endocrine System)*; Kumar, V., Abbas, A. K., Fausto, N., Aster, J. C., Eds.; Saunders: Philadelphia, **2005**; pp 1156–1226.
- (31) E. C. Chao, R. R. Henry., *Nature Reviews Drug Discovery*, **2010**, 9 (7), 551–559.
- (32) S. Vorberg, I. Koch, C. Buning., *Journal of Cheminformatics*, **2012**, 4 (S1), P41.
- (33) S. Faham, A. Watanabe, G. M. Besserer, D. Cascio, A. Specht, B. A. Hirayama, E. M. Wright, J. Abramson., *Science (1979)*, **2008**, 321 (5890), 810–814.



- (34) J. J. Marín-Peñalver, I. Martín-Timón, C. Sevillano-Collantes, F. J. del Cañizo-Gómez., *World Journal of Diabetes*, **2016**, 7 (17), 395.
- (35) I. D. Kuntz., *Science (1979)*, **1992**, 257 (5073), 1078–1082.
- (36) J. Drews., *Science*, **2000**, 287 (5460), 1960–1964.
- (37) I. Muegge, M. Rarey., In *Reviews in Computational Chemistry (Chap 1 - Small Molecule Docking and Scoring)*; Lipkowitz, K. B., Boyd, D. B., Eds.; John Wiley & Sons, Ltd: New York, **2001**; Vol. 17, pp 1–60.
- (38) S. F. Sousa, P. A. Fernandes, M. J. Ramos., *Proteins*, **2006**, 65 (1), 15–26.
- (39) A. D. Becke., *The Journal of Chemical Physics*, **1993**, 98 (7), 5648–5652.
- (40) C. Lee, W. Yang, R. G. Parr., *Physical Review B*, **1988**, 37 (2), 785–789.
- (41) M. J. Frisch, G. W. Trucks, H. B. Schlegel, G. E. Scuseria, M. A. Robb, J. R. Cheeseman, G. Scalmani, V. Barone, G. A. Petersson, H. Nakatsuji, X. Li, M. Caricato, A. v Marenich, J. Bloino, B. G. Janesko, R. Gomperts, B. Mennucci, H. P. Hratchian, J. v Ortiz, A. F. Izmaylov, J. L. Sonnenberg, D. Williams-Young, F. Ding, F. Lipparini, F. Egidi, J. Goings, B. Peng, A. Petrone, T. Henderson, D. Ranasinghe, V. G. Zakrzewski, J. Gao, N. Rega, G. Zheng, W. Liang, M. Hada, M. Ehara, K. Toyota, R. Fukuda, J. Hasegawa, M. Ishida, T. Nakajima, Y. Honda, O. Kitao, H. Nakai, T. Vreven, K. Throssell, J. A. Montgomery Jr., J. E. Peralta, F. Ogliaro, M. J. Bearpark, J. J. Heyd, E. N. Brothers, K. N. Kudin, V. N. Staroverov, T. A. Keith, R. Kobayashi, J. Normand, K. Raghavachari, A. P. Rendell, J. C. Burant, S. S. Iyengar, J. Tomasi, M. Cossi, J. M. Millam, M. Klene, C. Adamo, R. Cammi, J. W. Ochterski, R. L. Martin, K. Morokuma, O. Farkas, J. B. Foresman, D. J. Fox., *Gaussian, Inc., Wallingford CT, Gaussian 16 Revision C.01*, **2016**.
- (42) R. Dennington, T. A. Keith, J. M. Millam., *GaussView Version 6, Semichem Inc., Shawnee Mission, KS*, **2016**.
- (43) P. Sykes., *A Guidebook to Mechanism in Organic Chemistry*, 6th ed.; Pearson Education: New Delhi, India, **2004**.
- (44) K. B. Benzon, H. T. Varghese, C. Y. Panicker, K. Pradhan, B. K. Tiwary, A. K. Nanda, C. van Alsenoy., *Spectrochimica Acta Part A: Molecular and Biomolecular Spectroscopy*, **2015**, 151, 965–979.
- (45) S. W. Xia, X. Xu, Y.-L. Sun, Y.-H. Fan, C.-F. Bi, D. M. Zhang, L.-R. Yang., *Chinese Journal of Structural Chemistry*, **2006**, 25 (2), 197–203.
- (46) M. Snehathala, C. Ravikumar, I. Hubert Joe, N. Sekar, V. S. Jayakumar., *Spectrochimica Acta Part A: Molecular and Biomolecular Spectroscopy*, **2009**, 72 (3), 654–662.

- (47) T. A. Koopmans., *Physica*, **1934**, *1* (1–6), 104–113.
- (48) R. G. Parr, L. V. Szentpály, S. Liu., *J Am Chem Soc*, **1999**, *121* (9), 1922–1924.
- (49) R. G. Parr, R. G. Pearson., *J Am Chem Soc*, **1983**, *105* (26), 7512–7516.
- (50) R. G. Pearson., *Journal of Chemical Sciences*, **2005**, *117* (5), 369–377.
- (51) S. Mandal, D. K. Poria, D. K. Seth, P. S. Ray, P. Gupta., *Polyhedron*, **2014**, *73*, 12–21.
- (52) P. Jaramillo, P. Pérez, R. Contreras, W. Tiznado, P. Fuentealba., *Journal of Physical Chemistry A*, **2006**, *110* (26), 8181–8187.
- (53) N. P. G. Roeges., *A Guide to the Complete Interpretation of Infrared Spectra of Organic Structures*; John Wiley and Sons Inc.: New York, **1994**.
- (54) B. C. Smith., *Infrared Spectral Interpretation, A Systematic Approach*, 1st ed.; CRC Press: Washington, DC, **1999**; Vol. 2.
- (55) P. Politzer, D. G. Truhlar., *Chemical Applications of Atomic and Molecular Electrostatic Potentials*; Plenum Press: New York, **1981**.
- (56) E. Scrocco, J. Tomasi., *Advances in Quantum Chemistry*, **1978**, *11* (C), 115–193.
- (57) P. Politzer, J. S. Murray., In *Theoretical Biochemistry and Molecular Biophysics: A Comprehensive Survey, Protein*; Beveridge, D. L., Lavery, R., Eds.; Adenine Press: Schenectady, New York, **1991**.
- (58) E. Scrocco, J. Tomasi., *Topics in Current Chemistry*, **1973**, *42*, 95–170.
- (59) *Principles and Applications of Nonlinear Optical Materials*, 1st ed.; Munn, R. W., Ironside, C. N., Eds.; Springer Dordrecht: Netherlands, **1993**.
- (60) A. Migalska-Zalas, K. el Korchi, T. Chtouki., *Optical and Quantum Electronics*, **2018**, *50(11)* (Article no. 389), 1–10.
- (61) A. P. Caricato, W. Ge, A. D. Stiff-Roberts., In *Advances in the Application of Lasers in Materials Science, (Chap 10 - UV- and RIR-MAPLE: Fundamentals and applications)*; Ossi, P. M., Ed.; Springer Verlag, **2018**; pp 275–308.
- (62) L. Ferreira, R. dos Santos, G. Oliva, A. Andricopulo., *Molecules*, **2015**, *20* (7), 13384–13421.
- (63) (Editorial) Eric C. Westman., *Frontiers in Nutrition*, **2021**, *8* (827990), 1–5.
- (64) C. Hale, M. Wang., *Mini Reviews in Medicinal Chemistry*, **2008**, *8* (7), 702–710.
- (65) X.-Y. Meng, H.-X. Zhang, M. Mezei, M. Cui., *Current Computer-Aided Drug Design*, **2011**, *7* (2), 146–157.

- (66) R. Huey, G. M. Morris., *The Scripps Research Institute, USA*, **2008**, 8, 54–56.
- (67) S. Hari., *Journal of Applied Pharmaceutical Science*, **2019**, 9 (7), 18–26.
- (68) K. Boussery, F. M. Belpaire, J. van de Voorde., In *The Practice of Medicinal Chemistry*; Wermuth, C. G., Ed.; Elsevier Science, **2008**; pp 635–654.
- (69) F. Ntie-Kang, L. L. Lifongo, J. A. Mbah, L. C. Owono Owono, E. Megnassan, L. M. Mbaze, P. N. Judson, W. Sippl, S. M. N. Efange., *In Silico Pharmacology*, **2013**, 1(1) (Article 12), 1–11.
- (70) K. Ohtawara, H. Teramae., *Chemical Physics Letters*, **2004**, 390 (1–3), 84–88.
- (71) J. Eberhardt, D. Santos-Martins, A. F. Tillack, S. Forli., *Journal of Chemical Information and Modeling*, **2021**, 61 (8), 3891–3898.
- (72) O. Trott, A. J. Olson., *Journal of Computational Chemistry*, **2010**, 31 (2), 455–461.
- (73) G. M. Morris, D. S. Goodsell, R. S. Halliday, R. Huey, W. E. Hart, R. K. Belew, A. J. Olson., *Journal of Computational Chemistry*, **1998**, 19 (14), 1639–1662.
- (74) M. A. Alamri, M. Tahir ul Qamar, M. U. Mirza, R. Bhadane, S. M. Alqahtani, I. Muneer, M. Froeyen, O. M. H. Salo-Ahen., *Journal of Biomolecular Structure and Dynamics*, **2021**, 39 (13), 4936–4948.

## CHAPTER-V

### Section A

**An efficient and green protocol for the synthesis of 1-hydroxy-2-arylimidazole-3-oxide derivatives under solvent free condition using inexpensive Copper borate ( $\text{CuB}_4\text{O}_7$ ) catalyst.**

#### **5.A.1 Background of the present investigation:**

During the past, drugs containing heterocyclic scaffold has occupied a unique position because of their high therapeutic values. A lot of drug motif heterocyclic core are in clinical use to treat many infectious diseases<sup>1</sup>. Among a large and diverse variety of heterocyclic compounds, imidazole, five membered nitrogen containing heterocyclic compound has gained a lot of interest in the field of drug discovery and has occupied a special position in the field of heterocyclic chemistry<sup>2</sup>. A unique feature of the imidazole scaffold is its polar nature and this property could be largely exploited to improve the pharmacokinetic property of drug molecule containing imidazole core as this moiety could help in improving the aqueous solubility of many drugs which are poorly soluble in water<sup>3</sup>. A large variety of compounds containing imidazole scaffold shows a lot of promising therapeutic activities such as antiviral<sup>2</sup>, antitumor<sup>4</sup>, antiinflammatory<sup>5</sup>, antidiabetic<sup>6</sup>, anticonvulsant<sup>7</sup>, antiasthmatic<sup>8</sup> and antiamebic<sup>19</sup> etc. A large variety of drugs containing imidazole scaffold such as Etonitazene (analgesics)<sup>10</sup> (104), Enviroxime (antiviral)<sup>11</sup> (105), pantoprazole (antiulcer)<sup>10</sup>(106), Metronidazole (antibacterial)<sup>3</sup> (107) and Carbimazole (antithyroid)<sup>7</sup> (108) etc. are commercially available in the market (Fig. 5A.1). Among the various types of heterocyclic compounds consisting of imidazole core, 1-hydroxy-imidazole-3-oxide is regarded as a versatile heterocyclic compound as these compounds are mostly involved in the synthesis of room temperature ionic liquids<sup>11</sup>. Particularly, the incorporation of N-O moiety into the imidazolium based ionic liquid may give rise to greener solvent which is degradable by design and may fulfill the primary aspect of green chemistry principles<sup>12</sup>. Moreover, the imidazolium salt namely 1-alkoxy-3-alkyl-imidazolium salt were found to be liquid at room temperature and the synthesis of such room temperature ILs requires a two-step alkylation of the precursor 1-hydroxyimidazole<sup>13</sup>.

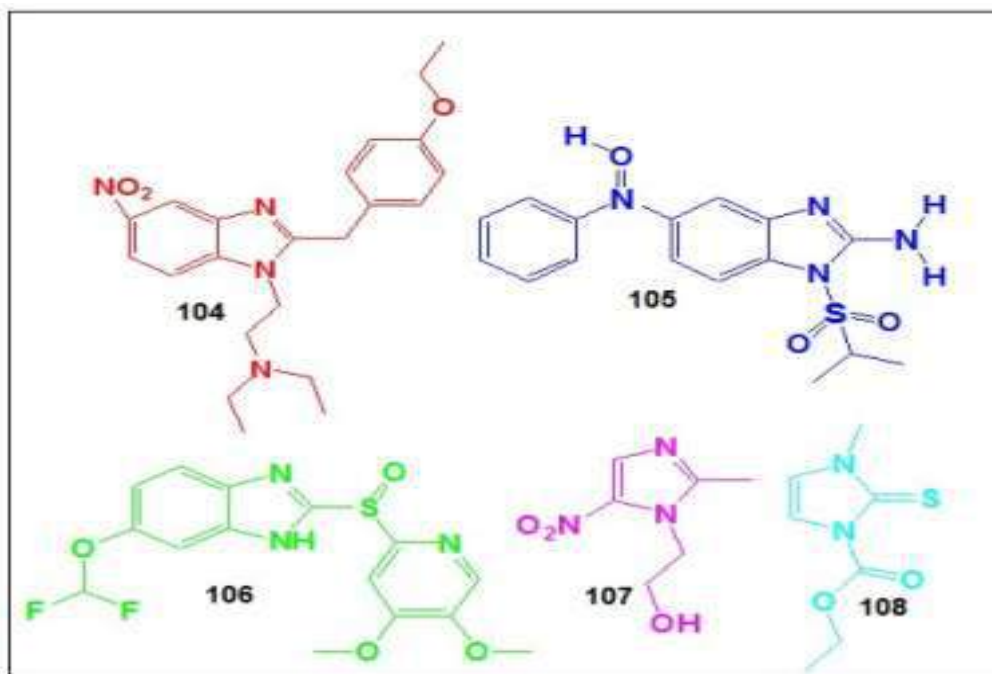
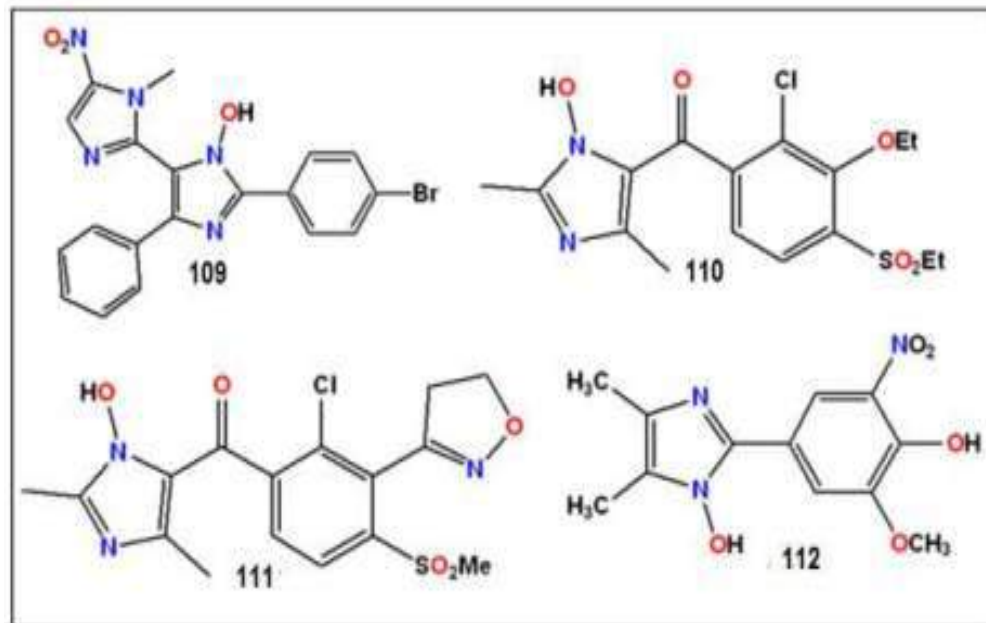


Fig. 5.A.1. Examples of drugs containing imidazole scaffold

The precursor 1-hydroxy-imidazole3-oxide could readily be obtained by cyclization of glyoxime and formaldehyde<sup>14</sup>. The employment of alkyl or aryl aldehydes in the synthesis of 1-hydroxyimidazole results in the formation of corresponding 1-hydroxy-2-alkylimidazole3-oxide and 1-hydroxy-2-arylimidazole-3-oxide derivatives respectively. In general, Heterocyclic compounds commonly containing a dipolar R<sub>3</sub>-N-O linkage in which the nitrogen either sp<sup>3</sup> or sp<sup>2</sup> hybridized are known as Heterocyclic-N-oxides<sup>15-16</sup>. Interestingly, the incorporation of a negative charge on oxygen changes most of the physical properties including the reactivity of the heterocyclic compounds and the most common Heterocyclic-N-Oxide is Pyridine-N-oxide which has excellent donor properties as compared to normal pyridine<sup>17-18</sup>. Imidazole -N-oxides are the compounds which have N-O group attached to the imidazole ring. Imidazole-N-oxides fall under the category of N-substituted imidazole which have a wide variety of applications. These compounds have gained popularity due to their anti-protozoal<sup>19</sup>, fungicidal, herbicidal, pesticidal<sup>20</sup>, hypotensive properties<sup>21</sup>, anti-tumor<sup>22</sup> and anti-viral<sup>23</sup> properties (Fig.5.A.2). Apart from its pharmaceutical applications, imidazole-N-oxides are also used for the generation of N-containing heterocyclic carbenes (NHCs) which acts as intermediates in various organic reactions<sup>24</sup>.

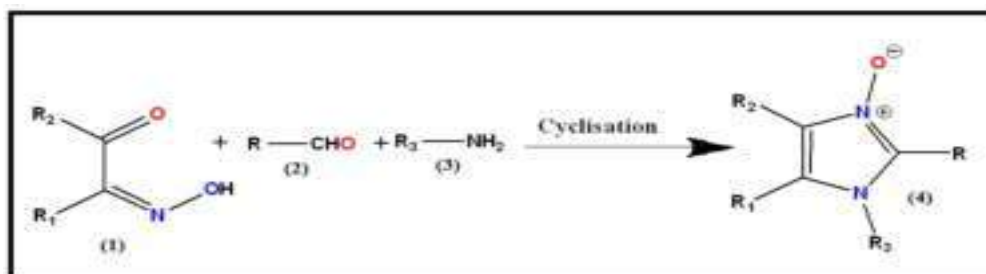


**Fig. 5.A.2.** Examples of 1-hydroxyimidazole compounds having biological activities.

The current literature survey revealed that only few works on the synthesis of 1-hydroxy-2-arylimidazole-3-oxide has been documented in the literature<sup>25</sup>. Thus, it was thought worthwhile to undertake the research work in the synthesis of 1-hydroxy-2-arylimidazole-3-oxide derivatives under green chemical condition by employing inexpensive and unconventional copper borate as a catalyst.

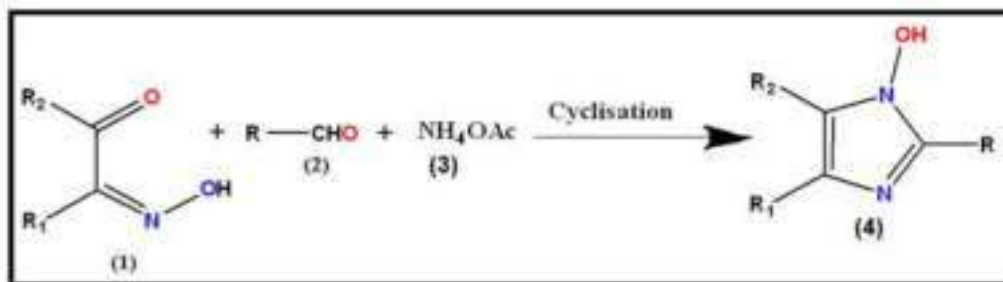
### 5.A.2 Result and Discussions

By looking at the diverse applications of Imidazole-3-oxides and 1-hydroxyimidazole-3-oxide, various methodologies have been developed in the past for the synthesis of these compounds. The most common and the conventional method for the synthesis of imidazole-3-oxides (4) is from mono-oximes ( $\alpha$ -hydroxyiminoketones) (1) and aldehydes (2) in the presence of amines (3)<sup>20,26</sup> (Scheme 5.A.1)



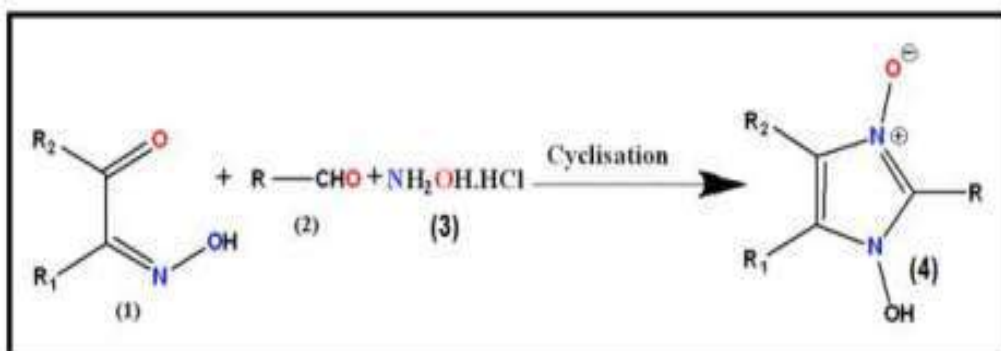
**Scheme. 5.A.1.** Method of synthesis of N-alkylimidazole-3-oxide (4)

Substitution of the amine precursor with  $\text{NH}_4\text{OAc}$  for the above reaction results in the formation of the 1-hydroxyimidazole derivatives (4)<sup>27-28</sup> (Scheme 5.A.2).



**Scheme. 5.A.2.** Synthesis of 1-hydroxyimidazole derivatives (4)

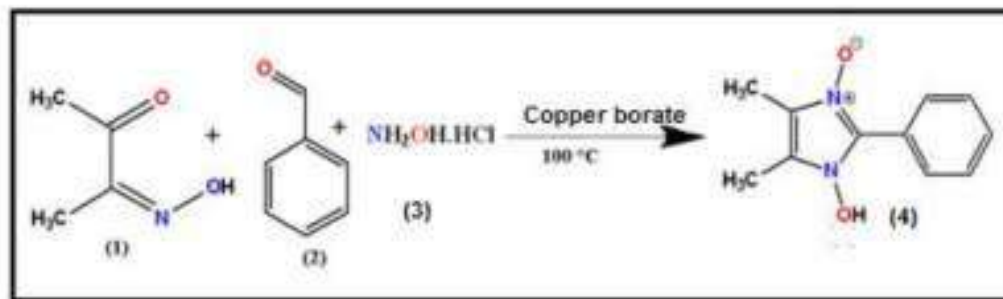
However, when hydroxylamine hydrochloride ( $\text{NH}_2\text{OH}\cdot\text{HCl}$ ) is used instead of amine and  $\text{NH}_4\text{OAc}$ , the corresponding 1-hydroxy-2-alkylimidazole 3-oxide (4) or 1-hydroxy-2-arylimidazole-3-oxide (4) is formed respectively depending upon the aldehyde precursor used<sup>29-30</sup> (Scheme 5.A.3).



**Scheme. 5.A.3.** Synthesis of 1-hydroxy-2-(aryl)-4,5-dimethylimidazole-3-oxide (4).

Although the above-mentioned procedures are widely used for the synthesis of imidazole-N-oxides and 1 hydroxy imidazole-3-oxides, yet there are a very few reports for the solvent free and green procedures for the synthesis of the above said compounds<sup>35</sup>. These factors prompted us to devise a synthetic method for the synthesis of 1-hydroxy-2-arylimidazole-3-oxide derivatives under solvent free conditions using copper borate as a catalyst. Thus, in this chapter we are representing the catalytic efficacy of the inexpensive copper borate ( $\text{CuB}_4\text{O}_7$ ) as a catalyst for the solvent free synthesis of 1-hydroxy-2-(aryl)-4,5-dimethylimidazole-3-oxide derivatives.

Initially, for the synthesis of 1-hydroxy-2-(aryl)-4,5-dimethylimidazole-3-oxide (4), we selected diacetylmonoxime (1), benzaldehyde (2) and hydroxylamine hydrochloride ( $\text{NH}_2\text{OH}\cdot\text{HCl}$ )(3) as a model compounds under different reaction conditions at 100 °C for 2 hours using varied amount of catalyst (0.5 to 3.5 mol %) (Scheme5.A.4).



**Scheme. 5.A.4.** Model reaction for the synthesis of 1-hydroxy-2-(aryl)-4,5-dimethylimidazole-3-oxide using diacetyl monoxime(1) 1mmol, benzaldehyde (2) 1mmol, hydroxylamine hydrochloride (3) 2.5 mmol under different mole % of catalyst.

Again, for the optimization of the reaction condition, we choose different solvent systems for the above reaction. At least we choose 5 polar protic and polar aprotic solvents to screen the efficacy of the employed catalyst for the desired reaction (Table 5.A.1). Interestingly we observed that the above reaction proceeds well in more polar protic and aprotic solvents like alcohol and DMF, DMSO respectively (Table 5.A.1. entry 1, 2, 3 and 4) but we encountered that under this reaction condition, the reaction needs more time for the completion. Therefore, we focused our study towards the green protocol by utilizing solvent free condition for the synthesis of the 1-hydroxy-2-arylimidazole3-oxide. Moreover, we observed that under solvent free condition, the reaction proceeds well and requires less time for completion without forming the by-product and therefore making the work-up procedure more facile and efficient (Table 5.A.1, entry 6).

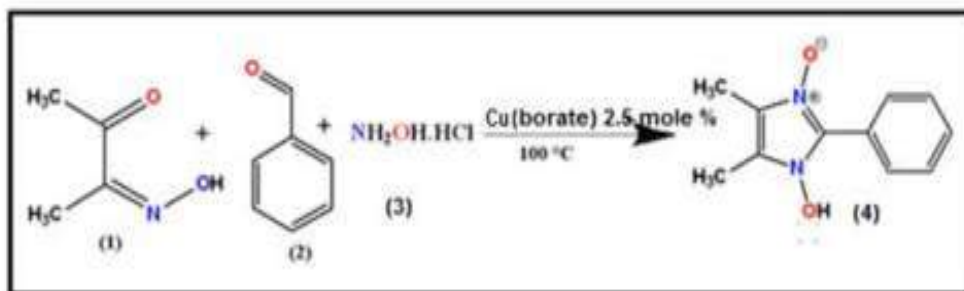


**Table. 5.A.1.** Screening of the reaction condition (solvent) for model reaction

Entry	Solvent <sup>a</sup>	Yield <sup>b</sup>
1	Ethanol	90
2	Methanol	86
3	DMF	88
4	DMSO	79
5	Water	55
6	<b>Neat</b>	<b>98</b>

<sup>a</sup>The reaction was carried out with diacetyl monoxime (1) (1 mmol), benzaldehyde (2) (1 mmol) and hydroxylamine hydrochloride (2.5 mmol) with the catalyst using different solvents at 100°C. After having recognized the optimum reaction conditions, we carried forward this protocol to other aromatic aldehydes to synthesize 1-hydroxy-2-(aryl)-4,5-dimethylimidazole-3-oxide derivatives (4) and in almost all the cases, the reaction proceeded in a short time with excellent yield of the products (90-98 %) and <sup>b</sup>isolated yields

We carried out the above reaction with model components using different mol % of the catalyst to optimize the catalyst loading for the desired product and we observed that the reaction proceeds well when the amount of catalyst loading is 2.5 mol % at the optimized reaction temperature of 100 °C (Table 5.A.2). Then we optimized the reaction time for the modelled reaction and we found that the reaction completes within 10 minutes under solvent free condition (Scheme 5.A.5). Therefore, we concluded that the model reaction goes for completion when the amount of catalyst loading is 2.5 mole % at 100 °C and 10 minutes of reaction time (Table 5.A.2, entry 5). It was also observed that only a negligible amount of product was formed without catalyst (Table 5.A.2, entry 1).



**Scheme. 5.A.5.** Optimized reaction condition for the synthesis of 1-hydroxy-2-(aryl)-4,5-dimethylimidazole-3-oxide

**Table. 5.A.2.** Screening of the amount of catalyst loading for the model reaction

Entry	Catalyst mol % <sup>a</sup>	Temperature (°C)	Time (Minutes)	Yield <sup>b</sup> (%)
1	0	100	10	12
2	0.5	100	10	59
3	1.0	100	10	62
4	2.0	100	10	85
<b>5</b>	<b>2.5</b>	<b>100</b>	<b>10</b>	<b>97</b>
6	3.0	100	10	95
7	3.5	100	10	94

<sup>a</sup>The reaction was carried out with diacetyl monoxime (1) (1 mmol), benzaldehyde (2) (1 mmol) and hydroxylamine hydrochloride (2.5 mmol) with the catalyst using different solvents at 100°C. After having recognized the optimum reaction conditions, we carried forward this protocol to other aromatic aldehydes to synthesize 1-hydroxy-2-(aryl)-4,5-dimethylimidazole-3-oxide derivatives (4) and in almost all the cases, the reaction proceeded in a short time with excellent yield of the products (90-98 %), <sup>b</sup>isolated yield

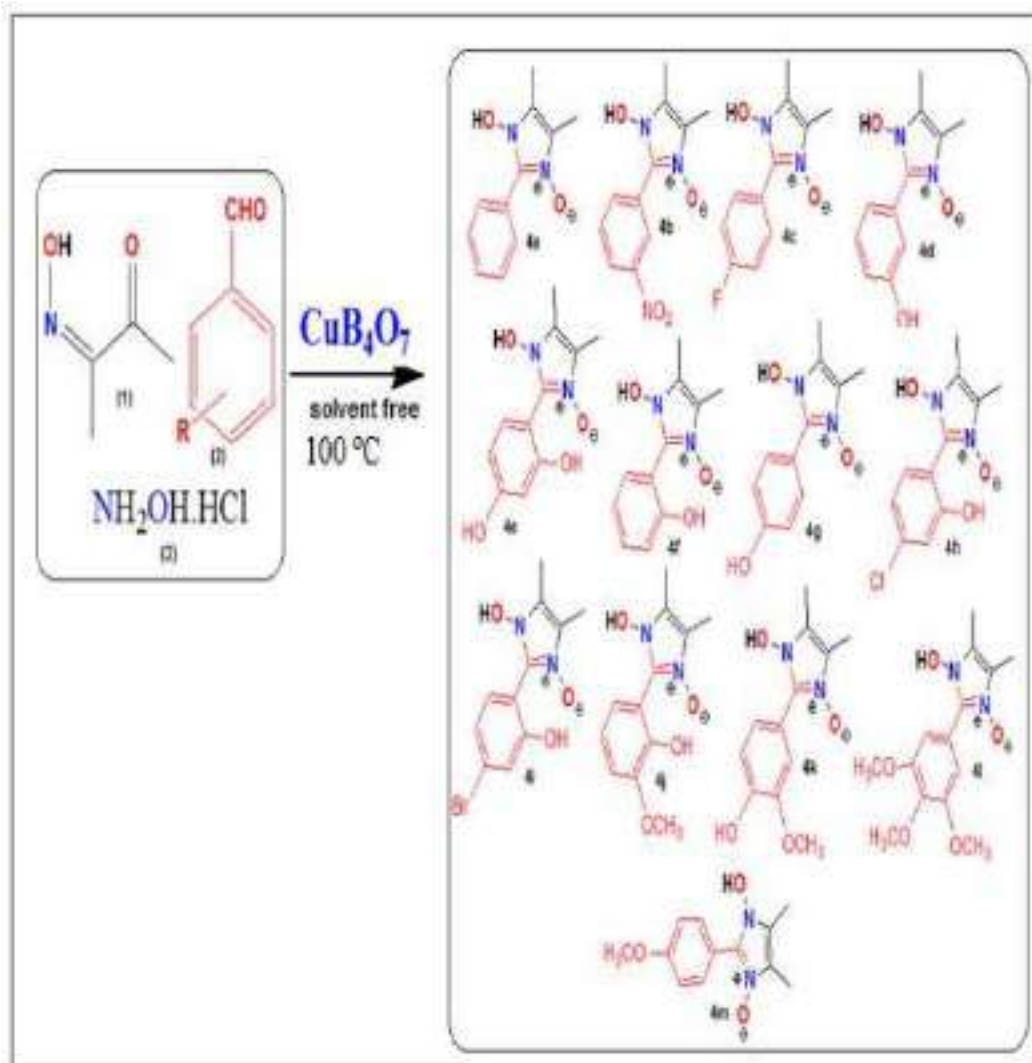
It was observed that when the amount of catalyst loading is more than or less than 2.5 mole %, the isolated yield of the product found to be decreased. Having recognized the optimized reaction condition, we therefore extended this reaction protocol for a number of aromatic aldehydes having electron withdrawing and electron releasing groups and we found that this catalytic protocol works well with both type of aldehyde precursors. However, it reflects from this study that aldehydes having electron withdrawing group successfully afforded the desired product more efficiently in excellent yield than the aldehydes having the electron releasing group (Table 5.A.3, Fig. 5.A.3).

**Table. 5.A.3.** CuB<sub>4</sub>O<sub>7</sub> catalyzed solvent free synthesis of 1-hydroxy-2-(aryl)-4,5-dimethylimidazole-3-oxide (4a-4m)

Entry	$\alpha$ -hydroxyiminoketone	Aldehyde	Product	Yield <sup>b</sup> (%)
1	Diacetyl monoxime	Benzaldehyde	4a	97
2	Diacetyl monoxime	3-nitro-benzaldehyde	4b	98
3	Diacetyl monoxime	4-fluoro-benzaldehyde	4c	98
4	Diacetyl monoxime	3-hydroxy-benzaldehyde	4d	95
5	Diacetyl monoxime	2,4-dihydroxy-benzaldehyde	4e	93
6	Diacetyl monoxime	2-hydroxy-benzaldehyde	4f	94
7	Diacetyl monoxime	4-hydroxybenzaldehyde	4g	94
8	Diacetyl monoxime	2-hydroxy-5-chloro-benzaldehyde	4h	96
9	Diacetyl monoxime	2-hydroxy-5-bromo-benzaldehyde	4i	95
10	Diacetyl monoxime	2-hydroxy-3-methoxy-benzaldehyde	4j	95
11	Diacetyl monoxime	4-hydroxy-3-methoxy-benzaldehyde	4k	94
12	Diacetyl monoxime	3,4,5-trimethoxy-benzaldehyde	4l	94
13	Diacetyl monoxime	4-methoxy-benzaldehyde	4m	93

<sup>b</sup>isolated yield

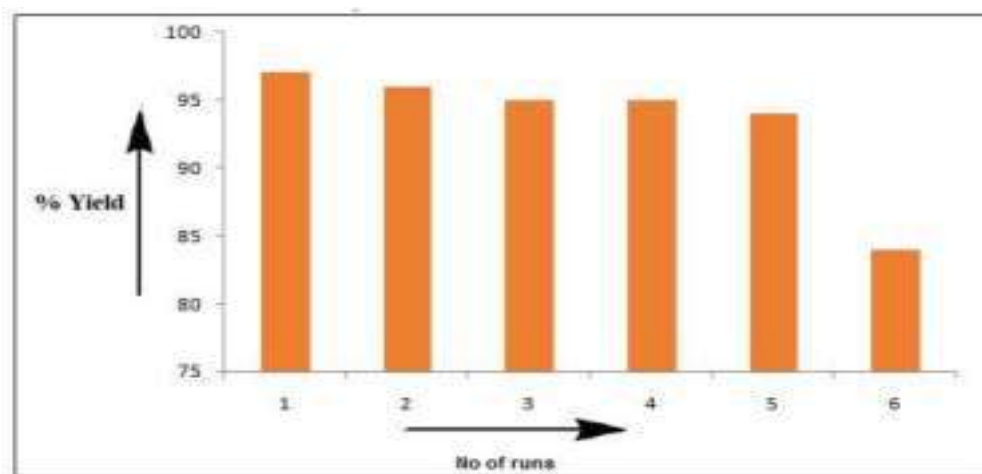
After recognizing the catalytic efficacy of the copper borate catalyst, we were interested to study the recyclability of the catalyst for the given reaction protocol and we observed that the catalyst is easily recoverable with simple filtration from the reaction mixture. Thus, we recovered the catalyst after the first run of the reaction and purified the catalyst by simply washing with methanol and dried at 100 °C in an oven. The recovered catalyst again used for further reaction and interestingly we observed that catalyst did not lose its efficiency up to 5<sup>th</sup> run of the reaction (Table 5.A.4). However, after the 5<sup>th</sup> run, we observed that the product yield changed little and from this we can infer that the catalyst could be used up to 5<sup>th</sup> run for the studied reaction protocol. The bar diagram for the catalytic recyclability of the studied catalyst is given in Fig. 5.A.4.



**Fig. 5.A.3.** Schematic representation of product formed under the stated reaction condition

**Table. 5.A.4.** Recyclability of copper borate in model reaction

Entry	No. of runs	Isolated yields (%)
1	1	97
2	2	96
3	3	95
4	4	95
5	5	94
6	6	84

**Fig. 5.A.4.** Recyclability of the catalyst

Interestingly, it has been observed that the 1-hydroxyimidazole derivatives and N-hydroxybenzimidazole derivatives know to show prototropic tautomerism and this type of tautomerism plays an important role in drug discovery. Therefore, due to prototropic tautomerism, either N-hydroxy (a/a') or N-oxide (b/b') tautomeric form exist for these type of molecules<sup>31-33</sup> (Fig.5A.5).

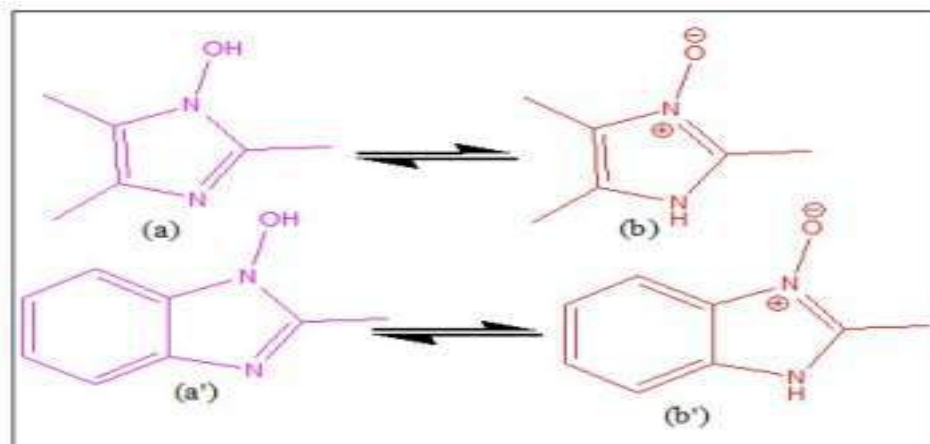


**Fig. 5.A.5.** Prototropic tautomeric equilibrium of 1-hydroxyimidazole and N-hydroxybenzimidazole, a/a') N-hydroxy form and b/b') N-oxide form.

While recrystallizing the synthesized 1-hydroxy-2-arylimidazole3-oxide derivatives using aqueous ethanol (20:80), we observed that the compound 4m crystallized in a needle shaped crystal and therefore, we carried out the X-ray single crystal diffraction study of 4m. From the single crystal diffraction study, it was revealed that the compound 4m exist as a 1, 3-dihydroxy form instead of 1-hydroxy 3-oxide form as shown in Fig 5.A.6.

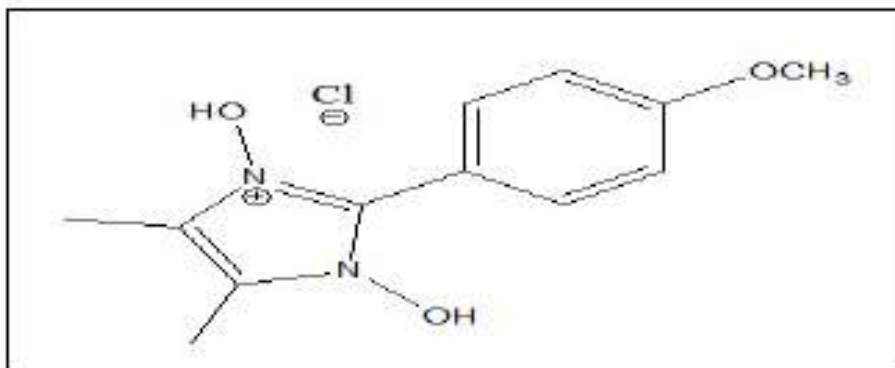


**Fig. 5.A.6.** Structure of 1,3-dihydroxy-2-(4-methoxyphenyl)-4,5-dimethyl-1H-imidazol-3-ium chloride (4m).

### 5.A.2.1 Description of crystal structure of (4m)

The compound, 1,3-dihydroxy-2-(4-methoxyphenyl)-4,5-dimethyl-1*H*-imidazol-3-ium chloride, **4m**, crystallizes in the monoclinic P 2<sub>1</sub>/n space group. Crystal data and experimental details for **4m** are listed in Table 5.A.5. Selected bond lengths and torsion angles are presented in Table 5.A.6. The asymmetric unit has been shown in Fig. 5.A.7. The three-dimensional packing arrangement of **4m** has been shown in Fig. 5.A.8. The molecule is not a planar molecule as is evident from the torsion angles around C1–C8 bond. There is puckering in the C1–C8 bond. The puckering is envisioned by the dihedral angle between the planes containing the phenyl and imidazole moiety which is *ca.* 44.62 (0.05). There are two intermolecular O–H···Cl interactions (Table 5.A.7, Fig. 5.A.9) which stabilizes the crystal packing and is further stabilized by an intermolecular C–H···Cg interaction (Table 5.A.8, Fig. 5.A.10) between C12–H12B and Cg2 (centroid of C1 – C6 ring).

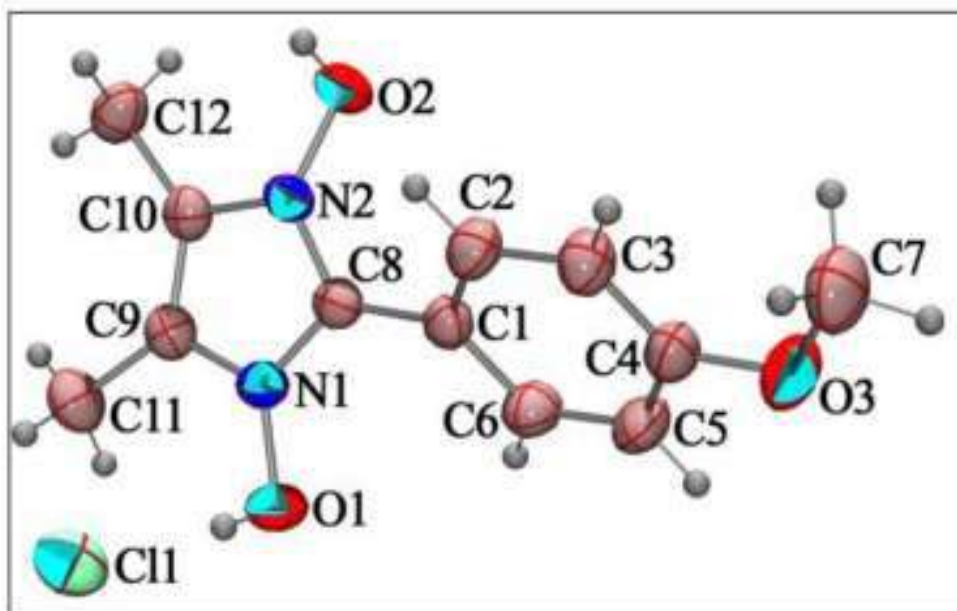


**Fig. 5.A.7.** Asymmetric unit of **4m** with displacement ellipsoids drawn at 50% probability level.

**Table. 5.A.5** Crystal data collection and structure refinement for (4m)

Crystal data	
CCDC reference number	2183509
Empirical formula	C <sub>12</sub> H <sub>15</sub> N <sub>2</sub> O <sub>3</sub> Cl
Moiety formula	C <sub>12</sub> H <sub>15</sub> N <sub>2</sub> O <sub>3</sub> , Cl
Formula weight	270.71
Crystal system	Monoclinic
Space group	P 21/n
Color, habit	Pale white, rod
Size, mm	0.28 × 0.26 × 0.25
Unit cell dimensions	
a = 8.5143(4)Å	α = 90°
b = 7.6289(4)Å	β = 94.228(4)°
c = 20.1962(9)Å	γ = 90°
Volume Å <sup>3</sup>	1308.27(11)
Z	4
Density (calculated), Mg/m <sup>3</sup>	1.374
Absorption coefficient, mm <sup>-1</sup>	0.294
F(000)	568
Data collection	
Temperature, K	293(2)
Theta range for data collection	3.35° to 25.00°
Index ranges	-10 ≤ h ≤ 9 -7 ≤ k ≤ 9 -24 ≤ l ≤ 23
Reflections collected	5168
Unique reflections	2299
Observed reflections (>2σ(I))	1890
R <sub>int</sub>	0.0169
Completeness to θ, %	25.00°, 99.8
Absorption correction	Multi-scan (SADABS; Bruker, 2000) T <sub>min</sub> = 0.922, T <sub>max</sub> = 0.923
Refinement	
Refinement method	Full-matrix least-squares on F <sup>2</sup>
Data / restraints / parameters	2299 / 0 / 223
Calculated weights, w	1/[σ <sup>2</sup> (F <sub>o</sub> <sup>2</sup> ) + (0.0378P) <sup>2</sup> + 0.3138P] where P = (F <sub>o</sub> <sup>2</sup> + 2F <sub>c</sub> <sup>2</sup> )/3
Goodness-of-fit on F <sup>2</sup>	1.051
Final R indices [I > 2σ(I)]	R <sub>1</sub> = 0.0356, wR <sub>2</sub> = 0.0843
R indices (all data)	R <sub>1</sub> = 0.0456, wR <sub>2</sub> = 0.0909
Largest diff. peak and hole	0.169 and -0.199 e.Å <sup>-3</sup>



**Table 5.A.6.** Selected bond lengths (Å), bond angles (°) and torsion angles (°) for (**4m**)

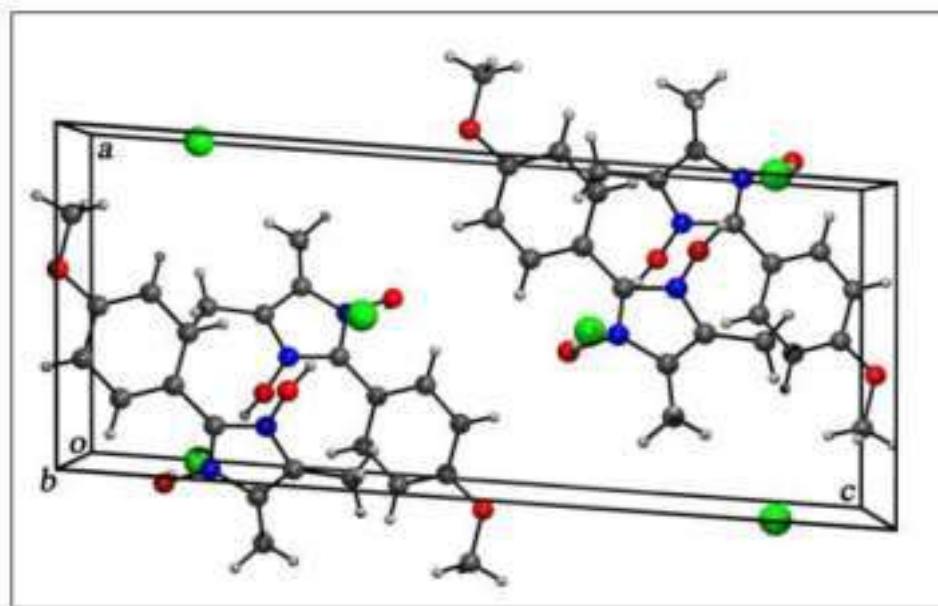
Bond lengths (Å)			
O(1)–N(1)	1.3798(18)	O(2)–N(2)	1.3716(18)
C(1)–C(8)	1.460(2)	C(9)–C(10)	1.356(2)
Torsion angles (°)			
N(1)–C(8)–C(1)–C(6)	46.1(3)	N(2)–C(8)–C(1)–C(2)	42.9(3)

**Table 5.A.7.** Hydrogen bonded geometries in (**4m**)

Bond	D - H	H···A	D···A	D - H···A
O(1)–H(1)···Cl(1) <sup>i</sup>	0.88(3)	2.10(3)	2.9732(16)	172(2)
O(2)–H(2A)···Cl(1) <sup>ii</sup>	1.00(3)	1.95(3)	2.9393(14)	170(2)

Symmetry codes: (i)  $-1+x, y, z$ ; (iii)  $3/2-x, 1/2+y, 1/2-z$ **Table 5.A.8** X–H···C<sub>g</sub> interactions in (**4m**)

X–H···C <sub>g</sub>	H···C <sub>g</sub>	H <sub>perp</sub>	$\gamma$	X–H···C <sub>g</sub>	X···C <sub>g</sub>
C(12)–H(12B)···C <sub>g</sub> (2) <sup>iii</sup>	2.93(2)	2.92	4.19	133.2(18)	3.669(2)

Symmetry codes: (iii)  $1/2-x, -1/2+y, 1/2-z$ Note: C<sub>g</sub> is the centroid of the C1–C6 ring.**Fig. 5.A.8.** The molecular arrangement of **4m** in the *ac* plane

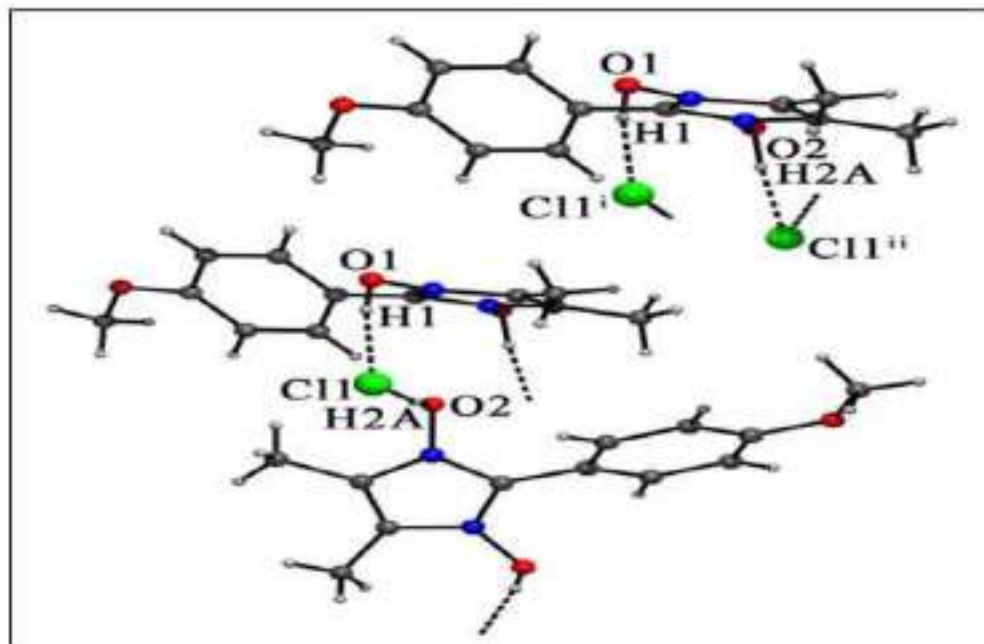


**Fig. 5.A.9.** Hydrogen bonding interaction in 4m, (dotted lines indicate the interionic C–H···Cl interactions in 4m).

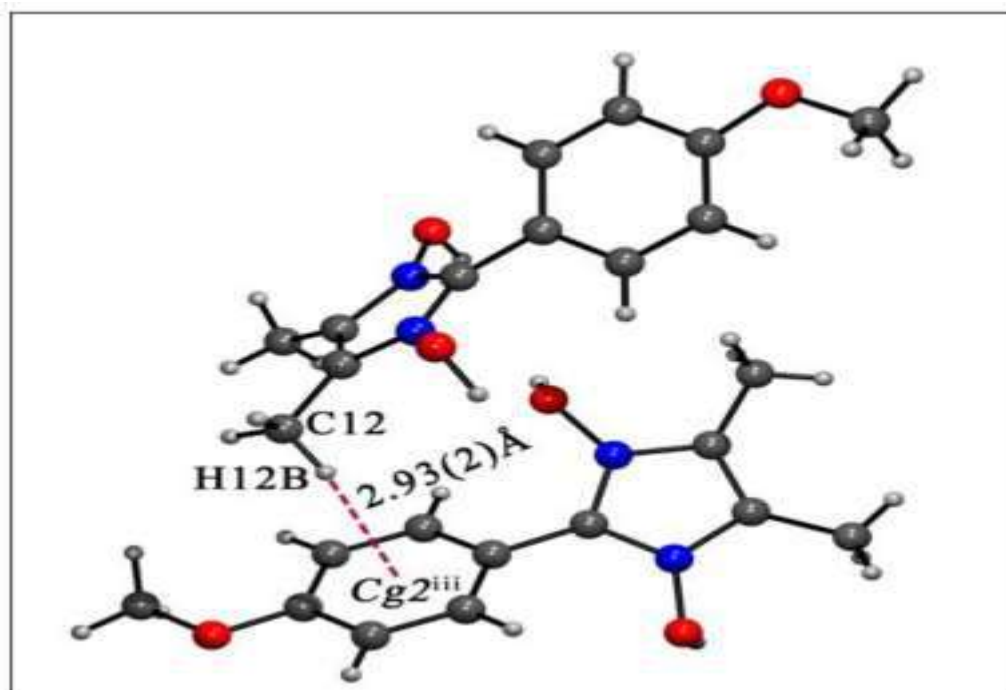


**Fig. 5.A.10.** C–H···Cg interaction in the cationic unit of 4m (Dotted line indicates the C–H···Cg interaction)

Thus, it is evident from the crystallography study that the title compound 4m exist as a 1,3-dihydroxy form in the solid state and more work towards the understanding of the tautomeric form of 1-hydroxy-2-arylimidazole3-oxide is under progress in our laboratory.

### 5.A.3 Experimental section

#### 5.A.3.1 Materials and methods:

All starting materials of high purity for the desired synthesis were purchased commercially and used as received. The FT-IR spectra of the prepared compounds were recorded in Bruker Alpha III spectrophotometer operating in the wave number region 4000 to 400  $\text{cm}^{-1}$  in dry KBr. The melting points of the synthesized compounds were determined by open capillary method.  $^1\text{H}$ NMR of the synthesized 1-hydroxy-2-arylimidazole-3-oxide derivatives were recorded at room temperature on a FT-IR (Bruker Advance-II 400 MHz) spectrometer by using  $\text{DMSO-d}_6$  as solvents and chemical shifts are quoted in ppm downfield of internal standard tetramethyl silane (TMS). X-ray single crystal study of 1,3-dihydroxy-2-(4-methoxyphenyl)-4,5-dimethyl-1*H*-imidazol-3-ium chloride (4m), was recorded on a Bruker SMART-APEX CCD diffractometer and the Diffraction data was collected using monochromatic  $\text{Mo K}\alpha$  radiation ( $\lambda = 0.71073 \text{ \AA}$ ) with the  $\omega$  and  $\phi$  scan technique. The unit cell was determined using Bruker SMART, the diffraction data were integrated with Bruker SAINT system and the data were corrected for absorption using SADABS<sup>34</sup>. The structure was solved by direct method and was refined by full matrix least squares based on  $F^2$  using SHELXL 97<sup>35</sup>. All the H atoms were localized from the difference electron-density map and refined isotropically. ORTEP-plot and packing diagram were generated with ORTEP-3 for Windows<sup>36</sup> and PLATON<sup>37</sup>. WinGX<sup>38-39</sup> was used to prepare the material for publication.

#### 5.A.3.2 General procedure for the synthesis of 1-hydroxy-imidazole-3-oxide derivatives (4a-4m):

In a typical green procedure, a mixture of diacetyl monoxime (1 mmol), substituted benzaldehyde (1 mmol), hydroxylamine hydrochloride (2.5 mmol) and copper borate (2.5 mmol) were thoroughly ground and mixed in a mortar and pestle to make a homogeneous mixture. The mixture was then transferred to a test tube. The reaction was heated at 100°C for 10 minutes. The progress of the reaction was monitored by TLC using hexane/ethyl acetate (80:20) solvent. After completion of the reaction, the reaction mixture was dissolved in methanol and filtered. The filtrate was evaporated under vacuum and subsequently dried to afford the desired product. All the synthesized products (4a-4m) were recrystallized from ethanol and have been characterized by their analytical (yield and melting point) and spectroscopic data (FT-IR and  $^1\text{H}$ NMR) and compared with the literature value.

### 5.A.3.2 Crystallization procedure for compound 4m

The compound 4m after recrystallized from ethanol were further dissolved in aqueous ethanol solution (20:80) and the solution was left for evaporation at room temperature. After 5 days a pale white needle shaped crystals were start appearing in the solution. After seven days, we obtained the crystals of compound 4m suitable for single crystal x-ray diffraction study.

### 5.A.4 Analytical and Spectroscopic data

**5.A.4.1 1-hydroxy-2-phenyl-4,5-dimethylimidazole-3-oxide (4a):** white solid, yield= 97 %, melting point found ( $^{\circ}\text{C}$ ) = 155-157, IR (KBr,  $\text{cm}^{-1}$ )  $\nu_{\text{max}}$ :3441 (br, OH), 3054, 3039 (C-H, Aromatic), 2969, 2927 (C-H, Aliphatic), 2231, 1713, 1639, 1545 (C=C), 1602, 1582 (C=N), 1347, 1253, 815,  $^1\text{HNMR}$  (400 MHz, DMSO  $d_6$ ):  $\delta\text{ppm}$  = 12.68 (s, 1H, OH), 6.81-7.69 (m, 4H, Ar-H), 3.15 (s, 3H, CH<sub>3</sub>), 2.31 (s, 3H, CH<sub>3</sub>).

**5.A.4.2 1-hydroxy-2-(3-nitrophenyl)-4,5-dimethylimidazole-3-oxide (4b):** Pale yellow solid, yield= 98 %, melting point found ( $^{\circ}\text{C}$ ) = 208-211, IR (KBr,  $\text{cm}^{-1}$ )  $\nu_{\text{max}}$ :3442 (br, OH), 3060 (C-H, Aromatic), 2974, 2926 (C-H, Aliphatic), 1657 (C=C), 1625, 1610 (C=N), 1394, 1267, 833,  $^1\text{HNMR}$  (400 MHz, DMSO  $d_6$ ):  $\delta\text{ppm}$  = 11.65 (s, 1H, OH), 7.66-8.40 (m, 4H, Ar-H), 3.36 (s, 3H, CH<sub>3</sub>), 1.96 (s, 3H, CH<sub>3</sub>).

**5.A.4.3 1-hydroxy-2-(4-fluorophenyl)-4,5-dimethylimidazole-3-oxide (4c):** Pale white solid, yield= 98 %, IR (KBr,  $\text{cm}^{-1}$ )  $\nu_{\text{max}}$ :3424 (br, OH), 3062 (C-H, Aromatic), 2984, 2926 (C-H, Aliphatic), 1632 (C=C), 1550, 1487 (C=N), 1391, 1257, 839,  $^1\text{HNMR}$  (400 MHz, DMSO  $d_6$ ):  $\delta\text{ppm}$  = 11.00 (s, 1H, OH), 7.07-7.80 (m, 4H, Ar-H), 3.34 (s, 3H, CH<sub>3</sub>), 2.24 (s, 3H, CH<sub>3</sub>).

**5.A.4.4 1-hydroxy-2-(3-hydroxyphenyl)-4,5-dimethylimidazole-3-oxide (4d):** Pale white solid, yield= 95 %, IR (KBr,  $\text{cm}^{-1}$ )  $\nu_{\text{max}}$ :3430 (br, OH), 3298, 3051 (C-H, Aromatic), 2995, 2962 (C-H, Aliphatic), 1627 (C=C), 1602, 1545 (C=N), 1334, 1243, 854,  $^1\text{HNMR}$  (400 MHz, DMSO  $d_6$ ):  $\delta\text{ppm}$  = 11.37 (s, 1H, OH), 9.99 (s, 1H, OH), 7.40-7.46 (m, 4H, Ar-H), 3.35 (s, 3H, CH<sub>3</sub>), 1.96 (s, 3H, CH<sub>3</sub>).

**5.A.4.5 1-hydroxy-2-(2,4-dihydroxyphenyl)-4,5-dimethylimidazole-3-oxide (4e):** Pale brown, yield= 93 %, IR (KBr,  $\text{cm}^{-1}$ )  $\nu_{\text{max}}$ :3549, 3452 (br, OH), 3288, 3112 (C-H, Aromatic), 2972, 2930 (C-H, Aliphatic), 1718, 1677 (C=C), 1618

(C=N), 1364, 1257, 810, <sup>1</sup>HNMR (400 MHz, DMSO d<sub>6</sub>): δppm = 13.57 (s, 1H, OH), 11.48 (s, 1H, OH), 11.37 (s, 1H, OH), 6.79-7.70 (m, 3H, Ar-H), 3.34 (s, 3H, CH<sub>3</sub>), 2.21 (s, 3H, CH<sub>3</sub>).

**5.A.4.6 1-hydroxy-2-(2-hydroxyphenyl)-4,5-dimethylimidazole-3-oxide (4f):**

Dirty white, yield= 94 %, IR (KBr, cm<sup>-1</sup>) ν<sub>max</sub>: 3430 (br, OH), 3098, 3064 (C-H, Aromatic), 2958, 2927 (C-H, Aliphatic), 1658, 1640 (C=C), 1615, 1542 (C=N), 1343, 1260, 832, <sup>1</sup>HNMR (400 MHz, DMSO d<sub>6</sub>): δppm = 12.16 (s, 1H, OH), 9.87 (s, 1H, OH), 6.87-7.67 (m, 4H, Ar-H), 3.26 (s, 3H, CH<sub>3</sub>), 2.42 (s, 3H, CH<sub>3</sub>).

**5.A.4.7 1-hydroxy-2-(4-hydroxyphenyl)-4,5-dimethylimidazole-3-oxide (4g):**

white flakes yield= 94 %, melting point found (°C) = 165-168, IR (KBr, cm<sup>-1</sup>) ν<sub>max</sub>: 3400 (br, OH), 3000 (C-H, Aromatic), 2671 (C-H, Aliphatic), 1611 (C=C), 1560 (C=N), 1382, 1252, 837, <sup>1</sup>HNMR (400 MHz, DMSO d<sub>6</sub>): δppm = 11.32 (s, 1H, OH), 9.88 (s, 1H, OH), 7.04-7.86 (m, 4H, Ar-H), 2.27 (s, 3H, CH<sub>3</sub>), 2.19 (s, 3H, CH<sub>3</sub>).

**5.A.4.8 1-hydroxy-2-(5-chloro-2-hydroxyphenyl)-4,5-dimethylimidazole-3-oxide (4h):**

Pale yellow solid yield= 96%, IR (KBr, cm<sup>-1</sup>) ν<sub>max</sub>: 3416 (br, OH), 3212, 3136, 3053 (C-H, Aromatic), 2929, 2855 (C-H, Aliphatic), 1691, 1630 (C=C), 1572 (C=N), 1381, 1261, 815, <sup>1</sup>HNMR (400 MHz, DMSO d<sub>6</sub>): δppm = 13.49 (s, 1H, OH), 10.29 (s, 1H, OH), 7.03-7.70 (m, 3H, Ar-H), 3.34 (s, 3H, CH<sub>3</sub>), 2.50 (s, 3H, CH<sub>3</sub>).

**5.A.4.9 1-hydroxy-2-(5-bromo-2-hydroxyphenyl)-4,5-dimethylimidazole-3-oxide (4i):**

Pale yellow solid yield= 95%, IR (KBr, cm<sup>-1</sup>) ν<sub>max</sub>: 3417 (br, OH), 3059, 3027 (C-H, Aromatic), 2924, 2853 (C-H, Aliphatic), 1658 (C=C), 1602, 1580 (C=N), 1384, 1252, 828, <sup>1</sup>HNMR (400 MHz, DMSO d<sub>6</sub>): δppm = 11.48 (s, 1H, OH), 10.31 (s, 1H, OH), 6.83-7.63 (m, 3H, Ar-H), 3.32 (s, 3H, CH<sub>3</sub>), 1.91 (s, 3H, CH<sub>3</sub>).

**5.A.4.10 1-hydroxy-2-(2-hydroxy-3-methoxyphenyl)-4,5-dimethylimidazole-3-oxide (4j):**

white solid, yield= 95%, IR (KBr, cm<sup>-1</sup>) ν<sub>max</sub>: 3335 (br, OH), 3097, 3065 (C-H, Aromatic), 2929, 2837 (C-H, Aliphatic), 1625 (C=C), 1578 (C=N), 1366, 1246, 839, <sup>1</sup>HNMR (400 MHz, DMSO d<sub>6</sub>): δppm = 12.87 (s, 1H, OH), 11.38 (s, 1H, OH), 6.87-7.17 (m, 3H, Ar-H), 3.81 (s, 3H, OCH<sub>3</sub>), 2.43 (s, 3H, CH<sub>3</sub>), 2.18 (s, 3H, CH<sub>3</sub>).

**5.A.4.11 1-hydroxy-2-(4-hydroxy-3-methoxyphenyl)-4,5-dimethylimidazole-3-oxide (4k):**

white solid, yield= 94%, melting point found (°C) = 200-202, IR (KBr,

cm<sup>-1</sup>)  $\nu_{\max}$ : 3389 (br, OH), 3076 (C-H, Aromatic), 2928 (C-H, Aliphatic), 1636 (C=C), 1596 (C=N), 1388, 1279, 856, <sup>1</sup>HNMR (400 MHz, DMSO d<sub>6</sub>):  $\delta_{\text{ppm}}$  = 12.65 (s, 1H, OH), 10.35 (s, 1H, OH), 6.64-8.52 (m, 3H, Ar-H), 3.76 (s, 3H, OCH<sub>3</sub>), 2.35 (s, 3H, CH<sub>3</sub>), 2.10 (s, 3H, CH<sub>3</sub>).

**5.A.4.12 1-hydroxy-2-(3,4,5-methoxyphenyl)-4,5-dimethylimidazole-3-oxide (4l):** white solid, yield= 94%, IR (KBr, cm<sup>-1</sup>)  $\nu_{\max}$ : 3424 (br, OH), 3001 (C-H, Aromatic), 2930, 2836 (C-H, Aliphatic), 1732, 1632 (C=C), 1586, 1534 (C=N), 1364, 1246, <sup>1</sup>HNMR (400 MHz, DMSO d<sub>6</sub>):  $\delta_{\text{ppm}}$  = 11.37 (s, 1H, OH), 7.33 (s, 2H, Ar-H), 3.78 (s, 6H, OCH<sub>3</sub>), 3.33 (s, 3H, OCH<sub>3</sub>), 2.49 (s, 3H, CH<sub>3</sub>), 1.37 (s, 3H, CH<sub>3</sub>).

**5.A.4.13 1-hydroxy-2-(4-methoxyphenyl)-4,5-dimethylimidazole-3-oxide (4m):** white solid, yield= 93%, melting point found (°C) = 196-198, IR (KBr, cm<sup>-1</sup>)  $\nu_{\max}$ : 3418 (br, OH), 3003 (C-H, Aromatic), 2929 (C-H, Aliphatic), 1610, 1541 (C=N), 1380, 1256, 837 <sup>1</sup>HNMR (400 MHz, DMSO d<sub>6</sub>):  $\delta_{\text{ppm}}$  = 10.95 (s, 1H, OH), 8.12 (d, 2H, Ar-H), 3.78 (s, 3H, OCH<sub>3</sub>), 1.83 (s, 6H, CH<sub>3</sub>).

## 5.A.5 Supporting spectra

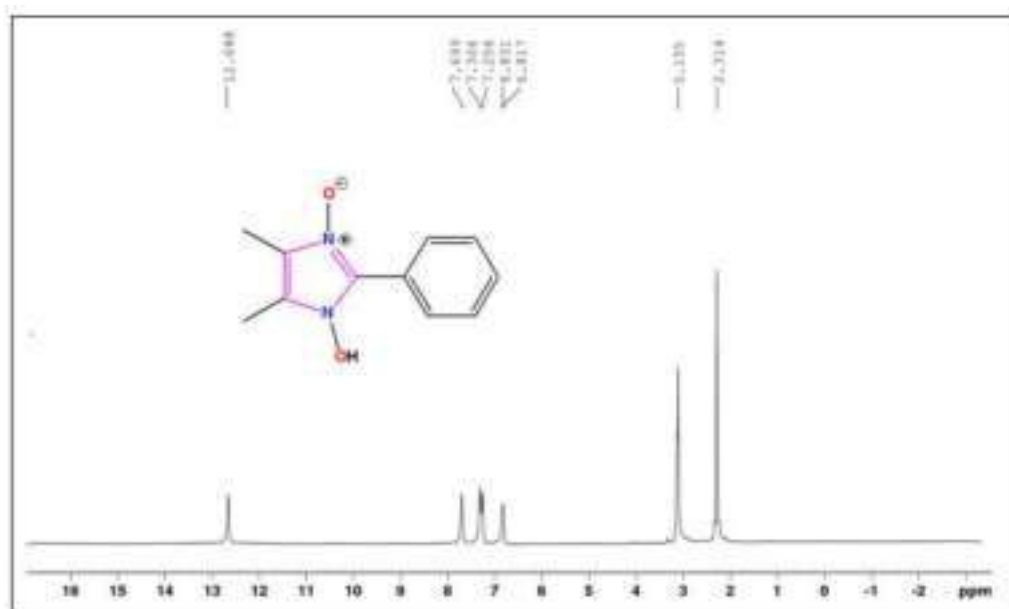


Fig. 5.A.5.1. <sup>1</sup>H NMR spectra of 1-hydroxy-2-phenyl-4,5-dimethylimidazole-3-oxide (4a)

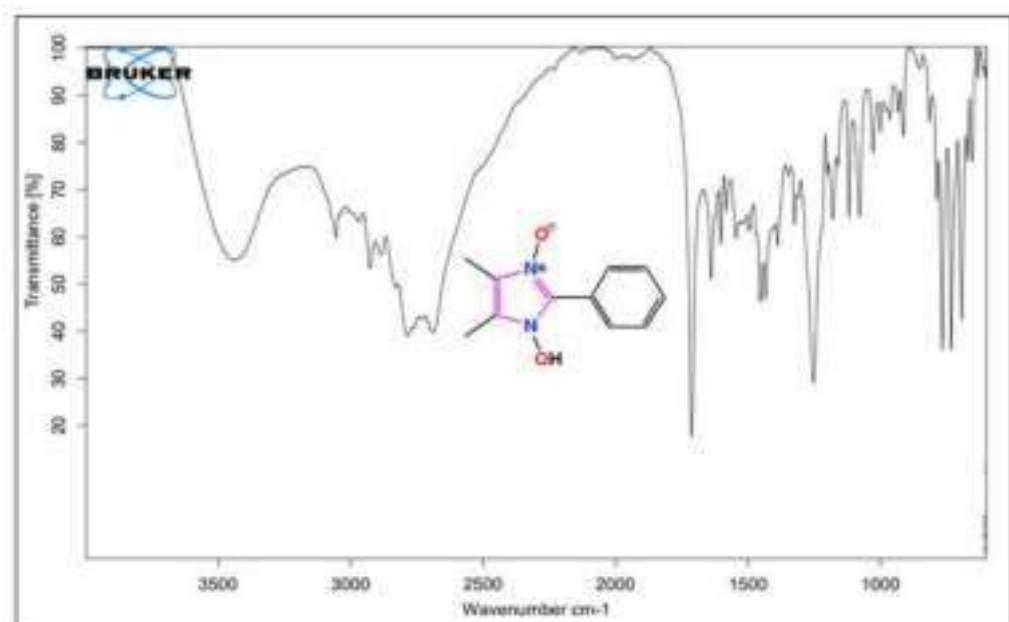
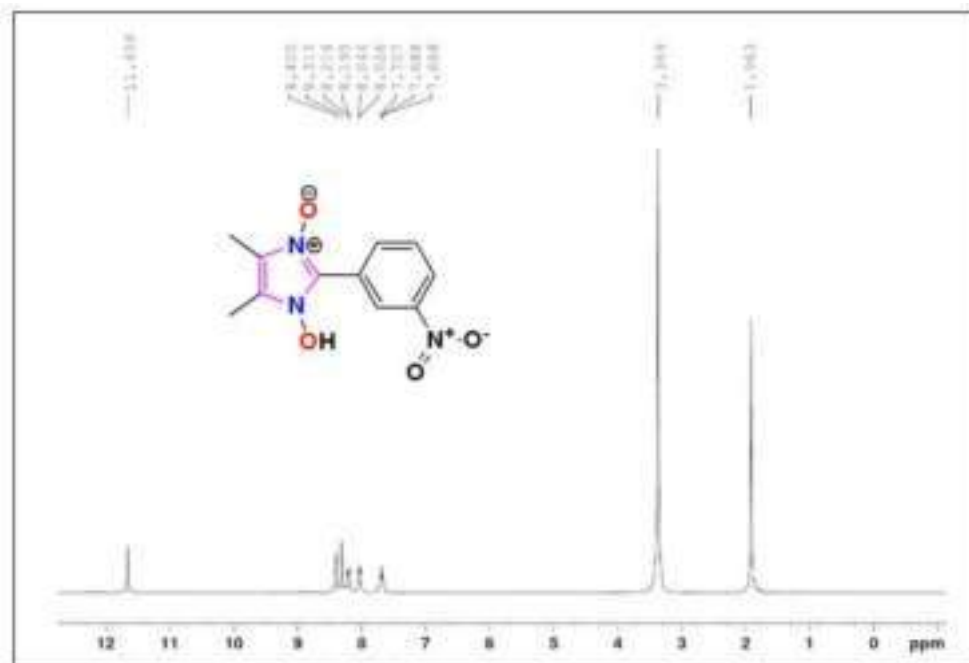
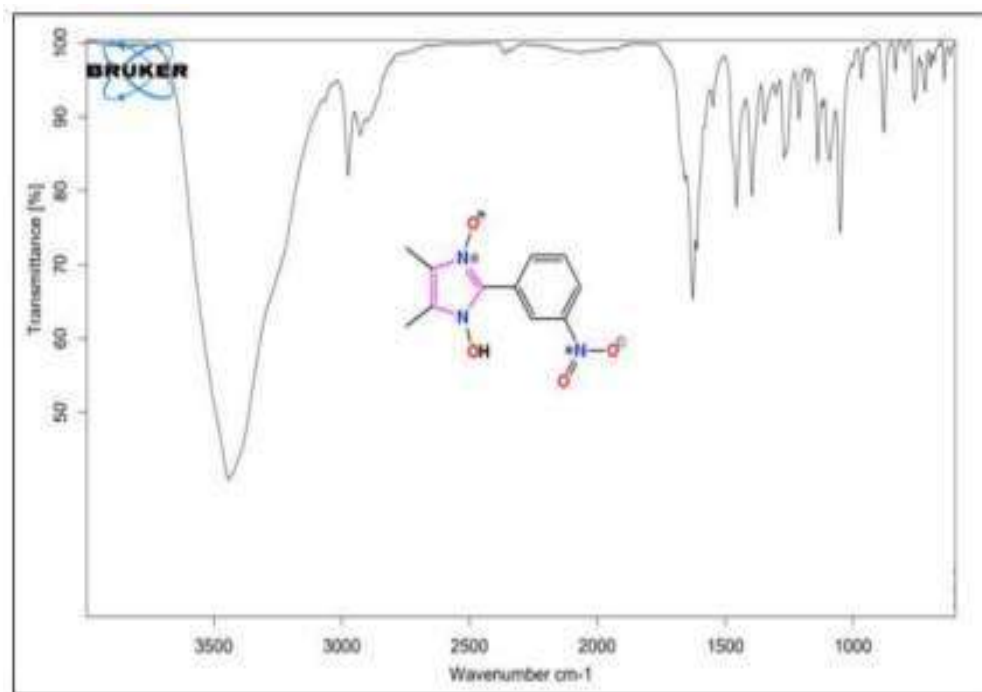


Fig. 5.A.5.2. FT-IR spectra of 1-hydroxy-2-phenyl-4,5-dimethylimidazole-3-oxide (4a)



**Fig. 5.A.5.3.**  $^1\text{H}$  NMR spectra of 1-hydroxy-2(3-nitrophenyl)-4,5-dimethylimidazole-3-oxide (4b)



**Fig. 5.A.5.4.** FT-IR spectra of 1-hydroxy-2(3-nitrophenyl)-4,5-dimethylimidazole-3-oxide (4b)



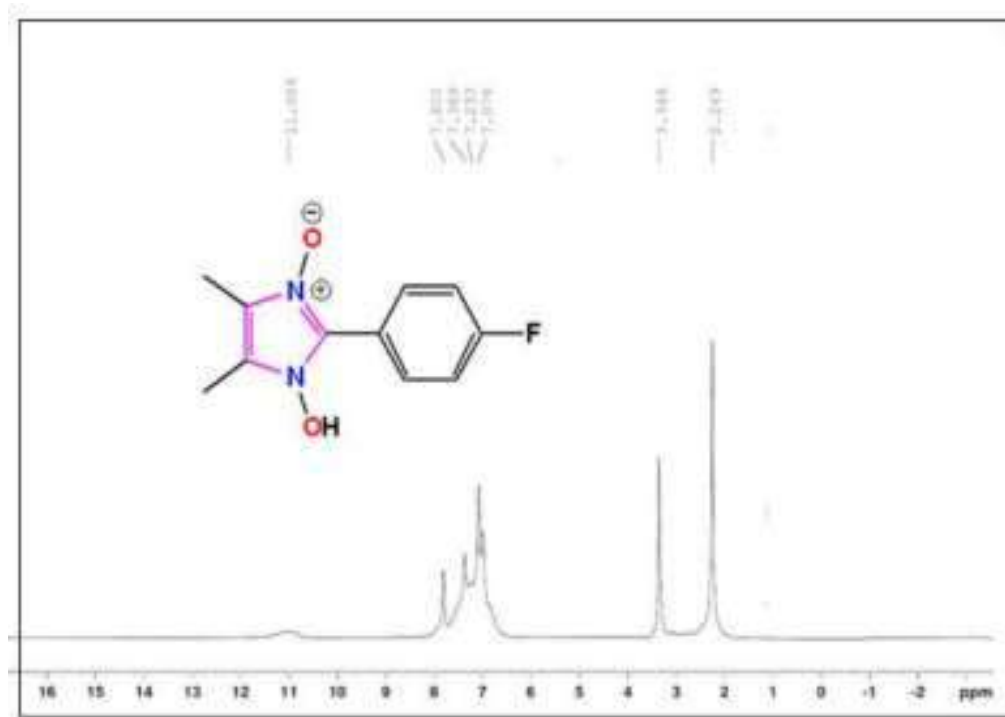


**Fig. 5.A.5.5.**  $^1\text{H}$ NMR spectra of 1-hydroxy-2(4-fluorophenyl)-4, 5-dimethylimidazole-3-oxide (4c)

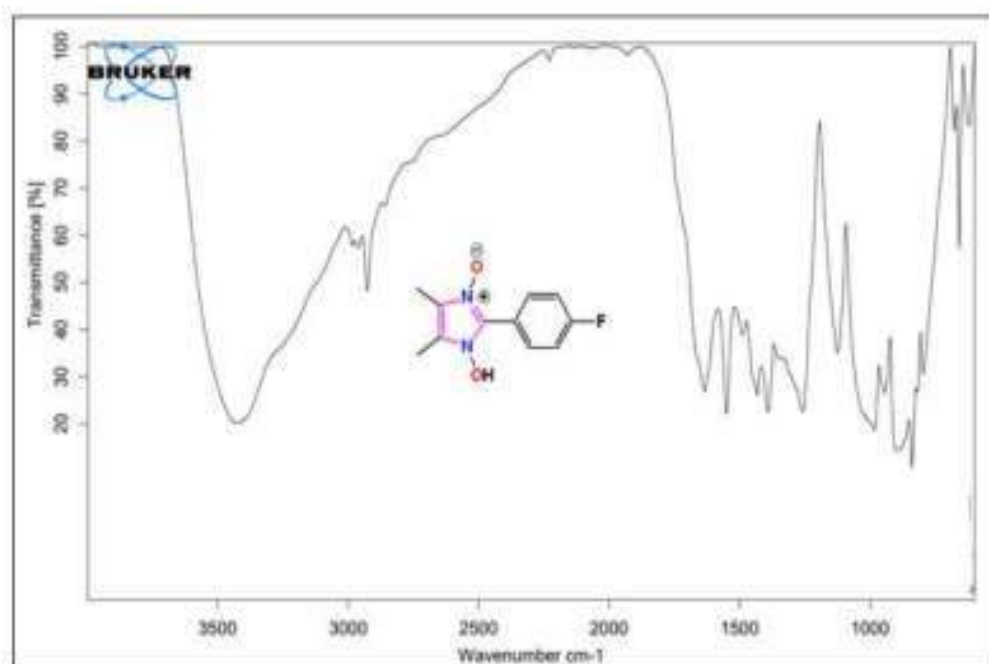


**Fig. 5.A.5.6.** FT-IR spectra of -hydroxy-2(4-fluorophenyl)-4,5-dimethylimidazole-3-oxide (4c)

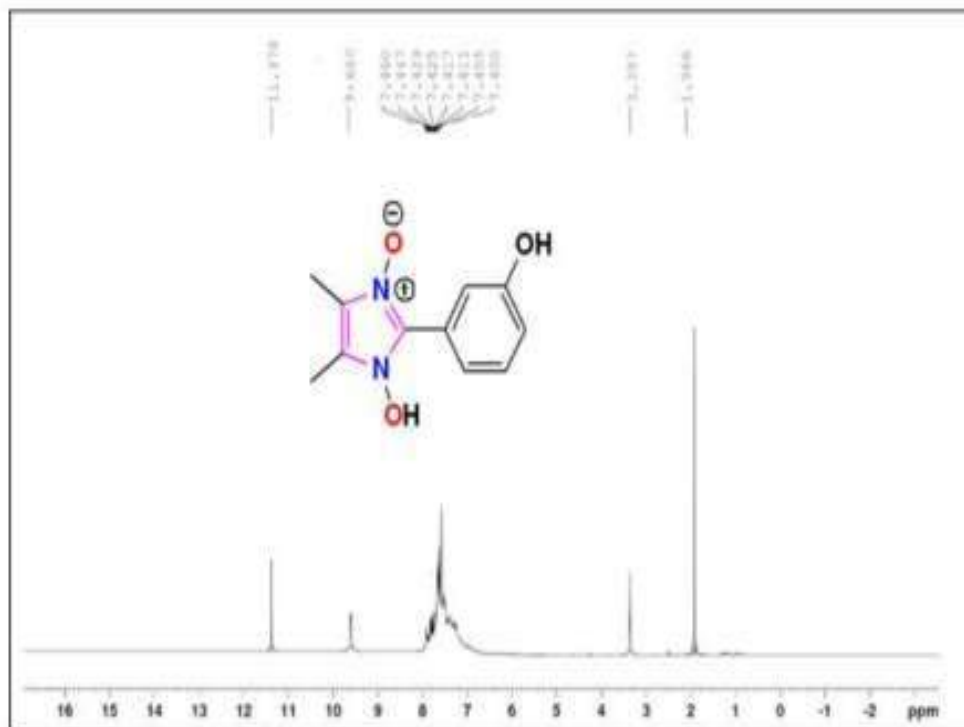


Fig. 5.A.5.7. <sup>1</sup>H NMR spectra of 1-hydroxy-2(3-hydroxyphenyl)-4, 5-dimethylimidazole-3-oxide (4d).

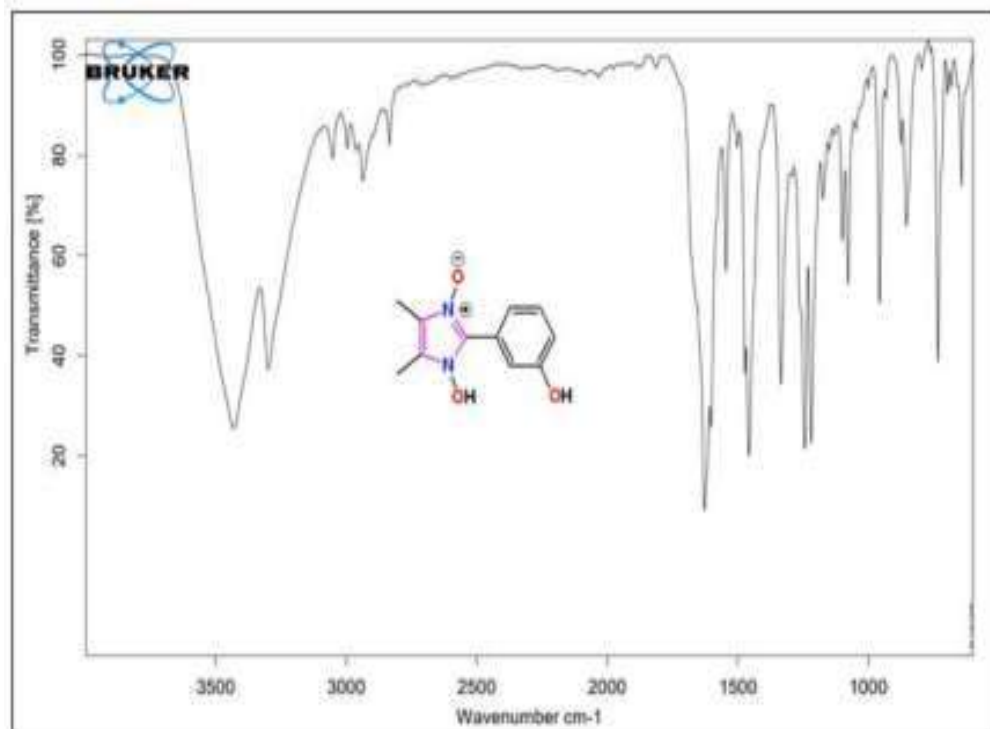


Fig. 5.A.5.8. FT-IR spectra of 1-hydroxy-2(3-hydroxyphenyl)-4,5-dimethylimidazole-3-oxide (4d)

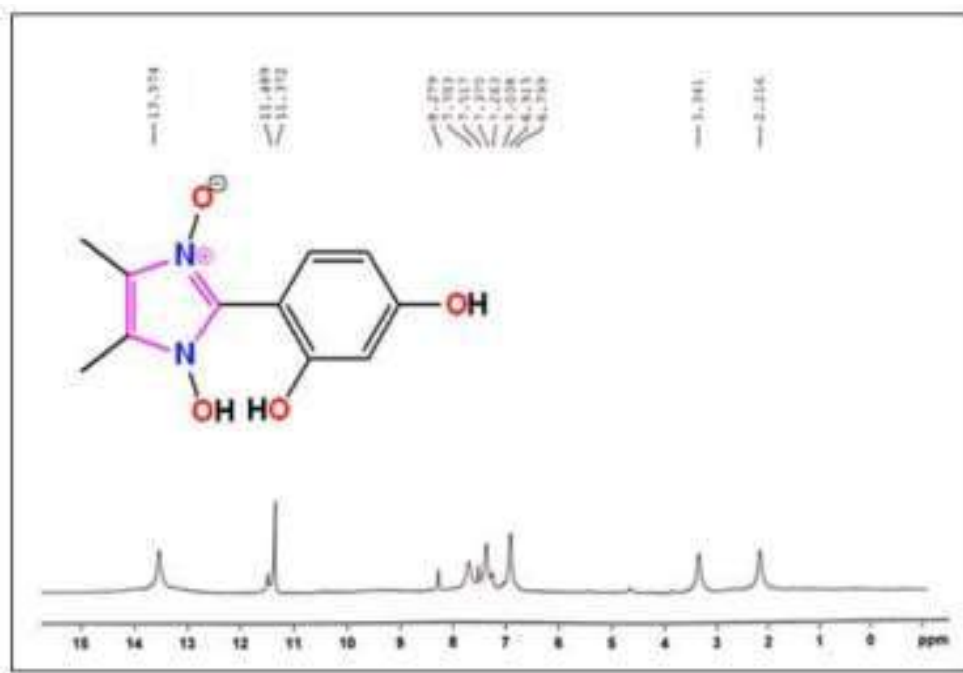


Fig. 5.A.9. <sup>1</sup>H NMR spectra of 1-hydroxy-2(2, 4-dihydroxyphenyl)-4, 5-dimethylimidazole-3- oxide (4e).

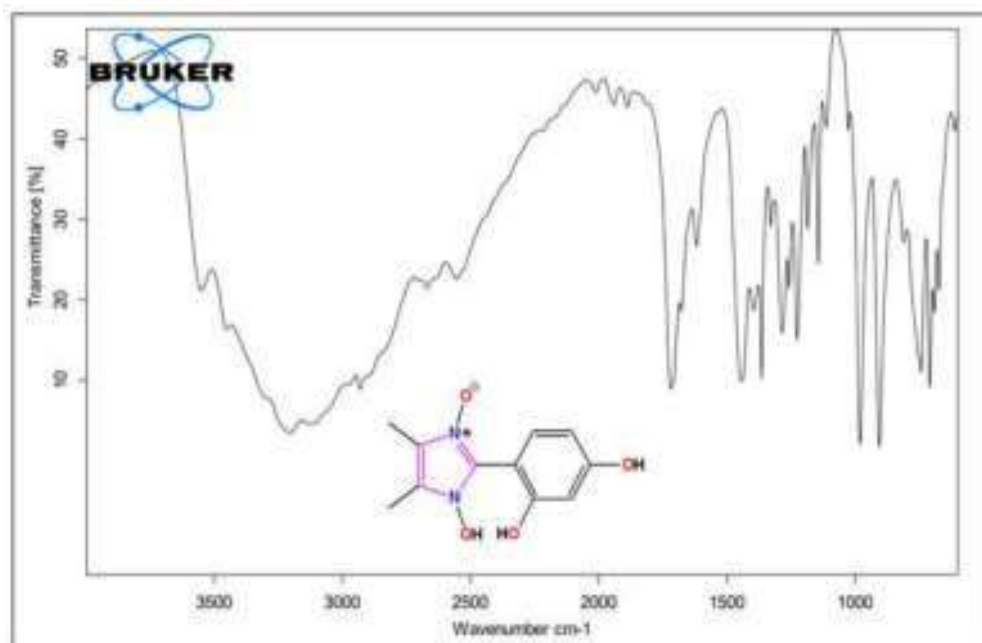
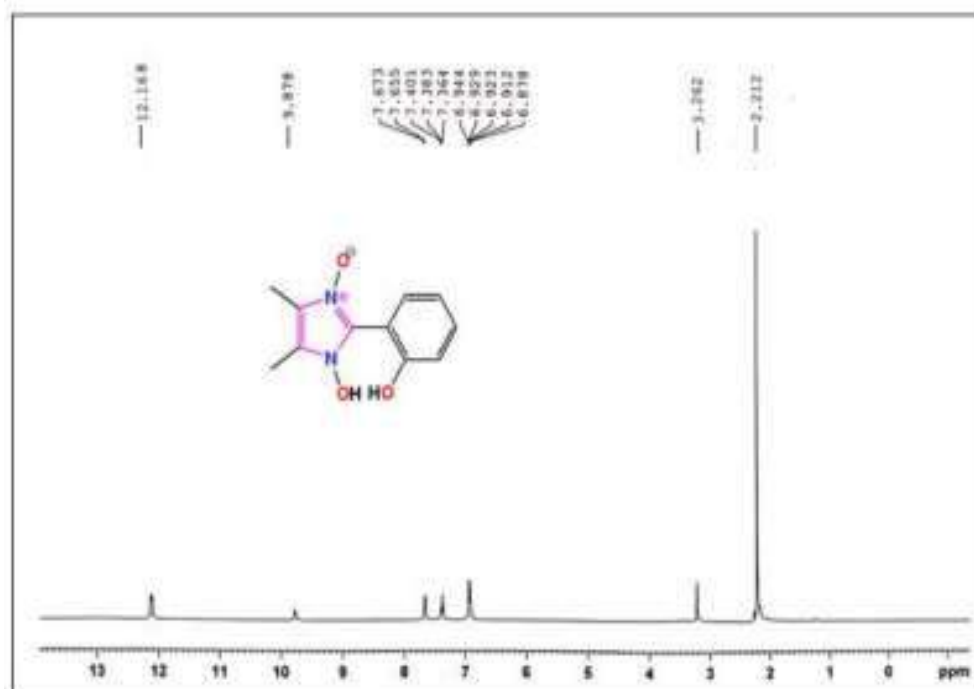
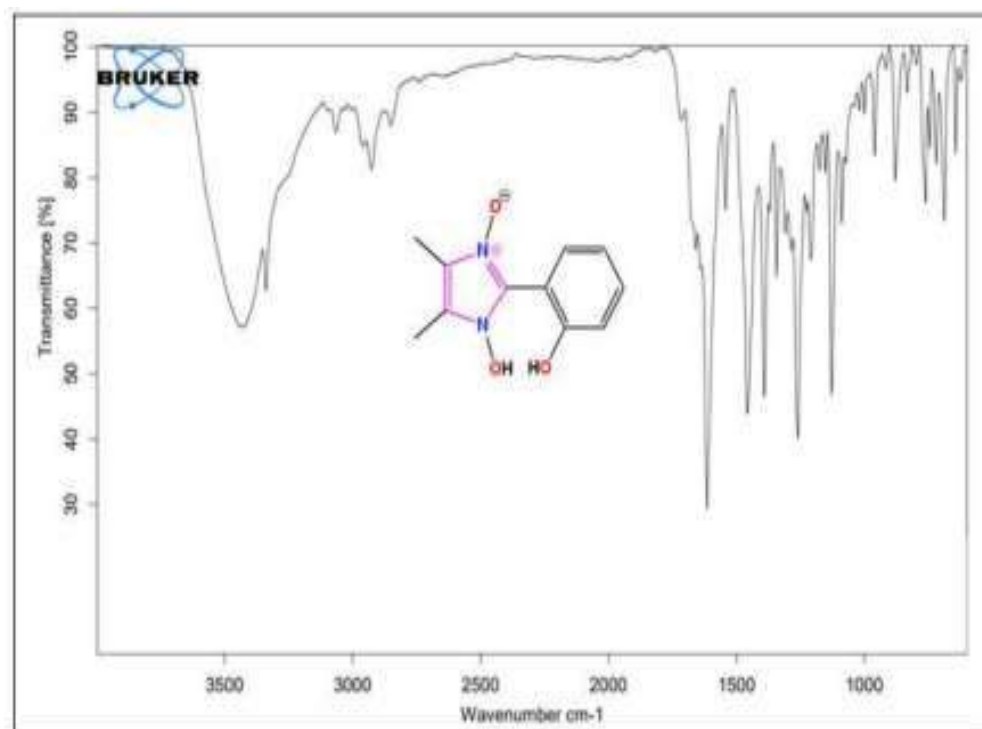


Fig. 5.A.5.10. FT-IR spectra of 1-hydroxy-2(2, 4-dihydroxyphenyl)-4, 5-dimethylimidazole-3- oxide (4e).



**Fig. 5.A.11.** <sup>1</sup>H NMR spectra of 1-hydroxy-2(2-hydroxyphenyl)-4, 5-dimethylimidazole-3- oxide (4f).



**Fig. 5.A.5.12.** FT-IR spectra of 1-hydroxy-2(2-hydroxyphenyl)-4, 5-dimethylimidazole-3- oxide (4f).

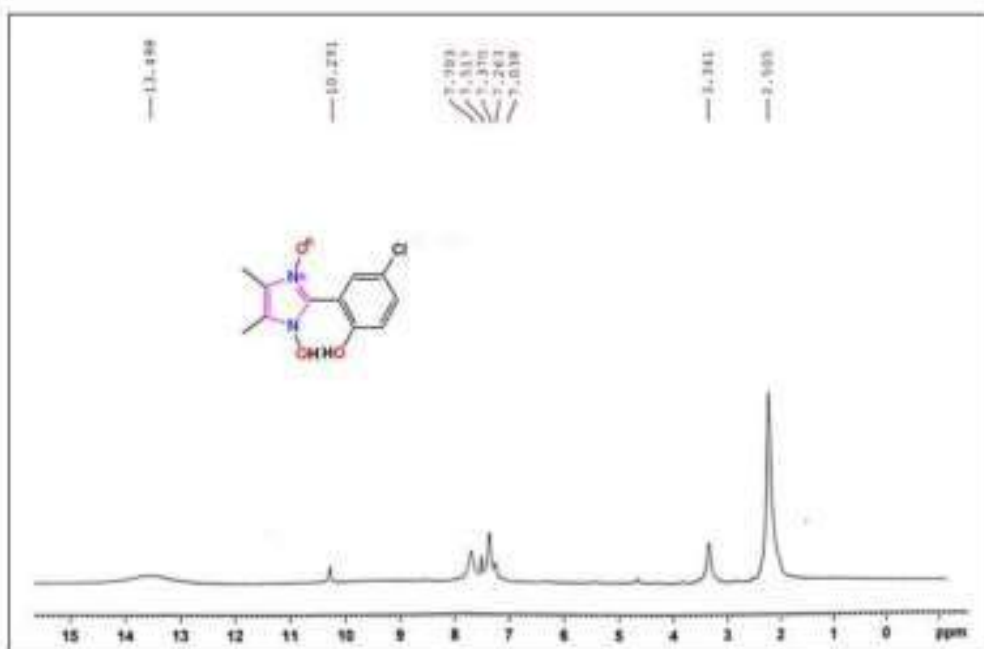


Fig. 5.A.5.13. <sup>1</sup>H NMR spectra of 1-hydroxy-2(5-chloro-2-hydroxyphenyl)-4, 5-dimethylimidazole-3- oxide (4h).

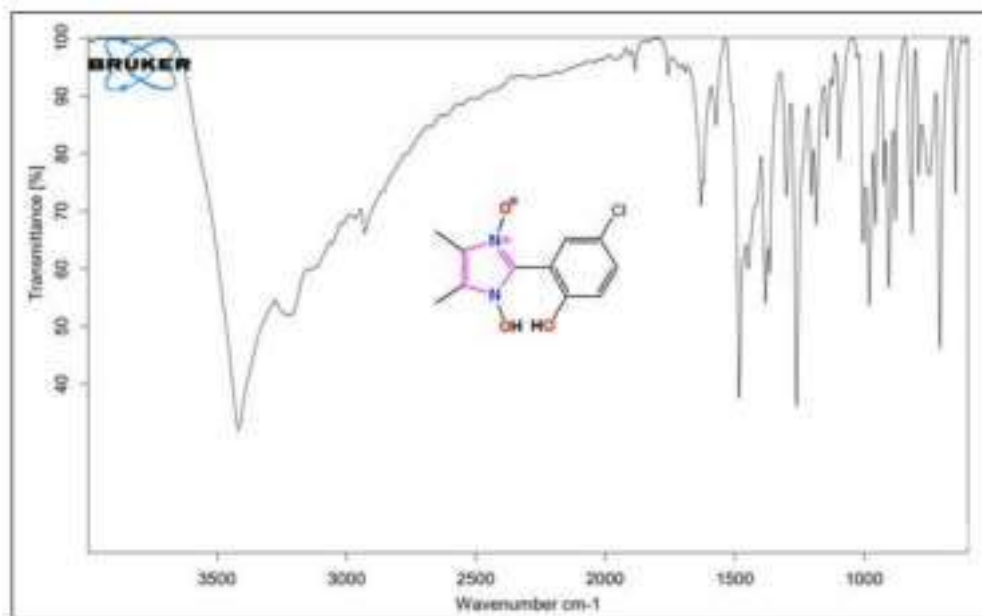


Fig. 5.A.5.14. FT-IR spectra of 1-hydroxy-2(5-chloro-2-hydroxyphenyl)-4, 5-dimethylimidazole-3- oxide (4h).

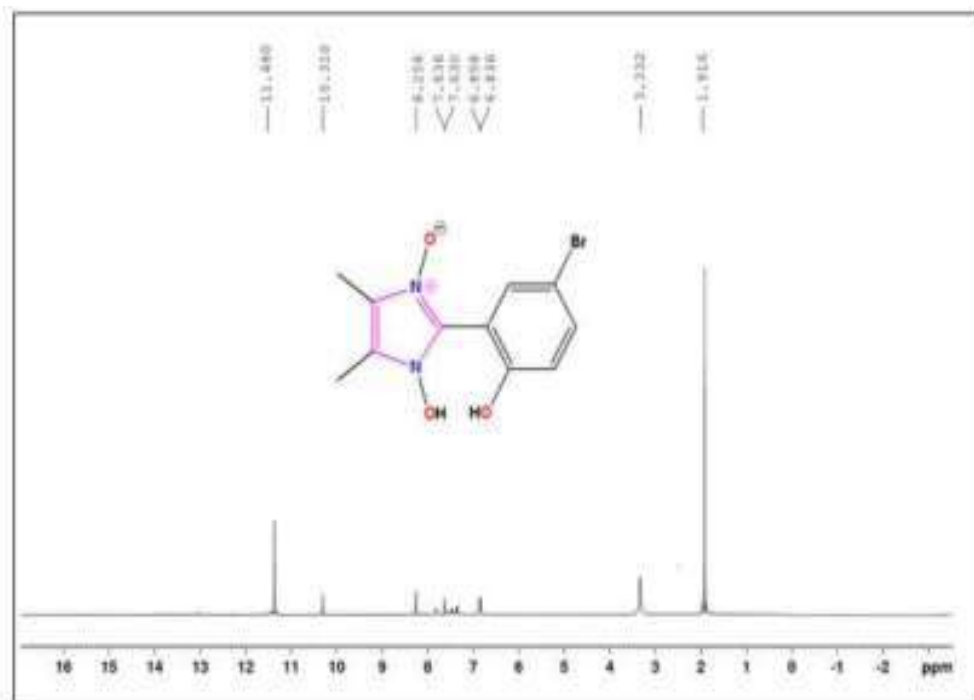


Fig. 5.A.5.15. <sup>1</sup>H NMR spectra of 1-hydroxy-2(5-bromo-2-hydroxyphenyl)-4, 5-dimethylimidazole-3- oxide (4i).

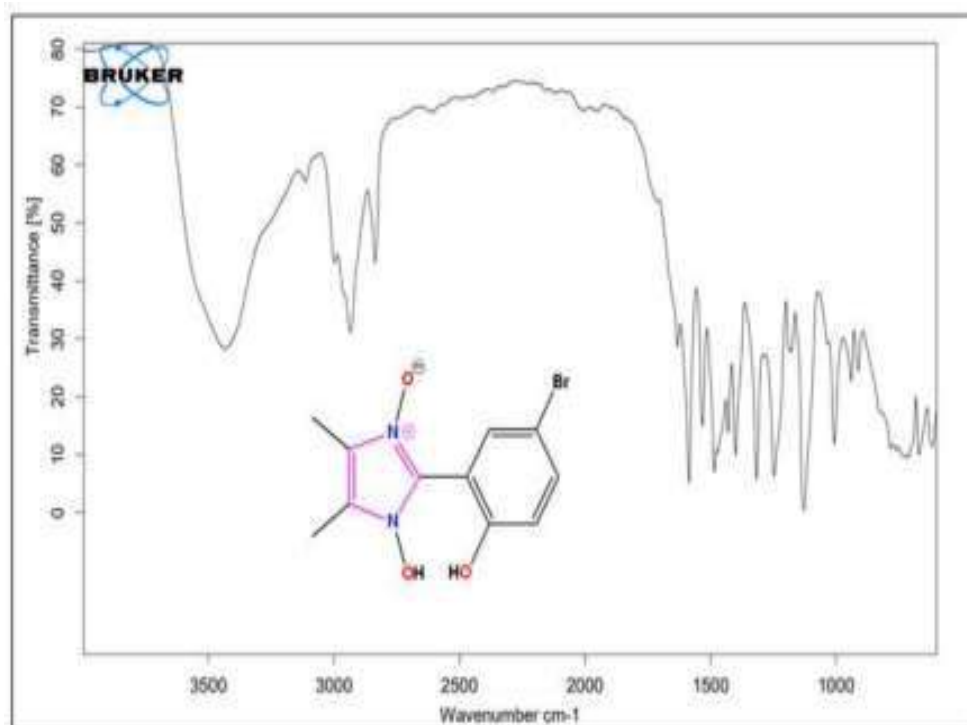


Fig. 5.A.5.16. FT-IR spectra of 1-hydroxy-2(5-bromo-2-hydroxyphenyl)-4, 5-dimethylimidazole-3- oxide (4i).

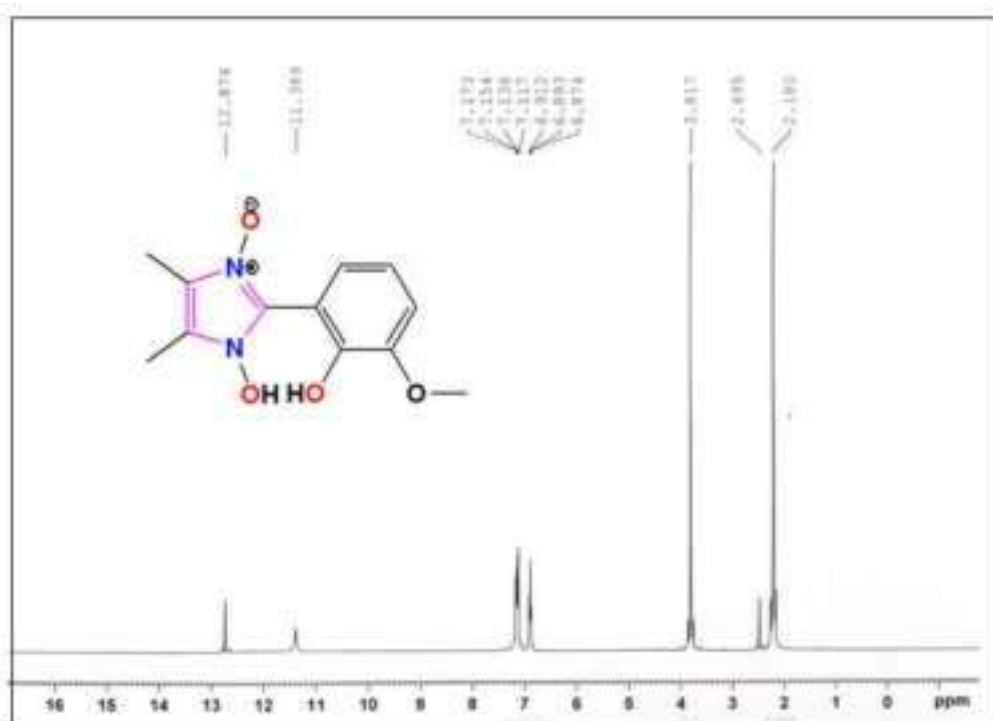


Fig. 5.A.5.17. <sup>1</sup>H NMR spectra of 1-hydroxy-2(2-hydroxy-3-methoxyphenyl)-4, 5-dimethylimidazole-3- oxide (4j).

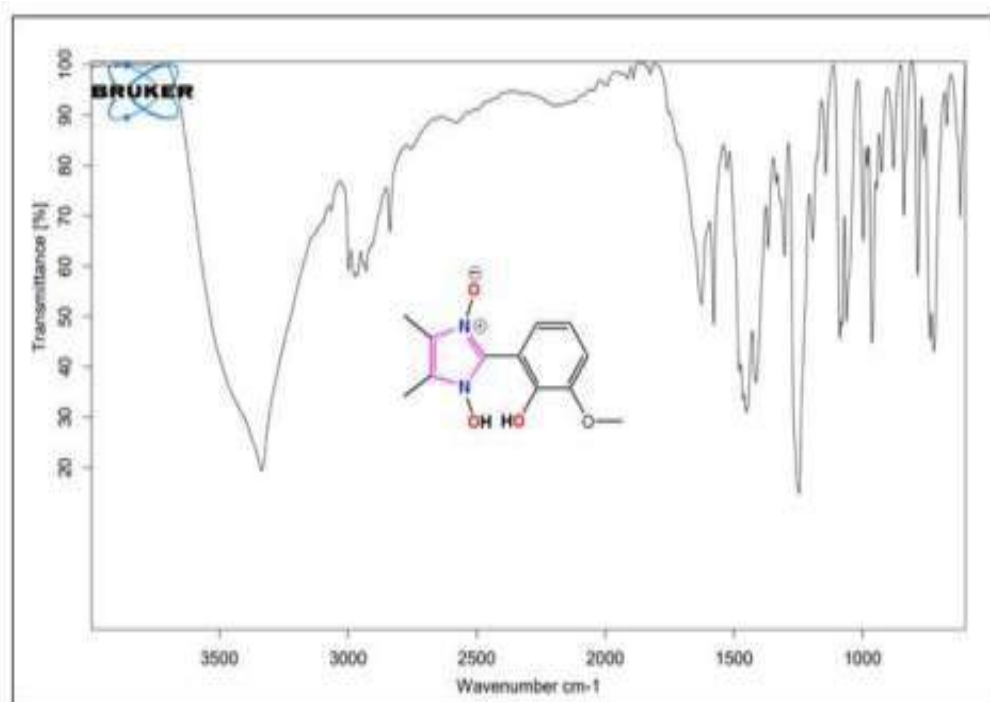
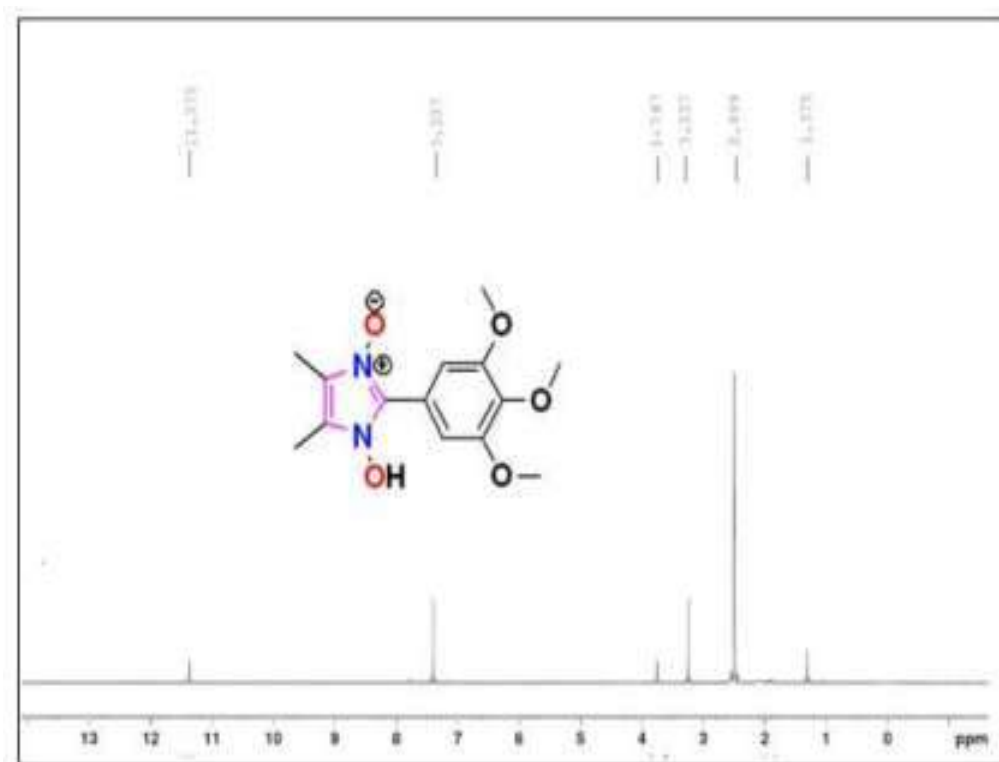
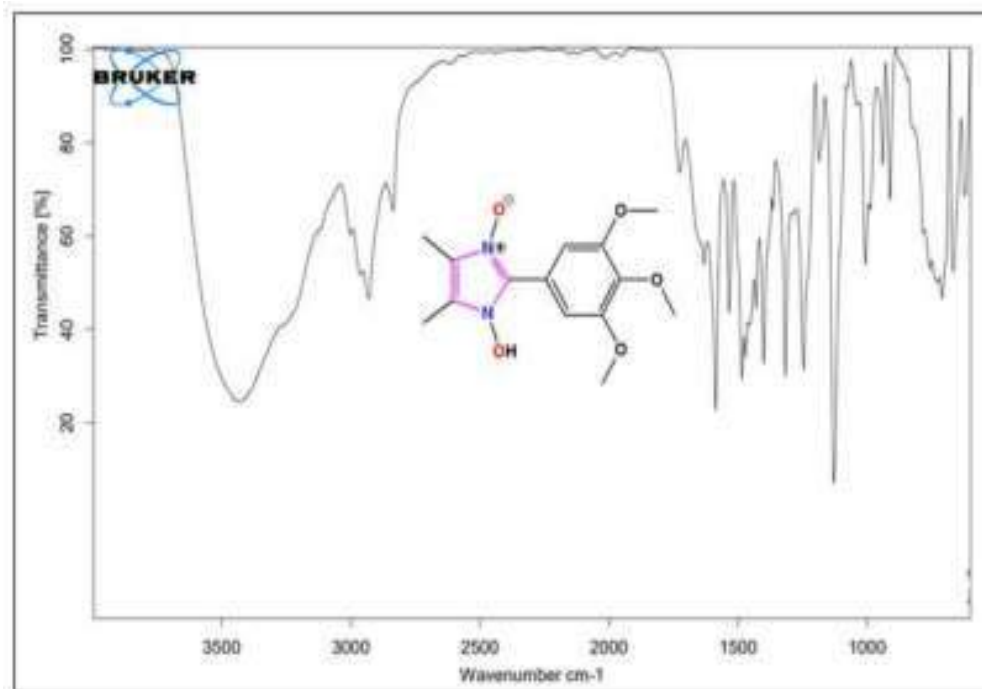


Fig. 5.A.5.18. FT-IR spectra of 1-hydroxy-2(2-hydroxy-3-methoxyphenyl)-4, 5-dimethylimidazole-3- oxide (4j).



**Fig. 5.A.5.19.** <sup>1</sup>H NMR spectra of 1-hydroxy-2(3, 4, 5-tri-methoxyphenyl)-4, 5-dimethylimidazole-3- oxide (41).



**Fig. 5.A.5.20.** FT-IR spectra of 1-hydroxy-2(3, 4, 5-tri-methoxyphenyl)-4, 5-dimethylimidazole-3- oxide (41).



## 5.A.6 References

- (1) H. Brahmhatt, M. Molnar, V. Pavić., *Karbala International Journal of Modern Science*, **2018**, 4 (2), 200–206.
- (2) A. Verma, S. Joshi, D. Singh., *Journal of Chemistry*, **2013**, 2013 (Article ID 392412).
- (3) P. Manocha, S. R. Wakode, A. Kaur, H. Kumar., *International Journal of Pharmaceutical Science and Research*, **2016**, 1 (7), 12–16.
- (4) A. Reyes-Arellano, O. Gómez-García, J. Torres-Jaramillo., *Medicinal Chemistry*, **2016**, 6 (9), 561–566.
- (5) D. H. Romero, V. E. T. Heredia, O. García-Barradas, Ma. E. M. López, E. S. Pavón., *Journal of Chemistry and Biochemistry*, **2014**, 2 (2), 45–83.
- (6) K. Anand, S. Wakode., *International Journal of Chemical Studies*, **2017**, 5 (2), 350–362.
- (7) B. K. Verma, S. Kapoor, U. Kumar, S. Pandey, P. Arya., *Indian Journal of Pharmaceutical and Biological Research*, **2017**, 5 (01), 1–9.
- (8) M. W. Bhade, P. R. Rajput., *International Journal of Applied and Pure Science and Agriculture*, **2016**, 2 (11), 80–84.
- (9) R. Katikireddy, R. Kakkerla, M. P. S. M. Krishna, G. Durgaiyah, Y. N. Reddy, M. Satyanarayana., *Heterocyclic Communications*, **2019**, 25 (1), 27–38.
- (10) A. Goyal, J. Singh, D. P. Pathak., *Journal of Pharmaceutical Technology, Research and Management*, **2013**, 1 (1), 69–79.
- (11) D. R. MacFarlane, K. R. Seddon., *Australian Journal of Chemistry*, **2007**, 60 (1), 3–5.
- (12) R. Rogers, G. Garau., *Materials world*, **2007**, 15 (12), 25–27.
- (13) G. Laus, J. Sladlwieser, W. Klötzer., *Synthesis (Stuttg)*, **1989**, 1989 (10), 773–775.
- (14) K. Hayes., *Journal of Heterocyclic Chemistry*, **1974**, 11 (4), 615–618.
- (15) A. Albini, S. Pietra., *Heterocyclic N-Oxides*; CRC Press: Boca Raton, Ann Arbor, Boston USA, **1991**.
- (16) A. Albini., *Synthesis (Stuttg)*, **1993**, 1993 (3), 263–277.
- (17) Y. Wang, L. Zhang., *Synthesis (Stuttg)*, **2015**, 47 (03), 289–305.

- (18) J. V. Quagliano, J. Fujita, G. Franz, D. J. Phillips, J. A. Walmsley, S. Y. Tyree., *J Am Chem Soc*, **1961**, 83 (18), 3770–3773.
- (19) R. B. da Silva, V. B. Loback, K. Salomão, S. L. de Castro, J. L. Wardell, S. M. S. V. Wardell, T. E. M. M. Costa, C. Penido, M. D. G. M. de Oliveira Henriques, S. A. Carvalho, E. F. da Silva, C. A. M. Fraga., *Molecules*, **2013**, 18 (3), 3445–3457.
- (20) M. Witschel., *Bioorganic & Medicinal Chemistry*, **2009**, 17 (12), 4221–4229.
- (21) T. B. Stensbøl, P. Uhlmann, S. Morel, B. L. Eriksen, J. Felding, H. Kromann, M. B. Hermit, J. R. Greenwood, H. Braüner-Osborne, U. Madsen, F. Junager, P. Krogsgaard-Larsen, M. Begtrup, P. Vedsø., *Journal of Medicinal Chemistry*, **2002**, 45 (1), 19–31.
- (22) M. L. Richardson, K. A. Croughton, C. S. Matthews, M. F. G. Stevens., *Journal of Medicinal Chemistry*, **2004**, 47 (16), 4105–4108.
- (23) O. K. Kim, L. K. Garrity-Ryan, V. J. Bartlett, M. C. Grier, A. K. Verma, G. Medjanis, J. E. Donatelli, A. B. Macone, S. K. Tanaka, S. B. Levy, M. N. Alekshun., *Journal of Medicinal Chemistry*, **2009**, 52 (18), 5626–5634.
- (24) G. Mloston, M. Celeda, M. Jasinski, K. Urbaniak, P. J. Boratynski, P. R. Schreiner, H. Heimgartner., *Molecules*, **2019**, 24 (23), 4398.
- (25) S. A. Amitina, A. Y. Tikhonov, I. A. Grigor'Ev, Y. V. Gatilov, B. A. Selivanov., *Chemistry of Heterocyclic Compounds*, **2009**, 45 (6), 691–697.
- (26) F. J. Allan, G. G. Allan., *Chemistry & Industry*, **1964**, 44, 1837–1837.
- (27) P. A. Nikitina, L. G. Kuz'Mina, V. P. Perevalov, I. I. Tkach., *Tetrahedron*, **2013**, 69 (15), 3249–3256.
- (28) P. A. Nikitina, A. S. Peregudov, T. Y. Koldaeva, L. G. Kuz'Mina, E. I. Adiulin, I. I. Tkach, V. P. Perevalov., *Tetrahedron*, **2015**, 71 (33), 5217–5228.
- (29) K. Pradhan, B. K. Tiwary, M. Hossain, R. Chakraborty, A. K. Nanda., *RSC Advances*, **2016**, 6 (13), 10743–10749.
- (30) S. Bartz, B. Blumenröder, A. Kern, J. Fleckenstein, S. Frohnapfel, J. Schatz, A. Wagner., *Zeitschrift für Naturforschung*, **2009**, 64b (6), 629–638.
- (31) S. O. Chua, M. J. Cook, A. R. Katritzky., *Journal of the Chemical Society B: Physical Organic*, **1971**, 2350–2355.
- (32) W. Schilf, L. Stefaniak, M. Witanowski, G. A. Webb., *Journal of Molecular Structure*, **1986**, 140 (3–4), 311–315.
- (33) M. Boiani, H. Cerecetto, M. Gonzalez, O. E. Piro, E. E. Castellano., *Journal of Physical Chemistry A*, **2004**, 108 (51), 11241–11248.

- (34) *SADABS, SMART and SAINT*; Bruker AXS Inc., Madison, Wisconsin, USA, **2000**.
- (35) G. M. Sheldrick., *SHELXS-97 and SHELXL-97, Program for Crystal Structure Solution and Refinement*; University of Gottingen, Gottingen: Germany, **1997**.
- (36) L. J. Farrugia., *Journal of Applied Crystallography*, **1997**, 30 (5), 565–565.
- (37) A. L. Spek., *Acta Crystallographica*, **2009**, D65 (2), 148–155.
- (38) L. J. Farrugia., *Journal of Applied Crystallography*, **1999**, 32 (4), 837–838.
- (39) L. J. Farrugia., *Journal of Applied Crystallography*, **2012**, 45 (4), 849–854.

## **CHAPTER-V**

### **Section B**

#### **DFT, Molecular Docking and Pharmacokinetic study of some selected 1-hydroxy-2-arylimidazole-3-oxide derivatives**

##### **5.B.1 Background of the present investigation**

The imidazole scaffold is an important moiety present in natural products and biologically active compounds<sup>1-2</sup>. Imidazole derivatives are present in various classes of anti-cancer, anti-diabetic, anti-viral and anti-diabetic drugs<sup>3-4</sup>. Apart from biological applications, imidazole derivatives also various other important properties like electroluminescence and hence can also be used in diodes<sup>5</sup>. Imidazole-3-oxide derivatives are important derivatives of imidazole compounds. These compounds have gained immense popularity due to their anti-protozoal<sup>6</sup>, fungicidal, herbicidal, pesticidal<sup>7</sup>, hypotensive properties<sup>8</sup>, anti-tumor<sup>9</sup> and anti-viral<sup>10</sup> properties. Furthermore, these compounds are also used as intermediates in some organic reactions<sup>11</sup>.

Theoretical studies based on quantum mechanics using computational methods is an emerging field of research for understanding mechanism, geometry and reaction pathways of organic molecules<sup>12-13</sup>. With the introduction of Computer Aided Drug Design (CADD), the process of drug designing taken a new dimension as this method reduces the time and is cost effective for drug design<sup>14</sup>. In order to understand the Thermodynamic properties and other important parameters like dipole moments, optical properties, vibration frequencies theoretically, DFT or Density Functional Theory is widely used<sup>15-17</sup> and the results obtained from DFT can be used for comparing with the experimental results.

##### **5.B.2 Results and Discussion**

###### **5.B.2.1 Computational Study**

The molecular geometry, molecular orbital (HOMO,LUMO), Non-linear Optical property (NLO), Global chemical descriptors and Molecular Electrostatic Potential (MEP) of the selected 1-hydroxy-2-arylimidazole-3-oxide derivatives namely, 1-hydroxy-2-(2-hydroxyphenyl)-4,5-dimethylimidazole-3-oxide(IMO-1), 1-hydroxy-2-(5-nitro-2-hydroxyphenyl)-4,5-dimethylimidazole-3-oxide(IMO-2), 1-hydroxy-2-(5-chloro-2-hydroxyphenyl)-4,5-dimethylimidazole-3-oxide(IMO-3), 1-hydroxy-2-(5-bromo-2-hydroxyphenyl)-4,5-dimethylimidazole-3-oxide(IMO-4), 1-hydroxy-2-(2,4-dihydroxyphenyl)-4,5-dimethylimidazole-3-oxide(NO-5) and 1-hydroxy-2-(2-hydroxy-3-methoxyphenyl)-4,5-dimethylimidazole-3-oxide(IMO-6) have been optimized by Density Functional Theory (DFT) using Becke's three-parameter hybrid method (B3) with Lee, Yang and Parr correlation functional methods (LYP) with B3LYP/631G+(d,2p) level of basis set<sup>18-19</sup>. All the

computational calculations were calculated by Gaussian 16, Revision A.03 programme package<sup>20</sup> and the results were visualized using GAUSSVIEW 6.0 software<sup>21</sup> on a hp-Z640 desktop P.C. with an Intel Xeon processor (Specifications: E5-2630 V4 @ 220GHz).

### 5.B.2.1.1 Optimization of Molecular Geometry

To the best of our knowledge, the X-Ray single crystal structure of only a few 1-hydroxy-2-arylimidazole-3-oxide derivatives have been reported so far, therefore, structure optimization using DFT method serves as a good alternative to ascertain the different geometrical parameters of the selected compounds under study. The geometrical parameters of the studied compounds (IMO-1 to IMO-6) were calculated by DFT assay using B3LYP/631G+(d,2p) level of basis set. The optimized gas phase molecular geometry of the compounds (IMO-1 to IMO-6) with atom labelling scheme is shown in Fig. 5.B.1 and Fig 5.B.2 and the structural parameters like bond lengths, bond angles and dihedral angles are listed in Table 5.B.1.

From the Table 5.B.1, the dihedral angles C6-C5-C7-N9 and C6-C5-C7-N12 in IMO-1 are 34.178° and -143.86° respectively. In IMO-2, the dihedral angles, C6-C5-C7-N9 and C6-C5-C7-N12 are -32.60° and 149.34° respectively. In IMO-3, the dihedral angles, C7-C6-C8-N13 and C7-C6-C8-N10 are -144.14° and 33.96° respectively. In IMO-4, the dihedral angles, C7-C6-C8-N13 and C7-C6-C8-N10 are -144.099° and 33.98° respectively. In IMO-5, the dihedral angles, C9-C8-C5-N4 and C9-C8-C5-N1 are -33.67° and 148.31° respectively. Finally for IMO-6, dihedral angles, C6-C5-C7-N9 and C6-C5-C7-N12 are -145.62° and 36.132° respectively. Therefore, from the analysis of the dihedral angles it is evident that the phenyl ring 2 is not planar with the imidazole ring 1. From the Table 5.B.1, it is seen that the C-N bond lengths of imidazole ring in all the studied compounds IMO-1, IMO-3 and IMO-4 namely C8-N10, C8-N13, C11-N10 and C11-N13 are 1.351 Å, 1.374 Å, 1.391 Å and 1.380 Å respectively. For the compounds IMO-2 and IMO-6, the C-N bond lengths, namely C7-N9, C7-N12, C10-N9 and C10-N12 are in the range 1.350 Å, 1.374 Å, 1.389-1.391 Å and 1.380-1.381 Å respectively. For the compound IMO-5, the C-N bond lengths namely, C5-N1, C5-N4, C2-N1 and C3-N4 are 1.350 Å, 1.374 Å, 1.391 Å and 1.382 Å respectively. The shortening of the C-N bond lengths reveals the effect of resonance in this part of the molecule and this can be attributed to the difference in hybridization state of different carbon atoms in the imidazole ring<sup>22</sup>.

**Table 5.B.1.** Structural parameters (bond lengths, bond angle and dihedral angle) of the studied compounds (IMO-1 to IMO-6)

<b>C-C bond length (Å)</b>					
<b>IMO-1</b>		<b>IMO-2</b>		<b>IMO-3</b>	
C1-C2	1.403	C1-C2	1.402	C2-C3	1.400
C2-C3	1.389	C2-C3	1.382	C3-C4	1.388
C3-C4	1.408	C3-C4	1.413	C4-C5	1.408
C4-C5	1.425	C4-C5	1.433	C5-C6	1.424
C5-C6	1.414	C5-C6	1.404	C6-C7	1.413
C6-C1	1.389	C6-C1	1.390	C7-C2	1.386
C5-C7	1.458	C5-C7	1.460	C6-C8	1.458
C10-C11	1.376	C10-C11	1.376	C11-C12	1.376
C10-C14	1.488	C10-C14	1.488	C11-C15	1.488
C11-C13	1.491	C11-C13	1.491	C12-C14	1.491
<b>IMO-4</b>		<b>IMO-5</b>		<b>IMO-6</b>	
C2-C3	1.399	C10-C11	1.404	C1-C2	1.401
C3-C4	1.387	C11-C12	1.391	C2-C3	1.391
C4-C5	1.407	C12-C13	1.405	C3-C4	1.419
C5-C6	1.424	C13-C8	1.426	C4-C5	1.423
C6-C7	1.413	C8-C9	1.414	C5-C6	1.414
C7-C2	1.385	C9-C10	1.385	C6-C1	1.387
C6-C8	1.457	C8-C5	1.455	C5-C7	1.459
C11-C12	1.376	C2-C3	1.375	C10-C11	1.375
C11-C15	1.488	C2-C6	1.488	C10-C14	1.488
C12-C14	1.491	C3-C7	1.491	C11-C13	1.491
<b>C-H, C-O, N-O, C-Cl, C-Br and O-H bond distances (Å)</b>					
<b>IMO-1(Å)</b>		<b>IMO-2(Å)</b>		<b>IMO-3(Å)</b>	
C1-H26	1.084	C2-H29	1.082	C3-H28	1.084
C2-H27	1.085	C3-H28	1.083	C4-H27	1.084
C3-H28	1.084	C6-H30	1.081	C7-H26	1.082
C6-H25	1.083	C13-H25	1.094	C14-H18	1.090
C13-H19	1.090	C13-H26	1.090	C14-H19	1.094
C13-H20	1.094	C13-H27	1.095	C14-H20	1.095
C13-H21	1.095	C14-H22	1.091	C15-H21	1.091

C14-H22	1.094	C14-H23	1.094	C15-H22	1.094
C14-H23	1.091	C14-H24	1.094	C15-H23	1.094
C14-H24	1.094	C4-O8	1.325	C5-O9	1.339
C4-O8	1.341	N17-O18	1.236	N10-O16	1.324
N9-O15	1.325	N17-O19	1.235	N13-O17	1.379
N12-O16	1.380	O8-H20	1.047	O17-H24	0.973
O16-H18	0.973	O16-H21	0.973	O9-H25	1.028
O8-H17	1.023			C2-Cl1	1.762
<b>IMO-4</b>		<b>IMO-5</b>		<b>IMO-6</b>	
C3-H19	1.084	C9-H24	1.083	C1-H27	1.084
C4-H29	1.084	C10-H25	1.083	C2-H28	1.085
C7-H18	1.082	C12-H26	1.086	C6-H26	1.083
C14-H25	1.090	C6-H18	1.091	C14-H22	1.094
C14-H26	1.094	C6-H19	1.094	C14-H23	1.091
				C14-H24	1.094
C14-H27	1.095	C6-H20	1.094	C13-H19	1.090
C15-H22	1.091	C7-H21	1.096	C13-H20	1.094
C15-H23	1.094	C7-H23	1.094	C13-H21	1.095
C15-H24	1.094	C7-H22	1.091	C18-H31	1.341
C5-O9	1.338	C13-O17	1.338	C18-H32	1.372
N10-O16	1.324	C11-O14	1.368	C18-H30	1.379
N13-O21	1.379	O17-H29	1.033	C4-O8	1.341
O9-H28	1.029	O14-H27	0.966	C3-O17	1.372
O17-H21	0.973	O16-H28	0.973	N12-O16	1.379
C2-Br1	1.909	N1-O15	1.327	N9-O15	1.326
		N4-O16	1.380	O16-H25	0.973
				O8-H29	1.034
<b>Bond Angle (°)</b>					
<b>IMO-1</b>		<b>IMO-2</b>		<b>IMO-3</b>	
C3-C2-C1	120.394	C3-C2-C1	118.925	C3-C2-Cl1	119.664
C4-C3-C2	121.156	C4-C3-C2	121.577	C4-C3-C2	119.340
C5-C4-C3	118.729	C5-C4-C3	118.765	C5-C4-C3	121.625
C6-C1-C2	119.394	C6-C1-C2	121.419	C6-C5-C4	118.525
C7-C5-C4	120.945	C7-C5-C4	121.125	C7-C2-Cl1	119.548
O8-C4-C3	118.214	O8-C4-C3	118.125	C8-C6-C5	121.008
N9-C7-C5	128.145	N9-C7-C5	127.966	O9-C5-C4	118.267

C10-N9-C7	111.037	C10-N9-C7	111.178	N10-C8-C6	127.940
C11-C10-N9	107.214	C11-C10-N9	107.080	C11-N10-C8	111.014
N12-C7-C5	127.429	N12-C7-C5	127.630	C12-C11-N10	107.199
C13-C11-C10	132.159	C13-C11- C10	132.156	N13-C8-C6	127.588
C14-C10-N9	120.287	C14-C10-N9	120.424	C14-C12-C11	132.145
O15-N9-C7	125.466	O15-N9-C7	125.461	C15-C11-C10	120.306
O16-N12-C7	125.099	O16-N12-C7	125.020	O16-N10-C8	125.492
H17-O8-C4	109.111	N17-C1-C6	118.967	O17-N13-C8	125.072
H19-C13- C11	109.651	O18-N17-C1	118.148	H18-C14-C12	109.660
H20-C13- C11	111.424	O19-N17-C1	117.846	H19-C14-C12	111.359
H21-C13- C11	111.739	H20-O8-C4	109.712	H20-C14-C12	111.760
H22-C14- C10	110.763	H21-O16- N12	106.313	H21-C15-C11	110.551
H23-C14- C10	110.565	H22-C14- C10	110.497	H22-C15-C11	110.604
H24-C14- C10	110.585	H23-C14- C10	110.746	H23-C15-C11	110.735
H25-C6-C1	119.627	H24-C14- C10	110.614	H24-O17-N13	106.168
H26-C1-C6	120.005	H25-C13- C11	111.227	H25-O9-C5	109.068
H27-C2-C1	120.026	H26-C13- C11	109.675	H26-C7-C2	119.659
H28-C3-C2	121.452	H27-C13- C11	111.789	H27-C4-C3	120.812
		H28-C3-C2	121.118	H28-C3-C2	120.126
		H29-C2-C1	119.618		
		H30-C6-C1	118.778		



IMO-4		IMO-5		IMO-6	
C3-C2-Br1	119.601	C3-C2-N1	107.213	C3-C2-C1	120.882
C4-C3-C2	119.352	N4-C3-C2	105.316	C4-C3-C2	120.487
C5-C4-C3	121.568	C5-N1-C2	111.122	C5-C4-C3	118.334
C6-C5-C4	118.500	C6-C2-N1	120.313	C6-C1-C2	119.712
C7-C2-Br1	119.501	C7-C3-C2	132.231	C7-C5-C4	120.320
C8-C6-C5	120.905	C8-C5-N1	128.168	O8-C4-C3	118.814
O9-C5-C4	118.281	C9-C8-C5	120.392	N9-C7-C5	128.310
N10-C8-C6	127.965	C10-C9-C8	122.059	C10-N9-C7	111.086
C11-N10-C8	111.010	C11-C10-C9	118.884	C11-C10-N9	107.176
C12-C11- N10	107.201	C12-C11- C10	120.592	N12-C7-C5	127.293
N13-C8-C6	127.556	C13-C12- C11	120.983	C13-C11-C10	132.183
C14-C12-C11	132.130	O14-C11- C10	117.094	C14-C10-N9	120.334
C15-C11- N10	120.356	O15-N1-C5	125.406	O15-N9-C7	125.466
O16-N10-C8	125.482	O16-N4-C3	122.928	O16-N12-C7	125.099
O17-N13-C8	125.073	O17-C13- C12	117.863	H17-O8-C4	109.111
H18-C7-C2	119.958	H18-C6-C2	110.548	H18-O16-N12	106.062
H19-C3-C2	120.341	H19-C6-C2	110.597	H19-C13-C11	109.651
H20-C4-C3	120.850	H20-C6-C2	110.782	H20-C13-C11	111.424
H21-O17- N13	106.189	H21-C7-C3	111.780	H21-C13-C11	111.739
H22-C15- C11	110.540	H22-C7-C3	109.649	H22-C14-C10	110.763
H23-C15- C11	110.610	H23-C7-C3	111.437	H23-C14-C10	110.565
H24-C15- C11	110.740	H24-C9-C8	119.060	H24-C14-C10	110.585
H25-C14-	109.658	H25-C10-C9	121.473	H25-C6-C1	119.627

C12					
H26-C14-	111.352	H26-C12-	121.380	H26-C1-C6	120.005
C12		C11			
H27-C14-	111.761	H27-O14-	109.656	H27-C2-C1	120.026
C12		C11			
H28-O9-C5	109.096	H28-O16-C4	106.050	H28-C3-C2	121.452
		H29-O17-	109.054		
		C13			
Selected dihedral angle (°)					
IMO-1		IMO-2		IMO-3	
O16-N12-C7-	-177.570	O16-N12-	-177.700	O17-N13-C8-	-
N9		C7-N9		N10	179.470
O16-N12-C7-	0.833	O16-N12-	3.880	O17-N13-C8-	-1.010
C5		C7-C5		C6	
C6-C5-C7-	-147.380	C6-C5-C7-	149.340	C7-C6-C8-	-
N9		N9		N10	147.580
C6-C5-C7-	34.579	C6-C5-C7-	-32.600	C7-C6-C8-	34.304
N12		N12		N13	
C4-C5-C7-	-143.860	C4-C5-C7-	145.390	C5-C6-C8-	33.960
N12		N12		N10	
C4-C5-C7-	34.178	C4-C5-C7-	-32.640	C5-C6-C8-	-
N9		N9		N13	144.140
C4-C3-C2-C1	0.913	C4-C3-C2-	-0.662	C5-C4-C3-C2	1.009
		C1			
C5-C4-C3-C2	0.344	C5-C4-C3-	-0.517	C6-C5-C4-C3	0.070
		C2			

Again, from the optimized geometry, it is evident that the C-C bond distance of all the aryl groups in the compounds IMO-1 to IMO-6 are in the range 1.382 to 1.433 Å which suggests that the carbon atoms are highly conjugated and electrons are delocalized through resonance<sup>23</sup>

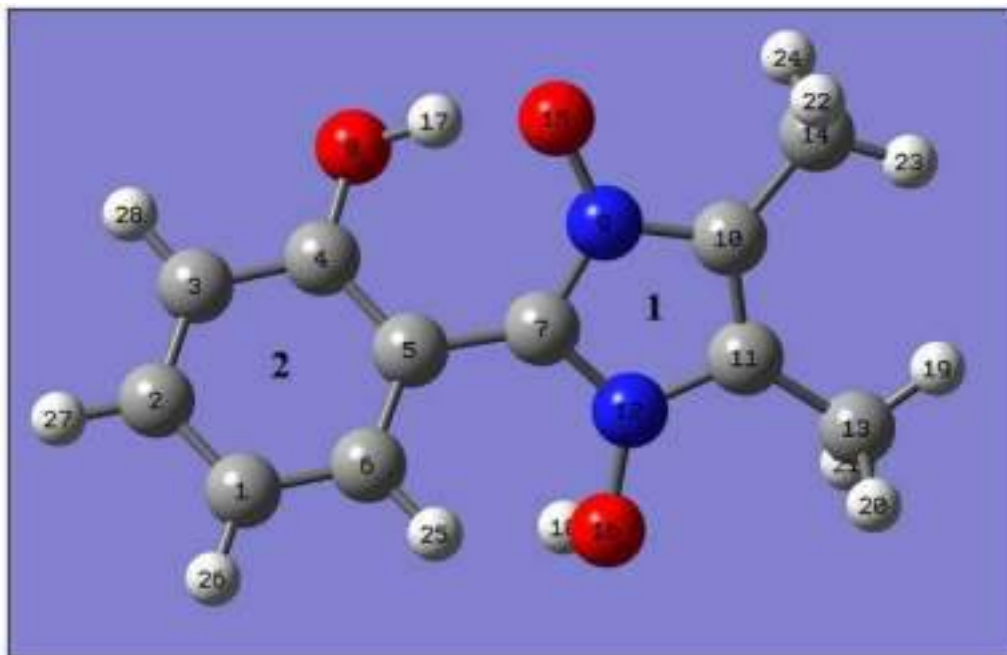


**Fig. 5.B.1.** Labeling of the phenyl ring and the imidazole ring in the studied compounds

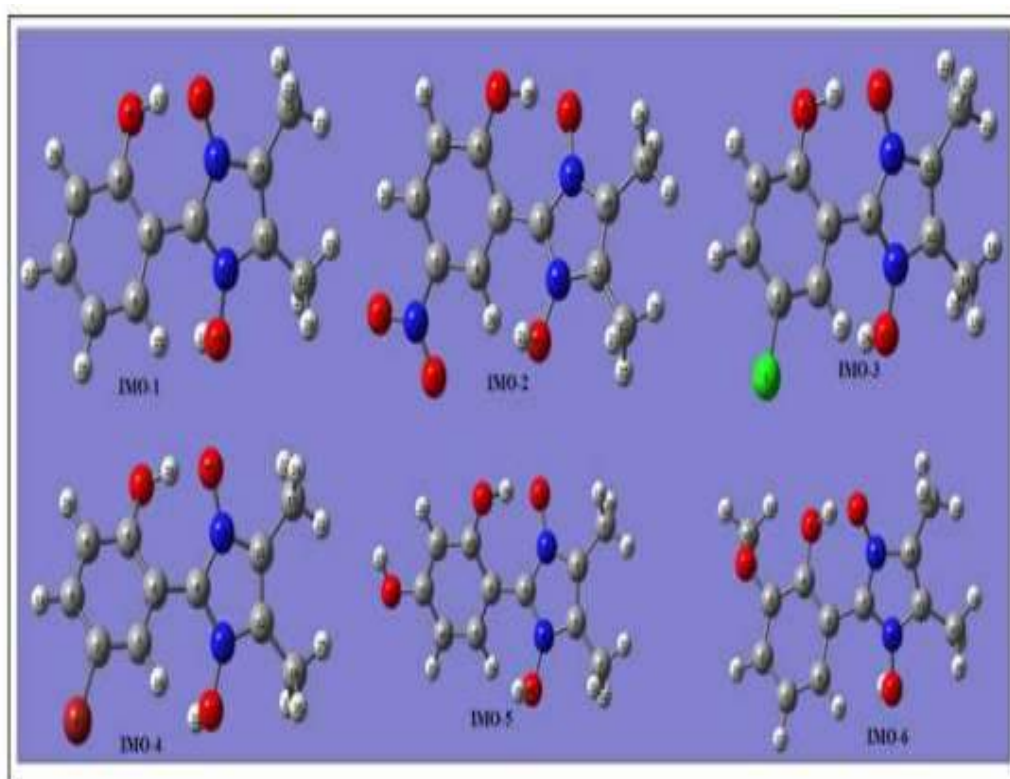


**Fig. 5.B.2.** DFT optimized geometry of the compounds IMO-1 to IMO-6 with atom labeling scheme

The N-O bond distance in the imidazole ring 1 of the studied compounds IMO-1 to IMO-6 are in the range 1.324-1.327 Å and the O-H bond distances in the imidazole ring1 of all the studied compounds are equal with a value of 0.973Å. The aromatic C-H, aliphatic C-H, C-O, O-H and C-Halogen bond distances for the studied compounds IMO-1 to IMO-6 are in the range 1.081-1.086 Å, 1.325-1.341Å, 1.023-1.047Å and 1.762-1.909 Å respectively.

#### 5.B.2.1.2 Frontier Molecular Orbitals

The Frontier Molecular Orbitals namely the Highest Occupied Molecular Orbital (HOMO) and the Lowest Unoccupied Molecular Orbital (LUMO) are essential for calculating the most reactive positions in  $\pi$ -electron conjugated systems, in which the HOMO acts as an electron donor and the LUMO acts as an electron acceptor, which determine whether a system is stable or instable<sup>24</sup>. The energy difference between the HOMO and the LUMO called the energy gap is an important parameter for analyzing the charge transfer within a molecule. For organic molecules having a low energy gap, there is a significant intramolecular charge transfer within the molecule<sup>25</sup>.

. The energies of HOMO and LUMO orbitals of the studied compounds (IMO-1 to IMO-6) are calculated using DFT/B3LYP method using 6-31G+ (d, 2p) level of basis set and shown in Fig.5.B.3. The energy of HOMO and LUMO orbitals of the studied compounds (IM-1 to IM-6) are listed in Table 5.B.2

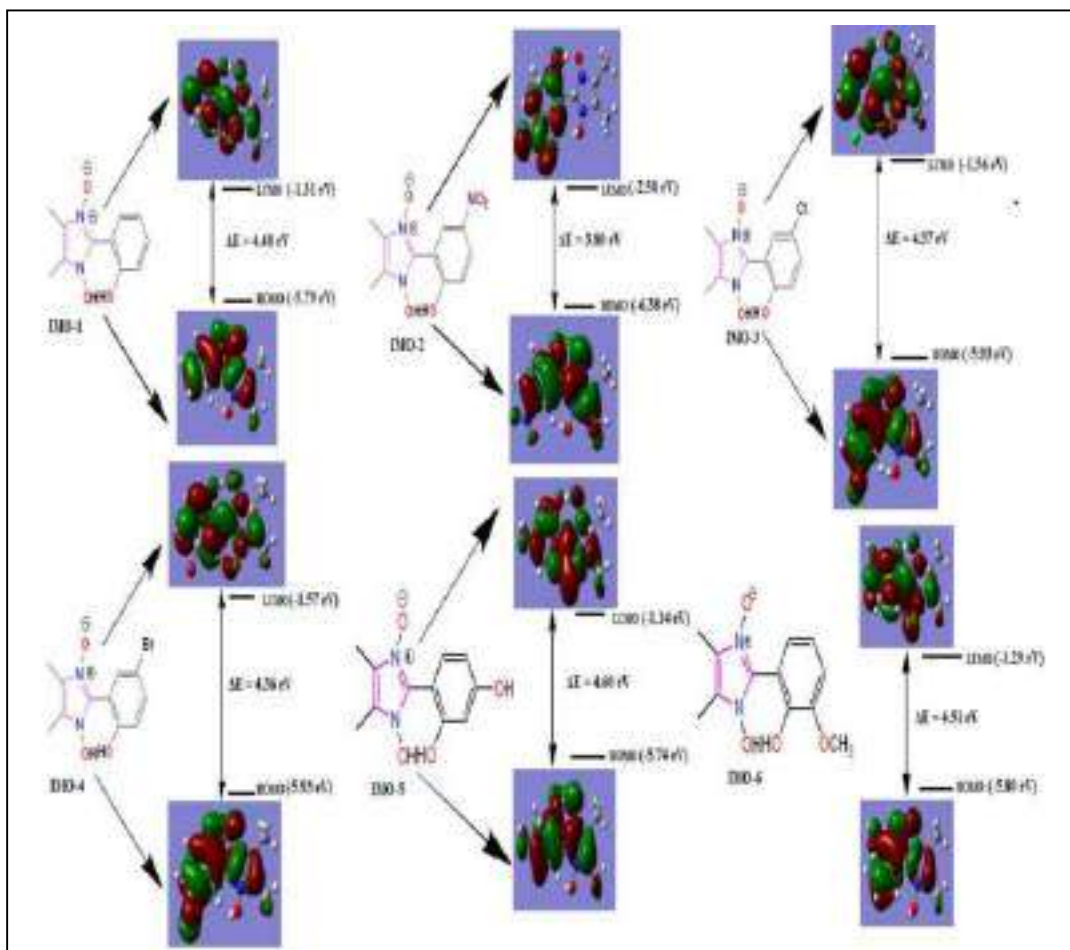


**Fig. 5.B.3.** Pictorial representation of the HOMO-LUMO of selected compounds (IMO-1 to IMO-6)

From the Table 5.B.2, it is evident that the energy of HOMO and LUMO orbitals are negative and this shows that the compounds under study (IMO-1 to IMO-6) are relatively stable<sup>46</sup> and the energy of HOMO and LUMO orbitals of the compounds are -5.79 eV(IMO-1), -6.38 eV(IMO-2), -5.93 eV(IMO-3), -5.93(IMO-4), -5.74(IMO-5), -5.80 eV(IMO-6) and -1.31 eV(IMO-1), -2.58 eV(IMO-2), -1.56 (IMO-3), -1.57(IMO-4), -1.14 eV (IMO-5), -1.29 eV( IMO-6). From the energies of the HOMO and LUMO, global chemical descriptors like chemical potential, global hardness and global electrophilicity can be determined which is helpful for understanding the reactivity and the structure of the molecule which in turn is essential for determination of the various pharmacological properties of the molecule for the process of drug design<sup>26</sup>. The ionization energy (I) and electron affinity (A) can be expressed in terms of HOMO and LUMO orbital energies as follows:

$$I = -E_{\text{HOMO}} \text{ and } A = -E_{\text{LUMO}}$$

The chemical reactivity descriptors such as chemical potential ( $\mu$ ), Electronegativity ( $\chi$ ), Global hardness ( $\eta$ ) and global electrophilicity power ( $\omega$ ) can be calculated with the help of following relation;

$$\text{Chemical potential } (\mu) = (E_{\text{HOMO}} + E_{\text{LUMO}})/2 = -(I-A)/2$$

$$\text{Electronegativity } (\chi) = (I+A)/2$$

$$\text{Global Hardness } (\eta) = (-E_{\text{HOMO}} + E_{\text{LUMO}})/2 = (I-A)/2$$

$$\text{electrophilicity power } (\omega) = \mu^2/2 \eta$$

Where I and A are the first ionization potential and electron affinity of the chemical species<sup>27-29</sup>. The ionization energy (I), electron affinity (A), Chemical potential ( $\mu$ ), Electronegativity ( $\chi$ ), Global hardness ( $\eta$ ) and Global electrophilicity power ( $\omega$ ) of the studied compounds (IMO-1 to IMO-6) are listed in Table 5.B.2

**Table. 5.B.2.** Energies of HOMO and LUMO orbitals, ionization energy (I), electron affinity (A), Chemical potential ( $\mu$ ), Electronegativity ( $\chi$ ), Global hardness ( $\eta$ ) and Global electrophilicity power ( $\omega$ ) of the studied compounds (IMO-1 to IMO-6)

Parameters (eV)	IMO-1	IMO-2	IMO-3	IMO-4	IMO-5	IMO-6
$E_{\text{HOMO}}$	-5.79	-6.38	-5.93	-5.93	-5.74	-5.80
$E_{\text{LUMO}}$	-1.31	-2.58	-1.56	-1.57	-1.14	-1.29
$\Delta E$	4.48	3.80	4.37	4.36	4.60	4.51
Ionization Energy (I)	5.79	6.38	5.93	5.93	5.74	5.80
Electron Affinity (A)	1.31	2.58	1.56	1.57	1.14	1.29
Chemical potential ( $\mu$ )	-3.55	-4.48	-3.74	-3.75	-3.44	-3.54
Electronegativity ( $\chi$ )	3.55	4.48	3.74	3.75	3.44	3.54
Global hardness( $\eta$ )	2.24	1.90	2.185	2.180	2.30	2.25
Electrophilicity power( $\omega$ )	2.81	5.28	3.20	3.22	2.57	2.78

It was observed that the chemical potential of all the studied molecules are negative and it suggest that they do not decompose spontaneously into its elements they are made up of.

Apparently, it is seen that the hard molecule has large HOMO-LUMO gap and soft molecule has small HOMO-LUMO gap<sup>30</sup>. Thus, from the table 5.B.2 it is evident that the hardness of the studied molecule follows the order IMO-5 > IMO-

6>IMO-1>IMO-3>IMO-4>IMO-2. Moreover, the hardness signifies the resistance towards the deformation of electron cloud of chemical systems under small perturbation that occur during the chemical reaction. Thus, hard system is less polarizable than soft system<sup>31</sup>. Again, a large value of electrophilicity is assigned for good electrophile whereas nucleophile is described by low value of nucleophilicity<sup>32</sup>.

### **5.B.2.1.3 FT-IR analysis**

Study of the molecular vibrations of organic compounds is an important area of research as it is possible to correlate the theoretical and experimental FT-IR spectra of the studied compounds to figure out the different structural features in the molecules.

The theoretical vibrational spectra of the studied compounds (IMO-1 to IMO-6) was calculated using B3LYP/631G+(d,2p) basis set on the optimized geometry of the molecules in the gas phase. The experimental and theoretical vibrational frequencies of the studied compounds (IMO-1 to IMO-6) are given in Table 5.B.3 with proper assignment of the observed peaks.

**Table 5.B.3** Theoretical vibrational spectra of the studied compounds (IMO-1 to IMO-6)

Unscaled frequency (cm <sup>-1</sup> ) (theoretical)	IR <sub>i</sub>	R(A)	IR Frequency (cm <sup>-1</sup> ) Experimental	Assignments
<b>IMO-1</b>				
3705.02	45.6127	107.6216	3431	v OH stretch
3214.65	8.1747	196.2786	3338	vAr-H stretch
3207.92	10.5946	126.254		v(as)Ar-H stretch
3196.54	11.179	137.9638		v(as)Ar-H stretch
3180.19	2.9544	71.0119		v(as)Ar-H stretch
3141.24	9.5178	79.2307		v(as)CH <sub>3</sub> stretch
3134.3	9.791	53.93		v (as)CH <sub>3</sub> stretch
3104.86	6.0324	81.7627		v (as)CH <sub>3</sub> stretch
3093.32	9.7373	103.3131	3098	v (as)CH <sub>3</sub> stretch
3048.73	22.8065	273.4913	3037	vCH <sub>3</sub> stretch
3041.98	30.0307	298.3652	3006	v CH <sub>3</sub> stretch
2645.32	957.6912	44.5108		vOH stretch
1671.45	25.2853	33.3528	1650	v C=C stretch
1653.62	51.9197	290.3311	1640	v Ar C=C stretch
1614.47	51.3607	22.1022	1615	v (as)Ar C=C stretch
1457.09	34.6840	78.6450	1457	υC-N stretch
1493.02	23.2802	13.2052	1542	υC-N stretch
1337.64	21.2356	61.8351	1343	v N-O stretch
<b>IMO-2</b>				
3708.7	54.7241	96.4733		v OH stretch
3251.26	6.0628	20.7603	3318	vAr-H stretch
3236.79	3.0491	119.7162		v (as)Ar-H stretch
3213.44	1.7457	109.6095		v (as)Ar-H stretch
3144.57	8.1638	80.5279	3150	v (as)CH <sub>3</sub> stretch
3137.92	8.1158	54.2632		v (as)CH <sub>3</sub> stretch
3107.87	4.8485	83.504	3102	v (as)CH <sub>3</sub> stretch
3098.01	7.3051	94.5127		v (as)CH <sub>3</sub> stretch



## Chapter-V B

3050.94	18.9379	280.0527	3049	v CH <sub>3</sub> stretch
3043.61	23.5196	287.2019		v CH <sub>3</sub> stretch
2301.78	1350.918	112.0266		v OH stretch
1670.03	32.1487	30.5226		v C=C stretch
1655.81	172.1217	199.7095	1635	v Ar C=C stretch
1623.32	139.5832	67.2111	1621	v (as)Ar C=C stretch
1397.38	47.9595	11.9295		C-N stretch
1471.94	17.3935	5.0781	1484	C-N stretch
1336.15	113.0832	90.2131	1327	v N-O stretch
<b>IMO-3</b>				
3706.21	48.4285	103.2254	3417	v OH stretch
3230.73	0.4683	38.2996	3238	vAr-H stretch
3217.85	2.7715	204.6611	3213	v (as)Ar-H stretch
3203.41	1.2489	69.7343		v (as)Ar-H stretch
3142.52	8.9493	79.5551	3143	v (as)CH <sub>3</sub> stretch
3135.4	9.2279	54.9416	3136	v (as)CH <sub>3</sub> stretch
3105.99	5.5806	82.8585		v (as)CH <sub>3</sub> stretch
3095.05	8.7991	100.241		v (as)CH <sub>3</sub> stretch
3049.44	21.6612	281.2927	3054	v CH <sub>3</sub> stretch
3042.59	27.531	295.8094		v CH <sub>3</sub> stretch
2607.67	998.2402	38.2402		v OH stretch
1670.39	27.7088	29.6206		v C=C stretch
1648.04	11.8571	312.3336	1692	v Ar C=C stretch
1608.44	32.1363	25.1459	1631	v (as)Ar C=C stretch
1479.80	29.9446	13.3081	1482	C-N stretch
1394.27	50.1501	6.0786	1381	C-N stretch
1336.38	31.8164	54.6673	1365	v N-O stretch
<b>IMO-4</b>				
3705.55	47.6898	101.883	3418	v OH stretch
3232.46	0.5041	31.1475	3366	vAr-H stretch
3217.69	2.5979	192.8309		v (as)Ar-H stretch
3203.16	1.0309	67.4351		v (as)Ar-H stretch
3142.52	9.0416	80.4962		v (as)CH <sub>3</sub> stretch

3135.67	9.1412	55.1417		v (as)CH <sub>3</sub> stretch
3105.89	5.5709	83.5943		v (as)CH <sub>3</sub> stretch
3095.15	8.7228	98.7825	3084	v (as)CH <sub>3</sub> stretch
3049.5	21.8497	285.2729	3060	v CH <sub>3</sub> stretch
3042.7	27.2933	293.7105	3027	v CH <sub>3</sub> stretch
2596.32	1025.3657	38.3236		v OH stretch
1670.38	27.986	29.6608	1658	v C=C stretch
1645.96	15.6418	323.3396		v Ar C=C stretch
1606.74	34.2417	21.1009	1602	v (as)Ar C=C stretch
1479.49	30.7870	13.4282	1488	C-N stretch
1394.38	52.5472	6.2468	1384	C-N stretch
1336.88	34.8166	55.404	1306	v N-O stretch

---

**IMO-5**


---

3819.82	87.7808	177.7733		v OH stretch
3703.1	44.3077	11.05166	3452	v OH stretch
3221.67	3.8053	139.191	3288	vAr-H stretch
3206.4	1.7675	58.2336	3205	v (as)Ar-H stretch
3183.19	9.1867	131.2378		v (as)Ar-H stretch
3140.49	9.8455	82.7708		v (as)CH <sub>3</sub> stretch
3133.95	9.9568	54.993	3126	v (as)CH <sub>3</sub> stretch
3104.61	6.1979	82.7744	3113	v (as)CH <sub>3</sub> stretch
3092	10.135	105.793		v (as)CH <sub>3</sub> stretch
3048.57	23.8552	279.8837		v CH <sub>3</sub> stretch
3040.99	32.4452	317.8999	2973	v CH <sub>3</sub> stretch
2528.27	1060.9586	53.2578		v OH stretch
1673.46	13.6042	43.8922	1678	v C=C stretch
1661.69	393.0675	318.5151		v Ar C=C stretch
1626.04	91.5295	2.8895	1619	v (as)Ar C=C stretch
1498.43	24.8828	52.003	1445	C-N stretch
1394.80	34.3140	11.8589	1394	C-N stretch
1342.65	7.7212	20.3365	1364	v N-O stretch

---

**IMO-6**


---

3707.9	45.7938	101.1333	3335	v OH stretch
--------	---------	----------	------	--------------

---

3218.18	6.1246	126.6136		vAr-H stretch
3204.66	7.5837	173.6928		v (as)Ar-H stretch
3189.44	5.0698	65.7592		v (as)Ar-H stretch
3146.69	13.9772	98.4095		v (as)CH <sub>3</sub> stretch
3141.23	9.6342	81.3277		v (as)CH <sub>3</sub> stretch
3134.51	9.681	53.8307		v (as)CH <sub>3</sub> stretch
3108.43	35.3624	96.6261		v (as)CH <sub>3</sub> stretch
3105.09	5.9275	80.2792		v (as)CH <sub>3</sub> stretch
3093.85	9.511	104.4622	3098	v (as)CH <sub>3</sub> stretch
3048.89	22.762	275.497	3065	v CH <sub>3</sub> stretch
3042.3	29.8785	305.75		v CH <sub>3</sub> stretch
3015.55	83.0457	145.7974	2998	v CH <sub>3</sub> stretch
2514.14	1180.046	59.5506		v OH stretch
1671.46	28.082	31.2389		v C=C stretch
1641.2	17.9565	285.0536	1626	v Ar C=C stretch
1622.17	11.2284	17.424		v (as)Ar C=C stretch
1479.33	41.6254	14.9933	1479	vC-N stretch
1393.52	35.2125	9.8195	1366	vC-N stretch
1343.14	1.95	27.1136	1336	v N-O stretch

### 5.B.2.1.3.1 C-H stretching vibrations

For the studied compounds (IMO-1 to IMO-6), C-H functional group is present at a number of positions. The characteristics region of C-H stretching vibration of aromatic ring falls in the range 3100-3000 cm<sup>-1</sup><sup>33</sup>. In the present investigation, theoretically calculated bands in the range 3214-3180 cm<sup>-1</sup>, 3251-3213 cm<sup>-1</sup>, 3230-3203 cm<sup>-1</sup>, 3232-3203 cm<sup>-1</sup>, 3221-3183- cm<sup>-1</sup> and 3218-3189- cm<sup>-1</sup> were assigned to aromatic C-H stretching vibrations for compounds IMO-1, IMO-2, IMO-3, IMO-4, IMO-5 and IMO-6 respectively. Pure symmetric bands were calculated at 3214 cm<sup>-1</sup> in IMO-1, 3251 cm<sup>-1</sup> in IMO-2, 3230 cm<sup>-1</sup> in IMO-3, 3232 cm<sup>-1</sup> in IMO-4, 3221 cm<sup>-1</sup> in IMO-5 and 3218 cm<sup>-1</sup> in IMO-6 respectively. Experimentally, symmetric bands were observed at 3338 cm<sup>-1</sup> in IMO-1, 3318 cm<sup>-1</sup> in IMO-3, 3366 cm<sup>-1</sup> in IMO-4, 3288 cm<sup>-1</sup> and 3205 cm<sup>-1</sup> in IMO-5 respectively. Asymmetric vibrational bands were calculated with stretching frequencies 3180 cm<sup>-1</sup>, 3196 cm<sup>-1</sup>, 3207 cm<sup>-1</sup> in IMO-1, 3213, cm<sup>-1</sup>, 3236 cm<sup>-1</sup> in IMO-2, 3217 cm<sup>-1</sup>, 3230 cm<sup>-1</sup> in IMO-3, 3203 cm<sup>-1</sup>, 3217 cm<sup>-1</sup> in IMO-4, 3183 cm<sup>-1</sup>, 3206 cm<sup>-1</sup> in IMO-5 and 3189 cm<sup>-1</sup> and 3204 cm<sup>-1</sup> in IMO-6 respectively. Experimentally,

Asymmetric vibrational bands were observed at 3213  $\text{cm}^{-1}$  in IMO-3 and 3205  $\text{cm}^{-1}$  in IMO-6 respectively (Table 5.B.3).

#### 5.B.2.1.3.2 Aromatic C-C stretching vibrations

Generally, the bands observed in the range 1650-1400  $\text{cm}^{-1}$  are assigned to C-C stretching mode of aromatic derivatives<sup>34</sup>. In our present study, the range for theoretically calculated C-C stretching vibrational mode showing sharp bands are in the range 1614-1671  $\text{cm}^{-1}$ , 1632-1670  $\text{cm}^{-1}$ , 1608-1670  $\text{cm}^{-1}$ , 1606-1670  $\text{cm}^{-1}$ , 1626-1673  $\text{cm}^{-1}$  and 1622-1671  $\text{cm}^{-1}$  for IMO-1, IMO-2, IMO-3, IMO-4, IMO-5 and IMO-6 respectively (Table 5.B.3). Experimentally, the aromatic C-C stretching frequencies for the studied compounds observed in the range 1615-1650  $\text{cm}^{-1}$  in IMO-1, 1621-1632  $\text{cm}^{-1}$  in IMO-2, 1631-1692  $\text{cm}^{-1}$  in IMO-3, 1602-1658  $\text{cm}^{-1}$  in IMO-4, 1619-1678  $\text{cm}^{-1}$  in IMO-5 and 1626  $\text{cm}^{-1}$  in IMO-6 respectively.

#### 5.B.2.1.3.3 C-N bond stretching vibrations

For imidazole scaffolds, several bands of variable intensity are observed in the range of 1660-1450  $\text{cm}^{-1}$  owing to C=N and C=C stretching vibrations<sup>35</sup>. Theoretically, for the studied compounds (IMO-1 to IMO-6), the C=N stretching vibrations are observed in the range of 1457-1493  $\text{cm}^{-1}$  for IMO-1, 1471-1397  $\text{cm}^{-1}$  for IMO-2, 1479-1394  $\text{cm}^{-1}$  for IMO-3 and IMO-4, 1498-1394  $\text{cm}^{-1}$  for IMO-5 and 1479-1393  $\text{cm}^{-1}$  for IMO-6. The experimentally observed values for C=N stretching vibrations are found in the range of 1542-1457  $\text{cm}^{-1}$  for IMO-1, 1484  $\text{cm}^{-1}$  for IMO-2, 1482-1381 for IMO-3, 1488-1384  $\text{cm}^{-1}$  for IMO-4, 1145-1394  $\text{cm}^{-1}$  for IMO-5 and 1479-1366  $\text{cm}^{-1}$  for IMO-6.

#### 5.B.2.1.3.4 N-O bond stretching vibrations

N-O stretching vibration is an important stretching vibration for 1-hydroxy-2-(2-hydroxyphenyl)-4,5-dimethylimidazole-3-oxide derivatives to ascertain their structure. Theoretically, the N-O stretching frequency observed were at 1337.64  $\text{cm}^{-1}$ , 1336.15  $\text{cm}^{-1}$ , 1336.38  $\text{cm}^{-1}$ , 1336.88  $\text{cm}^{-1}$ , 1342.65  $\text{cm}^{-1}$  and 1343.14  $\text{cm}^{-1}$  for the compounds IMO-1, IMO-2, IMO-3, IMO-4, IMO-5 and IMO-6 respectively.

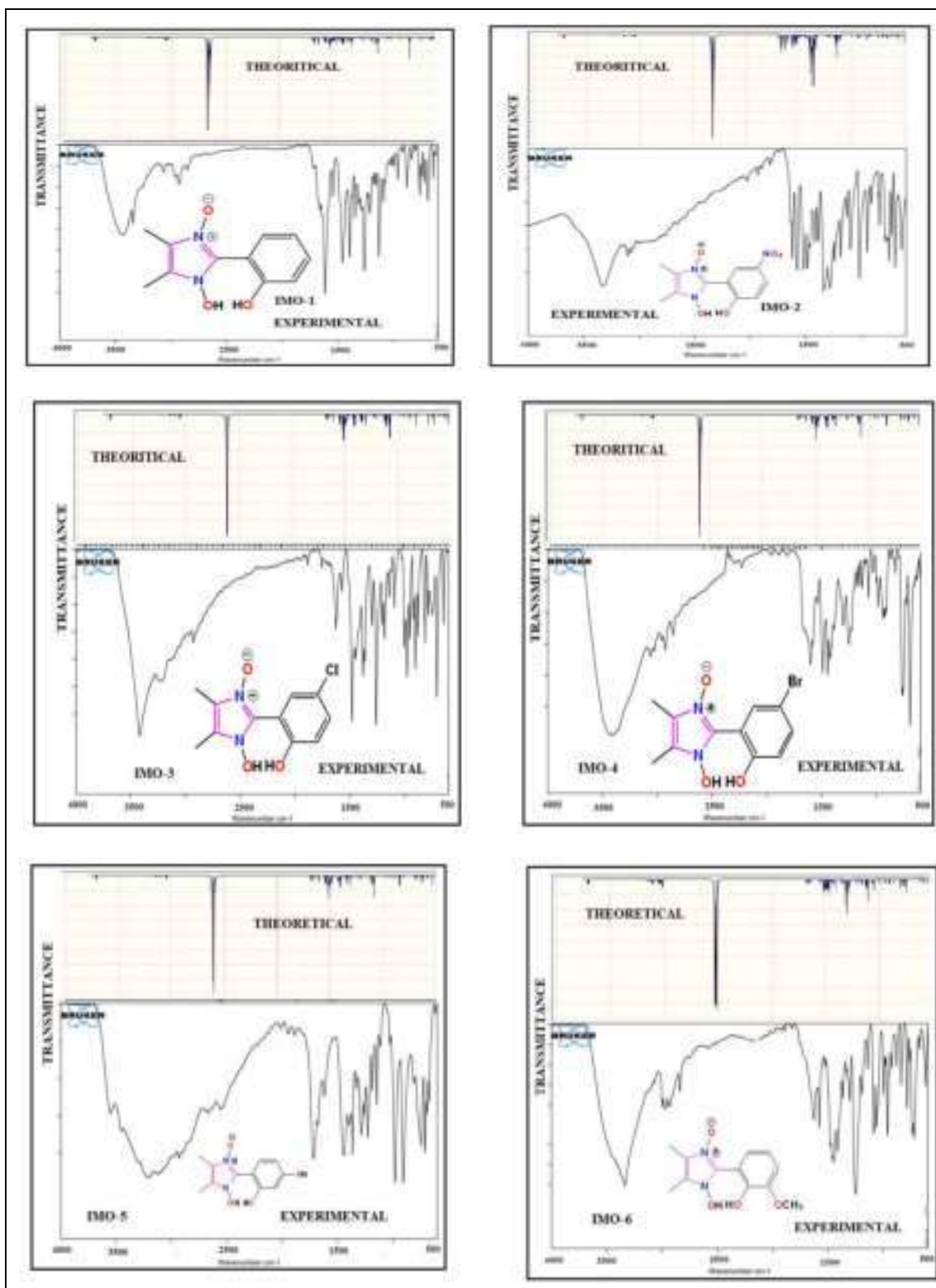


Fig. 5.B.4. Theoretical and experimental FTIR spectra of IMO-1 to IMO-6

The experimentally observed values for N-O stretching frequency were at 1343, 1327, 1365, 1306, 1364 and 1336  $\text{cm}^{-1}$  for the compounds IMO-1, IMO-2, IMO-3, IMO-4, IMO-5 and IMO-6 respectively.

Thus, from the above discussions it is evident that the theoretically calculated vibrational frequency matched well with the experimental results for the studied compounds (Fig. 5.B.4)

#### 5.B.2.1.4 Molecular Electrostatic Potential

Molecular Electrostatic Potential (MEP) is a useful parameter which gives information about the relative polarity of molecules along with other parameters like hydrogen bonding, reactivity, polarizability, sites for electrophilic and nucleophilic attack, etc<sup>36</sup>. To predict the reactive sites of electrophilic and nucleophilic attack for the investigated molecules (IMO-1 to IMO-6), MEP at B3LYP/6-31G+ (d, 2p) optimized geometry was calculated. The significance of MEP provides a visual method to understand the relative polarity of the given molecule and the different values of the electrostatic potential at the MEP surface are given by different colors such as red, blue and green. Red, blue and green color represents the region of most negative, most positive and zero electrostatic potential respectively. Thus, the electrostatic potential increases in the order blue > green > yellow > orange > red. The most negative electrostatic potential (red, orange and yellow region) in the MEP surface is assigned for the electrophilic reaction sites and the positive (blue region) corresponds to nucleophilic reaction site<sup>37-38</sup>. The MEP surface of the studied compounds (IMO-1 to IMO-6) is depicted in Fig. 5.B.5.

A detailed description of the MEP surface indicating the region of negative/electrophilic reaction sites and positive/nucleophilic reaction site for the studied compounds (IM-1 to IM-6) are listed in Table 5.B.4.

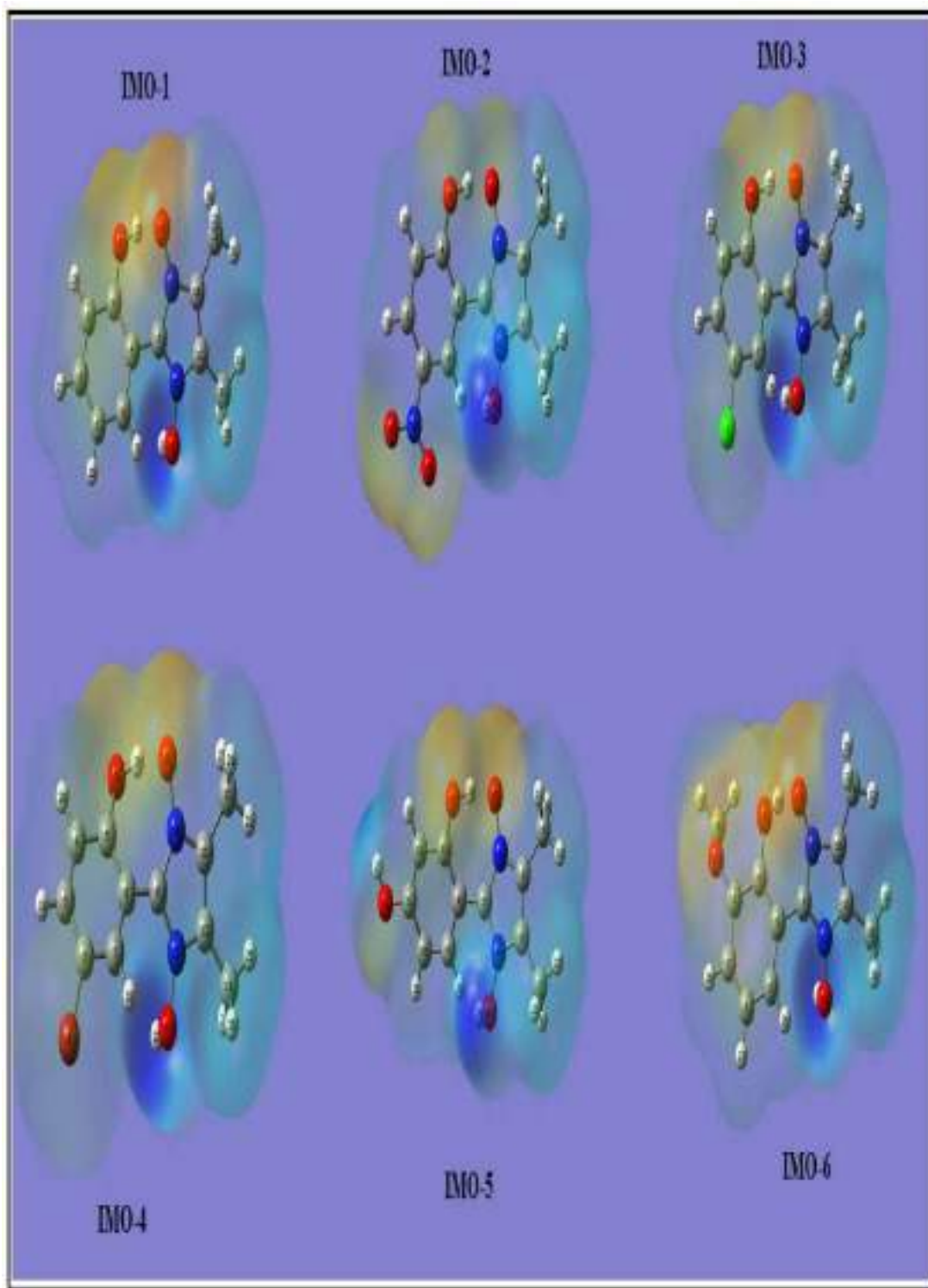
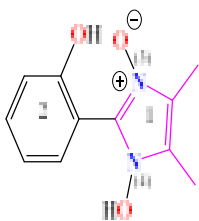


Fig. 5.B.5. MEP plot of studied compounds (IMO-1 to IMO-6)

**Table 5.B.4.** Detailed description of MEP surface for compounds IMO-1 to IMO-6

Entry	Negative region (red, orange, yellow)/Electrophilic reaction site	Positive region (blue)/Nucleophilic reaction site
IMO-1	-OH group of 2-phenyl ring and N(3)-O <sup>-</sup> group of imidazole core 1	-OH group attached to N(4) and two CH <sub>3</sub> groups of imidazole core 1
IMO-2	NO <sub>2</sub> group and -OH group of phenyl ring 2 and N(3)-O <sup>-</sup> group of imidazole core 1	-OH group attached to N(4) and two CH <sub>3</sub> groups of imidazole core 1
IMO-3	-OH group, Cl group of phenyl ring 2 and N(3)-O <sup>-</sup> group of imidazole core 1	-OH group attached to N(4) and two CH <sub>3</sub> groups of imidazole core 1
IMO-4	-OH group, Br group of phenyl ring 2 and N(3)-O <sup>-</sup> group of imidazole core 1	-OH group attached to N(4) and two CH <sub>3</sub> groups of imidazole core 1
IMO-5	-OH group at ortho position of phenyl ring 2 and N(3)-O <sup>-</sup> group of imidazole core 1	-OH group attached to N(4) and two CH <sub>3</sub> groups of imidazole core 1 and -OH group at para position of the phenyl ring 2
IMO-6	-OH group at ortho position and -OCH <sub>3</sub> at meta position of phenyl ring 2 and N(3)-O <sup>-</sup> group of imidazole core 1	-OH group attached to N(4) and two CH <sub>3</sub> groups of imidazole core 1





### 5.B.2.1.5 NLO Properties

With the rapid development in the field of non-linear optics, Organic molecules with strong non-linear properties has been a center of attention of many researchers working in the field of chemistry and material chemistry in the last few decades. Organic Molecules with  $\pi$ - conjugation has tremendous applications in the field of photonics, biomedicine, signal processing, etc<sup>39-40</sup>. Theoretically, the NLO properties of the given compound is calculated by determining the parameters such as magnitude of dipole moment ( $\mu$ ), polarizability ( $\alpha$ ), anisotropy of polarizability ( $\Delta\alpha$ ), first hyperpolarizability ( $\beta$ ) and second order hyperpolarizability ( $\gamma$ ). The polarizability tensors are calculated using the following relations:<sup>41</sup>

$$\text{Dipole moment } \mu = (\mu_x^2 + \mu_y^2 + \mu_z^2)^{1/2} \dots\dots\dots (1)$$

$$\alpha(\text{total}) \text{ or } \langle \alpha \rangle = \frac{1}{3} (\alpha_{xx} + \alpha_{yy} + \alpha_{zz}) \dots\dots\dots (2)$$

$$\Delta\alpha = 1/\sqrt{2} [(\alpha_{xx} - \alpha_{yy})^2 + (\alpha_{yy} - \alpha_{zz})^2 + (\alpha_{zz} - \alpha_{xx})^2 + 6(\alpha_{xy}^2 + \alpha_{xz}^2 + \alpha_{yz}^2) ]^{1/2} \dots\dots\dots (3)$$

$$\beta_x = \beta_{xxx} + \beta_{xyy} + \beta_{xzz} \dots\dots\dots (4)$$

$$\beta_y = \beta_{yyy} + \beta_{yzz} + \beta_{yxx} \dots\dots\dots (5)$$

$$\beta_z = \beta_{zzz} + \beta_{zxx} + \beta_{yyz} \dots\dots\dots (6)$$

$$\beta_{\text{total}} = (\beta_x^2 + \beta_y^2 + \beta_z^2)^{1/2} \dots\dots\dots (7)$$

$$\langle \gamma \rangle \text{ or } \gamma \text{ total} = 1/5 (\gamma_{xxxx} + \gamma_{yyyy} + \gamma_{zzzz} + 2(\gamma_{xxyy} + \gamma_{yyzz} + \gamma_{xxzz})) \dots\dots\dots (8)$$

Interestingly, 1-hydroxy-2-arylimidazole-3-oxide derivatives also consists of extended  $\pi$ -conjugated system carrying a phenyl ring in conjugation with imidazole core and therefore, it was thought worthwhile to study the NLO properties of these type of molecules. The nonlinear optical properties such as dipole moments, dipole polarizabilities, first- and second order hyperpolarizabilities of the studied compounds (IMO-1 to IMO-6) were calculated by B3LYP/ 6-31G + (d, 2p) basis set and the computed results are listed in Table 5.B.5

**Table 5.B.5.** Dipole moments, dipole polarizabilities, anisotropic polarizabilities and First order hyperpolarizabilities of IMO-1 to IMO-6

<b>Dipole moments, dipole polarizabilities and anisotropic polarizabilities</b>							
Entry	IMO-1	IMO-2	IMO-3	IMO-4	IMO-5	IMO-6	Ref.
$\mu_x$	-6.49	7.70	4.51	-4.83	-3.06	-3.82	0
$\mu_y$	-6.87	-4.20	-7.82	-5.92	3.93	-5.04	-4.06
$\mu_z$	0.02	0.01	-0.01	-0.02	1.80	3.35	0.0018
$\mu$	<b>9.45</b>	<b>8.77</b>	<b>9.03</b>	<b>7.64</b>	<b>5.31</b>	<b>7.16</b>	<b>4.06</b>
$\alpha_{xx}$	-70.30	-117.13	-87.40	-101.61	-80.72	-90.87	-16.62
$\alpha_{yy}$	-96.27	-111.77	-108.92	-107.58	-104.85	-111.97	-24.64
$\alpha_{zz}$	-98.43	-109.97	-109.87	-115.03	-100.28	-103.51	-27.03
$\alpha_{xy}$	-0.08	-28.44	-14.39	23.37	-8.48	-1.1319	-0.0003
$\alpha_{xz}$	-0.04	-0.08	-0.03	0.06	0.46	1.00	-0.07
$\alpha_{yz}$	-0.10	0.01	-0.02	0.23	2.23	1.77	0.01
$\alpha_{tot X}$	<b>-13.09</b>	<b>-16.59</b>	<b>-15.12</b>	<b>-16.00</b>	<b>-14.12</b>	<b>-15.11</b>	<b>-3.37</b>
$\Delta\alpha_x$	<b>4.01</b>	<b>7.36</b>	<b>4.92</b>	<b>6.24</b>	<b>4.43</b>	<b>2.79</b>	<b>1.39</b>
<b>First order hyperpolarizabilities</b>							
$\beta_{xxx}$	-58.13	179.99	82.57	4.60	-25.97	-66.73	-
$\beta_{xyy}$	-39.93	27.40	20.73	25.20	-0.24	9.33	-
$\beta_{xzz}$	-16.06	-2.99	7.50	22.88	-5.96	0.15	0.001
$\beta_{yyy}$	-62.87	-65.39	-106.74	-99.59	28.17	-17.20	-16.94
$\beta_{xxy}$	-38.03	12.15	-32.43	-51.72	-40.49	-1.66	-0.63
$\beta_{yzz}$	2.59	-6.63	-5.05	-13.39	13.10	-9.27	2.05
$\beta_{zzz}$	1.31	1.31	-0.04	-0.02	8.51	24.28	-0.01
$\beta_{xxxz}$	-0.49	-1.28	0.19	-0.46	18.98	27.00	-0.09
$\beta_{yyyz}$	-0.84	-1.11	-0.44	-0.26	8.06	10.61	-0.03
$\beta_{xyyz}$	0.27	0.11	0.07	-0.80	-5.41	14.32	0.05
$\beta_{total}$	<b>1.30</b>	<b>1.84</b>	<b>1.57</b>	<b>1.48</b>	<b>0.47</b>	<b>0.76</b>	<b>0.13</b>
$\times 10^{-30}$							
(esu)							

A comparative study of the dipole moment in the studied system indicates that they have different charge distributions for different directions. The theoretically calculated dipole moments of the studied compounds are 9.45 D (IMO-1), 8.77 D (IMO-2), 9.03 D (IMO-3), 7.64 D (IMO-4), 5.31 D (IMO-5) and 7.16 D (IMO-6) respectively and the dipole moment increases in the order IMO-1 > IMO-3 > IMO-2 > IMO-4 > IMO-6 > IMO-5. It is clearly seen that the studied compounds IMO-1 to IMO-6 have dipole moments greater than the reference material urea (4.06 D). Also, the total dipole polarizabilities value of the studied compounds along all three directions is listed in Table 3.C.5. From the Table 5.B.5,

it is evident that the dipole polarizability of the studied compounds follows the order IMO-2 ( $-16.59 \times 10^{-24}$  esu) > IMO-4 ( $-16.00 \times 10^{-24}$ ) > IMO-3 ( $-15.12 \times 10^{-25}$ ) > IMO-6 ( $-15.11 \times 10^{-24}$ ) > IMO-5 ( $-14.11 \times 10^{-24}$ ) > IMO-1 ( $-13.09 \times 10^{-24}$ ). The theoretically computed first-order hyperpolarizabilities and their individual components for the studied compounds (IMO-1 to IMO-6) are listed in Table 5.B.5. From the table, it is evident that the first-order hyperpolarizability of the studied compounds are IMO-1 ( $1.30 \times 10^{-30}$ ), IMO-2 ( $1.84 \times 10^{-30}$ ), IMO-3 ( $1.57 \times 10^{-30}$ ), IMO-4 ( $1.48 \times 10^{-30}$ ), IMO-5 ( $0.47 \times 10^{-30}$ ), IMO-6 ( $0.76 \times 10^{-30}$ ). A comparison of the first-order hyperpolarizability value of the studied compounds with the standard reference urea ( $0.134 \times 10^{-30}$  esu) have shown that the studied compounds have far greater value of first-order hyperpolarizability value than urea. Thus, the order for the first-order hyperpolarizability of the studied compounds are IMO-2 > IMO-3 > IMO-1 > IMO-4 > IMO-6 > IMO-5.

The second order hyperpolarizabilities of the compounds IMO-1 to IMO-6 are given in Table 5.B.6. The second order hyperpolarizability of the studied compounds are  $-0.85 \times 10^{-36}$  esu,  $-1.22 \times 10^{-36}$  esu,  $-1.17 \times 10^{-36}$  esu,  $-1.20 \times 10^{-36}$  esu,  $-0.94 \times 10^{-36}$  esu and  $-1.08 \times 10^{-36}$  esu for IMO-1, IMO-2, IMO-3, IMO-4, IMO-5 and IMO-6 respectively and the order of second-hyperpolarizability of the studied compounds is given by IMO-2 > IMO-4 > IMO-3 > IMO-6 > IMO-5 > IMO-1. Thus it is evident that the second-hyperpolarizability of the studied compounds are much greater than the reference NLO material urea (Table 5.B.6).

**Table. 5.B.6.** Second order hyperpolarizabilities of compound IMO-1 to IMO-6

Entry	Second order hyperpolarizabilities						$\gamma_{\text{total}}$ (x $10^{-36}$ ) esu
	$\gamma_{xxxx}$	$\gamma_{yyyy}$	$\gamma_{zzzz}$	$\gamma_{xxyy}$	$\gamma_{yyzz}$	$\gamma_{xxzz}$	
<b>IMO-1</b>	-3440.45	-1352.70	-121.08	-821.73	-264.63	-264.63	-0.85
<b>IMO-2</b>	-5333.19	-1970.72	-124.59	-1183.8	-352.36	-839.56	-1.22
<b>IMO-3</b>	-4767.79	-1950.03	-132.67	-1114.1	-360.95	-908.65	-1.17
<b>IMO-4</b>	-5037.13	-1907.64	-141.40	-1136.5	-361.76	-936.22	-1.20
<b>IMO-5</b>	-3958.78	-1308.62	-221.47	-900.79	-234.94	-791.54	-0.94
<b>IMO-6</b>	-4408.92	-1570.02	-463.25	-995.02	-321.04	-835.07	-1.08
<b>Urea</b>	-120.66	-117.90	-29.39	-44.02	-28.019	-39.86	-0.04

From the above discussion, it is evident that the studied molecules IMO-1 to IMO-6 have shown greater value of nonlinear optical parameters than the reference urea molecule and we may infer that this set of molecules could act as a better nonlinear optical material.

### 5. B.2.2 Molecular Docking study

According to Global Cancer Statistics 2020, Female breast cancer is the most commonly diagnosed cancer followed by lung cancer, colorectal cancer prostate cancer and stomach cancer<sup>42</sup>. In India alone, breast cancer contributes more than 27% of the total cancer patients<sup>43</sup>. Estrogens are a group of hormones which plays an important role in the sexual and reproductive development in women. They are also responsible for the regulation of growth and development of bone, breast and uterine pathology. Estrogen receptor is categorized into two subtypes, Er-alpha (Estrogen Receptor- $\alpha$ ) and Er-beta (Estrogen Receptor- $\beta$ ). Er-alpha is found in endometrial, mammary epithelial cells which are the origin for growth in most breast cancers, ovarian stromal cell and hypothalamus<sup>44</sup>. The excessive secretion of estrogen hormone leads to the multiplication of the ER- $\alpha$  which is responsible for responsible for breast cancer. In early stages of breast cancer, some of the prescribed drugs like cyclophosphamide, methotrexate, fluorouracil, and doxorubicin, etc. are usually used in combination as

Chemotherapeutic agents for first- and second-line treatment of patients with metastatic breast cancer<sup>45</sup>. These chemotherapeutic drugs have their own side effects. Now a days, modern anti-cancer drugs are in use which target specific receptors and tumors, thus reducing the side effects of the traditional chemo-drugs and hence increasing the efficiency of the treatment. Molecular Docking process is generally used to find out various interactions between the ligand and the protein in a faster and cheaper way and this has made molecular docking an important tool in drug designing<sup>46-47</sup>. In this chapter, we have reported the molecular docking study of the selected 1-hydroxy-2-arylimidazole-3-oxide derivatives against the estrogen receptor protein (PDB ID: 3ERT)

#### 5.B.2.2.1 Visualization of the Docking Result

Molecular docking study of the compounds (IMO-1 to IMO-6) against has been carried out using GUI interface programme of Autodock Tools (MGL tool or Molecular Graphics Laboratory tool developed by Scripps research Institute<sup>48</sup>. The docking results have been visualized with the help of Biovia Discovery Studio 2020 (DS), version 21.1.0.20298 and Edu Pymol version 2.5.2.

After successful docking of the compounds (IMO-1 to IMO-6) with the protein 3ERT, the docking result showed different types of protein-ligand interactions with particular binding energies. For better understanding of fitting of the ligand into the binding pocket of the protein, ligands are shown as blue green stick. The hydrogen bonding interactions between ligands and protein are shown by green dash line, the  $\pi$ -sulfur interaction as yellow dash line,  $\pi$ -anion/ $\pi$ -cation interactions as orange dash line,  $\pi$ -sigma interactions as purple dash line,  $\pi$ - $\pi$  stacking/  $\pi$ - $\pi$  T-shaped interactions as dark pink dash line and  $\pi$ -alkyl interactions as light pink dash line respectively. The binding energy ( $\Delta G$ ) and the predicted inhibitory constant ( $pK_i$ ) of the studied compounds (IMO-1 to IMO-6) are found to be -5.7Kcal/mole (IMO-1), -6.1Kcal/mole (IMO-2), -6.7Kcal/mole (IMO-3), -6.6Kcal/mole (IMO-4), -6.2Kcal/mole (IMO-5) and -5.7Kcal/mole (IMO-6) respectively and 54.14 $\mu$ M, 27.17 $\mu$ M, 9.66 $\mu$ M, 11.47 $\mu$ M, 22.87 $\mu$ M and 54.14 $\mu$ M respectively (Table 5.B.7)

**Table. 5.B.7.** Summary of docking of the compound (IM-1 to IM-6) against insulin receptor protein IIR3 with corresponding binding energy ( $\Delta G$ ), predicted inhibitory constant (**pKi**), interacting amino acid residues and type of interactions.

Ligands	Binding Energy (kcal/mol)	Predicted inhibitory constant ( <b>pKi</b> ) $\mu\text{M}$	Amino Acid residues	Types of interactions
IMO-1	-5.7	54.14	His513 Ala430, Arg434, Ile510	$\pi$ - Cation Alkyl, $\pi$ - Alkyl
IMO-2	-6.1	27.17	Ala493	$\pi$ -Sigma
IMO-3	-6.7	9.66	Met522 Trp383, Tyr526 Leu525	H-bonding, Alkyl, $\pi$ - Alkyl, Unfavorable Acceptor-Acceptor Alkyl, $\pi$ - Alkyl $\pi$ -Sigma, Alkyl, $\pi$ - Alkyl
IMO-4	-6.6	11.47	Lys481 Met315, Ile487 Ala312	H-bonding, Alkyl Alkyl $\pi$ -Sigma
IMO-5	-6.2	22.87	Ala312 Lys481 Met315	H-bonding, $\pi$ -Sigma H-bonding, Alkyl Alkyl
IMO-6	-5.7	54.14	Trp383, Met522 Leu525	H-bonding, Alkyl, $\pi$ - Alkyl Alkyl, $\pi$ - Alkyl

The visualization of the docking result of compound IMO-1 against the protein 3ERT showed an interaction with a binding constant value of -5.7 Kcal/mol and predicted inhibitory constant value of 54.14 $\mu\text{M}$ . For IMO-1, there were various types of interactions between the ligand and the protein. It was seen that a  $\pi$ -cation interaction was present between a phenyl ring of the ligand and amino acid His 513 at a distance of 4.88 $\text{\AA}$  (Fig. 5.B.6). Another significant interaction that was observed was the alkyl interactions between the two  $\text{CH}_3$  groups of the ligand and the  $\text{CH}_3$  group of Ala 430 at a distance of 4.18 and 4.27 $\text{\AA}$  respectively followed by the pi-alkyl type of interactions between the phenyl ring of the ligand and the sigma bond between two  $\text{CH}_2$  groups of the amino acid Arg 434 at a distance of

3.75 Å. Finally, a pi-alkyl interaction was also seen between the phenyl ring of the ligand and the sigma bond between the two CH<sub>2</sub> groups of Ile 510 amino acid at a distance of 4.85 Å.

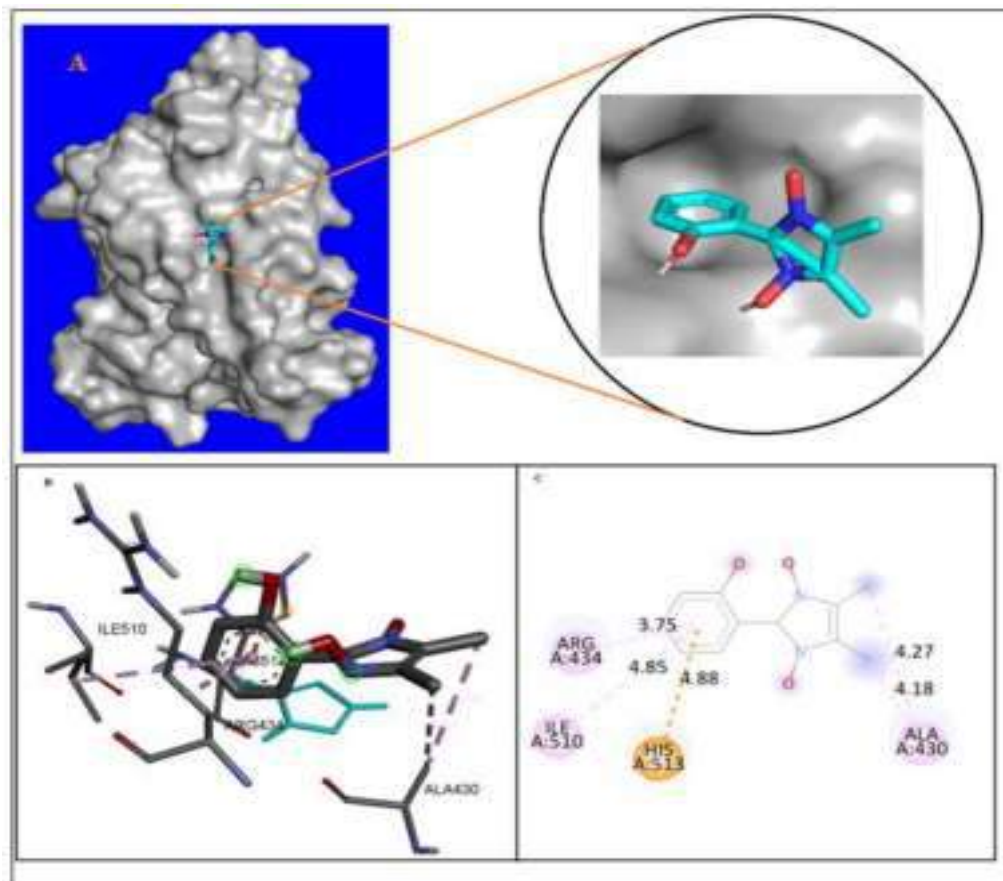


**Fig. 5.B.6.** Visualisation of docking results of ligand IMO-1 with the protein 3ERT : (A) Optimal binding mode of the protein with IMO-1 ligand (ligand shown as blue and green stick model), (B) Amino acid residues involved in different interactions (light pink dashed lines shows alkyl and pi-alkyl interactions and brown dashed lines show pi-cation interactions), (C) 2D representation of bonding interaction of ligand IMO-1 with different amino acid residues of protein 3ERT.

A close visualization of the docking result of ligand IMO-2 with the receptor protein 3ERT revealed that the ligand binds with the protein with a binding energy ( $\Delta G$ ) -6.1Kcal/mole and predicted inhibitory constant (**pKi**) 27.17 $\mu$ M. For IMO-2, it was found that there was only one kind of pi-sigma interaction between the phenyl ring of the ligand and the CH<sub>3</sub> group of the amino acid Ala 493 at a distance of 3.42Å (Fig. 5.B.7)

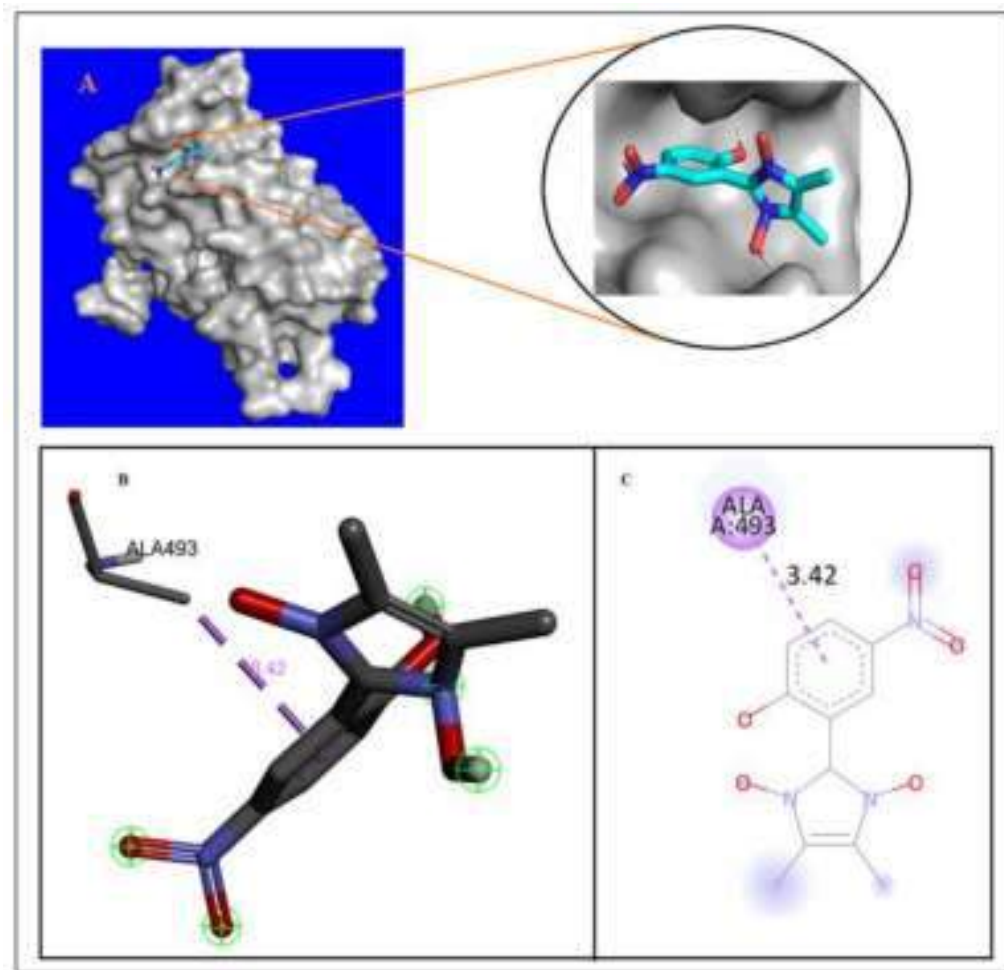


**Fig. 5.B.7.** Visualization of docking results of ligand IMO-2 with the protein 3ERT : (A) Optimal binding mode of the protein with IMO-2 ligand (ligand shown as blue and green stick model), (B) Amino acid residues involved in different interactions (purple dashed lines shows pi-sigma interactions (C) 2D representation of bonding interaction of ligand IMO-2 with different amino acid residues of protein 3ERT.

Docking results of the ligand IMO-3 shows the highest affinity interaction among the ligands IMO-1 to IMO-6 binding energy value of  $-6.7$  Kcal/mol and the predicted inhibitory constant was found to be  $9.66\mu\text{M}$ . A Conventional Hydrogen bonding was seen between the hydrogen atom of the  $-\text{OH}$  group attached to a nitrogen atom of the imidazole ring present in the ligand and the oxygen atom of the amino acid Lys 481 at a distance of  $2.87\text{\AA}$  (Fig. 5.B.8). A pi-sigma interaction was also seen between the phenyl ring of the ligand and the  $\text{CH}_3$  group of Ala 312 at a distance of  $3.79\text{\AA}$  followed by an alkyl interaction between the chlorine atom of the ligand with the sigma bond between the  $(\text{CH}_3)$  CH group and  $\text{CH}_2$  group of the Ile 487 amino acid at a distance of  $5.49\text{\AA}$ . Two more kinds of alkyl interactions were seen between the  $\text{CH}_3$  groups of the ligand and the sigma bond



between Sulfur atom and CH<sub>2</sub> group in Met315 at a distance of 4.31 Å and between the CH<sub>3</sub> groups of the ligand with the CH<sub>3</sub> group of the amino acid Lys 481 at a distance of 3.55 Å and 3.74 Å respectively.

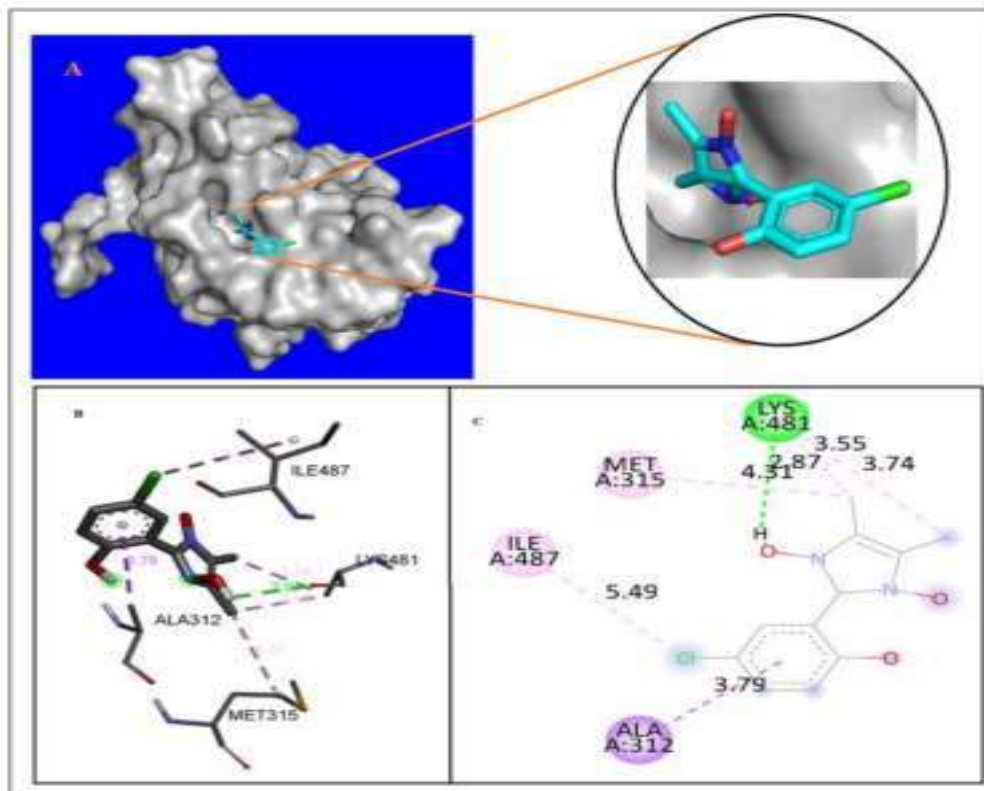


**Fig. 5.B.8.** Visualization of docking results of ligand IMO-3 with the protein 3ERT : (A) Optimal binding mode of the protein with IMO-3 ligand (ligand shown as blue and green stick model), (B) Amino acid residues involved in different interactions (purple dashed lines shows pi-sigma interactions, light pink dashed lines show alkyl interactions and green dashed lines show conventional hydrogen bonding interactions), (C) 2D representation of bonding interaction of ligand IMO-3 with different amino acid residues of protein 3ERT.

Docking results of the ligand IMO-4 shows the second highest affinity interaction after NO-3 with a binding energy value of -6.6 kcal/mol and the predicted inhibitory constant was found to be 11.47 μM. A Conventional Hydrogen bonding was seen between the hydrogen atom of the -OH group attached to a nitrogen atom of the imidazole ring present in the ligand and the sulfur atom of the amino acid Met 522 at a distance of 2.52 Å (Fig 5.B.9). A pi-sigma interaction was also seen between the phenyl ring of the ligand and the CH<sub>2</sub> group of Leu 525 at a distance of 3.61 Å followed by a pi-alkyl interaction between the CH<sub>3</sub> of the ligand with the phenyl ring of the amino acid Tyr 526 at a distance of 4.76 Å. Another pi-alkyl interaction was seen between the bromine atom of the ligand with the benzimidazole ring present in amino acid Trp 383 at a distance of 4.96 Å. Two

more alkyl interactions were also seen between the bromine atom of the ligand and the C(CH<sub>3</sub>)<sub>3</sub> group of the amino acid Leu 525 at a distance of 4.29 Å and between the CH<sub>3</sub> group of the ligand with the sigma bond present between the CH<sub>2</sub> group and Sulfur atom in the amino acid Met 522 at a distance of 4.57 Å. Finally, an unfavorable interaction was seen between the oxygen atom attached to the OH group in the ligand with the Oxygen atom present in amino acid Met 522 at a distance of 2.99Å.

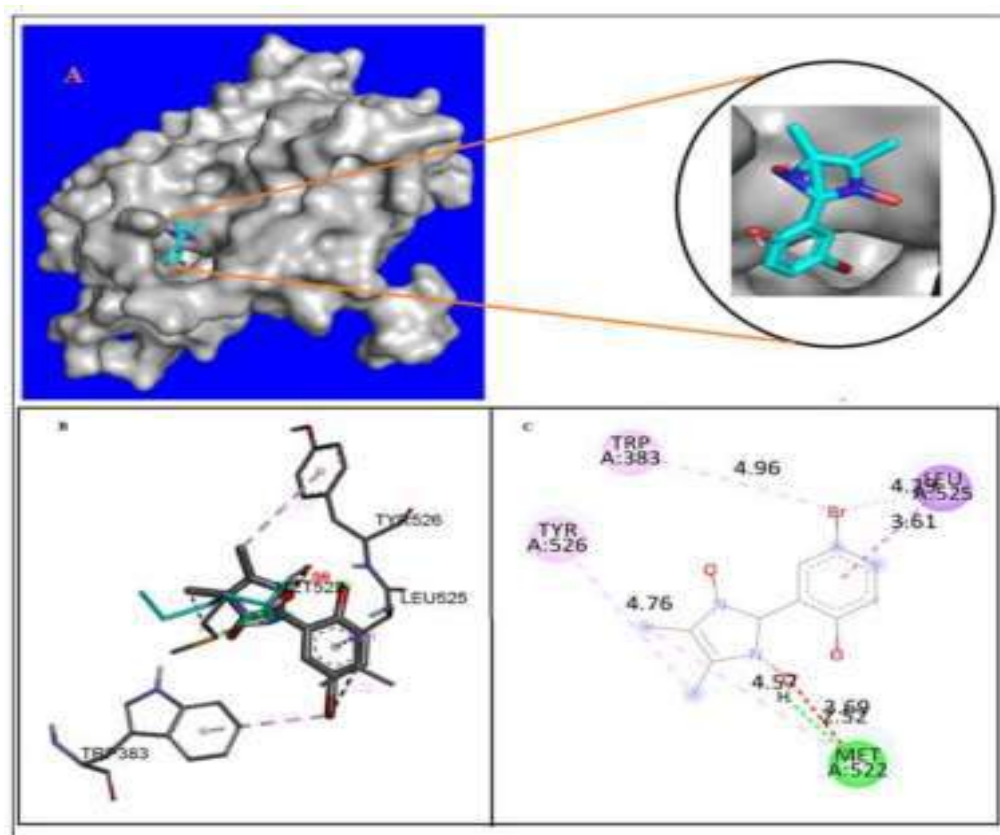


**Fig. 5.B.9.** Visualization of docking results of ligand IMO-4 with the protein 3ERT : (A) Optimal binding mode of the protein with IMO-3 ligand (ligand shown as blue and green stick model), (B) Amino acid residues involved in different interactions (purple dashed lines shows pi-sigma interactions, light pink dashed lines show alkyl and pi-alkyl interactions and green dashed lines show conventional hydrogen bonding interactions), (C) 2D representation of bonding interaction of ligand IMO-4 with different amino acid residues of protein 3ERT.

The interaction of ligand IMO-5 with 3ERT showed an interaction with a binding constant value of -6.2 Kcal/mol and predicted inhibitory constant value of 22.87 µM. For IMO-5, there were various types of interactions between the ligand and the protein. It was seen that a conventional Hydrogen bonding interaction was present between the oxygen atom of the ligand and the hydrogen atom of the NH<sub>2</sub>

group found in amino acid Ala 312 at a distance of 2.00Å. Another significant conventional hydrogen bonding interaction was also observed between the oxygen atom of the OH group of the ligand with the oxygen atom of the C=O group of the amino acid Lys 481 at a distance of 3.10Å. A pi-sigma interaction was also seen between the phenyl ring of the ligand with the CH<sub>3</sub> group of the amino acid Ala 312 at a distance of 2.00 Å followed by two alkyl interactions between the CH<sub>3</sub> group of the ligand with CH<sub>2</sub> group present in Lys 481 at a distance of 3.58Å and 3.65Å respectively. Finally, an alkyl interaction was also seen between the CH<sub>3</sub> group of the ligand with the sigma bond present between Sulfur and carbon atoms present in the amino acid Met 315 at a distance of 4.25Å (Fig. 5.B.10).

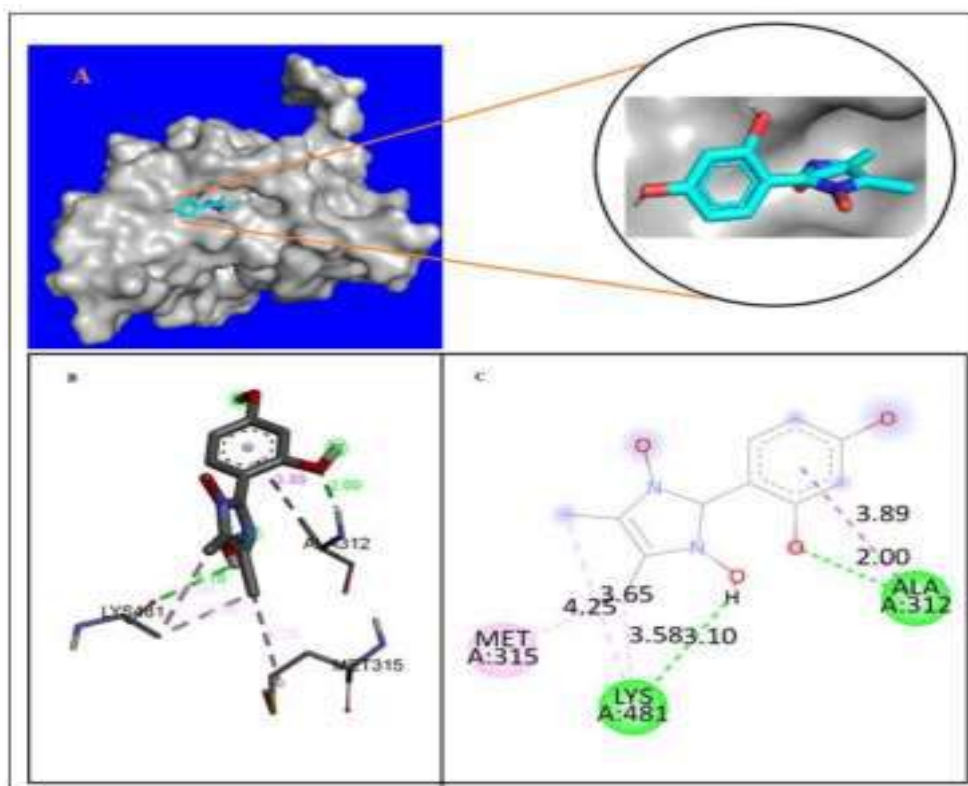


**Fig. 5.B.10.** Visualization of docking results of ligand IMO-5 with the protein 3ERT : (A) Optimal binding mode of the protein with IMO-5 ligand (ligand shown as blue and green stick model), (B) Amino acid residues involved in different interactions (purple dashed lines shows pi-sigma interactions, light pink dashed lines show alkyl and pi-alkyl interactions and green dashed lines show conventional hydrogen bonding interactions), (C) 2D representation of bonding interaction of ligand IMO-5 with different amino acid residues of protein 3ERT.

The interaction of IMO-6 with 3ERT showed an interaction with a binding constant value of -5.7 kcal/mol and predicted inhibitory constant value of 54.14  $\mu$ M. For IMO-6, there were various types of interactions between the ligand and the protein. It was seen that a conventional Hydrogen bonding interaction was present between the oxygen atom of the ligand and the hydrogen attached to nitrogen of the indole ring found in amino acid Trp 383 at a distance of 3.08Å.

Another significant conventional hydrogen bonding interaction was also observed between the hydrogen atom of the OH group of the ligand with the oxygen atom of the C=O group of the amino acid Met 522 at a distance of 2.24 Å. A pi-alkyl interaction was also seen between the phenyl ring of the ligand with the sigma bond between carbon and sulfur atoms in amino acid Met 522 at a distance of 4.98 Å followed by an alkyl interaction between the O-CH<sub>3</sub> group of the ligand with the sigma bond between carbon and sulfur atoms in amino acid Met 522 at a distance of 4.74 Å. Yet another pi-alkyl interaction was seen between the CH<sub>3</sub> group of the ligand with the indole ring in Trp 383 at a distance of 4.79 Å. Finally, an alkyl interaction was observed between the CH<sub>3</sub> group of the ligand with the -CH(CH<sub>3</sub>)<sub>2</sub> group of the amino acid Leu525 at a distance of 4.55 Å (Fig 5.B.11).

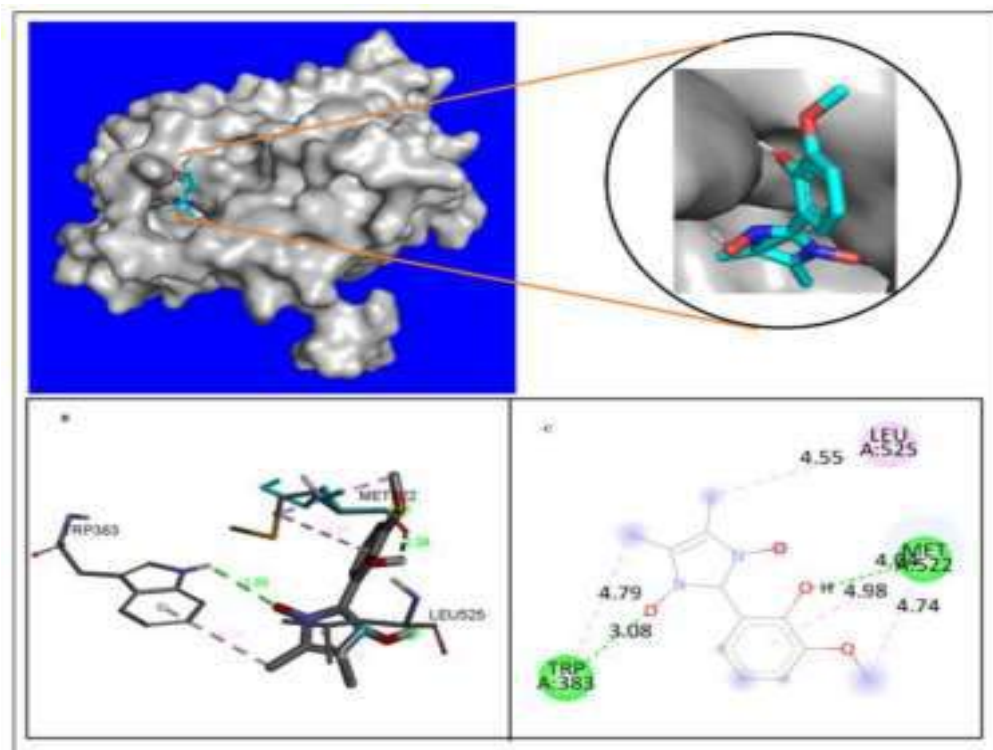


**Fig. 5.B.11:** Visualization of docking results of ligand IMO-6 with the protein 3ERT : (A) Optimal binding mode of the protein with IMO-6 ligand (ligand shown as blue and green stick model), (B) Amino acid residues involved in different interactions (purple dashed lines shows pi-sigma interactions, light pink dashed lines show alkyl and pi-alkyl interactions and green dashed lines show conventional hydrogen bonding interactions), (C) 2D representation of bonding interaction of ligand IMO-6 with different amino acid residues of protein 3ERT.

### 5.B.2.3 In silico Pharmacokinetics analysis of IMO-1 to IMO-6

In silico predictions of the pharmacokinetic ADMET properties like adsorption, distribution, metabolism, excretion and toxicity are very important for a molecule to be selected as a drug candidate in a much lesser time as compared to the conventional procedures<sup>49</sup>. Properties such as gastrointestinal adsorption (GI), water soluble capability (Log S), lipophilicity (Log P<sub>o</sub>/W), CYP1A2 inhibitor and Blood-Brain Barrier (BBB) are also very important for any compound to be considered as a drug candidate<sup>50</sup>. These pharmacokinetic properties of the studied ligands (IMO-1 to IMO-6) have been determined with the help of computer aided online SAR studies using SwissADME database (<http://www.swissadme.ch>) and the results of the pharmacokinetic properties as well as Lipinski's property have been summarized in the Table 5.B.8.

**Table 5.B.8.** Lipinski's properties and pharmacokinetic properties (ADME) of 1-hydroxy-2-arylimidazole-3-oxide derivatives (IMO-1 to IMO-6)

Properties	Compounds					
	IMO-1	IMO-2	IMO-3	IMO-4	IMO-5	IMO-6
<b>Molecular weight</b> (gm/mole)	220.22	406.35	254.67	299.12	236.22	250.25
<b>Rotatable bonds</b>	1	2	1	1	1	2
<b>H-bond acceptor</b>	3	5	3	3	4	4
<b>H-bond donor</b>	2	2	2	2	3	2
<b>Violations</b>	0	0	0	0	0	0
<b>Log P<sub>o</sub>/W</b>	1.40	0.68	1.68	2.03	1.00	1.47
<b>Log S</b>	-2.82(S)	-2.85(S)	-3.40(S)	-3.71(S)	-2.66(S)	-2.86(S)
<b>GI</b>	High	High	High	High	High	High
<b>BBB</b>	No	No	Yes	Yes	No	No
<b>CYP1A2</b>	Yes	No	No	Yes	No	Yes
<b>Bioavailability</b> Score	0.55	0.55	0.55	0.55	0.55	0.55
<b>Topological</b> Surface Area (Å <sup>2</sup> )	48.91	94.73	48.91	48.91	69.14	58.14

\*S: Soluble, BBB: Blood-Brain Barrier, CYP: Cytochrome P450, GI: Gastrointestinal absorption.

Analysis of Table 5.B.8, reveals that all the studied ligands (IMO-1 to IMO-6) with a bioavailability score in the range of 55 % have consensus lipophilicity (Log P<sub>o</sub>/W) value in the range of 0.68 to 1.68 and a high gastrointestinal absorption (GI). The positive value of the consensus lipophilicity indicates that all the ligands can pass through the lipid bilayer of the cellular membrane<sup>50</sup>. The solubility parameter (Log S) value of the ligands reveals that the ligands are soluble in water. This suggests that all the studied ligands could serve as a potential drug candidate with no violations of Lipinski's rule and hence qualifies the drug likeliness criteria.

#### **5.B.2.4 Computational details**

##### **5.B.2.4.1 DFT study**

All Quantum Mechanical calculations were carried out on a hp-Z640 desktop P.C. with an Intel Xeon processor (Specifications: E5-2630 V4 @ 220GHz) using Gaussian 16 W package. Density functional theory (DFT) with Becke's (B)three parameter hybrid model, Lee, Yang and Parr's (LYP) using 631G+(d,2p) basis set has been employed to optimize the geometry of the 1-hydroxy-2-arylimidazole-3-oxide derivatives (IMO-1 to IMO-6).

A set of theoretical calculations of selected compounds (IMO-1 to IMO-6) were performed with Gaussian 16W, Revision A.03 programme package using B3LYP/631G+(d,2p) basis sets to optimize geometry and minimize energy for faster and accurate calculations. With the optimized geometry, theoretical Raman and IR spectra were also calculated from the so chosen basis set. From the optimized geometry, the energy of HOMO and LUMO molecular orbitals along with the energy of HOMO-LUMO gap has also been measured. For analyzing the result of the theoretical calculations, a visual representation was obtained by Gauss View program 6.0 and it has been used to construct the molecular electrostatic potential surface (MESP) as well as the shape of HOMO and LUMO molecular orbitals. Also, nonlinear Optical property (NLO) of the selected 1-hydroxy-2-arylimidazole-3-oxide derivatives have also been calculated taking urea as a reference NLO material.

##### **5.B.2.4.2 Preparation of Protein and ligand for docking Study**

The X-ray crystallographic structures of the Estrogen receptor protein (PDB ID 3ERT) has been downloaded from the Protein Data Bank (PDB) (<http://www.pdb.org>.) database. Graphical User Interface program "Auto Dock Tools (ADT) 1.5.6" from Molecular Graphics Laboratory (MGL) developed by Scripps Research Institute has been used for the preparation of protein for docking study<sup>48</sup>. Input file of receptor protein for the blind docking study were created by taking specific chain (Chain A) of the protein (3ERT). In a typical receptor protein preparation, water molecules and hetero atoms along with the co-crystallized ligands in PDB crystal structure was removed and subsequently, the receptor

.pdbqt file has been prepared by adding polar hydrogen atoms and Kollman united atom charges<sup>46-47</sup>. The three-dimensional (3D) structures of ligands (IM-1 to IM-6) were drawn using Chemsketch (ACD/Structure Elucidator, version 12.01, Advanced Chemistry Development, Inc., Toronto, Canada, 2014, <http://www.acdlabs.com>.) and geometry optimization of the ligands (IM-1 to IM-6) were carried out using MM2 program incorporated in Chem. Draw Ultra 8.0 and further optimization of geometry of each molecule were carried out with the MOPAC 6 package using the semi-empirical AM1 Hamiltonian<sup>51</sup>. The input .pdbqt file of the ligands was generated using Auto Dock Tools (ADT). As the ligand molecules (IMO-1 to IMO-6) were non peptides, therefore, Gasteiger charge was assigned and then non-polar hydrogen was merged.

#### 5.B.2.4.3 Molecular docking study using Autodock vina

All molecular docking calculations of the studied ligands (IMO-1 to IMO-6) with protein 3ERT were carried out in the AutoDock Vina programme 1.1.2 developed by Scripps Research institute<sup>52-53</sup> and the results of the docking study and the intermolecular interactions between receptors protein and the ligand molecules were analyzed using BIOVIA Discovery Studio 2020 (DS), version 20.1.0.0 (Dassault Systèmes BIOVIA, Discovery Studio Modeling Environment, Release 2017, San Diego: Dassault Systèmes, 2016) and Edu pymol version 1.7.4.4<sup>52-53</sup>. The three-dimensional (3D) affinity (grid) maps and electrostatic a grid boxes of 100×100×100 Å grid points and grid centre (X, Y, Z) of 22.395 ,5.644, 21.987with a spacing of 1.00 Å generated by AutoGrid auxiliary program for each of the receptor protein for blind docking were generated to cover the entire active site of the receptor protein in order to eliminate biasness arising during the docking simulation<sup>54</sup>. Lamarckian genetic algorithm and a standard protocol with default setting of other run parameters were used for docking simulation. For each docking experiments, several runs were performed by the program with one predicted binding mode with each run. All the torsions were allowed to rotate. The predicted inhibitory constant (pK<sub>i</sub>) has been calculated using the following standardized equation<sup>55</sup>

$$pK_i = 10^{\frac{\text{Binding Energy Score}}{1.336}}$$

#### 5. B.4.4 Pharmacokinetic study

The pharmacokinetic properties like like absorption, distribution, metabolism, excretion and toxicity (ADMET) of the compounds (IMO-1 to IMO-6) have been studied using the computer aided online SwissADME database (<http://www.swissadme.ch>).

## 5.B.5 References

- (1) M. Waheed, N. Ahmed, M. A. Alsharif, M. I. Alahmdi, S. Mukhtar., *ChemistrySelect*, **2017**, 2 (26), 7946–7950.
- (2) A. Verma, S. Joshi, D. Singh., *Journal of Chemistry*, **2013**, 2013 (Article ID 392412).
- (3) L. H. Abdel-Rahman, A. A. Abdelhamid, A. M. Abu-Dief, M. R. Shehata, M. A. Bakheet., *Journal of Molecular Structure*, **2020**, 1200, 127034.
- (4) A. P. Taylor, R. P. Robinson, Y. M. Fobian, D. C. Blakemore, L. H. Jones, O. Fadeyi., *Organic & Biomolecular Chemistry*, **2016**, 14 (28), 6611–6637.
- (5) T. Shan, Z. Gao, X. Tang, X. He, Y. Gao, J. Li, X. Sun, Y. Liu, H. Liu, B. Yang, P. Lu, Y. Ma., *Dyes and Pigments*, **2017**, 142, 189–197.
- (6) R. B. da Silva, V. B. Loback, K. Salomão, S. L. de Castro, J. L. Wardell, S. M. S. V. Wardell, T. E. M. M. Costa, C. Penido, M. D. G. M. de Oliveira Henriques, S. A. Carvalho, E. F. da Silva, C. A. M. Fraga., *Molecules*, **2013**, 18 (3), 3445–3457.
- (7) M. Witschel., *Bioorganic & Medicinal Chemistry*, **2009**, 17 (12), 4221–4229.
- (8) T. B. Stensbøl, P. Uhlmann, S. Morel, B. L. Eriksen, J. Felding, H. Kromann, M. B. Hermit, J. R. Greenwood, H. Braüner-Osborne, U. Madsen, F. Junager, P. Krogsgaard-Larsen, M. Begtrup, P. Vedsø., *Journal of Medicinal Chemistry*, **2002**, 45 (1), 19–31.
- (9) M. L. Richardson, K. A. Crougton, C. S. Matthews, M. F. G. Stevens., *Journal of Medicinal Chemistry*, **2004**, 47 (16), 4105–4108.
- (10) O. K. Kim, L. K. Garrity-Ryan, V. J. Bartlett, M. C. Grier, A. K. Verma, G. Medjanis, J. E. Donatelli, A. B. Macone, S. K. Tanaka, S. B. Levy, M. N. Alekshun., *Journal of Medicinal Chemistry*, **2009**, 52 (18), 5626–5634.
- (11) G. Mloston, M. Celeda, M. Jasinski, K. Urbaniak, P. J. Boratynski, P. R. Schreiner, H. Heimgartner., *Molecules*, **2019**, 24 (23), 4398.
- (12) A. D. Bochevarov, M. A. Watson, J. R. Greenwood, D. M. Philipp., *Journal of Chemical Theory and Computation*, **2016**, 12 (12), 6001–6019.
- (13) M. Mutailipu, Z. Xie, X. Su, M. Zhang, Y. Wang, Z. Yang, M. R. S. A. Janjua, S. Pan., *J Am Chem Soc*, **2017**, 139 (50), 18397–18405.
- (14) M. Xiang, Y. Cao, W. Fan, L. Chen, Y. Mo., *Combinatorial Chemistry & High Throughput Screening*, **2012**, 15 (4), 328–337.



- (15) M. Evecen, H. Tanak., *Materials Science - Poland*, **2016**, 34 (4), 886–904.
- (16) X. Ma, D. Chang, C. Zhao, R. Li, X. Huang, Z. Zeng, X. Huang, Y. Jia., *Journal of Materials Chemistry C*, **2018**, 6 (48), 13241–13249.
- (17) S. Naseem, M. Khalid, M. N. Tahir, M. A. Halim, A. A. C. Braga, M. M. Naseer, Z. Shafiq., *Journal of Molecular Structure*, **2017**, 1143, 235–244.
- (18) A. D. Becke., *The Journal of Chemical Physics*, **1993**, 98 (7), 5648–5652.
- (19) C. Lee, W. Yang, R. G. Parr., *Physical Review B*, **1988**, 37 (2), 785–789.
- (20) M. J. Frisch, G. W. Trucks, H. B. Schlegel, G. E. Scuseria, M. A. Robb, J. R. Cheeseman, G. Scalmani, V. Barone, G. A. Petersson, H. Nakatsuji, X. Li, M. Caricato, A. v Marenich, J. Bloino, B. G. Janesko, R. Gomperts, B. Mennucci, H. P. Hratchian, J. v Ortiz, A. F. Izmaylov, J. L. Sonnenberg, D. Williams-Young, F. Ding, F. Lipparini, F. Egidi, J. Goings, B. Peng, A. Petrone, T. Henderson, D. Ranasinghe, V. G. Zakrzewski, J. Gao, N. Rega, G. Zheng, W. Liang, M. Hada, M. Ehara, K. Toyota, R. Fukuda, J. Hasegawa, M. Ishida, T. Nakajima, Y. Honda, O. Kitao, H. Nakai, T. Vreven, K. Throssell, J. A. Montgomery Jr., J. E. Peralta, F. Ogliaro, M. J. Bearpark, J. J. Heyd, E. N. Brothers, K. N. Kudin, V. N. Staroverov, T. A. Keith, R. Kobayashi, J. Normand, K. Raghavachari, A. P. Rendell, J. C. Burant, S. S. Iyengar, J. Tomasi, M. Cossi, J. M. Millam, M. Klene, C. Adamo, R. Cammi, J. W. Ochterski, R. L. Martin, K. Morokuma, O. Farkas, J. B. Foresman, D. J. Fox., *Gaussian, Inc., Wallingford CT, Gaussian 16 Revision C.01*, **2016**.
- (21) R. Dennington, T. A. Keith, J. M. Millam., *GaussView Version 6, Semichem Inc., Shawnee Mission, KS*, **2016**.
- (22) G. Varvounis, V. Gkalpinos, P. Theodorakopoulou, E. Tsemperlidou., In *Comprehensive Heterocyclic Chemistry IV (Chap 4.02 - Imidazoles)*; Black, D. S., Cossy, J., Stevens, C. V., Eds.; Elsevier: Oxford, **2022**; Vol. 4, pp 113–307.
- (23) P. Sykes., *A Guidebook to Mechanism in Organic Chemistry*, 6th ed.; Pearson Education: New Delhi, India, **2004**.
- (24) K. B. Benzon, H. T. Varghese, C. Y. Panicker, K. Pradhan, B. K. Tiwary, A. K. Nanda, C. van Alsenoy., *Spectrochimica Acta Part A: Molecular and Biomolecular Spectroscopy*, **2015**, 151, 965–979.
- (25) K. Fukui, T. Yonezawa, H. Shingu., *The Journal of Chemical Physics*, **2004**, 20 (4), 722–725.
- (26) L. G. Ferreira, R. N. dos Santos, G. Oliva, A. D. Andricopulo., *Molecules*, **2015**, 20 (7), 13384–13421.

- (27) M. Snehathala, C. Ravikumar, I. Hubert Joe, N. Sekar, V. S. Jayakumar., *Spectrochimica Acta Part A: Molecular and Biomolecular Spectroscopy*, **2009**, 72 (3), 654–662.
- (28) T. A. Koopmans., *Physica*, **1934**, 1 (1–6), 104–113.
- (29) R. G. Parr, R. G. Pearson., *J Am Chem Soc*, **1983**, 105 (26), 7512–7516.
- (30) R. G. Parr, L. V. Szentpály, S. Liu., *J Am Chem Soc*, **1999**, 121 (9), 1922–1924.
- (31) R. G. Pearson., *Journal of Chemical Sciences*, **2005**, 117 (5), 369–377.
- (32) S. Mandal, D. K. Poria, D. K. Seth, P. S. Ray, P. Gupta., *Polyhedron*, **2014**, 73, 12–21.
- (33) P. Jaramillo, P. Pérez, R. Contreras, W. Tiznado, P. Fuentealba., *Journal of Physical Chemistry A*, **2006**, 110 (26), 8181–8187.
- (34) N. P. G. Roeges., *A Guide to the Complete Interpretation of Infrared Spectra of Organic Structures*; John Wiley and Sons Inc.: New York, **1994**.
- (35) B. C. Smith., *Infrared Spectral Interpretation, A Systematic Approach*, 1st ed.; CRC Press: Washington, DC, **1999**; Vol. 2.
- (36) A. Madanagopal, S. Periandy, P. Gayathri, S. Ramalingam, S. Xavier, V. K. Ivanov., *Journal of Taibah University for Science*, **2017**, 11 (6), 975–996.
- (37) E. Scrocco, J. Tomasi., *Advances in Quantum Chemistry*, **1978**, 11 (C), 115–193.
- (38) P. Politzer, J. S. Murray., In *Theoretical Biochemistry and Molecular Biophysics: A Comprehensive Survey, Protein*; Beveridge, D. L., Lavery, R., Eds.; Adenine Press: Schenectady, New York, **1991**; Vol. 2.
- (39) E. Scrocco, J. Tomasi., *Topics in Current Chemistry*, **1973**, 42, 95–170.
- (40) E. M. Maya, A. W. Snow, J. S. Shirk, R. G. S. Pong, S. R. Flom, G. L. Roberts., *Journal of Materials Chemistry*, **2003**, 13 (7), 1603–1613.
- (41) Z. Sofiani, S. Khannyra, A. Boucetta, M. ElJouad, K. Bouchouit, H. Serrar, S. Boukhris, A. Souizi, A. Migalska-Zalas., *Optical and Quantum Electronics*, **2016**, 48 (282).
- (42) S. Muthu, T. Rajamani, M. Karabacak, A. M. Asiri., *Spectrochimica Acta Part A: Molecular and Biomolecular Spectroscopy*, **2014**, 122, 1–14.
- (43) H. Sung, J. Ferlay, R. L. Siegel, M. Laversanne, I. Soerjomataram, A. Jemal, F. Bray., *CA: A Cancer Journal for Clinicians*, **2021**, 71 (3), 209–249.
- (44) L. A. Torre, F. Bray, R. L. Siegel, J. Ferlay, J. Lortet-Tieulent, A. Jemal., *CA: A Cancer Journal for Clinicians*, **2015**, 65 (2), 87–108.

- (45) Z. Bai, R. Gust., *Arch Pharm (Weinheim)*, **2009**, 342 (3), 133–149.
- (46) N. Kerru, L. Gummidi, S. Maddila, K. K. Gangu, S. B. Jonnalagadda., *Molecules*, **2020**, 25 (8), 1909.
- (47) X.-Y. Meng, H.-X. Zhang, M. Mezei, M. Cui., *Current Computer-Aided Drug Design*, **2011**, 7 (2), 146–157.
- (48) R. Huey, G. M. Morris., *Using AutoDock 4 with AutoDocktools: A Tutorial.*; The Scripps Research Institute, Molecular Graphics Laboratory, pp. 54-56: La Jolla, CA, USA, **2008**.
- (49) S. Hari., *Journal of Applied Pharmaceutical Science*, **2019**, 9 (7), 18–26.
- (50) F. Ntie-Kang, L. L. Lifongo, J. A. Mbah, L. C. Owono Owono, E. Megnassan, L. M. Mbaze, P. N. Judson, W. Sippl, S. M. N. Efange., *In Silico Pharmacology*, **2013**, 1(1) (Article 12), 1–11.
- (51) K. Ohtawara, H. Teramae., *Chemical Physics Letters*, **2004**, 390 (1–3), 84–88.
- (52) J. Eberhardt, D. Santos-Martins, A. F. Tillack, S. Forli., *Journal of Chemical Information and Modeling*, **2021**, 61 (8), 3891–3898.
- (53) O. Trott, A. J. Olson., *Journal of Computational Chemistry*, **2010**, 31 (2), 455–461.
- (54) G. M. Morris, D. S. Goodsell, R. S. Halliday, R. Huey, W. E. Hart, R. K. Belew, A. J. Olson., *Journal of Computational Chemistry*, **1998**, 19 (14), 1639–1662.
- (55) M. A. Alamri, M. Tahir ul Qamar, M. U. Mirza, R. Bhadane, S. M. Alqahtani, I. Muneer, M. Froeyen, O. M. H. Salo-Ahen., *Journal of Biomolecular Structure and Dynamics*, **2021**, 39 (13), 4936–4948.

## CHAPTER-VI

### **Ni-borate catalyzed solvent free green synthesis of 2-substituted benzimidazole and 1, 2-disubstituted benzimidazole derivatives**

#### **6.1 Background of the present investigation**

Benzimidazole, an organic N-containing heterocyclic scaffold has gained a lot of interest during the past few decades due to its versatile pharmaceutical properties in medicinal chemistry<sup>1</sup>. The benzimidazole ring serves as one of the privileged scaffolds for the development and synthesis of libraries of novel molecules with potential therapeutic value<sup>2</sup>. The first synthesis of benzimidazole derivatives was reported by Hobrecker in 1872<sup>3</sup> and the first pharmacological properties of benzimidazole derivatives were studied by Godmann and Hart in 1943<sup>1</sup>. Having recognized the biological and medicinal properties of the benzimidazole scaffold, a numerous synthetic methodology has been developed for the synthesis of benzimidazole derivatives<sup>4-6</sup>. A large variety of benzimidazole derivatives have been known to show diverse biological activities such as anti-cancer<sup>3</sup>, anti-inflammatory<sup>7</sup>, analgesic<sup>8</sup>, anti-ulcer<sup>9</sup>, proton-pump inhibitors<sup>10</sup>, anti-microbial<sup>11</sup>, antioxidant<sup>12</sup>, antidiabetic<sup>13</sup>, antiviral<sup>14</sup> and anticoagulants<sup>15</sup> etc. A large variety of benzimidazole derivatives have been synthesized and their therapeutic potential has been examined during the past few decades<sup>16-19</sup>. A numerous clinically approved drugs which contains the benzimidazole scaffolds such as albendazole (113)<sup>20</sup> (anthelmintics), carbendazim (114) (fungicidal)<sup>21</sup>, telmisartan (115) (antihypertensives)<sup>22</sup> and astemizole (116) (antihistaminic)<sup>23</sup> are available in market (Fig 6.1.1). Among the diverse variety of benzimidazole derivatives, 1,2-disubstituted benzimidazole have attracted widespread interest due to their spacious applications in new drugs, including antihypertensive drugs (117)<sup>24</sup>, GABA<sub>A</sub> receptor agonists (118)<sup>25</sup> and the hepatitis C virus (HCV) NS5B polymerase inhibitors (119)<sup>26</sup> (Fig 6.1.2). Interestingly and specifically, 1, 2-disubstituted benzimidazole derivatives have significant pharmacological utility<sup>27</sup>. A numerous literature is available for the synthetic methodology for the synthesis of benzimidazole and 1, 2-disubstituted benzimidazole derivatives<sup>28-31</sup>. The reported procedure however suffers from some serious drawbacks such as use of harsh reaction condition, expensive catalyst, use of hazardous solvent, low yield, long reaction time and less atom economy<sup>32-34</sup>. Therefore, looking at the diverse application of the benzimidazole scaffold, development of a highly efficient and green protocol for the synthesis of this highly therapeutic agent is a current demand for the synthetic chemist.

Hence, it was thought worthwhile to develop an efficient, economical and green methodology for the synthesis of benzimidazole derivatives. Thus, in this section, we are representing the synthesis of 2-substituted benzimidazole and 1,2-

disubstituted benzimidazole derivatives using unconventional and inexpensive Ni-borate catalyst under solvent free condition.

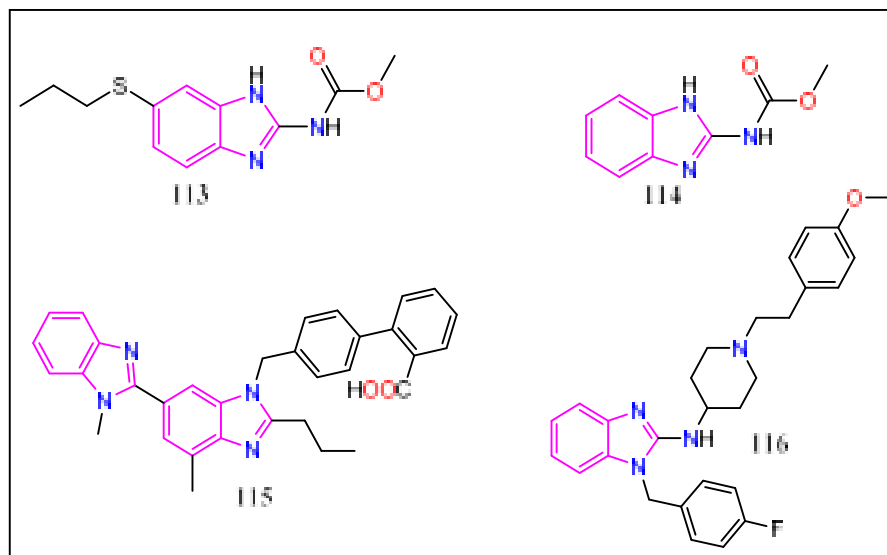


**Fig. 6.1.1.** Structures of some clinically approved drugs containing the benzimidazole scaffold

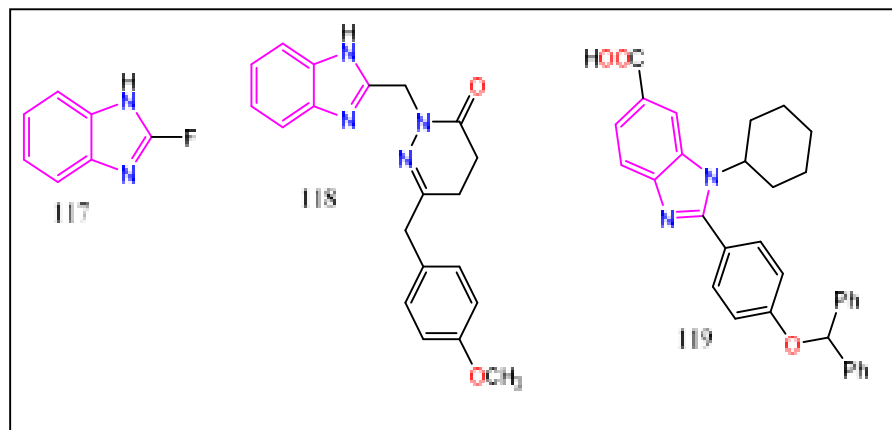
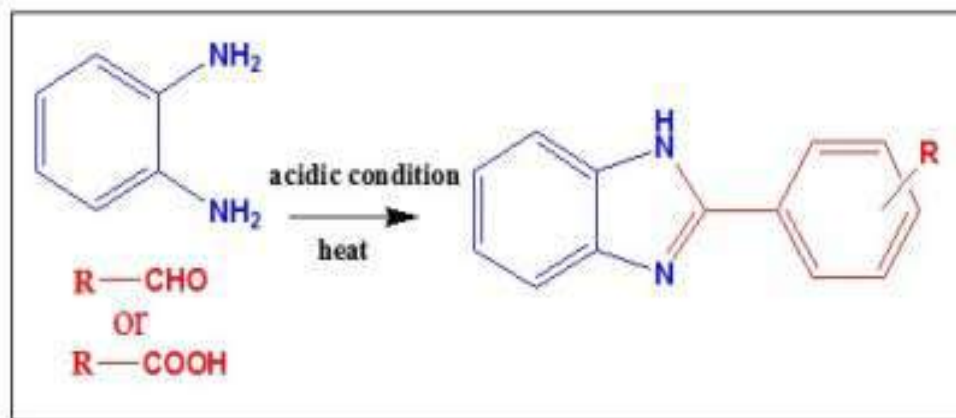


**Fig. 6.1.2.** Structures of some new drugs containing the benzimidazole scaffold

## 6.2 Results and discussions

### 6.2.1 2-Substituted benzimidazole derivatives

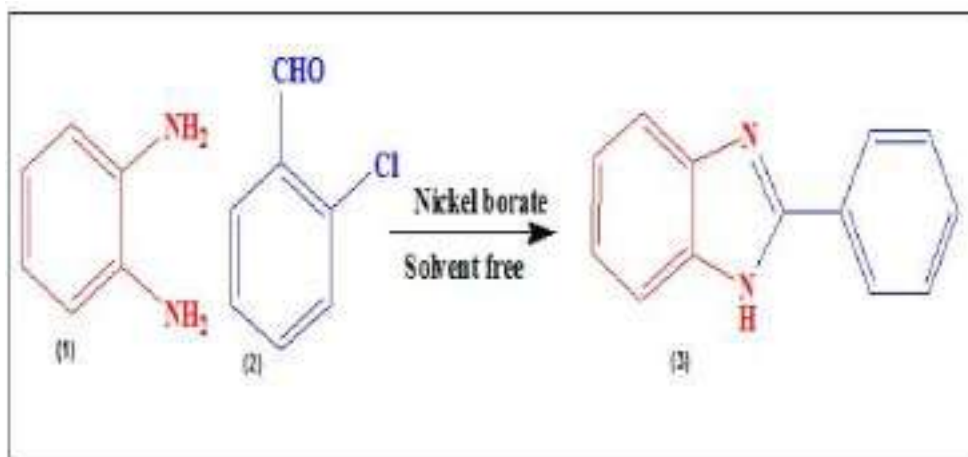
The classical method for the synthesis of 2-substituted benzimidazole derivatives involves the cyclization reaction of aromatic diamine with aldehydes, carboxylic acid or their derivatives at high temperature under strong acidic media<sup>35</sup> (Scheme 6.1.1).



**Scheme. 6.1.1.** Synthetic methodology for the synthesis of 2-substituted benzimidazole derivatives

There are several modified methods such as hydroformylation of N-alkenyl phenylenediamines using rhodium catalyst<sup>36</sup>, reductive cyclization of ortho-nitroaniline with aldehyde<sup>37</sup>, dehydration coupling of 2-bromoaniline<sup>35</sup> and carbonylation-cyclization of ortho-phenylenediamines using Pd catalyst<sup>38</sup> have been reported in the literature. However, the above cited modified methods has several major limitations such as use of expensive catalyst, harsh reaction condition, low yield, long reaction time and tedious work-up procedures etc.

Therefore, in this section, we are discussing the catalytic efficiency of Ni-borate for the green synthesis of 2-substituted benzimidazole and 1, 2-disubstituted benzimidazole derivatives under solvent free condition. Thus, optimization of the reaction was carried out by choosing ortho-phenylenediamine (1) and 2-chlorobenzaldehyde (2) as model reactants for the synthesis of benzimidazole (3) and the reaction was performed in presence of different amount of the catalyst under solvent free condition at different reaction condition such as amount of catalyst, time and temperature. In a typical model reaction, ortho-phenylenediamine (1 mmol) and 2-chlorobenzaldehyde (1mmol) was thoroughly mixed and ground in a mortar with the help of pestle in presence of the catalyst (Scheme 6.1.2).



**Scheme. 6.1.2.** Model reaction for the synthesis of 2-substituted benzimidazole (3)

The reaction mixture was then transferred into a 50 ml round bottomed flask and was allowed to stirrer at room temperature with the help of magnetic stirrer for 2 hours. The progress of the reaction was monitored with the help of TLC using ethyl acetate: hexane (20:80) mixture and we observed that the reaction did not go for completion and we isolated the reactant only. Therefore, we carried out the reaction at 60 °C and we found that a trace amount of the product was formed at this temperature (Table 6.1.1, entry 2). Further, we increased the reaction temperature to 80 °C and we observed that the reaction proceeds well and gets completed at 80 °C (Table 6.1.1, entry 3 and 4). After optimizing the reaction temperature, then we optimized the catalyst loading by varying the amount of catalyst for the same model reaction at optimized temperature and we observed that in absence of the catalyst no product has been formed (Table 6.1.2, entry 1). Then, we varied the amount of catalyst for the model reaction from 0.5 mol % to 4 mol % and we observed that the reaction proceeds well when the amount of the catalyst loading is 3 mol% (Table 6.1.2, entry 7). It was also observed that the increase and decrease of the catalyst loading has a remarkable effect on the yield of the product. An increase in the amount of catalyst loading from 3 mol % to higher result in the slight decrease of the yield of the product. However, decreases in the amount of catalyst loading from 3 mole% to less result in the significant decreases of the yield of the product. Thus, we observed that 3 mol % of catalyst loading at 80 °C for 2 hours was the optimum condition for the model reaction.

**Table. 6.1.1.** Optimization of reaction temperature for the model reaction

Entry	Temperature	Yield <sup>a</sup> (%)
1	Room Temperature	Nil
2	60 °C	Trace
3	70 °C	25
<b>4</b>	<b>80 °C</b>	<b>97</b>

\*<sup>a</sup>isolated yield**Table. 6.1.2.** Optimization of catalyst loading for the model reaction

Entry <sup>a</sup>	Amount of catalyst (mole %)	Time (hours)	Yield <sup>b</sup> (%)
<b>1</b>	<b>0</b>	<b>2</b>	<b>Nil</b>
2	0.5	2	15
3	1.0	2	20
4	1.5	2	32
5	2.0	2	50
6	2.5	2	60
<b>7</b>	<b>3.0</b>	<b>2</b>	<b>97</b>
8	3.5	2	89
9	4	2	88

\*<sup>a</sup>all the reaction were carried out using o-phenylenediamine (1, 1mmol) and aldehyde (2, 2 mmol) under solvent free condition at 120 °C for 3 hours using Ni-borate catalyst (2.5 mole %) and <sup>b</sup>isolated yield

Having recognized the optimum condition for the studied reaction, we extended catalytic reaction with o-phenylenediamine and a range of differently substituted aromatic aldehydes bearing electron donating as well as electron withdrawing groups. We observed that all the aldehydes gave well to excellent yields under the optimized reaction condition (Table 6.1.3 and Fig 6.1.3).

Again, we checked the recyclability of the catalyst for the given reaction by collecting the used catalyst after each run and subsequently purifying the catalyst by washing with methanol. We found that the catalyst was effective till 4<sup>th</sup> run of the reaction and after 4<sup>th</sup> run the catalyst lost its activity and the yield of the product decrease drastically. Thus, from this study we can infer that the studied catalyst efficiently yielded the desired product up to 4<sup>th</sup> run (Table 6.1.4, Fig 6.1.4).



**Table. 6.1.3.** Isolated yield and melting point of the synthesized benzimidazole derivatives (3a-3j)

Entry <sup>a</sup>	Diamine substrate	Aldehyde	Product	Yield <sup>b</sup> (%)	Melting point (°C)
1	o-phenylenediamine	Benzaldehyde	3a	93	295-298
2	o-phenylenediamine	2-chlorobenzaldehyde	3b	97	230-234
3	o-phenylenediamine	4-chlorobenzaldehyde	3c	96	290-298
4	o-phenylenediamine	2-nitrobenzaldehyde	3d	98	228-232
5	o-phenylenediamine	4-nitrobenzaldehyde	3e	98	315-319
6	o-phenylenediamine	4-methoxybenzaldehyde	3f	95	224-228
7	o-phenylenediamine	2-hydroxybenzaldehyde	3g	96	239-241
8	o-phenylenediamine	2-hydroxy-3-methoxybenzaldehyde	3h	95	197-201
9	o-phenylenediamine	2-hydroxy-5-nitrobenzaldehyde	3i	96	238-241
10	o-phenylenediamine	2-hydroxy-5-bromobenzaldehyde	3j	95	252-256

\*<sup>a</sup>all the reaction were carried out using o-phenylenediamine (1, 1mmol) and aldehyde (2, 1 mmol) under solvent free condition at 80 °C for 2 hours using Ni-borate catalyst (3 mole %) and <sup>b</sup>isolated yield.

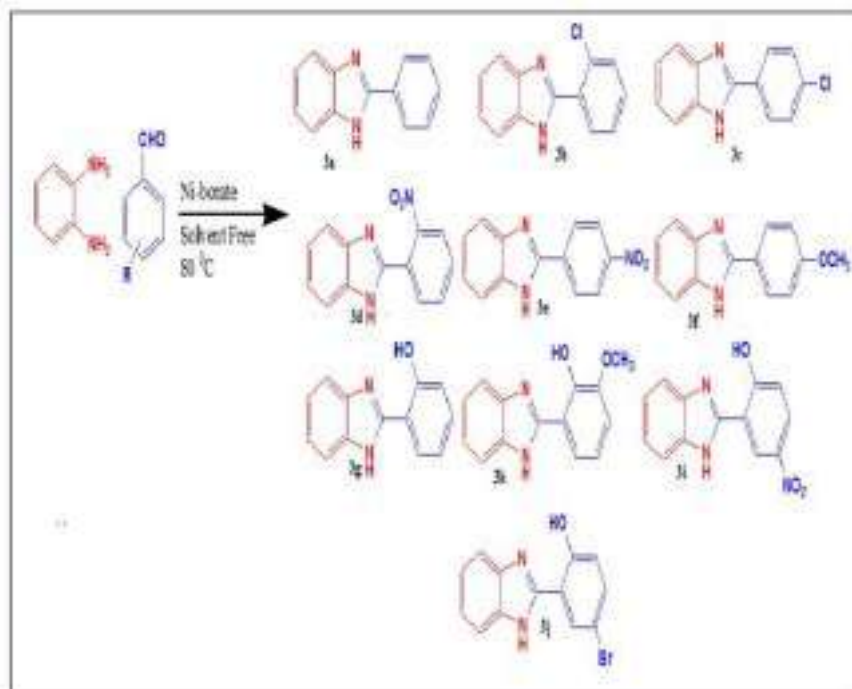


Fig. 6.1.3. Synthesized benzimidazole derivatives (3a-3j)

Table 6.1.4. Recyclability of the catalyst

Entry	Run	Yield <sup>b</sup> (%)
1	1	97
2	2	95
3	3	94
4	4	94
5	5	82
6	6	75

\*<sup>b</sup>isolated yield

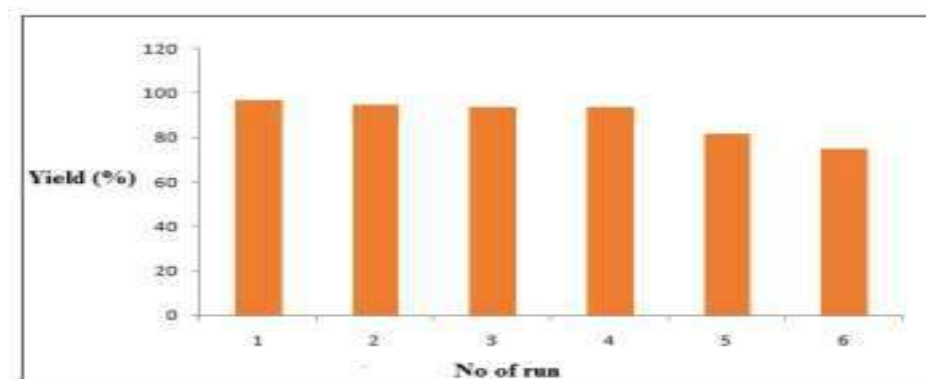
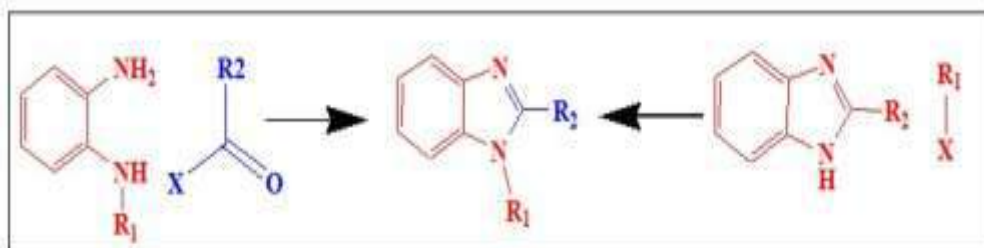


Fig. 6.1.4. Recyclability of the catalyst

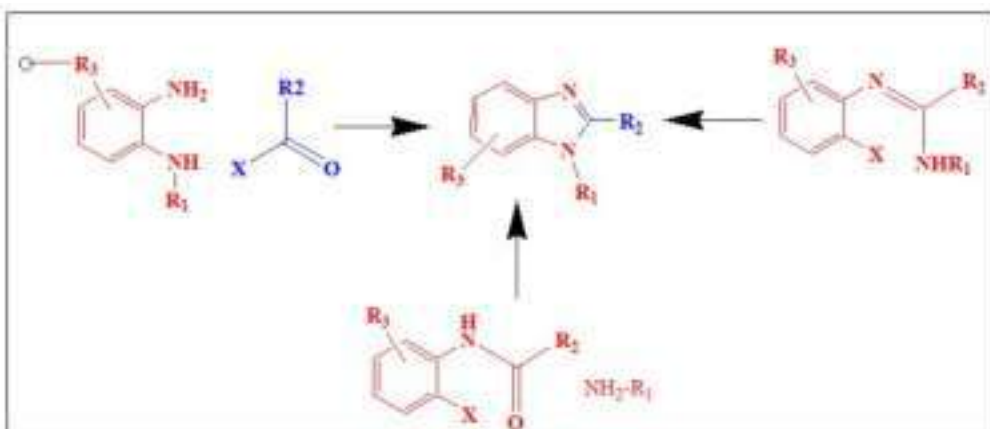
### 6.2.2 1, 2-disubstituted benzimidazole derivatives

1,2-disubstituted benzimidazole derivative represents a special class of the benzimidazole family and thus proven to be an important scaffold because of their diverse application in many fields such as drugs, dyes and polymers<sup>39</sup>. Undoubtedly, there are various methods for the synthesis of 1,2-disubstituted benzimidazole scaffold and the most common and traditional method involves the condensation of orthophenylene diamine with aldehyde or carboxylic derivatives. N-alkylation/N-arylation of benzimidazole serves as a frequent alternative for the synthesis of 1,2-disubstituted benzimidazole derivative<sup>40</sup> (Scheme 6.2.1).



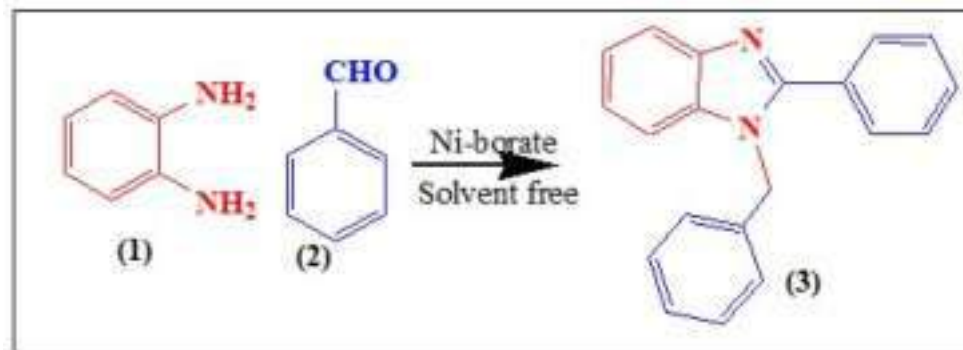
**Scheme. 6.2.1.** Classical method for the synthesis of 1,2-disubstituted benzimidazole

However, these methods are not very popular and suitable for the synthesis of 1,2-disubstituted benzimidazole as they are limited for few available substrates. Moreover, the traditional condensation method is not suitable for the synthesis of 1, 2-disubstituted benzimidazole derivatives because of the lack of difference between the two nitrogen atoms in the benzimidazole ring usually give rise to a mixture of regioisomers<sup>27</sup>. During the past few years, many improvements such as metal catalyzed aryl-amination and cascade arylamination/condensation methods have been formulated<sup>41</sup> (Scheme 6.2.2)



**Scheme. 6.2.2.** Modern methods for the synthesis of 1, 2-disubstituted benzimidazole derivatives.

Thus, the development and formulation of simple and region-selective synthesis of 1, 2-disubstituted benzimidazole derivatives have remains an active and emerging field of research. Therefore, in continuation to our research work for the synthesis of benzimidazole derivatives utilizing Ni-borate catalyst under solvent free condition, we were interested to examine the efficacy of the catalyst for the regioselective synthesis of 1,2-disubstituted benzimidazole derivatives. In order to optimize the reaction condition, orthophenylenediamine (1) and benzaldehyde (2) was chosen as a model reactant under solvent free condition (Scheme 6.2.3) using Ni-borate as a catalyst.



**Scheme. 6.2.3.** Model reaction for the synthesis of 1, 2-disubstituted benzimidazole.

For a model reaction, orthophenylenediamine (1 mmol) and benzaldehyde (2 mmol) was thoroughly mixed and ground in a mortar with the help of pestle in presence of the catalyst. The reaction mixture was then transferred into a 50 ml round bottomed flask and was allowed to stirrer at room temperature with the help of magnetic stirrer for 3 hours. The progress of the reaction was monitored with the help of TLC using ethyl acetate: hexane (20:80) mixture and we observed that the reaction did not go for completion and we isolated the reactant only. Therefore, we carried out the reaction at 80 °C and we found that a trace amount of the product has been formed along with 2-substituted benzimidazole at this temperature (Table 6.2.1, entry 2). Further, we increased the reaction temperature to 120 °C and we observed that the reaction proceeds well and gets completed at 120 °C without formation of the side product (Table 6.2.1, entry 3 and 4)

**Table 6.2.1.** Optimization of reaction temperature for the model reaction

Entry	Temperature	Yield <sup>a</sup> (%)
1	Room Temperature	Nil
2	80 °C	Trace
3	100 °C	20
4	120 °C	96

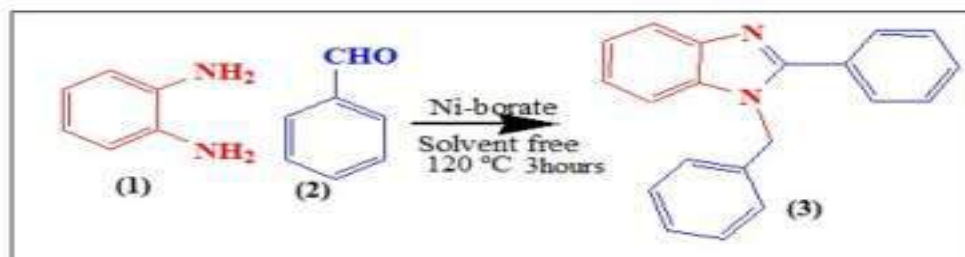
<sup>a</sup>isolated yield

After optimizing the reaction temperature, then we optimized the catalyst loading by varying the amount of catalyst for the same model reaction at optimized temperature and we observed that in absence of the catalyst no product was isolated (Table 6.2.2, entry 1). Then, we varied the amount of catalyst for the model reaction from 0.5 mol % to 4 mol % and we observed that the reaction proceeds well when the amount of the catalyst loading is 2.5 mol % (Table 6.2.2, entry 7). It was also observed that the increase and decrease of the catalyst loading has a remarkable effect on the yield of the product. An increase in the amount of catalyst loading from 2.5 mol % to higher result in the slight decrease of the yield of the product. However, decrease in the amount of catalyst loading from 2.5 mol % to less resulted in the significant decrease of the yield of the product. Thus, we were able to optimize the reaction condition as 2.5 mol % of catalyst at 120 °C for 3 hours reaction time for the formation of 1, 2-disubstituted benzimidazole (3) (Scheme 6.2.4).

**Table. 6.2.2.** Optimization of catalyst loading for the model reaction

Entry <sup>a</sup>	Amount of catalyst (mole %)	Time (hours)	Yield <sup>b</sup> (%)
<b>1</b>	<b>0</b>	<b>3</b>	<b>Nil</b>
2	0.5	3	10
3	1.0	3	22
4	1.5	3	37
5	2.0	3	66
<b>6</b>	<b>2.5</b>	<b>3</b>	<b>96</b>
7	3.0	3	92
8	3.5	3	80

\*<sup>a</sup>all the reaction were carried out using o-phenylenediamine (1, 1mmol) and aldehyde (2, 2 mmol) under solvent free condition at 120 °C for 3 hours using Ni-borate catalyst (2.5 mole %) and <sup>b</sup>isolated yield and <sup>b</sup>isolated yield



**Scheme. 6.2.4.** Optimization of reaction condition for model reaction to synthesize (3a'-3k')

**Table. 6.2.3.** Isolated yield and melting point of the synthesized benzimidazole derivatives (3a'-3k')

Entry <sup>a</sup>	Diamine substrate	Aldehyde	Product	Yield <sup>b</sup> (%)	Melting point (°C)
1	o-phenylenediamine	Benzaldehyde	3a'	96	132-136
2	o-phenylenediamine	4-methylbenzaldehyde	3b'	94	126-129
3	o-phenylenediamine	3-nitrobenzaldehyde	3c'	98	166-170
4	o-phenylenediamine	4-nitrobenzaldehyde	3d'	98	188-192
5	o-phenylenediamine	4-methoxybenzaldehyde	3e'	95	125-129
6	o-phenylenediamine	4-hydroxybenzaldehyde	3f'	94	255-258
7	o-phenylenediamine	4-chlorobenzaldehyde	3g'	96	138-141
8	o-phenylenediamine	2-hydroxybenzaldehyde	3h'	95	205-208
9	o-phenylenediamine	2-hydroxy-5-nitrobenzaldehyde	3i'	98	-
10	o-phenylenediamine	Indole-3-Carboxaldehyde	3j'	94	233-237
11	o-phenylenediamine	2-chlorobenzaldehyde	3k'	96	-

<sup>a</sup> all the reaction were carried out using o-phenylenediamine (1, 1mmol) and aldehyde (2, 2 mmol) under solvent free condition at 120 °C for 3 hours using Ni-borate catalyst (2.5 mole %) and <sup>b</sup>isolated yield.

After optimizing the reaction condition for the model reaction, we extended the catalytic reaction with a range of differently substituted aromatic aldehydes bearing electron donating as well as electron withdrawing groups. We observed

that all the aldehydes furnished 1, 2-disubstituted products in good to excellent yield under the optimized reaction condition (Table 6.2.3 and Fig 6.2.1).

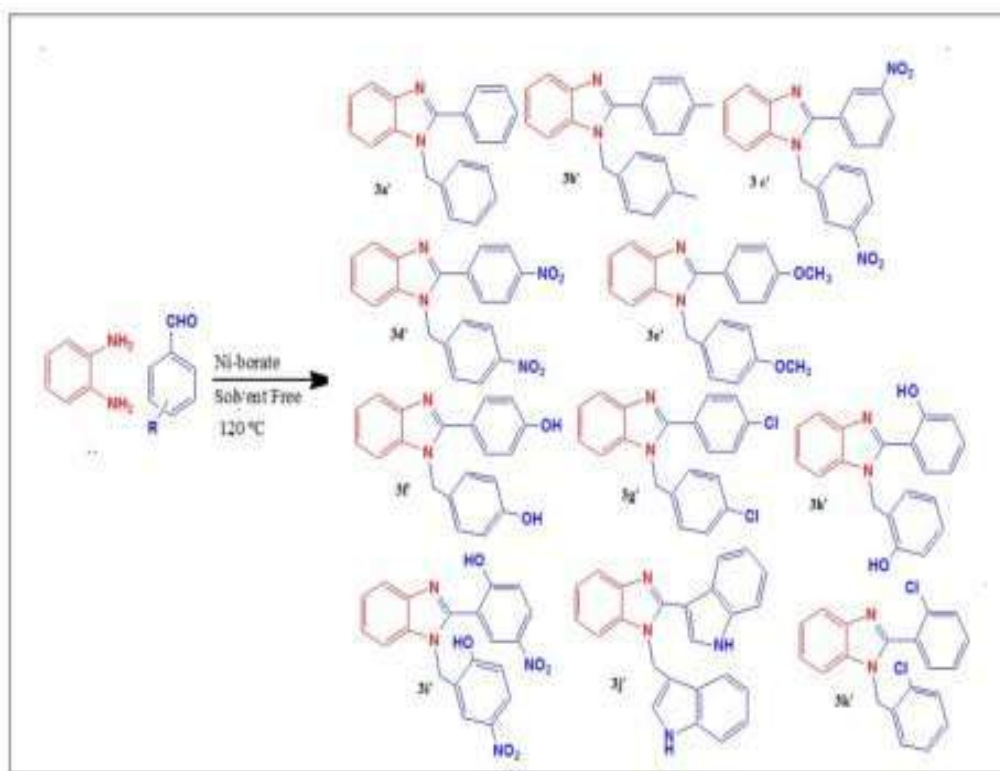


**Fig. 6.2.1.** Synthesized 1, 2-benzimidazole derivatives (3a'-3k')

Again, we examined the recyclability of the catalyst for the given reaction and we recover the catalyst after each run and subsequently purifying the catalyst by washing with methanol. We found that the catalyst was effective till 3<sup>rd</sup> run of the reaction and after 3<sup>rd</sup> run the catalyst lost its activity and the yield of the product varied drastically. Thus, we can infer that the studied catalyst efficiently yielded the desired product up to 3<sup>rd</sup> run (Table 6.2.4, Fig 6.2.2).

**Table. 6.2.4.** Recyclability of the catalyst

Entry	Run	Yield <sup>a</sup> (%)
1	1	96
2	2	95
3	3	94
4	4	82
5	5	75

<sup>a</sup>isolated yield

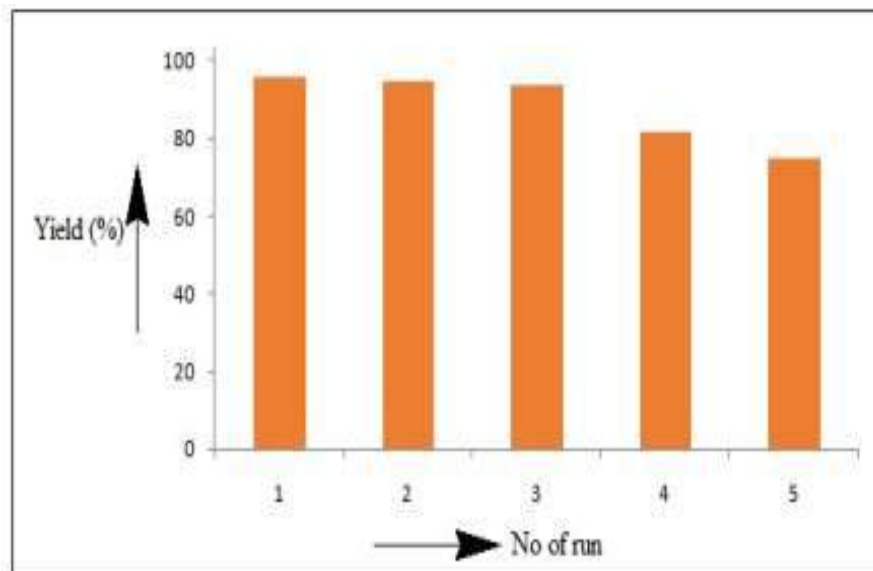


**Fig. 6.2.2** Recyclability of the catalyst

### 6.3 Experimental Section

#### 6.3.1 Materials

All starting materials of high purity for the synthesis of 2-substituted and 1, 2-disubstituted benzimidazole derivatives were purchased commercially and used as received. The FT-IR spectra of the prepared compounds were recorded in Bruker Alpha III spectrophotometer operating in the wave number region 4000 to 400  $\text{cm}^{-1}$  in dry KBr. The melting points of the synthesized compounds were determined by open capillary method.  $^1\text{H-NMR}$  spectra of the derivatives were recorded at room temperature on a FT-NMR (Bruker Advance-II 400 MHz) spectrometer by using  $\text{DMSO-d}_6$  as solvents and chemical shifts are quoted in ppm downfield of internal standard tetramethylsilane(TMS).

#### 6.3.2 General procedure for the synthesis of 2-substituted benzimidazole:

In a typical reaction procedure, a mixture of orthophenylenediamine (1, 1 mmol), substituted benzaldehyde (2, 1.0 mmol) and Nickel borate (3 mol %) thoroughly ground and mixed in a mortar and pestle to make a homogenous mixture. The mixture was then transferred to a test tube. The reaction was heated at 80  $^{\circ}\text{C}$  for 2 hours. The progress of the reaction was monitored by TLC using hexane/ethyl acetate (80:20) solvent. After completion of the reaction, the reaction mixture was dissolved in methanol and filtered. The filtrate was evaporated under vacuum and subsequently dried to afford desired product and the catalyst was recovered with simple filtration. The catalyst was again purified by washing with methanol and dried over an oven at 100  $^{\circ}\text{C}$  for 2 hours for further use. All the synthesized compounds (3a-3j) were recrystallized from ethanol and have been



characterized by their analytical (yield and melting point value) and spectroscopic data (FT-IR and <sup>1</sup>HNMR) and compared with the literature value.

### 6.3.3 General procedure for the synthesis of 1, 2-disubstituted benzimidazole

The synthesis of 1, 2-disubstituted benzimidazole derivatives have been accomplished by grinding the mixture of orthophenylenediamine (1, 1 mmol) and substituted aromatic aldehydes (2, 2.0 mmol) in presence of Ni-borate catalyst (2.5 mole %) in agate mortar and pestle. The reaction mixture was then transferred into the borosil test tube and subjected to heating at 120 °C for 3 hours. The progress of the reaction was monitored by TLC using hexane/ethyl acetate (80:20) solvent. After completion of the reaction, the reaction mixture was dissolved in methanol and filtered. The filtrate was evaporated under vacuum and subsequently dried to afford desired product and the catalyst was recovered with simple filtration. All the synthesized compounds (3a'-3k') were recrystallized from ethanol and have been characterized by their analytical (yield and melting point value) and spectroscopic data (FT-IR and <sup>1</sup>HNMR) and compared with the literature value.

### 6.4. Conclusion

In summary, we have reported a novel and unconventional Ni-borate catalyst for the synthesis of 2-substituted and 1, 2-disubstituted benzimidazole derivatives under solvent free condition. The catalyst was found to be an efficient and versatile for the synthesis of above-mentioned derivatives under green chemical condition. This process is advantageous due to its simple operational procedure and easy work-up of the product with minimal use of the hazardous solvent.

## 6.5 Analytical and Spectroscopic data

### 6.5.1 2-substituted benzimidazole

**6.5.1.1 2-Phenyl-1H-benzimidazole (3a):** white solid, yield= 93%, melting point found ( $^{\circ}\text{C}$ ) = 295-298, IR (KBr,  $\text{cm}^{-1}$ )  $\nu_{\text{max}}$ :3446 (br, NH), 3003 (C-H, Aromatic), 1622(C=N), 1590, 1445 (C=C, Aromatic),  $^1\text{HNMR}$  (400 MHz, DMSO  $d_6$ ):  $\delta\text{ppm}$  = 12.89 (S, 1H, OH), 8.15 (m, 2H, Ar-H), 7.52 (m, 2H, Ar-H), 7.46 (m, 3H, Ar-H), 7.17 (m, 2H, Ar-H).

**6.5.1.2 2-(2-Chlorophenyl)-benzimidazole (3b):** yellow solid, yield= 97%, melting point found ( $^{\circ}\text{C}$ ) = 230-234, IR (KBr,  $\text{cm}^{-1}$ )  $\nu_{\text{max}}$ :3444 (br, NH), 3031 (C-H, Aromatic), 1591(C=N), 1575, 1444 (C=C, Aromatic),  $^1\text{HNMR}$  (400 MHz, DMSO  $d_6$ ):  $\delta\text{ppm}$  = 12.77 (S, 1H, NH), 7.91 (m, 1H, Ar-H), 7.65-7.56 (m, 3H, Ar-H), 7.52-7.49 (m, 2H, Ar-H), 7.17-7.23 (m, 2H, Ar-H).

**6.5.1.3 2-(4-Chlorophenyl)-benzimidazole (3c):** yellow solid, yield= 96%, melting point found ( $^{\circ}\text{C}$ ) = 290-293, IR (KBr,  $\text{cm}^{-1}$ )  $\nu_{\text{max}}$ :3442 (br, NH), 3036 (C-H, Aromatic), 1598(C=N), 1580, 1429 (C=C, Aromatic),  $^1\text{HNMR}$  (400 MHz, DMSO  $d_6$ ):  $\delta\text{ppm}$  = 12.88 (S, 1H, NH), 8.13 (d, 2H, Ar-H), 7.64-7.49 (m, 4H, Ar-H), 7.20 (d, 2H, Ar-H).

**6.5.1.4 2-(2-Nitrophenyl)-benzimidazole (3d):** yellow solid, yield= 98%, melting point found ( $^{\circ}\text{C}$ ) = 228-232, IR (KBr,  $\text{cm}^{-1}$ )  $\nu_{\text{max}}$ :3428 (br, NH), 1620(C=N), 1528, 1457 (C=C, Aromatic),  $^1\text{HNMR}$  (400 MHz, DMSO  $d_6$ ):  $\delta\text{ppm}$  = 13.08 (S, 1H, NH), 8.04-7.85 (m, 2H, Ar-H), 7.89-7.63 (m, 4H, Ar-H), 7.225 (brs, 2H, Ar-H).

**6.5.1.5 2-(4-Nitrophenyl)-benzimidazole (3e):** pale yellow solid, yield= 98%, melting point found ( $^{\circ}\text{C}$ ) = 315-319, IR (KBr,  $\text{cm}^{-1}$ )  $\nu_{\text{max}}$ :3420 (br, NH), 1604(C=N), 1520, 1451 (C=C, Aromatic),  $^1\text{HNMR}$  (400 MHz, DMSO  $d_6$ ):  $\delta\text{ppm}$  = 13.20 (S, 1H, NH), 8.32 (d, 2H, Ar-H), 8.14 (d, 2H, Ar-H), 7.19-7.61 (m, 4H, Ar-H).

**6.5.1.6 2-(4-Methoxyphenyl)-benzimidazole (3f):** yellow solid; yield= 95%, melting point found ( $^{\circ}\text{C}$ ) = 224-228, IR (KBr,  $\text{cm}^{-1}$ )  $\nu_{\text{max}}$ :3342 (br, NH), 1605(C=N), 1506, 1459 (C=C, Aromatic),  $^1\text{HNMR}$  (400 MHz, DMSO  $d_6$ ):  $\delta\text{ppm}$  = 12.68 (S, 1H, NH), 8.12 (d, 2H, Ar-H), 7.04-7.75 (m, 6H, Ar-H), 3.82 (s, 3H, -OCH<sub>3</sub>).

**6.5.1.7 2-(2-Hydroxyphenyl)-benzimidazole (3g):** white solid; yield= 96%, melting point found ( $^{\circ}\text{C}$ ) = 239-241, IR (KBr,  $\text{cm}^{-1}$ )  $\nu_{\text{max}}$ :3330 (br, NH), 3054 (C-H, Aromatic), 1598(C=N), 1528, 1490 (C=C, Aromatic),  $^1\text{HNMR}$  (400 MHz,

DMSO  $d_6$ ):  $\delta$ ppm = 13.18 (s, 1H, NH), 12.98 (s, 1H, OH), 8.01 (m, 1H, Ar-H), 7.64 (m, 2H, Ar-H), 7.25-7.33 (m, 3H, Ar-H), 6.96-7.05 (m, 2H, Ar-H).

**6.5.1.8 2-(2-Hydroxy-3-methoxyphenyl)-benzimidazole (3h):** white solid; yield= 95%, melting point found ( $^{\circ}$ C) = 197-201, IR (KBr,  $cm^{-1}$ )  $\nu_{max}$ : 3152 (br, NH), 3004 (C-H, Aromatic), 1604(C=N), 1531, 1365 (C=C, Aromatic),  $^1$ HNMR (400 MHz, DMSO  $d_6$ ):  $\delta$ ppm = 9.55 (s, 1H, NH), 8.80 (s, 1H, OH), 6.78-7.88 (m, 7H, Ar-H), 3.42 (s, 3H, -OCH<sub>3</sub>).

**6.5.1.9 2-(2-Hydroxy-5-nitrophenyl)-benzimidazole (3j):** yellow solid; yield= 96%, melting point found ( $^{\circ}$ C) = 238-241, IR (KBr,  $cm^{-1}$ )  $\nu_{max}$ : 3284 (br, NH), 3000-2800 (OH), 1594(C=N), 1590, 1478 (C=C, Aromatic),  $^1$ HNMR (400 MHz, DMSO  $d_6$ ):  $\delta$ ppm = 14.08 (s, 1H, NH), 9.18 (s, 1H, OH), 8.22 (d, 2H, Ar-H), 8.17 (d, 2H, Ar-H), 7.21-7.71 (m, 3H, Ar-H).

**6.5.1.10 2-(2-Hydrox-5-bromophenyl)-benzimidazole (3k):** yellow solid; yield= 95%, melting point found ( $^{\circ}$ C) = 252-256, IR (KBr,  $cm^{-1}$ )  $\nu_{max}$ : 3364 (br, NH), 3065 C-H Aromatic), 1612(C=N), 1438 (C=C, Aromatic),  $^1$ HNMR (400 MHz, DMSO  $d_6$ ):  $\delta$ ppm = 10.28 (s, 1H, OH), 8.89 (s, 1H, NH), 6.72-7.52 (m, 7H, Ar-H).

## 6.5.2 1, 2-disubstituted benzimidazole

**6.5.2.1 1-benzyl-2-phenyl-1H-benzo[d]imidazole (3a<sup>l</sup>):** white solid; yield= 96%, melting point found ( $^{\circ}$ C) = 132-136, IR (KBr,  $cm^{-1}$ )  $\nu_{max}$ : 2924, 2853 (C-H Aromatic), 1632(C=N), 1469 (C=C, Aromatic),  $^1$ HNMR (400 MHz, DMSO  $d_6$ ):  $\delta$ ppm = 7.71-7.25 (m, 3H, Ar-H), 7.27-7.19 (m, 5H, Ar-H), 6.98 (d, 2H, Ar-H), 5.16 (s, 2H, -CH<sub>2</sub>).

**6.5.2.2 1-(4-methylbenzyl-2-p-tolyl-1H-benzo[d]imidazole (3b<sup>l</sup>):** white solid; yield= 94%, melting point found ( $^{\circ}$ C) = 126-129, IR (KBr,  $cm^{-1}$ )  $\nu_{max}$ : 2959, 2937 C-H Aromatic), 1626, 1587 (C=N), 1480 (C=C, Aromatic),  $^1$ HNMR (400 MHz, DMSO  $d_6$ ):  $\delta$ ppm = 7.64 (d, 1H, Ar-H), 7.58 (d, 2H, Ar-H), 7.38 (d, 1H, Ar-H), 7.33-7.19 (m, 4H, Ar-H), 7.04-6.85 (m, 4H, Ar-H), 5.48 (s, 2H, -CH<sub>2</sub>), 2.35 (s, 3H, CH<sub>3</sub>), 2.20 (s, 3H, CH<sub>3</sub>).

**6.5.2.3 1-(3-nitrobenzyl)-2-(3-nitrophenyl-1H-benzo[d]imidazole (3c<sup>l</sup>):** yellow solid; yield= 98%, melting point found ( $^{\circ}$ C) = 166-170, IR (KBr,  $cm^{-1}$ )  $\nu_{max}$ : 2882 C-H Aromatic), 1637(C=N), 1536, 1471 (C=C, Aromatic),  $^1$ HNMR (400 MHz,

DMSO  $d_6$ ):  $\delta$ ppm = 8.82 (s, 1H, Ar-H), 8.41 (d, 2H, Ar-H), 8.25 (d, 1H, Ar-H), 7.77-7.73 (m, 2H, Ar-H), 7.61-7.59 (m, 2H, Ar-H), 7.26-7.24 (m, 2H, Ar-H), 5.20 (s, 2H, -CH<sub>2</sub>).

**6.5.2.4 1-(4-nitrobenzyl)-2-(4-nitrophenyl-1H-benzo[d]imidazole (3d<sup>f</sup>):** bright yellow solid; yield= 98%, melting point found ( $^{\circ}$ C) = 188-192, IR (KBr,  $cm^{-1}$ )  $\nu_{max}$ : 3107 (C-H Aromatic), 1634, 1607 (C=N), 1540 (C=C, Aromatic), <sup>1</sup>HNMR (400 MHz, DMSO  $d_6$ ):  $\delta$ ppm = 8.32 (d, 2H, Ar-H), 8.23 (d, 2H, Ar-H), 8.10 (d, 2H, Ar-H), 7.88 (d, 1H, Ar-H), 7.62 (d, 1H, Ar-H), 7.28-7.20 (m, 2H, Ar-H), 7.02 (d, 2H, Ar-H), 5.18 (s, 2H, -CH<sub>2</sub>).

**6.5.2.5 1-(4-methoxybenzyl)-2-(4-methoxyphenyl-1H-benzo[d]imidazole (3e<sup>f</sup>):** white solid; yield= 95%, melting point found ( $^{\circ}$ C) = 125-129, IR (KBr,  $cm^{-1}$ )  $\nu_{max}$ : 2937 C-H Aromatic), 1626, 1587 (C=N), 1480, 1458 (C=C, Aromatic), <sup>1</sup>HNMR (400 MHz, DMSO  $d_6$ ):  $\delta$ ppm = 7.66 (d, 3H, Ar-H), 7.43 (d, 1H, Ar-H), 7.21-7.18 (m, 2H, Ar-H), 7.06 (d, 2H, Ar-H), 6.95(d, 2H, Ar-H), 6.82 (d, 2H, Ar-H), 5.39 (s, 2H, -CH<sub>2</sub>), 3.81 (s, 3H, -OCH<sub>3</sub>), 3.66 (s, 3H, -OCH<sub>3</sub>).

**6.5.2.6 1-(4-hydroxybenzyl) -1H-benzo[d]imidazol-2-yl)phenol (3f<sup>f</sup>):** yellow solid; yield= 94%, melting point found ( $^{\circ}$ C) = 255-258, IR (KBr,  $cm^{-1}$ )  $\nu_{max}$ : 2922 (C-H Aromatic), 1621, 1578 (C=N), 1506, 1463 (C=C, Aromatic), <sup>1</sup>HNMR (400 MHz, DMSO  $d_6$ ):  $\delta$ ppm = 10.77 (s, 1H, -OH), 9.58 (s, 1H, -OH), 7.82 (d, 1H, Ar-H), 7.78 (d, 1H, Ar-H), 7.74 (d, 2H, Ar-H), 7.54-7.51 (m, 2H, Ar-H), 7.12 (d, 2H, Ar-H), 6.94 (d, 2H, Ar-H), 6.65 (d, 2H, Ar-H) 5.61 (s, 2H, -CH<sub>2</sub>).

**6.5.2.7 1-(4-chlorobenzyl)-2-(4-chlorophenyl-1H-benzo[d]imidazole (3g<sup>f</sup>):** white solid; yield= 96%, melting point found ( $^{\circ}$ C) = 138-141, IR (KBr,  $cm^{-1}$ )  $\nu_{max}$ : 3070, 2847 C-H Aromatic), 1627, 1568 (C=N), 1505, 1462 (C=C, Aromatic), <sup>1</sup>HNMR (400 MHz, DMSO  $d_6$ ):  $\delta$ ppm = 7.71 (d, 3H, Ar-H), 7.60 (d, 2H, Ar-H), 7.46 (d, 1H, Ar-H), 7.32 (d, 2H, Ar-H), 7.26-7.24 (m, 2H, Ar-H), 7.01 (d, 2H, Ar-H), 5.54 (s, 2H, -CH<sub>2</sub>).

**6.5.2.8 2-(1-(2-hydroxybenzyl)-1H-benzo[d]imidazol-2-yl)phenol (3h<sup>f</sup>):** yellow solid; yield= 95%, melting point found ( $^{\circ}$ C) = 205-208, IR (KBr,  $cm^{-1}$ )  $\nu_{max}$ : 2923, 2852 (C-H Aromatic), 1635(C=N), 1495(C=C, Aromatic), <sup>1</sup>HNMR (400 MHz, DMSO  $d_6$ ):  $\delta$ ppm = 11.08 (s, 1H, -OH), 9.75 (s, 1H, -OH), 7.71 (d, 1H, Ar-H), 7.41-7.36 (m, 3H, Ar-H), 7.01 (d, 2H, Ar-H), 6.94-6.88 (m, 1H, Ar-H), 6.78 (d, 1H, Ar-H), 6.58-6.39 (m, 2H, Ar-H), 5.42 (s, 2H, -CH<sub>2</sub>).

**6.5.2.9**            **2-(1-(2-hydroxy-5-nitrobenzyl)-1H-benzo[d]imidazol-2-yl)-4-nitrophenol (3i')**: yellow solid, yield= 98%, IR (KBr,  $\text{cm}^{-1}$ )  $\nu_{\text{max}}$ : 2922, 2852 (C-H Aromatic), 1635, 1590 (C=N), 1481 (C=C, Aromatic),  $^1\text{HNMR}$  (400 MHz, DMSO  $d_6$ ):  $\delta_{\text{ppm}}$  = 13.98 (s, 2H, -OH), 9.11 (s, 2H, Ar-H), 8.77 (d, 2H, Ar-H), 8.21 (dd, 2H, Ar-H), 7.56-7.48 (m, 4H, Ar-H), 5.36 (s, 2H, -CH<sub>2</sub>).

**6.5.2.10**    **1-((1H-Indol-3-yl)methyl)-2-(1H-indol-3-yl)-1H-benzimidazole (3j')**: brown solid, yield= 94%, melting point found ( $^{\circ}\text{C}$ ) = 233-238, IR (KBr,  $\text{cm}^{-1}$ )  $\nu_{\text{max}}$ : 3032 C-H Aromatic), 1612, 1598(C=N), 1256 (C=C, Aromatic),  $^1\text{HNMR}$  (400 MHz, DMSO  $d_6$ ):  $\delta_{\text{ppm}}$  = 10.20 (s, 1H, -OH), 9.45 (s, 1H, -OH), 8.72 (s, 1H, Ar-H), 8.35 (t, 1H, Ar-H), 7.82 (d, 1H, Ar-H), 7.63 (s, 1H, Ar-H), 7.44-7.41 (m, 1H, Ar-H), 7.42 (t, 1H, Ar-H), 7.35-7.29 (m, 2H, Ar-H), 7.28-7.25 (m, 3H, Ar-H), 7.08-7.04 (m, 2H, Ar-H), 6.84 (t, 1H, Ar-H), 5.67 (s, 2H, -CH<sub>2</sub>).

**6.5.2.11**    **1-(2-chlorobenzyl)-2-(2-chlorophenyl)-1H-benzo[d]imidazole (3l')**: white solid, yield= 96%, IR (KBr,  $\text{cm}^{-1}$ )  $\nu_{\text{max}}$ : 3065 (C-H Aromatic), 1638 (C=N), 1446 (C=C, Aromatic),  $^1\text{HNMR}$  (400 MHz, DMSO  $d_6$ ):  $\delta_{\text{ppm}}$  = 7.93 (m, 1H, Ar-H), 7.72 (m, 2H, Ar-H), 7.68-7.65 (m, 4H, Ar-H), 7.62 (t, 1H, Ar-H), 7.56-7.50 (m, 2H, Ar-H), 7.32-7.27 (m, 1H, Ar-H), 7.25 (d, 1H, Ar-H), 5.43 (s, 2H, -CH<sub>2</sub>).

## 6.6 Supporting spectra

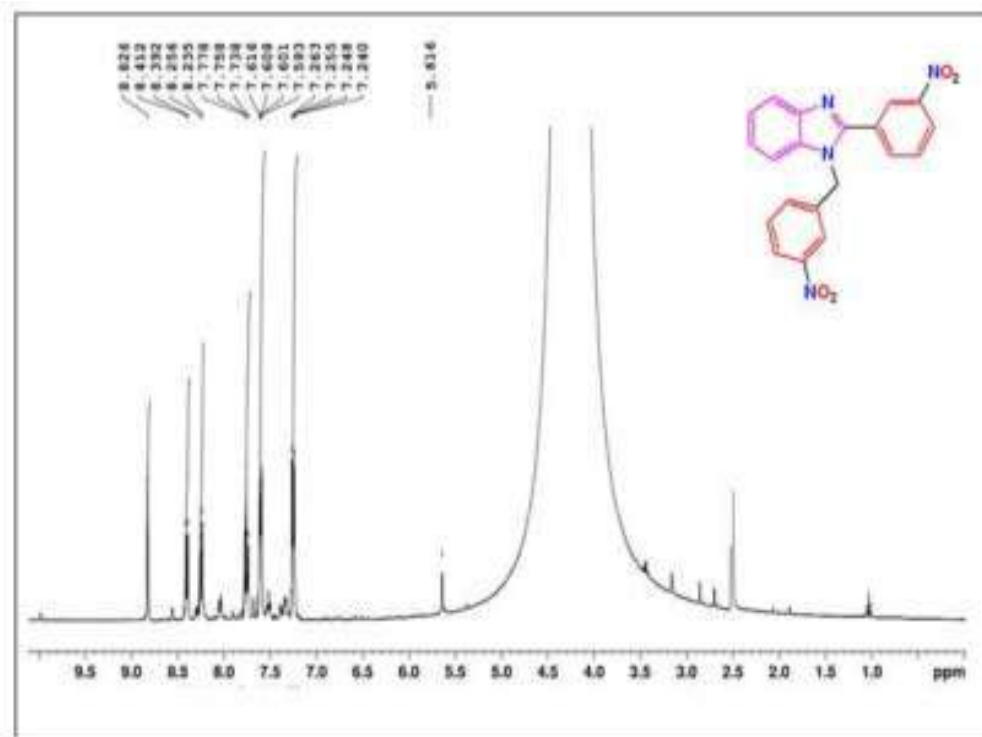


**Fig.6.6.1.** <sup>1</sup>HNMR of 1-(3-nitrobenzyl)-2-(3-nitrophenyl)-1H-benzo[d]imidazole (3c')

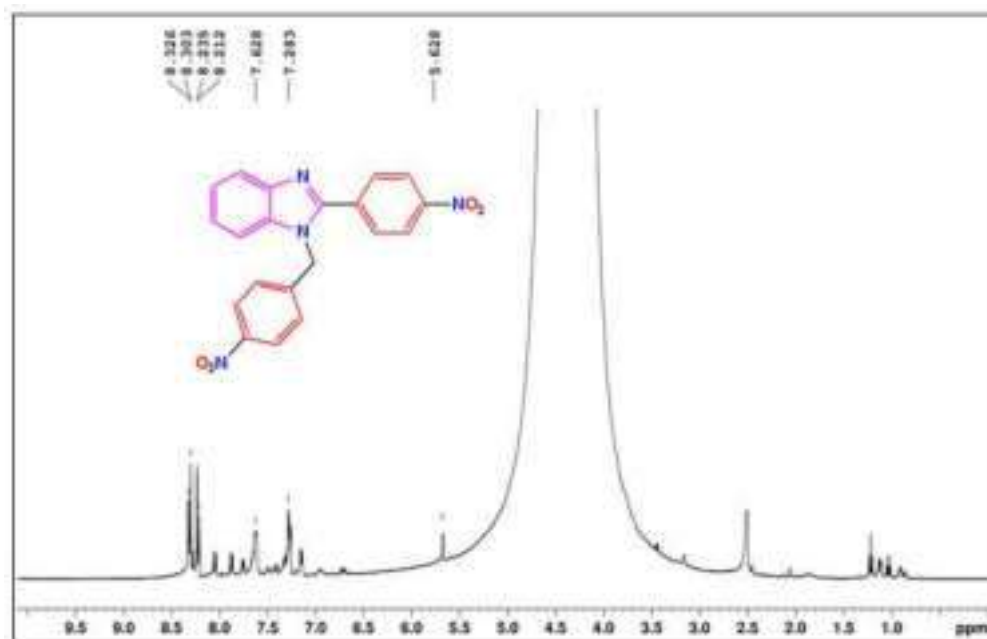


**Fig.6.6.2.** <sup>1</sup>HNMR of 1-(4-nitrobenzyl)-2-(4-nitrophenyl)-1H-benzo[d]imidazole (3d')

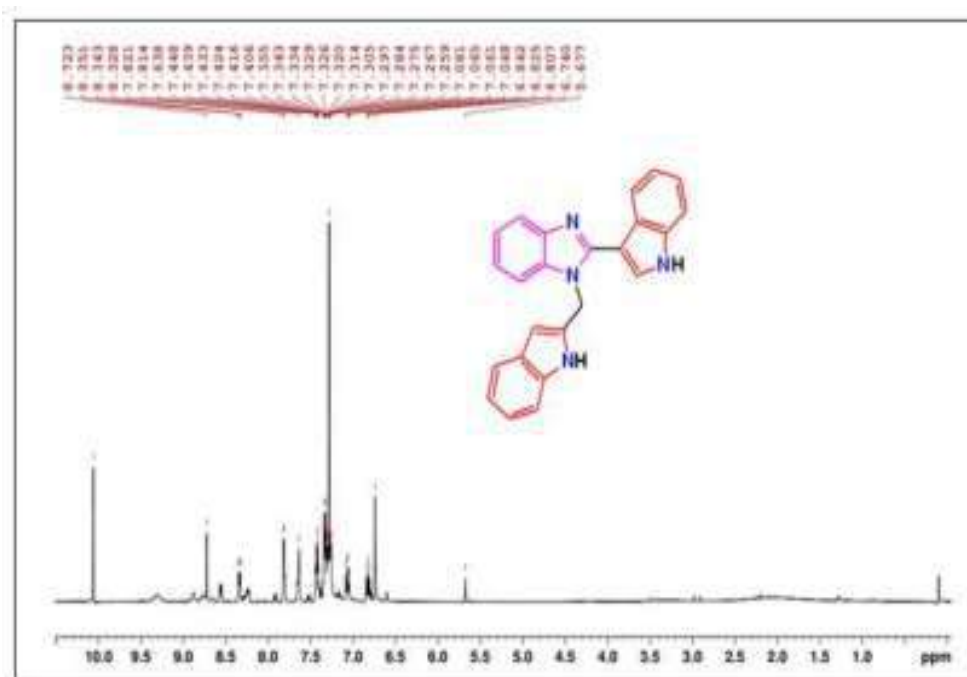


**Fig.6.6.3.** <sup>1</sup>HNMR of 1-((1H-Indol-3-yl)methyl)-2-(1H-indol-3-yl)-1H-benzimidazole (3j)

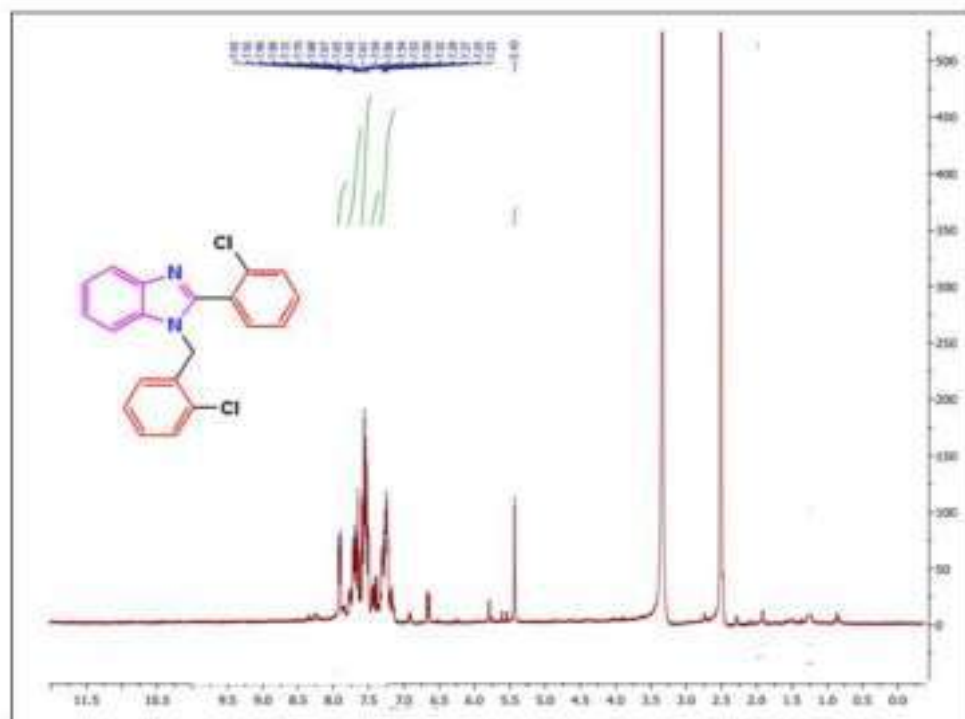


**Fig 6.6.4.** <sup>1</sup>HNMR of 1-(2-chlorobenzyl)-2-(2-chlorophenyl)-1H-benzo[d]imidazole (3l)

## 6.7 References

- (1) B. Pathare, T. Bansode., *Results in Chemistry*, **2021**, 3, 100200.
- (2) O. O. Ajani, D. v. Aderohunmu, C. O. Ikpo, A. E. Adedapo, I. O. Olanrewaju., *Arch Pharm (Weinheim)*, **2016**, 349 (7), 475–506.
- (3) A. R. Katritzky, X. Lan, J. Z. Yang, O. v. Denisko., *Chemical Reviews*, **1998**, 98 (2), 409–548.
- (4) Z. Wang, X. Deng, S. Xiong, R. Xiong, J. Liu, L. Zou, X. Lei, X. Cao, Z. Xie, Y. Chen, Y. Liu, X. Zheng, G. Tang., *Natural Product Research*, **2018**, 32 (24), 2900–2909.
- (5) G. R. Morais, E. Palma, F. Marques, L. Gano, M. C. Oliveira, A. Abrunhosa, H. V. Miranda, T. F. Outeiro, I. Santos, A. Paulo., *Journal of Heterocyclic Chemistry*, **2017**, 54 (1), 255–267.
- (6) V. Onnis, M. Demurtas, A. Deplano, G. Balboni, A. Baldisserotto, S. Manfredini, S. Pacifico, S. Liekens, J. Balzarini., *Molecules*, **2016**, 21 (5), 579.
- (7) R. Sharma, A. Bali, B. B. Chaudhari., *Bioorganic & Medicinal Chemistry Letters*, **2017**, 27 (13), 3007–3013.
- (8) M. M. Vandeputte, K. van Uytfanghe, N. K. Layle, D. M. st. Germaine, D. M. Iula, C. P. Stove., *ACS Chemical Neuroscience*, **2021**, 12 (7), 1241–1251.
- (9) A. Noor, N. G. Qazi, H. Nadeem, A. ullah Khan, R. Z. Paracha, F. Ali, A. Saeed., *Chemistry Central Journal*, **2017**, 11 (85), 1–13.
- (10) T. Iwahi, H. Satoh, M. Nakao, T. Iwasaki, T. Yamazaki, K. Kubo, T. Tamura, A. Imada., *Antimicrobial Agents and Chemotherapy*, **1991**, 35 (3), 490–496.
- (11) N. S. El-Gohary, M. I. Shaaban., *European Journal of Medicinal Chemistry*, **2017**, 131, 255–262.
- (12) M. Taha, A. Mosaddik, F. Rahim, S. Ali, M. Ibrahim, N. B. Almandil., *Journal of King Saud University - Science*, **2020**, 32 (1), 191–194.
- (13) B. Dik, D. Coşkun, E. Bahçivan, K. Üney., *Turkish Journal of Medical Sciences*, **2021**, 51 (3), 1585.
- (14) A. Kanwal, M. Ahmad, S. Aslam, S. A. R. Naqvi, M. J. Saif., *Pharmaceutical Chemistry Journal*, **2019**, 53 (3), 179–187.
- (15) H. Yang, Y. Ren, X. Gao, Y. Gao., *Chemical Research in Chinese Universities*, **2016**, 32 (6), 973–978.



- (16) Y. Bansal, O. Silakari., *Bioorganic & Medicinal Chemistry*, **2012**, 20 (21), 6208–6236.
- (17) K. P. Barot, S. Nikolova, I. Ivanov, M. D. Ghate., *Mini-Reviews in Medicinal Chemistry*, **2013**, 13 (10), 1421–1447.
- (18) W. Akhtar, M. F. Khan, G. Verma, M. Shaquiquzzaman, M. A. Rizvi, S. H. Mehdi, M. Akhter, M. M. Alam., *European Journal of Medicinal Chemistry*, **2017**, 126, 705–753.
- (19) E. Mulugeta, Y. Samuel., *Biochemistry Research International*, **2022**, 2022 (Article ID 7255299).
- (20) J. Horton., *Parasitology*, **2000**, 121 (Suppl. 1), S113–S132.
- (21) S. Singh, N. Singh, V. Kumar, S. Datta, A. B. Wani, D. Singh, K. Singh, J. Singh., *Environmental Chemistry Letters*, **2016**, 14 (3), 317–329.
- (22) P. Gosse., *Vascular Health and Risk Management*, **2006**, 2 (3), 195–201.
- (23) D. M. Richards, R. N. Brogden, R. C. Heel, T. M. Speight, G. S. Avery., *Drugs*, **1984**, 28 (1), 38–61.
- (24) H. Iqbal, A. K. Verma, P. Yadav, S. Alam, M. Shafiq, D. Mishra, F. Khan, K. Hanif, A. S. Negi, D. Chanda., *Frontiers in Pharmacology*, **2021**, 12 (Article ID 611109).
- (25) H. Y. Aboul-Enein, A. A. El Rashedy., *Current Drug Therapy*, **2013**, 8 (3), 145–154.
- (26) T. Ishida, T. Suzuki, S. Hirashima, K. Mizutani, A. Yoshida, I. Ando, S. Ikeda, T. Adachi, H. Hashimoto., *Bioorganic & Medicinal Chemistry Letters*, **2006**, 16 (7), 1859–1863.
- (27) B. A. Reddy., *E-Journal of Chemistry*, **2010**, 7(1) (Article ID 601929), 222–226.
- (28) M. Nardi, S. Bonacci, N. H. Cano, M. Oliverio, A. Procopio., *Molecules*, **2022**, 27 (5), 1751.
- (29) M. Taha, A. Ahmad Khan, F. Rahim, S. Imran, M. Salahuddin, N. Uddin, K. Mohammed Khan, S. Adnan Ali Shah, A. Zafar, Z. Amiruddin Zakaria., *Arabian Journal of Chemistry*, **2022**, 15 (1), 103505.
- (30) Y. Chen, F. Xu, Z. Sun., *RSC Advances*, **2017**, 7 (70), 44421–44425.
- (31) P. Thapa, P. M. Palacios, T. Tran, B. S. Pierce, F. W. Foss., *The Journal of Organic Chemistry*, **2020**, 85 (4), 1991–2009.
- (32) D. Kumar, D. N. Kommi, R. Chebolu, S. K. Garg, R. Kumar, A. K. Chakraborti., *RSC Advances*, **2013**, 3 (1), 91–98.

- (33) Y. R. Girish, K. S. Sharath Kumar, K. N. Thimmaiah, K. S. Rangappa, S. Shashikanth., *RSC Advances*, **2015**, 5 (92), 75533–75546.
- (34) R. Chebolu, D. N. Kommi, D. Kumar, N. Bollineni, A. K. Chakraborti., *Journal of Organic Chemistry*, **2012**, 77 (22), 10158–10167.
- (35) C. T. Brain, S. A. Brunton., *Tetrahedron Letters*, **2002**, 43 (10), 1893–1895.
- (36) D. Anastasiou, E. M. Campi, H. Chaouk, W. R. Jackson., *Tetrahedron*, **1992**, 48 (36), 7467–7478.
- (37) H. Naeimi, N. Alishahi., *Organic Chemistry International*, **2012**, 2012 (Article ID 498521), 1–5.
- (38) R. J. Perry, B. D. Wilson., *Journal of Organic Chemistry*, **1993**, 58 (25), 7016–7021.
- (39) M. J. Plater, P. Barnes, L. K. McDonald, S. Wallace, N. Archer, T. Gelbrich, P. N. Horton, M. B. Hursthouse., *Organic & Biomolecular Chemistry*, **2009**, 7 (8), 1633–1641.
- (40) K. Das, A. Mondal, D. Srimani., *Journal of Organic Chemistry*, **2018**, 83 (16), 9553–9560.
- (41) B. Zou, Q. Yuan, D. Ma., *Angewandte Chemie International Edition*, **2007**, 46 (15), 2598–2601.

## Chapter-VII

### 7.1 Concluding Remarks

In the present dissertation, the catalytic activity of some transition metal borates have been explored in some important organic reactions used for the green synthesis of some Nitrogen containing Heterocyclic Compounds. Looking at the diverse applications of Heterocyclic compounds there are several works on the synthesis of these compounds but most of the works suffer from serious drawbacks like harsh reaction conditions, low yield of the products, use of expensive solvents and non-recyclability of the catalysts. So, in this research work focus has been made on the green synthesis of some Nitrogen containing Heterocyclic compounds using some Transition metal borates like Copper Borate, Iron Borate and Nickel Borate as catalysts thereby investigating their catalytic properties which has not been explored much.

In **Chapter-I** of the thesis, a general introduction to a few Nitrogen containing heterocyclic compounds like 2,4,5-triaryl imidazoles, 3,4-dihydropyrimidin-2[1H]-ones, 1-hydroxy-2-arylimidazole-3-oxides and 2-substituted benzimidazole and 1, 2-disubstituted benzimidazole has been given with emphasis on Green Chemistry, Multicomponent Reactions and Solvent free synthesis. This chapter also includes the recent literature review on the various green protocols followed for the synthesis of these Nitrogen containing Heterocyclic Compounds. The literature review has also been separated into various parts depending on the type of method followed for their synthesis like Classical methods, Solvent free synthesis, Microwave assisted and Ultrasound assisted synthesis. A brief introduction to transition metal borates and their applications in various fields have also been discussed in this chapter.

**Chapter-II** of the thesis includes the experimental section wherein a brief description of the chemicals and solvents used in this research has been described. This chapter also contains the information about various analytical and spectroscopic techniques like melting point determination, FT-IR, <sup>1</sup>HNMR, X-Ray Crystallography along with the information about various theoretical calculations and techniques that were performed in this work like DFT, Molecular Docking and Pharmacokinetic studies.

**Chapter-III Section-A** of the thesis contains the multi-component green synthesis of 2,4,5 Tri-aryl imidazole derivatives using Copper Borate (CuB<sub>4</sub>O<sub>7</sub>) as a catalyst under solvent free conditions. This environmentally green approach provided access to substituted imidazole derivatives in good to excellent yield using an unconventional and inexpensive CuB<sub>4</sub>O<sub>7</sub> catalyst. The developed catalytic procedure was also found to be operative for a wide range of the aromatic aldehyde substrates.

In **Section-B** of **Chapter-III** the crystal structure of Bis[2-(4,5-diphenyl-1H-imidazol-2-yl)-4-nitro-phenolato] copper (II) dihydrate complex is discussed along with its synthesis and Hirschfeld Surface analysis. This section also covers the evidence for the in-situ conversion of  $\text{CuB}_4\text{O}_7$  into  $\text{Cu}(\text{OAc})_2 \cdot 2\text{H}_2\text{O}$  in presence of  $\text{NH}_4\text{OAc}$  and this evidence led to the finding that whenever copper salts are used as a catalyst for the synthesis of 2,4,5-triarylimidazole derivatives in presence of ammonium acetate, these salts are readily converted into copper acetate dihydrate in the reaction mixture.

**Chapter-III Section-C** of the thesis includes the theoretical studies and calculations like DFT, Molecular Docking, Non-linear Optical Properties and Pharmacokinetic Studies of the selected 2,4,5 triaryl imidazole derivatives. From DFT studies, the optimized geometry of the compounds were determined along with some important properties like bond lengths, bond angles, dihedral angles. DFT studies also were used to find out some interesting parameters like the energies of HOMO, LUMO, the energy gap between the HOMO and LUMO and global chemical descriptors of the studied compounds. Molecular Docking studies of these compounds were carried out with insulin receptor protein (PDB ID: 1IR3) and the compounds showed a very good binding interaction with the protein. The pharmacokinetic properties like ADMET of these compounds were determined with the help of SwissADME database (<http://www.swissadme.ch>) and they showed no violation of Lipinski's rule thus qualifying the drug likeliness criteria.

In **Chapter-IV Section-A**, we were able to explore the catalytic efficiency of Iron Borate in the synthesis of 3,4-dihydropyrimidine-2-(1H)-ones (DHPMs) and the catalyst showed very good results with excellent yield of the products and the catalyst showed remarkable recyclability and could be used efficiently up to the 4<sup>th</sup> run of the reaction

In **Section-B of Chapter-IV**, theoretical studies of the selected 3,4-dihydropyrimidine-2-(1H)-one derivatives (DP-1 to DP-3) have been done. The theoretical approach included DFT, Molecular Docking Studies, Non-Linear Optical Properties and Pharmacokinetic studies. Some theoretical Parameters like energies of Frontier Molecular orbitals (HOMO and LUMO), their energy gaps, global chemical descriptors, bond lengths, bond angles, dihedral angles, etc. which are very important for the study of structure of the complexes were calculated with the help of DFT. The compounds also showed promising NLO properties when compared with reference material Urea. Finally molecular docking study of these compounds was done with the protein 3DH4 and the compounds showed good interaction with the receptor protein.

**Chapter-V Section A** of the thesis includes synthesis of 1-hydroxy-2-arylimidazole-3-oxide derivatives under solvent free condition using inexpensive Copper borate ( $\text{CuB}_4\text{O}_7$ ) catalyst. As we were unable to recover the catalyst Copper Borate in the reaction for the synthesis of 2,4,5-triaryl imidazoles as

discussed in Chapter-I, it was again attempted to use copper borate as catalyst in yet another famous organic reaction for the synthesis of 1-hydroxy-2-arylimidazole-3-oxides under solvent free conditions and in this case, we were able to recover the catalyst successfully and the catalyst did not lose its efficiency up to 5<sup>th</sup> run of the reaction.

**Chapter-V Section-B** of the thesis includes the theoretical studies and calculations like DFT, Molecular Docking, Non-linear Optical Properties and Pharmacokinetic Studies of the selected and 1-hydroxy-2-arylimidazole-3-oxide derivatives. From the optimized geometry of these studied compounds various parameters like Bond length, Bond angles, energies of HOMO, LUMO and the energy gap between them, theoretical FT-IR vibrational frequencies, NLO properties, global chemical descriptors and MESP were calculated. The experimentally observed FT-spectra matched well with the theoretical FT-IR spectra for all the compounds under study. For Molecular Docking studies, the crystal structure of the protein 3ERT was downloaded from the Protein Data Bank (PDB). All the selected compounds under study showed good binding interactions with the chosen protein. For analyzing the drug likeliness of the selected compounds, their ADMET properties were also determined from online SwissADME database (<http://www.swissadme.ch>) and in no case any violation of Lipinski's Rule was observed.

Finally in **Chapter-VI** of the thesis, solvent free green synthesis of 2-substituted benzimidazole and 1, 2-disubstituted benzimidazole derivatives is reported using Nickel Borate as an efficient catalyst. The catalyst was found to be an efficient and versatile for the synthesis of the above-mentioned derivatives under green chemical condition. This process is advantageous due to its simple operational procedure and easy work-up of the product with minimal use of the hazardous solvent.

In Conclusion, we have been able to explore the catalytic activity of Copper Borate, Iron Borate and Nickel Borate in some solvent free multicomponent green reactions and thus we were able to prepare some very important Nitrogen Containing Heterocyclic Compounds like 2,4,5-triaryl imidazoles, 3,4-dihydropyrimidine-2-(1H)-ones, 1-hydroxy-2-arylimidazole-3-oxides, 2-substituted and 1, 2-disubstituted benzimidazoles in good yields. The borates that have been studied in this work have shown promising catalytic efficiency. Yet there are lot of other transition metal borates whose catalytic activity needs to be explored and in future more works in this field is highly expected.

## APPENDIX-I

### Supplementary spectra of Chapter III Section-A

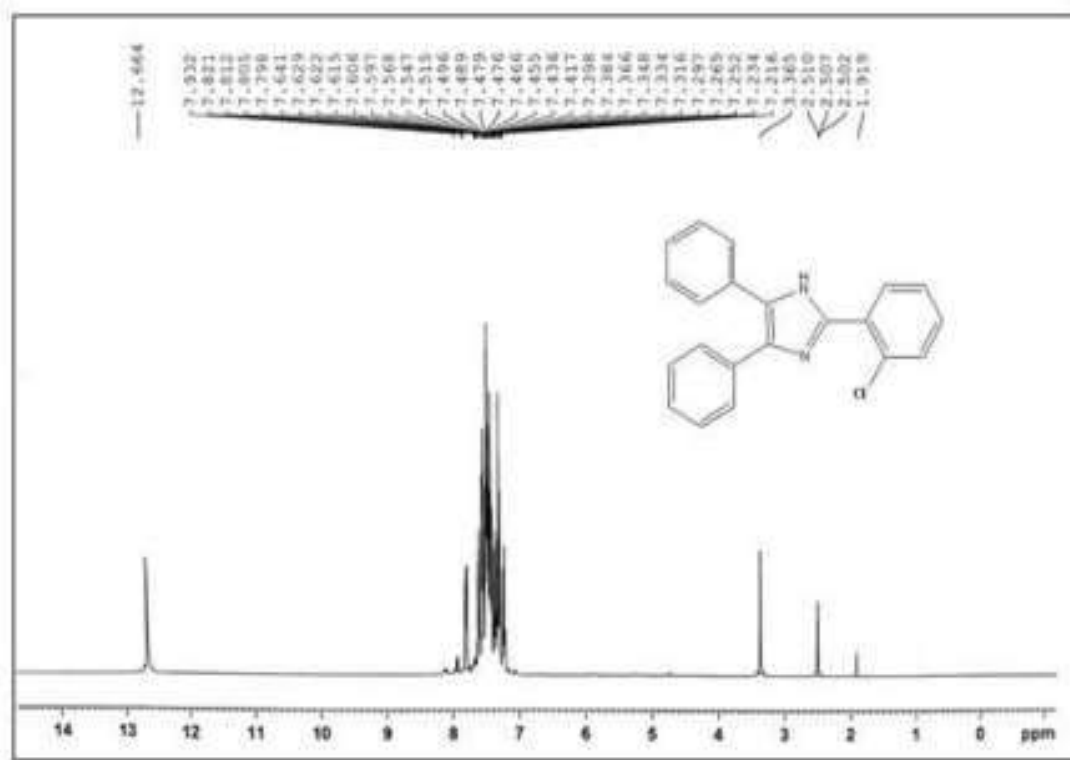


Fig. S. 3A.1. <sup>1</sup>H NMR spectra of 2-(2-chlorophenyl)-4,5-diphenyl-1H-imidazole (4e)

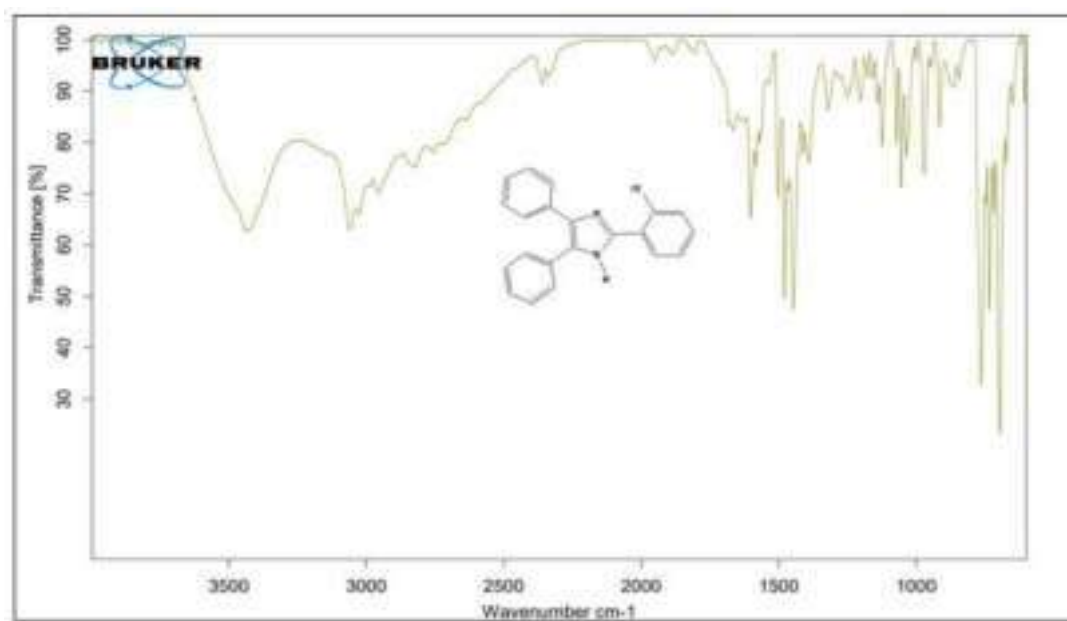
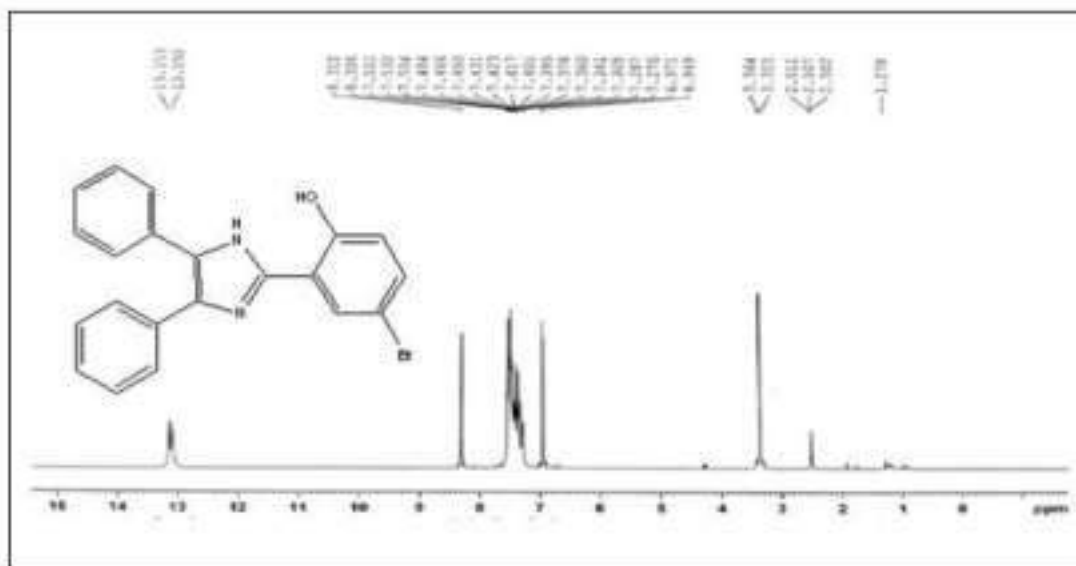
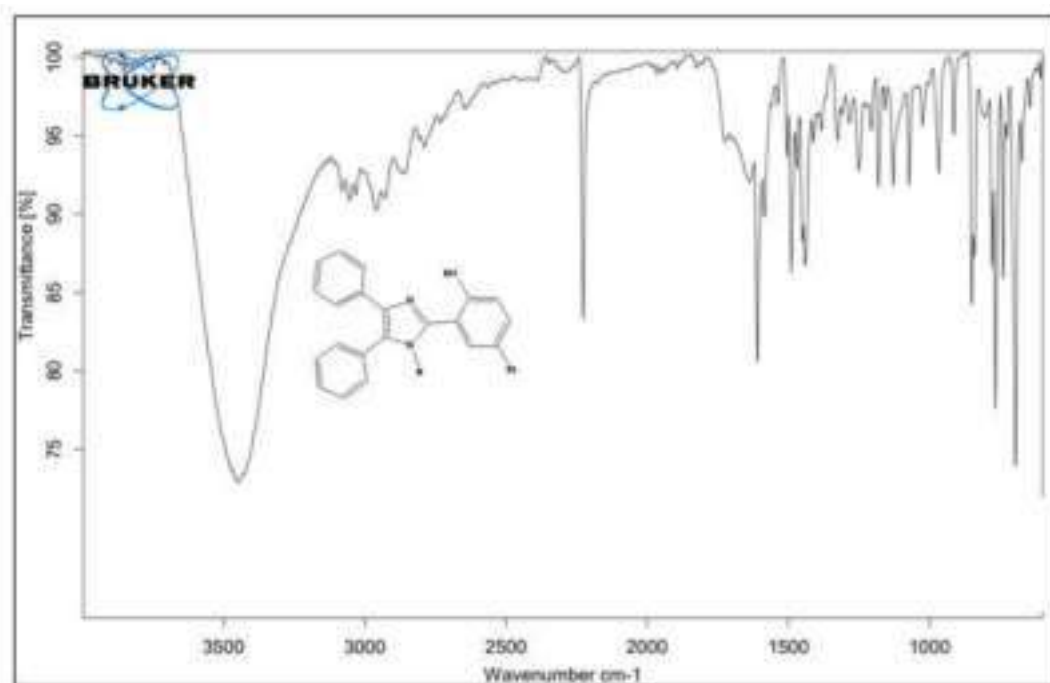


Fig. S. 3A.2. FT-IR spectra of 2-(2-chlorophenyl)-4,5-diphenyl-1H-imidazole (4e)



**Fig. S. 3A.3.** <sup>1</sup>H NMR spectra of 4-bromo-2-(4,5-diphenyl-1H-imidazol-2-yl)phenol (4m)



**Fig. S. 3A.4.** FT-IR spectra of 4-bromo-2-(4,5-diphenyl-1H-imidazol-2-yl)phenol (4m)

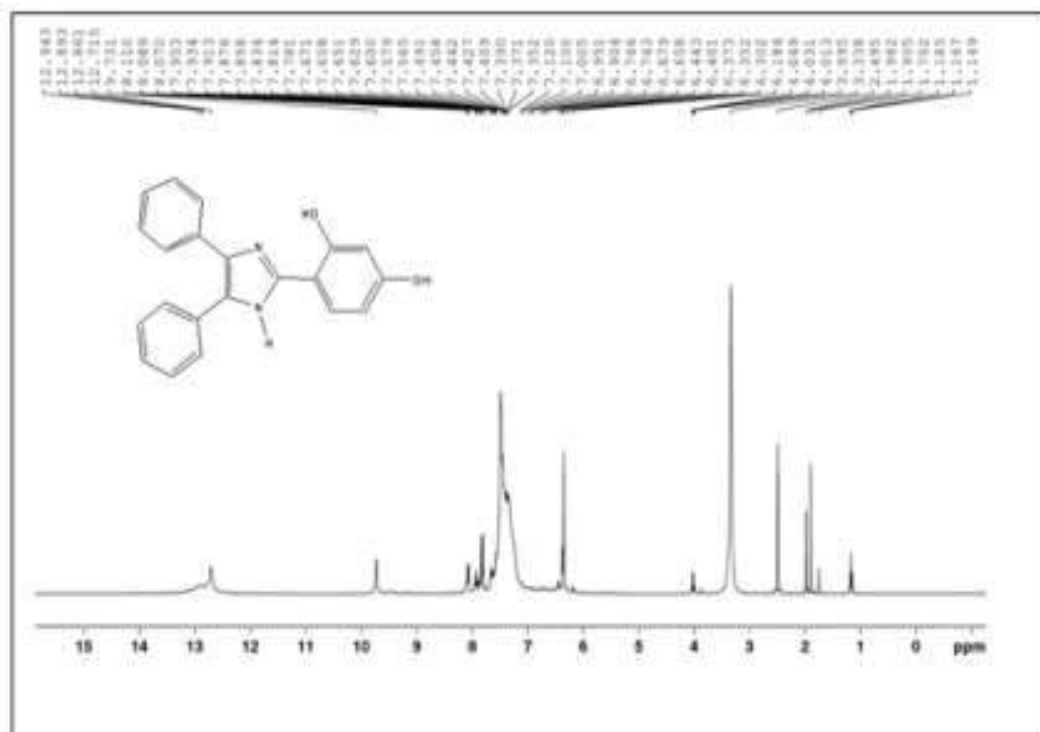


Fig. S. 3A.5.  $^1\text{H}$  NMR spectra of 4-(4,5-diphenyl-1H-imidazol-2-yl)benzene-1,3-diol (4o)

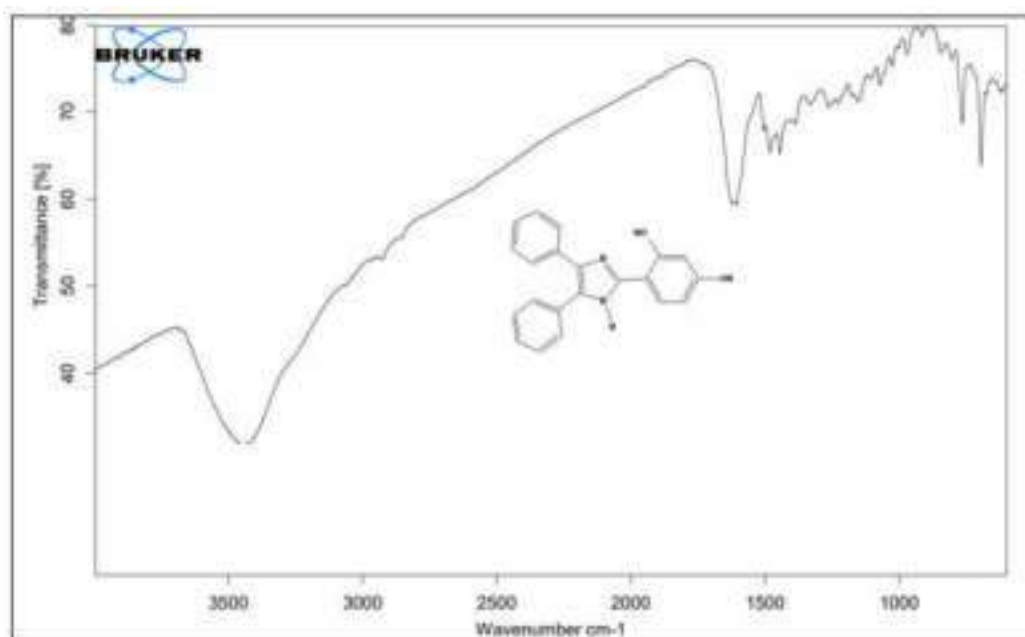


Fig. S. 3A.6. FT-IR spectra of 4-(4,5-diphenyl-1H-imidazol-2-yl)benzene-1,3-diol (4o)



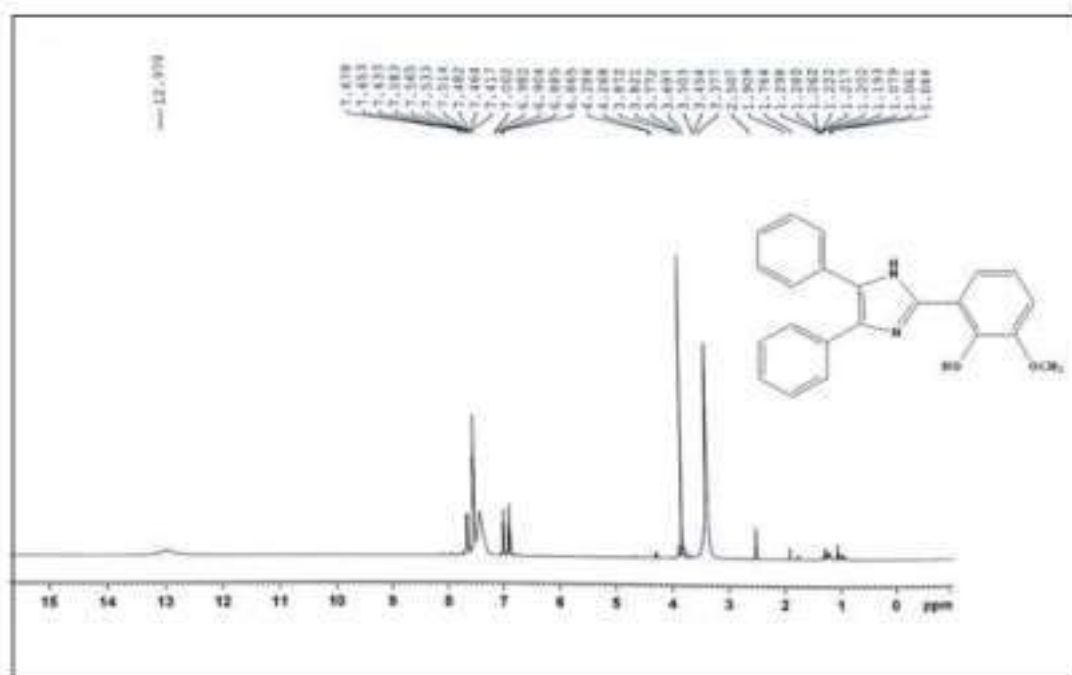


Fig. S. 3A.7. <sup>1</sup>H NMR spectra of 2-methoxy-6-(4,5-diphenyl-1H-imidazol-2-yl)phenol (4p)

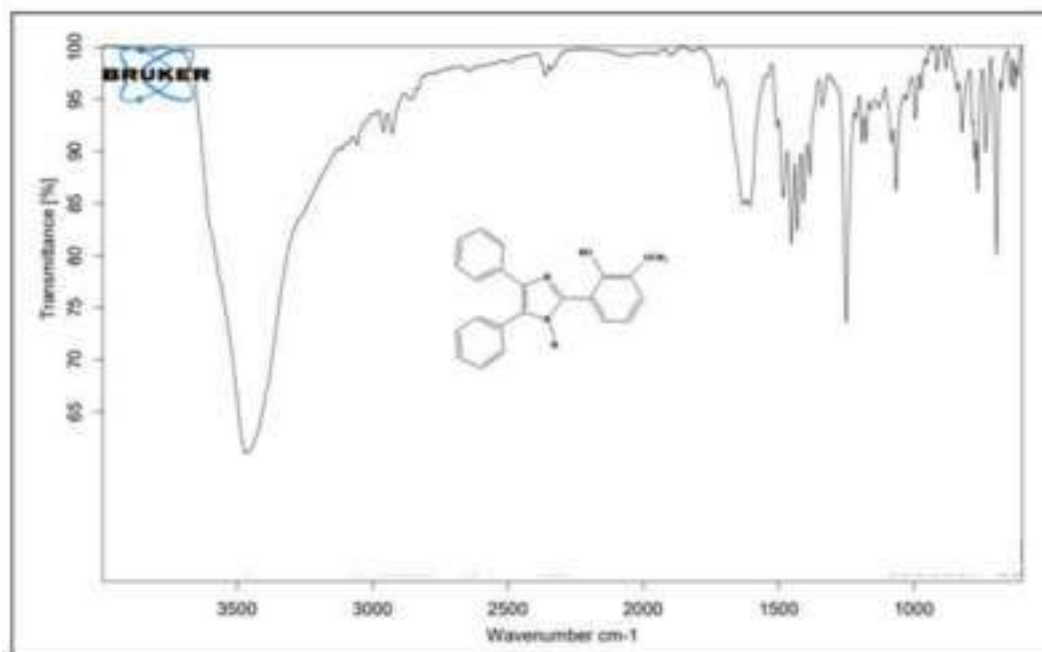
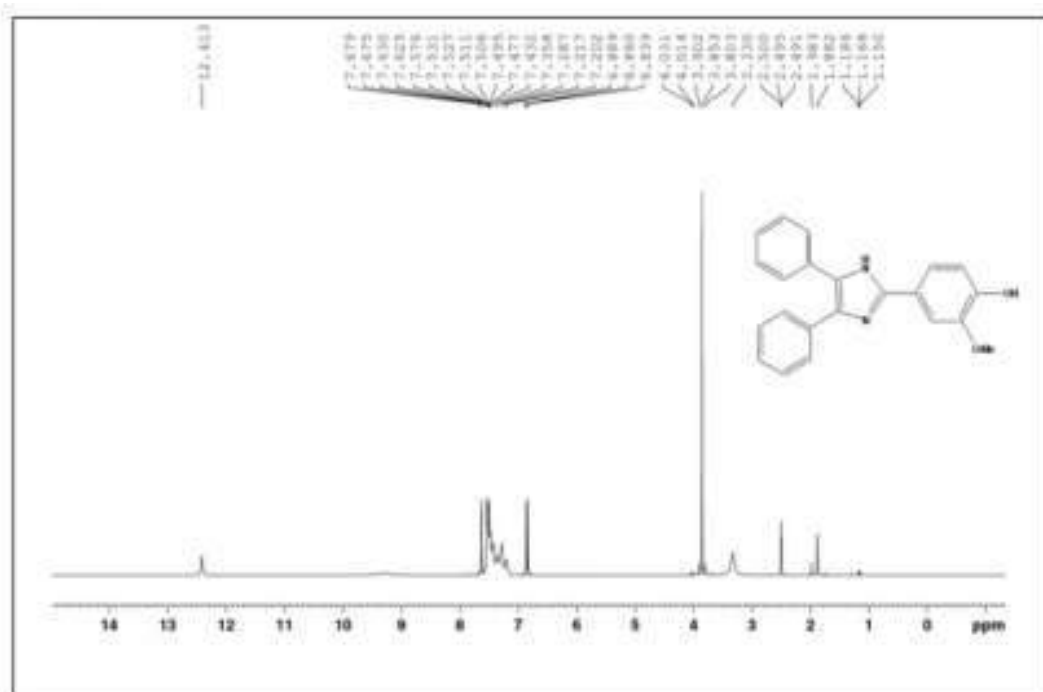
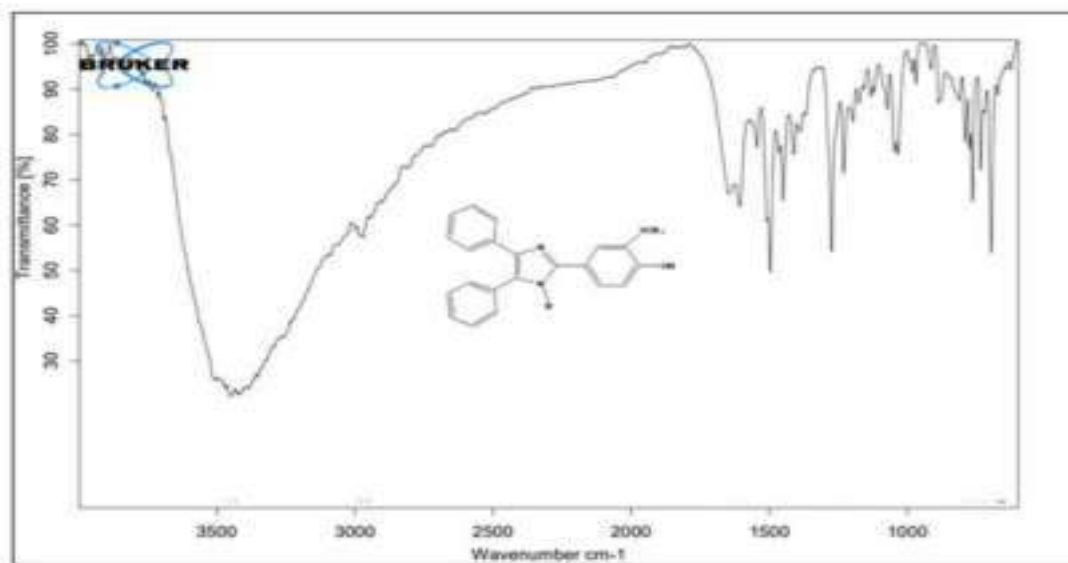


Fig. S. 3A.8. FT-IR spectra of 2-methoxy-6-(4,5-diphenyl-1H-imidazol-2-yl)phenol (4p)



**Fig. S. 3A.9.**  $^1\text{H}$  NMR spectra of 4-(4,5-diphenyl-1H-imidazol-2-yl)-2-methoxyphenol (4q)



**Fig. S. 3A.10.** FT-IR spectra of 4-(4,5-diphenyl-1H-imidazol-2-yl)-2-methoxyphenol (4q)

## APPENDIX-II

### List of Publications

1. Bis[2-(4,5-Diphenyl-1 H -Imidazol-2-Yl)-4-Nitrophenolato]Copper(II) Dihydrate: Crystal Structure and Hirshfeld Surface Analysis., **Sailesh Chettri**, Dhiraj Brahman, Biswajit Sinha, Mukesh.M.Jotani and Edward R.T.Tiekink *Acta Crystallographica Section E Crystallographic Communications* **2019**, **75 (11)**, **1664–1671**.
2. Exploration of Inhibitory Action of Azo Imidazole Derivatives against COVID-19 Main Protease (Mpro): A Computational Study., Abhijit Chhetri, **Sailesh Chettri**, Pranesh Rai, Biswajit Sinha and Dhiraj Brahman *Journal of Molecular Structure* **2021**, **1224**, **129178**.
3. Synthesis, Characterization and Computational Study on Potential Inhibitory Action of Novel Azo Imidazole Derivatives against COVID-19 Main Protease (Mpro: 6LU7)., Abhijit Chhetri, **Sailesh Chettri**, Pranesh Rai, Dipu Kumar Mishra, Biswajit Sinha and Dhiraj Brahman *Journal of Molecular Structure* **2021**, **1225**, **129230**.
4. Environmentally Benign Approach towards C–S Cross-Coupling Reaction by Organo-Copper(II) Complex., Rabindranath Singha, **Sailesh Chettri**, Dhiraj Brahman, Biswajit Sinha and Pranab Ghosh *Molecular Diversity*, **2022**, **26 (1)**, **505–511**.
5. [Diaquo{bis(p-hydroxybenzoato-κ1O1)}(1-methylimidazole-κ1N1)}copper(II)]: Synthesis, crystal structure, catalytic activity and DFT study., Amarjit Kamath, Dhiraj Brahman, **Sailesh Chettri**, Patrick McArdle and Biswajit Sinha *Journal of Molecular Structure* **2022**, **1247**, **131323**.

## APPENDIX-III

### List of Communicated Articles

1. Copper Borate ( $\text{CuB}_4\text{O}_7$ ) catalyzed multi-component green synthesis of 2,4,5 Tri-aryl imidazole derivatives and evidence of In-situ conversion of Copper Borate to Copper Acetate in presence of  $\text{NH}_4\text{OAc}$ . **(Communicated)**
2. DFT, Molecular Docking and Pharmacokinetic study of some selected 2, 4, 5-Tri-arylimidazole derivatives. **(Communicated)**
3. Synthesis, DFT, Molecular Docking and Pharmacokinetic study of some selected 3, 4-dihydropyrimidin-2(1H)-one (DHPM) derivatives. **(Communicated)**
4. Synthesis, DFT, Molecular Docking and Pharmacokinetic study of some selected 1- hydroxy-2-arylimidazole-3-oxide derivatives. **(Communicated)**

## APPENDIX-IV

### List of Seminars, Webinars, Symposiums and Conferences

#### Attended

1. National Seminar on “Frontiers in Chemistry-2019” organized by the Department of Chemistry, University of North Bengal, Darjeeling and CRSI North Bengal Local Chapter on 22<sup>nd</sup> May 2019.
2. International Seminar on the “International Year of the Periodic Table of Chemical Elements-2019” organized by the Department of Chemistry, University of North Bengal, Darjeeling on 22-23<sup>rd</sup> November 2019. **(Presented a Poster and got the award for One of the Best Poster Presentations).**
3. National Seminar on “Frontiers in Chemistry-2020” organized by the Department of Chemistry, University of North Bengal on 5<sup>th</sup> March 2020. **(Presented a Poster)**
4. National Seminar on “Material Chemistry-Today & Tomorrow” organized by the Indian Chemical Society, Kolkata & Department of Chemistry, Jadavpur University, Kolkata on 28<sup>th</sup> February – 1<sup>st</sup> March 2021. **(Presented a Poster).**
5. Interdisciplinary International Web Seminar on “Modern Trends in Humanities, Science & Technology and Social Sciences for Sustainable Development” organized by A.P.C. Roy Govt. College, Siliguri in collaboration with UGC-Human Resource Development Centre, University of North Bengal, Darjeeling on 23<sup>rd</sup> – 24<sup>th</sup> September 2021. **(Presented an oral presentation).**

## **BIBLIOGRAPHY**

- (1) X. Zhang, A. S. Shetty, S. A. Jenekhe., *Macromolecules*, **1999**, 32 (22), 7422–7429.
- (2) X. Wu, M. Li, Y. Qu, W. Tang, Y. Zheng, J. Lian, M. Ji, L. Xu., *Bioorganic & Medicinal Chemistry*, **2010**, 18 (11), 3812–3822.
- (3) I. M. El-Deeb, S. H. Lee., *Bioorganic & Medicinal Chemistry*, **2010**, 18 (11), 3860–3874.
- (4) O. O. Ajani, C. A. Obafemi, O. C. Nwinyi, D. A. Akinpelu., *Bioorganic & Medicinal Chemistry*, **2010**, 18 (1), 214–221.
- (5) M. M. Heravi, V. Zadsirjan., *RSC Advances*, **2020**, 10 (72), 44247–44311.
- (6) P. M. T. Ferreira, H. L. S. Maia, L. S. Monteiro., *Tetrahedron Letters*, **2002**, 43 (25), 4491–4493.
- (7) G. Daidone, B. Maggio, D. Schillaci., *Pharmazie*, **1990**, 45 (14), 441–442.
- (8) L. Gylbert., *Acta Crystallographica Section B Structural Crystallography and Crystal Chemistry*, **1973**, 29 (8), 1630–1635.
- (9) M. E. Prommer., *Journal of Opioid Management*, **2011**, 7 (5), 401–406.
- (10) H. Hotti, H. Rischer., *Molecules*, **2017**, 22 (11), 1962.
- (11) D. J. Sutor., *Acta Crystallographica*, **1958**, 11 (7), 453–458.
- (12) M. v. Djordjevic, K. D. Brunnemann, D. Hoffmann., *Carcinogenesis*, **1989**, 10 (9), 1725–1731.
- (13) M. Srivastava, J. Singh, S. B. Singh, K. Tiwari, V. K. Pathak, J. Singh., *Green Chemistry*, **2012**, 14 (4), 901–905.
- (14) D. Yang, B. An, W. Wei, L. Tian, B. Huang, H. Wang., *ACS Combinatorial Science*, **2015**, 17 (2), 113–119.
- (15) S. Shoja Shafti, M. Gilanipoor., *Schizophrenia Research and Treatment*, **2014**, 2014 (1), 1–5.
- (16) C. P. Tătaru, V. L. Purcărea., *J Med Life*, **2012**, 5 (3), 247–251.
- (17) C. le Tourneau, E. Raymond, S. Faivre., *Therapeutics and Clinical Risk Management*, **2007**, 3 (2), 341–348.
- (18) L. R. Wiseman, J. C. Adkins., *Drugs & Aging*, **1998**, 13 (4), 321–332.

- (19) J. W. Wheless, B. Vazquez., *Epilepsy Currents*, **2010**, *10* (1), 1–6.
- (20) N. Kerru, L. Gummidi, S. Maddila, K. K. Gangu, S. B. Jonnalagadda., *Molecules*, **2020**, *25* (8), 1909.
- (21) R. Kaur, S. Chaudhary, K. Kumar, M. K. Gupta, R. K. Rawal., *European Journal of Medicinal Chemistry*, **2017**, *132*, 108–134.
- (22) E. Vitaku, D. T. Smith, J. T. Njardarson., *Journal of Medicinal Chemistry*, **2014**, *57* (24), 10257–10274.
- (23) W.-Y. Fang, L. Ravindar, K. P. Rakesh, H. M. Manukumar, C. S. Shantharam, N. S. Alharbi, H.-L. Qin., *European Journal of Medicinal Chemistry*, **2019**, *173*, 117–153.
- (24) N. Kerru, A. Singh-Pillay, P. Awolade, P. Singh., *European Journal of Medicinal Chemistry*, **2018**, *152*, 436–488.
- (25) B. R. Smith, C. M. Eastman, J. T. Njardarson., *Journal of Medicinal Chemistry*, **2014**, *57* (23), 9764–9773.
- (26) S. A. Jenekhe, L. Lu, M. M. Alam., *Macromolecules*, **2001**, *34* (21), 7315–7324.
- (27) M. Balasubramanian, JG. Keay., *Comprehensive Heterocyclic Chemistry II*, 1st ed.; Oxford : New York [Pergamon Press], **1996**; Vol. 5.
- (28) J. P. Michael., *Natural Product Reports*, **1997**, *14* (6), 605–618.
- (29) G.-W. Wang, C.-S. Jia, Y.-W. Dong., *Tetrahedron Letters*, **2006**, *47* (7), 1059–1063.
- (30) A. R. Katritzky., *Handbook of Heterocyclic Chemistry*, 1st ed.; Oxford [Oxfordshire]: New York [Pergamon Press], **1985**.
- (31) C. T. Walsh., *Tetrahedron Letters*, **2015**, *56* (23), 3075–3081.
- (32) B. Zhang, A. Studer., *Chemical Society Reviews*, **2015**, *44* (11), 3505–3521.
- (33) R. Gaynes., *Emerging Infectious Diseases*, **2017**, *23* (5), 849–853.
- (34) N. Das, J. Madhavan, A. Selvi, D. Das., *3 Biotech*, **2019**, *9* (6), 231.
- (35) R. Aviner., *Comput Struct Biotechnol J*, **2020**, *18*, 1074–1083.
- (36) M. S. Saini, A. Kumar, J. Dwivedi, R. Singh., *International Journal of Pharma Sciences and Research*, **2013**, *4* (3), 66–77.
- (37) E. M. Flefel, W. I. El-Sofany, R. A. K. Al-Harbi, M. El-Shahat., *Molecules*, **2019**, *24* (13), 2511.

- (38) A. K. Dhingra, B. Chopra, J. S. Dua, D. N. Prasad., *Anti-Inflammatory & Anti-Allergy Agents in Medicinal Chemistry*, **2017**, *16* (3), 136–152.
- (39) N. Siddiqui, Andalip, S. Bawa, R. Ali, O. Afzal, M. Akhtar, B. Azad, R. Kumar., *Journal of Pharmacy And Bioallied Sciences*, **2011**, *3* (2), 194–212.
- (40) D. K. Lang, R. Kaur, R. Arora, B. Saini, S. Arora., *Anticancer Agents Med Chem*, **2020**, *20* (18), 2150–2168.
- (41) P. N. Kalaria, S. C. Karad, D. K. Raval., *Eur J Med Chem*, **2018**, *158*, 917–936.
- (42) T. K. Venkatachalam, E. A. Sudbeck, C. Mao, F. M. Uckun., *Bioorganic & Medicinal Chemistry Letters*, **2001**, *11* (4), 523–528.
- (43) A. H. M. Hussein, A. B. A. El-Adasy, A. M. El-Saghier, M. Olish, A. H. Abdelmonsef., *RSC Advances*, **2022**, *12* (20), 12607–12621.
- (44) N. B. Patel, H. R. Patel., *Indian Journal of Pharmaceutical Sciences*, **2010**, *72* (5), 620.
- (45) A. De, S. Sarkar, A. Majee., *Chem Heterocycl Compd (N Y)*, **2021**, *57* (4), 410–416.
- (46) D. Ma, Y. Yin, Y. L. Chen, Y. T. Yan, J. Wu., *RSC Advances*, **2021**, *11* (25), 15380–15386.
- (47) E. A. Ghareeb, N. F. H. Mahmoud, E. A. El-Bordany, E. A. E. El-Helw., *Bioorganic Chemistry*, **2021**, *112*.
- (48) A. P. Taylor, R. P. Robinson, Y. M. Fobian, D. C. Blakemore, L. H. Jones, O. Fadeyi., *Organic & Biomolecular Chemistry*, **2016**, *14* (28), 6611–6637.
- (49) W. Guo, M. Zhao, W. Tan, L. Zheng, K. Tao, X. Fan., *Organic Chemistry Frontiers*, **2019**, *6* (13), 2120–2141.
- (50) X. Chen, H. Yang, M. J. Hülsey, N. Yan., *ACS Sustainable Chemistry and Engineering*, **2017**, *5* (11), 11096–11104.
- (51) L. A. Aronica, G. Albano., *Catalysts*, **2022**, *12* (1), 68.
- (52) M. Henary, C. Kananda, L. Rotolo, B. Savino, E. A. Owens, G. Cravotto., *RSC Advances*, **2020**, *10* (24), 14170–14197.
- (53) I. K. Moiseev, M. N. Zemtsova, N. V. Makarova., *Chemistry of Heterocyclic Compounds*, **1994**, *30* (7), 745–761.
- (54) E. Chainikova, R. Safiullin, L. Spirikhin, A. Erastov., *Tetrahedron Letters*, **2013**, *54* (17), 2140–2142.



- (55) B. Lai, M. Ye, P. Liu, M. Li, R. Bai, Y. Gu., *Beilstein Journal of Organic Chemistry* 16:238, **2020**, 16 (1), 2888–2902.
- (56) R. Hili, A. K. Yudin., *Nat Chem Biol*, **2006**, 2 (6), 284–287.
- (57) J. Bariwal, E. van der Eycken., *Chemical Society Reviews*, **2013**, 42 (24), 9283–9303.
- (58) P. T. Anastas, J. C. Warner., *Green Chemistry: Theory and Practice*, 1st ed.; Oxford University Press, **1998**.
- (59) J. C. Warner, A. S. Cannon, K. M. Dye., *Environmental Impact Assessment Review*, **2004**, 24 (7–8), 775–799.
- (60) P. Anastas, N. Eghbali., *Chemical Society Reviews*, **2009**, 39 (1), 301–312.
- (61) P. T. Anastas., *Critical Reviews in Analytical Chemistry*, **2010**, 29 (3), 167–175.
- (62) A. M. Sanseverino., *Química Nova (New Chem.)*, **2000**, 23 (1), 102–107.
- (63) M. de La Guardia, S. Armenta., *Analytical and Bioanalytical Chemistry*, **2012**, 404 (3), 625–626.
- (64) E. J. Lenardão, R. A. Freitag, M. J. Dabdoub, A. C. Ferreira Batista, C. da Cruz Silveira., *Química Nova (New Chem.)*, **2003**, 26 (1), 123–129.
- (65) B. M. Trost., *Angewandte Chemie International Edition in English*, **1995**, 34 (3), 259–281.
- (66) R. A. Sheldon., *Pure and Applied Chemistry*, **2000**, 72 (7), 1233–1246.
- (67) P. Poehlauer, J. Manley, R. Broxterman, B. Gregertsen, M. Ridemark., *Organic Process Research and Development*, **2012**, 16 (10), 1586–1590.
- (68) M. Poliakoff, P. Licence., *Nature*, **2007**, 450 (7171), 810–812.
- (69) F. R. Nolasco, G. A. Tavares, J. A. Bendassolli., *Engenharia Sanitaria e Ambiental (Sanitary and Environmental Engineering)*, **2006**, 11 (2), 118–124.
- (70) A. de La Hoz, A. Díaz-Ortiz, P. Prieto., *Alternative Energy Sources for Green Chemistry. Chapter 1 - Microwave-Assisted Green Organic Synthesis*; pp. 1-33; The Royal Society of Chemistry, **2016**.
- (71) S. Tagliapietra, E. Calcio Gaudino, G. Cravotto., *Power Ultrasonics. Chapter 33 - The Use of Power Ultrasound for Organic Synthesis in Green Chemistry*; pp. 997–1022; Woodhead Publishing: Oxford, **2015**.
- (72) K. Tanaka, F. Toda., *Chemical Reviews*, **2000**, 100 (3), 1025–1074.

- (73) D. Friedmann, A. Hakki, H. Kim, W. Choi, D. Bahnemann., *Green Chemistry*, **2016**, *18* (20), 5391–5411.
- (74) Udayabhanu, H. Nagabhushana, D. Suresh, H. Rajanaika, S. C. Sharma, G. Nagaraju., *Materials Today: Proceedings*, **2017**, *4* (11), 11888–11893.
- (75) R. S. Varma., *ACS Sustainable Chemistry and Engineering*, **2016**, *4* (11), 5866–5878.
- (76) M. Jug, P. A. Mura., *Pharmaceutics*, **2018**, *10* (4), 189.
- (77) C. C. Piras, S. Fernández-Prieto, W. M. de Borggraeve., *Nanoscale Advances*, **2019**, *1* (3), 937–947.
- (78) A. Pettignano, A. Charlot, E. Fleury., *Polymers (Basel)*, **2019**, *11* (7), 1227.
- (79) G. K. Verma, K. Raghuvanshi, R. K. Verma, P. Dwivedi, M. S. Singh., *Tetrahedron*, **2011**, *67* (20), 3698–3704.
- (80) K. Tanaka., *Organic Process Research & Development*, **2003**, *7* (4), 612–612.
- (81) G. R. Desiraju., *Organic Solid State Chemistry*; Elsevier: Amsterdam; New York, **1987**; Vol. 32.
- (82) F. Wöhler., *Ann Phys*, **1828**, *88* (2), 253–256.
- (83) F. Toda, M. Yagi, K. Kiyoshige., *Journal of the Chemical Society, Chemical Communications*, **1988**, *14*, 958–959.
- (84) L. Claisen., *Berichte der deutschen chemischen Gesellschaft*, **1912**, *45* (3), 3157–3166.
- (85) B. S. Goud, K. Panneerselvam, D. E. Zacharias, G. R. Desiraju., *Journal of the Chemical Society, Perkin Transactions 2*, **1995**, No. 2, 325–330.
- (86) C. L. Raston, J. L. Scott., *Green Chemistry*, **2000**, *2* (2), 49–52.
- (87) K. Tanaka, T. Sugino, F. Toda., *Green Chemistry*, **2000**, *2* (6), 303–304.
- (88) K. Yoshizawa, S. Toyota, F. Toda., *Green Chemistry*, **2002**, *4* (1), 68–70.
- (89) D. C. Waddell, J. Mack., *Green Chemistry*, **2009**, *11* (1), 79–82.
- (90) X. Ma, Y. Zhou, J. Zhang, A. Zhu, T. Jiang, B. Han., *Green Chemistry*, **2008**, *10* (1), 59–66.
- (91) F. Toda, K. Tanaka, K. Hamai., *Journal of the Chemical Society, Perkin Transactions 1*, **1990**, No. 11, 3207–3209.
- (92) S. B. Zangade, S. S. Mokle, A. T. Shinde, Y. B. Vibhute., *Green Chemistry Letters and Reviews*, **2013**, *6* (2), 123–127.

- (93) J. M. Thomas, W. J. Thomas., *Principles and Practice of Heterogeneous Catalysis*, 1st ed.; Wiley-VCH: Weinheim, **1996**.
- (94) G. Nagendrappa., *Resonance* , **2002**, 7 (10), 59–68.
- (95) Z. Kibou, N. Cheikh, N. Choukchou-Braham, B. Mostefa-Kara, M. Benabdellah, D. Villemin., *Scientific Study & Research - Chemistry & Chemical Engineering, Biotechnology, Food Industry*, **2011**, 12 (2), 121–126.
- (96) S. Tu, B. Jiang, Y. Zhang, R. Jia, J. Zhang, C. Yao, F. Shi., *Organic & Biomolecular Chemistry*, **2007**, 5 (2), 355–359.
- (97) M. S Al-Ajely, A. M. Noori., *Biomedical Journal of Scientific & Technical Research*, **2020**, 29 (3), 22510–22516.
- (98) R. R. Wani, H. K. Chaudhari, B. S. Takale., *Journal of Heterocyclic Chemistry*, **2019**, 56 (4), 1337–1340.
- (99) V. Bhardwaj, D. Gumber, V. Abbot, S. Dhiman, P. Sharma., *RSC Advances*, **2015**, 5 (20), 15233–15266.
- (100) P. N. Rakendu, T. Aneeraja, G. Anilkumar., *Asian Journal of Organic Chemistry*, **2021**, 10 (9), 2318–2333.
- (101) C. K. Belwal, J. Patel., *Asian Journal of Green Chemistry*, **2019**, 3 (4), 483–491.
- (102) Y. L. N. Murthy, A. Rajack, K. Yuvaraj., *Arabian Journal of Chemistry*, **2016**, 9, S1740–S1746.
- (103) S. Yan, Y. Chen, L. Liu, N. He, J. Lin., *Green Chemistry*, **2010**, 12 (11), 2043–2052.
- (104) C. S. Jia, Y. W. Dong, S. J. Tu, G. W. Wang., *Tetrahedron*, **2007**, 63 (4), 892–897.
- (105) D. Kong, X. Wang, Z. Shi, M. Wu, Q. Lin, X. Wang., *Journal of Chemical Research*, **2016**, 40 (9), 529–531.
- (106) S. Martínez González, A. I. Hernández, C. Varela, S. Rodríguez-Aristegui, R. M. Alvarez, A. B. García, M. Lorenzo, V. Rivero, J. Oyarzabal, O. Rabal, J. R. Bischoff, M. Albarrán, A. Cebriá, P. Alfonso, W. Link, J. Fominaya, J. Pastor., *Bioorganic & Medicinal Chemistry Letters*, **2012**, 22 (5), 1874–1878.
- (107) P. H. Tran, T. P. Thi Bui, X. Q. Bach Lam, X. T. Thi Nguyen., *RSC Advances*, **2018**, 8 (63), 36392–36399.
- (108) E. A. Tiong, D. Rivalti, B. M. Williams, J. L. Gleason, E. A. Tiong, D. Rivalti, B. M. Williams, J. L. Gleason., *Angewandte Chemie International Edition*, **2013**, 52 (12), 3442–3445.

- (109) P. T. Anastas, J. B. Zimmerman., *Environmental Science & Technology*, **2003**, 37 (5), 94A-101A.
- (110) P. T. Anastas, E. S. Beach., *Green Chemistry Letters and Reviews*, **2008**, 1 (1), 9–24.
- (111) R. W. Armstrong, A. P. Combs, P. A. Tempest, S. D. Brown, T. A. Keating., *Accounts of Chemical Research*, **1996**, 29 (3), 123–131.
- (112) H. A. Younus, M. Al-Rashida, A. Hameed, M. Uroos, U. Salar, S. Rana, K. M. Khan., *Expert Opinion on Therapeutic Patents*, **2020**, 31 (3), 267–289.
- (113) B. A. D. Neto, R. O. Rocha, M. O. Rodrigues., *Molecules* , **2022**, 27 (1), 132.
- (114) Y. Volkova, S. Baranin, I. Zavarzin., *Advanced Synthesis & Catalysis*, **2021**, 363 (1), 40–61.
- (115) S. Siahrostami, S. J. Villegas, A. H. Bagherzadeh Mostaghimi, S. Back, A. B. Farimani, H. Wang, K. A. Persson, J. Montoya., *ACS Catalysis*, **2020**, 10 (14), 7495–7511.
- (116) L. Biesen, T. J. J. Müller., *Advanced Synthesis & Catalysis*, **2021**, 363 (4), 980–1006.
- (117) B. B. Touré, D. G. Hall., *Chemical Reviews*, **2009**, 109 (9), 4439–4486.
- (118) J. Zhu, H. Bienaymé., *Multicomponent Reactions*, 1st ed.; Wiley-VCH: Weinheim, Germany, **2005**.
- (119) L. F. Tietze., *Chemical Reviews*, **1996**, 96 (1), 115–136.
- (120) S. E. John, S. Gulati, N. Shankaraiah., *Organic Chemistry Frontiers*, **2021**, 8 (15), 4237–4287.
- (121) L. Biesen, T. J. J. Müller., *Advanced Synthesis & Catalysis*, **2021**, 363 (4), 980–1006.
- (122) M. Mamaghani, R. Hossein Nia., *Polycyclic Aromatic Compounds*, **2021**, 41 (2), 223–291.
- (123) A. Strecker., *Justus Liebigs Ann Chem*, **1850**, 75 (1), 27–45.
- (124) H. Debus., *Justus Liebigs Ann Chem*, **1858**, 107 (2), 199–208.
- (125) B. Radziszewski., *Berichte der deutschen chemischen Gesellschaft*, **1882**, 15 (2), 1493–1496.
- (126) B. Radziszewski., *Berichte der deutschen chemischen Gesellschaft*, **1882**, 15 (2), 2706–2708.

- (127) A. Hantzsch., *Berichte der deutschen chemischen Gesellschaft*, **1881**, 14 (2), 1637–1638.
- (128) A. Hantzsch., *Berichte der deutschen chemischen Gesellschaft*, **1890**, 23 (1), 1474–1476.
- (129) P. Biginelli., *Berichte der deutschen chemischen Gesellschaft*, **1891**, 24 (2), 2962–2967.
- (130) C. Mannich, W. Krösche., *Arch Pharm (Weinheim)*, **1912**, 250 (1), 647–667.
- (131) R. Robinson., *Journal of the Chemical Society, Transactions*, **1917**, 111 (0), 762–768.
- (132) H. T. Bucherer, H. T. Fischbeck., *J. Prakt. Chem*, **1934**, 140, 69–89.
- (133) F. Asinger., *Angewandte Chemie*, **1956**, 68 (12), 413–413.
- (134) I. Ugi, C. Steinbrückner., *Angewandte Chemie*, **1960**, 72 (7–8), 267–268.
- (135) L. S. Povarov., *Russian Chemical Reviews*, **1965**, 34 (9), 639–656.
- (136) K. Gewald, E. Schinke, H. Böttcher., *Chem Ber*, **1966**, 99 (1), 94–100.
- (137) “The academic pursuit of screening”, *Nature Chemical Biology*, **2007**, 3 (8), 433–433.
- (138) N. A. Petasis, I. Akritopoulou., *Tetrahedron Letters*, **1993**, 34 (4), 583–586.
- (139) J. E. Biggs-Houck, A. Younai, J. T. Shaw., *Curr Opin Chem Biol*, **2010**, 14 (3), 371–382.
- (140) Y. Chen, L. Li, X. He, Z. Li., *ACS Catalysis*, **2019**, 9 (10), 9098–9102.
- (141) H. Singh, J. Sindhu, J. M. Khurana, C. Sharma, K. R. Aneja, H. Singh, J. Sindhu, J. M. Khurana, C. Sharma, K. R. Aneja., *Australian Journal of Chemistry*, **2013**, 66 (9), 1088–1096.
- (142) M. Bararjanian, S. Balalaie, F. Rominger, B. Movassagh, H. R. Bijanzadeh., *The Journal of Organic Chemistry*, **2010**, 75 (9), 2806–2812.
- (143) S. Brauch, L. Gabriel, B. Westermann., *Chemical Communications*, **2010**, 46 (19), 3387–3389.
- (144) N. Elders, D. van der Born, L. J. D. Hendrickx, B. J. I. Timmer, A. Krause, E. Janssen, F. J. J. de Kanter, E. Ruijter, R. V. A. Orru., *Angewandte Chemie. International Edition*, **2009**, 48 (32), 5856–5859.
- (145) A. Dondoni, A. Massi., *Accounts of Chemical Research*, **2006**, 39 (7), 451–463.
- (146) M. S. Singh, S. Chowdhury., *RSC Advances*, **2012**, 2 (11), 4547–4592.

- (147) H. Eckert., *Molecules* 2012, Vol. 17, Pages 1074-1102, **2012**, 17 (1), 1074–1102.
- (148) A. Corma, H. García., *Chemical Reviews*, **2003**, 103 (11), 4307–4365.
- (149) B. Karimi, D. Zareyee., *Journal of Materials Chemistry*, **2009**, 19 (45), 8665–8670.
- (150) F. Bigi, S. Carloni, B. Frullanti, R. Maggi, G. Sartori., *Tetrahedron Letters*, **1999**, 40 (17), 3465–3468.
- (151) D. Koszelewski, W. Szymanski, J. Krysiak, R. Ostaszewski., *Synthetic Communications*, **2008**, 38 (7), 1120–1127.
- (152) L. el Kaïm, L. Gautier, L. Grimaud, L. M. Harwood, V. Michaut., *Green Chemistry*, **2003**, 5 (4), 477–479.
- (153) M. A. Zolfigol, E. Kolvari, A. Abdoli, M. Shiri., *Molecular Diversity*, **2010**, 14 (4), 809–813.
- (154) L. el Kaïm, L. Grimaud, S. Hadrot., *Tetrahedron Letters*, **2006**, 47 (23), 3945–3947.
- (155) K. Wang, D. Kim, A. Dömling., *Journal of Combinatorial Chemistry*, **2010**, 12 (1), 111–118.
- (156) P. Nun, J. Martinez, F. Lamaty., *Synthesis (Stuttg)*, **2010**, 2010 (12), 2063–2068.
- (157) J. Zimmermann, B. Ondruschka, A. Stark., *Organic Process Research and Development*, **2010**, 14 (5), 1102–1109.
- (158) J. G. Lombardino, E. H. Wiseman., *J Med Chem*, **1974**, 17 (11), 1182–1188.
- (159) A. R. Phillips, H. L. White, S. Rosen., European Patent Application EP 58 8901; Chemical Abstracts, 98, 53894z; **1982**.
- (160) G. Şerban Andrei, B. F. Andrei, P. R. Roxana., *Mini-Reviews in Medicinal Chemistry*, **2021**, 21 (11), 1380–1392.
- (161) P. Sharma, C. Larosa, J. Antwi, R. Govindarajan, K. A. Werbovets., *Molecules*, **2021**, 26 (14), 4213.
- (162) L. Zhang, X. M. Peng, G. L. V. Damu, R. X. Geng, C. H. Zhou., *Med Res Rev*, **2014**, 34 (2), 340–437.
- (163) H. C. Steel, G. R. Tintinger, R. Anderson., *Chemical Biology & Drug Design*, **2008**, 72 (3), 225–228.
- (164) T. G. Edwards, C. Fisher., *Antiviral Research*, **2018**, 152, 68–75.

- (165) P. R. Sawyer, R. N. Brogden, K. M. Pinder, T. M. Speight, G. S. Avery., *Drugs*, **1975**, 9 (6), 424–447.
- (166) R. C. Heel, R. N. Brogden, A. Carmine, P. A. Morley, T. M. Speight, G. S. Avery., *Drugs*, **1982**, 23 (1–2), 1–36.
- (167) D. S. Strand, D. Kim, D. A. Peura., *Gut and Liver*, **2017**, 11 (1), 27–37.
- (168) Y. Chen, S. Cui, H. Lin, Z. Xu, W. Zhu, L. Shi, R. Yang, R. Wang, Y. Dai., *International Journal of Impotence Research*, **2012**, 24 (6), 217–220.
- (169) P. Blankestijn, H. Rupp., *Cardiovascular & Hematological Agents in Medicinal Chemistry*, **2008**, 6 (4), 253–257.
- (170) S. L. Abrahams, R. J. Hazen, A. G. Batson, A. P. Phillips., *Journal of Pharmacology and Experimental Therapeutics*, **1989**, 249 (2), 359–365.
- (171) M. Holeček., *Nutrients* , **2020**, 12 (3), 848.
- (172) L. Maintz, N. Novak., *The American Journal of Clinical Nutrition*, **2007**, 85 (5), 1185–1196.
- (173) D. P. Patel, S. M. Swink, L. Castelo-Soccio., *Skin Appendage Disorders*, **2017**, 3 (3), 166–169.
- (174) Z. Haghhighijoo, O. Firuzi, S. Meili, N. Edraki, M. Khoshneviszadeh, R. Miri., *Iranian Journal of Pharmaceutical Research*, **2020**, 19 (1), 181–191.
- (175) F. Mostaghni, H. Shafiekhani, N. Madadi Mahani., *Acta Chimica Slovenica*, **2022**, 69 (1), 91–97.
- (176) L. H. Al-Wahaibi, B. G. M. Youssif, E. S. Taher, A. H. Abdelazeem, A. A. Abdelhamid, A. A. Marzouk., *Molecules*, **2021**, 26 (16), 4718.
- (177) L. L. Chang, K. L. Sidler, M. A. Cascieri, S. de Laszlo, G. Koch, B. Li, M. MacCoss, N. Mantlo, S. O’Keefe, M. Pang, A. Rolando, W. K. Hagmann., *Bioorg Med Chem Lett*, **2001**, 11 (18), 2549–2553.
- (178) T. F. Gallagher, S. M. Fier-Thompson, R. S. Garigipati, M. E. Sorenson, J. M. Smietana, D. Lee, P. E. Bender, J. C. Lee, J. T. Laydon, D. E. Griswold, M. C. Chabot-Fletcher, J. J. Breton, J. L. Adams., *Bioorganic & Medicinal Chemistry Letters*, **1995**, 5 (11), 1171–1176.
- (179) J. C. Lee, J. T. Laydon, P. C. McDonnell, T. F. Gallagher, S. Kumar, D. Green, D. McNulty, M. J. Blumenthal, J. R. Keys, S. W. Land Vatter, J. E. Strickler, M. M. McLaughlin, I. R. Siemens, S. M. Fisher, G. P. Livi, J. R. White, J. L. Adams, P. R. Young., *Nature*, **1994**, 372 (6508), 739–746.

- (180) M. S. Khan, S. A. Siddiqui, M. S. R. A. Siddiqui, U. Goswami, K. V. Srinivasan, M. I. Khan., *Chemical Biology & Drug Design*, **2008**, 72 (3), 197–204.
- (181) M. K. Kathiravan, A. B. Salake, A. S. Chothe, P. B. Dudhe, R. P. Watode, M. S. Mukta, S. Gadhwe., *Bioorganic & Medicinal Chemistry*, **2012**, 20 (19), 5678–5698.
- (182) T. Hussain, H. L. Siddiqui, M. Zia-ur-Rehman, M. Masoom Yasinzai, M. Parvez., *European Journal of Medicinal Chemistry*, **2009**, 44 (11), 4654–4660.
- (183) M. Tonelli, G. Paglietti, V. Boido, F. Sparatore, F. Marongiu, E. Marongiu, P. la Colla, R. Loddo., *Chemistry & Biodiversity*, **2008**, 5 (11), 2386–2401.
- (184) M. Tonelli, M. Simone, B. Tasso, F. Novelli, V. Boido, F. Sparatore, G. Paglietti, S. Pricl, G. Giliberti, S. Blois, C. Ibba, G. Sanna, R. Loddo, P. la Colla., *Bioorganic & Medicinal Chemistry*, **2010**, 18 (8), 2937–2953.
- (185) M. Tonelli, F. Novelli, B. Tasso, I. Vazzana, A. Sparatore, V. Boido, F. Sparatore, P. la Colla, G. Sanna, G. Giliberti, B. Busonera, P. Farci, C. Ibba, R. Loddo., *Bioorganic & Medicinal Chemistry*, **2014**, 22 (17), 4893–4909.
- (186) R. v. Shingalapur, K. M. Hosamani, R. S. Keri., *European Journal of Medicinal Chemistry*, **2009**, 44 (10), 4244–4248.
- (187) M. P. Wentland, D. M. Bailey, E. J. Alexander, M. J. Castaldi, R. A. Ferrari, M. H. Perrone, D. A. Luttinger, D. R. Haubrich., *Journal of Medicinal Chemistry*, **1987**, 30 (8), 1482–1489.
- (188) H. M. Refaat., *European Journal of Medicinal Chemistry*, **2010**, 45 (7), 2949–2956.
- (189) A. Leone-Bay, P. E. Timony, L. Green, L. Glaser., *Journal of Agricultural and Food Chemistry*, **1986**, 34 (4), 733–736.
- (190) H. Takemura, J. H. Choi, N. Matsuzaki, Y. Taniguchi, J. Wu, H. Hirai, R. Motohashi, T. Asakawa, K. Ikeuchi, M. Inai, T. Kan, H. Kawagishi., *Scientific Reports*, **2019**, 9 (1), 1–8.
- (191) H. J. Zhu, J. S. Wang, K. S. Patrick, J. L. Donovan, C. L. DeVane, J. S. Markowitz., *Journal of Chromatography B: Anal. Technol. Biomed. Life Sci.*, **2007**, 858 (1–2), 91–95.
- (192) Y. F. Sun, W. Huang, C. G. Lu, Y. P. Cui., *Dyes and Pigments*, **2009**, 81 (1), 10–17.
- (193) M. Stähelin, D. M. Burland, M. Ebert, R. D. Miller, B. A. Smith, R. J. Twieg, W. Volksen, C. A. Walsh., *Applied Physics Letters*, **1992**, 61 (14), 1628.
- (194) M. A. Babizhayev., *Life Sciences*, **2006**, 78 (20), 2343–2357.



- (195) J. v. Olsson, D. Hult, Y. Cai, S. García-Gallego, M. Malkoch., *Polymer Chemistry*, **2014**, 5 (23), 6651–6655.
- (196) L. Chen, B. Zhao, Z. Fan, X. Liu, Q. Wu, H. Li, H. Wang., *Journal of Agricultural and Food Chemistry*, **2018**, 66 (28), 7319–7327.
- (197) Z. Wang, P. Lu, S. Chen, Z. Gao, F. Shen, W. Zhang, Y. Xu, H. S. Kwok, Y. Ma., *Journal of Materials Chemistry*, **2011**, 21 (14), 5451–5456.
- (198) K. Mutoh, J. Abe., *Journal of Physical Chemistry A*, **2011**, 115 (18), 4650–4656.
- (199) M. M. Antonijevic, M. B. Petrovic., *International Journal of Electrochemical Science*, **2008**, 3 (1), 1–28.
- (200) A. Griffin, K. R. Hamling, K. Knupp, S. G. Hong, L. P. Lee, S. C. Baraban., *Brain*, **2017**, 140 (3), 669–683.
- (201) U. Eilers, J. Klumperman, H. P. Hauri., *Journal of Cell Biology*, **1989**, 108 (1), 13–22.
- (202) M. E. Suarez-Almazor, C. Spooner, E. Belseck., *Cochrane Database of Systematic Reviews*; (4):CD001461, **2000**, 2010 (1).
- (203) C. Li, X. Han., *Nanoscale Research Letters*, **2020**, 15 (1), 1–10.
- (204) W. Xiong, Z. Guo, B. Zeng, T. Wang, X. Zeng, W. Cao, D. Lian., *Frontiers in Bioengineering and Biotechnology*, **2022**, 10, 136.
- (205) J. Jayram, V. Jeena., *RSC Advances*, **2018**, 8 (66), 37557–37563.
- (206) F. R. Japp, H. H. Robinson., *Berichte der deutschen chemischen Gesellschaft*, **1882**, 15 (1), 1268–1270.
- (207) L. M. Wang, Y. H. Wang, H. Tian, Y. F. Yao, J. H. Shao, B. Liu., *Journal of Fluorine Chemistry*, **2006**, 127 (12), 1570–1573.
- (208) M. Kidwai, P. Mothra, V. Bansal, R. K. Somvanshi, A. S. Ethayathulla, S. Dey, T. P. Singh., *Journal of Molecular Catalysis A: Chemical*, **2007**, 265 (1–2), 177–182.
- (209) M. M. Heravi, K. Bakhtiari, H. A. Oskooie, S. Taheri., *Journal of Molecular Catalysis A: Chemical*, **2007**, 263 (1–2), 279–281.
- (210) A. F. Mohammed, N. D. Kokare, J. N. Sangshetti, D. B. Shinde., *Journal of the Korean Chemical Society*, **2007**, 51 (5), 418–422.
- (211) J. N. Sangshetti, N. D. Kokare, S. A. Kotharkara, D. B. Shinde., *Journal of Chemical Sciences*, **2008**, 120 (5), 463–467.
- (212) L. S. Gadekar, S. R. Mane, S. S. Katkar, B. R. Arbad, M. K. Lande., *Central European Journal of Chemistry*, **2009**, 7 (3), 550–554.

- (213) A. Yasodha, A. Sivakumar, G. Arunachalam, A. Puratchikody., *Journal of Pharmaceutical Science and Research*, **2009**, 1 (4), 127–130.
- (214) B. P. Bandgar, B. S. Hote, B. L. Korbadi, S. A. Patil., *E-Journal of Chemistry*, **2011**, 8 (3), 1339–1345.
- (215) J.-T. Li, B.-H. Chen, Y.-W. Li, X.-L. Sun., *International Journal of Advances in Pharmacy, Biology and Chemistry (IJAPBC)*, **2012**, 1 (3), 287–292.
- (216) S. D. Burungale, M. J. Bhitre., *International Journal of Pharmaceutical Sciences and Research (IJPSR)*, **2013**, 4 (10), 4051–4057.
- (217) P. D. Sanasi, D. Santhipriya, Y. Ramesh, M. R. Kumar, B. Swathi, K. J. Rao., *Journal of Chemical Sciences*, **2014**, 126 (6), 1715–1720.
- (218) J. Madhavi, S. Anita, M. Suresh, P. U. Rani., *Indian Journal of Research in Pharmacy and Biotechnology*, **2015**, 3 (2), 157–160.
- (219) N. Chouha, T. Boumoud, I. Tebabel, B. Boumoud, A. Debache., *Der Pharma Chemica*, **2018**, 8 (4), 202–206.
- (220) V. D. Patil, N. R. Sutar, K. P. Patil., *Journal of Chemical and Pharmaceutical Research*, **2016**, 8 (7), 728–732.
- (221) V. D. Patil, N. R. Sutar, K. P. Patil, P. Giddh., *Der Chemica Sinica*, **2016**, 7 (2), 23–28.
- (222) A. Parveen, M. R. S. Ahmed, K. A. Shaikh, S. P. Deshmukh, R. P. Pawar., *ARKIVOC*, **2007**, 2007 (16), 12–18.
- (223) R. Wang, C. Liu, G. Luo., *Green Chemistry Letters and Reviews*, **2010**, 3 (2), 101–104.
- (224) B. Karami, K. Eskandari, A. Ghasemi., *Turkish Journal of Chemistry*, **2012**, 36 (4), 601–613.
- (225) B. F. Mirjalili, A. Bamoniri, N. Mohaghegh., *Current Chemistry Letters*, **2013**, 2 (1), 35–42.
- (226) B. Maleki, H. K. Shirvan, F. Taimazi, E. Akbarzadeh, B. Maleki, H. K. Shirvan, F. Taimazi, E. Akbarzadeh., *International Journal of Organic Chemistry*, **2012**, 2 (1), 93–99.
- (227) B. F. Mirjalili, A. Bamoniri, M. A. Mirhoseini., *Scientia Iranica*, **2013**, 20 (3), 587–591.
- (228) J. Banothu, R. Gali, R. Velpula, R. Bavantula., *Arabian Journal of Chemistry*, **2017**, 10 (2), S2754–S2761.
- (229) G. Brahmachari, S. Das., *Indian Journal of Chemistry*, **2013**, 52 (B), 387–393.

- (230) A. A. Marzouk, S. Kamel Mohamed, V. M. Abbasov, A. H. Talybov., *World Journal of Organic Chemistry*, **2013**, 1 (1), 6–10.
- (231) P. v Maske, S. J. Makhija., *Asian Journal of Biomedical and Pharmaceutical Sciences*, **2013**, 3 (20), 63–65.
- (232) K. Nikoofar, M. Haghighi, M. Lashanizadegan, Z. Ahmadvand., *Journal of Taibah University for Science*, **2015**, 9 (4), 570–578.
- (233) M. Vosoughi, F. Mohebali, A. Pesaran, S. Bonakdar, H. A. Lordegani, A. R. Massah., *Bulgarian Chemical Communications*, **2015**, 47 (2), 607–612.
- (234) G. Mohammadi Ziarani, A. Badiei, N. Lashgari, Z. Farahani., *Journal of Saudi Chemical Society*, **2016**, 20 (4), 419–427.
- (235) M. Alikarami, M. Amozad., *Bull Chem Soc Ethiop*, **2017**, 31 (1), 177–184.
- (236) B. Alimenla, A. Kumar, L. Jamir, D. Sinha, U. B. Sinha., *Radiation Effects and Defects in Solids*, **2007**, 161 (12), 687–693.
- (237) C. R. Strauss, R. W. Trainor., *Australian Journal of Chemistry*, **1995**, 48 (10), 1665–1692.
- (238) J. L. Krstenansky, I. Cotterill., *Curr Opin Drug Discov Devel*, **2000**, 3 (4), 454–461.
- (239) A. Lew, P. O. Krutzik, M. E. Hart, A. R. Chamberlin., *Journal of Combinatorial Chemistry*, **2002**, 4 (2), 95–105.
- (240) S. Balalaie, A. Arabanian, M. S. Hashtroudi., *Monatshefte für Chemie*, **2000**, 131 (9), 945–948.
- (241) S. E. Wolkenberg, D. D. Wisnoski, W. H. Leister, Y. Wang, Z. Zhao, C. W. Lindsley., *Organic Letters*, **2004**, 6 (9), 1453–1456.
- (242) K. Shelke, G. Kakade, B. Shingate, M. Shingare., *Rasayan Journal of Chemistry*, **2008**, 1 (3), 489–494.
- (243) S. v. Nalage, M. B. Kalyankar, V. S. Patil, S. v. Bhosale, S. U. Deshmukh, R. P. Pawar., *Open Catalysis Journal*, **2010**, 3 (1), 58–61.
- (244) J. Safari, S. D. Khalili, S. H. Banitaba., *Journal of Chemical Sciences*, **2010**, 122 (3), 437–441.
- (245) K. F. Shelke, S. B. Sapkal, G. K. Kakade, B. B. Shingate, M. S. Shingare., *Green Chemistry Letters and Reviews*, **2010**, 3 (1), 27–32.
- (246) E. Chauveau, C. Marestin, F. Schiets, R. Mercier., *Green Chemistry*, **2010**, 12 (6), 1018–1022.

- (247) Z. Gordi, M. Vazan., *Journal of Particle Science & Technology*, **2015**, 1 (4), 253–263.
- (248) R. B. Sparks, A. P. Combs., *Organic Letters*, **2004**, 6 (14), 2473–2475.
- (249) J. Zhang, T. Q. Zhao, Y. Chen, X. D. Chen, H. K. Chang, Y. M. Zhang, S. C. Hua., *Chemical Papers*, **2017**, 69 (2), 325–338.
- (250) J. F. Zhou, Y. Z. Song, Y. L. Yang, Y. L. Zhu, S. J. Tu., *Synthetic Communications*, **2006**, 35 (10), 1369–1373.
- (251) K. M. El-Shaieb., *Heteroatom Chemistry*, **2006**, 17 (5), 365–368.
- (252) S. Puri, B. Kaur, A. Parmar, H. Kumar., *Current Organic Chemistry*, **2013**, 17 (16), 1790–1828.
- (253) K. F. Shelke, S. B. Sapkal, S. S. Sonar, B. R. Madje, B. B. Shingate, M. S. Shingare., *Bull Korean Chem Soc*, **2009**, 30 (5), 1057–1060.
- (254) K. F. Shelke, S. B. Sapkal, M. S. Shingare., *Chinese Chemical Letters*, **2009**, 20 (3), 283–287.
- (255) H. Zang, Q. Su, Y. Mo, B. W. Cheng, S. Jun., *Ultrasonics Sonochemistry*, **2010**, 17 (5), 749–751.
- (256) D. Nagargoje, P. Mandhane, S. Shingote, P. Badadhe, C. Gill., *Ultrasonics Sonochemistry*, **2012**, 19 (1), 94–96.
- (257) J. Safari, Z. Zarnegar., *Ultrasonics Sonochemistry*, **2013**, 20 (2), 740–746.
- (258) P. D. Sanasi, R. K. Majji, S. Bandaru, S. Bassa, S. Pinninti, S. Vasamsetty, R. B. Korupolu, P. D. Sanasi, R. K. Majji, S. Bandaru, S. Bassa, S. Pinninti, S. Vasamsetty, R. B. Korupolu., *Modern Research in Catalysis*, **2016**, 5 (1), 31–44.
- (259) M. Esmailpour, J. Javidi, F. Dehghani, S. Zahmatkesh., *Research on Chemical Intermediates*, **2017**, 43 (1), 163–185.
- (260) E. Eidi, M. Z. Kassae, Z. Nasresfahani., *Applied Organometallic Chemistry*, **2016**, 30 (7), 561–565.
- (261) B. S. Londhe, S. L. Khillare, A. M. Nalawade, R. A. Mane., *International Journal of Research in Engineering and Science (IJRES)*, **2021**, 9 (1), 79–84.
- (262) C. O. Kappe., *European Journal of Medicinal Chemistry*, **2000**, 35 (12), 1043–1052.
- (263) H. Cernecka, L. Veizerova, L. Mensikova, J. Svetlik, P. Krenek., *Journal of Pharmacy and Pharmacology*, **2012**, 64 (5), 735–741.

- (264) D. Kumarasamy, B. G. Roy, J. Rocha-Pereira, J. Neyts, S. Nanjappan, S. Maity, M. Mookerjee, L. Naesens., *Bioorganic & Medicinal Chemistry Letters*, **2017**, 27 (2), 139–142.
- (265) R. Kaur, S. Chaudhary, K. Kumar, M. K. Gupta, R. K. Rawal., *European Journal of Medicinal Chemistry*, **2017**, 132, 108–134.
- (266) M. Marinescu., *Molecules*, **2021**, 26 (19), 6022.
- (267) J. M. Wetzel, S. W. Miao, C. Forray, L. A. Borden, T. A. Branchek, C. Gluchowski., *Journal of Medicinal Chemistry*, **1995**, 38 (10), 1579–1581.
- (268) P. A. Halim, R. A. Hassan, K. O. Mohamed, S. O. Hassanin, M. G. Khalil, A. M. Abdou, E. O. Osman., *Journal of Enzyme Inhibition and Medicinal Chemistry*, **2022**, 37 (1), 189–201.
- (269) M. Salmón, R. Osnaya, L. Gómez, G. Arroyo, F. Delgado, R. Miranda., *Revista de la Sociedad Química de México*, **2001**, 45 (4), 206–207.
- (270) S. A. Haque, T. P. Hasaka, A. D. Brooks, P. v. Lobanov, P. W. Baas., *Cell Motility and the Cytoskeleton*, **2004**, 58 (1), 10–16.
- (271) C. Pothiraj, A. S. Velan, J. Joseph, N. Raman., *Mycobiology*, **2008**, 36 (1), 69.
- (272) K. S. Atwal, B. N. Swanson, S. E. Unger, D. M. Floyd, S. Moreland, A. Hedberg, B. C. O'Reilly., *Journal of Medicinal Chemistry*, **1991**, 34 (2), 806–811.
- (273) E. Ramu, V. Kotra, N. Bansal, R. Varala, S. R. Adapa., *Rasayan Journal of Chemistry*, **2008**, 1 (1), 188–194.
- (274) F. Cohen, L. E. Overman, S. K. Ly Sakata., *Organic Letters*, **1999**, 1 (13), 2169–2172.
- (275) B. C. Ranu, A. Hajra, U. Jana., *Journal of Organic Chemistry*, **2000**, 65 (19), 6270–6272.
- (276) R. S. Bhosale, S. v. Bhosale, S. v. Bhosale, T. Wang, P. K. Zubaidha., *Tetrahedron Letters*, **2004**, 45 (49), 9111–9113.
- (277) E. Rafiee, H. Jafari., *Bioorganic & Medicinal Chemistry Letters*, **2006**, 16 (9), 2463–2466.
- (278) R. Gupta, S. Paul, R. Gupta., *Journal of Molecular Catalysis A: Chemical*, **2007**, 266 (1–2), 50–54.
- (279) Suresh, A. Saini, D. Kumar, J. S. Sandhu., *Green Chemistry Letters and Reviews*, **2009**, 2 (1), 29–33.
- (280) H. Eshghi, A. Javid, A. Khojastehnezhad, F. Moeinpour, F. F. Bamoharram, M. Bakavoli, M. Mirzaei., *Chinese Journal of Catalysis*, **2015**, 36 (3), 299–307.

- (281) Z. Benzekri, R. Benhdidou, S. Hamia, H. Serrar, S. Boukhris, B. Sallek, A. Hassikou, A. Souizi., *J Mex Chem Soc*, **2017**, *61* (3), 217–221.
- (282) S. Prakash, N. Elavarasan, A. Venkatesan, K. Subashini, M. Sowndharya, V. Sujatha., *Advanced Powder Technology*, **2018**, *29* (12), 3315–3326.
- (283) S. Farooq, F. A. Alharthi, A. Alsalmeh, A. Hussain, B. A. Dar, A. Hamid, S. Koul., *RSC Advances*, **2020**, *10* (69), 42221–42234.
- (284) C. J. Liu, J. de Wang., *Molecules*, **2009**, *14* (2), 763–770.
- (285) S. K. Prajapati, K. K. Gupta, B. N. Babu., *Journal of Chemical Sciences*, **2015**, *127* (6), 1047–1052.
- (286) P. Biginelli., *Gazzetta Chimica Italiana*, **1893**, *23* (1), 360–413.
- (287) T. U. Mayer, T. M. Kapoor, S. J. Haggarty, R. W. King, S. L. Schreiber, T. J. Mitchison., *Science (1979)*, **1999**, *286* (5441), 971–974.
- (288) K. Folkers, H. J. Harwood, B. J. Treat., *J Am Chem Soc*, **1932**, *54* (9), 3751–3758.
- (289) Z. L. Shen, X. P. Xu, S. J. Ji., *Journal of Organic Chemistry*, **2010**, *75* (4), 1162–1167.
- (290) K.-Y. Lee, K.-Y. Ko., *Bull Korean Chem Soc*, **2004**, *25* (12), 1929–1931.
- (291) M. Kamal Raj, H. S. P. Rao, S. G. Manjunatha, R. Sridharan, S. Nambiar, J. Keshwan, J. Rappai, S. Bhagat, B. S. Shwetha, D. Hegde, U. Santhosh., *Tetrahedron Letters*, **2011**, *52* (28), 3605–3609.
- (292) A. Debache, M. Amimour, A. Belfaitah, S. Rhouati, B. Carboni., *Tetrahedron Letters*, **2008**, *49* (42), 6119–6121.
- (293) M. Kamali, A. Shockravi, M. S. Doost, S. E. Hooshmand., *Cogent Chemistry*, **2015**, *1* (1), 1081667.
- (294) B. S. Surendra, K. S. Prasad, T. R. S. Shekhar, A. A. Jahagirdar, S. C. Prashantha, N. Raghavendra, K. Gurushantha, N. Basavaraju, K. Rudresha., *Journal of Photochemistry and Photobiology*, **2021**, *8*, 100063.
- (295) M. Mittersteiner, F. F. S. Farias, H. G. Bonacorso, M. A. P. Martins, N. Zanatta., *Ultrasonics Sonochemistry*, **2021**, *79*, 105683.
- (296) K. S. Atwal, B. N. Swanson, S. E. Unger, D. M. Floyd, S. Moreland, A. Hedberg, B. C. O'Reilly., *Journal of Medicinal Chemistry*, **1991**, *34* (2), 806–811.
- (297) J. C. Barrow, P. G. Nantermet, H. G. Selnick, K. L. Glass, K. E. Rittle, K. F. Gilbert, T. G. Steele, C. F. Homnick, R. M. Freidinger, R. W. Ransom, P. Kling, D. Reiss, T. P. Broten, T. W. Schorn, R. S. L. Chang, S. S. O'Malley, T. v. Olah, J.

- D. Ellis, A. Barrish, K. Kassahun, P. Leppert, D. Nagarathnam, C. Forray., *Journal of Medicinal Chemistry*, **2000**, 43 (14), 2703–2718.
- (298) A. Shahid, N. S. Ahmed, T. S. Saleh, S. A. Al-Thabaiti, S. N. Basahel, W. Schwieger, M. Mokhtar., *Catalysts*, **2017**, 7 (3), 84.
- (299) H. Adibi, H. A. Samimi, M. Beygzadeh., *Catalysis Communications*, **2007**, 8 (12), 2119–2124.
- (300) B. C. Ranu, A. Hajra, S. S. Dey., *Organic Process Research and Development*, **2002**, 6 (6), 817–818.
- (301) F. Dong, L. Jun, Z. Xinli, Y. Zhiwen, L. Zuliang., *Journal of Molecular Catalysis A: Chemical*, **2007**, 274 (1–2), 208–211.
- (302) S. L. Jain, S. Singhal, B. Sain., *Green Chemistry*, **2007**, 9 (7), 740–741.
- (303) S. Verma, S. L. Jain, B. Sain., *Tetrahedron Letters*, **2010**, 51 (52), 6897–6900.
- (304) S. Patil, S. D. Jadhav, M. B. Deshmukh., *Archives of Applied Science Research*, **2011**, 3 (1), 203–208.
- (305) S. Patil, S. D. Jadhav, S. Y. Mane., *International Journal of Organic Chemistry*, **2011**, 1 (3), 125–131.
- (306) J. Lal, M. Sharma, S. Gupta, P. Parashar, P. Sahu, D. D. Agarwal., *Journal of Molecular Catalysis A: Chemical*, **2012**, 352, 31–37.
- (307) N. Azizi, S. Dezfuli, M. M. Hahsemi., *The Scientific World Journal*, **2012**, 2012 (Article ID 908702), 1–6.
- (308) H. Sachdeva, D. Dwivedi., *The Scientific World Journal*, **2012**, 2012 (Article ID 109432), 1–9.
- (309) A. Borse, M. Patil, N. Patil, R. Shinde., *ISRN Organic Chemistry*, **2012**, 2012 (Article ID 415645), 1–6.
- (310) M. Dewan, A. Kumar, A. Saxena, A. De, S. Mozumdar., *PLOS ONE*, **2012**, 7 (8), 1–8.
- (311) Z. Karimi-Jaberi, M. S. Moaddeli., *ISRN Organic Chemistry*, **2012**, 2012 (Article ID 474626), 1–4.
- (312) B. Mirjalili, L. Zamani., *South African Journal of Chemistry*, **2015**, 67 (1), 21–26.
- (313) Y. Zhang, B. Wang, X. Zhang, J. Huang, C. Liu., *Molecules*, **2015**, 20 (3), 3811–3820.
- (314) V. v Dabholkar, K. S. Badhe, S. K. Kurade., *Current Chemistry Letters*, **2017**, 6, 77–90.

- (315) M. Nasr-Esfahani, M. Taei., *RSC Advances*, **2015**, 5 (56), 44978–44989.
- (316) L. Z. Fekri, M. Nikpassand, M. Movaghari., *Bull Chem Soc Ethiop*, **2017**, 31 (2), 313–321.
- (317) H. Yuan, K. Zhang, J. Xia, X. Hu, S. Yuan., *Cogent Chemistry*, **2017**, 3 (1), 1318692.
- (318) T. S. Choudhare, D. S. Wagare, V. T. Kadam, A. A. Kharpe, P. D. Netankar., *Polycyclic Aromatic Compounds*, **2021**, 0:0, 1–8.
- (319) C. Simon, T. Constantieux, J. Rodriguez., *European Journal of Organic Chemistry*, **2004**, 2004 (24), 4957–4980.
- (320) A. K. Misra, G. Agnihotri, S. K. Madhusudan., *ChemInform*, **2005**, 36 (2).
- (321) V. Polshettiwar, R. S. Varma., *Tetrahedron Letters*, **2007**, 48 (41), 7343–7346.
- (322) H. R. Shaterian, A. Hosseinian, M. Ghashang, F. Khorami, N. Karimpoor., *Phosphorus, Sulphur, and Silicon and the Related Elements*, **2009**, 184 (9), 2333–2338.
- (323) H. W. Zhan, J. X. Wang, X. T. Wang., *Chinese Chemical Letters*, **2008**, 19 (10), 1183–1185.
- (324) D. Kumar, S. Suresh, J. S. Sandhu., *ChemInform*, **2010**, 41 (30).
- (325) K. K. Pasunooti, H. Chai, C. N. Jensen, B. K. Gorityala, S. Wang, X. W. Liu., *Tetrahedron Letters*, **2011**, 52 (1), 80–84.
- (326) A. Kuraitheerthakumaran, S. Pazhamalai, M. Gopalakrishnan., *Arabian Journal of Chemistry*, **2016**, 9 (Supplement 1), S461–S465.
- (327) R. K. Sharma, D. Rawat., *Inorganic Chemistry Communications*, **2012**, 17, 58–63.
- (328) V. Srivastava., *Green and Sustainable Chemistry*, **2013**, 3 (2A), 38–40.
- (329) M. Shingare, S. Dhanmane., *Chemistry and Materials Research*, **2015**, 7 (3), 27–31.
- (330) T. Pramanik, S. K. Padan., *International Journal of Pharmacy and Pharmaceutical Sciences*, **2016**, 8 (3), 396–398.
- (331) L. Moradi, M. Tadayon., *Journal of Saudi Chemical Society*, **2018**, 22 (1), 66–75.
- (332) T. J. Mason, J. Phillip. Lorimer., *Applied Sonochemistry: The Uses of Power Ultrasound in Chemistry and Processing*; Wiley-VCH: New York, **2003**.
- (333) A. Kotronarou, G. Mills, M. R. Hoffmann., *Journal of Physical Chemistry*, **1991**, 95 (9), 3630–3638.



- (334) M. S. Zhidovinova, O. v. Fedorova, G. L. Rusinov, I. G. Ovchinnikova., *Russian Chemical Bulletin*, **2003**, 52 (11), 2527–2528.
- (335) J. T. Li, J. F. Han, J. H. Yang, T. S. Li., *Ultrasonics Sonochemistry*, **2003**, 10 (3), 119–122.
- (336) J. S. Yadav, B. V. S. Reddy, K. B. Reddy, K. S. Raj, A. R. Prasad., *Journal of the Chemical Society, Perkin Transactions 1*, **2001**, Issue 16, 1939–1941.
- (337) H. A. Stefani, C. B. Oliveira, R. B. Almeida, C. M. P. Pereira, R. C. Braga, R. Cella, V. C. Borges, L. Savegnago, C. W. Nogueira., *European Journal of Medicinal Chemistry*, **2006**, 41 (4), 513–518.
- (338) C. J. Liu, J. de Wang., *Molecules*, **2010**, 15 (4), 2087–2095.
- (339) Z.-P. Lin, J.-S. Wang, J.-T. Li., *Letters in Organic Chemistry*, **2006**, 3 (7), 523–525.
- (340) A. Khanum, R.-R. Khan, M. M. M. A. Pasha., *Universal Journal of Pharmaceutical Research*, **2021**, 6 (5), 46–51.
- (341) V. S. Mityanov, A. v. Kutasevich, M. M. Krayushkin, B. v. Lichitsky, A. A. Dudinov, A. N. Komogortsev, T. Y. Koldaeva, V. P. Perevalov., *Tetrahedron*, **2017**, 73 (47), 6669–6675.
- (342) N. Xi, Q. Huang, L. Liu., In *Comprehensive Heterocyclic Chemistry III (Chap. 4.02 - Imidazoles)*; Katritzky, A. R., Ramsden, C. A., Scriven, E. F. V., Taylor, R. J. K., Eds.; Elsevier Science: New York, **2008**; Vol. 4, pp 143–364.
- (343) G. V. Nikitina, M. S. Pevzner., *Chemistry of Heterocyclic Compounds*, **1993**, 29 (2), 127–151.
- (344) T. R. Jensen, C. P. Schaller, M. A. Hillmyer, W. B. Tolman., *Journal of Organometallic Chemistry*, **2005**, 690 (24–25), 5881–5891.
- (345) G. Mloston, M. Celeda, M. Jasinski, K. Urbaniak, P. J. Boratynski, P. R. Schreiner, H. Heimgartner., *Molecules*, **2019**, 24 (23), 4398.
- (346) Y. Wang, L. Zhang., *Synthesis (Stuttg)*, **2015**, 47 (03), 289–305.
- (347) R. Kuhn, W. Blau., *Justus Liebigs Ann Chem*, **1958**, 615 (1), 99–107.
- (348) A. K. Sharma, S. N. Mazumdar, M. P. Mahajan., *Tetrahedron Letters*, **1993**, 34 (49), 7961–7964.
- (349) H. Cerecetto, A. Gerpe, M. González, Y. Fernández Sainz, O. E. Piro, E. E. Castellano., *Synthesis (Stuttg)*, **2004**, 2004 (16), 2678–2684.
- (350) P. Mucha, G. Mlostoń, M. Jasiński, A. Linden, H. Heimgartner., *Tetrahedron: Asymmetry*, **2008**, 19 (13), 1600–1607.

- (351) G. Mlostoń, P. Mucha, K. Urbaniak, K. Broda, H. Heimgartner., *Helvetica Chimica Acta*, **2008**, *91* (2), 232–238.
- (352) S. A. Amitina, A. Y. Tikhonov, I. A. Grigor'Ev, Y. V. Gatilov, B. A. Selivanov., *Chemistry of Heterocyclic Compounds*, **2009**, *45* (6), 691–697.
- (353) G. Mlostoń, M. Jasiński., *ARKIVOC*, **2010**, *2011* (6), 162–175.
- (354) V. S. Mityanov, V. P. Perevalov, I. I. Tkach., *Chemistry of Heterocyclic Compounds*, **2013**, *48* (12), 1793–1800.
- (355) K. Pradhan, B. K. Tiwary, M. Hossain, R. Chakraborty, A. K. Nanda., *RSC Advances*, **2016**, *6* (13), 10743–10749.
- (356) M. Gaba, S. Singh, C. Mohan., *European Journal of Medicinal Chemistry*, **2014**, *76*, 494–505.
- (357) Y. Bansal, O. Silakari., *Bioorganic & Medicinal Chemistry*, **2012**, *20* (21), 6208–6236.
- (358) J. B. Bariwal, A. K. Shah, M. K. Kathiravan, R. S. Somani, J. R. Jagtap, K. S. Jain., *Indian Journal of Pharmaceutical Education and Research*, **2008**, *42* (3), 225–231.
- (359) C. Kuş, N. Altanlar., *Turkish Journal of Chemistry*, **2003**, *27* (1), 35–40.
- (360) Y. S. Chhonker, B. Veenu, S. R. Hasim, N. Kaushik, D. Kumar, P. Kumar., *E-Journal of Chemistry*, **2009**, *6* (Suppl. 1, Article ID 604203), S342.
- (361) R. Vinodkumar, S. D. Vaidya, B. V. Siva Kumar, U. N. Bhise, S. B. Bhirud, U. C. Mashelkar., *European Journal of Medicinal Chemistry*, **2008**, *43* (5), 986–995.
- (362) B. G. Mohamed, M. A.-A. Abdel-Alim, M. A. Hussein., *Acta Pharmaceutica*, **2006**, *56* (1), 31–48.
- (363) B. Dik, D. Coşkun, E. Bahçivan, K. Üney., *Turkish Journal of Medical Sciences*, **2021**, *51* (3), 1585.
- (364) M. S. Yar, M. M. Abdullah, J. Majeed., *World Academy of Science, Engineering and Technology*, **2009**, *55*, 593–599.
- (365) Z. Kazimierczuk, J. A. Upcroft, P. Upcroft, A. Górska, B. Starościak, A. Laudy., *Acta Biochimica Polonica*, **2002**, *49* (1), 185–195.
- (366) Ş. Demirayak, U. Abu Mohsen, A. Çağrı Karaburun., *European Journal of Medicinal Chemistry*, **2002**, *37* (3), 255–260.
- (367) M. Faheem, A. Rathaur, A. Pandey, V. Kumar Singh, A. K. Tiwari., *ChemistrySelect*, **2020**, *5* (13), 3981–3994.

- (368) V. A. S. Pardeshi, N. S. Chundawat, S. I. Pathan, P. Sukhwal, T. P. S. Chundawat, G. P. Singh., *Synthetic Communications*, **2021**, *51* (4), 485–513.
- (369) M. M. Ramla, M. A. Omar, A. M. M. El-Khamry, H. I. El-Diwani., *Bioorganic & Medicinal Chemistry*, **2006**, *14* (21), 7324–7332.
- (370) R. Pedro Rothlin, H. Miguel Vetulli, M. Duarte, F. Germán Pelorosso., *Drug Development Research*, **2020**, *81* (7), 768–770.
- (371) H. Mostafavi, M. R. Islami, E. Ghonchepour, A. M. Tikdari., *Chemical Papers*, **2018**, *72* (12), 2973–2978.
- (372) D. Chianelli, N. Nikolaidis., WO 2001058878 A1. **2002**.
- (373) S. Vasiliou., *Drugs of Today (Barcelona, Spain : 1998)*, **2011**, *47* (9), 647–651.
- (374) A. K. Petersen, P. H. Olesen, L. B. Christiansen, H. C. Hansen, F. E. Nielsen., US 7915299 B2. **2008**.
- (375) Y. Li, M. Kataoka, M. Tatsuta, K. Yasoshima, T. Yura, K. Urbahns, A. Kiba, N. Yamamoto, J. B. Gupta, K. Hashimoto., *Bioorganic & Medicinal Chemistry Letters*, **2005**, *15* (3), 805–807.
- (376) T. Ishida, T. Suzuki, S. Hirashima, K. Mizutani, A. Yoshida, I. Ando, S. Ikeda, T. Adachi, H. Hashimoto., *Bioorganic & Medicinal Chemistry Letters*, **2006**, *16* (7), 1859–1863.
- (377) H. Zarrinmayeh, A. M. Nunes, P. L. Ornstein, D. M. Zimmerman, M. B. Arnold, D. A. Schober, S. L. Gackenheimer, R. F. Bruns, P. A. Hipskind, T. C. Britton, B. E. Cantrell, D. R. Gehlert., *Journal of Medicinal Chemistry*, **1998**, *41* (15), 2709–2719.
- (378) D. N. Kommi, P. S. Jadhavar, D. Kumar, A. K. Chakraborti., *Green Chemistry*, **2013**, *15* (3), 798–810.
- (379) T. B. Nguyen, L. Ermolenko, A. Al-Mourabit., *Green Chemistry*, **2013**, *15* (10), 2713–2717.
- (380) J. E. R. Sadig, R. Foster, F. Wakenhut, M. C. Willis., *Journal of Organic Chemistry*, **2012**, *77* (21), 9473–9486.
- (381) F. Fache, E. Schulz, M. L. Tommasino, M. Lemaire., *Chemical Reviews*, **2000**, *100* (6), 2159–2231.
- (382) Y. Chen, F. Xu, Z. Sun., *RSC Advances*, **2017**, *7* (70), 44421–44425.
- (383) H. Sharma, N. Kaur, N. Singh, D. O. Jang., *Green Chemistry*, **2015**, *17* (8), 4263–4270.
- (384) J. B. Wright., *Chemical Reviews*, **1951**, *48* (3), 397–541.

- (385) R. Wang, X. xia Lu, X. qi Yu, L. Shi, Y. Sun., *Journal of Molecular Catalysis A: Chemical*, **2007**, 266 (1–2), 198–201.
- (386) P. Thapa, P. M. Palacios, T. Tran, B. S. Pierce, F. W. Foss., *The Journal of Organic Chemistry*, **2020**, 85 (4), 1991–2009.
- (387) V. N. Mahire, P. P. Mahulikar., *Chinese Chemical Letters*, **2015**, 26 (8), 983–987.
- (388) V. Praneetha, S. U. Rani, K. Srinivas., *Asian Journal of Research in Chemistry*, **2016**, 9 (10), 468.
- (389) P. Saha, S. R. Brishty, S. M. A. Rahman., *Indian Journal of Pharmaceutical Sciences*, **2020**, 82 (2), 222–229.
- (390) K. Bahrami, M. M. Khodaei, A. Nejati., *Green Chemistry*, **2010**, 12 (7), 1237–1241.
- (391) Z. Y. Yu, J. Zhou, Q. S. Fang, L. Chen, Z. bin Song., *Chemical Papers*, **2016**, 70 (9), 1293–1298.
- (392) A. J. Blatch, O. v. Chetina, J. A. K. Howard, L. G. F. Patrick, C. A. Smethurst, A. Whiting., *Organic & Biomolecular Chemistry*, **2006**, 4 (17), 3297–3302.
- (393) S. Demirayak, I. Kayagil, L. Yurttas., *European Journal of Medicinal Chemistry*, **2011**, 46 (1), 411–416.
- (394) D. Yang, H. Fu, L. Hu, Y. Jiang, Y. Zhao., *Journal of Organic Chemistry*, **2008**, 73 (19), 7841–7844.
- (395) C. T. Brain, S. A. Brunton., *Tetrahedron Letters*, **2002**, 43 (10), 1893–1895.
- (396) M. L. di Gioia, R. Cassano, P. Costanzo, N. H. Cano, L. Maiuolo, M. Nardi, F. P. Nicoletta, M. Oliverio, A. Procopio., *Molecules*, **2019**, 24 (16), 2885.
- (397) G. Brasche, S. L. Buchwald., *Angewandte Chemie International Edition*, **2008**, 47 (10), 1932–1934.
- (398) P. Saha, T. Ramana, N. Purkait, M. A. Ali, R. Paul, T. Punniyamurthy., *Journal of Organic Chemistry*, **2009**, 74 (22), 8719–8725.
- (399) P. Saha, M. A. Ali, P. Ghosh, T. Punniyamurthy., *Organic & Biomolecular Chemistry*, **2010**, 8 (24), 5692–5699.
- (400) H. F. He, Z. J. Wang, W. Bao., *Advanced Synthesis & Catalysis*, **2010**, 352 (17), 2905–2912.
- (401) F. Wang, S. Cai, Q. Liao, C. Xi., *Journal of Organic Chemistry*, **2011**, 76 (9), 3174–3180.

- (402) J. Zhu, H. Xie, Z. Chen, S. Li, Y. Wu., *Chemical Communications*, **2009**, *17*, 2338–2340.
- (403) W. Shen, T. Kohn, Z. Fu, X. Jiao, S. Lai, M. Schmitt., *Tetrahedron Letters*, **2008**, *49* (51), 7284–7286.
- (404) C. Siddappa, V. Kambappa, A. K. C. Siddegowda, K. S. Rangappa., *Tetrahedron Letters*, **2010**, *51* (50), 6493–6497.
- (405) K. Bahrami, M. Mehdi Khodaei, F. Naali., *Journal of Organic Chemistry*, **2008**, *73* (17), 6835–6837.
- (406) C. Chen, C. Chen, B. Li, J. Tao, J. Peng., *Molecules*, **2012**, *17* (11), 12506–12520.
- (407) S. Bonacci, G. Iriti, S. Mancuso, P. Novelli, R. Paonessa, S. Tallarico, M. Nardi., *Catalysts*, **2020**, *10* (8), 845.
- (408) A. Procopio, C. Celia, M. Nardi, M. Oliverio, D. Paolino, G. Sindona., *Journal of Natural Products*, **2011**, *74* (11), 2377–2381.
- (409) T. J. Mason., *Philosophical Transactions of the Royal Society of London. Series A: Mathematical, Physical and Engineering Sciences*, **1999**, *357* (1751), 355–369.
- (410) M. S. Estevão, C. A. M. Afonso., *Tetrahedron Letters*, **2017**, *58* (4), 302–304.
- (411) K. Das, A. Mondal, D. Srimani., *Journal of Organic Chemistry*, **2018**, *83* (16), 9553–9560.
- (412) Y. R. Girish, K. S. Sharath Kumar, K. N. Thimmaiah, K. S. Rangappa, S. Shashikanth., *RSC Advances*, **2015**, *5* (92), 75533–75546.
- (413) S. Majumdar, M. Chakraborty, N. Pramanik, D. K. Maiti., *RSC Advances*, **2015**, *5* (63), 51012–51018.
- (414) C. Kathing, N. G. Singh, J. World Star Rani, R. Nongrum, R. Nongkhlaw., *Russian Journal of Organic Chemistry*, **2020**, *56* (9), 1628–1634.
- (415) B. Vieira, A. Barcellos, R. Schumacher, E. Lenardao, D. Alves., *Current Green Chemistry*, **2014**, *1* (2), 136–144.
- (416) A. de la Hoz, À. Díaz-Ortiz, A. Moreno., *Chemical Society Reviews*, **2005**, *34* (2), 164–178.
- (417) M. Nardi, S. Bonacci, N. H. Cano, M. Oliverio, A. Procopio., *Molecules*, **2022**, *27* (5), 1751.
- (418) D. Azarifar, M. Pirhayati, B. Maleki, M. Sanginabadi, R. N. Yami., *Journal of the Serbian Chemical Society*, **2010**, *75* (9), 1181–1189.

- (419) A. P. Sarkate, S. D. Shinde, A. O. Barde, A. P. Sarkate., *International Journal of ChemTech Research*, **2015**, 8 (2), 496–500.
- (420) R. G. Jacob, L. G. Dutra, C. S. Radatz, S. R. Mendes, G. Perin, E. J. Lenardão., *Tetrahedron Letters*, **2009**, 50 (13), 1495–1497.
- (421) P. Bandyopadhyay, M. Sathe, G. K. Prasad, P. Sharma, M. P. Kaushik., *Journal of Molecular Catalysis A: Chemical*, **2011**, 341 (1–2), 77–82.
- (422) B. Kumar, K. Smita, L. Cumbal., *Journal of Chemical Sciences*, **2014**, 126 (6), 1831–1840.
- (423) L. J. Zhang, J. Xia, Y. Q. Zhou, H. Wang, S. W. Wang., *Synthetic Communications*, **2012**, 42 (3), 328–336.
- (424) V. M. Rao, A. S. Rao, S. S. Rani, S. Yaraswi, M. Pal., *Mini Reviews in Medicinal Chemistry*, **2018**, 18 (14), 1233–1239.
- (425) A. A. Patil, S. B. Kamble, G. S. Rashinkar, R. S. Salunkhe., *Chemical Science Review and Letters*, **2014**, 3 (10), 214–220.
- (426) S. H. Nile, B. Kumar, S. W. Park., *Arabian Journal of Chemistry*, **2015**, 8 (5), 685–691.
- (427) W. Liu, S. Gao, Ph. Zhang, X. Zhou, C. Wang., *Asian Journal of Chemistry*, **2014**, 26 (7), 1980–1982.
- (428) K. Godugu, V. D. Sri Yadala, M. K. Mohinuddin Pinjari, T. R. Gundala, L. R. Sanapareddy, C. G. Reddy Nallagonda., *Beilstein Journal of Organic Chemistry*, **2020**, 16 (1), 1881–1900.
- (429) P. C. Keller, M. A. Banks, S. K. Boocock, J. R. Wermer, S. H. Lawrence, S. G. Shore., *Inorganic Chemistry*, **1986**, 25 (3), 367–372.
- (430) N. N. Greenwood, J. D. Kennedy., *Pure and Applied Chemistry*, **1991**, 63 (3), 317–326.
- (431) R. N. Grimes, A. P. E. York, P. E. Rakita, B. J. Coe, C. Nataro, M. A. Ferguson, K. M. Bocage, B. J. Hess, V. J. Ross, D. T. Swarr, K. Chwee, D. Tan, K. Goh, L. S. Chia, D. F. Treagust, J. E. Mcgrady, R. J. P. Williams, J. J. R. Fraústo Da Silva., *Journal of Chemical Education*, **2004**, 81 (5), 657–672.
- (432) H. Braunschweig, C. Kollann, D. Rais., *Angewandte Chemie International Edition*, **2006**, 45 (32), 5254–5274.
- (433) P. Becker., *Advanced Materials*, **1998**, 10 (13), 979–992.
- (434) Q. Li, F. Xue, T. C. W. Mak., *Inorganic Chemistry*, **1999**, 38 (18), 4142–4145.
- (435) H. Doweidar., *Journal of Materials Science*, **1990**, 25 (1), 253–258.

- (436) W. Vogel., *Glass Chemistry*; Springer-Verlag: Berlin Heidelberg, **1994**.
- (437) A. Thulasiramudu, S. Buddhudu., *Journal of Quantitative Spectroscopy and Radiative Transfer*, **2006**, *102* (2), 212–227.
- (438) B. H. Rudramadevi, S. Buddhudu., *Ferroelectrics Letters Section*, **2009**, *36* (3–4), 82–91.
- (439) V. Naresh, S. Buddhudu., *Ferroelectrics*, **2012**, *437* (1), 110–125.
- (440) X. X. Shi, X. J. Liu, L. J. Yuan., *Advanced Materials Research*, **2011**, *Vol. 236-238*, 876–879.
- (441) S. Li, L. Xu, Y. Zhai, H. Yu., *RSC Advances*, **2014**, *4* (16), 8245–8249.
- (442) P. Pascuta, R. Lungu, I. Ardelean., *Journal of Materials Science: Materials in Electronics*, **2010**, *21* (6), 548–553.
- (443) N. J. Kreidl., *Journal of Non-Crystalline Solids*, **1990**, *123* (1–3), 377–384.
- (444) C. L. Christ, J. R. Clark., *Physics and Chemistry of Minerals*, **1977**, *2* (1), 59–87.
- (445) P. C. Burns, J. D. Grice, F. C. Hawthorne., **1995**, *33*, 1131–1151.
- (446) L. Cui, W. Zhang, R. Zheng, J. Liu., *Chemistry – A European Journal*, **2020**, *26* (51), 11661–11672.
- (447) K. Saha, S. Ghosh., *Dalton Transactions*, **2022**, *51* (7), 2631–2640.
- (448) N. Wang, A. Xu, P. Ou, S. F. Hung, A. Ozden, Y. R. Lu, J. Abed, Z. Wang, Y. Yan, M. J. Sun, Y. Xia, M. Han, J. Han, K. Yao, F. Y. Wu, P. H. Chen, A. Vomiero, A. Seifitokaldani, X. Sun, D. Sinton, Y. Liu, E. H. Sargent, H. Liang., *Nature Communications*, **2021**, *12* : 6089, 1–9.
- (449) Organic Laboratory Techniques  
<http://www.chem.ucalgary.ca/courses/351/laboratory/meltingpoint.pdf> (accessed 2022 -07 -09).
- (450) *SADABS, SMART and SAINT*; Bruker AXS Inc., Madison, Wisconsin, USA, **2000**.
- (451) G. M. Sheldrick., *SHELXS-97 and SHELXL-97, Program for Crystal Structure Solution and Refinement*; University of Gottingen, Gottingen: Germany, **1997**.
- (452) L. J. Farrugia., *Journal of Applied Crystallography*, **1997**, *30* (5), 565–565.
- (453) A. L. Spek., *Acta Crystallographica*, **2009**, *D65* (2), 148–155.
- (454) L. J. Farrugia., *Journal of Applied Crystallography*, **1999**, *32* (4), 837–838.
- (455) L. J. Farrugia., *Journal of Applied Crystallography*, **2012**, *45* (4), 849–854.

- (456) M. J. Frisch, G. W. Trucks, H. B. Schlegel, G. E. Scuseria, M. A. Robb, J. R. Cheeseman, G. Scalmani, V. Barone, G. A. Petersson, H. Nakatsuji, X. Li, M. Caricato, A. v Marenich, J. Bloino, B. G. Janesko, R. Gomperts, B. Mennucci, H. P. Hratchian, J. v Ortiz, A. F. Izmaylov, J. L. Sonnenberg, D. Williams-Young, F. Ding, F. Lipparini, F. Egidi, J. Goings, B. Peng, A. Petrone, T. Henderson, D. Ranasinghe, V. G. Zakrzewski, J. Gao, N. Rega, G. Zheng, W. Liang, M. Hada, M. Ehara, K. Toyota, R. Fukuda, J. Hasegawa, M. Ishida, T. Nakajima, Y. Honda, O. Kitao, H. Nakai, T. Vreven, K. Throssell, J. A. Montgomery Jr., J. E. Peralta, F. Ogliaro, M. J. Bearpark, J. J. Heyd, E. N. Brothers, K. N. Kudin, V. N. Staroverov, T. A. Keith, R. Kobayashi, J. Normand, K. Raghavachari, A. P. Rendell, J. C. Burant, S. S. Iyengar, J. Tomasi, M. Cossi, J. M. Millam, M. Klene, C. Adamo, R. Cammi, J. W. Ochterski, R. L. Martin, K. Morokuma, O. Farkas, J. B. Foresman, D. J. Fox., *Gaussian, Inc., Wallingford CT, Gaussian 16 Revision C.01*, **2016**.
- (457) A. D. Becke., *Physical Review A*, **1988**, 38 (6), 3098–3100.
- (458) C. Lee, W. Yang, R. G. Parr., *Physical Review B*, **1988**, 37 (2), 785–789.
- (459) R. Dennington, T. A. Keith, J. M. Millam., *GaussView Version 6, Semichem Inc., Shawnee Mission, KS*, **2016**.
- (460) C. F. Leypold, M. Reiher, G. Brehm, M. O. Schmitt, S. Schneider, P. Matousek, M. Towrie., *Physical Chemistry Chemical Physics*, **2003**, 5 (6), 1149–1157.
- (461) C. Khantha, T. Yakhantip, C. M. Macneill, P. Pornprasit, V. Kruefu, N. Kungwan, R. C. Coffin, S. Phanichphant, D. L. Carroll., *Molecular Crystal and Liquid Crystals*, **2013**, 578 (1), 37–43.
- (462) P. Geerlings, F. de Proft, W. Langenaeker., *Chemical Reviews*, **2003**, 103 (5), 1793–1873.
- (463) R. G. Pearson., *Journal of Chemical Sciences*, **2005**, 117 (5), 369–377.
- (464) L. R. Domingo, M. Ríos-Gutiérrez, P. Pérez., *Molecules*, **2016**, 21 (6), 748.
- (465) A. B. Marahatta., *International Journal of Progressive Sciences and Technologies*, **2019**, 16 (1), 51–65.
- (466) M. Drissi, N. Benhalima, Y. Megrouss, R. Rachida, A. Chouaih, F. Hamzaoui., *Molecules*, **2015**, 20 (3), 4042–4054.
- (467) S. J. Luo, J. T. Yang, W. F. Du, A. Laref., *Journal of Physical Chemistry A*, **2011**, 115 (20), 5192–5200.
- (468) J. W. You, S. R. Bongu, Q. Bao, N. C. Panoiu., *Nanophotonics*, **2019**, 8 (1), 63–97.
- (469) Z. Miao, Y. Chu, L. Wang, W. Zhu, D. Wang., *Polymers (Basel)*, **2022**, 14 (8), 1516.



- (470) N. v. Kamanina, A. I. Plekhanov., *Optics and Spectroscopy*, **2002**, 93 (3), 408–415.
- (471) N. v. Kamanina, S. v. Serov, N. A. Shurpo, S. v. Likhomanova, D. N. Timonin, P. v. Kuzhakov, N. N. Rozhkova, I. v. Kityk, K. J. Plucinski, D. P. Uskokovic., *Journal of Materials Science: Materials in Electronics*, **2012**, 23 (8), 1538–1542.
- (472) L. Misoguti, A. T. Varela, F. D. Nunes, V. S. Bagnato, F. E. A. Melo, J. Mendes Filho, S. C. Zilio., *Opt Mater (Amst)*, **1996**, 6 (3), 147–152.
- (473) M. Fleck, A. M. Petrosyan., *Salts of Amino Acids: Crystallization, Structure and Properties*; Springer International Publishing: Switzerland, **2014**.
- (474) V. Kumar, N. Coluccelli, D. Polli., In *Molecular and Laser Spectroscopy (Chap 5-Coherent Optical Spectroscopy/Microscopy and Applications)*; Gupta, V. P., Ed.; Elsevier, **2018**; pp 87–115.
- (475) T. I. Kaya, U. Guvenc., *Dermatologic Therapy*, **2019**, 32 (3), e12907.
- (476) F. Liu, H. Xiao, H. Xu, S. Bo, C. Hu, Y. He, J. Liu, Z. Zhen, X. Liu, L. Qiu., *Dyes and Pigments*, **2017**, 136, 182–190.
- (477) Y. Sheng, Y. Jiang., *Journal of the Chemical Society, Faraday Transactions*, **1998**, 94 (13), 1829–1833.
- (478) A. H. G. Patel, A. A. K. Mohammed, P. A. Limacher, P. W. Ayers., *Journal of Physical Chemistry A*, **2017**, 121 (28), 5313–5323.
- (479) M. A. Spackman, D. Jayatilaka., *CrystEngComm*, **2009**, 11 (1), 19–32.
- (480) P. R. Spackman, M. J. Turner, J. J. McKinnon, S. K. Wolff, D. J. Grimwood, D. Jayatilaka, M. A. Spackman., *Journal of Applied Crystallography*, **2021**, 54 (3), 1006–1011.
- (481) S. L. Tan, M. M. Jotani, E. R. T. Tiekink., *Acta Crystallographica*, **2019**, E75 (3), 308–318.
- (482) S. K. Seth, N. C. Saha, S. Ghosh, T. Kar., *Chemical Physics Letters*, **2011**, 506 (4–6), 309–314.
- (483) N. E. Eltayeb, F. Şen, J. Lasri, M. A. Hussien, S. E. Elsilk, B. A. Babgi, H. Gökce, Y. Sert., *Journal of Molecular Structure*, **2020**, 1202, pp 127315.
- (484) R. Huey, G. M. Morris., *Using AutoDock 4 with AutoDocktools: A Tutorial.*; The Scripps Research Institute, Molecular Graphics Laboratory, pp. 54-56: La Jolla, CA, USA, **2008**.
- (485) J. Eberhardt, D. Santos-Martins, A. F. Tillack, S. Forli., *Journal of Chemical Information and Modeling*, **2021**, 61 (8), 3891–3898.

- (486) O. Trott, A. J. Olson., *Journal of Computational Chemistry*, **2010**, *31* (2), 455–461.
- (487) G. M. Morris, D. S. Goodsell, R. S. Halliday, R. Huey, W. E. Hart, R. K. Belew, A. J. Olson., *Journal of Computational Chemistry*, **1998**, *19* (14), 1639–1662.
- (488) P. T. Anastas, T. C. Williamson., *Green Chemistry : Frontiers in Benign Chemical Syntheses and Processes*; Oxford Science Publications: New York, **1998**.
- (489) M. Poliakoff, P. Anastas., *Nature*, **2001**, *413* (6853).
- (490) J. M. DeSimone., *Science (1979)*, **2002**, *297* (5582), 799–803.
- (491) R. A. Sheldon., *Green Chemistry*, **2016**, *18* (11), 3180–3183.
- (492) R. A. Sheldon., *Green Chemistry*, **2017**, *19* (1), 18–43.
- (493) P. Gupta, A. Mahajan., *RSC Advances*, **2015**, *5* (34), 26686–26705.
- (494) R. R. Magar, S. S. Choudhare, S. V. Padghan., *International Journal of Multidisciplinary Research (Epitome Journals)*, **2015**, *1* (7), 1–9.
- (495) E. Ezzatzadeh, F. Z. Hargalani, F. Shafaei., *Polycyclic Aromatic Compounds*, **2021**, *0* (0), 1–16.
- (496) T. Welton., *Green Chemistry*, **2011**, *13* (2), 225.
- (497) G. Centi, S. Perathoner., *Catalysis Today*, **2003**, *77* (4), 287–297.
- (498) P. T. Anastas, M. M. Kirchhoff, T. C. Williamson., *Applied Catalysis A: General*, **2001**, *221* (1–2), 3–13.
- (499) A. Dömling, U. Ivar., *Angewandte Chemie International Edition*, **2000**, *39* (18), 3168–3210.
- (500) J. E. Biggs-Houck, A. Younai, J. T. Shaw., *Current Opinion in Chemical Biology*, **2010**, *14* (3), 371–382.
- (501) B. Jiang, T. Rajale, W. Wever, S. J. Tu, G. Li., *Chemistry – An Asian Journal*, **2010**, *5* (11), 2318–2335.
- (502) S. Brauch, S. S. van Berkel, B. Westermann., *Chemical Society Reviews*, **2013**, *42* (12), 4948–4962.
- (503) C. de Graaff, E. Ruijter, R. V. A. Orru., *Chemical Society Reviews*, **2012**, *41* (10), 3969–4009.
- (504) M. C. Pirrung, K. das Sarma., *Tetrahedron*, **2005**, *61* (48), 11456–11472.
- (505) C. G. Neochoritis, T. Zarganes-Tzitzikas, K. Katsampoxaki-Hodgetts, A. Dömling., *Journal of Chemical Education*, **2020**, *97* (10), 3739–3745.

- (506) S. Garbarino, D. Ravelli, S. Protti, A. Basso., *Angewandte Chemie International Edition*, **2016**, 55 (50), 15476–15484.
- (507) G. van der Heijden, E. Ruijter, R. V. A. Orru., *Synlett*, **2013**, 24 (6), 666–685.
- (508) D. Insuasty, J. Castillo, D. Becerra, H. Rojas, R. Abonia., *Molecules*, **2020**, 25 (3), 576.
- (509) J. G. Lombardino, E. H. Wiseman., *Journal of Medicinal Chemistry*, **1974**, 17 (11), 1182–1188.
- (510) A. Chawla, A. Sharma, A. Kumar Sharma., *Der Pharma Chemica*, **2012**, 4 (1), 116–140.
- (511) R. Breslow., *Accounts of Chemical Research*, **1995**, 28 (3), 146–153.
- (512) A. P. Kulkarni, C. J. Tonzola, A. Babel, S. A. Jenekhe., *Chemistry of Materials*, **2004**, 16 (23), 4556–4573.
- (513) L. Streit, M. Moreau, J. Gaudin, E. Ebert, H. vanden Bossche., *Pesticide Biochemistry and Physiology*, **1991**, 40 (2), 162–168.
- (514) A. Husain, S. Drabu, N. Kumar, M. M. Alam, S. Bawa., *Journal of Pharmacy And Bioallied Sciences*, **2013**, 5 (2), 161.
- (515) T. Scior, D. M. Domeyer, K. Cuanalo-Contreras, S. A. Laufer., *Current Medicinal Chemistry*, **2011**, 18 (10), 1526–1539.
- (516) A. K. Takle, M. J. B. Brown, S. Davies, D. K. Dean, G. Francis, A. Gaiba, A. W. Hird, F. D. King, P. J. Lovell, A. Naylor, A. D. Reith, J. G. Steadman, D. M. Wilson., *Bioorganic & Medicinal Chemistry Letters*, **2006**, 16 (2), 378–381.
- (517) L. Wang, K. W. Woods, Q. Li, K. J. Barr, R. W. McCroskey, S. M. Hannick, L. Gherke, R. B. Credo, Y. H. Hui, K. Marsh, R. Warner, J. Y. Lee, N. Zielinski-Mozng, D. Frost, S. H. Rosenberg, H. L. Sham., *J Med Chem*, **2002**, 45 (8), 1697–1711.
- (518) R. A. Turner, C. F. Huebner, C. R. Scholz., *J Am Chem Soc*, **1949**, 71 (8), 2801–2803.
- (519) J. Miller., *Annals of Allergy*, **1963**, 21, 692–697.
- (520) A. Goyal, J. Singh, D. P. Pathak., *Journal of Pharmaceutical Technology, Research and Management*, **2013**, 1 (1), 69–79.
- (521) K. Gaffney, D. G. I. Scott., *British Journal of Rheumatology*, **1998**, 37 (8), 824–836.
- (522) J. Baharara, E. Amini, N. Nikdel, F. Salek-Abdollahi., *Avicenna Journal of Medical Biotechnology*, **2016**, 8 (3), 119.

- (523) J.-B. Tagne, S. Kakumanu, R. J. Nicolosi., *Molecular Pharmaceutics*, **2008**, 5 (6), 1055–1063.
- (524) R. S. Joshi, P. G. Mandhane, M. U. Shaikh, R. P. Kale, C. H. Gill., *Chinese Chemical Letters*, **2010**, 21 (4), 429–432.
- (525) C. Yu, M. Lei, W. Su, Y. Xie., *Synthetic Communications*, **2007**, 37 (19), 3301–3309.
- (526) S. D. Sharma, P. Hazarika, D. Konwar., *Tetrahedron Letters*, **2008**, 49 (14), 2216–2220.
- (527) J. N. Sangshetti, N. D. Kokare, S. A. Kotharkara, D. B. Shinde., *Journal of Chemical Sciences*, **2008**, 120 (5), 463–467.
- (528) S. N. Murthy, B. Madhav, Y. V. D. Nageswar., *Tetrahedron Letters*, **2010**, 51 (40), 5252–5257.
- (529) S. Samai, G. C. Nandi, P. Singh, M. S. Singh., *Tetrahedron*, **2009**, 65 (49), 10155–10161.
- (530) A. R. Khosropour., *Ultrasonics Sonochemistry*, **2008**, 15 (5), 659–664.
- (531) R. K. Sharma, C. Sharma., *Catalysis Communications*, **2011**, 12 (5), 327–331.
- (532) M. Kidwai, P. Mothsra, V. Bansal, R. K. Somvanshi, A. S. Ethayathulla, S. Dey, T. P. Singh., *Journal of Molecular Catalysis A: Chemical*, **2007**, 265 (1–2), 177–182.
- (533) G. H. Mahdavinia, A. M. Amani, H. Sepehrian., *Chinese Journal of Chemistry*, **2012**, 30 (3), 703–708.
- (534) H. Zang, Q. Su, Y. Mo, B. W. Cheng, S. Jun., *Ultrasonics Sonochemistry*, **2010**, 17 (5), 749–751.
- (535) M. Xia, Y. dong Lu., *Journal of Molecular Catalysis A: Chemical*, **2007**, 265 (1–2), 205–208.
- (536) M. Veerananarayana Reddy, Y. T. Jeong., *Journal of Fluorine Chemistry*, **2012**, 142, 45–51.
- (537) J. Jayram, V. Jeena., *Green Chemistry*, **2017**, 19 (24), 5841–5845.
- (538) J. Jayram, V. Jeena., *RSC Advances*, **2018**, 8 (66), 37557–37563.
- (539) K. Nikoofar, M. Haghghi, M. Lashanizadegan, Z. Ahmadvand., *Journal of Taibah University for Science*, **2015**, 9 (4), 570–578.
- (540) M. Kalhor, Z. Zarnegar., *RSC Advances*, **2019**, 9 (34), 19333–19346.

- (541) M. Kalhor, N. Khodaparast., *Research on Chemical Intermediates*, **2015**, *41* (5), 3235–3242.
- (542) A. Bamoniri, B. B. Fatemeh Mirjalili, S. Saleh., *RSC Advances*, **2018**, *8* (11), 6178–6182.
- (543) A. Khorramabadi-zad, M. Azadmanesh, S. Mohammadi., *South African Journal of Chemistry*, **2013**, *66* (1), 244–247.
- (544) N. V. Gandhare, R. G. Chaudhary, V. P. Meshram, J. A. Tanna, S. Lade, M. P. Gharpure, H. D. Juneja., *Journal of the Chinese Advanced Materials Society*, **2015**, *3* (4), 270–279.
- (545) Z. Varzi, M. S. Esmaili, R. Taheri-Ledari, A. Maleki., *Inorganic Chemistry Communications*, **2021**, *125*, 108465.
- (546) D. Kumar, D. N. Kommi, N. Bollineni, A. R. Patel, A. K. Chakraborti., *Green Chemistry*, **2012**, *14* (7), 2038–2049.
- (547) K. Sivakumar, A. Kathirvel, A. Lalitha., *Tetrahedron Letters*, **2010**, *51* (22), 3018–3021.
- (548) N. V. Shitole, K. F. Shelke, S. S. Sonar, S. A. Sadaphal, B. B. Shingate, M. S. Shingare., *Bull Korean Chem Soc*, **2009**, *30* (9), 1963–1966.
- (549) S. S. Dipake, M. K. Lande, A. S. Rajbhoj, S. T. Gaikwad., *Research on Chemical Intermediates*, **2021**, *47* (6), 2245–2261.
- (550) A. R. Khosropour., *Ultrasonics Sonochemistry*, **2008**, *15* (5), 659–664.
- (551) L. M. Wang, Y. H. Wang, H. Tian, Y. F. Yao, J. H. Shao, B. Liu., *Journal of Fluorine Chemistry*, **2006**, *127* (12), 1570–1573.
- (552) K. Nikoofar, M. Haghghi, M. Lashanizadegan, Z. Ahmadvand., *Journal of Taibah University for Science*, **2015**, *9* (4), 570–578.
- (553) M. Kidwai, P. Mothsra, V. Bansal, R. Goyal., *Monatshefte für Chemie / Chemical Monthly*, **2006**, *137* (9), 1189–1194.
- (554) M. Banazadeh, S. Amirnejat, S. Javanshir., *Frontiers in Chemistry*, **2020**, *8* (Article 596029), 1–15.
- (555) J. Safari, S. D. Khalili, S. H. Banitaba., *Synthetic Communications*, **2011**, *41* (16), 2359–2373.
- (556) J. Safari, S. D. Khalili, M. Rezaei, S. H. Banitaba, F. Meshkani., *Monatshefte für Chemie - Chemical Monthly*, **2010**, *141* (12), 1339–1345.
- (557) E. Eidi, M. Z. Kassae, Z. Nasresfahani., *Applied Organometallic Chemistry*, **2016**, *30* (7), 561–565.

- (558) R. Wang, C. Liu, G. Luo., *Green Chemistry Letters and Reviews*, **2010**, 3 (2), 101–104.
- (559) K. F. Shelke, S. B. Sapkal, S. S. Sonar, B. R. Madje, B. B. Shingate, M. S. Shingare., *Bull Korean Chem Soc*, **2009**, 30 (5), 1057–1060.
- (560) M. Vosoughi, F. Mohebbali, A. P. S. Bonakdar, H. A. Lordegani, A. R. Massah., *Bulgarian Chemical Communications*, **2015**, 47 (2), 607–612.
- (561) B. F. Mirjalili, A. Bamoniri, N. Mohaghegh., *Current Chemistry Letters*, **2013**, 2 (1), 35–42.
- (562) G. Brahmachari, S. Das., *Indian Journal of Chemistry - Section B*, **2013**, 52B, 387–393.
- (563) B. Maleki, H. K. Shirvan, F. Taimazi, E. Akbarzadeh., *International Journal of Organic Chemistry*, **2012**, 2 (1), 93–99.
- (564) N. V. Gandhare, R. G. Chaudhary, V. P. Meshram, J. A. Tanna, S. Lade, M. P. Gharpure, H. D. Juneja., *Journal of the Chinese Advanced Materials Society*, **2015**, 3 (4), 270–279.
- (565) A. Sedrpoushan, Z. Joshani, L. Fatollahi., *Letters in Organic Chemistry*, **2014**, 11 (4), 287–292.
- (566) F. Hatamjafari, H. Khojastehkouhi., *Oriental Journal of Chemistry*, **2014**, 30 (1), 329–331.
- (567) S. Balalaie, A. Arabanian, M. S. Hashtroudi., *Monatshefte für Chemie/Chemical Monthly*, **2000**, 131 (9), 945–948.
- (568) B. Valeur, I. Leray., *Coordination Chemistry Reviews*, **2000**, 205 (1), 3–40.
- (569) Y. Gabe, Y. Urano, K. Kikuchi, H. Kojima, T. Nagano., *J Am Chem Soc*, **2004**, 126 (10), 3357–3367.
- (570) S. L. Wiskur, H. Ait-Haddou, J. J. Lavigne, E. v. Anslyn., *Accounts of Chemical Research*, **2001**, 34 (12), 963–972.
- (571) E. L. Que, D. W. Domaille, C. J. Chang., *Chemical Reviews*, **2008**, 108 (5), 1517–1549.
- (572) E. L. Que, D. W. Domaille, C. J. Chang., *Chemical Reviews*, **2008**, 108 (10), 4328.
- (573) B. Sarkar., In *Metal Ions in Biological Systems Vol. 12 (Chap. 6 - Transport of Copper)*; Siegel, H., Siegel, A., Dekker, M., Eds.; New York, **1981**; pp 233–281.
- (574) F. M. Raymo., *Advanced Materials*, **2021**, 14 (6), 401–414.
- (575) D. J. Faulkner., *Natural Product Reports*, **2000**, 17 (1), 7–55.

- (576) J. Z. Ho, R. M. Mohareb, J. H. Ahn, T. B. Sim, H. Rapoport., *Journal of Organic Chemistry*, **2003**, *68* (1), 109–114.
- (577) A. R. Katritzky, C. W. Rees, E. F. V. Scriven., In *Comprehensive Heterocyclic Chemistry II, Vol. 2 (Chap 4.02 - Imidazoles)*; Katritzky, A. R., Rees, C. W., Scriven, E. F. V., Eds.; Oxford: New York, Pergamom, **1996**; pp 77–220.
- (578) L. de Luca., *Current Medicinal Chemistry*, **2006**, *13* (1), 1–23.
- (579) P. M. Colman, H. C. Freeman, J. M. Guss, M. Murata, V. A. Norris, J. A. M. Ramshaw, M. P. Venkatappa., *Nature*, **1978**, *272* (5651), 319–324.
- (580) E. I. Solomon, D. E. Heppner, E. M. Johnston, J. W. Ginsbach, J. Cirera, M. Qayyum, M. T. Kieber-Emmons, C. H. Kjaergaard, R. G. Hadt, L. Tian., *Chemical Reviews*, **2014**, *114* (7), 3659–3853.
- (581) M. Andersson, J. Hedín, P. Johansson, J. Nordström, M. Nydén., *Journal of Physical Chemistry A*, **2010**, *114* (50), 13146–13153.
- (582) V. Pascanu, G. González Miera, A. K. Inge, B. Martín-Matute., *J Am Chem Soc*, **2019**, *141* (18), 7223–7234.
- (583) Y. Li, R. T. Yang., *Langmuir*, **2007**, *23* (26), 12937–12944.
- (584) Q. Wang, Q. Gao, A. M. Al-Enizi, A. Nafady, S. Ma., *Inorganic Chemistry Frontiers*, **2020**, *7* (2), 300–339.
- (585) C. Chen, W. Zhang, J. Cong, M. Cheng, B. Zhang, H. Chen, P. Liu, R. Li, M. Safdari, L. Kloo, L. Sun., *ACS Energy Letters*, **2017**, *2* (2), 497–503.
- (586) S. S. Nadar, V. K. Rathod., *International Journal of Biological Macromolecules*, **2018**, *120* (Part B), 2293–2302.
- (587) S. Charoensuk, J. Tan, M. Sain, H. Manuspiya., *Nanomaterials*, **2021**, *11* (9), 2281.
- (588) S. Chettri, D. Brahman, B. Sinha, M. M. Jotani, E. R. T. Tiekink., *Acta Crystallographica*, **2019**, *E75* (11), 1664–1671.
- (589) G. M. Brown, R. Chidambaram., *Acta Crystallographica*, **1973**, *B29* (11), 2393–2403.
- (590) L. Yang, D. R. Powell, R. P. Houser., *Dalton Transactions*, **2007**, *Issue 9*, 955–964.
- (591) S. L. Tan, M. M. Jotani, E. R. T. Tiekink., *Acta Crystallographica*, **2019**, *E75* (3), 308–318.
- (592) C. B. Pinto, L. H. R. dos Santos, B. L. Rodrigues., *Acta Crystallographica*, **2019**, *C75* (Part 6), 707–716.

- (593) D. Das., *ChemistrySelect*, **2016**, *1* (9), 1959–1980.
- (594) S. V. Ley, A. W. Thomas., *Angewandte Chemie International Edition*, **2003**, *42* (44), 5400–5449.
- (595) R. Singha, S. Chettri, D. Brahman, B. Sinha, P. Ghosh., *Molecular Diversity*, **2022**, *26* (1), 505–511.
- (596) G. M. Sheldrick., *Acta Crystallographica*, **2015**, *C71* (1), 3–8.
- (597) M. Waheed, N. Ahmed, M. A. Alsharif, M. I. Alahmdi, S. Mukhtar., *ChemistrySelect*, **2017**, *2* (26), 7946–7950.
- (598) T. S. Rajasekar, P. Navamani, K. Jayamoorthy, N. Srinivasan., *Journal of Inorganic and Organometallic Polymers and Materials*, **2017**, *27* (4), 962–967.
- (599) S. Chauhan, V. Verma, D. Kumar, A. Kumar., *Synthetic Communications*, **2019**, *49* (11), 1427–1435.
- (600) A. Z. al Munsur, H. N. Roy, M. K. Imon., *Arabian Journal of Chemistry*, **2020**, *13* (12), 8807–8814.
- (601) S. H. Gebre., *Synthetic Communications*, **2021**, *51* (11), 1669–1699.
- (602) M. A. Zayed, M. A. Abdallah., *Egyptian Journal of Chemistry*, **2019**, *62* (11), 2143–2162.
- (603) D. Gustinčič, A. Kokalj., *Physical Chemistry Chemical Physics*, **2015**, *17* (43), 28602–28615.
- (604) L. Fabbrizzi, F. Foti, S. Patroni, P. Pallavicini, A. Taglietti., *Angewandte Chemie International Edition*, **2004**, *43* (38), 5073–5077.
- (605) Z. Li, X. Lou, H. Yu, Z. Li, J. Qin., *Macromolecules*, **2008**, *41* (20), 7433–7439.
- (606) Z. Song, W. Zhang, M. Jiang, H. H. Y. Sung, R. T. K. Kwok, H. Nie, I. D. Williams, B. Liu, B. Z. Tang., *Advanced Functional Materials*, **2016**, *26* (6), 824–832.
- (607) S. Suresh, N. Bhuvanesh, A. Raman, P. Sugumar, D. Padmanabhan, S. Easwaramoorthi, M. N. Ponnuswamy, S. Kavitha, R. Nandhakumar., *Journal of Photochemistry and Photobiology A: Chemistry*, **2019**, *385*, 112092.
- (608) Y. H. Lam, Y. Abramov, R. S. Ananthula, J. M. Elward, L. R. Hilden, S. O. Nilsson Lill, P. O. Norrby, A. Ramirez, E. C. Sherer, J. Mustakis, G. J. Tanoury., *Organic Process Research and Development*, **2020**, *24* (8), 1496–1507.
- (609) M. Evecen, H. Tanak., *Materials Science - Poland*, **2016**, *34* (4), 886–904.
- (610) S. Gümüş, L. Türker., *Heterocyclic Communications*, **2012**, *18* (1), 11–16.



- (611) P. Lienard, J. Gavartin, G. Boccardi, M. Meunier., *Pharmaceutical Research*, **2015**, 32 (1), 300–310.
- (612) H. J. Huang, H. W. Yu, C. Y. Chen, C. H. Hsu, H. Y. Chen, K. J. Lee, F. J. Tsai, C. Y. C. Chen., *J Taiwan Inst Chem Eng*, **2010**, 41 (6), 623–635.
- (613) D. Giugliano, A. Ceriello, K. Esposito., *The American Journal of Clinical Nutrition*, **2008**, 87 (1), 217S–222S.
- (614) G. S. Mohiuddin, S. Palaian, P. R. Shankar, K. G. Sam, M. Kumar., *International Journal of Pharmaceutical Sciences and Research*, **2019**, 10 (9), 4145–4148.
- (615) J. Ganugapati, A. Baldwa, S. Lalani., *Bioinformation*, **2012**, 8 (5), 220.
- (616) N. Satheesha Rai, B. Kalluraya, B. Lingappa, S. Shenoy, V. G. Puranic., *European Journal of Medicinal Chemistry*, **2008**, 43 (8), 1715–1720.
- (617) A. D. Becke., *The Journal of Chemical Physics*, **1993**, 98 (7), 5648–5652.
- (618) G. Varvounis, V. Gkalpinos, P. Theodorakopoulou, E. Tsemperlidou., In *Comprehensive Heterocyclic Chemistry IV (Chap 4.02 - Imidazoles)*; Black, D. S., Cossy, J., Stevens, C. V., Eds.; Elsevier: Oxford, **2022**; Vol. 4, pp 113–307.
- (619) P. Sykes., *A Guidebook to Mechanism in Organic Chemistry*, 6th ed.; Pearson Education: New Delhi, India, **2004**.
- (620) M. Belletête, J. F. Morin, M. Leclerc, G. Durocher., *Journal of Physical Chemistry A*, **2005**, 109 (31), 6953–6959.
- (621) D. Zhenming, S. Heping, L. Yufang, L. Diansheng, L. Bo., *Spectrochimica Acta Part A: Molecular and Biomolecular Spectroscopy*, **2011**, 78 (3), 1143–1148.
- (622) K. B. Benzon, H. T. Varghese, C. Y. Panicker, K. Pradhan, B. K. Tiwary, A. K. Nanda, C. van Alsenoy., *Spectrochimica Acta Part A: Molecular and Biomolecular Spectroscopy*, **2015**, 151, 965–979.
- (623) S. W. Xia, X. Xu, Y.-L. Sun, Y.-H. Fan, C.-F. Bi, D. M. Zhang, L.-R. Yang., *Chinese Journal of Structural Chemistry*, **2006**, 25 (2), 197–203.
- (624) M. Snehalatha, C. Ravikumar, I. Hubert Joe, N. Sekar, V. S. Jayakumar., *Spectrochimica Acta Part A: Molecular and Biomolecular Spectroscopy*, **2009**, 72 (3), 654–662.
- (625) T. A. Koopmans., *Physica*, **1934**, 1 (1–6), 104–113.
- (626) R. G. Parr, R. G. Pearson., *J Am Chem Soc*, **1983**, 105 (26), 7512–7516.
- (627) R. G. Parr, L. V. Szentpály, S. Liu., *J Am Chem Soc*, **1999**, 121 (9), 1922–1924.

- (628) S. Mandal, D. K. Poria, D. K. Seth, P. S. Ray, P. Gupta., *Polyhedron*, **2014**, *73*, 12–21.
- (629) P. Jaramillo, P. Pérez, R. Contreras, W. Tiznado, P. Fuentealba., *Journal of Physical Chemistry A*, **2006**, *110* (26), 8181–8187.
- (630) N. P. G. Roeges., *A Guide to the Complete Interpretation of Infrared Spectra of Organic Structures*; John Wiley and Sons Inc.: New York, **1994**.
- (631) B. C. Smith., *Infrared Spectral Interpretation, A Systematic Approach*, 1st ed.; CRC Press: Washington, DC, **1999**; Vol. 2.
- (632) P. Politzer, D. G. Truhlar., *Chemical Applications of Atomic and Molecular Electrostatic Potentials*; Plenum Press: New York, **1981**.
- (633) E. Scrocco, J. Tomasi., *Advances in Quantum Chemistry*, **1978**, *11* (C), 115–193.
- (634) P. Politzer, J. S. Murray., In *Theoretical Biochemistry and Molecular Biophysics: A Comprehensive Survey, Protein*; Beveridge, D. L., Lavery, R., Eds.; Adenine Press: Schenectady, New York, **1991**; Vol. 2.
- (635) E. Scrocco, J. Tomasi., *Topics in Current Chemistry*, **1973**, *42*, 95–170.
- (636) *Principles and Applications of Nonlinear Optical Materials*, 1st ed.; Munn, R. W., Ironside, C. N., Eds.; Springer Dordrecht: Netherlands, **1993**.
- (637) A. Migalska-Zalas, K. el Korchi, T. Chtouki., *Optical and Quantum Electronics*, **2018**, *50(11)* (Article no. 389), 1–10.
- (638) M. U. Khan, M. Khalid, S. Asim, Momina, R. Hussain, K. Mahmood, J. Iqbal, M. N. Akhtar, A. Hussain, M. Imran, A. Irfan, A. Ali, M. F. ur Rehman, Y. Jiang, C. Lu., *Frontiers in Materials*, **2021**, *8* (Article 719971), 287.
- (639) M. R. S. A. Janjua., *Journal of the Iranian Chemical Society*, **2017**, *14* (9), 2041–2054.
- (640) V. M. Geskin, C. Lambert, J. L. Brédas., *J Am Chem Soc*, **2003**, *125* (50), 15651–15658.
- (641) M. Beytur, F. Kardaş, O. Akyıldırım, A. Özkan, B. Bankoğlu, H. Yüksek, M. L. Yola, N. Atar., *Journal of Molecular Liquids*, **2018**, *251*, 212–217.
- (642) S. Muthu, T. Rajamani, M. Karabacak, A. M. Asiri., *Spectrochimica Acta Part A: Molecular and Biomolecular Spectroscopy*, **2014**, *122*, 1–14.
- (643) L. G. Ferreira, R. N. dos Santos, G. Oliva, A. D. Andricopulo., *Molecules*, **2015**, *20* (7), 13384–13421.
- (644) X.-Y. Meng, H.-X. Zhang, M. Mezei, M. Cui., *Current Computer-Aided Drug Design*, **2011**, *7* (2), 146–157.

- (645) A. T. Kharroubi, H. M. Darwish., *World J Diabetes*, **2015**, 6 (6), 867.
- (646) A. B. Olokoba, O. A. Obateru, L. B. Olokoba., *Oman Medical Journal*, **2012**, 27 (4), 269–273.
- (647) S. A. Ashraf, A. E. O. Elkhalfa, K. Mehmood, M. Adnan, M. A. Khan, N. E. Eltoun, A. Krishnan, M. S. Baig., *Molecules*, **2021**, 26 (19), 5957.
- (648) R. Chaturvedi, C. Desai, P. Patel, A. Shah, R. K. Dikshit., *Perspectives in Clinical Research*, **2018**, 9 (1), 15–22.
- (649) J. C. Lee, J. T. Laydon, P. C. McDonnell, T. F. Gallagher, S. Kumar, D. Green, D. McNulty, M. J. Blumenthal, J. R. Keys, S. W. Land Vatter, J. E. Strickler, M. M. McLaughlin, I. R. Siemens, S. M. Fisher, G. P. Livi, J. R. White, J. L. Adams, P. R. Young., *Nature*, **1994**, 372 (6508), 739–746.
- (650) K. L. Binns, P. P. Taylor, F. Sicheri, T. Pawson, S. J. Holland., *Molecular and Cellular Biology*, **2000**, 20 (13), 4791–4805.
- (651) S. Hari., *Journal of Applied Pharmaceutical Science*, **2019**, 9 (7), 18–26.
- (652) K. Boussey, F. M. Belpaire, J. van de Voorde., In *The Practice of Medicinal Chemistry*; Wermuth, C. G., Ed.; Elsevier Science, **2008**; pp 635–654.
- (653) F. Ntie-Kang, L. L. Lifongo, J. A. Mbah, L. C. Owono Owono, E. Megnassan, L. M. Mbaze, P. N. Judson, W. Sippl, S. M. N. Efange., In *Silico Pharmacology*, **2013**, 1(1) (Article 12), 1–11.
- (654) K. Ohtawara, H. Teramae., *Chemical Physics Letters*, **2004**, 390 (1–3), 84–88.
- (655) J. Eberhardt, D. Santos-Martins, A. F. Tillack, S. Forli., *Journal of Chemical Information and Modeling*, **2021**, 61 (8), 3891–3898.
- (656) G. M. Morris, D. S. Goodsell, R. S. Halliday, R. Huey, W. E. Hart, R. K. Belew, A. J. Olson., *Journal of Computational Chemistry*, **1998**, 19 (14), 1639–1662.
- (657) S. Zangade, P. Patil., *Current Organic Chemistry*, **2019**, 23 (21), 2295–2318.
- (658) T. T. Nguyen, P. H. Tran., *RSC Advances*, **2020**, 10 (16), 9663–9671.
- (659) L. Biesen, T. J. J. Müller., *Advanced Synthesis & Catalysis*, **2021**, 363 (4), 980–1006.
- (660) B. M. Sahoo, B. V. V. R. Kumar, J. Panda, S. C. Dinda., *Journal of Nanoparticles*, **2013**, 2013 (Article ID 780786), 1–6.
- (661) P. Costanzo, M. Nardi, M. Oliverio., *European Journal of Organic Chemistry*, **2020**, 2020 (26), 3954–3964.
- (662) B. Mohammadi, F. K. Behbahani., *Molecular Diversity*, **2018**, 22 (2), 405–446.

- (663) R. Kaur, S. Chaudhary, K. Kumar, M. K. Gupta, R. K. Rawal., *European Journal of Medicinal Chemistry*, **2017**, *132*, 108–134.
- (664) J. Lloyd, H. J. Finlay, K. Atwal, A. Kover, J. Prol, L. Yan, R. Bhandaru, W. Vaccaro, T. Huynh, C. S. Huang, M. L. Conder, T. Jenkins-West, H. Sun, D. Li, P. Levesque., *Bioorganic & Medicinal Chemistry Letters*, **2009**, *19* (18), 5469–5473.
- (665) J. Lloyd, H. J. Finlay, W. Vacarro, T. Hyunh, A. Kover, R. Bhandaru, L. Yan, K. Atwal, M. L. Conder, T. Jenkins-West, H. Shi, C. Huang, D. Li, H. Sun, P. Levesque., *Bioorganic & Medicinal Chemistry Letters*, **2010**, *20* (4), 1436–1439.
- (666) E. W. Hurst, R. Hull., *Journal of Medicinal Chemistry*, **1961**, *3* (2), 215–229.
- (667) C. O. Kappe., *European Journal of Medicinal Chemistry*, **2000**, *35* (12), 1043–1052.
- (668) L. M. Ramos, B. C. Guido, C. C. Nobrega, J. R. Corrêa, R. G. Silva, H. C. B. de Oliveira, A. F. Gomes, F. C. Gozzo, B. A. D. Neto., *Chemistry – A European Journal*, **2013**, *19* (13), 4156–4168.
- (669) R. Sharma, S. S. Jadav, S. Yasmin, S. Bhatia, H. Khalilullah, M. J. Ahsan., *Medicinal Chemistry Research*, **2015**, *24* (2), 636–644.
- (670) C. A. Bewley, S. Ray, F. Cohen, S. K. Collins, L. E. Overman., *Journal of Natural Products*, **2004**, *67* (8), 1319–1324.
- (671) S. Tcherniuk, R. van Lis, F. Kozielski, D. A. Skoufias., *Biochemical Pharmacology*, **2010**, *79* (6), 864–872.
- (672) G. Fitzharris., *Curr Biol*, **2012**, *22* (5), 437–444.
- (673) B. N. Acharya, G. B. D. Rao, D. Kumar, P. Kumar, M. P. Kaushik., *Medicinal Chemistry Research*, **2015**, *24* (4), 1763–1775.
- (674) P. Lacotte, D. A. Buisson, Y. Ambroise., *European Journal of Medicinal Chemistry*, **2013**, *62*, 722–727.
- (675) N. Singh, J. Kaur, P. Kumar, S. Gupta, N. Singh, A. Ghosal, A. Dutta, A. Kumar, R. Tripathi, M. I. Siddiqi, C. Mandal, A. Dube., *Parasitology Research*, **2009**, *105* (5), 1317–1325.
- (676) K. L. Dhumaskar, S. N. Meena, S. C. Ghadi, S. G. Tilve., *Bioorganic & Medicinal Chemistry Letters*, **2014**, *24* (13), 2897–2899.
- (677) A. Khan, J. Hashim, N. Arshad, I. Khan, N. Siddiqui, A. Wadood, M. Ali, F. Arshad, K. M. Khan, M. I. Choudhary., *Bioorganic Chemistry*, **2016**, *64*, 85–96.
- (678) F. Celik, M. Arslan, M. O. Kaya, E. Yavuz, N. Gencer, O. Arslan., *Artificial Cells, Nanomedicine and Biotechnology*, **2014**, *42* (1), 58–62.

- (679) A. O. Bryzgalov, M. P. Dolgikh, I. v. Sorokina, T. G. Tolstikova, V. F. Sedova, O. P. Shkurko., *Bioorganic & Medicinal Chemistry Letters*, **2006**, *16* (5), 1418–1420.
- (680) F. Cohen, L. E. Overman, S. K. Ly Sakata., *Organic Letters*, **1999**, *1* (13), 2169–2172.
- (681) S. Mondal, M. A. Mondal., *Journal of Heterocyclic Chemistry*, **2020**, *57* (12), 4175–4180.
- (682) M. Khashaei, L. Kafi-Ahmadi, S. Khademinia, A. Poursattar Marjani, E. Nozad., *Scientific Reports*, **2022**, *12* (1), 1–15.
- (683) Z. Karimi-Jaberi, M. S. Moaddeli., *ISRN Organic Chemistry*, **2012**, *2012* (Article ID 474626).
- (684) S. J. Kim, S. R. McAlpine., *Molecules*, **2013**, *18* (1), 1111–1121.
- (685) S. S. Panda, P. Khanna, L. Khanna., *Current Organic Chemistry*, **2012**, *16* (4), 507–520.
- (686) E. Kolvari, N. Koukabi, O. Armandpour., *Tetrahedron*, **2014**, *70* (6), 1383–1386.
- (687) B. K. Banik, A. T. Reddy, A. Datta, C. Mukhopadhyay., *Tetrahedron Letters*, **2007**, *48* (41), 7392–7394.
- (688) V. Polshettiwar, R. S. Varma., *Tetrahedron Letters*, **2007**, *48* (41), 7343–7346.
- (689) K. K. Pasunooti, H. Chai, C. N. Jensen, B. K. Gorityala, S. Wang, X. W. Liu., *Tetrahedron Letters*, **2011**, *52* (1), 80–84.
- (690) F. Dong, L. Jun, Z. Xinli, Y. Zhiwen, L. Zuliang., *Journal of Molecular Catalysis A: Chemical*, **2007**, *274* (1), 208–211.
- (691) A. Kuraitheerthakumaran, S. Pazhamalai, M. Gopalakrishnan., *Arabian Journal of Chemistry*, **2016**, *9* (Suppl. 1), S461–S465.
- (692) X. Chen, Y. Peng., *Catalysis Letters*, **2008**, *122* (3–4), 310–313.
- (693) S. L. Jain, J. K. Joseph, B. Sain., *Catalysis Letters*, **2007**, *115* (1–2), 52–55.
- (694) C. Ramalingan, S. J. Park, I. S. Lee, Y. W. Kwak., *Tetrahedron*, **2010**, *66* (16), 2987–2994.
- (695) F. Tamaddon, Z. Razmi, A. A. Jafari., *Tetrahedron Letters*, **2010**, *51* (8), 1187–1189.
- (696) H. Valizadeh, A. Shockravi., *Heteroatom Chemistry*, **2009**, *20* (5), 284–288.
- (697) S. P. Bahekar, P. B. Sarode, M. P. Wadekar, H. S. Chandak., *Journal of Saudi Chemical Society*, **2017**, *21* (4), 415–419.

- (698) A. Khorshidi, K. Tabatabaiean, H. Azizi, M. Aghaei-Hashjin, E. Abbaspour-Gilandeh., *RSC Advances*, **2017**, 7 (29), 17732–17740.
- (699) M. M. Khodaei, A. R. Khosropour, M. Beygzadeh., *Synthetic Communications*, **2004**, 34 (9), 1551–1557.
- (700) S. Asghari, M. Tajbakhsh, B. J. Kenari, S. Khaksar., *Chinese Chemical Letters*, **2011**, 22 (2), 127–130.
- (701) X. H. Chen, X. Y. Xu, H. Liu, L. F. Cun, L. Z. Gong., *J Am Chem Soc*, **2006**, 128 (46), 14802–14803.
- (702) J. Safaei Ghomi, R. Teymuri, A. Ziarati., *Monatshefte fur Chemie*, **2013**, 144 (12), 1865–1870.
- (703) M. Zeinali-Dastmalbaf, A. Davoodnia, M. M. Heravi, N. Tavakoli-Hoseini, A. Khojastehnezhad, H. A. Zamani., *Bull Korean Chem Soc*, **2011**, 32 (2), 656–658.
- (704) S. D. Salim, K. G. Akamanchi., *Catalysis Communications*, **2011**, 12 (12), 1153–1156.
- (705) S. Rostamnia, A. Morsali., *RSC Advances*, **2014**, 4 (21), 10514–10518.
- (706) S. Chancharunee, P. Pinhom, M. Pohmakotr, P. Perlmutter., *Synthetic Communications*, **2009**, 39 (5), 880–886.
- (707) N. Firoozeh, S. Rezazadeh, C. Izanloo., *J Mex Chem Soc*, **2017**, 61 (3), 241–249.
- (708) M. Nasr-Esfahani, M. Montazerozohori, M. Aghel-Mirrezaee, H. Kashi., *Journal of the Chilean Chemical Society*, **2014**, 59 (1), 2311–2314.
- (709) I. S. Zorkun, S. Saraç, S. Çelebi, K. Erol., *Bioorganic & Medicinal Chemistry*, **2006**, 14 (24), 8582–8589.
- (710) K. S. Atwal, G. C. Rovnyak, B. C. O'Reilly, J. Schwartz., *Journal of Organic Chemistry*, **1989**, 54 (25), 5898–5907.
- (711) Z. Maliga, T. M. Kapoor, T. J. Mitchison., *Chemistry & Biology*, **2002**, 9 (9), 989–996.
- (712) S. DeBonis, J. P. Simorre, I. Crevel, L. Lebeau, D. A. Skoufias, A. Blanzzy, C. Ebel, P. Gans, R. Cross, D. D. Hackney, R. H. Wade, F. Kozielski., *Biochemistry*, **2003**, 42 (2), 338–349.
- (713) M. Brands, R. Endermann, R. Gahlmann, J. Krüger, S. Raddatz., *Bioorganic & Medicinal Chemistry Letters*, **2003**, 13 (2), 241–245.
- (714) M. M. Ghorab, S. M. Abdel-Gawad, M. S. A. El-Gaby., *Il Farmaco*, **2000**, 55 (4), 249–255.

- (715) C. Oliver Kappe, W. M. F. Fabian, M. A. Semones., *Tetrahedron*, **1997**, 53 (8), 2803–2816.
- (716) A. D. Patil, N. V. Kumar, W. C. Kokke, M. F. Bean, A. J. Freyer, C. de Brosse, S. Mai, A. Truneh, D. J. Faulkner, B. Carte, A. L. Breen, R. P. Hertzberg, R. K. Johnson, J. W. Westley, B. C. M. Potts., *Journal of Organic Chemistry*, **1995**, 60 (5), 1182–1188.
- (717) S. K. Sam, S. C. Bo, H. L. Jae, K. L. Ki, H. L. Tae, H. K. Young, H. Shin., *Synlett*, **2009**, 2009 (4), 599–602.
- (718) K. Yamamoto, Y. G. Chen, F. G. Buono., *Organic Letters*, **2005**, 7 (21), 4673–4676.
- (719) X. Wang, Z. Quan, Z. Zhang., *Tetrahedron*, **2007**, 63 (34), 8227–8233.
- (720) X.-C. Wang, Z.-J. Quan, Z. Zhang, Y.-J. Liu, P.-Y. Ji., *Letters in Organic Chemistry*, **2007**, 4, 370–373.
- (721) R. Pérez, T. Beryozkina, O. I. Zbruyev, W. Haas, C. O. Kappe., *Journal of Combinatorial Chemistry*, **2002**, 4 (5), 501–510.
- (722) A. Lengar, C. O. Kappe., *Organic Letters*, **2004**, 6 (5), 771–774.
- (723) B. Khanetsky, D. Dallinger, C. O. Kappe., *Journal of Combinatorial Chemistry*, **2004**, 6 (6), 884–892.
- (724) A. D. Bochevarov, M. A. Watson, J. R. Greenwood, D. M. Philipp., *Journal of Chemical Theory and Computation*, **2016**, 12 (12), 6001–6019.
- (725) M. Mutailipu, Z. Xie, X. Su, M. Zhang, Y. Wang, Z. Yang, M. R. S. A. Janjua, S. Pan., *J Am Chem Soc*, **2017**, 139 (50), 18397–18405.
- (726) A. K. Sharma, W. M. C. Sameera, M. Jin, L. Adak, C. Okuzono, T. Iwamoto, M. Kato, M. Nakamura, K. Morokuma., *J Am Chem Soc*, **2017**, 139 (45), 16117–16125.
- (727) N. D. Yilmazer, M. Korth., *Journal of Physical Chemistry B*, **2013**, 117 (27), 8075–8084.
- (728) M. Evecen, H. Tanak., *Materials Science - Poland*, **2016**, 34 (4), 886–904.
- (729) X. Ma, D. Chang, C. Zhao, R. Li, X. Huang, Z. Zeng, X. Huang, Y. Jia., *Journal of Materials Chemistry C*, **2018**, 6 (48), 13241–13249.
- (730) S. Naseem, M. Khalid, M. N. Tahir, M. A. Halim, A. A. C. Braga, M. M. Naseer, Z. Shafiq., *Journal of Molecular Structure*, **2017**, 1143, 235–244.
- (731) M. Zheng, X. Liu, Y. Xu, H. Li, C. Luo, H. Jiang., *Trends in Pharmacological Sciences*, **2013**, 34 (10), 549–559.

- (732) A. Daina, M. C. Blatter, V. Baillie Gerritsen, P. M. Palagi, D. Marek, I. Xenarios, T. Schwede, O. Michielin, V. Zoete., *Journal of Chemical Education*, **2017**, *94* (3), 335–344.
- (733) M. Xiang, Y. Cao, W. Fan, L. Chen, Y. Mo., *Combinatorial Chemistry & High Throughput Screening*, **2012**, *15* (4), 328–337.
- (734) A. Maitra, A. K. Abbas., In *Robbins & Cotran Pathologic Basis of Disease (Chapter 24 - Endocrine System)*; Kumar, V., Abbas, A. K., Fausto, N., Aster, J. C., Eds.; Saunders: Philadelphia, **2005**; pp 1156–1226.
- (735) E. C. Chao, R. R. Henry., *Nature Reviews Drug Discovery*, **2010**, *9* (7), 551–559.
- (736) S. Vorberg, I. Koch, C. Buning., *Journal of Cheminformatics*, **2012**, *4* (S1), P41.
- (737) S. Faham, A. Watanabe, G. M. Besserer, D. Cascio, A. Specht, B. A. Hirayama, E. M. Wright, J. Abramson., *Science (1979)*, **2008**, *321* (5890), 810–814.
- (738) J. J. Marín-Peñalver, I. Martín-Timón, C. Sevillano-Collantes, F. J. del Cañizo-Gómez., *World Journal of Diabetes*, **2016**, *7* (17), 395.
- (739) I. D. Kuntz., *Science (1979)*, **1992**, *257* (5073), 1078–1082.
- (740) J. Drews., *Science*, **2000**, *287* (5460), 1960–1964.
- (741) I. Muegge, M. Rarey., In *Reviews in Computational Chemistry (Chap 1 - Small Molecule Docking and Scoring)*; Lipkowitz, K. B., Boyd, D. B., Eds.; John Wiley & Sons, Ltd: New York, **2001**; Vol. 17, pp 1–60.
- (742) S. F. Sousa, P. A. Fernandes, M. J. Ramos., *Proteins*, **2006**, *65* (1), 15–26.
- (743) A. P. Caricato, W. Ge, A. D. Stiff-Roberts., In *Advances in the Application of Lasers in Materials Science, (Chap 10 - UV- and RIR-MAPLE: Fundamentals and applications)*; Ossi, P. M., Ed.; Springer Verlag, **2018**; pp 275–308.
- (744) L. Ferreira, R. dos Santos, G. Oliva, A. Andricopulo., *Molecules*, **2015**, *20* (7), 13384–13421.
- (745) (Editorial) Eric C. Westman., *Frontiers in Nutrition*, **2021**, *8* (827990), 1–5.
- (746) C. Hale, M. Wang., *Mini Reviews in Medicinal Chemistry*, **2008**, *8* (7), 702–710.
- (747) R. Huey, G. M. Morris., *The Scripps Research Institute, USA*, **2008**, *8*, 54–56.
- (748) M. A. Alamri, M. Tahir ul Qamar, M. U. Mirza, R. Bhadane, S. M. Alqahtani, I. Muneer, M. Froeyen, O. M. H. Salo-Ahen., *Journal of Biomolecular Structure and Dynamics*, **2021**, *39* (13), 4936–4948.
- (749) H. Brahmhatt, M. Molnar, V. Pavić., *Karbala International Journal of Modern Science*, **2018**, *4* (2), 200–206.



- (750) A. Verma, S. Joshi, D. Singh., *Journal of Chemistry*, **2013**, 2013 (Article ID 392412).
- (751) P. Manocha, S. R. Wakode, A. Kaur, H. Kumar., *International Journal of Pharmaceutical Science and Research*, **2016**, 1 (7), 12–16.
- (752) A. Reyes-Arellano, O. Gómez-García, J. Torres-Jaramillo., *Medicinal Chemistry*, **2016**, 6 (9), 561–566.
- (753) D. H. Romero, V. E. T. Heredia, O. García-Barradas, Ma. E. M. López, E. S. Pavón., *Journal of Chemistry and Biochemistry*, **2014**, 2 (2), 45–83.
- (754) K. Anand, S. Wakode., *International Journal of Chemical Studies*, **2017**, 5 (2), 350–362.
- (755) B. K. Verma, S. Kapoor, U. Kumar, S. Pandey, P. Arya., *Indian Journal of Pharmaceutical and Biological Research*, **2017**, 5 (01), 1–9.
- (756) M. W. Bhade, P. R. Rajput., *International Journal of Applied and Pure Science and Agriculture*, **2016**, 2 (11), 80–84.
- (757) R. Katikireddy, R. Kakkerla, M. P. S. M. Krishna, G. Durgaiyah, Y. N. Reddy, M. Satyanarayana., *Heterocyclic Communications*, **2019**, 25 (1), 27–38.
- (758) D. R. MacFarlane, K. R. Seddon., *Australian Journal of Chemistry*, **2007**, 60 (1), 3–5.
- (759) R. Rogers, G. Garau., *Materials world*, **2007**, 15 (12), 25–27.
- (760) G. Laus, J. Sladlwieser, W. Klötzer., *Synthesis (Stuttg)*, **1989**, 1989 (10), 773–775.
- (761) K. Hayes., *Journal of Heterocyclic Chemistry*, **1974**, 11 (4), 615–618.
- (762) A. Albini, S. Pietra., *Heterocyclic N-Oxides*; CRC Press: Boca Raton, Ann Arbor, Boston USA, **1991**.
- (763) A. Albini., *Synthesis (Stuttg)*, **1993**, 1993 (3), 263–277.
- (764) Y. Wang, L. Zhang., *Synthesis (Stuttg)*, **2015**, 47 (03), 289–305.
- (765) J. V. Quagliano, J. Fujita, G. Franz, D. J. Phillips, J. A. Walmsley, S. Y. Tyree., *J Am Chem Soc*, **1961**, 83 (18), 3770–3773.
- (766) R. B. da Silva, V. B. Loback, K. Salomão, S. L. de Castro, J. L. Wardell, S. M. S. V. Wardell, T. E. M. M. Costa, C. Penido, M. D. G. M. de Oliveira Henriques, S. A. Carvalho, E. F. da Silva, C. A. M. Fraga., *Molecules*, **2013**, 18 (3), 3445–3457.
- (767) M. Witschel., *Bioorganic & Medicinal Chemistry*, **2009**, 17 (12), 4221–4229.

- (768) T. B. Stensbøl, P. Uhlmann, S. Morel, B. L. Eriksen, J. Felding, H. Kromann, M. B. Hermit, J. R. Greenwood, H. Braüner-Osborne, U. Madsen, F. Junager, P. Krogsgaard-Larsen, M. Begtrup, P. Vedsø., *Journal of Medicinal Chemistry*, **2002**, 45 (1), 19–31.
- (769) M. L. Richardson, K. A. Croughton, C. S. Matthews, M. F. G. Stevens., *Journal of Medicinal Chemistry*, **2004**, 47 (16), 4105–4108.
- (770) O. K. Kim, L. K. Garrity-Ryan, V. J. Bartlett, M. C. Grier, A. K. Verma, G. Medjanis, J. E. Donatelli, A. B. Macone, S. K. Tanaka, S. B. Levy, M. N. Alekshun., *Journal of Medicinal Chemistry*, **2009**, 52 (18), 5626–5634.
- (771) G. Mloston, M. Celeda, M. Jasinski, K. Urbaniak, P. J. Boratynski, P. R. Schreiner, H. Heimgartner., *Molecules*, **2019**, 24 (23), 4398.
- (772) F. J. Allan, G. G. Allan., *Chemistry & Industry*, **1964**, 44, 1837–1837.
- (773) P. A. Nikitina, L. G. Kuz'Mina, V. P. Perevalov, I. I. Tkach., *Tetrahedron*, **2013**, 69 (15), 3249–3256.
- (774) P. A. Nikitina, A. S. Peregudov, T. Y. Koldaeva, L. G. Kuz'Mina, E. I. Adiulin, I. I. Tkach, V. P. Perevalov., *Tetrahedron*, **2015**, 71 (33), 5217–5228.
- (775) S. Bartz, B. Blumenröder, A. Kern, J. Fleckenstein, S. Frohnapfel, J. Schatz, A. Wagner., *Zeitschrift für Naturforschung*, **2009**, 64b (6), 629–638.
- (776) S. O. Chua, M. J. Cook, A. R. Katritzky., *Journal of the Chemical Society B: Physical Organic*, **1971**, 2350–2355.
- (777) W. Schilf, L. Stefaniak, M. Witanowski, G. A. Webb., *Journal of Molecular Structure*, **1986**, 140 (3–4), 311–315.
- (778) M. Boiani, H. Cerecetto, M. Gonzalez, O. E. Piro, E. E. Castellano., *Journal of Physical Chemistry A*, **2004**, 108 (51), 11241–11248.
- (779) L. H. Abdel-Rahman, A. A. Abdelhamid, A. M. Abu-Dief, M. R. Shehata, M. A. Bakheet., *Journal of Molecular Structure*, **2020**, 1200, 127034.
- (780) T. Shan, Z. Gao, X. Tang, X. He, Y. Gao, J. Li, X. Sun, Y. Liu, H. Liu, B. Yang, P. Lu, Y. Ma., *Dyes and Pigments*, **2017**, 142, 189–197.
- (781) K. Fukui, T. Yonezawa, H. Shingu., *The Journal of Chemical Physics*, **2004**, 20 (4), 722–725.
- (782) A. Madanagopal, S. Periandy, P. Gayathri, S. Ramalingam, S. Xavier, V. K. Ivanov., *Journal of Taibah University for Science*, **2017**, 11 (6), 975–996.
- (783) E. M. Maya, A. W. Snow, J. S. Shirk, R. G. S. Pong, S. R. Flom, G. L. Roberts., *Journal of Materials Chemistry*, **2003**, 13 (7), 1603–1613.

- (784) Z. Sofiani, S. Khannyra, A. Boucetta, M. ElJouad, K. Bouchouit, H. Serrar, S. Boukhris, A. Souizi, A. Migalska-Zalas., *Optical and Quantum Electronics*, **2016**, 48 (282).
- (785) H. Sung, J. Ferlay, R. L. Siegel, M. Laversanne, I. Soerjomataram, A. Jemal, F. Bray., *CA : A Cancer Journal for Clinicians*, **2021**, 71 (3), 209–249.
- (786) L. A. Torre, F. Bray, R. L. Siegel, J. Ferlay, J. Lortet-Tieulent, A. Jemal., *CA: A Cancer Journal for Clinicians*, **2015**, 65 (2), 87–108.
- (787) Z. Bai, R. Gust., *Arch Pharm (Weinheim)*, **2009**, 342 (3), 133–149.
- (788) B. Pathare, T. Bansode., *Results in Chemistry*, **2021**, 3, 100200.
- (789) O. O. Ajani, D. v. Aderohunmu, C. O. Ikpo, A. E. Adedapo, I. O. Olanrewaju., *Arch Pharm (Weinheim)*, **2016**, 349 (7), 475–506.
- (790) A. R. Katritzky, X. Lan, J. Z. Yang, O. v. Denisko., *Chemical Reviews*, **1998**, 98 (2), 409–548.
- (791) Z. Wang, X. Deng, S. Xiong, R. Xiong, J. Liu, L. Zou, X. Lei, X. Cao, Z. Xie, Y. Chen, Y. Liu, X. Zheng, G. Tang., *Natural Product Research*, **2018**, 32 (24), 2900–2909.
- (792) G. R. Morais, E. Palma, F. Marques, L. Gano, M. C. Oliveira, A. Abrunhosa, H. V. Miranda, T. F. Outeiro, I. Santos, A. Paulo., *Journal of Heterocyclic Chemistry*, **2017**, 54 (1), 255–267.
- (793) V. Onnis, M. Demurtas, A. Deplano, G. Balboni, A. Baldisserotto, S. Manfredini, S. Pacifico, S. Liekens, J. Balzarini., *Molecules*, **2016**, 21 (5), 579.
- (794) R. Sharma, A. Bali, B. B. Chaudhari., *Bioorganic & Medicinal Chemistry Letters*, **2017**, 27 (13), 3007–3013.
- (795) M. M. Vandeputte, K. van Uytfanghe, N. K. Layle, D. M. st. Germaine, D. M. Iula, C. P. Stove., *ACS Chemical Neuroscience*, **2021**, 12 (7), 1241–1251.
- (796) A. Noor, N. G. Qazi, H. Nadeem, A. ullah Khan, R. Z. Paracha, F. Ali, A. Saeed., *Chemistry Central Journal*, **2017**, 11 (85), 1–13.
- (797) T. Iwahi, H. Satoh, M. Nakao, T. Iwasaki, T. Yamazaki, K. Kubo, T. Tamura, A. Imada., *Antimicrobial Agents and Chemotherapy*, **1991**, 35 (3), 490–496.
- (798) N. S. El-Gohary, M. I. Shaaban., *European Journal of Medicinal Chemistry*, **2017**, 131, 255–262.
- (799) M. Taha, A. Mosaddik, F. Rahim, S. Ali, M. Ibrahim, N. B. Almandil., *Journal of King Saud University - Science*, **2020**, 32 (1), 191–194.

- (800) A. Kanwal, M. Ahmad, S. Aslam, S. A. R. Naqvi, M. J. Saif., *Pharmaceutical Chemistry Journal*, **2019**, 53 (3), 179–187.
- (801) H. Yang, Y. Ren, X. Gao, Y. Gao., *Chemical Research in Chinese Universities*, **2016**, 32 (6), 973–978.
- (802) Y. Bansal, O. Silakari., *Bioorganic & Medicinal Chemistry*, **2012**, 20 (21), 6208–6236.
- (803) K. P. Barot, S. Nikolova, I. Ivanov, M. D. Ghate., *Mini-Reviews in Medicinal Chemistry*, **2013**, 13 (10), 1421–1447.
- (804) W. Akhtar, M. F. Khan, G. Verma, M. Shaquiquzzaman, M. A. Rizvi, S. H. Mehdi, M. Akhter, M. M. Alam., *European Journal of Medicinal Chemistry*, **2017**, 126, 705–753.
- (805) E. Mulugeta, Y. Samuel., *Biochemistry Research International*, **2022**, 2022 (Article ID 7255299).
- (806) J. Horton., *Parasitology*, **2000**, 121 (Suppl. 1), S113–S132.
- (807) S. Singh, N. Singh, V. Kumar, S. Datta, A. B. Wani, D. Singh, K. Singh, J. Singh., *Environmental Chemistry Letters*, **2016**, 14 (3), 317–329.
- (808) P. Gosse., *Vascular Health and Risk Management*, **2006**, 2 (3), 195–201.
- (809) D. M. Richards, R. N. Brogden, R. C. Heel, T. M. Speight, G. S. Avery., *Drugs*, **1984**, 28 (1), 38–61.
- (810) H. Iqbal, A. K. Verma, P. Yadav, S. Alam, M. Shafiq, D. Mishra, F. Khan, K. Hanif, A. S. Negi, D. Chanda., *Frontiers in Pharmacology*, **2021**, 12 (Article ID 611109).
- (811) H. Y. Aboul-Enein, A. A. El Rashedy., *Current Drug Therapy*, **2013**, 8 (3), 145–154.
- (812) T. Ishida, T. Suzuki, S. Hirashima, K. Mizutani, A. Yoshida, I. Ando, S. Ikeda, T. Adachi, H. Hashimoto., *Bioorganic & Medicinal Chemistry Letters*, **2006**, 16 (7), 1859–1863.
- (813) B. A. Reddy., *E-Journal of Chemistry*, **2010**, 7(1) (Article ID 601929), 222–226.
- (814) M. Taha, A. Ahmad Khan, F. Rahim, S. Imran, M. Salahuddin, N. Uddin, K. Mohammed Khan, S. Adnan Ali Shah, A. Zafar, Z. Amiruddin Zakaria., *Arabian Journal of Chemistry*, **2022**, 15 (1), 103505.
- (815) D. Kumar, D. N. Kommi, R. Chebolu, S. K. Garg, R. Kumar, A. K. Chakraborti., *RSC Advances*, **2013**, 3 (1), 91–98.

- (816) Y. R. Girish, K. S. Sharath Kumar, K. N. Thimmaiah, K. S. Rangappa, S. Shashikanth., *RSC Advances*, **2015**, 5 (92), 75533–75546.
- (817) R. Chebolu, D. N. Kommi, D. Kumar, N. Bollineni, A. K. Chakraborti., *Journal of Organic Chemistry*, **2012**, 77 (22), 10158–10167.
- (818) D. Anastasiou, E. M. Campi, H. Chaouk, W. R. Jackson., *Tetrahedron*, **1992**, 48 (36), 7467–7478.
- (819) H. Naeimi, N. Alishahi., *Organic Chemistry International*, **2012**, 2012 (Article ID 498521), 1–5.
- (820) R. J. Perry, B. D. Wilson., *Journal of Organic Chemistry*, **1993**, 58 (25), 7016–7021.
- (821) M. J. Plater, P. Barnes, L. K. McDonald, S. Wallace, N. Archer, T. Gelbrich, P. N. Horton, M. B. Hursthouse., *Organic & Biomolecular Chemistry*, **2009**, 7 (8), 1633–1641.
- (822) K. Das, A. Mondal, D. Srimani., *Journal of Organic Chemistry*, **2018**, 83 (16), 9553–9560.
- (823) B. Zou, Q. Yuan, D. Ma., *Angewandte Chemie International Edition*, **2007**, 46 (15), 2598–2601.

## INDEX

<b>TERMS</b>	<b>Page No.</b>
ADMET	195,198,260,263,334,336,365,366
Asinger Reaction	18
Asymmetric unit	140,143,149,153,280
Benzil	34,99,113,114,115,117,119, 121,140,158,159
Bigenelli	17,23,36,37,38,39,41,44,45,204,206,207,235,237
Bucherer and Bergs synthesis	18
Catalysis	8,9,46
Classical method	14,28,30,38,39,41,66,206,343
Copper Borate	111,113,121,136,137,140,159,269,271,272,273,278,284, 364,365,366
C–S cross-coupled	155
Debus-Raziszewski Synthesis	16
Dihedral angles	143,164,237,238,241,302,365
DFT	23,104,162,164,172,175,197,235,237,238,261,301,302, 309,335,364,365,366
DHPM	37,38,41,204,205,235,238,239,251,257,258,365,
Gewald's Synthesis	19
Hantzsch Synthesis	16
Heterocyclic compounds	1,2,3,4,6,7,9,12,13,23,24,69,90,91,98,99,100,101,103, 112,206,237,272,273,302,368,370
Mannich Reaction	17
MEP	163,164,180,181,237,238,249,250,251,301,319,320,321
Molecular Docking Study	23,106,107,163,185,187,198,255,262,325,326,336,365
Multicomponent Reactions	13,14,15,19,20,22,23,37,111,204,364
N-oxide	46,47,48,49,50,260,272,278,279

Petasis	21
Multicomponent Reaction	
Pharmacokinetic	162,163,195,196,198,235,260,261,263,269,301,334,336, 366,365,366
Povarov's reaction	19
Robinson's synthesis	17,18
Solvent free synthesis	9,12,30,41,42,50,63,64,117,206,272,276,364
Strecker's Reaction	15
Ugi Reaction	18
Wohler's Synthesis	10



# Bis[2-(4,5-diphenyl-1*H*-imidazol-2-yl)-4-nitrophenolato]copper(II) dihydrate: crystal structure and Hirshfeld surface analysis

Sailesh Chettri,<sup>a</sup> Dhiraj Brahman,<sup>a</sup> Biswajit Sinha,<sup>b</sup> Mukesh M. Jotani<sup>c</sup> and Edward R. T. Tiekink<sup>d,\*</sup>

Received 7 October 2019

Accepted 8 October 2019

Edited by W. T. A. Harrison, University of Aberdeen, Scotland

‡ Additional correspondence author: dhirajslg2@gmail.com

**Keywords:** crystal structure; copper(II); coordination complex; Hirshfeld surface analysis; computational chemistry.

**CCDC reference:** 1958158

**Supporting information:** this article has supporting information at journals.iucr.org/e

<sup>a</sup>Department of Chemistry, St. Joseph's College, Darjeeling 734 104, India, <sup>b</sup>Department of Chemistry, University of North Bengal, Darjeeling 734 013, India, <sup>c</sup>Department of Physics, Bhavan's Sheth R. A. College of Science, Ahmedabad, Gujarat 380 001, India, and <sup>d</sup>Research Centre for Crystalline Materials, School of Science and Technology, Sunway University, 47500 Bandar Sunway, Selangor Darul Ehsan, Malaysia. \*Correspondence e-mail: edwardt@sunway.edu.my

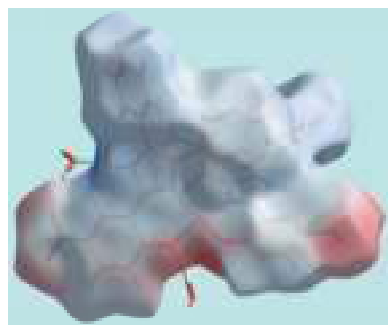
The crystal and molecular structures of the title Cu<sup>II</sup> complex, isolated as a dihydrate, [Cu(C<sub>21</sub>H<sub>14</sub>N<sub>3</sub>O<sub>3</sub>)<sub>2</sub>·2H<sub>2</sub>O], reveals a highly distorted coordination geometry intermediate between square-planar and tetrahedral defined by an N<sub>2</sub>O<sub>2</sub> donor set derived from two mono-anionic bidentate ligands. Furthermore, each six-membered chelate ring adopts an envelope conformation with the Cu atom being the flap. In the crystal, imidazolyl-amine-N—H···O(water), water—O—H···O(coordinated, nitro and water), phenyl-C—H···O(nitro) and  $\pi$ (imidazolyl)— $\pi$ (nitrobenzene) [inter-centroid distances = 3.7452 (14) and 3.6647 (13) Å] contacts link the components into a supramolecular layer lying parallel to (101). The connections between layers forming a three-dimensional architecture are of the types nitrobenzene-C—H···O(nitro) and phenyl-C—H··· $\pi$ (phenyl). The distorted coordination geometry for the Cu<sup>II</sup> atom is highlighted in an analysis of the Hirshfeld surface calculated for the metal centre alone. The significance of the intermolecular contacts is also revealed in a study of the calculated Hirshfeld surfaces; the dominant contacts in the crystal are H···H (41.0%), O···H/H···O (27.1%) and C···H/H···C (19.6%).

## 1. Chemical context

The title copper(II) complex, (I), was isolated during an ongoing research programme on the catalytic activity of copper borate (CuB<sub>4</sub>O<sub>7</sub>) for C—N heterocyclic bond formation reactions. Complex (I) was formed during the attempted synthesis of a triarylimidazole derivative using benzil and the respective aromatic aldehyde with copper borate, using ammonium acetate as a nitrogen source. The single-crystal analysis of the synthesized product revealed that in the copper(II) complex, the triarylimidazole moiety acts as a bidentate ligand for the copper atom. During the successful synthesis of the triarylimidazole, the desired product formed in good yield at a temperature in the range 100–110 °C. However, when the reaction was conducted at 130 °C and above, the title copper(II) complex formed instead of the targeted triarylimidazole. The crystal and molecular structures of (I) are described herein, along with a detailed analysis of the molecular packing *via* an analysis of the calculated Hirshfeld surfaces.

## 2. Structural commentary

The crystallographic asymmetric unit of (I) comprises a complex molecule and two water molecules of crystallization.

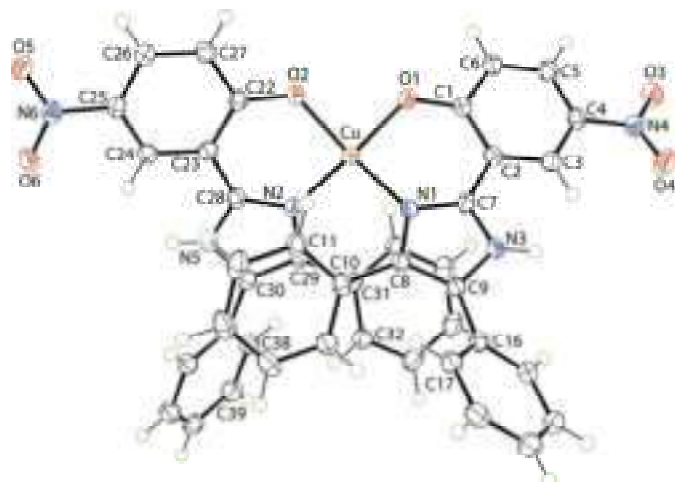




**Table 1**  
 Selected geometric parameters (Å, °).

Cu—O1	1.9291 (17)	Cu—N1	1.9586 (19)
Cu—O2	1.9304 (17)	Cu—N2	1.957 (2)
O1—Cu—O2	89.36 (7)	O2—Cu—N1	144.41 (8)
O1—Cu—N2	147.34 (8)	O2—Cu—N2	93.56 (7)
O1—Cu—N1	92.83 (8)	N1—Cu—N2	103.14 (8)

The copper(II) centre in (I), Fig. 1, is bis-*N,O*-chelated by two 2-(4,5-diphenyl-1*H*-imidazol-2-yl)-4-nitrophenolate monoanions. The resulting N<sub>2</sub>O<sub>2</sub> donor set defines a highly distorted coordination geometry, as seen in the angles included in Table 1 and in the view of Fig. 2. The angles range from a narrow 89.36 (7)°, for O1—Cu—O2, to a wide 147.34 (8)°, for O1—Cu—N2. The distortion is highlighted in the dihedral angle between the best planes through the two chelate rings of 49.82 (7)°. The value of  $\tau_4$  is a geometric measure of the distortion of a four-coordinate geometry (Yang *et al.*, 2007). For (I), the value computes as 0.48 which is almost exactly intermediate between the values of  $\tau_4 = 0$  for an ideal tetrahedron and  $\tau_4 = 1.0$  for an ideal square-planar geometry. In fact, the six-membered chelate rings are not planar, each adopting an envelope conformation with the Cu atom being the flap atom. In this description, the r.m.s. deviation for the least-squares plane through the O1/N1/C1/C2 atoms is 0.036 Å with the Cu atom lying 0.410 (3) Å out of the plane. The comparable parameters for the O2-chelate ring are 0.033 and 0.354 (3) Å, respectively. The dihedral angle formed between the two planar regions of the chelate rings is 49.38 (8)°. The dihedral angles between the best plane through the O1-chelate ring and each of the fused six- and five-membered rings are 9.18 (12) and 5.54 (14)°, respectively; the equivalent angles for the O2-chelate rings are 8.44 (8) and 2.71 (9)°, respectively. The N1-imidazol-2-yl ring forms dihedral angles of 41.20 (11) and 37.46 (10)° with the C10- and C16-phenyl substituents, respectively, and the dihedral angle between the


**Figure 1**  
 The molecular structure of the complex molecule in (I), showing the atom-labelling scheme and with displacement ellipsoids drawn at the 70% probability level.

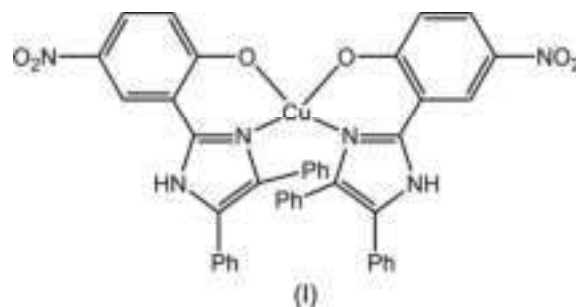
**Table 2**  
 Hydrogen-bond geometry (Å, °).

Cg1 is the ring centroid of the C16–C21 ring.

<i>D</i> — <i>H</i> ··· <i>A</i>	<i>D</i> — <i>H</i>	<i>H</i> ··· <i>A</i>	<i>D</i> ··· <i>A</i>	<i>D</i> — <i>H</i> ··· <i>A</i>
N3—H3N···O1W <sup>i</sup>	0.89 (2)	1.91 (2)	2.790 (3)	173 (3)
N5—H5N···O2W	0.88 (2)	1.95 (2)	2.822 (3)	172 (3)
O1W—H1W···O2	0.85 (2)	1.92 (2)	2.745 (2)	164 (2)
O1W—H2W···O2W <sup>ii</sup>	0.85 (2)	2.21 (2)	2.868 (2)	134 (2)
O2W—H3W···O1 <sup>iii</sup>	0.84 (2)	2.01 (2)	2.841 (2)	172 (2)
O2W—H4W···O3 <sup>iii</sup>	0.84 (2)	2.27 (2)	2.938 (2)	136 (2)
C3—H3···O1W <sup>i</sup>	0.95	2.57	3.435 (3)	151
C33—H33···O5 <sup>iv</sup>	0.95	2.48	3.345 (3)	151
C5—H5···O6 <sup>v</sup>	0.95	2.50	3.361 (3)	151
C34—H34···Cg1 <sup>vi</sup>	0.95	2.49	3.426 (3)	168

Symmetry codes: (i)  $-x + 2, -y + 1, -z + 1$ ; (ii)  $-x + 1, -y + 1, -z + 1$ ; (iii)  $x - 1, y, z - 1$ ; (iv)  $-x + 1, y + \frac{1}{2}, -z + \frac{1}{2}$ ; (v)  $x + 1, y, z + 1$ ; (vi)  $x, -y + \frac{1}{2}, z - \frac{1}{2}$ .

phenyl rings is 59.92 (8)°, *i.e.* all indicating splayed relationships. A similar situation pertains to the N2-imidazol-2-yl ring, where the comparable dihedral angles formed with the C31- and C37-phenyl rings are 38.29 (10), 48.5 (9) and 50.84 (7)°, respectively. Finally, the nitro groups are not strictly coplanar with the benzene rings to which they are connected, as seen in the dihedral angles of 14.2 (4)° for C1–C6/N4/O3/O4 and 5.9 (3)° for C22–C27/N6/O5/O6.



### 3. Supramolecular features

As each component of the asymmetric unit has hydrogen-bonding functionality, conventional hydrogen bonds are found in the crystal of (I); the geometric parameters characterizing the identified intermolecular interactions operating in the crystal of (I) are collated in Table 2. Each of the imidazolyl-amine-N—H atoms forms a donor interaction to a water molecule to generate a three-molecule aggregate. The O1W water molecule forms donor interactions to the coordinated O2 atom and to a symmetry-related O2W water molecule. The O2W water molecule connects to the coordinated O1 atom as well as to a nitro-O3 atom. Hence, the O2W water molecule is involved in four hydrogen-bonding interactions. The fourth contact involving the O1W water molecule, a C—H···O acceptor contact, is provided by the nitrobenzene ring. There is also a phenyl-C—H···O(nitro) contact of note, Table 2. The aforementioned interactions combine to stabilize a supramolecular layer lying parallel to (101), as shown in Fig. 3(a). There are also  $\pi$ – $\pi$  stacking and C—H···O interactions in the crystal, Fig. 3(b). Within layers, there are  $\pi$ – $\pi$  interactions occurring between the imidazolyl and nitrobenzene rings

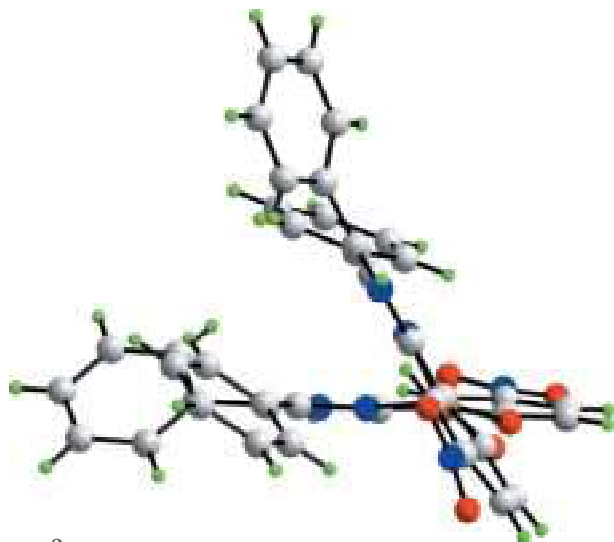


**Figure 2**  
A view of the molecular structure of the complex molecule in (I), highlighting the distorted coordination geometry about the copper(II) atom.

[inter-centroid distances:  $Cg(N1/N3/C7-C9) \cdots Cg(C1-C6) = 3.7452(14) \text{ \AA}$  and angle of inclination =  $9.70(13)^\circ$  for symmetry operation  $(-x + 2, -y + 1, -z + 1)$ ;  $Cg(N2/N5/C28-C30) \cdots Cg(C22-C27) = 3.6647(13) \text{ \AA}$  and angle of inclination =  $8.15(12)^\circ$  for  $(-x + 1, -y + 1, -z + 1)$ ]. The connections between layers along  $[010]$  are of the type nitrobenzene-C—H $\cdots$ O(nitro) and phenyl-C—H $\cdots\pi$ (phenyl), as detailed in Table 2.

#### 4. Hirshfeld surface analysis

The Hirshfeld surface calculations for (I) were performed with *CrystalExplorer17* (Turner *et al.*, 2017) and published proto-

cols (Tan *et al.*, 2019), and serve to indicate the significant role of the two water molecules in the supramolecular association in the crystal. The involvement of both the water molecules in hydrogen bonds, Table 2, are evident as bright-red spots near the respective atoms on the Hirshfeld surfaces mapped over  $d_{\text{norm}}$  for the O1W-, Fig. 4(a), and O2W-water, Fig. 4(b), molecules. In addition, the presence of faint-red spots near the O1W, O2W and H1W atoms in Figs. 4(a) and 4(b) are indicative of the other contacts of these atoms with those of the Cu<sup>II</sup> complex molecule (Table 2). The donors and acceptors of the hydrogen bonds involving atoms of the complex molecule are also apparent as bright-red spots near the participating atoms in the views of the Hirshfeld surfaces calculated for the complex molecule shown in Figs. 4(c)–(e).

The presence of a short interatomic C $\cdots$ C contact between atoms C22 and C28 (Table 3) arises from  $\pi$ – $\pi$  stacking between symmetry-related imidazole and nitrobenzene rings, and is observable as the faint-red spots near these atoms on the  $d_{\text{norm}}$ -mapped Hirshfeld surface in Fig. 4(c). The pair of faint-red spots appearing near the phenyl-C36 and H36 atoms, and also near the nitro-O5 atom on the surface indicating short interatomic contacts that characterize the weak C—H $\cdots$ O interaction, Table 3. The influence of the C—H $\cdots\pi$  contact on the molecular packing is recognized from the three faint-red spots in the phenyl-(C16–C21) ring and another near atom H34 in Fig. 4(e). The donors and acceptors of this interaction are also evident as the blue bump and a bright-orange spot enclosed within the black circle on the Hirshfeld surface mapped with the shape-index property in Fig. 5(a). The bright-orange region enclosed within a black circle in Fig. 5(b) is also an indication of the O2W—H4W $\cdots$ Cg(C16–C21) contact. The Hirshfeld surfaces mapped over the calculated electrostatic potential for the water and complex molecules in Fig. 6 also illustrate the donors and acceptors of

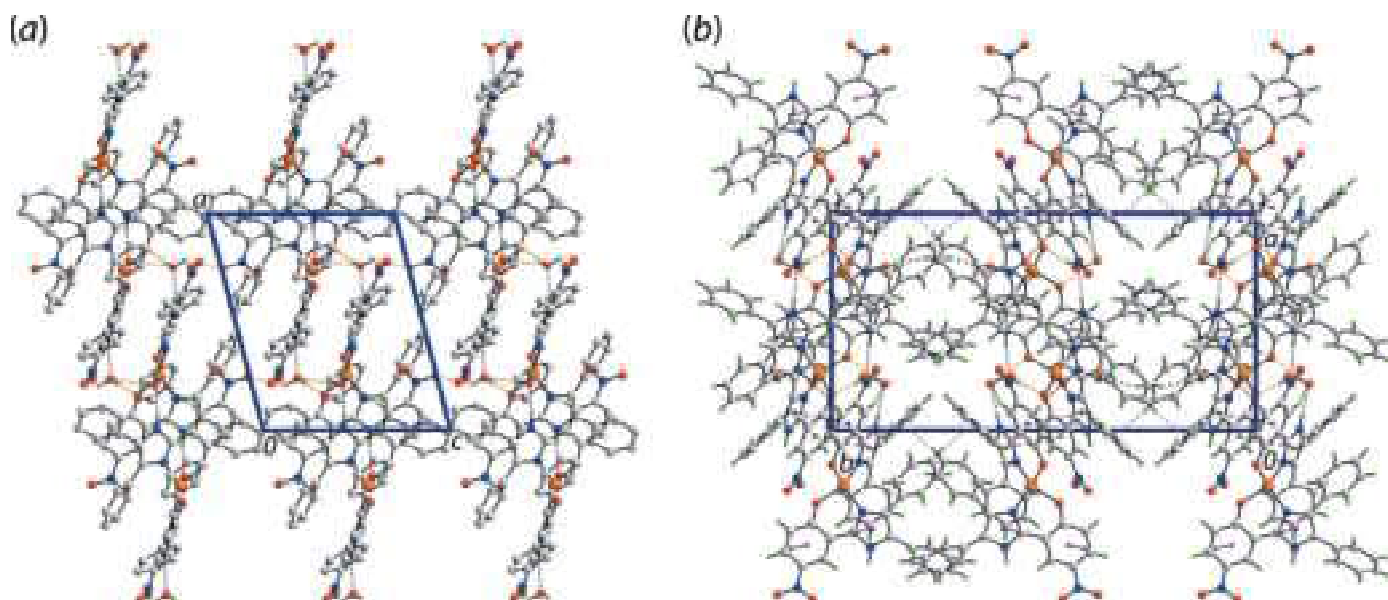


**Figure 3**  
The molecular packing in the crystal of (I): (a) a supramolecular layer parallel to (101) sustained by O—H $\cdots$ O, N—H $\cdots$ O and C—H $\cdots$ O interactions shown as orange, blue and green dashed lines, respectively, and (b) a view of the unit-cell contents in projection down the  $c$  axis, with  $\pi$ – $\pi$  and C—H $\cdots\pi$  interactions shown as purple and pink dashed lines, respectively.

intermolecular interactions through blue and red regions corresponding to positive and negative electrostatic potentials, respectively. The  $\pi$ - $\pi$  stacking between symmetry-related imidazolyl and nitrobenzene rings are viewed as the flat regions enclosing them on the Hirshfeld surfaces mapped over curvedness in Fig. 7. On the Hirshfeld surfaces mapped over  $d_{\text{norm}}$  illustrated in Figs. 4(c)–(e), faint-red spots also appear near other atoms indicating their involvement in other short interatomic contacts, as summarized in Table 3.

The Hirshfeld surfaces also provide an insight into the distortion in the coordination geometry formed by the  $\text{N}_2\text{O}_4$  donor set about the copper(II) centre in the complex molecule. This is performed by considering the Hirshfeld surface about the metal centre alone (Pinto *et al.*, 2019). The distortion in the coordination geometry is observed on the Hirshfeld surface mapped with the shape-index property as the bright-orange patches of irregular shape covering a major region for the Cu–O bonds in Fig. 8(a) and the small orange regions on the surface relatively far from the Cu–N bonds in Fig. 8(b). The different curvature of the Hirshfeld surfaces coordinated by the  $\text{N}_2\text{O}_4$  donor set in Figs. 8(c) and 8(d) also support this observation. The Cu–O and Cu–N bonds are rationalized in the two-dimensional fingerprint plot taking into account only the Hirshfeld surface for the copper atom shown in Fig. 9. The distribution of points in the fingerprint plot through the pair of

aligned red points at different inclinations from  $d_c + d_i \sim 2.0$  Å for the Cu–N bonds (upper region) and the Cu–O bonds (lower region) are indicative of the distorted geometry (Pinto *et al.*, 2019).

The overall two-dimensional fingerprint plot for (I), *i.e.* the entire asymmetric unit, Fig. 10(a), and those delineated into  $\text{H}\cdots\text{H}$ ,  $\text{O}\cdots\text{H}/\text{H}\cdots\text{O}$ ,  $\text{C}\cdots\text{H}/\text{H}\cdots\text{C}$ ,  $\text{C}\cdots\text{C}$  and  $\text{C}\cdots\text{O}/\text{O}\cdots\text{C}$  contacts are illustrated in Figs. 10(b)–(f), respectively. The percentage contribution from different interatomic contacts to the Hirshfeld surfaces of the complex molecule and for overall (I) are summarized in Table 4. The presence of water molecules in the crystal of (I) increases the percentage contribution from  $\text{O}\cdots\text{H}/\text{H}\cdots\text{O}$  contacts (Table 4) to the Hirshfeld surface of the asymmetric unit compared with the complex molecule alone. This results in slight decreases in the percentage contributions from other interatomic contacts for (I) (Table 4). A single conical tip at  $d_c + d_i \sim 1.9$  Å in the fingerprint plot delineated into  $\text{H}\cdots\text{H}$  contacts shown in Fig. 10(b) is the result of the involvement of the H12 atom in a short interatomic  $\text{H}\cdots\text{H}$  contact, Table 3. The points due to short interatomic contacts between amine hydrogen-H3N and water hydrogen atoms, H1W and H2W, Table 3, are merged within the plot. Although the molecular packing of (I) is influenced by several intermolecular  $\text{O}-\text{H}\cdots\text{O}$  and  $\text{C}-\text{H}\cdots\text{O}$  interactions, the presence of a pair of long spikes at  $d_c +$

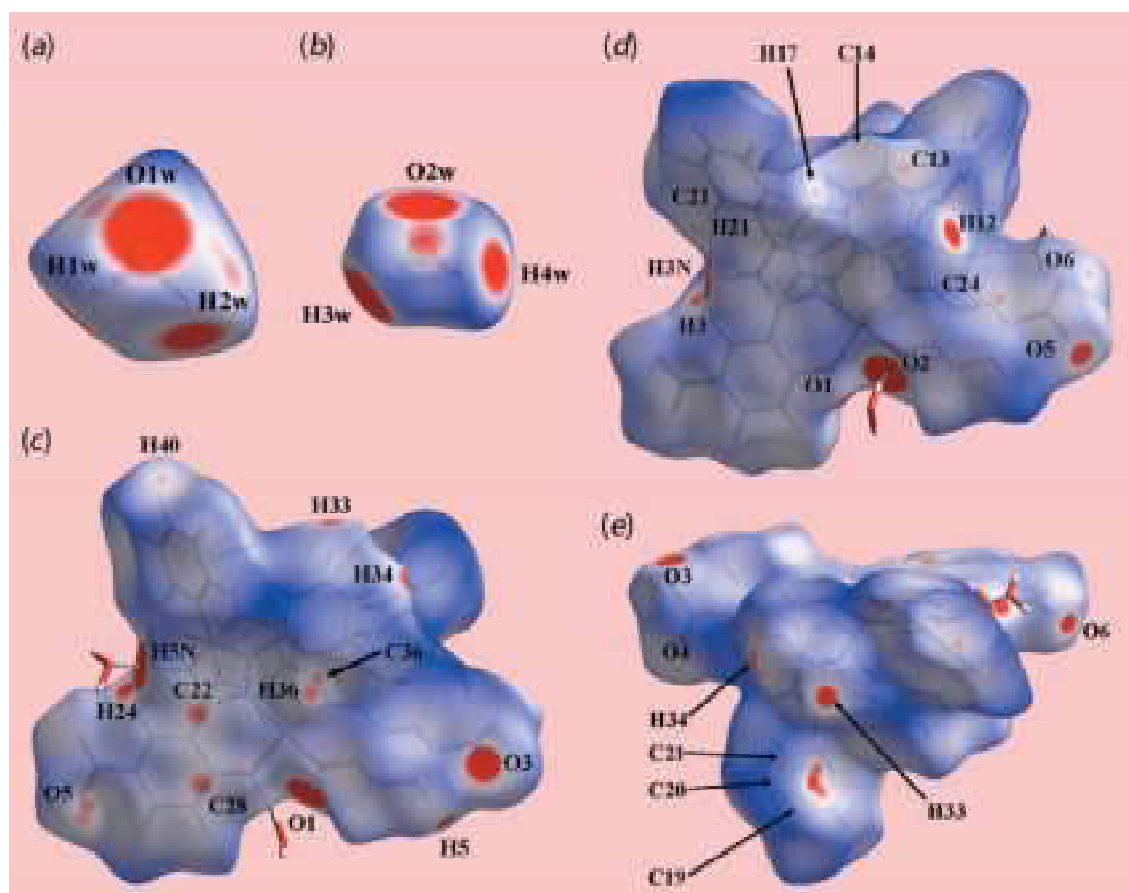
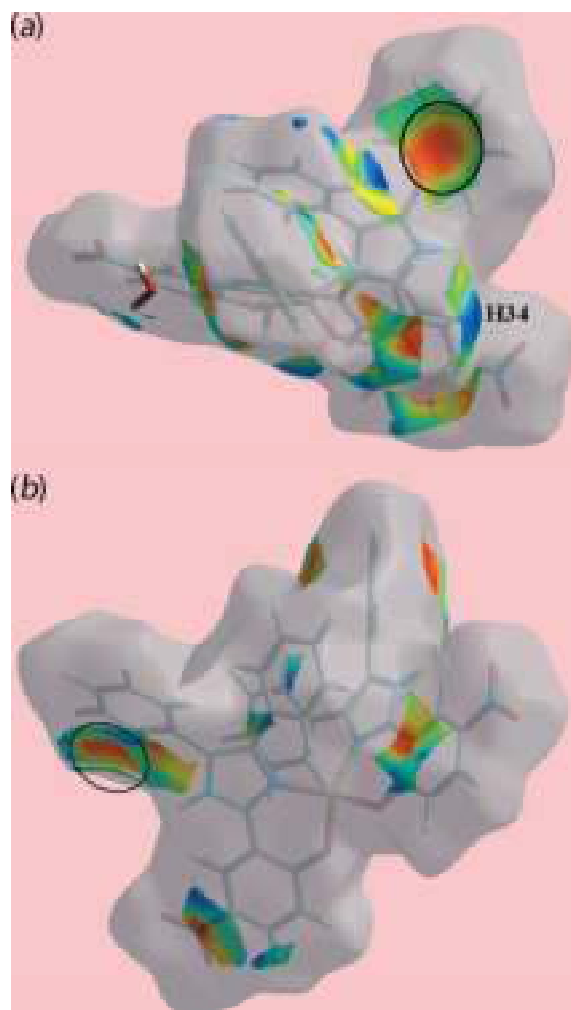


Figure 4

Different views of the Hirshfeld surfaces for the constituents of (I) mapped over  $d_{\text{norm}}$  for the (a) water-O1W molecule [in the range  $-0.2369$  to  $+1.2173$  arbitrary units (au)], (b) water-O2W molecule ( $-0.2114$  to  $+0.7500$  au) and (c)–(e) complex molecule ( $-0.1170$  to  $+1.6287$  au).


**Figure 5**

Two views of the Hirshfeld surface mapped with the shape-index property for the complex molecule in (I) from  $-1.0$  to  $+1.0$  arbitrary units highlighting (a) the donor and acceptor atoms of the  $C-H\cdots\pi$  interaction through a blue bump near the H34 atom and bright-orange curvature, enclosed within the black circle, and (b) the  $O2W-H4W\cdots\pi$  interaction by the bright-orange region enclosed within the black circle.

$d_i \sim 1.8 \text{ \AA}$  in the plot delineated into  $O\cdots H/H\cdots O$  contacts, Fig. 10(c), arise from the  $N-H\cdots O$  hydrogen bond, while the merged points correspond to other interactions at greater interatomic distances. The significant contribution from interatomic  $C\cdots H/H\cdots C$  contacts (Table 4) to the Hirshfeld surface of (I) reflect the combined influence of intermolecular  $C-H\cdots\pi$  interactions (Table 2) and the short interatomic  $C\cdots H/H\cdots C$  contacts, summarized in Table 3, and viewed as the distribution of points in the form of characteristic wings in Fig. 10(d). The presence of short interatomic  $C\cdots C$  contacts are evident as the points near a rocket shape tip at  $d_e + d_i \sim 3.2 \text{ \AA}$  in the respective delineated fingerprint plot, Fig. 10(e), while the points corresponding  $\pi-\pi$  stacking between the imidazole and nitrobenzene rings are distributed about  $d_e = d_i = 1.7 \text{ \AA}$  in the plot. The small, *i.e.* 2.7%, contribution from  $C\cdots N/N\cdots C$  contacts to the surface is also due to these  $\pi-\pi$  stacking interactions (delineated plot not shown). The

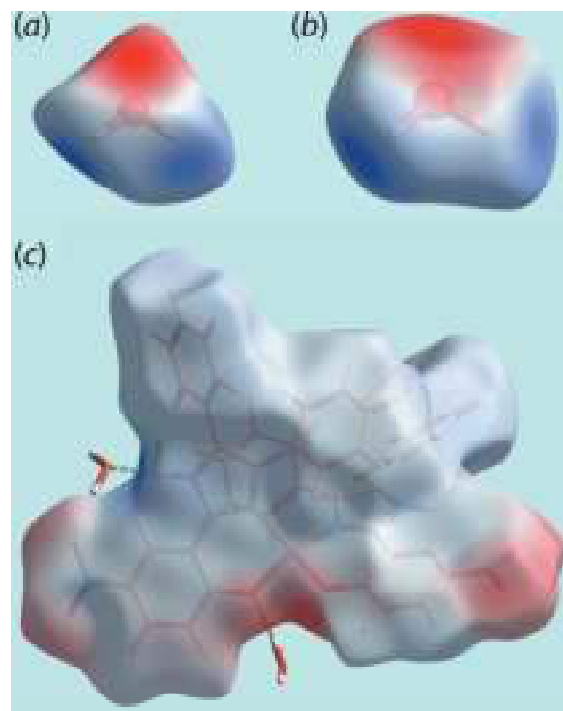
**Table 3**

Summary of short interatomic contacts ( $\text{\AA}$ ) in (I)<sup>a</sup>.

Contact	Distance	Symmetry operation
H12 $\cdots$ H12	1.92	$-x + 1, -y + 1, -z + 1$
H1W $\cdots$ H3N	2.22	$-x + 2, -y + 1, -z + 1$
H2W $\cdots$ H3N	2.26	$-x + 2, -y + 1, -z + 1$
O4 $\cdots$ H40	2.54	$x + 1, -y + \frac{3}{2}, z + \frac{1}{2}$
C1 $\cdots$ H3W	2.74	$-x + 1, -y + 1, -z + 1$
C6 $\cdots$ O6	3.206 (3)	$-x + 1, -y + 1, -z + 1$
C12 $\cdots$ H12	2.55	$-x + 1, -y + 1, -z$
C13 $\cdots$ C25	3.347 (3)	$-x + 1, -y + 1, -z$
C14 $\cdots$ O5	3.197 (3)	$-x + 1, -y + 1, -z$
H17 $\cdots$ O6	2.55	$-x + 1, -y + 1, -z$
C19 $\cdots$ H34	2.68	$x, -y + \frac{3}{2}, z - \frac{1}{2}$
C20 $\cdots$ H34	2.60	$x, -y + \frac{3}{2}, z - \frac{1}{2}$
C21 $\cdots$ H34	2.67	$x, -y + \frac{3}{2}, z - \frac{1}{2}$
C21 $\cdots$ H2W	2.64	$-x + 2, -y + 1, -z + 1$
C21 $\cdots$ O1W	3.161 (3)	$-x + 2, -y + 1, -z + 1$
C22 $\cdots$ C28	3.267 (3)	$-x + 1, -y + 1, -z + 1$
C36 $\cdots$ O5	3.146 (3)	$-x + 1, -y + 1, -z + 1$
H36 $\cdots$ O5	2.49	$-x + 1, -y + 1, -z + 1$
C41 $\cdots$ H20	2.76	$-x + 1, y, z$

Notes: (a) the interatomic distances are calculated in *CrystalExplorer17* (Turner *et al.*, 2017), whereby the  $X-H$  bond lengths are adjusted to their neutron values.

contribution of 3.2% from  $C\cdots O/O\cdots C$  contacts is due to the presence of short interatomic contacts involving nitro-O atoms, Table 2, and are apparent as the pair of parabolic tips at  $d_e + d_i \sim 3.2 \text{ \AA}$  in the delineated plot of Fig. 10(f). The


**Figure 6**

Different views of the Hirshfeld surfaces for the constituents of (I) mapped over the electrostatic potential (the red and blue regions represent negative and positive electrostatic potentials, respectively) for the (a) water-O1W molecule [in the range  $-0.1001$  to  $+0.1943$  atomic units (a.u.)], (b) water-O2W molecule ( $-0.1013$  to  $+0.1751$  a.u.) and (c) complex molecule ( $-0.1209$  to  $+0.2076$  a.u.). The hydrogen bonds involving water molecules in (c) are indicated by green dashed lines.

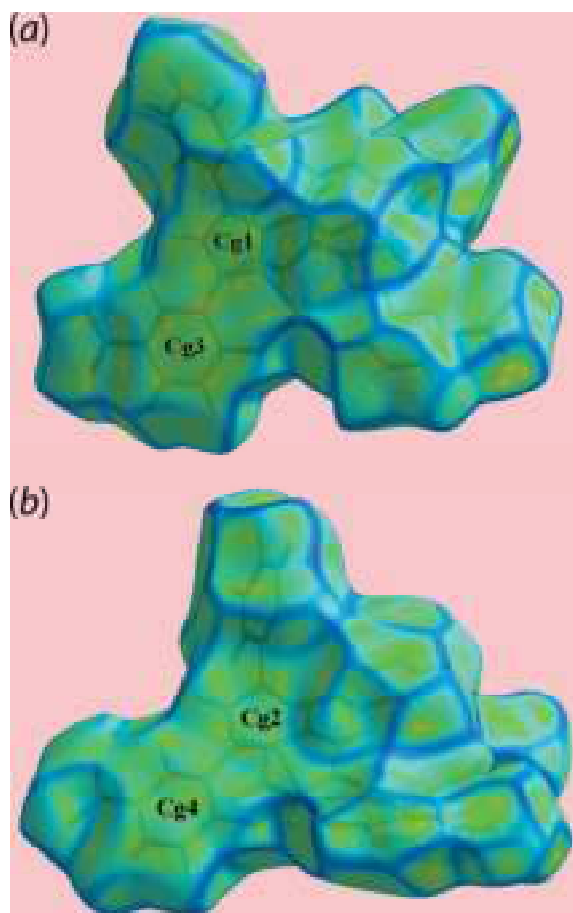


**Figure 7**  
Two views of the Hirshfeld surface mapped over curvedness for the complex molecule in (I), highlighting flat regions enclosing symmetry-related imidazole and nitrobenzene rings involved in  $\pi$ - $\pi$  stacking, labelled Cg1 and Cg3 for one pair of rings in (a), and Cg2 and Cg4 for the other pair in (b).

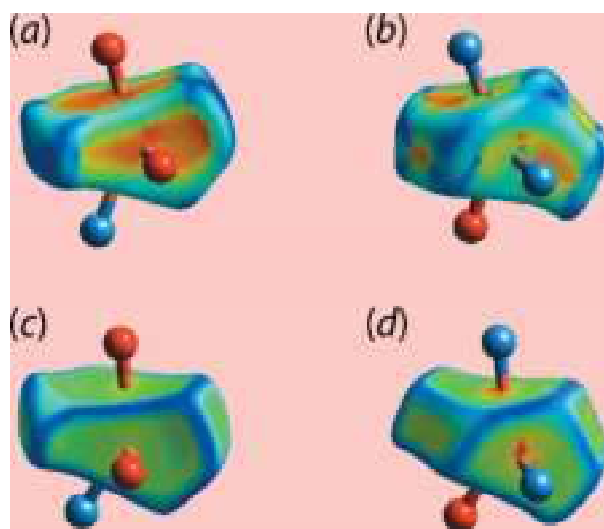


**Figure 8**  
Different views of the Hirshfeld surfaces calculated for the copper(II) centre in (I) highlighting the coordination by the  $N_2O_4$  donor set mapped over (a)/(b) shape-index in the range  $-1.0$  to  $+1.0$  arbitrary units and (c)/(d) curvedness in the range  $-4.0$  to  $+0.4$  arbitrary units.

**Table 4**  
Percentage contributions of interatomic contacts to the Hirshfeld surface for the complex molecule in (I) and overall (I).

Contact	Percentage contribution	
	complex molecule	(I)
H...H	41.3	41.0
O...H/H...O	25.6	27.1
C...H/H...C	19.8	19.6
C...C	3.5	3.3
C...O/O...C	3.4	3.2
C...N/N...C	2.8	2.7
N...H/H...N	2.2	2.1
O...O	0.6	0.5
N...O/O...N	0.2	0.2
Cu...O/O...Cu	0.0	0.3
Cu...C/C...Cu	0.3	0.0

contribution from other interatomic contacts to the surface summarized in Table 4 have negligible influence on the molecular packing.

## 5. Database survey

There are five crystal structures of copper complexes with related 2-(4,5-diphenyl-1*H*-imidazol-2-yl)phenolate ligands in the literature [Cambridge Structural Database (CSD): Groom *et al.*, 2016]. The first of these is the 4-bromo derivative of (I), isolated as a dimethylformamide solvate [(II); CSD refcode YUKSOO] (Parween *et al.*, 2015). The remaining four structures are 2,4-(*t*-Bu)<sub>2</sub>-phenolate derivatives, three of which are copper(II) complexes and the other, a copper(III) complex. Three of these four species have no additional substitution (Benisvy *et al.*, 2003). One was isolated as a methanol trisolvate [(III); JADZUK], another as a dimethylformamide tetrasolvate [(IV); NEPLAV01] and the third an oxidized species, *i.e.* a copper(III) complex, was isolated as a tetrafluoroborate salt/dichloromethane disolvate [(V); NEPLEZ01]; complex (IV) has crystallographic twofold symmetry. The final structure, a copper(II) complex (Benisvy *et al.*, 2006), has additional 4-methoxyphenyl substituents on the imidazol-

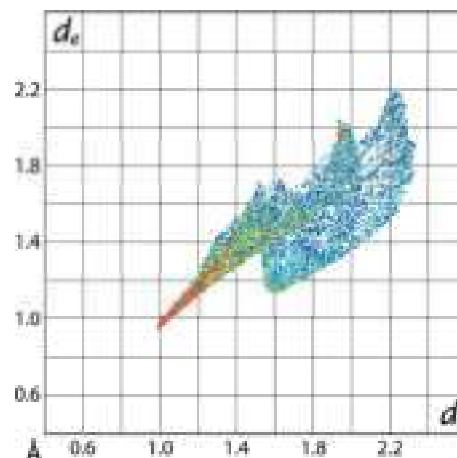


**Figure 9**  
The two-dimensional fingerprint plot taking into account only the Hirshfeld surface calculated about the copper(II) atom.

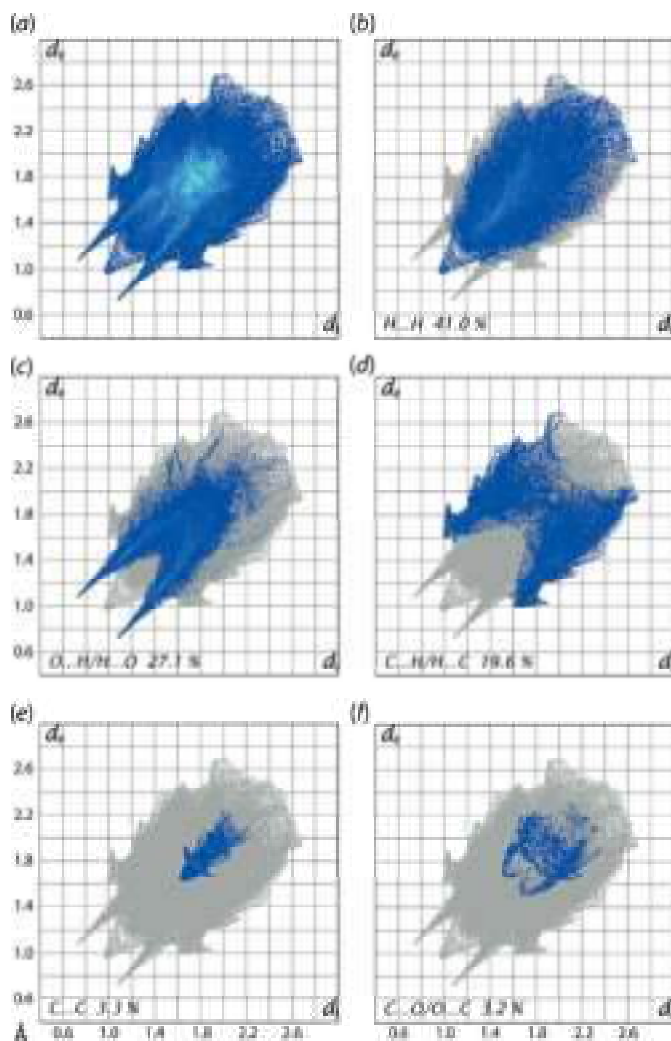


**Figure 10**  
 (a) A comparison of the full two-dimensional fingerprint plot for (I) and those delineated into (b) H...H, (c) O...H/H...O, (d) C...H/H...C, (e) C...C and (f) C...O/O...C contacts.

2-yl rings and was isolated as a methanol disolvate [(VI); JEBRUE]. The common feature of all the structures is the 'cis'-N<sub>2</sub>O<sub>2</sub> set but the coordination geometries are highly distorted, as seen in the sequence of  $\tau_4$  values for (I)–(VI) of 0.48, 0.53, 0.44, 0.37, 0.47 and 0.35, respectively.

## 6. Synthesis and crystallization

In a typical procedure, benzil (0.3 g, 1 mmol), ammonium acetate (0.19 g, 2.5 mmol), 2-hydroxy-5-nitrobenzaldehyde (0.167 g, 1 mmol) and copper(II) borate (0.218 mg, 1 mmol) were ground in an agate mortar with a pestle. To this mixture, about 1.5 g of dried silica gel (column chromatography, 60–120 mesh) was added and the reaction mixture was ground again for 30 min. The whole reaction mixture was then transferred to a 100 ml round-bottomed flask and heated at 130 °C with constant stirring for 4 h. The reaction mixture was then extracted with dry acetone and dried over MgSO<sub>4</sub>. After a few

**Table 5**  
 Experimental details.

Crystal data	
Chemical formula	[Cu(C <sub>21</sub> H <sub>14</sub> N <sub>3</sub> O <sub>3</sub> ) <sub>2</sub> ].2H <sub>2</sub> O
$M_r$	812.27
Crystal system, space group	Monoclinic, $P2_1/c$
Temperature (K)	100
$a, b, c$ (Å)	13.2752 (2), 25.1602 (4), 11.1166 (2)
$\beta$ (°)	104.256 (1)
$V$ (Å <sup>3</sup> )	3598.68 (10)
$Z$	4
Radiation type	Cu $K\alpha$
$\mu$ (mm <sup>-1</sup> )	1.42
Crystal size (mm)	0.14 × 0.11 × 0.07
Data collection	
Diffractometer	XtaLAB Synergy, Dualflex, AtlasS2
Absorption correction	Gaussian (CrysAlis PRO; Rigaku OD, 2018)
$T_{\min}, T_{\max}$	0.757, 1.000
No. of measured, independent and observed [ $I > 2\sigma(I)$ ] reflections	46023, 7490, 6420
$R_{\text{int}}$	0.058
$(\sin \theta/\lambda)_{\text{max}}$ (Å <sup>-1</sup> )	0.631
Refinement	
$R[F^2 > 2\sigma(F^2)], wR(F^2), S$	0.047, 0.128, 1.05
No. of reflections	7490
No. of parameters	532
No. of restraints	8
H-atom treatment	H atoms treated by a mixture of independent and constrained refinement
$\Delta\rho_{\text{max}}, \Delta\rho_{\text{min}}$ (e Å <sup>-3</sup> )	0.61, -0.74

Computer programs: CrysAlis PRO (Rigaku OD, 2018), SHELXS (Sheldrick, 2015a), SHELXL2014 (Sheldrick, 2015b), ORTEP-3 for Windows (Farrugia, 2012), DIAMOND (Brandenburg, 2006) and publCIF (Westrip, 2010).

days, a dark-brown solid was obtained. The product was recrystallized from dry dimethylformamide and, after 5 d, light-blue crystals of (I) were obtained (yield 60%; m.p. > 300 °C).

## 7. Refinement

Crystal data, data collection and structure refinement details are summarized in Table 5. Carbon-bound H-atoms were placed in calculated positions (C–H = 0.95 Å) and were included in the refinement in the riding-model approximation, with  $U_{\text{iso}}(\text{H})$  values set at  $1.2U_{\text{eq}}(\text{C})$ . The O- and N-bound H atoms were located in a difference Fourier map but were refined with distance restraints of O–H =  $0.84 \pm 0.01$  Å and N–H =  $0.88 \pm 0.01$  Å, respectively, and with  $U_{\text{iso}}(\text{H})$  set at  $1.5U_{\text{eq}}(\text{O})$  or  $1.2U_{\text{eq}}(\text{N})$ .

## Acknowledgements

The authors thank the Research Centre of Crystalline Materials X-ray crystallography laboratory for the X-ray intensity data. Crystallographic research at Sunway University is supported by Sunway University Sdn Bhd.

## Funding information

Funding for this research was provided by: Sunway University Sdn Bhd (grant No. STR-RCTR-RCCM-001-2019).

## References

- Benisvy, L., Bill, E., Blake, A. J., Collison, D., Davies, E. S., Garner, C. D., McArdle, G., McInnes, E. J. L., McMaster, J., Ross, S. H. K. & Wilson, C. (2006). *Dalton Trans.* pp. 258–267.
- Benisvy, L., Blake, A. J., Collison, D., Stephen Davies, E., David Garner, C., McInnes, E. J. L., McMaster, J., Whittaker, G. & Wilson, C. (2003). *Dalton Trans.* pp. 1975–1985.
- Brandenburg, K. (2006). *DIAMOND*. Crystal Impact GbR, Bonn, Germany.
- Farrugia, L. J. (2012). *J. Appl. Cryst.* **45**, 849–854.
- Groom, C. R., Bruno, I. J., Lightfoot, M. P. & Ward, S. C. (2016). *Acta Cryst.* **B72**, 171–179.
- Parween, A., Mandal, T. K., Guillot, R. & Naskar, S. (2015). *Polyhedron*, **99**, 34–46.
- Pinto, C. B., Dos Santos, L. H. R. & Rodrigues, B. L. (2019). *Acta Cryst.* **C75**, 707–716.
- Rigaku OD (2018). *CrysAlis PRO*. Rigaku Oxford Diffraction Ltd, Yarnton, Oxfordshire, England.
- Sheldrick, G. M. (2015a). *Acta Cryst.* **A71**, 3–8.
- Sheldrick, G. M. (2015b). *Acta Cryst.* **C71**, 3–8.
- Tan, S. L., Jotani, M. M. & Tiekink, E. R. T. (2019). *Acta Cryst.* **E75**, 308–318.
- Turner, M. J., Mckinnon, J. J., Wolff, S. K., Grimwood, D. J., Spackman, P. R., Jayatilaka, D. & Spackman, M. A. (2017). *CrystalExplorer*. Version 17. The University of Western Australia.
- Westrip, S. P. (2010). *J. Appl. Cryst.* **43**, 920–925.
- Yang, L., Powell, D. R. & Houser, R. P. (2007). *Dalton Trans.* pp. 955–964.